In vitro studies on HIV-1 infection of Astrocytes.

Jennifer Clarke

B.Sc. (Hons)

Infectious Diseases Laboratories
Institute of Medical and Veterinary Science
Adelaide
South Australia

Department of Microbiology
School of Molecular Biosciences
University of Adelaide
Adelaide
South Australia

****

A thesis submitted to the University of Adelaide in fulfilment of the requirements for the degree of Doctor of Philosophy

July, 2006

Table of Contents

Table of Figures

Table of Tables

THESIS SUMMARY

HIV-1 infection of astrocytes is involved in HIV-1 induced neurological diseases and is a possible source of viral persistence. *In situ* studies of post mortem brain tissue indicate that HIV-1 infection of astrocytes does occur, but is restricted. Previous *in vitro* studies have revealed intrinsic intracellular blocks to HIV-1 transcription and translation in astrocytes. Co-culture of infected astrocytes with permissive $CD4^+$ cells has been shown to "rescue" infectious HIV-1 from the restricted infection of astrocytes, resulting in transmission of infection to the $CD4^+$ cells. However, the early viral replication steps of entry, reverse transcription and integration have not been previously characterised in detail in astrocytes, and are the focus of this study.

In this thesis, two routes of initiation of *in vitro* HIV-1 infection of astrocyte cell lines were employed; i) "cell-to-cell" infection (involving coculture of astrocytes with HIV-1 infected macrophages or T-cell lines), and ii) "cell-free" infection (direct application of cell-free virus to the astrocytes). In the cell-to-cell infection model, the process of HIV-1 reverse transcription was investigated but could not be clearly demonstrated to occur within the astrocyte cell population. The cell-free infection model permitted a more detailed analysis of the interaction between astrocytes and HIV-1, focussing on the entry and post entry HIV-1 replication steps of reverse transcription and integration. In cell-free infection, uptake of HIV-1 by astrocytes occurred within vesicles. Although infectious virus was subsequently released from these cells, there was no evidence that viral replication had occurred. Extrachromosomal viral DNA could be detected in these cells, however the level of viral DNA associated with the astrocytes declined with time and was unaffected by inhibitors of HIV-1 reverse transcription. This astrocyte-associated viral DNA was subsequently shown to be due to HIV-1 DNA in the viral inoculum. Using specific assays to detect integrated forms of HIV-1 DNA, no evidence was found for viral integration in these cells. Unspliced viral RNA was present, and declined with time post infection. Despite the striking absence of integrated HIV-1 DNA in these cells, the majority of infected astrocyte cultures sporadically released infectious virus. This demonstrated that an alternative, replication-independent pathway of HIV-1 infection and transmission, previously reported in dendritic and epithelial cells, can also occur in astrocytes.

The identification and characterisation of this replication-independent pathway of astrocyte infection in this thesis may have significant ramifications for our understanding of the entry and spread of HIV-1 through the central nervous system (a major viral reservoir). The possibility that this pathway of infection occurs in astrocytes in the CNS may also impact upon the management of viral persistence and anti-retroviral therapy evasion by the virus. The effect of this replication-independent process on astrocyte function, and the relevance of this in the pathogenesis of HIV-1 associated dementia, remains to be determined.

Declaration

All work reported in this thesis was performed by myself unless otherwise stated. Monocyte derived macrophages were prepared by Dr Jillian Carr and Ms Helen Hocking. Stocks of the HIV-1 strains BaL and YU-2 were prepared by Dr Jillian Carr, and strain IIIB by Dr Nick Vandegraaff. Ms Helen Hocking, Ms Linda Mundy and Mr Adrian Purins maintained T-cell line cultures. All electron microscope sample processing and image capture was performed by Dr Peter Sutton-Smith. Dr Ghafar Sarvestani assisted in the capture of confocal microscope images and Ms Peta Grant assisted in the preparation of these images for print publication. All of the above work was performed at the Institute of Medical and Veterinary Science.

This thesis contains no material that has been accepted for the award of any other degree or diploma in any university or other tertiary institution.

To the best of my knowledge, this thesis contains no material previously published or written by any other person, except where due reference is made in the text of the thesis.

In accordance with the University of Adelaide regulations, I give my consent to this thesis being made available for photocopying and loan if accepted for the award of the degree.

Jennifer Clarke

Acknowledgments

To my Mum and Dad, for their un-ending support, encouragement, and understanding.....

To my boyfriend, Matt, for his continuous support, encouragement and understanding.....

To my dear friend, Julie-anne Lake, both for her expert scientific advice and for her friendship, especially in the difficult periods of my PhD. For her support and assistance in devising a new project when my original project could not be continued, her help in initially getting the project in this thesis "off the ground", and the confidence she instilled in my ideas and results.....

To my dear friend, Kate Thompson, for her friendship, support and understanding, our exchange of ideas, and our mini "HIV Neurovirology" meetings on Rundle Street.....

To entire IMVS HIV lab, past and present, for the invaluable positive, cooperative and friendly work environment. Especially Julie, Adrian, Nick, Jill, Adam and Raman for project and technical advice, and Helen and Jill for Macrophage preparation. A special thankyou to Kelly and Adrian for their moral support as fellow PhD students, and whose motivation, and understanding was invaluable.....

To my immediate supervisor at the IMVS, Li Peng, for his support of my ideas and the freedom he gave me to take the project in the direction it unravelled, and encouraging and supporting my attendence at conferences to expose my work and further my career.

To my Melbourne-based supervisor, Steve Wesselingh, especially for the exposure of my work, and the expert advice gained from introductions to members of the HIV-1 Pathogenesis group at the Burnet Institute. Also for assistance in career development and for contacting potential postdoctoral supervisors, and expert advice in manuscript preparation.

To my Adelaide University supervisor, Chris Burrell, for the freedom he gave me to pursue my project in the direction it unravelled, for his expert advice in manuscript preparation and for his support in exposing my work at conferences and furthering my career by this exposure and by contacting potential postdoctoral supervisors.

To the IMVS and Adelaide University for financial support to attend national and international scientific meetings, which provided valuable exposure and enabled instrumental scientific contacts to be formed.

To Ruth Brack-Werner and Tony Cunningham, for the inspiration offered by their interest in my work.....

~ THANKYOU ~

This work was supported in part by a NHMRC Dora Lush Biomedical Research Scholarship and part by the HIV-1 Research Laboratory, Institute of Medical and Veterinary Science, Adelaide and the HIV Neurovirology Laboratory, Burnet Institute, Melbourne.

Abbreviations

~	approximately
<	less than
>	greater than
°C	degrees Celcius
ACH2	Australian Centre for HIV and Hepatitis Virology Research
AIDS	Acquired Immune Deficiency Syndrome
APS	AIDS patient sera (pooled)
ATCC	American Type Culture Collection
AZT	3'-azido-3'-deoxythymidine
BBB	blood-brain barrier
bp	base pair
BSS	basal salt solution
GalC	galactocerebroside
CD	cluster designation
Ci	curie
cpm	counts per minute
CSF	cerebral spinal fluid
CTL	cytotoxic T lymphocyte
dATP	2'-deoxyadenosine 5'-triphosphate
dCTP	2'-deoxycytidine 5'-triphosphate
dH_20	de-ionised water
dGTP	2'-deoxyguanosine 5'-triphosphate
DMEM	Dulbecco modified Eagle medium
DNA	deoxyribonucleic acid
dNTP	2'-deoxynucleoside 5'-triphosphate
dpi	days post infection
DTT	dithiothreitol
dTTP	2'-deoxythymidine 5'-triphosphate
EDTA	ethylene-diamine-tetra-acetic acid
ELISA	enzyme linked immunosorbent assay
EM	electron microscopy
EMEM	Eagles Minimum Essential Media
ER	endoplasmic reticulum
FACS	fluorescence activated cell sorting
FCS	fetal calf serum
FITC	Fluorescein isothiocyanate
g (units)	gravity force
GFAP	glial fibrillary acidic protein
GM-CSF	granulocyte-macrophage colony-stimulating factor
h	hour
HEA	human embryonic astrocytes
HFA	human fetal astrocytes
HIV-1	Human Immunodeficiency Virus Type 1
HIV-VIG	Human Immunodeficiency Virus Virology Interest Group
hpi	hours post infection
IAA	isoamyl alcohol

ICAM-1	intercellular adhesion molecule-1
IFA	immunofluorescent assay
IFN	interferon
IgG	immunoglobulin G
IL	interleukin
kb	kilobase-pair
LB	Luria-Bertani medium
MCP-1	monocyte chemoattractant protein-1
M-CSF	macrophage colony-stimulating factor
MDM	monocyte-derived macrophage
MEM	Minimum Essential medium
-MG	malignant glioma
μg	microgram
μM	micromolar (micromoles per litre)
min	minute(s)
MIP-1β	Macrophage inflammatory protein 1β
ml	millilitre
mM	millimolar (millimoles per litre)
mpi	minutes post infection
NCHVR	National Centre for HIV Virology Research
NDS	normal donkey serum
ng	nanogram
NGF	nerve growth factor
NGS	normal goat serum
NHS	normal human serum
NIH	National Institutes of Health
NMDA	N-methyl-D-aspartate
OD	optical density
nt	nucleotide
^{32}P	radioactive phosphorous (mass number: 32)
PAGE	polyacrylamide gel electrophoresis
PBL	peripheral blood lymphocytes
PBMC	peripheral blood mononuclear cells
pBS	plasmid pBluescript (KS)
PBS	phosphate buffered saline
PC2	physical containment laboratory level 2
PC3	physical containment laboratory level 3
PCR	polymerase chain reaction
PHA	phytohemagglutinin
pi	post infection
PIC	pre-integration complex
PMA	phorbal myristic acid
PNK	polynucleotide kinase
RANTES	regulated upon activation normal T cell expressed and secreted
RNA	ribonucleic acid
rpm	revolutions per minute
RT	reverse transcriptase
SDS	sodium dodecyl sulphate
s	second(s)
SSC	standard saline citrate

ssDNA	salmon sperm DNA
std	standard
STE	sodium tris EDTA
T4 PNK	T4 polynucleotide kinase
TAE	tris-acetate EDTA
TBE	tris-boric acid EDTA
$TCID_{50}$	50% tissue culture infectious dose
TE	tris EDTA
TGF	transforming growth factor
TNF	tumour necrosis factor
VCAM-1	vascular cell adhesion molecule-1
v/v	volume per volume
w/v	weight per volume

Publications and presentations arising from this thesis

Publications:

Clarke JN, Lake J, Burrell CJ, Wesselingh SL, Gorry PR and Li P. (2006) Novel pathway of human immunodeficiency virus type 1 uptake and release in astrocytes - *Virology*. **348** pp141-155.

Conference Presentations:

Clarke JN, Lake J, **Burrell CJ**, Wesselingh SL and Li P. (2005) A new concept in restricted HIV-1 infection of astrocytes. Oral presentation at the XIIIth International Congress of Virology.

Clarke JN, Lake J, Burrell CJ, Wesselingh SL and Li P. (2004) A new concept in restricted HIV-1 infection of astrocytes. Oral presentation at the 6th International Symposium on NeuroVirology, Sardinia, Italy, September 2004. I was awarded the Volker ter Meulen Investigator in Training Lectureship Award for this presentation.

Clarke JN, Lake J, Burrell CJ, Wesselingh SL and Li P. (2004) A new concept in restricted HIV-1 infection of astrocytes. Oral presentation at the Australian Society for HIV-1 Medicine National Conference, Canberra, September 2004.

Clarke JN, Lake J, Burrell CJ, Wesselingh SL and Li P. (2004) A new concept in restricted HIV-1 infection of astrocytes. Oral presentation at the National HIV Virology Interest Group Conference, Barossa, July 2004.

Clarke JN, Lake J, Burrell CJ, Wesselingh SL and Li P. (2004) A new concept in restricted HIV-1 infection of astrocytes. Oral presentation at the Australian Society for Medical Research South Australian branch meeting, June 2004.

Clarke JN, Lake J, Burrell CJ, Wesselingh SL and Li P. (2004) A new concept in restricted HIV-1 infection of astrocytes. Oral presentation at the Australian Society for Microbiology South Australian branch meeting, April 2004. I was awarded the Becton Dickinson Award for this presentation.

Clarke JN, Lake J, Burrell CJ, Wesselingh SL and Li P. (2004) A new concept in restricted HIV-1 infection of astrocytes. Invited speaker at the HIV-1 Pathogenesis Seminar Series, Burnet Institute, Melbourne, February 2004.

Chapter 1

Introduction

1.1 Background on HIV

1.1.1 Discovery and classification of the Human Immunodeficiency Virus

During the late 1970s and early 1980s an unusual syndrome, characterised by lymphadenopathy, opportunistic infections such as *Pneumocystis carinii* pneumonia and a variety of unusual cancers (including non-Hodgkin's lymphoma and Kaposi's sarcoma), began to present in previously healthy individuals in the USA and Europe. This immunodeficiency syndrome was first reported by the Centres for Disease Control, USA in 1981 (1981). A similar "Acquired Immunodeficiency Syndrome" (AIDS) was seen in male homosexuals, intravenous drug users, hemophiliacs and other blood transfusion recipients, and their partners and children. A common laboratory finding in these patients was a reduced number of $CD4^+$ T-cells in their peripheral blood. In 1983 three similar infectious agents were isolated from such patients; "lymphadenopathy-associated virus" (LAV) (Barre-Sinoussi *et al*, 1983), "Human T-cell Leukemia Virus Type III (HTLV-III)" (Gallo *et al*, 1984; Popovic *et al*, 1984) and "AIDS-associated retrovirus" (ARV) (Levy *et al*, 1984). The similarity of these three viruses, and differences from HTLV, lead to the renaming of this new group of viruses as Human Immunodeficiency Virus (HIV) (Coffin *et al*, 1986).

The presence of a virus-associated reverse transcriptase together with the morphology of this agent upon electron microscopy (refer Section 1.1.5) indicated that HIV was a member of the Retroviridae Family (Barre-Sinoussi *et al*, 1983; Gonda *et al*, 1985). Like previously described retroviruses, mature HIV-1 particles were observed to have an electron dense core and a diameter of approximately 100nm (Coffin *et al*, 1997). Subsequent sequence analysis of the proviral DNA further classified this virus as a member of the Lentivirus genus (Ratner *et al*, 1985). This lead to the identification of a number of other, genetically distint, primate lentiviruses, including simian immunodeficiency virus (SIV) and a less virulent human immunodeficiency virus (HIV-2). Accordingly the human immunodeficiency virus described above was renamed HIV-1.

HIV-1 is thought to have originated from SIV infected chimpanzees in certain parts of Africa (Eigen and Nieselt-Struwe, 1990; Holmes, 2001; Myers *et al*, 1992; Sharp *et al*, 2005; Vidal *et al*, 2000). HIV-1, like all retroviruses, exhibits a high degree of genetic variation. Phylogenetic comparisons between HIV-1 strains found worldwide have identified eleven distinct subtypes or clades. The predominant subtype in the Western world is type B. The predominant subtype in India and Africa, and globally, is type C. Whilst subtype B is the most studied, the general course of disease progression due to the different subtypes appears similar, and involves degeneration of the immune system. The pathogenesis of HIV-1 described in this thesis pertains to subtype B.

1.1.2 Prevalence of HIV-1 infection

In December 2005 the estimated number of people living with HIV was between 36.7-45.3 million (2005). An estimated 3.1 million people with AIDS died in 2005, whilst approximately 4.9 million people became newly infected. Across the world, the number of people living with HIV has continued to increase. In particular, the prevalence of HIV-1 has significantly increased in India, China, Papua New Guinea, Vietnam, Ukraine and the Russian Federation in the last few years. Globally, the number of women living with HIV has also increased significantly in this period. The Sub-Saharan region of Africa is the worst affected region, with around 25.8 million people living with HIV (Figure 1.1).

Whilst the advent of effective highly active anti-retroviral therapy / anti-retroviral therapy (HAART / ART) has dramatically improved the care and prognosis of people living with HIV-1 in the developed world, at the end of 2003 only around 400 000 of the people living with HIV-1 (ie only 1%) were being treated. Treatment programs are under way in many developing countries, however access to and delivery of treatment is hindered by several factors including cost, availability of trained staff, and cultural and political barriers. The access to anti-retroviral therapy has improved significantly in many developing countries in the last two years, but it is still only estimated that, at best, only one person in ten in Africa, and one person in seven in Asia in need of anti-retroviral therapy were receiving it in mid-2005 (2005).

Figure 1.1 Prevalence of HIV

Global distribution and number of people estimated to be living with HIV at the end of 2005. The range of estimates for each region is indicated within brackets, with the mean estimate indicated above, in bold.

Adapted from www.unaids.org

1.1.3 Clinical course of HIV-1 infection

HIV-1 is transmitted via body fluids and blood products. The predominant routes of transmission are direct sexual contact, needle-sharing, and vertical transmission from mother to child. Infected cells and cell-free virus come into contact with mucosal surfaces or the blood stream. Direct access to the blood enables the virus to come into contact with circulating immune cells including T-cells and monocytes. These cells express both the main receptor for HIV-1 (CD4) and a "coreceptor" which facilitate virus entry and infection (Section 1.1.6i). Contact of the virus with mucosal surfaces leads uptake of the virus by the resident immune cells of the mucosa; Dendritic cells. These macrophage-related cells also express CD4 and a coreceptor for HIV-1. They take up the virus for antigen presentation and can become directly infected. After taking up HIV-1, dendritic cells migrate to local draining lymph nodes where they come into contact with circulating immune cells, enabling the virus to spread to T-cells and monocytes. Viremia results and circulation of infected T-cells and monocytes rapidly distributes the virus throughout the body.

A burst of viral replication occurs in the first few weeks of infection, accompanied by a sharp drop in the number of circulating $CD4^+$ T-cells and a clinical syndrome which resembles acute mononucleosis, with fever, malaise, and lymphadenopathy. Approximately 3-6 weeks after the initial infection, a specific anti-HIV-1 CTL immune response is detectable, followed by an antibody response, and a concomitant decline in viremia ensues (Figure 1.2). Symptoms usually resolve, and the number of circulating $CD4^+$ T-cells stabilises temporarily.

Typically over the next 8 to 12 years few, if any, clinical manifestations are experienced. Throughout this period of "clinical latency" steady viral replication continues and the number of $CD4^+$ T-cells decline. In the majority of untreated infected individuals, the number of $CD4^+$ T-cells eventually reaches a critically low level, and plasma virus titres simultaneously escalate. The dysfunction and severe depletion of vital immune cells renders the individual highly susceptible to reactivation of other latent infections and the onset of opportunistic diseases. This clinical presentation of late stage HIV-1 infection is known as Acquired Immunodeficiency Syndrome (AIDS). This syndrome may include protozoal,

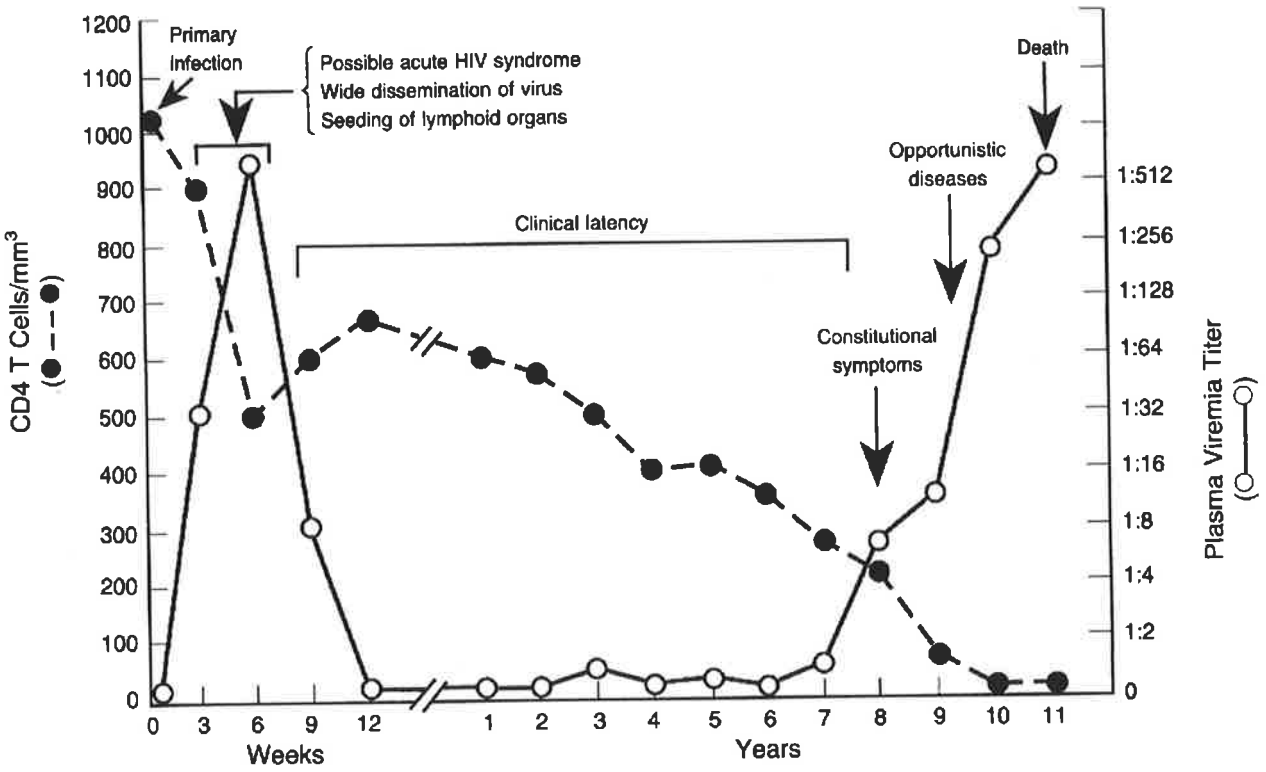

Figure 1.2 Typical course of HIV-1 disease progression in an untreated patient.
Primary infection of an individual initially results in a burst of viral replication giving rise to viremia, with a concomitant loss of $CD4^+$ T cells. This may be accompanied by general symptoms resembling acute mononucleosis. By three to six weeks after the initial infection, a HIV-1 specific immune response has been generated which, temporarily, restricts the viremia. Correspondingly, the number of $CD4^+$ T cells in the peripheral blood stabilises, and the individual is asymptomatic for several years. As the number of $CD4^+$ T cells falls below 300 / mm^3, symptoms begin to develop. This is paralleled by the re-emergence of viremia. When the $CD4^+$ T cell count eventually falls below a critical level (approximately 200 / mm^3), the individual becomes highly susceptible to both reactivation of latent infections and to new, opportunistic infections.

Adapted from Pantaleo *et al.* 1993.

bacterial, fungal and viral infections, the development of malignancies and a variety of neurological symptoms (see Section 1.3).

Treatment with a single antiretroviral drug is only effective for a short time (weeks to months), as "drug-escape" viral mutants readily emerge (Wei *et al*, 1995). HAART involves treatment with a combination of 3 or more drugs that target at least two different steps in viral replication. A treatment regime that inhibits the viral reverse transcriptase and viral protease is highly effective at suppressing viral replication and delaying the onset of AIDS. However, whilst plasma virus levels can be suppressed below detection, virus can still be recovered from $CD4^+$ T cells (Chun *et al*, 1997; Finzi *et al*, 1997; Wong *et al*, 1997). Complete virus eradication is not achieved, and virus levels rebound upon removal of therapy (Chun *et al*, 1999). This indicates that the virus or provirus is able to persist in certain population(s) of cells despite extended therapy.

1.1.4 HIV-1 persistence

The ability of HIV-1 to gain access to virtually all organs of the body, to infect a variety of cell types, and to integrate its proviral DNA into the cellular chromosomes, form the basis for long term persistence of the infection. Indeed, even in patients whose viral loads have been undetectable during treatment for several years, cessation of antiretroviral therapy results in a rebound of HIV-1 viremia (Chun *et al*, 2000; Davey *et al*, 1999; Harrigan *et al*, 1999; Imamichi *et al*, 2001; Rosenberg *et al*, 2000; Zhang *et al*, 2000). This indicates that either an undetectable level of viral replication continues in the presence of effective HAART therapy, and / or that the virus can persist in latent reservoirs or sanctuaries, evading eradication by therapy, for extended periods of time. Evidence for a low level of ongoing viral replication in the presence of HAART includes genetic sequence evolution (Gunthard *et al*, 1999; Zhang *et al*, 1999) unintegrated DNA levels (Chun *et al*, 1997) and the continued presence of cell-associated viral RNA (Furtado *et al*, 1999). There is also evidence that viral reservoirs, which enable long-term persistence of the virus in a stable, replication-competent form, are established early in the course of HIV-1 infection (Chun *et al*, 1998; Finzi *et al*, 1997; Lisziewicz *et al*, 1998; Lori *et al*, 1999) and can persist despite extended therapy (Chun *et al*, 1999; Chun *et al*, 2000; Davey *et al*, 1999; Harrigan *et al*, 1999; Imamichi *et al*, 2001; Rosenberg *et al*, 2000; Zhang *et al*, 2000). Ongoing low level

viral replication in the presence of HAART may also serve to continually reseed viral reservoirs (Dornadula *et al*, 1999; Furtado *et al*, 1999; Sharkey *et al*, 2000; Yerly *et al*, 2000; Zhang *et al*, 1999).

Long-lived, resting memory $CD4^+$ T-cells are the most studied reservoir of HIV-1. This reservoir alone is reported to be sufficient for extended persistence of HIV-1 in the majority of patients on HAART (Finzi *et al*, 1999; Zhang *et al*, 1999). Sequence analysis of the viral strains which emerge upon cessation of therapy have been reported to be similar to the genotypes that pre-existed in the latent $CD4^+$ T-cell reservoir in some, but, notably, not all patients (Chun *et al*, 2000; Imamichi *et al*, 2001; Siliciano and Siliciano, 2000; Zhang *et al*, 2000). This indicates that HIV-1 replication can also be reactivated from other sources of persistence.

Sources of viral persistence (or "viral reservoirs") may be considered from a cellular or anatomical point of view (Blankson *et al*, 2002). In addition to resting memory $CD4^+$ T-cells, postulated cellular reservoirs include macrophages, follicular dendritic cells, and probably also quiescent $CD4^+$ T-cells, monocytes, $CD8^+$ T-cells, blood-derived dendritic cells, B-cells, astrocytes and microglia (Blankson *et al*, 2002; Brack-Werner, 1999). Anatomical reservoirs include the Central Nervous System (CNS), Gut-associated lymphoid tissue, bone marrow, genito-urinary tract and the kidneys (Blankson *et al*, 2002; Brack-Werner, 1999; Cavert and Haase, 1998; Schrager and D'Souza, 1998).

It has been suggested that the central nervous system may be a major anatomical source of viral persistence (Brack-Werner, 1999; Schrager and D'Souza, 1998). HIV-1 enters the CNS early in the course of infection, where it infects microglia / macrophages and astrocytes (discussed in detail in Section 1.3). Viral replication in the CNS may not be restricted by HAART as well as it is systemically, because the blood-brain barrier hinders the access of many (but not all) antiretroviral agents (Brew, 2001). The frequency of infection of these cell types is moderate (around 7.5% and 2.6% for microglia and astrocytes, respectively), and, as there are around 10^{12} cells in each of these two populations present in the adult brain, these represent two major cellular reservoirs of viral persistence. Indeed, the number of HIV-1 infected microglia, and the number of HIV-1 infected astrocytes, have each been estimated to be similar to the number of infected lymphocytes in untreated patients (Table 1.1) (Brack-Werner, 1999).

HIV Target Cell			HIV DNA Positive Cells	
Compartment	**Type**	**Total number in compartment**	**Frequency (%)**	**Calculated number in compartment**
Brain	Astrocyte	$0.4\text{-}2.0\text{x}10^{12}$	2.6	$1.0\text{-}5.0\text{x}10^{10}$
Brain	Microglia	$0.2\text{-}1.0\text{x}10^{12}$	7.5	$1.0\text{-}7.5\text{x}10^{10}$
Lymph Nodes	Lymphocytes	$2.0\text{x}10^{11}$	15-30	$1.0\text{-}6.0\text{x}10^{10}$
Blood	PBMC	$1.0\text{x}10^{10}$	4.6	$5.0\text{x}10^{8}$

Table 1.1 Central nervous system cells represent a major potential source of virus persistence.

The CNS has been postulated to be a key anatomical reservoir for HIV-1. Indeed, in untreated HIV-1 individuals, the estimated number of microglia and astrocytes which may harbour HIV-1 DNA is similar to the estimated number of infected lymphocytes. The tabulated frequency of HIV-1 positive astrocytes and HIV-1 positive microglia in the CNS of HIV-1 infected individuals represents the mean frequency of HIV-1 positive astrocytes or microglia from two independent studies covering 26 cases of AIDS (Bagasra *et al.* 1996), by *in situ* DNA-PCR.

Adapted from Brack-Werner *et al.* 1999.

1.1.5 The HIV-1 Virus

The HIV-1 genome is composed of two identical copies of a 9.2kb single stranded, positive sense, non-segmented RNA. Upon infection of a target cell, this genomic RNA is reverse transcribed into linear, double stranded DNA that is subsequently integrated into the host cell chromosome and established as provirus (for a detailed description refer to Section 1.1.6). In the virion, the two identical positive sense RNA molecules exist in close association with the nucleocapsid protein and the viral enzymes reverse transcriptase, integrase and protease (Figure 1.3). Capsid proteins encapsulate this nucleoprotein complex, forming a condensed core structure. In mature virions this appears as a dense cone shape upon electron microscopy (Figure 1.4).

The transcriptionally active proviral DNA genome is around 9.7kb, and, like all retroviruses, has three main structural genes; *gag*, *pol* and *env* (Figure 1.5). *Gag* (**g**roup specific **a**nti**g**en) encodes structural proteins including the matrix, capsid and nucleoproteins, *pol* (**pol**ymerase) encodes the protease, reverse transcriptase and integrase enzymes, and *env* (**env**elope) encodes the surface and the transmembrane glycoproteins. HIV-1 is a complex retrovirus, with additional regulatory (Rev, Tat and Nef) and accessory (Vpr, Vpu and Vif) proteins being derived from multiply spliced RNA transcripts. Repeating sequences (R) occur at both the 5' and 3' end of the RNA genome. The duplication of this repeating region at both ends of the genomic RNA is important in facilitating reverse transcription of the genome (Section 1.1.6ii). During reverse transcription sequences from both 3' (U3; **u**nique **3**') and 5' (U5; **u**nique **5**') end of the RNA genome are also duplicated, forming a region (U3-R-U5) known as the LTR (**l**ong **t**erminal **r**epeat) at each end of the genomic DNA. The LTR region includes promoter, enhancer and regulatory elements for viral transcription.

1.1.6 HIV-1 Replication

The life cycle of HIV-1 is representative of the Retroviridae, and is depicted in Figure 1.6. In summary, to enter a target cell, the envelope of the virus needs to attach to specific cell-surface receptors. The expression of these receptors defines the cell tropism of the virus. Upon this interaction, the viral and cellular membranes fuse, facilitating the entry of the viral core into the cell cytoplasm where reverse transcription of the viral RNA genome can

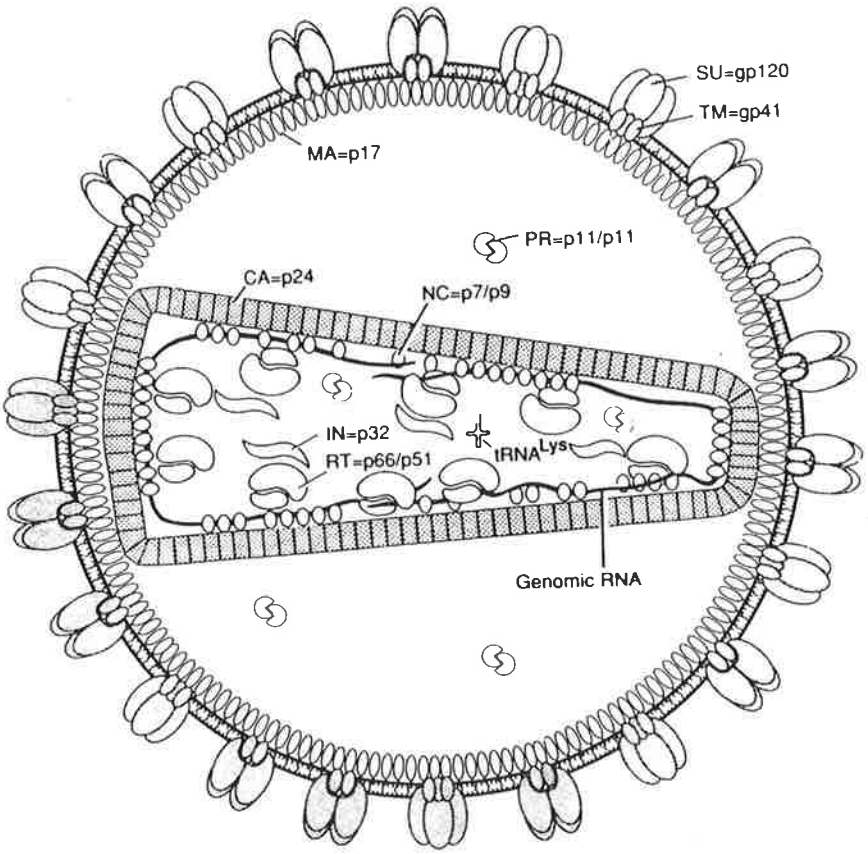

LEGEND:

= MA = p17 = matrix protein
= CA = p24 = capsid protein
= NC = p7/p9 = nucleocapsid protein
= PR = p11/p11 = protease
= RT = p65/p51 = reverse transcriptase
= IN = p32 = integrase
= SU = gp120 = envelope protein (surface glycoprotein)
= TM = gp41 = transmembrane protein
= host cell-derived $tRNA_3^{lys}$

Figure 1.3 Model of the structure of the mature HIV-1 virion. Relative distribution of the viral components are indicated.

Adapted from Arnold and Arnold, 1991.

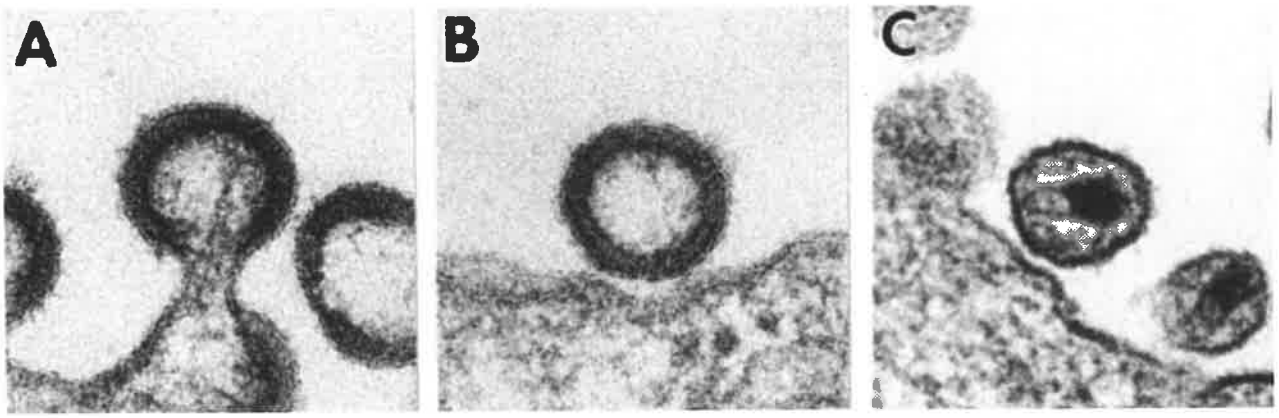

Figure 1.4 Ultrastructure of the HIV-1 virus particle.

Transmission electron microscopy illustrating the ultrastructure of the HIV-1 virus particle; new virions budding from an infected cell (**A**) and newly released virions (**B**) exhibit an "immature" morphology with an electron dense circumference. Mature HIV-1 virions (**C**) exhibit an electron dense perimeter and cone-shaped core.

Adapted from Gonda *et al.* 1989.

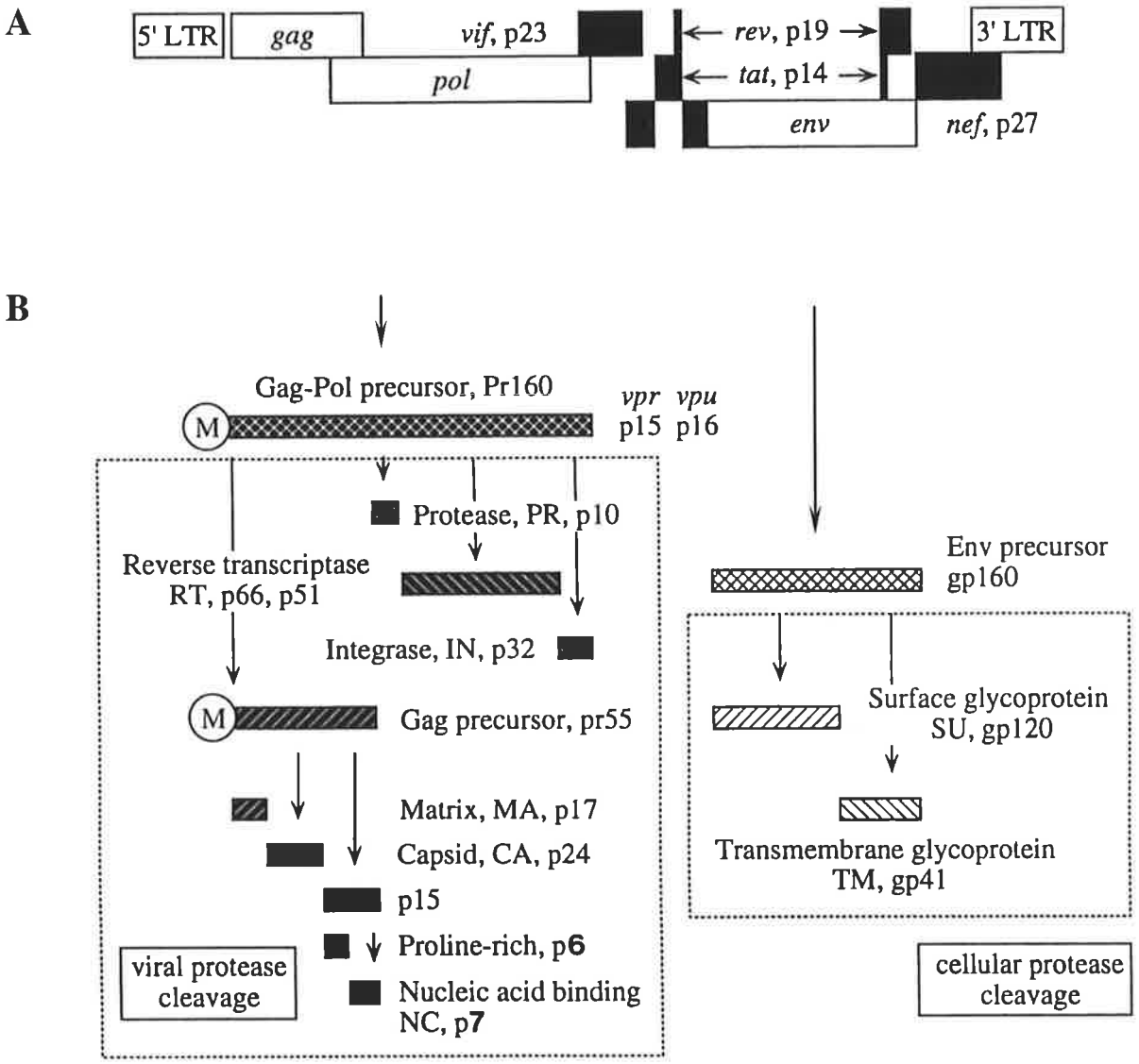

Figure 1.5 Genomic organisation of HIV-1 and viral protein processing. The HIV-1 genome contains 9 overlapping open reading frames (**A**). This gives rise to 10 distinct viral transcripts (the Gag and Gag-Pol polyprotein share the same open reading frame). The structural and enzymatic protein precursors are processed by viral and cellular proteases (**B**). The viral protease is responsible for the processing of the 160kDa Gag-Pol polyprotein into four Gag proteins (Matrix, Capsid, Nucleocapsid and Proline-rich) and 3 enzymes (Protease, Reverse Transcriptase / RNase and Integrase). The Env precursor is cleaved by a cellular protease into the surface and transmembrane glycoproteins. The viral regulatory (Tat, Rev and Nef) and accessory proteins (Vif, Vpu and Vpr) are not processed by proteases.

Adapted from Levy J.A. (1998)

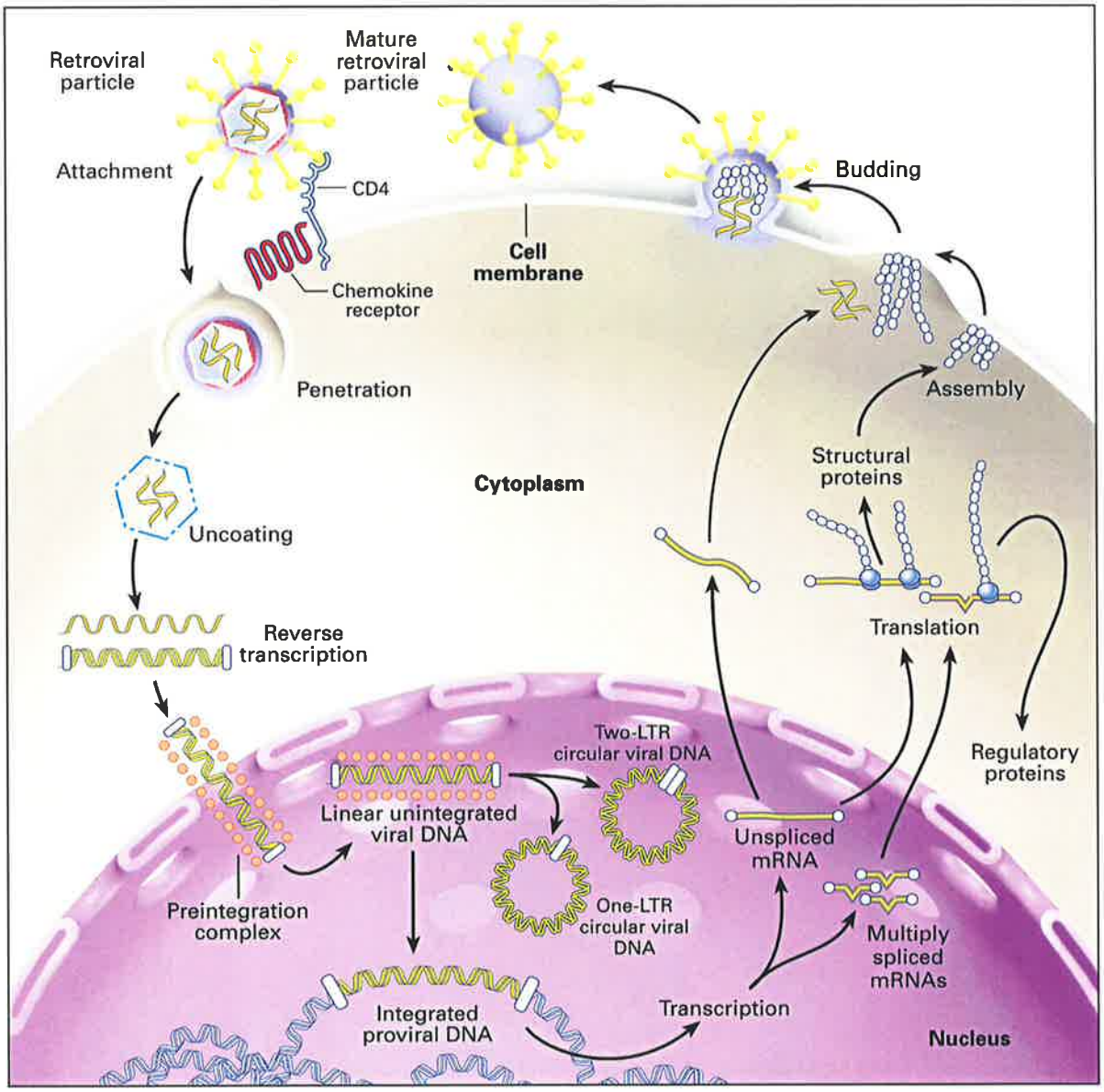

Figure 1.6 Life-Cycle of HIV-1

Cell-free HIV-1 infection of a CD4+ and coreceptor expressing cell. Attachment and the fusion of viral and cell membranes occurs via interaction of the viral gp120 and gp41 with a CD4 and coreceptor molecule on the cell surface. This enables the viral core to access the cell cytoplasm, where viral reverse transcription can proceed. Newly synthesised viral DNA is targeted to the nucleus, where it may either self-ligate to form circular forms, or integrate into the host genome. Viral replication proceeds from integrated proviral DNA. Viral early gene products (regulatory proteins) enable transcription and translation of larger HIV-1 RNAs. Upon assembly, the immature, enveloped virions are released by budding, and subsequently undergo maturation.

Adapted from Furtado *et al* 1999.

proceed. The DNA copy of the viral genome becomes integrated into a cell chromosome, and regulated transcription and translation of the viral genes subsequently result in the production and release of viral progeny. The individual steps of the HIV-1 life cycle are described below.

1.1.6i Cell attachment and entry

Cell-free HIV-1 infection is initiated through the binding of the viral surface glycoproteins, gp120 trimers, with the cellular receptor, CD4 (McDougal *et al*, 1986). The majority of infection events require this high affinity CD4-gp120 interaction, although CD4 independent virus entry has also been described in several cell types, including astrocytes (see Section 1.5.1) (Bagasra *et al*, 1996; Brack-Werner, 1999; Saha *et al*, 2001; Speck *et al*, 1999). Whilst the interaction of gp120 with CD4 is usually essential for infection, this interaction alone is insufficient for virus entry (Clapham and Weiss, 1997; James *et al*, 1996) and interaction with an additional cell surface receptor (termed a "co-receptor") is also required. Several chemokine receptors are able to act as co-receptors for HIV-1, including members of the seven membrane-spanning CC and CXC families of chemokine receptors.

The two major co-receptors used by HIV-1 are CXCR4 (present on T-cells) and CCR5 (present on both primary T-cells and macrophages). Based on the co-receptor usage HIV-1 strains can be broadly classified as either T-cell tropic (syncytia-inducing, "SI") or macrophage tropic (non-syncytia-inducing, "NSI"). The interaction of the variable V3 loop of gp120 with the co-receptor triggers conformation changes in the gp120 complex which exposes a hydrophobic fusion peptide in the viral gp41 transmembrane protein (Schulz *et al*, 1992). This mediates the fusion of the viral and cellular membranes, which usually occurs at the plasma membrane of the cell surface (Maddon *et al*, 1988), resulting in the release of the viral core into the cytoplasm of the cell.

Interaction of the virus with CD4 and a coreceptor can similarly occur within a vesicle, for example, macrophages have been reported to uptake HIV-1 virus by macropinocytosis, and infection can subsequently result by fusion of the virus with the CD4 and coreceptors on the membrane of the macropinosome, which has been directly derived from the plasma membrane (Marechal *et al*, 2001). Indeed, vesicular uptake of HIV-1 by a variety of

endocytic mechanisms has been demonstrated in several cell types including macrophages, endothelial cells, T-cell lines and HeLa cells, (Fredericksen *et al*, 2002; Grewe *et al*, 1990; Liu *et al*, 2002; Marechal *et al*, 1998; Marechal *et al*, 2001; Pauza and Price, 1988; Schaeffer *et al*, 2001). HIV-1 entry by macropinocytosis has also been demonstrated in brain microvascular endothelial cells (Liu *et al*, 2002), and HeLa cells have been reported to take up HIV-1 by clathrin dependent endocytosis (Schaeffer *et al*, 2001). It now appears that a significant amount of HIV-1 virus enters several cell types via endocytosis (Fredericksen *et al*, 2002). However fusion of the virion with cellular membranes is not pH dependent, and unless CD4 and a coreceptor are available to mediate membrane fusion within the vesicle, endocytic uptake of HIV-1 is reported to result in lysosome-mediated viral degradation and not productive infection (Fredericksen *et al*, 2002; Schaeffer *et al*, 2001).

Cell-to-cell infection refers to the transmission of infection through physical contact between an infected cell and an uninfected cell. *In vitro* studies indicate that the mechanism of virus entry via cell-to-cell mode of infection may differ from cell-free infection with respect to CD4 dependence. Neutralising anti HIV-1 antibodies (Fu *et al*, 1999; Gupta *et al*, 1989; Phillips and Bourinbaiar, 1992) and drugs which interfere with CD4, (Matthias *et al*, 2002) can prevent cell-free but not cell-to-cell transmission of infection. Interestingly, it has been reported that HIV-1 can infect CD4 negative cells when CD4 is provided *in trans*, either as soluble CD4 or by contact with CD4 positive cells (Speck *et al*, 1999). *In vitro* HIV-1 infection of a naive cell via direct contact with an infected cell has been reported to result in a faster progression of the early steps of virus replication than in cell-free infection paradigms (Li and Burrell, 1992). The relevance of these specific observations to the spread of infection *in vivo* is unclear. Direct contact of uninfected cells with infected cells occurs in several anatomical sites important for viral spread, including the contact between dendritic cells and T-cells in lymphoid tissue. Contact between uninfected cells and cells infected with certain "syncytia-inducing" strains of HIV-1 typically results in the fusion of cells ("syncytia") *in vitro*. Again, the precise relevance of this cell fusion phenomenon *in vivo* is unclear, but the formation of multinucleated giant cells in the brain, a hallmark of HIV-1 encephalitis (Fenyo *et al*, 1989; Sharer, 1992), may be the *in vivo* equivalent of syncytia. A number of *in vitro* infection models have utilised the cell-to-cell mode of infection (Barbosa *et al*, 1994; Karageorgos *et al*, 1993; Karageorgos *et al*, 1995; Li *et al*, 1993a; Li and Burrell, 1992; Li *et al*, 1992; Li *et al*, 1994).

1.1.6ii Reverse transcription

Reverse transcription occurs in a structure refered to as the "replication complex" (Bowerman *et al*, 1989). This complex includes viral RNA / DNA, reverse transcriptase, integrase, nucleocapsid, matrix and Vpr proteins (Bukrinsky *et al*, 1993; Karageorgos *et al*, 1993; Miller *et al*, 1997). The viral reverse transcriptase enzyme has both RNA- and DNA-dependent DNA polymerase activity as well as RNase H activity. The binding of a cell-derived $tRNA_3^{lys}$ to the viral **p**rimer **b**inding **s**ite (PBS) located immediately downstream of the U5 region (refer to Figure 1.7 panel A) primes the initiation of DNA synthesis from the viral genomic RNA. A short minus sense strand of DNA is produced, known as "strong-stop DNA". During this DNA synthesis, the RNA template strand is degraded by the RNase H activity of reverse transcriptase. The R region in the strong-stop DNA is complementary to the R region in the 3' viral RNA. This permits the strong-stop DNA species to be transferred and bind to the 3' end of the viral RNA (Figure 1.7 panel B). This transfer of templates is known as the "first template switch", and may occur to either the same strand from which the DNA was synthesised (intramolecular switch) or on the other RNA strand (intermolecular switch) (Hu and Temin, 1990). This primes the continuation of the viral minus strand DNA synthesis (Figure 1.7 panel C). The majority of the RNA template is concomitantly degraded by the reverse transcription, however two short regions known as **poly**purine **t**racts (PPT) upstream of the U3 region are resistant to digestion and remain associated with the newly synthesised DNA. The PPTs then act to prime the synthesis of incomplete plus sense DNA strands (Figure 1.7 panels C and D). The downstream plus sense DNA synthesis continues over the tRNA attached to minus strand, generating a DNA copy of the PBS. The upstream plus sense DNA strand displaces the downstream strand, which is then available for transfer to the 3' end of the newly synthesised minus strand DNA (second template switch), facilitated by annealing of the complementary PBS regions (Li *et al*, 1993b) (Figure 1.7 panels E and F). Synthesis of both plus and minus sense DNA strands is completed to generate the dsDNA, with the LTR region (U3-R-U5) duplicated at both ends (Figure 1.7 panel G).

HIV-1 reverse transcription occurs within the cytoplasm of the infected cell, however the process of reverse transcription can commence within the virion itself, and the presence of reverse transcribed DNA in a small proportion of virions has been reported

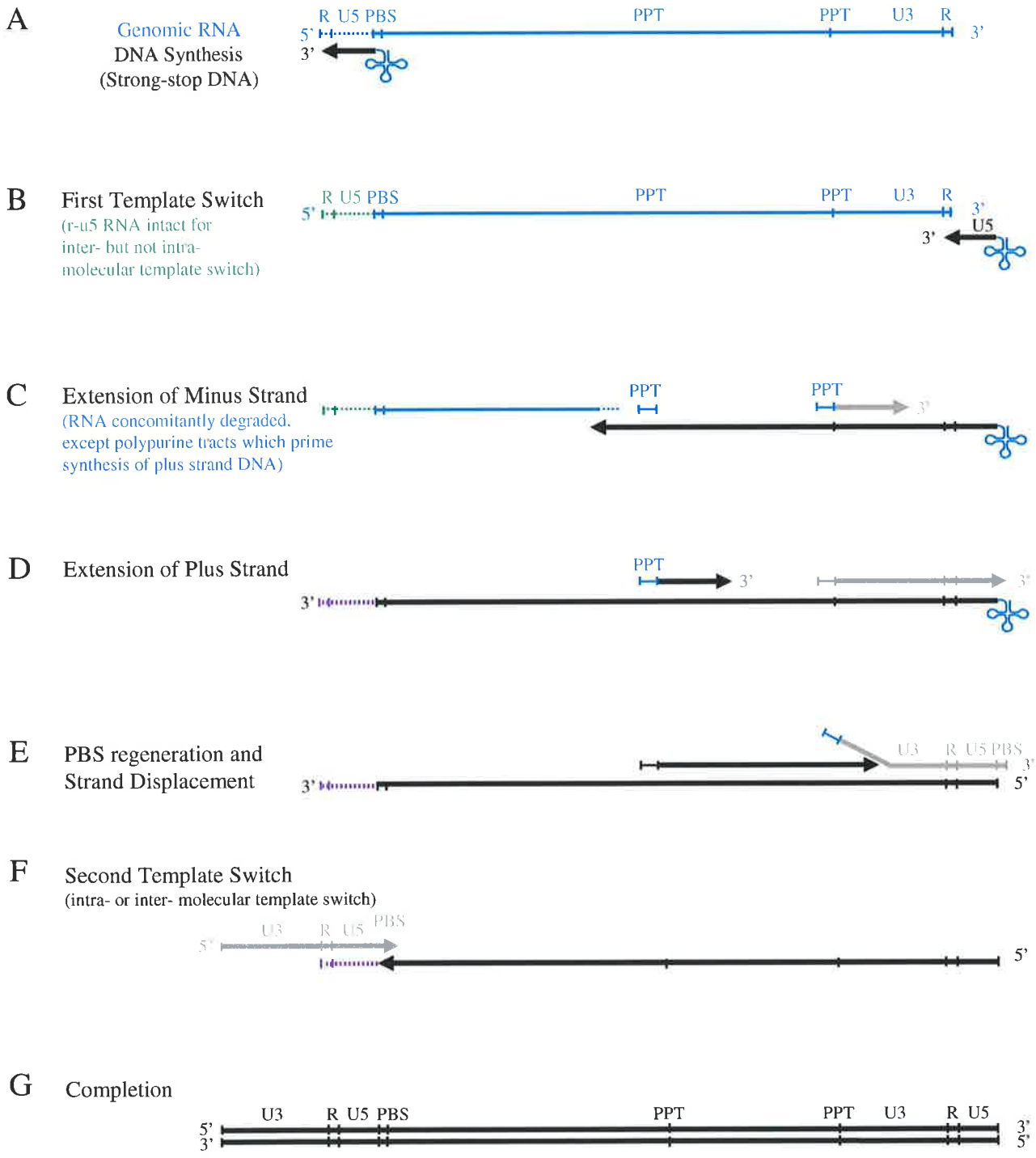

Figure 1.7 Reverse Transcription of the HIV-1 genome.

The RNA genome of HIV-1 is shown in blue (and dashed green). In panel (A) DNA synthesis (represented in black, grey and dashed purple) is primed by the annealing of the $tRNA_3^{lys}$ ( ) to the primer binding site (PBS). The dashed lines indicate RNA (green) or DNA (purple) which may or may not be present, depending on whether the template switching has occurred within the same RNA template or between the two identical genomic RNA strands. Refer to the text, Section 1.1.6ii for a detailed description of the process of reverse transcription.

Adapted from Karageorgos *et al.*, 1993.

(Arts *et al*, 1994; Lori *et al*, 1992; Trono, 1992; Zhang *et al*, 1994; Zhang *et al*, 1996a; Zhang *et al*, 1996b; Zhang *et al*, 1993). The availability of dNTPs for DNA synthesis appears to be one of the limitations to intravirion reverse transcription. Recently the viral reverse transcriptase has also been reported to reverse transcribe virion-derived singly or multiply spliced viral transcripts which may be packaged in the virion at low levels (see Section 1.1.6v) (Liang *et al*, 2004).

1.1.6iii Integration

The viral proteins integrase, matrix and Vpr remain associated with the reverse trancribed viral dsDNA, in a structure known as the "pre-integration complex" (PIC). Integrase, matrix and Vpr contain nuclear localisation signals which facilitate the transport of the PIC to the nucleus of the infected cell (Depienne *et al*, 2001; Depienne *et al*, 2000; Fouchier and Malim, 1999). This nucleoprotein complex is actively transported across the nuclear membrane (Bukrinsky *et al*, 1992) via the karyopherin transporter pathway (Barbosa *et al*, 1994; Fouchier and Malim, 1999). Nuclear transport of the pre-integration complex is thought to commence shortly after the initiation of reverse transcription. As this nuclear transport is an active process, mitosis of the cell is not required, enabling HIV-1 to infect non-dividing cells such as macrophages.

Once inside the nucleus, the linear viral dsDNA has four potential fates; i) integration in a collinear fashion into the cellular chromosome, ii) circularisation via recombination of the terminal LTRs (forming a circular molecule with one LTR), iii) circularisation via direct end-to-end ligation (forming a circular molecule with two LTR regions), or iv) persisting as a linear viral dsDNA molecule (Barbosa *et al*, 1994). Integration of the viral DNA into the cell chromosome is mediated by the viral integrase enzyme, and the chromosomal sites of integration appear semi-random. Although limited transcription of some viral genes from unintegrated templates has been demonstrated (Kok *et al*, 1998; Wu and Marsh, 2001; Wu and Marsh, 2003a; Wu and Marsh, 2003b), integration of HIV-1 proviral DNA is required to establish productive infection. Not all integrated HIV-1 DNA proviruses are transcriptionally active, and activity appears to be dependent, in part, on the transcriptional activity (or inactivity) of the integration site.

1.1.6iv Transcription and Translation

The HIV-1 provirus is a single transcriptional unit and the proviral LTR acts as a strong promoter for viral transcription. In addition to the transcriptional activity of the integration site, the level of transcription may depend on the activation state of the cell and the level of cellular transcription factors available to interact with the viral promoter and enhancer elements in the LTR (Levy, 1998).

The HIV-1 genome has 9 overlapping open reading frames (ORFs) (Figure 1.5). Three of these encode structural proteins or enzymes and six encode regulatory proteins. However, multiple splicing patterns give rise to at least 30 distinct RNA species (Purcell and Martin, 1993; Schwartz *et al*, 1990). These transcripts can be categorised into three groups based on their size and degree of splicing; multiply spliced transcripts (1.7-2kb; encoding Tat, Rev and Nef), singly spliced transcripts (4.3-5.6kb; encoding Vpr, Vpu, Vif and Env) and unspliced transcripts (9.2kb; forming genomic RNA and encoding the Gag-Pol polyprotein).

Multiply spliced transcripts are the first to be produced (at around 12 hours post infection (hpi)), and encode the major regulatory proteins; Tat (**trans**activator of **t**ranscription), Rev (**re**gulator of **v**irus expression) and Nef (**ne**gative **f**actor) (Davis *et al*, 1997; Greene, 1991; Kim *et al*, 1989). These proteins are translated from different monocistronic 1.7-2kb mRNAs. The most abundant of these transcripts is *nef*. The roles of the Nef protein are not fully understood. Nef may both enhance and decrease viral replication in certain situations, and has been associated with viral latency and the down-modulation of both CD4 (preventing super-infection) (Garcia and Miller, 1991; Guy *et al*, 1987) and MHC expression (aiding in immune escape) (Schwartz *et al*, 1996). Viral isolates from a cohort of long term survivors (Hartley *et al*, 1996; Kirchhoff *et al*, 1995; Pandori *et al*, 1996; Welker *et al*, 1996) and some blood transfusion recipients who were slow to progress to disease have exhibited *nef* deletions (Deacon *et al*, 1995; Michael *et al*, 1995).

Tat protein is essential for virus production (Dayton *et al*, 1986; Fisher *et al*, 1986), and transactivates HIV-1 LTR-directed transcription. Tat interacts with two cellular factors, cyclin T and the kinase CDK9. The Tat/cyclin T/CDK9 complex interacts with a stem loop structure (**trans**activation **r**esponse region, or "TAR") in the 5' terminus of all HIV-1 RNA

transcripts. The interaction of the Tat/cyclin T/CDK9 complex with the TAR region mediates the phosphorylation of the carboxy terminal domain of RNA Pol II, which dramatically improves the rate of complete viral transcript production. In the absence of Tat, HIV-1 LTR-directed RNA synthesis results in the accumulation of prematurely terminated transcripts (Knipe and Howley, 2001). Interestingly, cellular expression of cyclin T and CDK9 is increased in peripheral blood mononuclear cells (PBMCs) upon activation (with PHA or PMA) (Herrmann *et al*, 1998).

Rev protein is required for efficient transport of the larger, incompletely spliced and unspliced genome length viral transcripts out of the nucleus. In the absence of Rev, the unspliced genomic RNA, unspliced *gag/pol* and the partially spliced *vif*, *vpr* and *vpu/env* mRNAs do not accumulate in the cytoplasm (Felber *et al*, 1989; Hammarskjold *et al*, 1989; Sodroski *et al*, 1986). The HIV-1 infection of astrocytes appears to display this "Rev-defective" phenotype (Sections 1.3.2ii, 1.4.2 and 1.5.3) (Brack-Werner, 1999). In eucaryotic cells modifications of RNA transcripts, including splicing, occur in the nucleus prior to the export of the transcripts to the cytoplasm. Complete splicing of retrovirus transcripts is impeded by suboptimal splice sites, and, in the absence of Rev, these incompletely spliced transcripts (containing unused splice donor and acceptor sequences) may be retained by the cellular splicing machinery, hindering their nuclear export (Nakielny *et al*, 1997). All unspliced and partially spliced HIV-1 RNAs include a Rev response element (RRE). In the cytoplasm, Rev protein possesses a NLS that targets it for import into the nucleus. In the nucleus, Rev binds and oligomerises to the RRE structure on viral transcripts. This oligomerisation exposes the nuclear export signal (NES) domain of the Rev proteins, forming a "Rev export complex" which is shuttled to the cytoplasm. The complex is disassembled in the cytoplasm; the unspliced or partially spliced transcripts are available for translation or assembly into progeny virions, and the Rev proteins are available for repeat nuclear import (Knipe and Howley, 2001).

Singly-spliced and unspliced HIV-1 transcripts appear around 16 to 24 hpi (Davis *et al*, 1997; Kim *et al*, 1989), and, as described above, are dependent on Rev for nuclear export. The Env gp160 polyprotein is translated (and simultaneously glycosylated) from singly spliced 4.3kb mRNA at the rough endoplasmic reticulum (ER). The glycosylated polyprotein is targeted to the Golgi apparatus, where it is assembled into oligomers (Coffin *et al*, 1997) and cleaved by cellular enzymes into the transmembrane gp41 and surface

gp120 glycoproteins (Knipe and Howley, 2001). Spontaneous interaction with CD4 molecules in the Golgi is prevented by the viral accessory protein, Vpu (Luo *et al*, 1997). After cleavage, gp120 and gp41 molecules are weakly associated by a non-covalent interaction, and transported to the plasma membrane for incorporation into budding virions. The precursor to Gag (p55 Gag) is translated from the unspliced 9.2kb RNA. The p160 Gag-Pol polyprotein is also translated from the unspliced 9.2 kb RNA by the occurrence of a frame shift in translation, which occurs during formation of approximately 5% of these nascent polyproteins. Gag and the less abundant Gag-Pol polyproteins are targeted to the cell membrane via the ER. The mature Gag (Matrix, Capsid and Nucleocapsid) and Pol (Protease, Reverse transcriptase and Integrase) are formed by cleavage events by the virally encoded protease during assembly and maturation of the virion (see below) (Knipe and Howley, 2001). This proteolysis and maturation of the virion is essential for the infectivity of the virus.

1.1.6v Assembly, Release and Maturation

The assembly, release and maturation of virions involves noncovalent intermolecular interactions of the viral components and proteolytic cleavages of viral polyproteins. Identical genomic RNA sequences associate in pairs by virtue of an interaction near their 5' end. Specific sequences in the 5' region of the genomic RNA contain *cis*-acting packaging or encapsidation signals ("ψ"), which facilitate an interaction with the nucleocapsid portion of Gag polyprotein. The nucleocapsid may also be responsible for the annealing of cell-derived $tRNA_3^{lys}$ to the PBS site of the genomic RNA (Bieth *et al*, 1990; Meric and Spahr, 1986; Prats *et al*, 1988). The matrix portion of the Gag polyprotein may interact with the transmembrane region of env, gp41. This assembly of structural polyproteins and the paired RNA strands forms a viral "pre-core". The cell membrane, containing gp41 and gp120 oligomers, forms a protrusion above the forming immature viral core. As the virion buds it acquires an envelope derived from the cell plasma membrane with incorporated transmembrane gp41 and the associated surface gp120 molecules. Complete cleavage of the viral polyproteins by the viral protease, to form the individual structural proteins (Matrix, Capsid and Nucleocapsid) and the active viral enzymes (Reverse transcriptase and Integrase) is thought to occur during and after pre-core assembly and budding from the cell (von Schwedler *et al*, 1998; Wiegers *et al*, 1998). This protease-mediated maturation of viral

structural proteins is visible by electron microscopy as the formation of a condensed, cone shaped viral core (Figure 1.4).

Several additional cellular and viral components may be actively or passively packaged into the forming virions. Singly and multiply spliced viral RNAs contain some packaging elements, and are consequently packaged, at low levels, into virions (Clever *et al*, 1999; Clever and Parslow, 1997; Luban and Goff, 1994). Incorporation of several additional viral proteins into the virion, including Tat (Knipe and Howley, 2001), Nef (Bukovsky *et al*, 1997; Pandori *et al*, 1996; Welker *et al*, 1996), and Vif (Kao *et al*, 2003; Khan *et al*, 2001; Liu *et al*, 1995) have been reported. As mentioned above, cellular $tRNA_3^{lys}$ is actively associated with the unspliced viral RNA and incorporated into the virion. Incorporation of additional cellular factors, such as APOBEC3G, may influence the ability of the virion to replicate in the next cycle of infection (Harris *et al*, 2003; Lecossier *et al*, 2003; Mariani *et al*, 2003). It is possible for reverse transcription to commence within the mature virion (Section 1.1.6ii) (Arts *et al*, 1994; Lori *et al*, 1992; Trono, 1992; Zhang *et al*, 1994; Zhang *et al*, 1996a; Zhang *et al*, 1996b; Zhang *et al*, 1993), indicating that cellular dNTPs may also be incorporated into the virion.

1.2 Background to the Central Nervous System

1.2.1 Cellular Organisation of the Central Nervous System

The Central Nervous System (CNS) is primarily comprised of neurons and non-neuronal cell types that are collectively referred to as "glia". There are up to $1x10^{11}$ neurons in the adult human brain (Williams and Herrup, 1988), and 10-50 times as many glial cells (Kandel *et al*, 1991). Glial cells in the CNS include the macroglia (oligodendrocytes and astrocytes) and microglia. Neurons and neuronal networks have received significant scientific attention for their unique property of electrical excitability. Glial cells, which provide structural support, are now known to also provide metabolic and trophic support to neurons, and it has been hypothesised that astrocytes may also play a direct role in information processing (Barres, 1991; Kimelberg and Norenberg, 1989; Laming, 1989; Teichberg, 1991).

1.2.1i Neurons

Neurons are highly polarised cells which communicate with each other by translating electrical impulses, which travel along the cell, into either chemical or electrical signals at synapses (connections with adjoining cells), which can result in perpetuation of the impulse or signal. These highly specialised cells have an array of processes extending out from the cell body, known as dendrites. These processes receive excitatory input, and neurons are usually classified by their dendrite morphology. A single axon, which may branch into "collaterals", extends out from the cell body of a neuron, along which impulses are rapidly transmitted to the axon terminus. Some axons are surrounded by an insulating myelin sheath (see Section 1.2.1iii and below). Axons end in a number of processes (terminal ramifications), each of which terminate in a small swelling ("bouton") containing neurotransmitter-filled vesicles. Boutons come into close physical contact with membranes of other cells, at a region known as a synapse. Electrical impulses travel down the axons via a wave of membrane depolarisation, or by "jumping" between gaps in the myelin sheath. Upon reaching a terminal synapse, the membrane depolarisation enables a Ca^{2+} influx into the bouton, which induces exocytosis of the neurotransmitter-filled vesicles into the synapse. This chemical release may stimulate excitation of the contacting cell(s) via the respective neurotransmitter receptors. On neurons, these receptors are usually closely associated with ion channels that convert the signal back to an electrical impulse.

Neurons have very specialised metabolic requirements, and are highly susceptible to damage by changes in the extracellular millieu. Neurons are terminally differentiated cells and are, in general, non-renewable in the adult CNS. The blood-brain-barrier (BBB) and cerebrospinal fluid (CSF) -brain-barrier (Section 1.2.3)) strictly regulate the passage of factors and cells between the CNS and the rest of the body and permit tight control of the environment in the CNS. Myelin coating of axons serve to protect neurons, in addition to facilitating faster electrical conduction (Section 1.2.1iii). Astrocytes provide intimate protection of neurons at unmyelinated sites. Astrocytes also support the highly specialised metabolic requirements of neurons, including the provision of energy, waste removal, neurotransmitter recycling, and the maintainance of synaptic homeostasis (Sections 1.2.1iv and 1.2.2).

1.2.1ii Microglia

Microglia serve as resident tissue macrophages of the CNS and are thought to differentiate from bone-marrow derived monocytes (i.e. of macrophage lineage) which enter the brain parenchyma during early stages of brain development (Chugani *et al*, 1991; Esiri and McGee, 1986; Gehrmann *et al*, 1995; Miyake *et al*, 1984; Perry *et al*, 1985; Zigmond *et al*, 1999). Microglia resemble monocytes and macrophages immunophenotypically, and express many of the same markers (including F4/80, 2.4G2 (FcIgG1/2b) receptor, MAC-1 (C3 receptor) and MAC-3) (Esiri and McGee, 1986; Gehrmann *et al*, 1995; Giulian and Baker, 1986; Perry *et al*, 1985), which can make it difficult to distinguish microglia from macrophages which may have infiltrated the CNS from the periphery. Microglia play an important role in the remodeling of the CNS during early development, and as an immune effector cell in response to disease or injury of the CNS (refer to Section 1.2.4i). Microglia retain their ability to divide and to be phagocytic, and have multiple morphological and functional states (Davis *et al*, 1994; Gehrmann *et al*, 1995). They are CD4 and MHC Class I positive, and respond quickly and dramatically to alterations in the CNS microenvironment, and can be rapidly induced to express high levels of MHC Class II. Their role in normal homeostasis of the CNS is less understood. They are distributed throughout the brain, with an increased frequency in grey matter and more recently evolved regions of the CNS (Davis *et al*, 1994; Gehrmann *et al*, 1995; Lawson *et al*, 1990). Microglia comprise approximately 20% of the CNS cell population, forming a network which spans most of the CNS parenchyma (Gehrmann *et al*, 1995; Kandel *et al*, 1991; Zigmond *et al*, 1999).

1.2.1iii Macroglia; oligodendrocytes and astrocytes

The macroglia include both oligodendrocytes and astrocytes. Oligodendrocytes are involved in axonal guidance during development and regeneration of the CNS. They are also responsible for myelin formation in the CNS (analogous to the Schwann cells of the peripheral NS), which insulates regions of nerve axons. This enables faster nerve conduction as the action potential can "leap" (by saltatory conduction) between nodes of Ranvier (unmyelinated regions of axons). Not all axons in the CNS are myelinated, and the regulatory determinants which underlie this are not clear (Zigmond *et al*, 1999). It is also unclear whether all oligodendrocytes form myelin. They have receptors for certain

neurotransmitters, implying they may have additional roles which are not yet known (Brodal, 1998; Marcoux and Choi, 2002).

Oligodendrocytes are usually identified on the basis of their morphology and the expression of galactocerebroside (GalC). They are thought to be derived from the multipotent neural stem cell population. Studies of the rat optic nerve indicate that oligodendrocytes and Type 2 astrocytes are both derived from a common precursor, the O-2A progenitor cell (Raff *et al*, 1984; Raff *et al*, 1987). The differentiation of this precursor into either oligodendrocytes or Type 2 astrocytes seems to be regulated by Type 1 astrocytes (Raff and Lillien, 1988).

1.2.1iv Astrocytes

Astrocytes are the most abundant cell type in the human brain. In the adult human brain there is an estimated $0.4\text{-}2.0\text{x}10^{12}$ astrocytes, comprising approximately 40% of cells in the CNS (Kandel *et al*, 1991; Rutka *et al*, 1997). A diverse array of functions have been attributed to astrocytes, at various stages of ontogeny, in different regions of the brain, and under both normal and pathological conditions (Wilkin *et al*, 1990). The roles of astrocytes include regulation of the barriers of the CNS, direct physical, metabolic, neurotropic and homeostatic support of neurons and immunological responses to injury or infection (described in detail below and in Sections 1.2.2, 1.2.3 and 1.2.4). It has also been proposed that astrocytes, in addition to neurons, are actively involved in information processing (Barres, 1991; Bezzi and Volterra, 2001; Kimelberg and Norenberg, 1989; Laming, 1989; Teichberg, 1991; Yu *et al*, 1992).

Astrocytes form a complex intercellular communication network through the CNS (Figure 1.8) and signal via "gap junctions" (electrical synapses) between themselves and other cell populations in the CNS (Zigmond *et al*, 1999). Astrocytes respond to Ca^{2+} and astrocyte networks can transmit waves of Ca^{2+} conduction (Yu *et al*, 1992) via their tightly coupled intercellular gap junctions (Zigmond *et al*, 1999). Astrocytes possess a wide variety of neurotransmitter-gated ion channels and neurotransmitter receptors (Barres, 1991; Barres *et al*, 1990). It is possible that astrocytes also synthesise and release certain neurotransmitters (Barres, 1991).

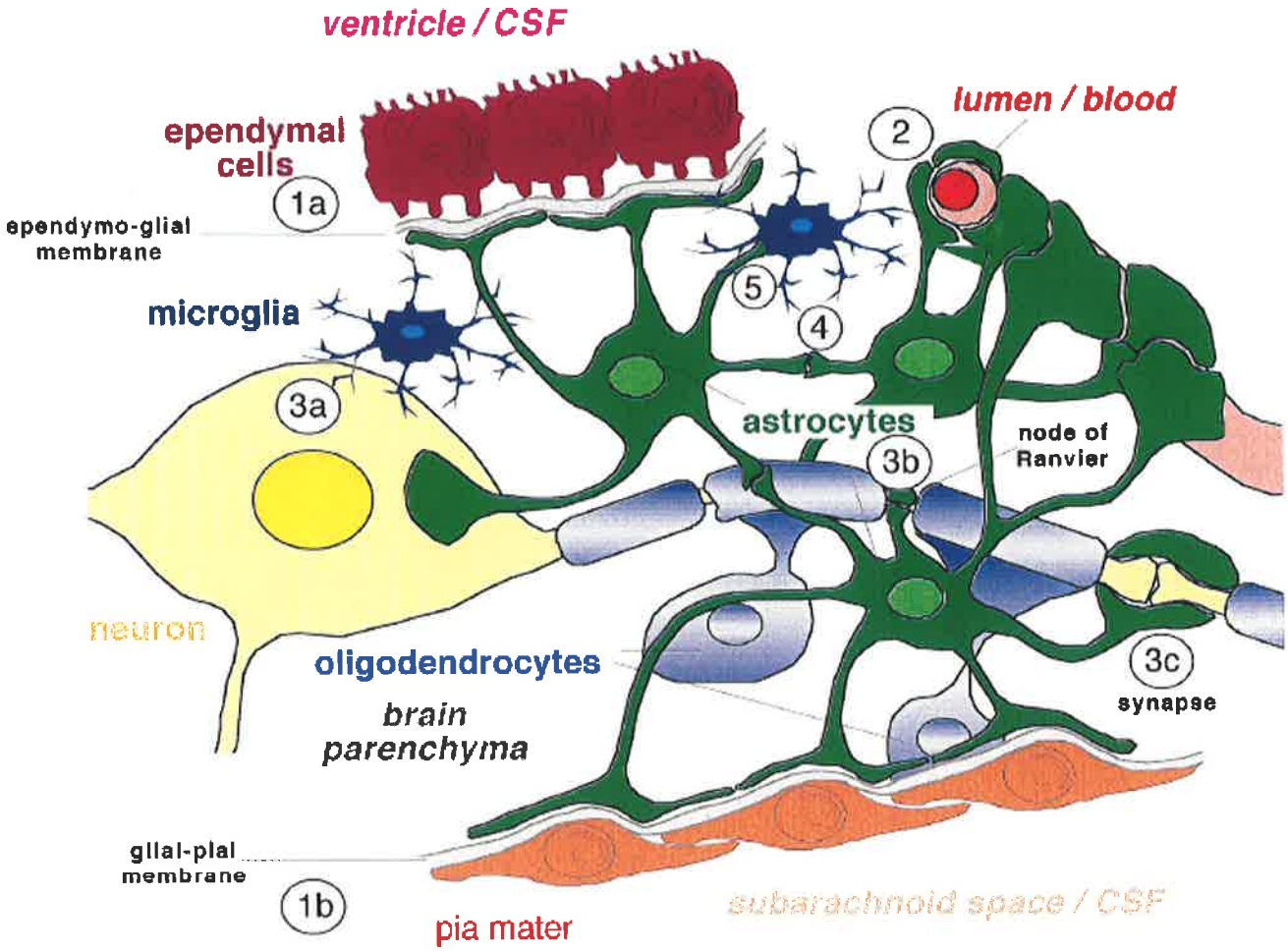

Figure 1.8 Diagrammatic representation of the intercellular contacts of astrocytes in the CNS. Astrocyte processes form connections with other astrocytes and all other cell types within the brain. Astrocyte endfeet ensheath the coverings of the brain, covering the ependymal cells which line the ventricles (**1a**) and the cells of the pia mater (**1b**), which collectively form the brain-CSF barrier. Astrocyte podia also form tight junctions around the endothelial cells which line the capillaries of the brain and comprise the blood-brain barrier (**2**). Astrocytes also surround neurons, providing a protective covering where myelin is absent; on cell bodies (**3a**), nodes of ranvier (**3b**) and at synapses (**3c**). Astrocyte podia form contacts between astrocytes, enabling intercellular signalling via gap junctions (**4**). Astrocytes also form contacts with neighbouring microglial cells (**5**).

Adapted from Brack-Werner, 1999.

Astrocytes also play multifaceted roles of neuronal support. They guide neurons and axons during growth and development of the CNS, and contact and surround neurons, providing protection where the myelin sheath is absent, ie. on cell bodies, nodes of Ranvier, and at synapses (Raff *et al*, 1987; Zigmond *et al*, 1999). Astrocytes play a vital role in maintaining homeostasis of the extracellular milieu and synaptic microenvironment, and thus assist normal neuronal function. To this end, astrocytes are involved in recycling of spent neurotransmitters (including glutamate) (Pfrieger and Barres, 1996), provision of neuronal growth factors (such as NGF and TGF-β) (Frei *et al*, 1989), spatial buffering of ions (K^+, Na^+, Cl^-, HCO3 and Ca^{2+}) (Zigmond *et al*, 1999) removal and recycling of toxic metabolites (eg ammonium) and regulation of energy metabolism (glycogen synthesis, storage and catabolism) (Pellerin *et al*, 1997).

In addition, astrocytes also form, regulate and maintain the protective barriers of the brain. Their podia form a sheath ("glia limitans" or limiting membrane) around the endothelial cells lining brain capillaries which comprise the blood-brain barrier (BBB) and around the ependymal cells which form the CSF-brain barrier (Zigmond *et al*, 1999) (Section 1.2.3). As a result, astrocytes are involved in the control of which substances enter the brain parenchyma, and the rate at which they enter. Astrocytes may be induced to express various chemokine receptors and cellular adhesion molecules (including VCAM-1, ICAM-1 and MCP-1) and thereby regulate trafficking of immune cells across the BBB (Persidsky *et al*, 1997; Weiss *et al*, 1998; Weiss *et al*, 1999; Woodman *et al*, 1999; Wu *et al*, 2000). In addition, astrocytes act as immune effector cells in the CNS. They become activated in response to injury or infection, can be induced to express MHC Class II Antigen, can express and respond to a number of cytokines, and may have antigen presenting capabilities (see Section 1.2.4ii).

Astrocytes are derived from two distinct progenitor cell types, giving rise to Type-1 astrocytes (from 1A progenitor cells, thought to be derived from neuroepithelial cells) and Type-2 astrocytes (from 0-2A progenitor cells) (Chu *et al*, 2001; Linskey, 1997). The differentiation of O-2A progenitors into either oligodendrocytes or Type 2 astrocytes seems to be regulated by Type 1 astrocytes (Raff and Lillien, 1988). These two types of astrocytes differ with respect to their morphology in culture, their antigen expression and their functional attributes (Wilkin *et al*, 1990). Type 1 astrocytes form the glial limiting

membrane and are involved in the formation of the BBB (Janzer and Raff, 1987). Type 2 astrocytes are associated with nodes of Ranvier (Ffrench-Constant *et al*, 1986). Both Type 1 and 2 astrocytes (and proliferating O-2A progenitors) are present in the white matter of the adult CNS (Raff *et al*, 1987). A variety of functionally distinct subtypes of astrocytes also appears to exist (Wilkin *et al*, 1990).

Astrocytes are traditionally identified on the basis of their morphology and the expression of the astrocyte specific marker, glial fibrillary acidic protein (GFAP). However, whilst both Type 1 and Type 2 astrocytes can express GFAP (Raff *et al*, 1984), not all astrocytes express GFAP, and consequently studies of astrocytes are biased towards the subset of astrocytes which are GFAP positive. The level of GFAP expression in these astrocytes varies according to their activation state. It is difficult to ascertain the extent to which astrogliosis (synonymous with astrocytosis; the increase in size and number of GFAP positive cells, and considered to be a property of Type 1 astrocytes (Wilkin *et al*, 1990)) indicates a proliferation of GFAP positive astrocytes as opposed to induction of GFAP expression in formerly GFAP negative astrocytes.

The enormous diversity of astrocyte function, their multiple origins and the variations in their biological features (antigenic markers, enzyme, transporter, receptor and ion-channel profiles) (Raff *et al*, 1987; Wilkin *et al*, 1990) suggest they are highly heterogeneous population of cells. It has been postulated that sub-types of astrocytes with specific functions exist in the CNS (Brack-Werner, 1999; Wilkin *et al*, 1990). In summary, astrocytes form a complex intercellular communication network amongst themselves and with neurons, microglia, oligodendrocytes, endothelial cells and ependymal cells. They play numerous roles in development, homeostasis and disease of the CNS and may even be involved in neural information processing.

1.2.2 Metabolic relationships between Neurons and Astrocytes

Glucose is the obligatory energy substrate for the CNS, although in certain circumstances, ketone bodies can also be metabolised in the brain (Zigmond *et al*, 1999). Regional neuronal activity, blood flow and energy metabolism is tightly coupled. This is thought to be regulated in part by nitric oxide (NO), which may be released upon neurotransmitter

stimulus of neurons and glial cells, and can act as a local vasodilator (Iadecola, 1992). Additionally, the coupling of regional neuronal activity and energy metabolism is thought to be regulated by astrocytes, which have specialised processes that surround brain capillaries (Peters *et al*, 1991a) and other processes which encompass neuronal synapses (Barres, 1991). The synaptic astrocyte processes have receptors for and can uptake neurotransmitters (Barres, 1991), including the main excitatory neurotransmitter, glutamate (Figure 1.9). The uptake of glutamate by astrocytes drives a Na^+, K^+ ATPase, which promotes glycolysis. This in turn stimulates uptake of glucose by the astrocyte endfeet surrounding the capillary (Pellerin and Magistretti, 1994). Glycolysis generates the intermediates lactate and, to a lesser extent, pyruvate, which can be released by the astrocyte and taken up by neurons for further energy conversion. Neurons can also metabolise glucose directly. In addition, astrocytes store glycogen as an energy reservoir (Vaughn and Grieshaber, 1972).

The involvement of astrocytes at glutamatergic synapses has been well characterised. Uptake of glutamate at synapses by astrocytes rapidly restores the homeostasis of the synaptic millieu. The majority of glutamate taken up by astrocytes is converted back to glutamine (synaptically inert), which is released and taken up by neurons (Figure 1.9). This coordinated "glutamate-glutamine shuttle" between astrocytes and neurons functions not only to remove the potentially excitotoxic build up of glutamate in synapses and to replenish the neurons supply of the neurotransmitter precursor, glutamine, but also to prevent the build up of the neuronal metabolic waste product, ammonium. Astrocytes are also able to synthesise new glutamine (Zigmond *et al*, 1999). Astrocytes are thought to play similar roles in maintaining the extracellular millieu of other types of synapses, and have been shown to uptake and recycle other neurotransmitters, including γ-Aminobutyric acid (GABA) and aspartate (Nicholls and Attwell, 1990; Zigmond *et al*, 1999). Future studies of the complexities of information processing in the CNS are likely to reveal additional intimate relationships between astrocytes and neurons.

1.2.3 Barriers of the CNS

The fastidious requirements of the CNS environment for normal neuron function are maintained, in part, by regulated barriers which segregate the brain from the rest of the body. These include the blood-brain, CSF-brain and CSF-blood boundaries. The majority of the

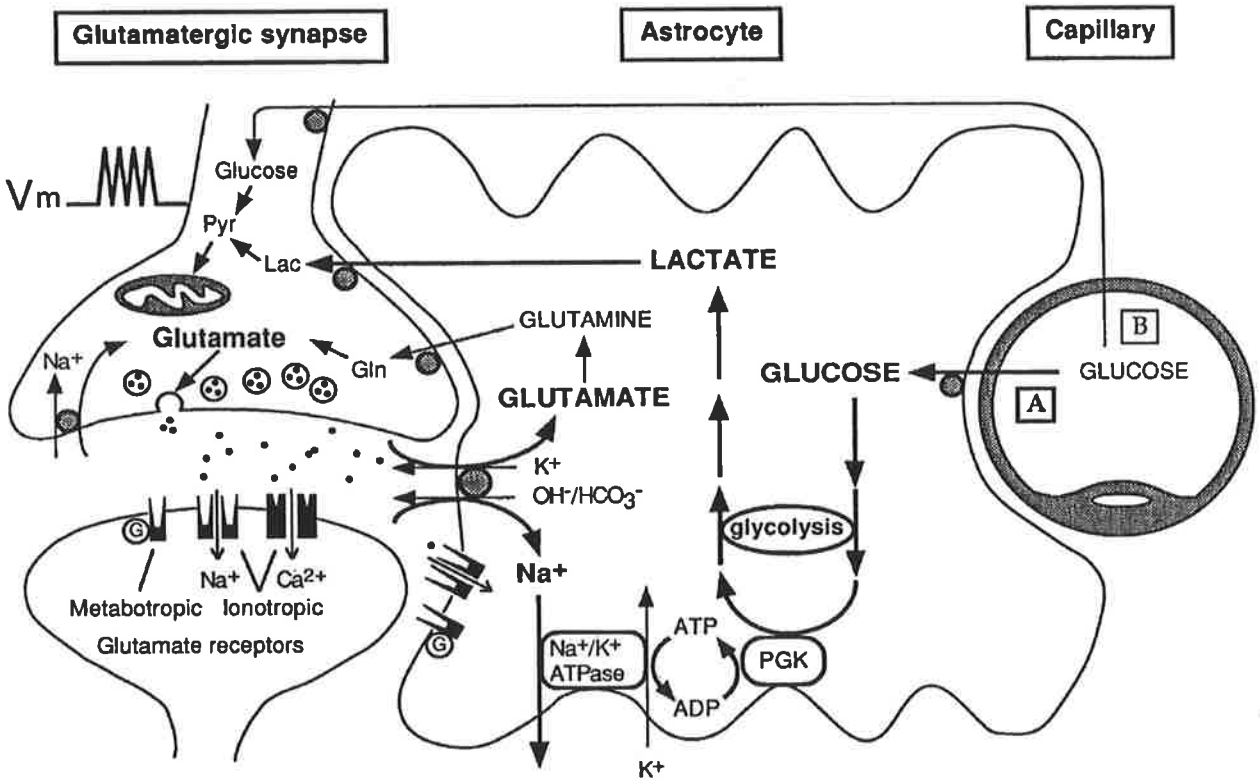

Figure 1.9 Schema of metabolic relationships between astrocytes and neurons. During activation of glutamatergic synapses, the excitatory neurotransmitter, glutamate, is released into the neuronal synapse. Astrocyte cell projections surround the synaptic cleft, and efficiently uptake the glutamate from the synapse. In the astrocyte, glutamate is cotransported with Na^+. In addition to removing the spent neurotransmitter from the synapse, this drives a a Na^+/K^+ ATPase, which activates glycolysis in the astrocyte cell, promoting increased uptake of glucose from the local brain capillaries (**A**) and generating lactate. Lactate is released from astrocytes and can be directly taken up by neurons, efficiently replenishing their energy supply. Astrocytes convert glutamate back to glutamine, and this inactive precursor is shuttled back to the neuron. During basal (**B**) conditions, glucose can be taken up and metabolised by neurons directly.

Adapted from Pellerin and Magistretti, 1994

brain is protected by these barriers, except certain regions (area postrema, periventricular organs, median eminence, posterior pituitary and pineal body), where rapid release of neuronal factors into the systemic circulation is required (Brodal, 1998). At these regions the neurons are in direct contact with the perivascular space, and the endothelial cells are fenestrated and contain an abundance of pinocytotic vesicles.

1.2.3i Blood-brain barrier

The BBB serves to restrict exchange of solutes between the blood and the brain, and acts as an interface between the systemic immune system and the CNS. The redundancy of some intercellular signalling molecules means that, in the absence of a BBB, systemic hormones and cytokines could act as neurotransmitters in the brain and vice versa. Disruptions to the BBB (in, for example, Multiple Sclerosis, AIDS, lead poisoning and perhaps Alzheimers disease) leads to edema and subsequent neurological impairment (Buee *et al*, 1994; Claudio *et al*, 1995).

The endothelial cells of the BBB capillaries are unique. They lack fenestrations and form unique tight junctions which act as gates; allowing certain small molecules to enter and restricting the entry of macromolecules (Zigmond *et al*, 1999). These endothelial cells are less permeable and have a reduced level of transcytosis than their systemic counterparts (Zigmond *et al*, 1999). A basement membrane, comprised of collagen and other proteins, surrounds the endothelia and pericytes of the BBB capillaries. BBB pericytes can control vascular tone and have phagocytic activity, which is heightened upon BBB injury. Astrocyte projections surround the basement membrane, and astrocytes are involved in inducing and maintaining the integrity of the BBB and associated endothelia (Arthur *et al*, 1987; Dallasta *et al*, 1999; Fontana *et al*, 1984; Hickey, 1991; Janzer and Raff, 1987). The endothelia and astrocytes of the BBB have specialised transport mechanisms for molecules such as glucose which are required by the CNS (Zigmond *et al*, 1999). These cells facilitate the transport and distribution of these molecules according to the regional and metabolic requirements of the CNS.

1.2.3ii The CSF-blood barrier and the CSF/brain boundary

The CSF is produced by the choroid plexus. This fluid fills the subarachnoid space (between the pia mater and arachnoid mater, layers of the outer covering of the brain), the ventricles of the brain and the central canal of the spinal cord. The CSF is continuous between these compartments and around the entire brain. The choroid plexus is a region where the ependymal cells of the ventricles fuse with the pia and arachnoid mater (Zigmond *et al*, 1999). The choroid plexus is formed by invaginations of the pia mater into the ventricles, and is lined with epithelium that has tight junctions. The epithelium of the choroid plexus is continuous with the ependymal lining inside of the ventricles. The epithelium of the choroid plexus represents a barrier between the blood and the CSF (Brodal, 1998). Astrocyte podia line the inner side of the ependymal cells, forming a boundary between the CSF and the brain (Brack-Werner, 1999). The ependymal cells themselves are freely permeable to water and small protein molecules, facilitating exchange of water and soluble molecules between the CSF and the interstitial fluid of the CNS (Brodal, 1998). Because of this, the composition of the CSF can provide an insight into the millieu within the brain.

1.2.4 Immune System of the CNS

The CNS was originally considered to be an immunoprivileged site, however it is now well established that antigenic challenge in the CNS can trigger a rapid and rigorous immune response. The immune system and its regulation in the CNS, however, differs significantly from the systemic immune system (Binder and Griffin, 2003; Gehrmann *et al*, 1995; Irani and Griffin, 1996). This has been attributed to the unique requirements and attributes of the CNS. These include i) the paucity of MHC Ag expression in the brain, ii) the restricted access of systemic cells and molecules to the CNS by the BBB, iii) the non-renewable and essential nature of neurons, iv) the absence of a structured lymphatic drainage system in the CNS, and v) the rigid confines of the skull.

Microglia are the main intrinsic immune effector cell of CNS, in addition to astrocytes and circulating immune cells which may be induced to cross the BBB (Gehrmann *et al*, 1995). The immune response in the CNS is considered to be biased towards the preservation of

neurons, as these cells are, in general, non-renewable. Neurons lack MHC expression altogether, and effective antigen presenting cells and costimulation are deficient in the brain (Irani *et al*, 1996). Neurons normally express apoptotis-inhibiting factors, such as Bcl-2 and Bcl-x_L (Levine *et al*, 1996; Levine *et al*, 1994). Neurotrophins, such as NGF, BDNF, NT-4/5 and NT-3, promote neuronal survival, and are produced locally in the brain (Zigmond *et al*, 1999). The removal of infected cells, by apoptosis (Vaux and Hacker, 1995) or cell-mediated lysis, is usually an effective way to control infection in the body. However, the preferential immune response to virus-infected neurons in the CNS appears to involve control of viral replication by non-cytolytic antibody and cytokine mediated mechanisms which preserve the neurons, rather than by cell-mediated lysis (Binder and Griffin, 2003; Levine and Griffin, 1992; Levine *et al*, 1994).

The high expression of TGFβ1 in the normal brain may contribute to its relative immunoprivilege (Taylor and Streilein, 1996) by acting as an IL-1 receptor antagonist, preventing the development of cytotoxic T-cells and inhibiting adhesion molecule expression (VCAM-1) on astrocytes (Marcoux and Choi, 2002; Winkler and Beveniste, 1998). Moreover, TGFβ1 appears to have a direct protective effect on neurons (Flanders *et al*, 1998; Henrich-Noack *et al*, 1994). Gangliosides which are produced in the brain also act to limit inflammation in the brain by suppressing lymphocyte proliferation (Irani *et al*, 1996).

The brain is subject to continual leucocyte surveillance (Lassmann, 1997), but to a lesser extent than other organs (Griffin *et al*, 1987; Wekerle *et al*, 1987) as the level of adhesion molecule expression (required for extravasation of leucocytes) on the BBB and cerebral capillaries is very low (Belayev *et al*, 1996). Upon injury or infection, however, the BBB may become compromised. Expression of leucocyte adhesion molecules, including ICAM-1 and VCAM-1, may increase, with a corresponding increase in the number of infiltrating immune cells (Belayev *et al*, 1996; Irani and Griffin, 1996). The synthesis of complement in the brain upon injury, including C3a and C5a (Barnum, 1995; Bellander *et al*, 1996; Lindsberg *et al*, 1996), can also act to enhance vascular permeability, as these molecules are potent chemoattractants for neutrophils and macrophages. Prostaglandins (Giulian *et al*, 1996a) and platelet activating factors (Nishida and Markey, 1996; Pettigrew *et al*, 1995) can also be produced by glial cells in the brain. Cytokine, chemokine and chemokine receptor

expression is very low in the normal brain (Marcoux and Choi, 2002). In response to injury or infection, however, several cytokines and chemokines can be expressed by glial cells, including the proinflammatory cytokines IL1 and TNFα, as well as IL6 and IL8. IL6 can act to down-modulate the immune response by inducing immunosuppressive cytokines such as TGFβ1 (Marcoux and Choi, 2002), and it has been reported to have both neuroprotective and neurodestructive properties (Gadient and Otten, 1997). IL8, a CXC chemokine, may be chemotactic for neutrophil recruitment and neuroprotective through stimulating increased astrocyte production of the neurotropin, NGF (Marcoux and Choi, 2002).

Overall, the brain may be considered a site with its own distinct immunological properties. It is capable of a complex immune response, which is biased towards neuron survival and restriction of cytotoxicity. The profile of chemokine and cytokine expression in the CNS during insult or injury seem to underlie the monocyte-rich inflammation which follows (Marcoux and Choi, 2002). The immunological attributes of the two intrinsic immune effector cell types in the brain are considered briefly below.

1.2.4i Role of Microglia in CNS Immune Responses

Resting microglia functionally resemble highly down-regulated macrophages (Section 1.2.1ii). Upon challenge to the integrity of the CNS microglia respond rapidly, proliferating and changing morphology and phenotype to express increased levels of MHC Class I and II molecules. They may become either reactive non-phagocytic microglia or reactive phagocytic microglia. The latter are functionally analogous to fully functional macrophages (Gehrmann *et al*, 1995; Kreutzberg, 1996). Accordingly, reactive microglia can produce and respond to a number of cytokines including IL1, IL6, TNFα, IFNγ and TGFβ and quinolinic acid (Frei *et al*, 1989; Gehrmann *et al*, 1995; Giulian and Baker, 1986; Giulian *et al*, 1986; Levy, 1998; Stanley *et al*, 1994). Additionally, they can act as antigen presenting cells (Gehrmann *et al*, 1995), produce and respond to several complement components (Barnum, 1995; Gasque *et al*, 1995; Gasque *et al*, 1998) and produce the prostaglandin thromboxane A2 (Giulian *et al*, 1996a). In addition to CD4, they also express the chemokine receptors CCR3 and CCR5, which can be used as coreceptors by HIV-1.

1.2.4ii Role of Astrocytes in CNS Immune Responses

In the normal brain, astrocytes help maintain an immuno-dormant state. They produce a number of neurotrophic factors, including NGF, LIF and IL6 (see below) (Wesselingh *et al*, 1990) and maintain microglia in a latent, ramified state (Giulian *et al*, 1995; Hori *et al*, 1999; Nottet *et al*, 1995; Schilling *et al*, 2001), in addition to maintaining the integrity of the BBB (Sections 1.2.1iv and 1.2.3i).

In addition, astrocytes have an immunological capacity and become activated in response to injury or infection in the CNS or to perturbations in the BBB (Yu *et al*, 1992). The activation of astrocytes is known as astrogliosis. They respond to a number of cytokines, including IL1, IL6, TNFα and TGFβ (Botchkina *et al*, 1997; da Cunha *et al*, 1993; Frei *et al*, 1989; Giulian *et al*, 1986; Liu *et al*, 1996; Stanley *et al*, 1994). Similarly they are capable of producing a range of cytokines, including IL1, IL6 (Frei *et al*, 1989; Sairanen *et al*, 1997), IFNα, IFNβ, TGF-β and lymphotoxin (Levy, 1998), and chemokines (Barnes *et al*, 1996; Chiodi *et al*, 1996; Eddleston and Mucke, 1993; Kutsch *et al*, 2000; Lee *et al*, 1993; Nitta *et al*, 1994; Peterson *et al*, 1997; Ridet *et al*, 1997; Weiss *et al*, 1998; Wu *et al*, 2000). Astrocytes may be induced to express various chemokine receptors, including CXCR4 (Sanders *et al*, 2000; Wu *et al*, 2000), CCR5 (Rottman *et al*, 1997), CXCR1, CXCR2 and CCR2b (Cota *et al*, 2000). Upon stimulation, they can also produce MCP-1 (Weiss *et al*, 1998; Weiss *et al*, 1999; Wu *et al*, 2000) and both granulocyte-macrophage and macrophage colony-stimulating factors (GM-CSF and M-CSF) (Frei *et al*, 1989; Malipiero *et al*, 1990).

Astrocytes can be induced to express MHC Class II antigen (Malipiero *et al*, 1990), and there is some evidence to suggest astrocytes may capable of antigen presentation (Fierz *et al*, 1985; Fontana *et al*, 1986; Fontana *et al*, 1984; Gehrmann *et al*, 1995; Shrikant and Benveniste, 1996) and phagocytosis (Shrikant and Benveniste, 1996). Given their intrinsic role in the BBB (Sections 1.2.1iv and 1.2.3), and that, upon activation, they can express ICAM-1 and VCAM-1 (Rosenman *et al*, 1995; Woodman *et al*, 1999) and MCP-1 (Weiss *et al*, 1998; Weiss *et al*, 1999; Wu *et al*, 2000), astrocytes are also involved in regulating the trafficking of systemic immune cells into the CNS (Persidsky *et al*, 1997; Weiss *et al*, 1998; Weiss *et al*, 1999; Woodman *et al*, 1999; Wu *et al*, 2000).

1.3 HIV-1 infection of the CNS and HIV-1 induced Neurological Diseases

CNS involvement in HIV infection was recognised as early as 1983 (Snider *et al*, 1983), and was observed in the majority of untreated AIDS patients. In approximately half of the cases the neuropathology could be accounted for by opportunistic diseases (predominantly cerebral toxoplasmosis, CMV encephalitis and cryptococcal meningitis (Johnson *et al*, 1988; Petito *et al*, 1986)) or lymphoma in the CNS (Booss and Esiri, 2003; Snider *et al*, 1983). However, in around 20-30% of HIV-1 patients, CNS disorders were observed which could not be attributed to another etiology (Navia and Price, 1987; Petito *et al*, 1986; Price *et al*, 1988). These were subsequently attributed to neuropathological effects of the HIV-1 virus itself. It is now known that HIV-1 enters the brain early in the course of infection, where it persists for life. HIV-1 can induce a range of neurological disorders including sensory neuropathy of the peripheral nerves, vacuolar myelopathy and myelitis of the spinal cord, paediatric encephalopathy, HIV-1 encephalitis (HIVE) and, the most devastating neurological manifestation, HIV-1 associated dementia (HAD) (Power and Johnson, 1995). The neurological manifestations of HIV-1 do not usually present until the patient has developed AIDS and the BBB has become compromised, but in some patients HAD may present as the first AIDS defining illness. The introduction of HAART in the developed world has seen a significant reduction in the incidence of HAD (from 21% to 10%) (Sacktor *et al*, 2001). However, the onset of HAD as the first AIDS defining illness, and the development of HAD in patients whose T-cell levels are above 200/ml, has increased in frequency (Dore *et al*, 1999; Sacktor *et al*, 2001), indicating that continued research into this debilitating consequence of HIV-1 is required.

1.3.1 Entry of HIV-1 into the CNS

HIV-1 enters the CNS within the first few weeks of infection (An *et al*, 1999b; Chiodi *et al*, 1996; Davis *et al*, 1992; Palmer *et al*, 1994), and this subsequently becomes an important site of viral replication (Shaw *et al*, 1985) and persistence (Brack-Werner, 1999; Pierson *et al*, 2000). The main route of entry of HIV-1 into the CNS remains to be determined. HIV-1 may initially gain access to the CNS by trafficking infected macrophages or T-cells (the "Trojan Horse" hypothesis) (Figure 1.10) (Haase, 1986; Nottet *et al*, 1996; Persidsky *et al*,

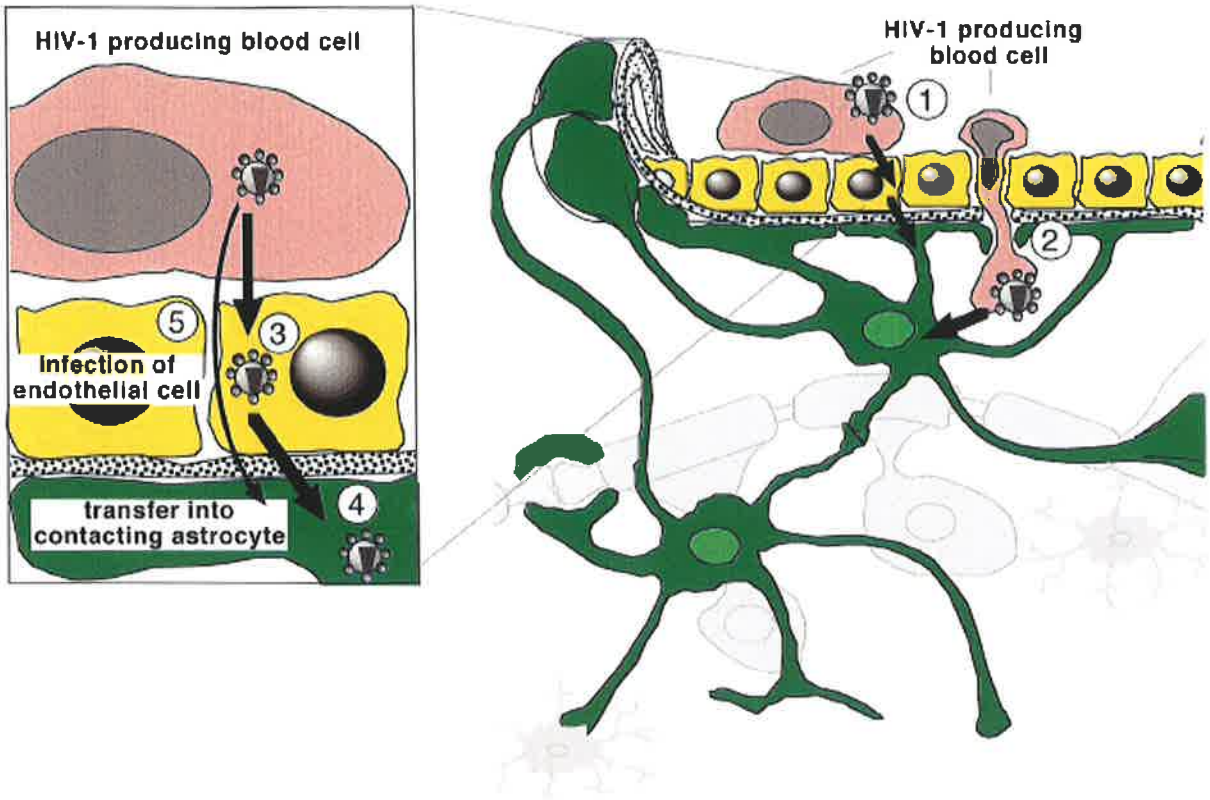

Figure 1.10 Involvement of astrocytes in the entry of HIV-1 into the CNS. HIV-1 may gain access to the CNS from the blood as either free or cell associated virus. Infected cells, trafficking in the blood, may adhere to adhesion molecules expressed by brain capillary endothelial cells. The expression of these adhesion molecules on the endothelial cells may be, at least in part, regulated by the adjacent astrocytes. Additionally, under certain conditions, astrocytes themselves can also express adhesion molecules and can secrete chemoattractants. Infected cells may then either transmit virus to the endothelial cells (**1**), or extravasate into the brain parenchyma (**2**). Virus which gains access to these endothelial cells, as either free virus or by cell-cell contact, may gain access to astrocytes in the brain parenchyma via infection or transcytosis of brain endothelial cells (**3**, **4**), or, if the integrity of the tight junctions between the endothelial cells has been compromised, virus may access the brain parenchyma directly (**5**), enabling subsequent infection of the local astrocytes.

Adapted from Brack-Werner, 1999.

1997; Williams and Hickey, 1995). This may be facilitated by upregulation of adhesion molecules on the brain endothelial cells, which can be stimulated by the products of activated cells (eg TNFα, IL6 and IL10) (Nottet *et al*, 1996; Persidsky *et al*, 1997) or perturbation of the BBB by viral products (eg HIV-1 Tat protein) (Hofman *et al*, 1994; Lafrenie *et al*, 1996). Alternatively, blood-derived free virus may transcytose (Bomsel, 1997) or infect (Owens *et al*, 1991) epithelial cells, it is possible that HIV-1 may transcytose the epithelial cells which line the choroid plexus or the endothelial cells of the BBB, and thus gain access to the brain parenchyma (Figure 1.10). Given the intimate relationship of brain capillary endothelial cells with astrocytes at the BBB (Sections 1.2.1iv, 1.2.3i and 1.2.4ii), astrocytes are believed to play a crucial role in the passage of infected cells and free virus into the CNS. Modulation of adhesion molecule expression by astrocytes (and endothelial cells) comprising the BBB (as a consequence of viral factors or systemic factors altered by systemic HIV-1 infection) may induce the passage of HIV-1 infected or inflammatory cells into the brain (Weiss *et al*, 1999; Woodman *et al*, 1999). Similarly, systemic affects of HIV-1 infection may also influence the ability of endothelial cells to transcytose free virus (the potential role of astrocytes in this process has not been explored), enabling subsequent spread of infection to BBB astrocytes. Once HIV-1 has gained access to the brain parenchyma, spread of virus presumably occurs via cell to cell spread through the vast CNS network of astrocytes and microglia.

1.3.1i Neurotropism

To infect the CNS, in addition to gaining access to the brain parenchyma, a virus needs to display neurotropism. CCR5 and CCR3 coreceptor-using HIV-1 has the propensity to infect microglia in the CNS. Indeed the majority of HIV-1 isolates derived from the CNS display macrophage tropism, and microglia and infiltrating macrophages are the main producers of HIV-1 within the brain. A number of *in vitro* studies have suggested a preferential infection of astrocytes by T-cell tropic strains, however they can also be infected *in vitro* by certain macrophage tropic strains (McCarthy *et al*, 1998; Nath *et al*, 1995; Schweighardt *et al*, 2001). A recent comparison of HIV-1 V3 envelope sequences from astrocytes and macrophages / microglia from the same patients found that the viral sequences isolated from astrocytes corresponded to CCR5 usage, yet they were distinct from the viral sequences

isolated from neighbouring macrophages (Thompson *et al*, 2004). Preferential microglial tropism has also been reported (Strizki *et al*, 1996).

Once in the CNS, HIV-1 evolves separately from the systemic virus population, as brain and CSF derived isolates display distinct biological, serological and molecular properties compared to blood-derived strains (Cheng-Mayer *et al*, 1989; Epstein *et al*, 1991; Hughes *et al*, 1997; Keys *et al*, 1993; Korber *et al*, 1994; Power *et al*, 1994; Steuler *et al*, 1992). A recent study indicated that the choroid plexus contained a range of virus isolates, some with homology to brain derived HIV-1 sequences and some with homology to blood-derived HIV-1 sequences from the same patient (Burkala *et al*, 2005; Chen *et al*, 2000). This indicates that the choroid plexus may act as an interface between blood and brain derived strains and that this region is involved in the entry (and exit) of HIV-1 into the brain. Differences in the envelope sequences of viral isolates from the brains of demented and non-demented patients has also been reported (Power *et al*, 1994), indicating that particular neurovirulent attributes of certain strains may mediate HIV-1 induced neurological disorders (Power and Johnson, 1995; Power *et al*, 1994). The envelope sequences from the "demented" isolates were also found to be mediate greater neurotoxicity *in vitro* than the "non-demented" isolates, when cloned into a common HIV-1 plasmid backbone (Power *et al*, 1998).

1.3.2 Identification of CNS cells infected by HIV-1 in post mortem brain sections.

1.3.2i Productively infected cells in the CNS in vivo

Microglia are the only CD4-expressing cell type in the CNS, and they also express the chemokine receptors CCR3 and CCR5 which can act as co-receptors for HIV-1. Microglia (and infiltrating macrophages) comprise the majority of productively HIV-1 infected cells in the brain (An *et al*, 1999a; Bagasra *et al*, 1996; Gartner *et al*, 1986; Glass *et al*, 1995; Koenig *et al*, 1986; Kure *et al*, 1990; Nuovo *et al*, 1994; Takahashi *et al*, 1996; Vazeux *et al*, 1987; Wang *et al*, 2001; Wiley, 1996; Wiley *et al*, 1986). Early studies of HIV-1 positive post mortem brain tissue using double labelling for cell markers and HIV markers (immunolabelling for the late HIV-1 proteins Gag and Env) demonstrated HIV-1 mainly in

macrophage/microglial cells (at a frequency of around 7.5%), and multinucleated giant cells derived from these cells (see Section 1.3.3). Only rarely were HIV-1 late proteins detected in astrocytes, oligodendrocytes or neurons. However subsequent studies detecting HIV nucleic acids (by *in situ* hybridisation, *in situ* PCR and *in situ* RT-PCR) demonstrated the presence of HIV-1 nucleic acid in a significant number of astrocytes, indicating that astrocytes but rarely neurons or oligodendrocytes, are also a major target for HIV-1 infection in the CNS (An *et al*, 1999a; An *et al*, 1999b; Chiodi *et al*, 1996; Epstein *et al*, 1984; Nuovo *et al*, 1994; Ranki *et al*, 1995; Saito *et al*, 1994; Sharer *et al*, 1986; Takahashi *et al*, 1996; Tornatore *et al*, 1994a; Wiley *et al*, 1986).

1.3.2ii Restricted HIV-1 infection of astrocytes in vivo

The detection of HIV-1 nucleic acid, but the absence of detection of structural HIV-1 proteins in astrocytes, indicated that the HIV-1 infection of astrocytes *in vivo* is restricted. HIV-1 DNA has been detected in around 1-7% of astrocytes (x=2.6%, n=22) by *in situ* PCR on HIV-1 positive brains (Bagasra *et al*, 1996; Brack-Werner, 1999). Of further note, *in situ* immunohistochemical studies have revealed that around 40% of astrocytes harbouring HIV-1 nucleic acid also express detectable levels of early (regulatory) HIV-1 gene products (Bagasra *et al*, 1996; Blumberg *et al*, 1994; Brack-Werner, 1999), in particular Nef (Blumberg *et al*, 1994; Ranki *et al*, 1995; Saito *et al*, 1994; Tornatore *et al*, 1994a). Even though the percentage of infected cells is low to moderate, the sheer number of astrocytes present in the brain ($0.4\text{-}2.0\text{x}10^{12}$ (Kandel *et al*, 1991; Rutka *et al*, 1997)), make them, numerically, a major potential reservoir of HIV-1 (Brack-Werner, 1999) (Section 1.1.4 and Table 1.1). Whether or not astrocytes *in vivo* can produce viable virus is not known. However, astrocytes also exhibit a similar pattern of restricted infection *in vitro*, and yet they can transmit infectious virus to uninfected cells (Sections 1.4.3 and 1.5). This supports the notion that infected astrocytes, *in vivo*, may act as a reservoir of viral persistence (Cheng-Mayer *et al*, 1987; Dewhurst *et al*, 1987b; Di Rienzo *et al*, 1998; Sabri *et al*, 1999; Tornatore *et al*, 1991) (Section 1.1.4).

1.3.3 HIV-1 Encephalitis and neuropathology of HIV-1

HIV-1 encephalitis (HIVE) is detected in around 10-50% of AIDS patients upon autopsy (Bell, 1998; Booss and Esiri, 2003; Budka, 1991; Petito *et al*, 1986). HIVE predominantly occurs in the late stage of HIV infection (Bell, 1998), when the breakdown in the integrity of the BBB may facilitate an increase in the CNS viral load (Booss and Esiri, 2003). The extent of the neuropathology does not correlate well with the severity of clinical presentation (see Section 1.3.4 below), and in many cases, HIVE is asymptomatic. The pathology and symptoms of HIVE in children (pediatric encephalopathy) is more prevalent, and generally more pronounced, than in adults. The gross pathology of HIVE typically involves brain atrophy with sulcal widening and ventricular dilatation. Histologically, the most common pathological findings in HIVE is white matter pallor (Navia *et al*, 1986a; Petito *et al*, 1986), and the most distinguishing feature is usually the presence of multinucleated giant cells (MNGC) (Budka *et al*, 1991; Petito *et al*, 1986). Macrophage / microglial activation, astrogliosis, and neuronal damage, ranging from subtle changes to apoptosis, is also commonly observed (Nathanson *et al*, 1994; Sharer, 1992). A range of additional pathology may also be present. Diagnosis of HIVE is based upon the observation of multiple disseminated foci of microglia, macrophages and MNGCs.

The presence of MNGC has become a hallmark of HIVE, as they are common in most (Bell, 1998; Budka, 1991; Sharer *et al*, 1986), but not all (Anders *et al*, 1986a; Anders *et al*, 1986b), HIVE brains. These unusual cells are HIV-1 positive, and are reported to be formed by fusion of infected macrophages and microglia (Michaels *et al*, 1988; Price *et al*, 1988; Sharer *et al*, 1985). MNGC are predominantly found in the cerebral white matter, and are also prevalent in the subcortical grey matter and the cerebral cortex (Bell, 1998). They are usually clustered around capillaries, but are also commonly found in normal neutropils, gliomesenchymal cell nodules and cavitating lesions (Rhodes, 1987).

Myelin pallor, although not diagnostic, is a common finding, and appears to be the result of perivascular demyelination. It is mainly found in the periventricular and central white matter, and is usually associated with astrogliosis. Oligodendrocyte damage is normally only apparent with advanced disease and severe myelin damage, which is rare (Gray *et al*, 1991Kato, 1987 #528). An increase in the number of microglia and astrocytes is often

observed in the white matter, and the extent of pathology in the white matter has been reported to correlate with the level of astrogliosis in this region (Ciardi *et al*, 1990).

The clinical presentations of HIVD (see below) indicate that brain dysfunction occurs in the cortex and subcortex, and hence many studies have focussed on these areas. Indeed, some autopsies have demonstrated the highest concentration of virus in the subcortical region (Wiley *et al*, 1998). Neuronal damage and loss has been observed in the neocortex (Masliah *et al*, 1992b; Wiley *et al*, 1991), frontal cortex (Everall *et al*, 1991; Giangaspero *et al*, 1989; Gray *et al*, 1991), basal ganglia and substantia nigra (Reyes *et al*, 1991). The processes which may cause this neuronal damage are discussed in Section 1.3.5.

1.3.4 HIV-1 Associated Dementia

HIV-1-Associated Dementia (HAD), now also referred to as HIV Dementia (HIVD) and AIDS Dementia Complex (ADC), was originally called AIDS Subacute Encephalopathy. It presents clinically as a subcortical dementia, progressing from impaired memory and concentration loss, apathy, psychomotor slowing and motor disabilities to incontinence, mutism and paraplegia (McArthur, 1987; Navia *et al*, 1986a; Navia *et al*, 1986b). In the absence of therapy, HAD occurs in around 20%-30% of patients (McArthur *et al*, 1993; Navia *et al*, 1986b), and has a very poor prognosis of, on average, 6 to 7 months (McArthur *et al*, 1993; Power and Johnson, 1995). HAD usually presents during AIDS, when plasma T-cell levels fall below 200/μl, however the presentation of HAD as the first AIDS defining illness is not uncommon (Navia, 1997; Navia and Price, 1987). The introduction of Highly Active Anti-Retroviral Therapy (HAART) in the developed world has seen a decrease in the incidence of HAD in HIV-1 positive patients (from 21% to 10%) (Sacktor *et al*, 2001), yet the relative incidence of HAD as an AIDS defining illnesses has increased (Dore *et al*, 1999). With HAART, the prognosis of HAD is also considerably improved, with a median survival time of 44 months. A milder form of neurological impairment has also arisen, termed HIV-associated minor cognitive disorder (MCMD). A striking feature of HAD is the absence of correlation between the presence and severity of symptoms or pathology and the CNS viral load (Glass *et al*, 1993; Gray *et al*, 1988; Navia *et al*, 1986a) (discussed in Sections 1.3.4i-ii below). This, taken together with the virtual absence of infection of

neurons, has lead to the concept that HIV-1 induces neuronal dysfunction indirectly (mechanisms discussed in detail in Section 1.3.5).

1.3.4i Lack of correlation of HAD with neuropathology

Whilst HIV-1 is present in the brains of patients with HAD, there is no apparent correlation between the presence / severity of clinical HAD and the neuropathology seen at autopsy (Bell, 1998; Navia *et al*, 1986a; Vago *et al*, 1990; Wiley *et al*, 1986). In many severely demented patients the histopathology may be "surprisingly bland and unremarkable" (Navia *et al*, 1986a; Wiley *et al*, 1986). Conversely, many non-demented patients show considerable neuropathology (as described in Section 1.3.3 above), which is similar to that found in some severely demented patients. (Navia *et al*, 1986a; Wiley *et al*, 1986). The number of HIV-1 infected cells or MNGC do not correlate well with loss of cognitive function, and neither does the amount of viral antigen in the CNS tissue (Glass *et al*, 1995; Masliah *et al*, 1997). For example, whilst most patients with MNGC and diffuse myelin pallor have HAD, 50% of patients with HAD have neither MNGC or diffuse myelin pallor (Glass *et al*, 1993). The CNS viral load does not correlate with the clinical symptoms either (Power and Johnson, 1995), and indeed, often remarkably little virus is found in the brains of demented patients (Pumarola-Sune *et al*, 1987). This has lead to the consideration of viral and cellular factors as potential indirect mediators of the neuronal dysfunction (Section 1.3.5). The involvement of soluble factors has been further implicated by the lack of co-localisation of apoptotic neurons with HIV-1 infected microglia (Shi *et al*, 1996). There are however a limited number of factors which have been found to correlate with the clinical presentation of HAD, and these are outlined below.

1.3.4ii Factors which do correlate with HAD

In general, the brains of demented patients have been found to have a higher level of macrophage / microglial activation than brains from non-demented patients. Elevated TNFα mRNA expression in microglia and astrocytes, and diminished IL4 expression in the CNS have also been found to correlate with dementia (Wesselingh *et al*, 1997). This suggests that the pathogenesis of HAD may involve CNS immune activation or dysregulation. Levels of nitric oxide synthase (NOS) and eicosanoids have also been reported to be elevated in the

brains of demented patients (Adamson *et al*, 1996). The expression of HIV-regulatory proteins (Rev and Nef) in astrocytes (Ranki *et al*, 1995), and a heightened level of astrocyte apoptosis (Pemberton and Brew, 2001; Thompson *et al*, 2001), also correlate with presence and severity of dementia. This indicates that HAD also involves the infection and depletion of the astrocyte population, which is vital to the maintenance of CNS homeostasis and normal neuronal function (Sections 1.2.1-1.2.3). There is also evidence that elevation of the excitoxins Ntox (neurotoxic amine) and quinolinic acid (Giulian *et al*, 1996b; Heyes *et al*, 1991) correlate with the degree of cognitive impairment. Neuron damage, in the form of decreased dendritic and synaptic density (Everall *et al*, 1999; Masliah *et al*, 1997) and selective neuronal loss (Fox *et al*, 1997; Masliah *et al*, 1992a) has also been shown to correlate with clinical presentation. High levels of β_2-microglobulin, neopterin (Brew *et al*, 1996) and the β-chemokines MCP-1 and RANTES (Cinque *et al*, 1998; Kelder *et al*, 1998) in the CSF and the presence of $CD16^+$ and $CD69^+$ monocytes in the peripheral blood (Pulliam *et al*, 1997) (which may be able to traffic through the normal BBB (Gartner, 2000)), have also been correlated with the presentation of HAD.

1.3.5 Mechanisms underlying HAD

For the reasons outlined above, the neuronal dysfunction which underpins HAD is thought to be mediated indirectly. This may occur via excess production of host molecules by infected or activated astrocytes and macrophage / microglial cells, in addition to the direct and indirect neurotoxic effects attributed to many HIV-1 proteins (Epstein and Gendelman, 1993; Nathanson *et al*, 1994; Sharer, 1992; Wiley *et al*, 1986; Zhang *et al*, 2003). How the latter occurs, given that viral load does not correlate with symptoms, remains an anomaly. It is convenient to postulate that individual host factors or individual viral strains, which evolve during the course of CNS infection, may determine the outcome. Alternatively, a small amount of a viral component ("virotoxin") at some stage of infection may trigger a cascade of events within the CNS, a so-called "hit and run" phenomenon (Nath, 2002), which ultimately leads to cellular dysfunction. A current concept is that the compensatory mechanisms in the CNS can cope with and enable the brain to recover from a certain number of assaults, but that a threshold of neurological assaults is reached in HAD where the compensatory mechanisms become insufficient (Brew, 2004). Another emerging hypothesis is that the pathogenesis of HAD may involve neuronal channelopathies (Gelman *et al*,

2004). Toxic viral and cellular factors that may play a role in HIV-1 induced neurological dysfunction are discussed below.

1.3.5i Toxic viral proteins

A number of HIV-1 proteins have been shown to have toxic effects on CNS cells *in vitro* and *in vivo*. In particular, gp120 (Benos *et al*, 1994; Berrada *et al*, 1995; Lipton *et al*, 1991; Pulliam *et al*, 1991; Pulliam *et al*, 1993; Toggas *et al*, 1994), gp41 (Magnuson *et al*, 1995; Sabatier *et al*, 1991), Tat (Magnuson *et al*, 1995; Sabatier *et al*, 1991) and Nef (Kort and Jalonen, 1998; Trillo-Pazos *et al*, 2000) have demonstrated neurotoxic properties. Some viral proteins, such as gp120 and Tat, have been shown to be directly toxic to neurons (Liu *et al*, 2000; Meucci *et al*, 1998), however the greatest neurotoxicity is seen in cultures where macrophages / microglia and astrocytes are also present (Dreyer *et al*, 1990; Giulian *et al*, 1990; Giulian *et al*, 1993; Kaul and Lipton, 1999; Lipton and Gendelman, 1995). In addition to production of these viral proteins within the brain, Tat (Schwarze *et al*, 1999) and gp120 (Banks *et al*, 1998; Banks *et al*, 1999) can transverse the intact BBB and enter the brain from the periphery. More viral proteins may enter the CNS upon the breakdown of the BBB which occurs in AIDS (Power *et al*, 1993). There is also evidence which suggests that extracellular Vpr (Huang *et al*, 2000; Patel *et al*, 2000) and Rev (Mabrouk *et al*, 1991) may contribute to the neurotoxicity.

The direct effect of gp120 appears to be specific to particular populations of neurons (eg dopaminergic neurons) (Bennett *et al*, 1995; Diop *et al*, 1995), however it also exerts neurotoxicity indirectly by affecting microglia and astrocytes (Lipton, 1993). In astrocytes, gp120 has been reported to induce NOS expression, upregulate adhesion molecule expression and induce cytoskeletal changes (Nath and Geiger, 1998). Gp120 also alters ion exchange in and arachidonic acid release from astrocytes, both of which disrupt the ability of astrocytes to take up the excitotoxin, glutamate (Lipton, 1994; Patton *et al*, 2000) (refer Figures 1.9 and Section 1.2.2). In macrophages and microglia, gp120 induces production of the proinflammatory and neurotoxic cytokines TNFα and IL1β, and neurotoxic arachidonic acid metabolites (Ilyin and Plata-Salaman, 1997; Kolson *et al*, 1998)).

Elevated levels of gp41 have been associated with severe HAD (Adamson *et al*, 1996). Gp 41 may exert neurotoxic effects by elevating iNOS expression in glial cells (Adamson *et al*, 1996). It may also contribute to excitotoxicity by stimulating release of glutamate from astrocytes (Kort, 1998).

Tat is actively released by infected cells, including infected glia (Tardieu *et al*, 1992), and can directly affect neurons and cause their depolarisation (Cheng *et al*, 1998; Magnuson *et al*, 1995). Tat stimulates production of several cytokines and chemokines in both macrophages / microglia (TNFα, IL1) and astrocytes (IL6, IL8, RANTES, MCP-1 and TNFα) (Kutsch *et al*, 2000; Nath *et al*, 1999), and can be taken up by uninfected glia and affect cellular function (Wortman *et al*, 2000). This stimulation of glial cells by Tat is highly sensitive, and a brief exposure of Tat (a few minutes) is sufficient to induce heightened cytokine release from macrophages and astrocytes which can last for several hours (Nath *et al*, 1999).

Nef can be toxic to neurons and glial cells (Kort and Jalonen, 1998; Trillo-Pazos *et al*, 2000), and is expressed by infected astrocytes *in vivo* (Bagasra *et al*, 1996; Blumberg *et al*, 1994; Brack-Werner, 1999; Ranki *et al*, 1995; Saito *et al*, 1994; Tornatore *et al*, 1994a). The number of Nef-expressing astrocytes *in vivo* has been reported to correlated with HAD (Ranki *et al*, 1995).

Whilst there is very good evidence that several HIV-1 proteins have neurotoxic properties, the anomaly that the viral load in the CNS does not correlate with the clinical symptoms remains (Glass *et al*, 1995; Masliah *et al*, 1997; Power and Johnson, 1995; Pumarola-Sune *et al*, 1987). Possible explanations for this apparent discrepancy which have been hypothesised include i) the evolution of strains with particular neurotoxic attributes (Power *et al*, 1994; Power *et al*, 1998), ii) a "hit and run" phenomenon, where a brief transient exposure to viral proteins may set up a cascade of long lasting effects in CNS (Nath, 2002; Nath *et al*, 1999), and iii) viral-induced over-activation and dysregulation of macrophages / microglia and astrocytes in the brain which may become self-perpetuating (Gorry *et al*, 2003) and iv) a threshold of neurotoxic assaults, beyond which the brain cannot recover (Brew, 2004). These hypotheses are not mutually exclusive, and the cellular factors thought

to be involved in these processes are discussed below. Additionally, the development of viral-triggered chronic activation and dysregulation in the CNS may depend on host factors.

1.3.5ii Toxic cellular factors and the immune dysregulation hypothesis

In striking contrast to the systemic immunodeficiency induced by HIV-1, the scenario in the brain appears to be chronic over-activation of the resident immune cells, microglia and astrocytes, and of infiltrated macrophages. These cells may become activated by infection, by contact with viral proteins, or by factors produced by other activated cells (Lipton and Gendelman, 1995). Several of the products of activated macrophages / microglia and astrocytes are neurotoxic and thought to participate in the pathology of HAD (Gartner, 2000; Lipton and Gendelman, 1995; Williams and Hickey, 2002). Candidate neurotoxic cellular products include TNFα, IL1β, IL6, TGFα, TGF β, GM-CSF, quinolinic acid, arachidonic acid metabolites (eicosinoids), PAF, NOS and endothelin 1 (Figure 1.11). Indeed, an elevated level of some of these factors has been correlated with HAD (Section 1.3.4ii).

Activated macrophages and microglia (and to a lesser extent, astrocytes) produce TNFα and IL1β. These two proinflammatory and neurotoxic cytokines may act in synergistic and autocrine fashions to induce further cell activation, and may promote further viral replication. Activated macrophage / microglial cells may also produce IL6, GM-CSF, PAF, TGFβ, arachidonic acid and free radicals such as NO. It has been suggested that TNFα and IL1, in combination with IL6 and GM-CSF, could account for many of the clinical and histopathological findings in HIVE (Merrill and Chen, 1991). In addition to activating additional glial cells, several of these molecules may, directly or indirectly, contribute to neuronal damage and apoptosis (Sections 1.2.4, 1.3.3 and 1.3.4ii). Activated microglia also release excitatory amino acids (EAAs) and related substances, including glutamate, quinolinate, cysteine and the amine Ntox (Brew *et al*, 1995; Giulian *et al*, 1990; Giulian *et al*, 1993; Lipton *et al*, 1991; Yeh *et al*, 2000). These EAAs are excitotoxic to N-methyl-D-aspartate (NMDA) glutamate receptors on neurons and can induce neuronal dysfunction and apoptosis (Bonfoco *et al*, 1995).

The activation of astrocytes (by infection or exposure to certain viral and cellular factors) would result in further cytokine, chemokine MCP-1, arachidonic acid and free radical (NO)

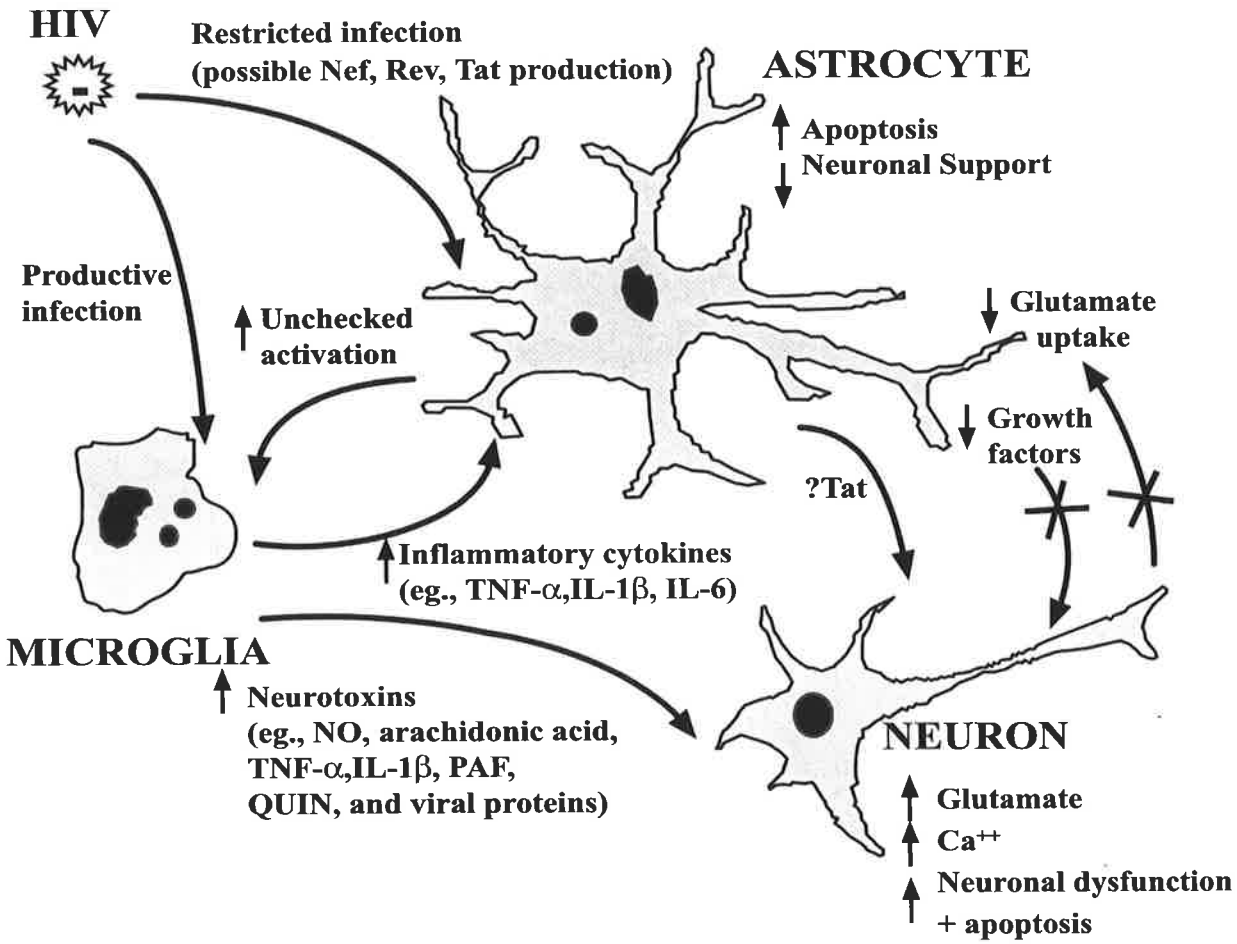

Figure 1.11 Model of the role of astrocytes in the pathogenesis of HAD

HIV-1 productively infects microglia and macrophages in the CNS, and causes a limited infection in astrocytes resulting in the production of viral regulatory proteins. Infected microglia and macrophages become activated, and, in addition to producing virus and viral proteins, produce a number of neurotoxins. These factors activate additional microglia, macrophages and astrocytes. Astrocytes become activated, either by infection and / or the products of activated microglia / macrophages, and their functions of neuronal support become impaired. In particular their capacity to remove excess excitotoxins, such as glutamate, and to produce neurotrophins, such as NGF, is altered. A proportion of astrocytes undergo apoptosis, further reducing the capacity for neuronal support. The products of activated microglia / macrophages may also be directly toxic to neurons. This, in addition to the toxicity of glutamate excess and dysregulated ion concentrations in the extracellular milieu, and lack of neurotrophic support, may lead to neuronal dysfunction, degeneration, and, in some neurons, apoptosis.

Adapted from Gorry *et al.* 2003

release (Adamson *et al*, 1996; Conant *et al*, 1998; Genis *et al*, 1992; Stella *et al*, 1997). Importantly, some of these factors (and several viral proteins) interfere with several crucial astrocyte functions. Critically, TNFα and arachidonic acid perturb the ability of astrocytes to re-uptake and maintain homeostasis of the EEA, glutamate (Fine *et al*, 1996; Genis *et al*, 1992), and can even cause glutamate release (Bezzi *et al*, 1998) by altering the ion-gradients needed for these processes. Local glutamate excess is directly detrimental to neuron function (Section 1.2.2 and Figure 1.9). Additionally, the ability of astrocytes to provide neurotrophic factors, to sustain and promote neuron survival, may be compromised. The apoptosis of astrocytes observed in HAD would further exacerbate the lack of neuron support. The immunoregulatory role of astrocytes (limiting microglial activation (Giulian *et al*, 1995; Hori *et al*, 1999; Nottet *et al*, 1995; Schilling *et al*, 2001), and inactivation of PAF and TGFβ produced by activated macrophages / microglia (Nottet *et al*, 1995)) is impaired. The diminished presence of immunosuppressive IL4 (involved in the down-regulation of astrocyte activation (Eng *et al*, 1989)) and IL10 in HAD brains (Wesselingh *et al*, 1993) also indicates that the immune response in HAD has become unchecked.

In summary, the current concept of the pathogenesis of HAD involves chronic activation and dysregulation of immune cells in the CNS (Figure 1.11). This is supported by the correlation between intensity of macrophage / microglial activation and the products of these cells, with HAD (Glass *et al*, 1993; Wesselingh *et al*, 1993) and the dysfunction and loss of astrocytes (Gorry *et al*, 2003; Thompson *et al*, 2001). A major role for astrocyte dysfunction has been implicated in other neurological disorders, including hepatic encephalopathy and Alzheimer type II disease (Zigmond *et al*, 1999). In HAD, this concept of dysregulation may explain the lack of correlation between either CNS virus load or pathology and the clinical severity. The vital role of astrocytes for normal neuronal function (Section 1.2.2) and regulation of the CNS immune response (Section 1.2.4ii), and their demise in HAD (Thompson *et al*, 2001) (Section 1.3.4ii) support their importance in the pathogenesis of HAD. Further elucidation of the effects of cellular and viral factors, and restricted HIV-1 infection on astrocyte function will be important in the development of a comprehensive treatment strategy for HIVE and HAD. *In situ* analyses of post mortem brains has been extremely valuable in delineating the cells and potential mechanisms involved in HAD, but only end stage disease can be observed. Animal models, in particular primate models, have also been exceedingly valuable, however the cost of such studies

limits their use and the highly specific interaction between HIV-1 and human astrocytes limits their applicability. *In vitro* infection systems fail to represent the intact cellular interactions of the brain, but permit specific mechanistic questions to be addressed. A combination of these three modes of analysis is required for a comprehensive understanding of the interactions between HIV-1 and astrocytes and roles of astrocytes in the pathogenesis of HAD.

1.4 *In vitro* HIV-1 infection of Astrocytes

Human fetal and progenitor derived astrocytes are susceptible to *in vitro* infection by a number of HIV-1 strains, and exhibit three stages of infection; i) initial release of HIV-1 core protein, p24, ii) a period of restricted infection, which, like post mortem *in situ* findings, is characterised by undetectable or low level virus production, detectable HIV-1 DNA, frequent detection of HIV-1 regulatory proteins and the absence of HIV-1 structural proteins, and iii) "reactivation" or "rescue" of productive infection upon coculture with HIV-1 susceptible cells (Cheng-Mayer *et al*, 1987; Dewhurst *et al*, 1987b; Di Rienzo *et al*, 1998; Messam and Major, 2000; Sabri *et al*, 1999; Tornatore *et al*, 1991). The efficiency of this infection is low (Brack-Werner, 1999; Di Rienzo *et al*, 1998), and it is not cytopathic (Brack-Werner, 1999; Dewhurst *et al*, 1987b; Di Rienzo *et al*, 1998; Nath *et al*, 1995). Some astrocyte cell lines are refactory to HIV-1 infection (Cheng-Mayer *et al*, 1987; Keys *et al*, 1991), whilst other astrocyte cell lines display the restricted infection described above, reportedly depending on the which viral strain is used (Sabri *et al*, 1999; Shahabuddin *et al*, 1996). The variation in susceptibility of astrocyte cell lines to HIV-1 infection may also reflect the heterogeneity and stage of differentiation of the astrocytes, and possibly their surface receptor expression.

1.4.1 Initial release of HIV-1 core protein

When primary and susceptible continuous astrocyte cultures are infected *in vitro* with HIV-1, HIV-1 core protein, p24, is released into the culture supernatant, and supernatant p24 protein levels are routinely used as an indicator of virus release. Typically the amount of HIV-1 p24 detected in the astrocyte culture supernatants during the first few days of infection is very low (for example <200 pg/ml (Di Rienzo *et al*, 1998; Nath *et al*, 1995)), but

up to 1400 pg/ml has been reported (Lawrence *et al*, 2004; Sabri *et al*, 1999). After around 4-6 dpi, p24 secretion diminishes to undetectable levels (typically <6 pg/ml). This initial "p24 release" from infected astrocytes is thought to represent a brief phase of productive infection and virus release (Messam and Major, 2000), although the potential for surface bound virus to be released needs to be considered (Lawrence *et al*, 2004). Where human fetal astrocyte preparations are used, the level of HIV-1 replication that may occur in contaminating microglia may also need to be taken into account. The amount of p24 protein released from HIV-1 infected astrocytes during this early phase of infection is much less than that from HIV-1 susceptible cells, such as monocytes or T-cells (Brack-Werner *et al*, 1992; McCarthy *et al*, 1998).

Primary and continuous astrocyte cultures that are transfected with plasmid DNA encoding the HIV-1 virus also exhibit this pattern of transient initial p24 release. Transfection of HIV-1-encoding plasmid DNA bypasses the viral replication steps of virus-cell attachment, entry and reverse transcription (refer Sections 1.1.6 and 1.6.1v). Integration may proceed, but not in the natural context of the PIC (Section 1.1.6iii). Other cell types which are not suseptible to HIV-1 infection (for example, 293T murine and HeLa human epithelial cells) can also be transfected with HIV-1-encoding plasmid DNA and can subsequently produce large amounts of HIV-1. Whilst the level of p24 protein released from HIV-1 transfected astrocytes is much higher than that from infected astrocytes (Lawrence *et al*, 2004), it is still low compared to HIV-1 transfection of other cell types (Gorry *et al*, 1999). Like HIV-1 infected astrocytes, transfected astrocytes also appear to enter a state of "viral latency" after the initial period of p24 release. This is restriction is not apparent upon transfection of the HIV-1 provirus into 293T or HeLa cells.

1.4.2 Restricted infection

After the initial burst of p24 release, HIV-1 infection of astrocytes enters a "restricted" or "latent" stage. This occurs in both primary astrocytes and susceptible astrocyte cell lines. This is also observed in transfected astrocytes and a chronically infected astrocyte cell line. The features of this latent phase of infection appear to mimic those observed in *in situ* infected astrocytes in post mortem brain sections with respect to the detection of HIV-1 DNA (Brengel-Pesce *et al*, 1997; Di Rienzo *et al*, 1998; Keys *et al*, 1991; Kort, 1998; Nath

et al, 1995; Sabri *et al*, 1999), viral regulatory transcripts (Gorry *et al*, 1998) and regulatory proteins (Kohleisen *et al*, 1992; Kort, 1998), and the noticeable absence of viral structural proteins (Brack-Werner *et al*, 1992; Kohleisen *et al*, 1992; Kohleisen *et al*, 1999; Kort, 1998; Tornatore *et al*, 1994b; Tornatore *et al*, 1991). The phrase "restricted infection" is often used as the infection is not necessarily truly latent, as some viral regulatory gene expression may be detectable (Di Rienzo *et al*, 1998; Kohleisen *et al*, 1999). The number of HIV-1 antigen positive cells (Brengel-Pesce *et al*, 1997; Keys *et al*, 1991), and amount of HIV-1 RNA (Di Rienzo *et al*, 1998) and DNA (Di Rienzo *et al*, 1998 Keys, 1991 #123; Nath *et al*, 1995; Sabri *et al*, 1999) which can be detected in astrocyte cultures declines with time post infection (discussed in detail in Chapter 5).

This restricted infection resembles a Rev-defective phenotype (see Section 1.1.6iv), in which viral gene expression is limited to transcription of the early, multiply-spliced mRNAs encoding the regulatory proteins (*tat*, *rev* and *nef*). The expression of singly and multiply spliced viral transcripts, including a predominance of the *nef* mRNA, and low or absent expression of unspliced viral transcripts has been noted in other, so called, latent infection models based on T cells and macrophages (Klotman *et al*, 1991; Muesing *et al*, 1985; Pomerantz *et al*, 1990; Robert-Guroff *et al*, 1990). A study by Tornatore *et al* indicated, however, that the profile of HIV-1 transcript expression upon reactivation of infection in HIV-1 transfected astrocytes differs from that of reactivation in T-cells and macrophages (Tornatore *et al*, 1994b). Stimulation of promonocyte U1 cells results in a pronounced increase in the multiply spliced viral mRNAs, followed by an increase in unspliced RNA species (Muesing *et al*, 1985; Pomerantz *et al*, 1990). In contrast, cytokine stimulation of transfected astrocytes also leads to an increase in multiply spliced viral transcripts (*rev* and *nef*) but no increase in unspliced viral RNA (Tornatore *et al*, 1994b).

To analyse the restricted HIV-1 infection of astrocytes, Brack-Werner *et al* (1992) established a chronically HIV-1_{IIIB} infected astrocyte line cell line, TH4-7-5, from the 85HG-66 astrocyte cell line (Brack-Werner *et al*, 1992). This stably HIV-1 infected cell line contains one integrated copy of the provirus per cell, and displays the same pattern of restricted infection seen in infected and transfected astrocytes. TH4-7-5 cells express HIV-1 regulatory proteins, including a disproportionately high level of Nef expression, but their expression of viral structural proteins is limited. Stimulation of TH4-7-5 cells with TNFα

and phorbal esters only had a modest effect on virus production (Kleinschmidt *et al*, 1994). This is concordant with the stimulation of other persistently HIV-1 infected astrocytes (Shahabuddin *et al*, 1992; Tornatore *et al*, 1994b), and in contrast with latently infected monocyte (U1) and T-cell lines (Folks *et al*, 1988; Michael *et al*, 1991; Poli *et al*, 1990; Pomerantz *et al*, 1990).

The restriction of HIV-1 in astrocytes, which comes into effect after an apparent brief initial productive infection, appears to be distinct from the prototypic models of HIV-1 latency in T-cells and cells of the monocyte lineage. This indicates that astrocytes have unique intrinsic mechanisms which can control the replication of the HIV-1 virus.

1.4.3 "Rescue" or "Reactivation" upon coculture with permissive cells

When infected (or transfected) astrocytes in the restricted phase are cocultured with cells that are susceptible to HIV-1 infection, (T-cells or monocyte derived cells), the cocultured cells become productively infected. This "rescue" of productive infection is thought to arise from a "reactivation" of the restricted infection in the astrocyte cells, stimulated by the coculture. Detection of productive infection (by p24 protein or reverse transcriptase activity in the coculture supernatants, or by cytopathic effect (formation of syncytia) in the susceptible cell population) typically requires at least 2, and up to 6, days of coculture (Cheng-Mayer *et al*, 1987; Di Rienzo *et al*, 1998; Sabri *et al*, 1999). In TH4-7-5 cells approximately two weeks of coculture was required for the detection of productive infection in the susceptible cells (Brack-Werner *et al*, 1992). HIV-1 infection of astrocytes can be "rescued" as long as 4 or 5 months after the original infection (Chiodi *et al*, 1987; Dewhurst *et al*, 1987b), although the amount of virus released appears to diminish with time post original infection (Chiodi *et al*, 1987). This rescue of productive infection has also been demonstrated when the HIV-1 susceptible cells are separated from latently infected (transfected) astrocytes by a 0.4μm transwell (Tornatore *et al*, 1991). This suggested that the "rescue" of infection from astrocytes could be induced by soluble factors.

The cytokine IL1β and, in some models, TNFα (but not TNFβ, GM-CSF, FGFβ, IFN, IL2 or IL6), have been reported to induce a transient burst of p24 release from astrocytes which are in the restricted phase of infection (Lawrence *et al*, 2004; Tornatore *et al*, 1991). This

suggests that some proinflammatory cytokines, which may be released by T-cells or macrophages upon coculture, can mediate reactivation of virus production in astrocytes. The underlying mechanism of this appears to be different to reactivation of latent infection in other cell types (refer Section 1.4.2). Similar to the rescue of infection by coculture, it takes at least 4 days for the p24 release from IL1β or TNFα treated astrocytes to be detectable (Lawrence *et al*, 2004; Tornatore *et al*, 1991). This cytokine-induced p24 release is transient, and lasts around 2-3 days. The presence of infectious virus has been demonstrated in supernatants collected from IL1β or TNFα treated, HIV-1 transfected astrocytes, during the period of cytokine induced p24 release (Tornatore *et al*, 1991). IL1β can act to upregulate transcription of HIV-1 proviral DNA through an interaction with the viral LTR (Swingler *et al*, 1992; Tornatore *et al*, 1994b; Tornatore *et al*, 1991), and so it is possible that IL1β "rescues" productive infection from astrocytes by this mechanism.

The potential for HIV-1 to be "rescued" from restricted astrocyte infection implies that the cellular block(s) to HIV-1 infection of astrocytes can be temporarily overcome. The ability of astrocytes to transmit virus upon coculture or cytokine stimulus suggests that astrocytes may be capable of transmitting virus *in vivo*, as they come into contact with HIV-1 susceptible cells (including microglia and infiltrated macrophages and lymphocytes) in the brain parenchyma and at the boundaries of the brain, and, during HIVE and HAD, they become exposed to IL1β and TNFα. This supports the notion that HIV-1 infection of astrocytes may be a significant source of viral persistence and rebound (Section 1.1.4). The current literature on the replication (and the restrictions to the replication) of HIV-1 in astrocytes is outlined below.

1.5 Mechanisms of HIV-1 replication in astrocytes *in vitro*

1.5.1 Virus Entry

Astrocyte infection is independent of CD4, the main receptor for HIV-1. Astrocytes do not express detectable surface CD4 (Harouse *et al*, 1989; Peudenier *et al*, 1991; Tornatore *et al*, 1991) and, whilst some astrocyte cultures may express CD4 transcripts, neither anti-CD4 monoclonal antibodies nor soluble CD4 block astrocyte infection (Clapham *et al*, 1989; Di Rienzo *et al*, 1998; Harouse *et al*, 1989; Ma *et al*, 1994; Tornatore *et al*, 1991). Whilst some

astrocytes can be induced to express various HIV-1 co-receptors (Rottman *et al*, 1997; Sanders *et al*, 2000) these do not appear to be involved in astrocyte infection either (Sabri *et al*, 1999).

HIV-1 gp120 has been demonstrated to bind to galactosyl ceramide (also known as galactocerebroside) (Bhat *et al*, 1993; Harouse *et al*, 1991), which may be present on the surface of astrocytes. In one report, antibodies to galactosyl ceramide were shown to inhibit HIV-1 infection of an astrocyte cell line, U373-MG (Harouse *et al*, 1989), however infection of human fetal astrocytes has been repeatedly shown to be independent of this molecule (Hao *et al*, 1997; Hao and Lyman, 1999; Ma *et al*, 1994). This molecule is expressed in much greater abundance on oligodendrocyte cells, yet these are rarely, if ever, infected (Section 1.3.2i). The binding of HIV-1 to other surface molecules present on human fetal astrocytes has been reported, including a 65kDa and a 260kDa cell surface protein (Hao and Lyman, 1999; Ma *et al*, 1994), however whether or not this binding facilitates astrocyte infection is yet to be demonstrated. In one report, HIV-1 virions were observed to be clustered near clathrin coated pits and within endocytic vesicles. The morphology of these vesicles appeared consistent with viral uptake by clathrin-mediated endocytosis (Hao and Lyman, 1999). Whether this mode of viral uptake by astrocytes results in infection, or whether, as with endocytic uptake of HIV-1 reported in several other cell types (refer to Section 1.1.6i) (Fredericksen *et al*, 2002; Marechal *et al*, 2001; Schaeffer *et al*, 2001), this mode of uptake results in lysosome-mediated viral degradation (Fredericksen *et al*, 2002; Schaeffer *et al*, 2001), remains to be determined.

The mannose receptor has recently been identified as being involved in astrocyte infection, and the involvement of additional receptors, yet to be identified, has also been implicated (Liu *et al*, 2004). The mannose receptor, like the dendritic cell HIV-1 receptor DC-SIGN, is a member of the large C-type lectin superfamily. The mannose receptor is involved in phagocytosis by macrophages and microglia, and is reported to be involved in pinocytosis by astrocytes (Regnier-Vigouroux, 2003).

The relevance of specific receptor and coreceptor usage to astrocyte infection is unclear. Some reports imply that astrocytes are more susceptible to infection by CXCR4-using "T-cell tropic" strains of HIV-1 virus than "macrophage-tropic" strains (McCarthy *et al*, 1998; Nath *et al*, 1995; Schweighardt *et al*, 2001). Given the apparent independence of astrocyte

infection from CD4 and the known T cell and macrophage viral coreceptors (see above), the molecular mechanism for this is unclear. Other reports observe similar infections of astrocytes with both T-cell tropic and macrophage tropic virus strains (Di Rienzo *et al*, 1998).

1.5.1i Cell to cell transmission of HIV-1 to astrocytes

It has been suggested that infection of astrocytes may be more efficient by the cell-to-cell infection route than by cell-free infection (Brack-Werner, 1999; Nath *et al*, 1995). Given the close proximity of cells within the CNS, it is more likely that *in vivo* infection of astrocytes occurs by direct cell-to-cell contact rather than by free virus. Up to four times more astrocytes have been reported to express HIV-1 antigens following cell-to-cell infection compared to cell-free infection (Nath *et al*, 1995), although the respective viral dose for each of these models cannot be directly compared. One hypothesis for the apparent increased efficiency of cell-to-cell HIV-1 infection of astrocytes could involve the provision of the CD4 receptor *in trans*, by the infected "viral donor" cell to the astrocyte (Speck *et al*, 1999). This may enable the virus to enter the astrocyte via the interaction of gp120 with CD4 (provided *in trans*) and a coreceptor for HIV-1, some of which may be expressed by astrocytes under certain conditions. The *in vivo* relevance of this is unclear.

1.5.2 Reverse transcription and integration

The occurrence of viral reverse transcription and integration is implicit in the concept that the initial phase of astrocyte infection, *in vitro*, is productive. The detection of a low level of HIV-1 DNA in infected astrocytes (Brengel-Pesce *et al*, 1997; Di Rienzo *et al*, 1998; Keys *et al*, 1991; Kort, 1998; Nath *et al*, 1995; Sabri *et al*, 1999) confirms that reverse transcription has occurred. The derivation of the TH4-7-5 cell line, with one integrated copy of HIV-1 DNA / cell (Brack-Werner *et al*, 1992), is further evidence that HIV-1 genomic RNA can reverse transcribe within astrocytes. Infection models that induce fusion of the viral and astrocyte membranes (Section 1.6.1vi) result in productive infection, further indicating that reverse transcription and integration can proceed in astrocytes. The kinetics of reverse transcription, and the possibility that astrocytes may be able to limit this process, has not been explored.

Further evidence that the reverse transcribed HIV-1 DNA can integrate into astrocytes is based on i) the detection of HIV-1 DNA in some astrocyte cultures as long as a week (Brengel-Pesce *et al*, 1997; Keys *et al*, 1991; Sabri *et al*, 1999), or even almost a month (Di Rienzo *et al*, 1998), after infection, and ii) that productive viral infection may be rescued upon coculture or cytokine stimulus. The presence of integrated HIV-1 DNA has been formally demonstrated in TH4-7-5 cells (by restriction analysis) (Brack-Werner *et al*, 1992). The kinetics of HIV-1 integration in astrocytes has not been investigated.

1.5.3 Transcription and Translation and mechanisms of restriction

The frequent detection of early, multiply-spliced HIV-1 proteins, in the absence of structural viral proteins, in HIV-1 infected astrocytes, both *in vivo* (see Section 1.3.2ii) and *in vitro* (Section 1.4.2), resembles a "Rev defective" phenotype. This is because Rev is required to transport the incompletely spliced transcripts, which encode the viral structural proteins, from the nucleus to the cytoplasm for translation (Section 1.1.6iv). Analysis of the restricted infection of the TH4-7-5 cell line and of HIV-1 transfected astrocytes has identified two different mechanisms, specific to astrocytes, which can explain the expression of regulatory HIV-1 proteins and the lack of expression of structural HIV-1 proteins, in astrocytes.

1.5.3i Aberrant Rev / RRE regulatory axis in astrocytes

Transcription and translation of HIV-1 have been studied extensively in the chronically HIV-1_{IIIB} infected astrocyte cell line, TH4-7-5 (Brack-Werner *et al*, 1992; Kleinschmidt *et al*, 1994; Neumann *et al*, 1995) (refer to Section 1.4.2). Consistent with other models of astrocyte infection, these cells are able to transmit virus to HIV-1 susceptible cells upon coculture despite exhibiting a restricted infection (Section 1.4.3). The *rev* gene and Rev-responsive element (RRE) of the HIV-1 provirus in this chronically infected cell line have been shown to be intact, and overexpression of Rev by a Rev-expressing plasmid did not alter the "Rev-defective" infection phenotype (Neumann *et al*, 1995). Rev protein, which is normally localised mainly to the nucleous and nucleolus, was also present in the cytoplasm (Neumann *et al*, 1995). Further analysis revealed a defect in the nuclear export of the Rev-dependent structural HIV-1 transcripts in these cells (Neumann *et al*, 1995). This process is normally dependent on the ability of Rev to shuttle between the nucleus and cytoplasm

(Section 1.1.6iv). Transfection experiments with Rev-reporter and Rev-expressing constructs have demonstrated that this aberrant cellular distribution of Rev and apparent block in the Rev-RRE regulatory axis also occurs in human fetal astrocytes and several astrocyte cell lines, including the parental cell line to TH4-7-5 (85HG-66, U251-MG, U87-MG, U138-MG and U373-MG) (Ludwig *et al*, 1999; Neumann *et al*, 1995). Further studies using the U87-MG astrocyte cell line suggests this astrocyte specific aberration of the Rev-RRE regulatory axis may be partly due to a lower level of expression of a constitutive cellular protein, Sam86, in astrocytes (Li *et al*, 2002b). Sam68 can interact with both HIV-1 Rev and the RRE, and is involved in the nuclear export of Rev (Li *et al*, 2002b). Whilst exogenous expression of Sam68 can partially alleviate the Rev function block in U87-MG astrocytes (Li *et al*, 2002b) and the down-modulation of Sam68 inhibits HIV-1 gene expression, replication and Rev function in several cell types (Li *et al*, 2002a), the molecular mechanism of Sam68's involvement in Rev-mediated nuclear export, and whether this relates to the accumulation of Rev in the cytoplasm, is yet to be elucidated.

1.5.3ii Low TRBP levels in astrocytes

An aberrant Rev/RRE axis is not observed in all models of astrocyte infection. In another transfection base model of astrocyte infection (using the U251-MG astrocyte cell line), HIV-1 structural transcripts were found to be correctly processed and efficiently transported to the cytoplasm (Gorry *et al*, 1998; Gorry *et al*, 1999). Despite efficient nuclear export, however, the translation of these structural genes was highly inefficient (Gorry *et al*, 1998; Gorry *et al*, 1999). In this paradigm, the block in translation of HIV-1 structural genes has been attributed to a reduced level of transcription of a cellular *trans*-activation-responsive RNA-binding protein (TRBP) in astrocytes (Gorry *et al*, 2003; Ong *et al*, 2005), which is a potent inhibitor of double-stranded RNA induced, interferon-regulated, protein kinase (PKR) activation (Bannwarth *et al*, 2001). TRBP enhances viral replication by both activating the HIV-1 long terminal repeat (LTR) promoter (Daher *et al*, 2001) and by blocking the inhibitory effects of PKR on viral translation (Park *et al*, 1994). Co-expression of TRBP or a catalytically inactive PKR mutant has been reported to restore HIV-1 replication in astrocytes, indicating that the very low endogenous level of TRBP in astrocytes may be responsible for the limited translation of HIV-1 structural proteins in these cells (Ong *et al*, 2005). The regulatory transcripts *Rev* and *Tat* have polypyrimidine tracts

near their initiating codons which may enable them to evade this cap-dependent PKR inhibition of translation (Gorry *et al*, 1999).

Curiously, transcription and translation of HIV-1 proteins appears unhindered in astrocytes in infection models which induce fusion of the viral and astrocyte membranes, such as VSV-envelope pseudotyped virons (Section 1.6.1vi). TRBP has been shown to be incorporated into VSV-pseudotyped HIV-1 virions, which may, in part, explain the lack of restriction observed upon infection of astrocytes with VSV-pseudotyped HIV-1 (Thorpe, 2001) (Dr Damien Purcell, personal communication).

1.5.4 Release of infectious virus

During the initial phase of *in vitro* infection, astrocyte cultures release p24 protein, a marker of HIV-1 virus production, into the supernatant (Section 1.4.1). Hence these supernatants are thought to contain infectious virus, although this has not been formally demonstrated. During the restricted phase of infection (and transfection), astrocyte supernatants are non-infectious when added to HIV-1 susceptible cells. The evidence that astrocytes can produce and release fully competent and infectious virus comes from coculture studies (Section 1.4.3) and the demonstration that transfected astrocytes can release infectious virus to susceptible cells across a transwell or upon cytokine stimulation (Tornatore *et al*, 1991). Fully competent, infectious virus is also released from astrocytes where productive infection was induced by fusion of the viral and cell membranes (Section 1.6.1vi). Taken together, this indicates that all the necessary factors for complete and competent virus production exist in astrocytes, yet virus replication is normally restricted.

1.6 *In vitro* models of astrocyte infection

1.6.1 Consideration of the limitations of current HIV-1 astrocyte infection models

The majority of human astrocyte infection models appear to display the restricted paradigm of infection observed *in vivo*. However, some observations vary between models, confounding the interpretation of the literature. The variation seen may be largely attributed

to the different astrocyte sources, virus strains and infection methods. The advantages and limitations of the respective astrocyte infection models need to be considered for interpretation of the literature, and are discussed below.

1.6.1i Primary Astrocytes

Primary human astrocytes are usually derived from human fetal material (HFA), or occasionally, human embryonic material (HEA). In addition to being primary cells, they have the advantage of representing the heterogeneity of astrocytes present in the CNS. Most reports document the purity of their HFA (or HEA) cultures as ≥95% or 99% by GFAP immunoreactivity, however the potential for a low level of contamination by HIV-1 susceptible microglia and macrophages cannot be completely excluded. The relevance of this depends on the exact nature of the study. HFA and HEA are actively dividing cells, and therefore the extrapolation of these studies to the HIV-1 infection of adult astrocytes (AA), which are terminally differentiated and do not divide at the same rate (if at all), is uncertain. AA cultures are seldom used due to the inavailability of fresh adult brain tissue. They may also contain a very low percentage of HIV-1 susceptible microglia / macrophages. Recently it has become possible to derive astrocytes from precursor cells, usually from fetal brain material. These progenitor-derived astrocyte (PDA) cultures have the distinct advantage of being pure, as well as representing primary cells.

1.6.1ii Astrocyte cell lines

A number of astrocyte cell lines have been derived from gliomas, gliocytomas and astrocytomas. Astrocyte cell lines usually represent a clonal cell population derived from adult tissue. As such, they are unable to represent the heterogeneity of astrocytes in the CNS. They also have chromosomal abnormalities and a rapidly dividing phenotype. Many of the available astrocyte cell lines express GFAP, the prototypic astrocyte marker. Some astrocyte cell lines do not express GFAP however, but neither is this expressed on all primary astrocytes, *in vivo* or *ex vivo*, and its expression may be lost upon culture (Cheng-Mayer *et al*, 1987; Collins, 1983; Keys *et al*, 1991). The cell lines SF609 and U138-MG, thought to be of astrocytic origin in earlier studies, do not appear to be pure astrocyte cell lines (Cheng-Mayer *et al*, 1987; Collins, 1983; Keys *et al*, 1991), and have been excluded

from consideration in this thesis. The chronically HIV-1_{IIIB} infected astrocyte cell line, TH4-7-5, was derived by coculture of the 85HG-66 astrocyte cell line with persistently HIV-1_{IIIB} infected H9 cells. The TH4-7-5 cell line has been highly valuable for studying post integrational events in astrocytes, and these cells model the characteristic attributes of astrocyte infection (preferential expression of multiply-spliced viral transcripts, with only a low level of virus structural protein expression, and transmission of infection upon coculture with HIV-1 susceptible cells) (Sections 1.4.2 and 1.4.3). The derivation of TH4-7-5 cells indicate that the earlier virus replication steps were possible in 85HG-66 astrocytes, however it should be noted that the derivation of this cell line by single cell cloning represented a rare clone which persistently expressed viral antigens (Brack-Werner *et al*, 1992).

1.6.1iii Virus strain and phenotype

Findings from several *in vitro* studies (McCarthy *et al*, 1998; Nath *et al*, 1995; Sabri *et al*, 1999; Schweighardt *et al*, 2001; Shahabuddin *et al*, 1996), and a recent *in vivo* study (Thompson *et al*, 2004), indicate that astrocyte infection may be dependent on the strain of HIV-1. Most strains are either unable to infect astrocytes or are capable of establishing a restricted infection. In a few instances, however, productive infection has been documented (Canki *et al*, 1997; Nath *et al*, 1995). This appears to depend on either the virus strain itself, or, in case of astrocyte cell lines, the particular cell line. Some virus strains appear selective as to which astrocyte cell lines they are able to infect in a restricted manner. Additionally, whilst the strain HIV-1_{SF2} has been reported to productively infect several astrocyte cell lines (Nath *et al*, 1995) (Prof Cecilia Cheng-Mayer, personal communication), possibly due to its unique membrane fusion properties (Fackler and Peterlin, 2000), it is not able to productively infect all astrocyte cell lines (Shahabuddin *et al*, 1996). Conversely, HIV-1_{NL4-3}, which has been reported to establish a restricted infection in a variety of astrocyte cell lines and by several different research groups (Cheng-Mayer *et al*, 1987; Clapham *et al*, 1989; Dewhurst *et al*, 1987b; Dewhurst *et al*, 1988; Gorry *et al*, 1998; Gorry *et al*, 1999; Kort, 1998), has also been reported to productively infect an astrocyte cell line which is refractory to productive infection by HIV-1_{SF2} (Shahabuddin *et al*, 1996). This adds further support to the concept that multiple mechanisms of virus restriction occur in astrocytes, and that different mechanisms of restriction may be evident in different astrocyte cell lines. Alternatively, given host cell factors can be incorporated into virions and affect the

subsequent replication ability of the virus (Harris *et al*, 2003; Lecossier *et al*, 2003; Mariani *et al*, 2003; Thorpe, 2001), the variation in susceptibility of different cell lines to the same virus strain in different studies may involve differing viral phenotypes according to the producer cell in which the virus stock was generated.

1.6.1iv In vitro *models for astrocyte infection*

Astrocyte cultures can be infected by inoculation with cell free virus or by coculture with infected cells. (Infections initiated by transfection of proviral DNA or by induction of viral fusion at the cell membrane occur through different mechanisms and are discussed separately below.) It has been suggested that it is more physiologically relevant (and more efficient) to infect astrocytes by contact with infected cells, however the presence of a mixed culture limits the aspects of astrocyte infection which can be studied. While cell-free infections permit a wider scope of study, this route is reportedly even less efficient than cell-to-cell infection. To overcome the apparent inefficiency of cell-free infection, highly concentrated cell-free virus stocks are sometimes used (for example, 2μg HIV-1 p24 protein / ml (Nath *et al*, 1995), ~10^5-10^6 cpm / Reverse transcriptase activity / ml (Brack-Werner *et al*, 1992; Cheng-Mayer *et al*, 1987; Chiodi *et al*, 1987)), and it should be noted that the amount of virus subsequently released by the infected astrocyte cultures may be much less than what was in the initial inoculum. Occasionally, infections are performed in the presence of agents which interfere with the cell membrane and promote interaction of viral and cellular membranes, such as polybrene and DEAE dextran (Cheng-Mayer *et al*, 1987; Kort, 1998).

In early studies the viral inocula were not pretreated with DNase (Brengel-Pesce *et al*, 1997; Cheng-Mayer *et al*, 1987; Di Rienzo *et al*, 1998; Keys *et al*, 1991; Nath *et al*, 1995) and in some studies the excess inoculum may not have been removed (Brengel-Pesce *et al*, 1997). This is important in the assessment of HIV-1 DNA by sensitive techniques such as PCR, as HIV-1 DNA may be present in the viral inoculum, derived from the degradation of infected producer cells, and, where virus stocks are derived from molecular clones, the from original plasmid.

1.6.1v Transfection of viral DNA

To improve the efficiency of viral expression, and to circumvent the restrictions to HIV-1 entry in astrocytes, several studies of HIV-1 infection of astrocytes establish a restricted infection by *transfecting* the astrocytes with viral DNA. This has been a highly effective tool for, in particular, studying the transcription and translation of HIV-1 in astrocytes. Transfection studies are limited to post-integrational events, as the processes of viral attachment, entry and reverse transcription are bypassed (Sections 1.5.1 and 1.5.2). Whilst full length proviral plasmid DNA can integrate into the host cell DNA after transfection, the process of plasmid integration is fundamentally different to the proviral integration that occurs during viral replication, as the plasmid DNA is not in the context of pre-formed viral proteins. During HIV-1 infection, the process of integration is highly organised sequence of events, guided by pre-formed viral and cellular proteins in the PIC. (Sections 1.1.6ii-iii). Other cellular and virion factors, which are normally packaged by the virus producer cell and may affect the new round of infection, are also absent in transfection models of astrocyte infection. Additionally, the process of transfection causes considerable metabolic stress to the cells and their membranes.

1.6.1vi Induction of viral fusion at the cell membrane

The efficiency of virus expression in astrocytes has also been increased by inducing fusion of the virus with the cell membrane, in the receptor–dependent manner by which HIV-1 enters T-cells and macrophages. This has been achieved by transfecting astrocytes to express CD4 and, where necessary, a coreceptor for HIV-1. Curiously, expression of CD4 alone permits productive infection of some astrocyte cell lines by some viral strains (Chesebro *et al*, 1990; Shahabuddin *et al*, 1996). The requirement to also transfect the astrocytes to express a coreceptor may depend on the endogenous coreceptor expression of the cells and the coreceptor usage of the isolate. When transfected to express both CD4 and a coreceptor, susceptibility to productive infection by HIV-1 is reportedly conferred to HFA and astrocyte cell lines (Schweighardt and Atwood, 2001).

MLV and VSV envelope pseudotyped HIV-1 virions induce membrane fusion at the plasma membrane surface (McClure *et al*, 1990) or at endocytosed membranes (Matlin *et al*, 1982),

respectively. Infection by these pseudotyped virions is independent of HIV-1 receptor and coreceptor expression. These pseudotyped virions productively infect astrocytes (Canki *et al*, 2001; Chesebro *et al*, 1990), as does the HIV-1_{SF2} virus strain (Cheng-Mayer *et al*, 1987; Nath *et al*, 1995) which has since been shown to have unique membrane fusion properties (Fackler and Peterlin, 2000).

Models which manupulate HIV-1 entry into astrocyte cells by fusion-based approaches such as transfecting the astrocytes to express CD4 and a coreceptor, or pseudotyping the virus with MLV and VSV envelopes, have some advantages over proviral plasmid DNA transfection methods. Specifically, fusion-based methods deliver the viral core, in the context of pre-formed virus proteins, into the cytoplasm of the cell. In considering the interpretation of these pseudotype virus based studies, however, the potential for the producer cell to affect the virus phenotype needs to be considered. This is highlighted by the observation that producer-cell derived TRBP protein (see Section 1.5.3ii) could be incorporated into VSV pseudotyped HIV-1 virions. Exogenous TRBP alone has been shown to relieve the restrictions to HIV-1 replication in both HFA and the U251-MG astrocyte cell line (Bannwarth *et al*, 2001; Ong *et al*, 2005) (Dr Damien Purcell, personal communication) illustrating the potential for artifacts to occur with a pseudotyped virus approach.

Taken together, however, these HIV-1 membrane fusion models indicate that HIV-1 entry (or, more specifically, the mode of HIV-1 entry) is a major restriction to HIV-1 replication in astrocytes. These models also indicate that if the viral genome is delivered to the cytoplasm of astrocytes in the context of the intact viral core and pre-integration complex, productive infection can occur. This seems to indicate that, in these models, there are no intrinsic cellular restrictions to virus replication. However, these fusion-based models of productive astrocyte infection do not resemble the paradigm of restricted astrocyte infection observed in post mortem tissue. The fact that CD4 (and HIV-1 coreceptor) expression on astrocytes results in a productive infection rather than a restricted infection is also consistent with the notion that astrocyte infection, *in vivo*, occurs through a mechanism which is independent of CD4 and coreceptor expression.

1.6.2 Choice of Astrocyte cell lines and HIV-1 strains for this thesis

1.6.2i Astrocyte cell lines

The U251-MG astrocyte cell line was chosen for the majority of the work in this thesis as it is a well characterised, GFAP positive (and CD4 negative) astrocyte cell line (Bigner *et al*, 1981) (Section 2.1.1). It has been used by several other groups to study HIV-1 infection of astrocytes (Cheng-Mayer *et al*, 1987; Clapham *et al*, 1989; Dewhurst *et al*, 1987b; Dewhurst *et al*, 1988; Gorry *et al*, 1998; Gorry *et al*, 1999; Kort, 1998). Initially it was intended that the studies with this cell line would be repeated in human fetal astrocyte cultures, however the progression of results from the reverse transcription and integration studies made it imperative that the pure astrocyte cultures be used. The use of progenitor-derived astrocytes would have been ideal, however the preparation of these is highly tedious and very expensive. So, to determine whether results from the U251-MG astrocytes were particular to this cell line or representative of astrocytes in general, the pertinent results of this thesis were repeated in two additional astrocyte cell lines, CCF-STTG1 and U87-MG. These two astrocyte cell lines are also well characterised (Section 2.1.1) and have been used in several previous studies of HIV-1 infection of astrocytes (Brengel-Pesce *et al*, 1997; Chesebro *et al*, 1990; Clapham *et al*, 1989; Liu *et al*, 2004; Ludwig *et al*, 1999).

1.6.2ii HIV-1 strains

Cell-free infections were performed with the NL4-3 strain of HIV-1. This strain was selected as it is a fully competent strain, and available as a molecular clone. As such, virus stocks could be prepared with limited cell passage from transfection of the clone, ensuring minimum genetic variation of the virus stock from the published strain. It was also chosen as it has been previously demonstrated to infect U251-MG cells in a restricted manner typical of astrocyte infection (Gorry *et al*, 1998; Gorry *et al*, 1999). This strain was also chosen as it is a T-cell tropic strain, and the literature at the time indicated a preference for astrocyte infection by T-cell tropic strains (McCarthy *et al*, 1998; Nath *et al*, 1995; Schweighardt *et al*, 2001). Initially it was intended that the scope of the cell-free infections studies in this thesis would extend to other T-cell tropic virus strains (including SF2 and

IIIB, and the CSF derived primary isolate; JR-CSF) and to macrophage-tropic virus strains (including BaL and primary isolates derived from the CNS; HIV-1 JR-FL and YU2).

Cell-to-cell infections with primary monocyte-derived macrophages (MDM) utilised the macrophage tropic strain BaL, as cell-to-cell transmission of infection with HIV-1_{BaL} infected MDM has been used previously to successfully analyse the transmission of HIV-1 from macrophages to lymphocytes (Carr *et al*, 1999). Cell-to-cell infections with T-cell lines used the established and well characterised clonal HIIIB cell line, derived from HIV-1 IIIB infection of H9 cells. This cell line has also been used successfully to study cell-to-cell transmission of HIV-1 in the analysis of T-cell infection (Karageorgos *et al*, 1993; Karageorgos *et al*, 1995; Li *et al*, 1993a; Li and Burrell, 1992; Li *et al*, 1992; Li *et al*, 1994). As a comparison, the E12 cell line, which is persistently infected with the T-cell tropic HIV-1 strain, SF2, was also used. It was originally envisaged that pertinent results from cell-to-cell studies with chronically infected T-cell lines would be repeated with infected PBMC or PBL cultures and HFA.

1.7 *In vivo* significance of restricted HIV-1 infection of astrocytes

Characterisation of the restricted HIV-1 infection of astrocytes is imperative to understanding the entry and spread of HIV-1 into the CNS, HIV-1 persistence and HIV-1 induced neurological diseases. Additionally, understanding the cell-specific restrictions to HIV-1 replication in these cells may lead to novel antiviral strategies. Furthermore, a greater understanding of astrocyte function and dysfunction is likely to be help clarify our understanding of the pathogenesis of HAD.

Astrocytes regulate the barriers to the brain and are integrally involved in the entry of HIV-1 into the central nervous system, both as free virus and within infected cells (Section 1.3.1). As astrocytes are the first CNS cell type encountered by the virus upon passage through the BBB, they may facilitate the spread of HIV-1 through the brain parenchyma (Section 1.3.1). HIV-1 is known to be able to persist within the human body for extended periods of time (years), even whilst plasma viral loads are kept below the level of detection by antiretroviral therapy (Section 1.1.4). The brain is perhaps the major anatomical sanctuary for HIV-1 during therapy, as the BBB can prevent several therapeutic agents from reaching effective

concentrations within the brain (Section 1.1.4). Numerically, the number of HIV-1 infected astrocytes and microglia within the brain represent a major cellular source of potential viral persistence (Section 1.1.4). The restricted nature of astrocyte infection may also assist the virus in evading therapy. *In vitro* studies indicate that, even though infection is restricted in astrocytes, these cells can transmit infectious virus upon contact with susceptible cells, or upon stimulation with TNFα and IL1β (Section 1.4.3). Exposure of astrocytes to HIV-1 susceptible cells and these proinflammatory cytokines occurs in the brain environment during HIVE (Sections 1.3.3-5).

HIV-1 induces several neurological syndromes, the most devastating of which is HAD (Section 1.3). This disease appears to be the result of immune over-activation and dysregulation within the CNS (Section 1.3.5). Astrocyte activation and dysfunction, as well as the over-activation of microglia and macrophages, is involved in this process. Direct infection and exposure to viral proteins and the products of activated cells mediates this activation. This dysfunction of astrocytes is critical as it interferes with their support of neurons and control of the CNS milieu, vital for normal neuronal function (Sections 1.3.5, 1.2.2 and 1.2.3). Similar dysfunction of astrocytes have been implicated in other neurological diseases including Alzheimer's disease and hepatic encephalopathy (Zigmond *et al*, 1999), and so the elucidation of the mechanisms involved in HAD may be applicable to other neurological diseases.

Cellular mechanisms, which are unique and intrinsic to astrocytes, can restrict astrocyte infection *in vivo* and *in vitro* (Sections 1.3.2ii, 1.4 and 1.5). Multiple mechanisms of virus restriction by astrocytes are apparent, at several steps of virus replication including entry, transcription and translation (Sections 1.5.1 and 1.5.3). Analysis of astrocyte-specific blocks in the Rev-RRE regulatory axis of HIV-1 (Section 1.5.3i) indicate that astrocytes express factors which can control HIV-1 replication. Further analysis of these factors, and other mechanisms of viral restriction in astrocytes, may reveal novel antiretroviral strategies. The development of new and improved antiretroviral therapies is imperative given the high prevalence of HIV-1 globally, and the fact that the number of people infected with HIV-1 continues to increase (Section 1.1.2).

To further current understanding of the restricted HIV-1 infection of astrocytes, the work in this thesis analyses the processes of HIV-1 reverse transcription and integration in astrocytes, and investigates the mode of viral entry and phenomenon of transmission of infection from astrocytes.

1.8 Scope of this thesis

1.8.1 Hypotheses

The HIV-1 infection of astrocytes exhibits a number of fundamental differences compared to the infection of CD4 and coreceptor expressing HIV-1 susceptible cells. Several restrictions to HIV-1 replication in astrocytes have been described, but these restrictions are not entirely consistent, indicating that additional mechanisms of virus restriction may occur in astrocytes. Viral entry appears to be a major block to astrocyte infection, although little is known about the mode of HIV-1 attachment and entry in astrocytes. The viral replication steps of reverse transcription and integration have not been specifically investigated in astrocytes. More than one mechanism for the restricted expression of viral proteins has been described, and the underlying determinants for the observation of different mechanisms in different infection models are not known. This thesis addresses the possibility that additional mechanisms of restriction of viral replication may exist at earlier stages in the virus life cycle in astrocytes. Characterisation of the early events of virus replication, specifically virus entry, reverse transcription and integration, may explain the discrepancies in the literature regarding the mechanisms of restriction of viral gene expression. Understanding the processes of virus entry, reverse transcription, integration, and subsequent virus release upon coculture, will provide valuable knowledge pertaining to the effectiveness of antiretroviral drugs in HIV-1 infected astrocytes. Understanding these early steps of virus replication, and potential virus release, together with the current literature on the later stages of viral replication in astrocytes, will further current knowledge of astrocyte infection in the CNS and the dissemination and persistence of HIV-1 in the brain.

Specifically, the hypotheses addressed in this thesis are

i) That the process of viral entry is more efficient in astrocytes infected by the cell-to-cell infection route than the cell-free infection route, and that more efficient viral entry results in a greater level of subsequent viral reverse transcription.

ii) That, because the mode of virus entry in astrocytes is fundamentally different to that in CD4 and coreceptor expressing HIV-1 susceptible cells, the susceptibility of astrocytes to HIV-1 infection does not relate to the classification of HIV-1 strains as either T-cell tropic or Macrophage tropic.

iii) That, upon entry, HIV-1 undergoes reverse transcription in astrocytes, but that the kinetics of HIV-1 reverse transcription in astrocytes may differ to that in $CD4^+$, coreceptor expressing, HIV-1 susceptible cells. Potential differences in the kinetics and regulation of viral reverse transcription in astrocytes may be due to the different mechanisms of virus entry and / or the presence of astrocyte-specific restrictions to normal viral reverse transcription.

iv) That, following reverse transcription, the reverse transcribed HIV-1 genome undergoes integration in astrocytes, but that the kinetics of HIV-1 integration in astrocytes may differ to that in $CD4^+$, coreceptor expressing, HIV-1 susceptible cells. Potential differences in the kinetics and regulation of viral integration in astrocytes may be due to upstream differences in virus entry and reverse transcripton, and / or the presence of astrocyte-specific restrictions to normal viral integration.

v) That, under certain circumstances, integrated proviral HIV-1 DNA in astrocytes can be transcriptionally active, and under certain stimuli, the virus life cycle may proceed to completion with the release of infectious virions.

1.8.2 Aims

The main aims of this study were to characterise the entry, reverse transcription and integration of HIV-1 in astrocytes, and the subsequent transmission of HIV-1 from astrocytes. A minor aim of this thesis was to compare the relative efficiency of cell-free and cell-to-cell transmission of infection to astrocytes.

1.8.3 Overview of experimental approach

Entry and reverse transcription of HIV-1 in astrocytes was first studied with a cell-to-cell route of infection with the U251-MG astrocyte cell line. The kinetics of virus entry and subsequent reverse transcription was assessed by measurement of HIV-1 DNA transcripts during the course of astrocyte infection or exposure to HIV-1 secreting cells. This study included both T-cell tropic and macrophage tropic strains of HIV-1.

A cell-free infection model was also established, and used to study the virus entry and reverse transcription steps in more detail, in three astrocyte cell lines (U251-MG, CCF-STTG1 and U87-MG astrocytes). Immunofluorescent, confocal microscopy and electron microscopy approaches were employed to study virus entry. The kinetics of viral reverse transcription was assessed by measurement of HIV-1 DNA transcripts during the course of infection, and by employing inhibitors of transcription and reverse transcription. The later viral replication steps of integration and virus release were also investigated. Specific assays to detect integrated and total chromosome-associated HIV-1 DNA were employed to characterise the kinetics of viral integration in astrocytes. Sensitive assays to detect the release of infectious virus from the astrocyte cultures were developed, and coupled to the analysis of viral integration. Finally, to gain a more comprehensive understanding of the viral processes occurring within the astrocytes, the kinetics of viral RNA expression was also assessed during the course of infection.

Chapter 2

Materials and Methods

2.1 Materials

2.1.1 Cells and Cell Culture

2.1.1i Astrocyte cell lines

U251-MG cells are a GFAP positive, CD4 negative, astrocyte cell line derived from a malignant glioma, by Bigner et al 1981 (Bigner *et al*, 1981). They were kindly supplied by Dr Damien Purcell, Melbourne University, at passage 3 from his original U251-MG source; Dr Jens Kort, Department of Medicine, Albany Medical College, Albany, N.Y., USA. These U251-MG cells have the same origin, but are at an earlier passage, as those held by the Australian National Centre in HIV-1 Virology Research (NCHVR) Research Reagent Program (also donated by Dr Purcell). U251-MG cells were maintained as recommended by Dr Purcell and as described previously (Bigner *et al*, 1981; Gorry *et al*, 1998). Specifically, they were maintained in Dulbecco modified Eagle medium (DMEM, Gibco BRL) supplemented with 10mM Hepes, 0.37% sodium bicarbonate, 2mM L-glutamine, 1.2 μg/ml penicillin, 1.6 μg/ml gentamycin, 10% heat inactivated fetal calf serum (CSL).

The CCF-STTG1 cell line were established from a Grade IV astrocytoma of a 68 year old Caucasian female (Barna *et al*, 1985). 70-80% of cells are positive for GFAP expression, and HLA-DR is present on approximately 20-30% of cells after 48 hours of culture, and they are CD4 negative. They were obtained from the American Type Culture Collection (ATCC), and maintained according to their recommendations. Specifically they were maintained in RPMI 1640 media (Gibco BRL) supplemented with 1.5 g/L sodium bicarbonate, 10mM Hepes, 2mM L-glutamine, 1mM Sodium Pyruvate, 4.5g/L glucose, 1.2 μg/ml penicillin, 1.6 μg/ml gentamycin, 10% heat inactivated fetal calf serum (CSL).

U87-MG cells are an astrocyte cell line derived from a Grade IV malignant glioma of a 44 year old female, originally characterised by Ponten and MacIntyre (Ponten and Macintyre,

1968). They were obtained from the ATCC, and maintained according to their recommendations. Specifically they were maintained in Eagles Minimum Essential Medium (EMEM, Gibco BRL) with Earles Basal Salt Solution (BSS, Gibco BRL) supplemented with 1.5 g/L sodium bicarbonate, 2mM L-glutamine, 0.1mM non-essential amino acids, 1.2 μg/ml penicillin, 1.6 μg/ml gentamycin, 10% heat inactivated fetal calf serum (CSL). They have been reported by some to be GFAP positive (Clapham *et al*, 1989), and by others to be GFAP negative (Chesebro *et al*, 1990; Ludwig *et al*, 1999).

All astrocyte cell lines were cultured in a humidified cell culture incubator at 37°C with 5% CO_2. Astrocyte cell lines passaged approximately 18 hours prior to experiments to reach a confluency of around 80% at time of use, to ensure cells were in the log phase of growth. For all experiments, astrocyte cell lines were used at passage 5-8 from their source to ensure accurate representation of the phenotype of the cell line. Repeat experiments were performed on cells of the same passage number derived from a common stock stored in liquid nitrogen, to minimise inter-experimental variation.

The CD4 receptor negative status of U251-MG, U87-MG and CCF-STTG1 cells was confirmed by FACS analysis using FITC-conjugated anti-human CD4 IgG_1 antibodies (Immunotech, France) and FITC-conjugated anti-human IgG_1 isotype controls (Immunotech, France) (Table 4.1). HuT-78 and 293T cells (see below) were included as positive and negative controls respectively.

U251-MG, U87-MG and CCF-STTG1 cells were confirmed to be positive for the astrocyte specific intermediate filament protein; glial fibrillary acidic protein (GFAP) by immunofluorescence assay (IFA) as described in Sections 2.3.3 and 2.3.4 and shown in Figure 4.1.

2.1.1ii Uninfected T-cell lines

HuT-78 cells are a $CD4^+$ human T-lymphoblastoid cell line (Gazdar *et al*, 1980). They were obtained from the National Institutes of Health (NIH) AIDS Research and Reference Reagent Program, from Dr Robert Gallo. They were maintained according to NIH recommendations, specifically they were maintained in RPMI 1640 (Gibco BRL)

supplemented with 20mM Hepes, 0.12% sodium bicarbonate, 2mM L-glutamine, 1.2 μg/ml penicillin, 1.6 μg/ml gentamycin, 10% heat inactivated fetal calf serum (CSL).

CEM-SS cells are a derivative of the CEM human CD4+ lymphoblastoid cell line (Foley *et al*, 1965; Nara and Fischinger, 1988; Nara *et al*, 1987) which has been cloned for viral-induced syncytial / fusigenic sensitivity following HIV infection. They were also obtained from the NIH AIDS Research and Reference Reagent Program, from Dr Peter L. Nara, and maintained according to NIH recommendations, as described above for the maintenance of HuT-78 cells.

A3.01 cells are a subclone of the CEM human CD4+ lymphoblastoid cell line (see above) (Buttke and Folks, 1992; Folks *et al*, 1985). They were also obtained NIH AIDS Research and Reference Reagent Program, from Dr Thomas Folks, and maintained according to NIH recommendations, as described above for the maintenance of HuT-78 cells.

All T-cell lines were maintained in a humidified atmosphere of 5% CO_2 at 37°C. T-cell lines were subcultured approximately 18 hours prior to use at a density of $5x10^5$ cells/ml to ensure that the cells were in the log phase of growth.

2.1.1iii HIV-1 infected T-cell lines

The HIIIB cell line is a laboratory clone of H9 cells (Popovic *et al*, 1984) persistently infected with the IIIB strain of HIV-1 (formerly known as HTLV-IIIB (Li and Burrell, 1992). HIIIB cells secrete approximately 0.01 $TCID_{50}$ virus / hour and are >95% positive for the HIV-1 core antigen, p24, by immunofluorescence. They contain 2 integrated copies of HIV-1 provirus per cell and undetectable levels of unintegrated viral DNA by Southern blot hybridisation (Li and Burrell, 1992).

ACH-2 is a clonal cell line derived from A3.01 cells persistently infected with HIV-1 (Clouse *et al*, 1989; Folks *et al*, 1989), obtained from the NIH AIDS Research and Reference Reagent Program, from Dr Thomas Folks. They contain 1 integrated copy of HIV-1 provirus per cell.

8E5 is a clonal cell line persistently infected with HIV-1_{LAV} (Folks *et al*, 1986), obtained from the NIH AIDS Research and Reference Reagent Program. They contain 1 integrated copy of HIV-1 provirus per cell.

E12 cells are from a clone of persistently HIV-1_{SF2} infected HuT-78 cells, originally obtained from Dr Jay Levy. Characterisation of these cells for use in this thesis demonstrated that approximately 30% of these cells were p24 positive (FACS for intracellular p24). They secreted infectious virus and detectable p24 protein into the supernatant, and formed syncytia upon coculture with HuT-78 cells.

All persistently infected T-cell lines were maintained according to the provider's specifications, as described for uninfected T-cell lines (Section 2.1.1ii).

2.1.1iv Additional cell lines

293T cells, obtained from the ATCC, were maintained in DMEM supplemented with 10mM Hepes, 0.37% sodium bicarbonate, 2mM L-glutamine, 1.2 μg/ml penicillin, 1.6 μg/ml gentamycin, 10% heat inactivated fetal calf serum (CSL). They were cultured in a humidified cell culture incubator at 37°C with 5% CO_2, and passaged approximately 18 hours prior to experiments to reach a confluency of around 80% at time of use.

2.1.1v Primary cells

Peripheral blood mononuclear cells (PBMCs) and monocyte derived macrophages (MDMs) were prepared and infected by Dr Jillian Carr and Ms Helen Hocking. Specifically, peripheral blood leucocytes (PBLs) were prepared by density gradient centrifugation of buffy coat blood packs from healthy blood donors, generously provided by the Australian Red Cross Blood Bank. The volume of the buffy coat blood pack was diluted with an equal volume of cold Hanks Balanced Salt Solution (HBBS, Gibco). The diluted blood was overlaid onto ficoll lymphoprep, and centrifuged (800xg for 30 min at 4°C with low brake) to separate the red blood cells (pellet) from the PBLs ("buffy coat" layer immediately above the lymphoprep) and plasma (top). The PBL layer was collected and washed once with cold HBBS. To culture PBMCs, the cells were resuspended and cultured in RPMI 1640 with

20mM Hepes, 0.12% (v/v) sodium bicarbonate, 2mM L-glutamine, 1.2μg/ml penicillin, 1.6μg/ml gentamycin and 10% (v/v) heat inactivated FCS and maintained in a humidified atmosphere of 5% CO_2 at 37°C.

To isolate MDMs, the cells were washed twice more with cold HBBS then once with MDM serum-free medium (DMEM with 10mM Hepes, 0.12% (v/v) sodium bicarbonate, 2mM L-glutamine, 1.2μg/ml penicillin, 1.6μg/ml gentamycin), resuspended in pre-warmed MDM adherence medium (as above with 20% (v/v) FCS), seeded into tissue culture flasks at a density of $1x10^7$ cells/ml, and incubated in a humidified cell culture incubator at 37°C with 5% CO_2. After approximately one hour the non-adherent cells were removed, and the adherence medium replaced. After a second hour the supernatant containing non-adherent cells was again removed, and the adhered monocytes washed 3 to 6x with $HBSS^+$ (HBBS with $CaCl_2$ and $MgSO_4$ (Gibco)). The monocytes were then cultured overnight in complete macrophage medium (DMEM with 10mM Hepes, 10% (v/v) FCS and 7.5% (v/v) human serum (HS)). The next day the monocytes were gently detached by cell scraping in $HBSS^+$, pooled and cultured in complete macrophage medium, allowing differentiation into macrophages. The MDMs were re-seeded for infection 5 to 7 days after isolation.

2.1.2 Plasmids

pNL4-3 is an infectious molecular clone of the NL4-3 T-cell tropic strain of HIV-1, obtained from the NIH AIDS Research and Reference Reagent Program.

pBS-tat, pBS-rev and pBS-nef are respective laboratory HIV_{HXB2} derived cDNA clones in pBluescript II (SK) phagemid (pBS) (Stratagene) (Davis *et al*, 1997), generously provided by Dr Adam Davis. pBS-β–actin is a construct with a clone of the human *β–actin* cDNA, also kindly provided by Dr Davis. Briefly, the respective cDNAs were cloned into pBS by the T-A cloning strategy (Ausubel *et al*, 1995) of respective RT-PCR products with restriction enzyme sites engineered into the 5' and 3' primers, and the identity of the plasmid inserts was confirmed by sequence analysis.

pGEM-DenCap is a laboratory clone of pGEM-3Zf(-) (Promega) with a 428bp Dengue Virus Capsid cDNA insert, constructed by Ms Robyn Taylor and Dr Jillian Carr.

pEGFP-Vpr (Schaeffer *et al*, 2001) is a kind gift from Prof Warner Greene, San Fransico, CA, USA, with permission from Dr Carlos de Noronha who constructed this plasmid. It is a derivative of pEGFP (Clonetech) with a cDNA insert encoding HIV-1_{NL4-3} Vpr, which is expressed as a C-terminal fusion protein with EGFP.

2.1.3 Oligonucleotide Sequences

All oligonucleotides were synthesised by GeneWorks. Oligonucleotides for use in real time PCR were HPLC purified by GeneWorks. Lyophilised oligonucleotide pellets were resuspended in dH_20 to a stock concentration of 1mM (1 nmol/µl), aliquoted and stored at –20°C. Oligonucleotide stocks were further diluted to 25 pmol/µl or 10pmol/µl for used as primers in conventional and real time PCR respectively, or to 40 ng/µl for use as probes. The sequences and nucleotide positions of oligonucleotide primers and probes used in this study are presented in Table 2.1 below.

Table 2.1 Primers

	Oligo Name	Sequence	Sequence Coordinate Reference
Conventional PCR	β-glo1 (+) β-glo2 (-)	5'-CAACTTCATCCACGTTCACC-3' 5'-GAAGAGCCAAGGACAGGTAC-3'	nt 938-918[a] nt 671-690[a]
	Mit1 (+) Mit2 (-)	5'-GACGTTAGGTCAAGGTGTAG-3' 5'-GGTTGTCTGGTAGTAAGGTG-3'	nt 1320-1340[b] nt 1715-1695[b]
	Gag-P1 (+) Gag-III (-)	5'-GAGGAAGCTGCAGAATGGG-3' 5'-CTGTGAAGCTTGCTCGGCTC-3'	nt 1408-1426[c] nt 1722-1703[c]
	PBS-659 (-) Alu164 (+)	5'-TTTCAGGTCCCTGTTCGGGCGCCAC-3' 5'-TCCCAGCTACTCGGGAGGCTGAGG-3'	nt 659-635[c] nt 164-187[e]
	NI-1 NI-2	5'-CACACACAAGGCTACTTCCCT-3' 5'-GCCACTCCCCIGTCCCGCCC-3'	nt 57-77[c,f] nt 408-389[c,f]
	U3.1 (+) Gag3 (-)	5'-GGAAGGGCTAATTCACTCC-3' 5'-TGCACACAATAGAGGGTTGC -3'	nt 2-20[c] nt 1055-1036[c]
	RU5-1 (+) RU5-2 (-)	5'-GTCTCTCTGGTTAGACCAGATCTG-3' 5'-CTGCTAGAGATTTTCCACACTGAC-3'	nt 456-479[c] nt 635-612[c]
	β-actin1 (+) β-actin2 (-)	5'-CAACTCCATCATGAAGTGTGAC-3' 5'-CCACACGGAGTACTTGCGCTC-3'	nt 2597-2618[g] nt 2892-2872[g]
	$adp1_{JC}$ (+) $adx2_{JC}$ (-)	5'-TCTCGACGCAGGACTCGGCTT-3' 5'-ATTCCTTCGGGCCTGTCGGGT-3'	230-248[h] 7967-7949[h]
	$ex2_{JC}$ (-)	5'-TCATCAATATCCCAAGGAGCATGGTGCC-3'	nt 8422-8402[c,h] (8412-8392[d,h])
	DenCapF (+) DenCapR (-)	5'-GCAGATCTCGATGAATAACCAC-3' 5'-GTTCTGCGTCTCCTGTTCAAG-3'	nt 86-107[i] nt 377-398[i]
Real Time PCR	β-glo1 (+) β-glo2 (-)	5'-CAACTTCATCCACGTTCACC-3' 5'-GAAGAGCCAAGGACAGGTAC-3'	nt 938-918[a] nt 671-690[a]
	SS1 (+) (R) SS2a (-) (U5)	5'-CTAACTAGGGAACCCACTGC-3' 5'-CTGCTAGAGATTTTCCACAC-3'	nt 498-517[c,d] nt 616-635[c,d]
	U5-P1 (+) U5-P2 (-)	5'-GGTAACTAGAGATCCCTCAG-3' 5'-AGAGCTCCTCTGGTTTCCCT-3'	nt 583-602[c] nt 664-684[c]

Symbols (+) and (-) indicate sense and antisense sequences respectively.

[a]Human *β-globin* sequence genebank accession number L26462
[b]Human Mitochondrial sequence genebank accession number NC_001807
[c]Human Immunodeficiency Virus Type 1 (HXB2) genebank accession number K03455
[d]Human Immunodeficiency Virus Type 1 (NL4-3) genebank accession number M19921
[e]*Alu* consensus sequence (Jurka and Smith, 1988)
[f](Chun *et al*, 1997)
[g]Human *β-actin* sequence genebank accession number M10277
[h]Adapted from (Davis *et al*, 1997)
[i]DEN-2 capsid sequence genebank accession number AF038403

Table 2.2 Probes

	Probe Name	Sequence	Sequence Coordinate / Reference
Fragment Probes	βGlo	Flanked by primers β-glo 1 and β-glo 2	nt 671-938[a]
	Mit	Flanked by primers M1 and M2	nt 1320-1715[b]
	Gag	Flanked by primers Gag-P1(+) and Gag-III(-)	nt 1408-1722[c]
	LTR	Constructed from U5 and U3 regions of HIV-1	nt 9648-9718 (U5)[c] ligated to nt 1-376 (U3)[c]
	DenCap	DenCap cDNA insert from pGEM-DenCap	
	β–actin	β–actin cDNA insert from pBS-β–actin	
	Rev	Rev cDNA insert from pBS-Rev	
	Tat	Tat cDNA insert from pBS-Tat	
	Nef	Nef cDNA insert from pBS-Nef	
Splice Junction Oligo Probees[g]	1.4	5'-TGTCGACACCCAATT/CAGTCGCCGCCCCTC-3'	nt 5338-5324/289-274[c,e]
	1.4a	5'-AGGAGATGCCTAAGG/CAGTCGCCGCCCCTC-3'	nt 5515-5501/289-274[c,e]
	1.5	5'-CGCTGTCTCCGCTTCTTC/CAGTCGCCGCCCCTC-3'	nt 5537-5523/289-274[c,e]
	4.7	5'-GGAGGTGGGT/TGCTTTGATA-3'	nt 8378-8369/6047-6058[c,f] (nt 8388-8379/6046-6057[h,f])

[a]Human *β-globin* sequence genebank accession number L26462
[b]Human Mitochondrial sequence genebank accession number NC_001807
[c]Human Immunodeficiency Virus Type 1 (HXB2) genebank accession number K03455
[d]from Ms Robyn Tailor and Dr Jillian Carr
[e](Davis *et al*, 1997)
[f]oligo designed to span the junction between Splice Donor 4 and Splice Acceptor 7
[g]Splice junction oligonucleotides; first number denotes splice donor and second number denotes splice acceptor site.
[h]Human Immunodeficiency Virus Type 1 (NL4-3) genebank accession number M19921

2.1.4 Commonly used buffers and solutions

DNase Buffer (1x) for RNA:

0.1M sodium acetate, 5mM $MgSO_4$, pH 5.0, in dH_20, autoclaved.

Ethidium bromide stock solution:

10 mg/ml ethidium bromide (Sigma) dissolved in dH_20. Stored at 4°C in a dark bottle.

Gel Loading Buffer (10×):

60% Glycerol; 100mM EDTA (pH 8.0); 100mM Tris (pH 7.5); Bromphenol blue; Xylene cyanol.

Hirt Solution 1 (1×):

5mM Tris pH 7.7; 10mM EDTA.

Hirt Solution 2 (1×):

10mM EDTA; 5mM Tris pH 7.7; 1.2% SDS.

Hybridisation Solution (for use with oligonucleotide probes):

2.5x Denhardts, 6x SSC, 0.5% SDS and 100 μg/ml ssDNA.

LB (1×):

10 g/L bacto-tryptone, 5 g/L bacto-yeast extract, 10 g/L NaCl; sterilised by autoclaving.

Non-denaturing polyacrylamide gel solution:

8% acrylamide (Bio-Rad), 0.22% N,N'-methylenebisacrylamide (National Diagnostic), 1×TBE. Gels were polymerised by the addition of ammonium persulfate (Bio-Rad) to 0.1% and TEMED (N,N,N',N'-Tetramethylethylenediamine; Bio-Rad) to 0.075%.

PBS:

140mM NaCl, 3mM KCl, 1mM KH_2PO_4, 8mM Na_2HPO_4. Sterilised if required.

Phenol:

Tris-equilibrated Phenol was prepared according to suppliers instructions (Sigma).

Prehybridisation Solution (for use with oligonucleotide probes):

25x Denhardts, 6x SSC, 0.5% SDS and 100 μg/ml ssDNA.

SSC (1×):

150mM NaCl, 15mM trisodium citrate, pH 8.0.

STE:

100mM NaCl, 10mM Tris pH 7.6, 1mM EDTA.

SOB:

20 g/L bacto-tryptone, 5 g/L bacto-yeast extract, 0.584 g/L NaCl (10mM final), 0.186 g/L KCl (2.5mM final); sterilised by autoclaving. Filter steriled $MgSO_4$ was added after autoclaving to a final concentration of 20mM.

SOC:

SOC medium is identical to SOB except that it also contains 20mM glucose (filter sterilised).

Solution D:

4M guanidinium thiocyanate, 25 mM sodium citrate pH 7.0, 0.5% sarcosyl, stored in the dark. 2-mercaptoethanol (Sigma) was added immediately prior to use to a final concentration of 0.1M.

TAE (1x):

40mM Tris-acetate, 1mM EDTA.

TBE (1x):

90mM Tris, 90mM Boric acid, 2.4mM disodium ETDA.

TE (1x):

10mM Tris, 1mM EDTA, pH 8.0.

Transformation Buffer:

10mM Pipes, 15mM $CaCl_2$, 250mM KCl; heated to dissolve, cooled, pH adjusted to 6.7 with KOH, then $MnCl_2$ added to 55mM. Filter sterilised.

2.2 Preparation and Analysis of HIV-1 Virus Stocks

2.2.1 Quantification of HIV-1 core protein antigen (p24)

p24 levels in viral stocks and infected cell culture supernatant were measured to indicate HIV-1 virus concentration and virus release, respectively. Triton-X100 was added to samples to a final concentration of 0.5% (v/v) and vortexed (to inactivate virus and stabilise p24 protein content). Where required, samples were stored at 4°C, and serial dilutions were performed in fresh culture media / 0.5% Triton-X100. p24 concentration was determined using a commercially available HIV-1 p24 Enzyme Linked Immunosorbent Assay (ELISA) (Perkin Elmer Life Sciences).

2.2.2 Titration of HIV-1 virus stocks

2.2.2i Syncytia determined $TCID_{50}$ of HIV-1 NL4-3

Six independent replicate serial four-fold dilutions (50µl virus + 150 µl media) of virus stocks were made in 48-well cell culture trays (Falcon) in cell culture media, including both negative and positive controls. $5x10^4$ CEM-SS cells (in 50 µl) were added to each well (final total volume of 200µl / well). The next day 200µl of fresh media was added to each well. The cells were subcultured as required (usually every second day) by mixing the cells (pipetting up and down), discarding 200µl of cells and spent media and replacing with 200µl fresh media. The wells were observed over 10 days from establishment of the $TCID_{50}$, and wells in which syncytia formed scored as positive. $TCID_{50}$ was calculated by the following equation (adapted from Grist (Grist *et al*, 1974));

$Log_xTCID_{50} = L-d(s-0.5)$

Where L is the negative log of the lowest dilution (at which 100% of wells are infected)
d is the difference between log dilutions
s is the sum of positive tests
x is the serial dilution factor

For example:

Dilution	proportion of +ve wells
4^{-1}	6/6 ie 1.00
4^{-2}	5/6 ie 0.83
4^{-3}	1/6 ie 0.17
4^{-4}	0/6 ie 0.00

Therefore the sum of positive tests (s) is 2.00

$TCID_{50}$ calculation

$Log_4TCID_{50} = L-d(s-0.5)$
$= -1-1(2-0.5)$
$= -2.5$

ie $4^{2.5}$ $TCID_{50}$ /37.5µl

ie 32 $TCID_{50}$ /37.5µl

(x26.67 to convert from 37.5ul to 1ml)

ie $8.5x10^2$ $TCID_{50}$ /ml

2.2.2ii Syncytia determined $TCID_{50}$ of HIV-1 IIIB:

$1.5x10^5$ HuT-78 cells were aliquoted into a series of 1.6ml tubes, and pelleted by centrifugation. The supernatant was removed and the cells in each tube resuspended in 600µl of a respective dilution of a prepared serial 10-fold dilutions of virus stock. Cells in virus dilutions were incubated (humidified 37°C, 5% CO_2) with loose lids for 2 hours. Cells were then pelleted by centrifugation, viral supernatant removed, the cells washed twice with media then resuspended in 1200µl media. The resuspended cells from each tube were

aliquoted into 6 wells of a 48-well cell culture tray, i.e. 200 µl/well. The following day a further 200µl fresh media was added to each well. Over the following 10 days of culture the cells were subcultured as required by replacing half of the culture volume with fresh media. The $TCID_{50}$ was maintained and scored as described above (Note; log_{10} used in calculation instead of log_4, according to the serial the dilution factor).

2.2.2iii p24-determined $TCID_{50}$ (Macrophage tropic strains)

MDMs were seeded into 48 well cell culture trays in 200µl of media/well. After adherence (~18 hours), 100µl of media was removed and replaced with 100µl of ten-fold serially diluted virus stock in fresh MDM culture media. MDM inoculations with each virus dilution were performed with 6 replicate wells. Positive and negative controls were also established. Half media changes (100µl) were performed every second day. Nine days after the $TCID_{50}$ was set up, supernatants were sampled and assayed from each well, and scored as positive (≥12.5pg/ml) or negative (≤12.5pg/ml). $TCID_{50}$ was calculated by the equation given in Section 2.2.2i above (Note; log_{10} used in calculation instead of log_4, according to the serial dilution factor).

2.2.3 Preparation of cell free T-cell tropic HIV-1 Stocks

2.2.3i HIV-1_{NL4-3} Virus Stock

HIV-1_{NL4-3} virus stocks were prepared as described (Clarke *et al*, 2006); 293T cells were transfected with HIV-1 pNL4-3 proviral plasmid DNA (Section 2.1.2), using Effectene (Gibco BRL). Transfection parameters and viral harvest time were optimised according to the manufacturer's instructions and determined according to subsequent p24 levels. HIV-1 containing supernatants were harvested at 28-36 hours post transfection and filtered (0.2µm) to remove cell-debris. This viral inoculum was amplified by culture in CEM-SS cells. Infected CEM-SS cells were maintained with 0.5 volume media changes and media additions as appropriate to maintain cells in a concentrated but logarithmic phase of growth. The optimal time to commence virus collection was determined to be from 9 days onwards, with maximal virus titres usually obtained between day 9 and 13. Eight days post infection

a complete media change was performed and the culture volume reduced 5 to 10 fold. From day 9, the virus-containing culture supernatant were collected daily by centrifugation and the cells re-seeded in fresh medium. Immediately after each collection, the virus-containing medium was clarified by centrifugation at 2800g for 10 min, filtered (0.2μm) (Ministart Filters, Sartorius) to remove cell-debris, aliquoted and stored at -80°C. The virus stocks was subsequently characterised by $TCID_{50}$ and p24 content determination (Sections 2.2.1, 2.2.2).

Titres of these viral stocks on peak days of virus production ranged from $0.3\text{-}1.1x10^5$ CEM-SS $TCID_{50}$/ml, and 0.7-1.7 μg/ml p24. One particular stock had a p24 content of 5.9 μg/ml, and was reserved for electron microscopy (Chapter 4). For cell-free infections, virus stocks were treated with 50 μg/ml DNase 1 (Roche) in the presence of 10mM $MgCl_2$ for 30 minutes at room temperature. A sample of DNase treated virus stock and virus stock with the DNase omitted (but otherwise treated identically) was taken and added to an equal volume of phenol-chloroform-isoamyl alcohol (25:24:1), vortexed, and stored for subsequent analysis of the DNase treatment.

2.2.3.ii HIV-1_{IIIB} Virus Stock

$HIV\text{-}1_{IIIB}$ virus stock was prepared as described previously (Vandegraaff *et al*, 2001b). Specifically HIIIB cells were grown in log phase until $\geq 10^9$ cells were available. Cells were then pooled and re-seeded at a concentration of $\geq 5x10^7$ cells/ml in a 50ml centrifuge tube and incubated with a loose lid (humidified 37°C, 5% CO_2). A complete media change was performed by centrifugation every 45 min. The virus-containing culture media, harvested every 45 min, was pooled and stored ice. After ≥8 consecutive media collections, the virus-containing media was clarified by centrifugation at 2800g for 10 min, filtered (0.2μm) to remove cell-debris, aliquoted and stored at –80°C. The titre of these viral stocks were up to $3.16x10^6$ HuT-78 $TCID_{50}$/ml.

2.2.3.iii Production of Vpr-EGFP-labelled chimeric HIV-$1_{NL4\text{-}3}$ Virions

Production of chimeric $HIV\text{-}1_{NL4\text{-}3}$ virions which would contain both wild type Vpr and EGFP-Vpr fusion proteins was achieved by dual transfection of pEGFP-Vpr and pNL4-3 (Section 2.1.2) (Schaeffer *et al*, 2001). Such virions were expected to be fluorescent for a

single round of replication, and were produced for use in studies of the mode of HIV-1 entry into astrocyte cells (Chapter 4). Dual transfections were optimised by comparing 3 different transfection products (Effectine (Gibco Life Technologies), Lipofectamine (Gibco Life Technologies) and Superfect (Qiagen), two cell lines (HeLa-Tat and 293T cells), a range of transfection parameters according to the respective manufacturer's instructions. The efficiency of the dual transfection was measured by the percent of EGFP positive cells (as observed under a Olympus inverted UV microscope) and the HIV-1 p24 content of the supernatant. Chimeric HIV-1 NL4-3/Vpr-EGFP containing supernatants were harvested at 36 hours post transfection, and filtered (0.2μm) to remove cell-debris, aliquoted and stored in liquid nitrogen.

2.2.4 Preparation of cell free macrophage tropic HIV-1 stocks

2.2.4i Preparation of HIV-1_{JR-CSF} and HIV-1_{JR-FL} virus stocks

500μl of each of HIV-1_{JR-CSF} and HIV-1_{JR-FL} virus were obtained from the NCHVR Research Reagent Program (donated by Dr Dale McPhee), and amplified according to instructions from the provider. Each aliquot of virus was incubated with $1x10^7$ 2 day phytohemagglutinin (PHA) stimulated PBMCs in a total volume of 1.5ml for 2 hours. After 2 hours, 8.5ml fresh media with 2.5% human IL2 (RPMI 1640 with 20mM Hepes, 0.12% (v/v) sodium bicarbonate, 2mM L-glutamine, 1.2μg/ml penicillin, 1.6μg/ml gentamycin and 10% (v/v) heat inactivated FCS) was added to culture the cells at a density of $1x10^6$ cells/ml. The following day an additional 10ml media (with IL2) was added to maintain the cells at ~$1x10^6$ cells/ml. Half volume media changes were performed twice per week and the viral-containing supernatant clarified (by centrifugation at 2800g for 10 min), aliquoted and stored at -80°C. Viral infected PBMC cultures were maintained for 28 days after infection. Viral harvests were characterised by HIV-1 p24 content (ELISA), which peaked at day 11 (HIV-1_{JR-CSF} ; 375ng p24/ml, HIV-1_{JR-FL}; 700 ng p24/ml).

HIV-1_{JR-FL} viral stock produced by amplification in PBMCs (above) was then passaged in MDMs to maintain the macrophage tropism of this strain. A medium flask ($75cm^2$) of 6 day old MDMs was inoculated with 8ml of the 11dpi virus stock derived from the infected PBMCs. After 5 hours the viral inoculum was replaced with 20ml MDM media (DMEM

with 10% FCS and 7.5% HS). Viral stocks were harvested weekly with almost complete (18ml) media changes, for 4 weeks. The MDM passaged stock with the highest HIV-1 p24 content was then re-amplified in PBMCs, as outlined above.

2.2.4ii Preparation of HIV-1_{BaL} and HIV-1_{YU2} virus stocks

HIV-1_{BaL} and HIV-1_{YU2} virus stocks were prepared by Dr Jillian Carr by MDM passage and PBMC amplification, similar to the method employed for JR-CSF and JR-FL described above. The titre of the HIV-1_{BaL} virus stock was in the order of 10^5-10^6 $TCID_{50}$ U/ml on MDMs. HIV-1_{YU2} virus stock has a p24 content of 267 pg/ml.

2.3 Infection Protocols

2.3.1 Cell to cell infections; persistently infected T-cell viral donors

The chonically HIV-1 infected T-cell lines HIIIB and E12 were used as "virus-donor" cells. These cells were mixed with uninfected "virus-recipient" U251-MG astrocyte cells at a ration of 1:2 ($8.3x10^5$ HIIIB or E12 cells and $1.67x10^6$ U251-MG cells in 6-well trays). Negative controls (uninfected U251-MG cells alone), controls to determine the level of HIV-1 replication within the viral donor cells alone, and positive controls (donor cells cocultured with the HIV-1 susceptible HuT-78 T-cell line) were set up in parallel. U251-MG cells were either pre-seeded at density of $1.1x10^6$ 18 hours prior to the experiment (to give ~1. $7x10^6$ U251-MG cells / well at the time of coculture), or detached with trypsin (0.1% for 3-5 min at RT) immediately prior (<1 h) to cell-mixing.

Any viral replication in the persistently infected T-cell lines which may occur upon coculture could potentially mask the detection of viral replication in the astrocyte population. Therefore in some experiments, to minimise this, the virus donor T-cells were removed after a period of coculture (Section 2.3.1i), and in other experiments transcription in the donor cell population was inhibited with Actinomycin C_1 ($ActC_1$; Roche) (Section 2.3.1ii). To further ascertain whether detected HIV-1 DNA species may represent *de novo* reverse transcription in the U251-MG astrocyte cells, some experiments were performed in

the presence or absence of the reverse transcriptase inhibitor, zidovudine (3'-azido-3'-deoxythymidine, or AZT) (Sigma) (Section 2.3.1iii).

At designated times post coculture the cells were harvested for Hirt extraction of extrachromosomal DNA (Sections 2.6.2-2.6.3). The inter-sample extraction efficiency was assessed by semi-quantitative mitochondrial PCR followed by Southern hybridisation. The level of HIV-1 reverse transcribed DNA products was analysed by semi-quantitative HIV-1 *gag* PCR and Southern hybridisation (Sections 2.7.2-2.7.3).

2.3.1i Removal of viral donor T-cells from astrocytes post coculture.

In some experiments, to minimise the contribution of potential HIV-1 replication within the donor cell population in the U251-MG astrocyte cocultures, the donor cells were removed after 1-24 hours of coculture. This was performed by washing the suspension donor cells off the adherent U251-MG cells and, in some experiments, treating the remaining adherent cells with trypsin and removing the remaining donor cells with anti-CD3 antibody coated magnetic beads (Dynal). In the latter experiments, cells were trypsined briefly (0.1% v/v) to detach all cells, washed with 2% FCS / PBS to inactivate the trypsin and resuspended in 400µl 2% FCS / PBS. Anti-CD3 coated beads were added according to the manufacturers directions; to a final concentration of $2x10^7$ beads / ml, as determined to ensure the beads were in ~50x excess compared to the estimated number of CD3 positive target cells present. Beads and cells were incubated whilst gently rotating for 30 min at 4°C. A magnet was held against the side of the tube for 2 min to attract beads and adhered cells, and the non-bound supernatant (containing the free, $CD3^-$ cells) transferred to a new tube. The cells in this tube were again subjected to magnetic force, and the resulting CD3-depleted population re-seeded.

2.3.1ii Treatment of HIV-1 Donor T-cells with Actinomycin C_1

In some cell to cell infection experiments, viral donor cells were pretreated with $ActC_1$ (Roche) for 2 hours prior to coculture with U251-MG cells, to prevent new transcription and reverse transcription of HIV-1 occurring in the donor-cell population during the period of coculture. $ActC_1$ specifically inhibits DNA-dependent DNA and RNA synthesis (Reich and

Goldberg, 1964; Rill and Hecker, 1996; Sambrook *et al*, 1989). The concentration of $ActC_1$ to be used was optimised to determine the minimal concentration required to inhibit transcription in each donor cell line, as measured by [5,6-^{3}H]-Uridine (Amersham) uptake (see below). This was to ensure that any potential effect of the $ActC_1$ on the U251-MG cells was minimised. Excess $ActC_1$ was removed from the viral donor cells by two media washes, immediately prior to cell-mixing. The optimal $ActC_1$ treatment of HIIIB cell and E12 cells was determined to be 8 μg/ml /10^6 cells /2 h. To allow for inter-experimental variation, $ActC_1$ was routinely used at 12 μg/ml /10^6 cells /2h. For each experiment in which $ActC_1$ was used, a sample of the treated cells, along with untreated control cells, and cells treated with twice the amount of $ActC_1$, were assayed by tritiated uridine uptake to confirm the effective inhibition of transcription by treatment with 12 μg/ml /10^6 cells /2 h of $ActC_1$.

Assessment of $ActC_1$ inhibition of transcription by tritiated uridine uptake determination

1x10^6 cells (in 1ml) were treated with various concentrations (0, 2, 4, 6, 8, 10, 12, 16, 20, 24 and 48 μg/ml) of $ActC_1$ for 2 hours. Cells were then washed with PBS to remove excess $ActC_1$ and resuspended in 1ml media with 4μl [5,6-^{3}H]-Uridine (^{3}H-U) (Amersham) and incubated overnight (~18h). To remove un-incooporated ^{3}H-U, cells were then washed once with PBS, once with 10% (w/v) TrichloroAcetic Acid in PBS (TCA; 100% TCA made by 50g TCA in 27.7ml dH_20), and resuspended in 500μl 0.3M NaOH, 1% SDS. Scintillation fluid was added, and ^{3}H-U was measured with a scintillation counter. The level of incorporated ^{3}H-U indicated the transcriptional activity of the cells, and the minimum concentration of $ActC_1$ which resulted in maximal inhibition of transcription was determined.

2.3.1iii AZT treatment

In some cell-to-cell infection experiments, both donor and recipient cells were pre-treated overnight (~18 hours) with or without the nucleoside analogue zidovudine (3'-azido-3'-deoxythymidine, or AZT) (Sigma). AZT was diluted to 10mM in DMSO, and further diluted in serum free medium. It was used at 20μM, a concentration previously shown to be effective for the inhibition of HIV-1 reverse transcription (Coates *et al*, 1992; Li *et al*, 1992).

This concentration was maintained for the duration of the experiment. AZT is a thymidine analogue that specifically inhibits reverse transcription, and was used to identify the level of pre-existing reverse transcribed DNA.

2.3.2 Cell to cell infections; chronically infected macrophage donor cells

MDMs were prepared as described in Section 2.1.1v, seeded into 12- or 24-well cell culture trays and, after 5 to 7 days, infected with HIV-1_{BaL} by Ms Helen Hocking. 13 days later, when a chronic infection of the MDMs was established, they were treated with 5 μg/ml DNase I (Roche) overnight (to minimise potentional carry-over of HIV-1 DNA due to the turn-over of infected MDMs in the culture) then cocultured with U251-MG astrocytes. To coculture these cell populations, U251-MG cells were detached by either trypsin treatment (0.1% for 3-5 min at RT) or by gentle cell scraping, and added to the infected MDMs. The MDMs had been pre-seeded in either cell culture trays (promoting adherence) or in telfon pots (preventing adherence). Cocultures were performed at a ratio of 1 MDM : 5-10 U251-MG cells. Specifically, cell mixes comprised either 1-2x10^5 MDMs and 1x10^6 U251-MG cells, or 5x10^4 MDMs and 5x10^5 U251-MG cells.

Hirt extrachromosomal DNA was harvested at various times up to 24 hours post cell mixing. "Mock" coculture controls were set up simultaneously; these were replica wells of DNase treated, infected MDMs and U251-MG cells which were kept separated until the designated time for harvest and Hirt extrachromosomal DNA extraction (Sections 2.6.2-2.6.3), when both cell populations were pooled. "Mock" cocultures controlled for the contribution of any ongoing viral replication in the MDMs in the HIV-1 replication assays. Hirt extrachromosomal DNA extractions were assayed for mitochondrial DNA content (conventional mitochondrial PCR and Southern hybridisation) to determine the relative efficiency of the extrachromosomal DNA extractions. The level of HIV-1 reverse transcribed DNA products was analysed by HIV-1 *gag* PCR and Southern hybridisation (Sections 2.7.2-2.7.3).

2.3.2i Minimising the detection of HIV-1 replication in the infected MDMs.

The detection of HIV-1 replication in the infected MDM population could potentially mask any viral replication that might be occurring in the U251-MG cells upon cell mixing. To minimise the potential detection of HIV-1 replication in the infected MDMs in the cell mixes, the separation of the two cell populations, after a period of mixing, was attempted. This was achieved by i) trypsin treatment of the cell mixes to separate the trypsin sensitive U251-MG cells from the trypsin resistant MDMs, ii) culturing the MDMs and performing the cell mix in the teflon pots to prevent adherence, followed by the removal of the MDMs with anti-CD14 magnetic beads (Dynal; as described for anti-CD3 magnetic beads in Section 2.3.1i), or iii) pretreating the MDMs for 2 days ± AZT (20μM) to distinguish between pre-existing HIV-1 DNA and *de novo* reverse transcribed HIV-1 DNA.

2.3.3 Cell-free infections for immunofluorescent analysis of viral entry

U251-MG, CCF-STTG1 or U87-MG astrocyte cells were cultured on either glass chamber slides (Lab-Tek) or on sterile glass coverslips in cell-culture dishes overnight to reach 80% - 90% confluence, then infected with re-filtered (0.2μm) HIV-1_{NL4-3} for 15, 30, 45, 60 or 75 minutes at 37°C. Uninfected cells were prepared simultaneously as controls. Immediately following the designated infection time, cells were gently rinsed with PBS to remove excess virus inoculum and fixed by submersion in 1% formalin / PBS overnight at 4°C.

2.3.3i with AlexaFluor546-conjugated Human Transferrin

In some experiments AlexaFluor-546-conjugated Human Transferrin (Molecular Probes) was included at 25 μg/ml during the infection, to label clathrin-dependent endocytosis. Infection of HeLa cells were included as a positive control for the colocalisation of internalised HIV-1 with labelled transferrin (Schaeffer *et al*, 2001). These experiments (and all subsequent processing) were performed with minimal exposure to light, in order to preserve the fluorescent properties of the fluorophore conjugate.

2.3.4 Cell-free infections for Electron Microscopy Analysis of viral entry

2.3.4i Preparation of HIV-1 virus stocks for Electron Microscopy and optimisation of infections for EM

Virus stocks of the highest titres were used for infection for EM analysis, in order to maximise the probability of locating virions. Of these, the HIV-1_{IIIB} stock had the highest titre; 3.16 x 10^6 $TCID_{50}$/ml in HuT-78 cells. The most concentrated HIV-1_{NL4-3} stock available had a p24 content of 5.97 µg/ml. Titres of available HIV-1_{BaL}, HIV-1_{YU2} and HIV-1_{JR-FL} were unfortunately lower (10^5-10^6 $TCID_{50}$/ml and 267 and 700 ng/ml of p24 respectively – see Section 2.2.4), but were included in the hope of gaining insight into the mode of entry of macrophage tropic strains as well as T-cell tropic strains of HIV-1 into astrocytes. In initial experiments, neat virus stock was applied to the astrocyte cells. In subsequent experiments infection conditions were optimised to achieve good cell morphology upon EM analysis. The HIV-1_{IIIB} stock was used for the optimisation as it was in the greatest abundance. To improve the morphology of the cells, the virus stock was diluted in fresh medium (½, ¼, ⅛). Additionally various cell recovery times (0.5, 1, 2, 4, 6, 8 hours) in fresh medium, after infection, were trialed.

To increase the probability of locating virus upon E.M analysis, virus stocks were concentrated and resuspended / diluted in fresh medium. Methods of virus concentration included ultracentrifugation and centifugation of the virus stock on high molecular weight retention columns (10 000 Da cut-off 2ml capacity column, (Centricon) and 15ml Amicon Ultra 100 000 MWCO column (Millipore)). For ultracentrifugation, 1.5ml virus was loaded onto a 4.5ml ultracentrifuge tube containing 3ml of 20% (w/v) sucrose. The virus was pelleted by centrifugation at 40 000 rpm for 90 min at 4°C. The supernatant was gently drained off and the virus pellet resuspended in 200µl fresh medium. For the columns, the respective manufacturers' instructions were followed. Specifically, up to 15ml of 0.2µm filtered virus was applied and the columns centrifuged at 3700 x g for 30 minutes, after which the flow through of the columns was assessed. The Centricon column required six such spins to reduce the retainate from 2ml to ~250µl, after which the concentrated virus was diluted 1 in 2 in fresh medium. The virus retainate reduced from 10ml to ~250µl Amicon column within the first 30 minute spin and 3 subsequent spins were performed to

wash the virus stock (2 washes in PBS and 1 in media) before the retainate of ~250µl was diluted 1 in 2 in fresh medium for infection. In subsequent experiment, virus stocks were concentrated approximately 10-fold by the latter Amicon method. HIV-1_{IIIB} stocks concentrated by this method were shown to maintain infectivity by infection of HuT-78 cells, resulting in consequent syncytia formation and p24 secretion within 40 hpi.

2.3.4ii Infection of astrocyte cells for Electron Microscopy

Sixteen-well cell-culture glass chamber slides (LabTek) were seeded with U251-MG, CCF-STTG1 or U87-MG cells and cultured overnight to reach 80% - 90% confluence. The cells were infected by gently replacing all or half of the culture medium with HIV-1 virus stock. The infection was allowed to proceed for 40 min (humidified 37°C, 5% CO_2). Viral inoculum was then removed, the cells gently rinsed three times with PBS, then fixed *in situ* by submersion of the entire chamber slide in 2.5% glutaraldehyde in sodium cacodylate buffer overnight at 4°C. Uninfected cells were prepared simultaneously in an identical manner for control purposes.

2.3.5 Cell free infections for the analysis of HIV-1 DNA, RNA and transmission of infection.

2.3.5i Conventional Infection

Culture media of pre-seeded (≥18 hours) U251-MG cells (in 6-well cell culture trays) was removed and replaced with HIV-1_{IIIB} or HIV-1_{NL4-3} virus stock, and incubated for 2-6 hours, after which virus stock was either removed and replaced with fresh media, or fresh media added. Culture supernatant samples were taken daily or every second day for the determination of p24 content. Media changes were performed as required. Duplicate infected cultures were harvested on designated days post infection for Hirt DNA extraction. Cultures which were maintained for ≥5 days post infection (dpi) were rinsed with PBS and split with 1.0% trypsin on day 5, the cells pooled and re-seeded into 3x as many fresh wells. On day 7, $1x10^6$ HuT-78 cells were added to each of at least two infected U251-MG cultures, and monitored over the subsequent 9 days for evidence of transmission of HIV-1 infection to the permissive HuT-78 cell population (by syncytia formation and supernatant

p24 levels). Negative (uninfected U251-MG cells alone, treated with media in place of virus stock) and positive controls (infection of the HIV-1 susceptible HuT-78 T-cell line) were set up in parallel.

2.3.5ii Centrifugally enhanced Infection

To enhance the efficiency of virus inoculation, a modified centrifugal enhancement protocol (also known as "spinoculation") was used (Vandegraaff *et al*, 2001b). This reportedly increases the effective multiplicity of infection by approximately ten-fold (Ho *et al*, 1993; Li and Burrell, 1992; Pietroboni *et al*, 1989). Astrocyte cells (U251-MG, CCF-STTG1 or U87-MG cells) were treated with trypsin, resuspended in a minimal volume and aliquoted into 10ml teflon tubes (Savillex) (typically $1.6x10^6$ cells in a volume of 100 – 300 µl per tube). Re-filtered (0.2µm) viral inoculum (DNase treated in latter experiments, see Section 2.3.5iii, below) was added to the tubes, (usually 1.5 ml, giving a typical multiplicity of infection of 0.1-0.3 $TCID_{50}U$/cell, or 0.4-1.2 pg p24 / cell), and incubated for 30 minutes at 4°C. This 4°C incubation was designed to permit attachment of virions to the cells, to facilitate a synchronous infection upon warming to 37°C. Cells and virus were then centrifuged at 2500xg for 1 hour at 37°C in a prewarmed centrifuge, after which the inoculum was removed and the cells were allowed recover in prewarmed fresh media for 15 min at 37°C. Cells were then washed 3 times with fresh media to remove excess virus. In latter experiments the stringency of removal of excess / surface bound virus was increased by further washing steps and the inclusion of a trypsin treatment. Specifically, after the 15 minute recovery step, cells were washed twice with (complete) media, twice with serum-free media, and resuspended in 200µl serum free media. 200µl 0.1% trypsin was added, and the cells incubated for 5 min. Complete media was then added, followed by 3 further washes with complete media. This procedure did not appear to be detrimental to the cells (see below). Like cells from multiple tubes were pooled, 2 aliquots of $4x10^5$ cells harvested for analysis of HIV-1 DNA and RNA intermediates at this time (the earliest possible time-point, typically 3½ - 4 hours since the first contact of cells with virus at 4°C, and 3 - 3½ since contact at 37°C), and remaining cells seeded into 6-well cell-culture trays at a density of $4x10^5$ cells / well (in 4ml media/well) for subsequent harvest and analysis. Supernatants were sampled daily or every second day for p24 content by HIV-1 p24 ELISA (Section 2.2.1). The cultures were confluent by four days post infection (dpi), so at 5dpi the

remaining cultures were rinsed with PBS, treated with trypsin (0.1% for 3-5 minutes or until all the cells were detached), resuspended in complete media, pooled, and re-seeded into 3x as many fresh wells. To confirm successful infection, at 7dpi $1x10^6$ HuT-78 cells were added to 2 of the astrocyte cultures from each infection. These cocultures were analysed over the subsequent 6 days for evidence of transmission of infection to the HuT-78 cells (by supernatant p24 levels and syncytia formation). In some experiments, 10 U/ml IL1β (Roche) was added to the infected astrocytes at 7dpi and maintained (daily 0.5 volume media changes) for the remainder of the experiment (until 16dpi). Supernatants from wells ± IL1β treatment were assayed for infectious virus (Infectivity Assay, Section 2.8) and p24 protein content (HIV-1 p24 ELISA).

Negative (uninfected U251-MG cells alone, with media in place of virus stock) and positive controls (infection of the HIV-1 susceptible HuT-78 T-cell line) were set up simultaneously and processed identically.

U251-MG cell tolerance of the centrifugally enhanced infection procedure

To assess the impact of the procedure on cell viability, two teflon tubes were seeded with i) 2.5×10^6 and ii) 1.0×10^7 U251-MG cells respectively, and the centrifugally enhanced infection protocol performed, using culture medium in place of virus stock. At the end of the procedure (approximately 3 hours later), a sample of cells was taken from each tube to assess cell viability. The counts extrapolated to i) 2.8×10^6 and ii) 1.04×10^7 cells / tube, with a normal cell viability (97.5% and 96.4% respectively, by trypan blue exclusion). The appearance and degree of confluence (by light microscopy) of the U251-MG cells during the next 5 days of culture did not appear to differ to cells which had not been subjected to the spinoculation procedure, indicating that this procedure did not seem to be detrimental to the cells. A seeding density of 4.0×10^5 cells / well was chosen as cultures seeded at this density were approximately 50% confluent after 24 hours, and ≥90% confluent after 4 days.

2.3.5iii DNase I treatment of viral inoculum

For experiments from Section 5.3 onwards, the filtered viral stocks were treated with filter sterilised DNase 1 (Boehringer Mannheim) at 50 μg/ml in the presence of 10mM filter

sterilised $MgCl_2$ for 30 minutes at RT (16°C). The purpose of this step was to remove any contaminating HIV-1 DNA from the virus stock. HIV-1 DNA could be present in the virus stock due to either i) persistence of the pNL4-3 used to transfect the cells to obtain virus stock, and / or ii) may have arisen from lysis of virus-producer cells and release of partly degraded chromosomal DNA during amplification of the virus stock. To assess the effectiveness of the DNase I treatment, a sample of the treated virus stock was taken along with a sample of mock treated virus stock (prepared simultaneously and identically except for the omission of the DNase 1). Phenol / Chloroform / Isoamyl Alcohol (IAA) (25:24:1) was added at a 1:1 volume to both ±DNase I treated virus samples at the same time the DNased virus stock was added to the cells in cell free infection experiments. The phenol/chloroform/IAA virus samples were vortexed and stored at –80°C for subsequent extraction (Section 2.6.4) and analysis by PCR and Southern hybridisation (Sections 2.7.3 and 2.7.4).

The effectiveness of this batch of DNase I on pNL4-3 plasmid was also tested by addition of 50 µg/ml DNase 1 (Boehringer Mannheim) in the presence of 10mM $MgCl_2$ to a range of pNL4-3 DNA for 30 minutes at RT, followed by phenol/chloroform/IAA DNA extraction (Section 2.6.4) and PCR analysis (Section 2.7.3).

2.4 Immunofluorescence Assay and Microscopic Analysis

2.4.1 Immunoflourescence Assay Protocol

Cells grown, infected and fixed *in situ* in 1% formalin / PBS overnight at 4°C on chamber slides or coverslips for Immunofluorescence Assay (IFA) (see Section 2.3.3) were dipped in 80% (v/v) ethanol, at which stage they were relocated from PC3 to PC2 laboratories. Uninfected controls were prepared simultaneously. For infections that included fluorophore-conjugated transferrin (Section 2.3.3i) all steps were performed with minimal exposure to light, to preserve the fluorophore. The chamber apparatus of chamberslides was removed whilst submersed in ethanol. They were then washed at least 3x with PBS. Slides were washed in a continuously stirring slide bath and coverslips were washed by serial submersion through PBS baths. Cells were permeablised with 0.05% IPEGAL CA-630 (Sigma) / PBS for 20-30 minutes, washed with PBS and blocked with 2% serum* / PBS for

30-45 minutes. The blocking solution was then replaced with the respective primary antibody or primary antibody combinations (see Section 2.4.1i below) in 2% serum* / PBS for 60-90 minutes. Cells were then rewashed with PBS (≥3x), briefly re-blocked with 2% serum* / PBS (~10min), then incubated with the respective fluorophore-conjugated secondary antibody or secondary antibody combinations (see Section 2.4.1ii below) in 2% serum* / PBS for 60-75 minutes. To preserve the fluorophores, this and all subsequent steps were performed with minimal exposure to light. After subsequent PBS washes the nuclei of the cells were counterstained by with 5 μg/ml Hoechst 33342 (Molecular Probes) / PBS for 15-20 minutes. The cells were then washed extensively with PBS (≥8x over ≥90min) prior to mounting with ProLong AntiFade Mounting Medium (Molecular Probes). After the mounting medium dried (~1 – 5 hours) the coverslips were sealed with nail polish and the slides stored in the dark at 4°C (or -20°C) until examination by confocal microscopy (Section 2.4.2).

* the serum used usually reflected the species the secondary antibodies were raised in, which was inert with respect to the target species of all antibodies used. The blocking serum was either normal goat sera (NGS) or normal donkey sera (NDS) for use with Cyanine-conjugated or AlexaFluor-conjugated secondary antibodies, respectively.

2.4.1i Primary Antibodies

For HIV-1 staining, either pooled AIDS patient sera (APS) or a monoclonal antibody raised against HIV-1 p24 was used. APS was used at a dilution of 1/1000, and pooled normal human sera (NHS) was used at the same concentration on replica infected cell-coated coverslips / chamber-slides to control for any non-HIV-1 specific binding of the APS (or the secondary antibodies) to the cells. The murine monoclonal anti HIV-1 p24 $IgG_{1\kappa}$ (NIH AIDS Research and Reference Reagent Catalogue Number 6458) was used at a dilution of 1/100 (92 μg/ml final). To control for any non-specific binding of this monoclonal antibody (or the secondary antibodies), purified mouse $IgG_{1\kappa}$ (PharMingen) was used as an isotype control on replica infected cell coverslips / chamber-wells, also at a final concentration of 92 μg/ml.

For GFAP staining, Rabbit Anti-Human GFAP polyclonal antibody (Zymed, catalogue number 18-0063) was used at a dilution of 1/50. This antibody was omitted in replica infected cell-coated coverslips / chamber-slides to control for any non-specific binding of the secondary antibodies.

All antibody dilutions were performed in blocking solution, ie 2% NGS or NDS in PBS (see * above). Where combinations of mulitple primary antibodies were used, final concentrations of each antibody in the mix was as described above, and controls were tailored to mimic the antibody combination.

2.4.1ii Secondary Antibodies

APS (and NHS controls) were detected with either Cyanine-2-conjugated donkey anti-human IgG_1 or AlexaFluor-488-conjugated goat anti-human IgG_1, both of which emit light in the green spectrum. Binding of murine monoclonal anti-HIV-1 p24 IgG_1 (and isotype control) were detected with AlexaFluor-546-conjugated goat anti-mouse IgG_1, which emits light in the orange / red spectrum. Anti-GFAP antibodies were detected with either Cyanine3-conjugated anti-rabbit (red) for dual immunofluorescence with APS, or AlexaFluor-488-conjugated goat anti-rabbit IgG_1 (green) for dual immunofluorescence with anti HIV-1 p24.

Cyanine-conjugated antibodies (Jackson ImmunoResearch Laboratories) were used at a dilution of 1/100. AlexaFluor-conjugated antibodies (Molecular Probes) were used at 10 μg/ml (1/200). In multiple-labelling experiments, incubations were performed with the respective combination of antibodies. Dilutions were performed in 2% NDS* or NGS* / PBS.

2.4.2 Confocal Microscopic Analysis of IFA

Cells were viewed and images captured with a BioRad Radiance 2100 confocal microscope with the expert assistance of Dr Ghafar Sarvestani at the Detmold Imaging Core Facility, Hanson Institute, Adelaide. This confocal microscope is equipped with three lasers (Argon ion 488nm (14mw); Green HeNe 543nm (1.5mw); Red Diode 637nm (5 mw)), a mercury

UV lamp and an Olympus IX70 inverted microscope. 40x UPLAPO (with NA=1.15 water) or 60X UPLAPO (with NA=1.4 water) objectives were used, in combination with a 10x eyepiece objective. Multiple fluorescent labelling was imaged with separate channels (PMT tubes) in a sequential setting. The green fluorescence (Cyanine 2, AlexaFluor 488 or EGFP) was excited with Argon 488 nm laser line and the emission was viewed through a HQ515/30 nm narrow band barrier filter in PMT1. The red fluorescence (Cyanine 3 or AlexaFluor 546) was excited with Green HeNe 543 nm laser line and the emission was viewed through a long pass barrier filter (570LP) to allow only red light wavelengths longer than 570 nm to pass through PMT2. Blue fluorescence (Hoechst 33342) was excited with UV light from the mercury lamp. Control images (infected cells with control sera and uninfected cells with specific sera) were captured with identical settings to experimental images. Image data was analysed with Confocal Assistant software program for the Microsoft® Windows™ (Todd Clark Brelje. USA) and converted to CMYK tiff files by Peta Grant, Photography Department, Institute of Medical and Veterinary Science, Adelaide.

2.5 Electron Microscope Analysis

Cells grown in chamber slides, infected and fixed *in situ* in 2.5% (v/v) glutaraldehyde in sodium cacodylate buffer overnight at 4°C for Electron Microscopy (EM) (see Section 2.3.4). The next day, whilst still submersed in the fixative, they were relocated from PC3 to PC2 facilities. Subsequent preparation of cells for EM were performed by Dr Peter Sutton-Smith of the Department of Tissue Pathology, Institute of Medical and Veterinary Science, Adelaide. In brief, the cells were post-fixed in 2% (v/v) osmium tetroxide and embedded *in situ* in Spurr's Epoxy Resin. In order to obtain multiple sections from this thin cell monolayer, the cells embedded in resin blocks were removed from the chamber slide and re-embedded perpendicular to the plane of the cells. Ultrathin sections were cut and stained with uranyl acetate and lead citrate. Sections were analysed with a Jeol Jem-1200 EXII Transmission Electron Microscope.

2.6 Nucleic Acid Purification / Extraction

2.6.1 Plasmid DNA preparations

2.6.1i Bacterial Culture and preparation of competent cells.

Escherichia coli (*E. Coli*) strain DH5α were propagated in 1x LB broth or 1x LB agar plates (15 g/L bacto-agar) at 37°C for 12-18 hours. DH5α *E. coli* transformed with pBS constructs or pNL4-3 were grown in the presence of 100 μg/ml ampicillin (Boehringer Mannheim).

Competent DH5α cells were prepared essentially by the method of Inoue *et al* (Inoue *et al*, 1990). Specifically, DH5α cells were subcultured overnight on blood agar. The next morning, 250ml of SOB medium (Section 2.1.4) was inoculated with several colonies from the blood agar plate, and grown at 18°C to a density of 0.6 A_{600}. The culture was then rapidly chilled on ice for 10 min. The bacterial cells were pelleted by centrifugation at 2500 x g for 10 min at 4°C, resuspended in 80ml Transformation Buffer (Section 2.1.4), and incubated on ice for 10 min. Cells were pelleted by centrifugation again, and resuspended in 20ml transformation buffer. 1.4ml of DMSO was added drop-wise and the cell suspension aliquoted (1 or 2 ml aliquots) and snap-frozen in liquid nitrogen.

2.6.1ii Transformation, propagation and isolation of plasmid DNA

Respective plasmids were transformed into competent DH5α *E.coli* by heat shock. Specifically, competent cells were thawed at room temperature then placed on ice. Competent cells were dispensed in 200μl aliquots into pre-chilled 1.6ml polypropylene tubes. 1 to 5 μl of ligation mix or plasmid was added, mixed gently, and incubated on ice for 30 min. Cells were then heat shocked at 42°C for exactly 90 sec, then returned immediately to ice for ~10 min. 800μl of SOC was added, and the cells incubated with shaking at 37°C for 1 hour. A portion of the cells were then plated on LB agar with the appropriate selection agent.

Small scale preparation of plasmid DNA from bacteria was performed by the alkali lysis method (Sambrook *et al*, 1989). Larger scale plasmid preparations were prepared using Qiagen Plasmid Extraction Kit (Qiagen) according to the manufacturer's instructions.

2.6.2 Cell harvests for DNA and RNA extractions

2.6.2i Cell harvests for solo Hirt DNA extractions or dual DNA and RNA extractions from the same cultures.

At respective times post infection astrocyte cells were harvested by media collection, PBS rinse, trypsin treatment (0.1% v/v for 3-5 min, or until all cells were detached) and resuspension in complete media. Cells and media/PBS/trypsin from all these steps and a final PBS rinse of the emptied well, were collected into a 10ml centrifuge tube, to ensure all cells were collected. Suspension T-cell line positive control cells were collected into 10ml tubes along with a PBS rinse of the well to ensure collection of all cells. Cells were pelleted by low speed centrifugation (930 rpm-Hereus / 6500 rpm benchtop for 3-5 min), washed once by resuspension in PBS and transferred to 1.6ml centrifuge tubes. Where RNA extractions were to be prepared from the same cultures, the PBS suspended cells were divided into equal portions in two 1.6ml centrifuge tubes, one for RNA and one for DNA extraction. For RNA extractions, the cells were pelleted and resuspended in 500µl Solution D (Section 2.1.4), which lyses the cells and protects the RNA, and stored at -80°C until further extraction was performed (Section 2.6.5). For DNA extractions see Section 2.6.3 below.

2.6.2ii Cell harvests for solo RNA extractions

The medium from astrocyte cells was removed and any loose cells collected by low speed centrifugation. To harvest the adherent cells, Solution D applied directly to the cell monolayer, lysing the cells. The Solution D lysed cells and a subsequent Solution D rinse of the well were added to the pelleted loose cells from the same well, to maximise the collection of cells. The final volume of Solution D was 500µl. Suspension T-cell line positive control cells were pelleted by low speed centrifugation and the pellet resuspended directly in Solution D. At this stage the cells are lysed and the RNA is protected by Solution

D, and if required samples could be stored at -80°C at this stage, until further extraction was performed (Section 2.6.5).

2.6.3 Hirt Extrachromosomal and Chromosomal DNA extractions.

Chromosomal and extrachromosomal DNA was separated by the method of Hirt (Hirt, 1967). PBS cell suspensions designated for DNA extraction from Section 2.4.2i were pelleted and gently resuspended in 160µl Hirt Solution 1 (see Section 2.1.4). 20µl of 10 mg/ml Proteinase K (Merck) was then added, followed by 200µl Hirt Solution 2 (Section 2.1.4). Reagents were mixed by gently inverting the tubes 5x (to minimise chromosomal DNA shearing), and the tubes incubated for ≥30 min at 37°C. 100µl of 5M NaCl was added, reagents mixed by gentle inversion, and incubated at 4°C ≥overnight. Samples were then centrifuged at 17 000xg for 60 min at 4°C to separate the extrachromosomal DNA (Hirt Supernatant) from the chromosomal DNA (Hirt Pellet). With the samples kept on ice, the Hirt supernatants were separated into fresh tubes. At this stage potential cross-contamination of chromosomal / extrachromosomal DNA has been reported to be <10% (Kumar *et al*, 2002). Hirt pellets were then re-spun briefly (17 000xg for 15 min at 4°C) to enable subsequent collection of remaining supernatant and minimisation of extrachromosomal contamination of the chromosomal fraction. Hirt supernatant was then also re-spun briefly (17 000xg for 15 min at 4°C) and transferred to fresh tubes, leaving behind any trace of pelleted material to minimise any chromosomal contamination of the extrachromosomal fraction. If necessary, separated Hirt supernatants and Hirt pellets were stored at –80°C at this stage, until the rest of the DNA extraction (below) was performed.

2.6.3i Extrachromosomal Hirt DNA (Hirt Supernatant)

Hirt supernatant fractions were extracted by addition of an equal volume (500µl) phenol / chloroform / IAA (25:24:1), mixed by vortexing and the aqueous and organic phases separated by centrifugation (room temperature). The aqueous phase removed into a fresh tube (on ice) and the extrachromosomal DNA precipitated at by the addition of 2x volumes (1ml) chilled absolute ethanol (A/R grade), 0.05 volumes (25µl) 4M NaCl (0.2M final) and 1µl glycogen (10 mg/ml) to aid visualisation of the subsequent pellet, and centrifuged at approximately 13000xg for 15 min to pellet the precipitate. The pellet was washed with

chilled 80% ethanol (v/v), air dried, resuspended in 100µl dH_20 and stored at –80°C until use. (Note: NaCl was used as the salt component for DNA precipitation instead of Sodium Acetate in order to minimise SDS precipitation, as SDS is carried over into the Hirt supernatant from Hirt Solution 2.)

2.6.3ii Chromosomal Hirt DNA (Hirt Pellet)

500µl dH2O was added to Hirt pellet fractions, and heated to 70°C for 20min, with occasional gentle vortexing, to resuspend the chromosomal DNA. An equal volume (500µl) phenol / chloroform / IAA (25:24:1) was added, samples vortexed thoroughly but gently, then the aqueous and organic layers separated by centrifugation. Chromosomal DNA was extracted from the aqueous phase as described for extrachromosomal DNA (Section 2.4.2i above), with the exception that all steps prior to storage were performed at room temperature, with room temperature reagents (to prevent precipitation of residual SDS carried over with the Hirt pellet from Hirt Solution 2).

2.6.4 DNA extraction from DNased virus stocks

The stored ± DNase I treated virus stock samples (from Section 2.3.5iii) were spiked with equivalent amounts of an irrelevant plasmid DNA, pGEM-DenCap (Section 2.1.2), to enable subsequent normalisation of DNA extraction efficiency. Total DNA was then prepared in the same manner as Hirt supernatant DNA extractions (Section 2.6.3i).

The ± DNase treated virus stock DNA was analysed for DenCap DNA, *β–globin* DNA and three stages of HIV-1 reverse transcribed DNA; early strong-stop (RU5), extended minus strand (*gag*) and complete (*gag*-U3). For positions of the primers demonstrating the stages of reverse transcription amplified by the respective primer pairs see refer Figure 2.1 (and Figure 1.7 and Section 1.1.6ii).

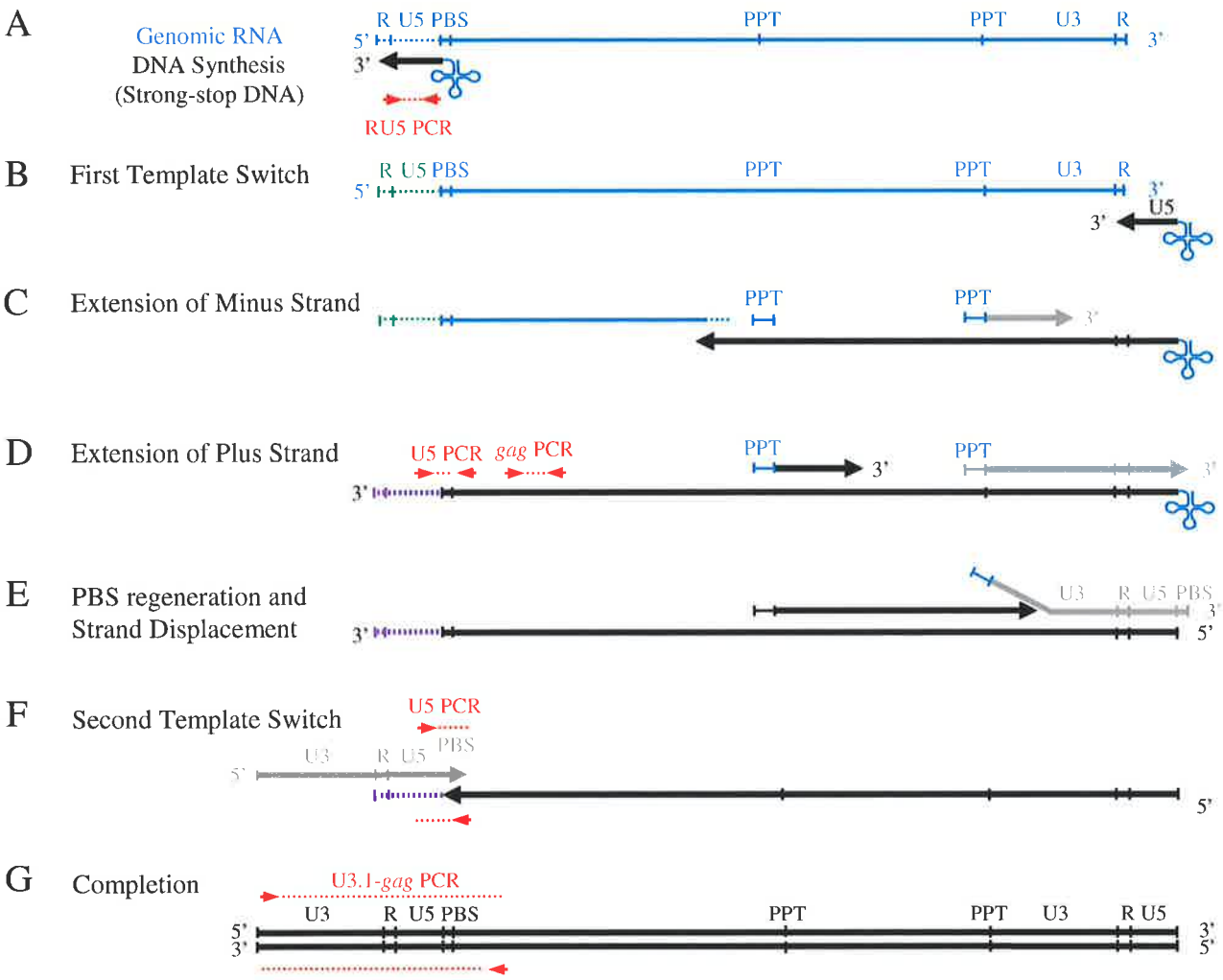

Figure 2.1 Primer positions and PCR amplification specific to various stages of reverse transcription. Primers sites (►) and PCR product amplifications (·····) are superimposed on the schema of reverse transcription. The RU5 PCR (**A**) amplifies the first region of the HIV-1 genome to be reverse transcribed, the minus strand strong-stop DNA, which encompasses the RU5 region of the LTR. RU5 amplification also occurs at all subsequent stages of reverse transcription. *Gag* DNA is synthesised near the 3' end of the extended minus strand, post first strand transfer (**D**). Primers which target *gag* recognise this and all subsequent stages of reverse transcription. In the event of an intermolecular first template switch, the U5 primers, which span either side of the PBS, also detect late extended strand post first strand transfer HIV-1 DNA and all subsequent forms (**D**). In the event of an intramolecular first template switch, amplification of these primers does not occur until after the second template switch has occurred (**F**). The U3.1-*gag* PCR spans a region of DNA which can only be amplified upon virtual completion of reverse transcription (**G**), as the sense primer anneals to the 2nd nucleotide of the U3 region and the antisense primer is in the Gag region. Refer to the text, Section 1.1.6ii, and Figure 1.7 for a detailed description of the process of reverse transcription.

Adapted from Karageorgos *et al.* 1993.

2.6.4i Confirmation of DNase I susceptibility of pNL4-3 plasmid DNA

DNA samples from the DNase I treated pNL4-3 samples in phenol/chloroform/IAA were also prepared in the same manner as Hirt supernatant DNA extractions (Section 2.6.3i). Persistence of pNL4-3 DNA was assessed by HIV-1 *gag* PCR.

2.6.5 Cellular and Viral RNA Extractions and cDNA preparation

RNA was extracted from virus stocks or infected cells at designated times by a modified method of Chomczynski and Sacchi, 1987 (Chomczynski and Sacchi, 1987). Specifically, an equal volume (500µl) of Solution D was added to respective virus stock samples, which were then vortexed vigorously and stored at –80°C if required. RNA was extracted from such virus samples, or from cells which had been harvested, lysed and stored in 500µl of Solution D (Section 2.6.2i-ii) by the sequential addition of 50µl 2M sodium acetate (pH 4.0), 500µl tris-saturated phenol (pH 8.0) and 100µl chloroform / isoamyl alcohol (49:1). Reagents were mixed by gentle vortexing and incubated on ice for 15 min. Samples were centrifuged at 10 000xg for 15 min at 4°C, and the aqueous phase (~700µl), containing the RNA, transferred to a fresh pre-chilled tube. 0.7 x volumes of chilled isopropanol (500µl) was immediately added, mixed by inversion, and incubated at -20°C for an hour (or -80°C for shorter incubations or for storage) to precipitate RNA. The precipitate was pelleted by centrifugation at 10 000xg for 20 min at 4°C, washed with 150µl of 80% (v/v) ethanol, briefly air-dried and immediately resuspended in DNase treatment (Section 2.6.5i below);

2.6.5i DNase treatment of RNA and re-extraction

The RNA pellet was resuspended in 1.0U/µl Rnase-free DNase (Roche), 0.4U/µl RNase Inhibitor and DNase Buffer for RNA (Section 2.1.4) and incubated for 120 minutes at room temperature. 500µl Solution D was then added to inactivate the DNase (stored at –80°C temporarily if required) then re-extracted as outlined above (Section 2.6.5). Subsequent pellets were resuspended in 25µl dH_2O with 0.4U/µl RNase Inhibitor. 8µl of the RNA was immediately added to a reverse transcription reaction mix (Section 2.4.5ii below), 8µl to a mock reverse transcription reaction mix and the remainder of the RNA stored at –80°C.

2.6.5ii Conversion of RNA to cDNA

cDNA was prepared immediately from DNase treated RNA (Section 2.6.5i above) with 0.8 U/µl RT-AMV (Roche) (omitted in "RT-minus" mock reverse transcription controls which were prepared simultaneously), 0.4 U/µl RNase Inhibitor (Roche), 1 pmol/µl each 3' primer (ba2, $adx2_{JC}$, gagHIII, Table 2.1), 1mM each dNTP (Promega) in 1x AMV RT buffer (Roche) (total reaction volume 20µl) at 42°C for 50 min, followed by RT AMV inactivation at 95°C. Samples were made up to 60µl with dH_2O and stored at either -20°C (short term) or -80°C (long term).

2.7 Analysis of HIV-1 DNA and cDNA to investigate HIV-1 Reverse Transcription, Integration and Transcription.

2.7.1 Copy Number Standards and Normalisation of Samples

2.7.1i HA8 Standards; for all HIV species, and normalisation according to β–globin content

HA8 standards were used for all HIV-1 DNA, *β–globin* and PCRs were prepared by Dr Raman Kumar, Dr Nicolas Vandergraaff and Ms Linda Mundy, and have been described previously (Vandegraaff *et al*, 2001b). The HA8 standard is chromosomal DNA extracted from equal cell numbers from each of three persistently HIV-1 infected cell lines; **H**IIIB, **A**CH-2 and **8**E5 (see Section 2.1.1iii). These well characterised cell lines containing two, one and one copies of integrated HIV-1 per cell, respectively (Clouse *et al*, 1989; Folks *et al*, 1986; Li and Burrell, 1992). Single use aliquots of HA8 standard DNA and stored at -80°C at 4000 cells-worth of DNA / µl (≡ 5333.3 HIV-1 DNA copies / µl), and diluted appropriately for use as PCR standards.

The DNA content of chromosomal DNA preparations was estimated by PCR amplification of the single-copy human *β-globin* gene compared to HA8 standards. Samples were normalised if required according to their *β–globin* content.

2.7.1ii Mitochondrial Standards for normalisation of samples.

For extrachromosomal DNA extractions; samples were quantified according to their level of mitochondrial DNA by comparison to the mitochondrial level from a known number of cells of the same cell line, by PCR. HuT-78 cells were determined to contain approximately 5x the level of mitochondrial DNA / cell compared to U251-MG cells.

cDNA samples were normalised according to their level of *β-actin* cDNA by comparison to *β-actin* cDNA levels from a known number of cells of the same cell line.

2.7.1iii Rev, Tat, Nef Standards

For HIV-1 *tat*, *rev* and *nef* standards; tat, rev and nef cDNA fragments were purified from plasmids which encoded the respective cDNAs (pBS-tat/rev/nef, see Section 2.1.2). Following propagation of these plasmids, isolation of the respective plasmid DNA (Section 2.6.1) and sequencing to confirm the identity of the inserts, the respective cDNA fragments were obtained by restriction digest, separated from the plasmid backbone by agarose gel electrophoresis and purified from the gel with QiaQuick Spin Columns (Qiagen). The fragments were quantified by both spectrometry and comparison to DNA markers of known mass (2 log DNA ladder, 1kb DNA ladder and 100bp DNA ladder; New England Biolabs) by ethidium bromide stained polyacrylamide gel electrophoresis, followed by quantification using Typhoon 9410 (Molecular Dynamics) fluorescence scanning and ImageQuant software (Molecular Dynamics) (Section 2.7.3iii). Concentrated, single use aliquots were stored at -80°C and diluted appropriately for use as PCR standards.

2.7.1iv pGEM-DenCap Standards for normalisation of viral DNA extractions

Viral stock DNA extractions were normalised according to their content of pGEM-DenCap by as determined by PCR compared to dilutions of the pGEM-DenCap plasmid which had been quantified by spectrometry.

2.7.2 Conventional PCR Procedures

2.7.2i Standard PCR Conditions for Conventional PCR

Conventional PCRs were performed in a Perkin-Elmer GeneAmp PCR 9600 system. In this thesis, standard PCR conditions refer to PCR amplification with 1x PCR Buffer (Perkin Elmer), 2.5mM $MgCl_2$, 0.2mM each dNTP (Promega), 25pmol of each primer and 2.5U AmpliTaq Gold DNA Polymerase (Perkin Elmer). Final reaction volume was 25µl. Reactions were performed in thin bottom tubes (Axygen), and no oil was required as the GeneAmp PCR 9600 system has a hot lid. The AmpliTaq Gold DNA Polymerase requires heat activation at 95°C, thus acting to provide a hot start and minimise non-specific amplifications. Standard cycling parameters were an initial denaturation of 12 min at 95°C, followed by X cycles of 95°C 45 sec, Y°C 30 sec, 72°C 35 sec; and a final extension of 72°C 10 min. X, the cycle number, was adjusted as required to maintain amplification within the exponential phase to enable semi-quantification of results, and is specified in the text. The optimal annealing temperature (Y) was determined for each PCR, and was usually between 58-61°C.

2.7.2ii Mitochondrial PCR

Mitochondrial PCR was performed with Mit1 and Mit2 primers (Table 2.1) on extrachromosomal DNA extracted from approximately 50-200 cells, in a reaction volume of 20µl and an annealing temperature of 59°C, but otherwise according to standard PCR procedures. Amplification in linear range was usually achieved with 15-19 cycles.

2.7.2iii HIV-1 R-U5 PCR

R-U5 PCR (RU5-1 and RU5-2 primers, Table 2.1) detects the early "strong stop" HIV-1 reverse transcribed DNA species, and all subsequent HIV-1 DNA species, extrachromosomal and integrated (refer to Figure 2.1), and was performed according to standard procedures, with an annealing temperature of 58°C. This PCR was used to analyse reverse transcribed HIV-1 DNA species present in the virus stock.

2.7.2iv HIV-1 Gag PCR

HIV-1 *gag* PCR with primers Gag-P1 and Gag-III has been previously described (Vandegraaff *et al*, 2001b). These primers amplify a region of the HIV-1 *gag* gene, as such they detect HIV-1 reverse transcribed DNA which has undergone the first template switch and extended to this region of the *gag* gene ("extended minus strand") (Figure 2.1). This PCR does not detect earlier stages of reverse transcription. However this PCR detects all later stages of HIV-1 DNA, both extrachromosomal and integrated. For reverse transcription analysis, typically ~2500 cells-worth of extrachromosomal DNA were analysed by this PCR. This PCR was also used to analyse the extent of HIV-1 reverse transcribed DNA in the virus stock, and the level of unspliced, genomic HIV-1 RNA present throughout infections (typically on ~10 000 cells-worth of cDNA). Typically 22-26 cycles of this PCR was required for semi-quantitative amplification, with an annealing temperature of 59°C.

2.7.2v HIV-1 U3-Gag PCR

"Complete" HIV-1 reverse transcription products were detected by PCR with a primer to the U3 region (U3.1) and to the *gag* region (Gag3). These primers have been described previously (Karageorgos *et al*, 1995), and span the region of the HIV-1 genome which is only reverse transcribed after the second template switch has occurred (Figure 2.1). Stringent binding of the U3.1 primer is only possible once reverse transcription is complete and the full length HIV-1 DNA template is available. The design of this PCR requires amplification of a 1.054 kb region of HIV-1 DNA. Consequently a longer PCR extension time of 1 min 45 sec was required, but otherwise standard conditions were employed, with an annealing temperature of 59°C and 25-30 cycles. This PCR was used to detect "complete" reverse transcribed HIV-1 DNA on ~2500 cells-worth of extrachromosomal DNA and to analyse the extent of HIV-1 reverse transcribed DNA in the virus stock.

2.7.2vi β–globin PCR

β–globin PCR with β-glo1 and β-glo2 primers (Table 2.1) has been described previously (Vandegraaff *et al*, 2001b). This PCR was used on chromosomal DNA extracted from

approximately 100-200 cells, according to standard PCR procedures with an annealing temperature of 58°C. Amplification in linear range was usually achieved with 20-25 cycles.

2.7.2vii Alu PCR

Alu PCR is a nested PCR designed to specifically and selectively detect the integrated form of HIV-1 DNA, and was originally described Chun *et al.* (1997) (Chun *et al*, 1997). It has been modified in our laboratory by Dr Nicholas Vandergraaff and Dr Raman Kumar (Vandegraaff *et al*, 2001b). For a diagrammatic schema of this PCR please refer to Figure 2.2. The first round of PCR uses a sense primer (Alu164) which specifically anneals to the highly conserved *Alu* repeat elements of the human genome (approximately 9×10^5 elements / haploid genome), and an antisense primer (PBS-659) (Table 2.1) which binds the PBS region of the HIV-1 genome. This first round PCR was set up in two stages; primers and dNTPs to a total volume of 10µl were aliquoted into PCR tubes and a wax bead (PCR Gem 50; Perkin Elmer) placed over the reagents. Tubes were heated to 75°C for 1 min then cooled to 4°C in the PCR machine allowing a solid wax layer to form over the reagents. Reactions were then made up to 50µl (including the 10µl lower phase) with PCR reaction Buffer II, 1.2mM (final) Magnesium Acetate, 1.6U rTth DNA Polymerase (Perkin Elmer) and respective sample / standard DNA. Reactions were cycled as follows; 94°C 3 min; 22 cycles of 94°C 30 sec, 66°C 30 sec, 70°C 5 min; and a final extension of 72°C 10 min. Sample chromosomal DNA input represented ~10 000 cells-worth. A background of ~10 000 cells-worth of uninfected cellular chromosomal DNA was included in the HA8 standards.

Following 1st-round amplification, the PCR product was diluted 1 in 200, and 5µl used in the 2nd-round of PCR. Given the input DNA in the first round PCR is already diluted 1 in 10 (5µl in 50µl reaction), the total dilution factor of original DNA template in the 2nd round PCR is 1 in 2000. This 2nd round of PCR was performed with a set of nested PCR primers (NI-1 and NI-2; Table 2.1) specific to the U3 region of the HIV-1 LTR (Figure 2.2). This nested PCR was performed with 1.25mM $MgCl_2$, an annealing temperature of 63°C and a 1 minute extension time, but otherwise according to standard PCR procedures, with 31 cycles. This is greater than the cycle number required for accurate quantification from the standards but was performed intentionally to ensure maximum sensitivity of the assay, which was the

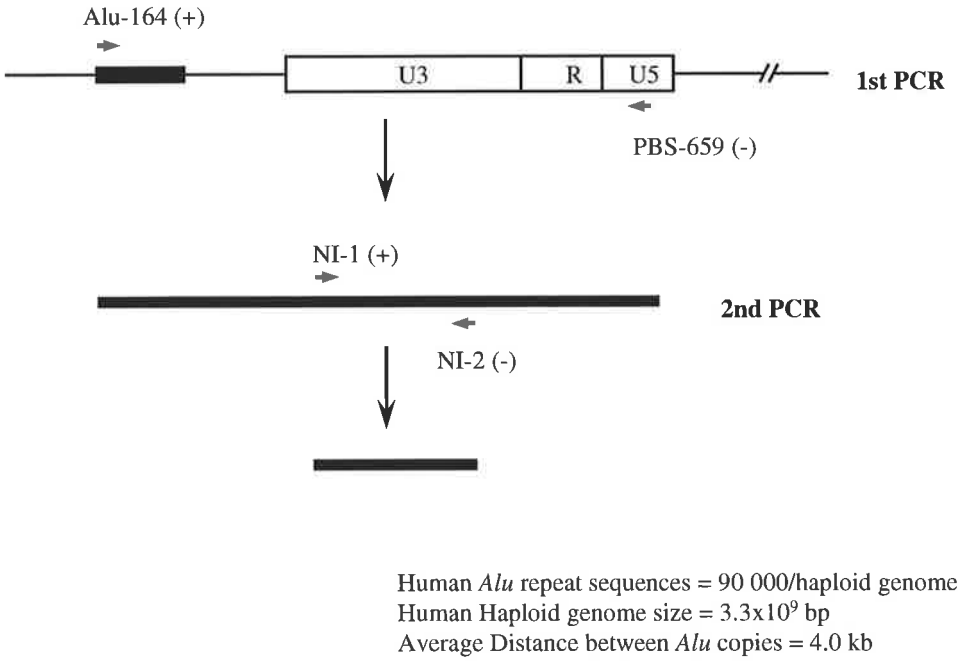

Figure 2.2 The nested-*Alu* PCR Method for the Detection of Integrated HIV-1 DNA. In the first round of PCR, the 5'primer is designed to anneal within a conserved *Alu* repeat sequence and the 3' primer is designed to anneal within the HIV-1 LTR sequence (primers Alu-164 5' and PBS-659 3', respectively). This reaction amplifies across the integration site, including both cellular DNA upstream of the integration site and integrated HIV-1 LTR DNA. The product size is variable, depending on the distance from the integration site to the nearest *Alu* sequence, which occurs on average every 4.0 kb. To increase sensitivity and to generate a product of a defined size, a second (nested) round of PCR (primers NI-1 and NI-2) is performed on a dilution of the product from the first amplification. This second round product is detected by means of a [α-^{32}P]dATP labelled probe generated by Klenow amplification of a DNA fragment of the HIV-1 LTR

incorporating the region flanked by NI-1 and NI-2.

Adapted from Chun *et al.* 1997, incorporating the modifications of Vandergraaff *et al.* 2001

priority in this study. Amplification was confirmed to be specific to the integrated form of HIV-1 and not unintegrated forms by control reactions in which the Alu164 primer was omitted in the first round of PCR ("Alu-minus" controls).

Alternatively, 2nd round amplification could also be performed with Real Time HIV-1 RU5 PCR (Section 7.4iv).

2.7.2viii β–actin PCR

cDNA *β-actin* content was determined by amplification of a segment of the *β-actin* gene with primers β-actin-1 and β-actin-2 (Table 2.1) which have been described previously (Davis *et al*, 1997). PCR amplification was performed on ~200 cells-worth of cDNA, with an annealing temperature of 60°C and typically 20-25 cycles.

2.7.2ix HIV-1 2kb transcript RT-PCR

HIV-1 2kb transcript cDNAs (*tat*, *rev* and *nef*) were detected by a modified version of the method of Davis *et al* (Davis *et al*, 1997). The primers adp1 and adx2 were modified to exclude unnecessary accessory 5' sequences (renamed $adp1_{JC}$ and $adx2_{JC}$) (Table 2.1). All three multiply spliced (2kb) transcript species are co-amplified by these primers, yielding products of three different sizes (tat 393bp; rev 216bp and nef 194bp). PCR amplification was performed on ~250 000 cells-worth of cDNA, with an annealing temperature of 60°C and typically 28 cycles.

2.7.2x DenCap PCR

Dengue Capsid cDNA was amplified from pDenCap template, which was used to spike viral stock DNA extractions to monitor DNA extraction efficiency. Standard PCR procedures were used with DenCap-F and DenCap-R primers (Table 2.1), an annealing temperature of 58°C, and 30 cycles.

2.7.3 Southern Transfer and Hybridisation Techniques

All conventional PCR products (5µl) were subjected to 8% polyacrylamide gel electrophoresis (PAGE) and then Southern transfer (Bio-Rad electroblot apparatus) onto Hybond N+ nylon membranes (Amersham). Large (18x16 cm) PAGE gels were electrophoresed at 160v for ~60 min in 1x TBE. Semi-dry electroblot transfer was performed by sequentially layering pre-soaked Whatman paper (2 sheets), nylon membrane and the gel, then Whatman paper (2 sheets) onto the base of the apparatus. The Whatman paper, membrane and gel were all briefly pre-soaked in 0.3x TBE. The DNA was transferred electrophoretically to the membrane at 50mA for 90 min. Following denaturation and fixation of the DNA to the membrane by placing the membrane on Whatman paper pre-soaked in 0.4M NaOH for 20 min, the filters were washed in 2x SSC, and prehybridised and hybridised with respective probes. Two distinct methods were followed for prehybridisation and subsequent steps, depending on the nature of the probe to be used. *β–actin*, *tat*, *rev* and *nef* RT-PCR products were prehybridised with Prehybridisation Solution (see Section 2.1.4) overnight at 55°C, and hybridised with oligonucleotide probes. All other PCR products (Mitochondrial, RU5, *gag*, U3-*gag*, *β–globin*, nested *Alu* and DenCap) were prehybridised in Ultrahyb™ solution (Ambion) for ≥30min at 42°C and hybridised with respective cloned DNA fragment probes. Prehybridisation, hybridisation and subsequent washes were performed in roller bottles in a rotating Hybaid Oven to ensure continuous mixing.

2.7.3i Hybridisation with DNA fragment probes

Mitochondrial, *β–globin*, HIV-1 and HIV-1 LTR DNA fragments for probe synthesis were prepared by Dr Raman Kumar, Dr Nick Vandergraaff, Ms Kelly Cheney and Ms Linda Mundy. Mitochondrial, *β–globin* and HIV-1 fragments were used to synthesise probes for the PCR products of the same name. The HIV-1 LTR fragment was used to synthesise probes for the detection of nested *Alu* PCR, RU5 PCR and U3-*gag* PCR products. Briefly, after generating these fragments by PCR, they were purified and cloned into plasmid vectors. For use as probes, the fragments were re-obtained from the plasmid vector by restriction digest, electrophoretic agarose gel separation from the plasmid backbone and Qiaquick spin column purification (Qiagen). For use in this thesis the relevant dengue

capsid cDNA fragment and *β–actin* fragment were obtained from pGEM-DenCap and pBS-β–actin and prepared as above.

These double stranded DNA probe fragments were labelled with [α-^{32}P]dATP using the Megaprime DNA Labelling Kit (Amersham), according to the manufacturer's instructions. Reaction mixes contained ~120ng DNA template which was denatured at 100°C in the presence of 5µl random nonamers, 5µl reaction buffer, 4µl each dGTP, dTTP and dCTP, 2µl DNA polymerase (Klenow fragment) and 5µl of [α-^{32}P]dATP (10µCi/ml, Geneworks), and were incubated for 45 min at 37°C. Probes were then purified through a G-25 Sephadex spun column stored for up to 2 weeks at -20°C. Immediately prior to use, these double stranded probes were denatured by heating to 100°C in a boiling water bath for a few minutes followed immediately by incubation on ice.

After prehybridisation of membranes the respective labelled and denatured probe was added and hybridised overnight at 42°C. Membranes were then washed, initially with prewarmed 5xSSC, 0.5% SDS for 15 min at 55°C, then twice with prewarmed 0.5xSSC, 0.1% SDS for 20 min at 55°C. Membranes were then exposed to Storage Phospor Screens (Molecular Dynamics) for between 30 min and 16 hours, depending on the signal strength.

2.7.3ii Hybridisation with oligonucleotide probes

Specific oligonucleotides were used for the hybridisation of multiply spliced 2kb HIV-1 transcripts (*rev*, *tat* and *nef*) RT-PCR products. The sequence for the *rev*, *tat* and *nef* probes has been previously described (Davis *et al*, 1997), and is given in Table 2.2. Specifically the *rev* (p1.4a), *tat* (p1.4) and *nef* (p1.5) probes span the splice junction sites which characterise the respective transcripts, and their nomenclature identifies the respective Splice Donor and Splice Acceptor sites. These oligonucleotides were labelled at the 5' termini with [γ-^{32}P]dATP using T4 polynucleotide kinase (PNK) as follows; 200ng probe was end labelled with 20U PNK (Roche) in 1x PNK buffer with 5µl [γ-^{32}P]dATP (10 µCi/ml, Geneworks) (total volume 20µl). The reaction was incubated for 50 min at 37°C, after which 500µl of 6x SSC was added to terminate the reaction. Probes were then purified through a G-25 Sephadex spun column for immediate use or stored for up to 2 weeks at -20°C.

After prehybridisation of membranes, the prehybridisation solution was replaced with prewarmed hybridisation solution (see Section 2.1.4), and the respective labelled oligonucleotide probe added. For detection of all three 2kb transcript cDNA species on the same membrane, all three probes were added. Hybridisation was performed at 55°C for ≥4 hours. Membranes were initially washed for 20 min with prewarmed 2xSSC, 0.1%SDS at 65°C, then twice for 15 min with 0.2xSSC, 0.1%SDS at 65°C, then twice with 0.1xSSC, 0.1%SDS at 70°C. Membranes were then exposed to Storage Phospor Screens (Molecular Dynamics) for between 30 min and 16 hours, depending on the signal strength.

2.7.3iii Phosphor or fluorescent analysis of band intensity

The intensity of the bands detected by the use of labelled [α-^{32}P] fragment probes or [γ-^{32}P] labelled oligonucleotide probes and subsequent exposure to phosphorous coated screens was measured by phosphor scanning with a PhosphorImager (Molecular Dynamics) or Typhoon 9410 (Molecular Dynamics) machine. In most cases an approximate conversion from band intensity to respective copy numbers could be determined by comparison to the standards. Where interpretations were more complex or a greater degree of accuracy required, the intensity of the bands was quantified with ImageQuant software (Molecular Dynamics). Briefly, a rectangle was drawn around the band of highest intensity. The rectangle was the copied and placed over each band to be quantified to ensure the same area (volume) was to be quantified for each band. The pixel number was then quantified within each rectangle (employing the "integrate volume" function) and transferred to Microsoft Excel for analysis. The pixel count from negative control lanes was subtracted from all counts to correct for the background level of pixels in the defined area. A standard curve of pixel number versus input copy number was generated from the pixel counts from the standards. Pixel counts of the experimental were converted to copy number by regression analysis using the standard curve.

The Typhoon 9410 was also used to fluorescently scan ethidium bromide stained PAGE gels in some instances. Where a high degree of accuracy was required (for example, determination of the intensity of rev, tat and nef fragments for subsequent use as standards), the intensity of bands were quantified with ImageQuant software as above.

2.7.4 Real Time PCR Procedures

2.7.4i Standard Real Time PCR Procedures

10µl real time PCR reactions were prepared with Quantitect SYBER green (Qiagen) 1x PCR mix ($MgCl_2$ and dNTPs included), 1pmol each primer (HPLC purified) and respective standard or sample DNA. Reactions were run in a 72 tube carousel in a Rotor-Gene cycler machine (Corgette Research). Optimal gain settings were determined for each batch of Quantitect SYBER green, and typically set at either 5 or 10. Standard cycling parameters were 50°C for 2 min, 95°C for 15 min then 40 cycles of (94°C 20 sec, Y°C 20 sec, 72°C 20 sec), followed by a final hold of 72°C for 30 sec, where Y is the optimal annealing temperature, typically 58-61°C. The Rotor-Gene cycler measures the fluorescence of each tube every cycle. At the conclusion of cycling, the machine measures the melting curve for the products in each tube, again by virtue of fluorescence. Analysis was subsequently performed with Rotor-Gene software (Corgette Research). Specifically, negative controls and standards were checked for expected results, and the melting curves of each tube were checked to confirm that only single melting temperature occurred at the expected temperature. Rotor-Gene software was used to automatically determine the threshold fluorescent values from negative controls ("NTC"; no template control). Next it determined the optimal cycle number for interpolation from standards, generating a standard curve of normalised fluorescence versus copy number. From this, the respective copy numbers of all samples was derived. Where required, further analysis and graphical representation was done by importing this data into Microsoft Excel.

2.7.4ii Real Time Mitochondrial PCR

Mitochondrial PCR was performed with MitA and MitB primers (ref Table 2.1) on extrachromosomal DNA extracted from approximately 50-200 cells, with standard real time PCR procedures and an annealing temperature of 58°C.

2.7.4iii Real Time β–globin PCR

For *β–globin* real time PCR the same primer sequences were used as for conventional *β–globin* PCR (Table 2.1). Standard real time PCR parameters were used on approximately 100-200 cells-worth of chromosomal DNA, with an annealing temperature of 58°C.

2.7.4iv Real Time HIV-1 RU5 PCR

To assay for the presence of any HIV-1 DNA a sense primer to the R region of HIV-1 (SS1) was used in conjunction with an antisense primer to the U5 region (SS2a) (Table 2.1). Thus it amplified minus strand strong stop DNA and all subsequent stages of reverse transcribed HIV-1 DNA (Figure 2.1). This PCR was performed with standard real time PCR parameters and an annealing temperature of 60°C. These primers detect early strong stop reverse transcribed HIV-1 DNA and all subsequent forms. They were used to detect the presence of HIV-1 DNA in chromosomal preparations, directly or after the first round of *Alu* PCR (Section 2.7.2vii), typically on ~20 000 or ~10 000 cells-worth of chromosomal DNA respectively.

2.7.4v Real Time HIV-1 U5 PCR

To amplify late reverse transcribed and subsequent forms of HIV-1 DNA, the primer pair U5-P1 and U5-P2 were used. These both anneal to the U5 region of HIV-1 DNA, to either side of the PBS region, as such they only detect reverse transcribed HIV-1 DNA which has proceeded beyond the second template switch (Figure 2.1). This PCR does not detect earlier stages of reverse transcription, but does detect all later stages of HIV-1 DNA, extrachromosomal and integrated. For reverse transcription analysis, typically ~2000 cells-worth of extrachromosomal DNA were analysed by this PCR, with standard real time PCR parameters and an annealing temperature of 60°C.

2.7.5 HIV-1 Reverse Transcription Analysis

Hirt extrachromosomal DNA was harvested from cells at designated times post cell-to-cell or cell-free HIV-1 infection, typically 2½-3½, 26 and 48-52hpi (Section 2.3.1, 2.3.2, 2.3.5,

2.6.2, 2.6.3). The extrachromosomal DNA content of each of the samples was assessed by mitochondrial PCR and Southern (typically performed on ~50-200 cells-worth of extrachromosomal DNA) and normalised accordingly (Sections 2.7.1ii, 2.7.2-2.7.4).

DNA was extracted from viral stocks (Section 2.6.4) which had been treated with or without DNase I (Section 2.3.5iii) and, after inactivation of the DNase, spiked with a known amount of pGEM-DenCap DNA (2.6.4). The relative efficiency of the DNA extractions was determined according to the pGEM-DenCap content, by DenCap PCR and Southern hybridisation. If necessary, samples were normalised accordingly (Sections 2.7.1iv, 2.7.2-2.7.3).

Samples were analysed for the presence and level of various species of HIV-1 reverse transcribed DNA, specifically "early" (minus strand strong-stop), "extended minus strand" (post first strand transfer) and "complete" (end-stage post second strand transfer) species (Figure 2.1, 1.7 and Section 1.1.6ii) by conventional RU5, *gag* (or U5 real time) and *gag*-U3 PCRs and Southern hybridisation respectively (Sections 2.7.1i, 2.7.2-2.7.4). These conventional PCR assays were typically performed on ~2500 cells-worth of extrachromosomal DNA.

In order to ensure accuracy, a two step dilution of Hirt extrachromosomal DNA was performed so that the same dilution series could be used for normalisation and HIV-1 DNA assessment. An initial dilution of 1/10 was made (subsequently used in PCRs assessing HIV-1 DNA), from which a further dilution of 1/25 (total dilution factor of 250) was performed on which the mitochondrial PCRs were initially performed.

2.7.5i Infections with nucleoside analogue reverse transcriptase inhibitors

To further characterise HIV-1 reverse transcription, two nucleoside analogue inhibitors of reverse transcription were used; an analogue of thymidine; zidovudine (3'-azido-3'-deoxythymidine, or AZT) (Sigma) and an analogue of cytidine; lamivudine (cis-1-[2'-Hydroxymethyl-5'-(1,3-oxathiolanyl)] cytosine, or 3TC) (kind gift from David Bourke, Department of Medicinal Chemistry, Victorian College of Pharmacy, Australia). Both drugs were made to 10mM stocks in DMSO, and further diluted in serum free media to the

working concentration. The final concentrations used (20μM for AZT and 50μM for 3TC) were based on concentrations shown to inhibit viral release following infection of T cells (Coates *et al*, 1992; Hazuda *et al*, 2000).

At these concentrations these drugs had been previously demonstrated to be non-toxic to HuT-78 cells in our laboratory (by Dr Nick Vandegraaff). For the purpose of this thesis, cell cytotoxicity experiments were also performed with these drugs on the astrocyte cell lines U251-MG, CCF-STTG1 and U87-MG. These experiments were performed in triplicate by incubating astrocytes with concentrations of drugs ranging from 5-fold above and below the intended concentration for use. After 24h, 48h and 72h in the presence of absence of the drug, cultures were assessed for cell death by trypan blue exclusion and cell growth by total cell number. Drugs were considered non-toxic if there was <5% inhibition of cell growth over 52h (LD_5) compared to drug-free cultures.

These analogues require phosphorylation by a constitutively expressed kinase to be converted into their active triphosphate form (Brinkman *et al*, 1998; Kakuda, 2000; Lewis *et al*, 2003) Section 2.7.5i).. To enable conversion of these analogues into their respective active triphosphates, the cells were pre-incubated in the presence of the respective drug or drug carrier (identical dilution of DMSO to that present with the drug) overnight prior to the infection. Centrifugally enhanced cell-free infections were then performed as described in Section 2.3.5ii. The designated concentration of the drug was maintained through out all steps of the infection, washes and subsequent culture until the cells were harvested for DNA extraction. HuT-78 cells were included as controls to confirm the antiviral activity of the drugs.

2.7.6 HIV-1 Integration Analysis

Hirt chromosomal DNA was harvested from cells at designated times post cell free HIV-1 infection, typically 3-3½ hpi, 1, 2, 7, 10, 13, 16 dpi (Section 2.3.5, 2.6.2, 2.6.3). *β–globin* DNA content of chromosomal DNA was determined by semi-quantitative conventional PCR and Southern hybridisation or quantitative real time PCR, and samples normalised accordingly (Sections 2.7.1i, 2.7.2-2.7.4). HIV integration was assayed by nested *Alu* PCR or real time HIV-1 RU5 PCR on ~10 000 or ~20 000 cells-worth of chromosomal DNA

respectively (Sections 2.7.1i, 2.7.2-2.7.4). Samples were diluted for *β–globin* analysis, and usually used neat in these HIV-1 DNA analyses.

2.7.7 HIV-1 RNA Analysis

RNA was extracted from virus stocks or cells at designated times post cell free HIV-1 infection, typically 3-3½ hpi, 1, 2, 7, 10, 13, 16 dpi, and reverse transcribed into cDNA (Section 2.3.5, 2.6.2, 2.6.5). Mock reverse transcription reactions were also performed to confirm that DNase treatment of the RNA was effective and that subsequent amplification was derived from cDNA and not pre-existing DNA. Cellular cDNA preparations were assayed for their level of *β–actin* by semi quantitative conventional PCR and Southern hybridisation, and samples normalised accordingly if required. Mock cDNA preparations were confirmed not to contain any detectable *β–actin* DNA. Mock and genuine cDNA preparations were assayed to determine levels of unspliced, genomic HIV cDNA and multiply spliced rev, tat and nef cDNA by semi-quantitative conventional PCRs and Southern hybridisation (Section 2.7.1, 2.7.2, 2.7.3). To maintain accuracy, samples were diluted in two stages. The second dilution was used for *β–actin* analysis, and either the neat or the first dilution (of the same dilution series) was used to assess HIV-1 cDNA levels.

2.8 Detection of release of infectious virus (Infectivity Assay)

In experiments where the astrocyte culture supernatants were tested for infectivity, half of the supernatant (2ml) was collected daily from 7 dpi to 16 dpi (replaced with fresh media ± IL1β as appropriate). Collected supernatants were immediately filtered (0.2μm) and applied to $5x10^5$ cells of an HIV-1 susceptible T-cell line. A3.01 cells were initially used in addition to HuT-78 cells, as the potential for A3.01 cells to become infected was not expected to be affected by the presence of IL1β in some of the supernatants (Tornatore *et al*, 1991). Initially this was unknown for HuT-78 cells. Media alone and diluted viral stock controls were also included. Initially infectivity assays were performed by direct application of the filtered supernatant to the cells. In latter experiments the filtered supernatants were applied to the cells by a modified centrifugally enhanced infection protocol as described in Section 2.3.5ii, except the initial 4°C incubation and the post centrifugation washes were omitted. Instead, after centrifugation, half of the supernatant (1ml) was replaced and the cell pellet

resuspended in the remaining supernatant and seeded into 48-well culture dishes. Centrifuge tubes were rinsed with 1ml fresh complete cell culture medium, which was then added to the respective to ensure minimal loss of cells. These T-cell line cultures were maintained, with half media changes / cell splitting as required, for up to 12 days and monitored for evidence of HIV-1 infection (syncytia formation, HIV-1 p24 ELISA (Section 2.2.1)).

2.9 List of Suppliers

ABI, Applied Biotechnology Inc., Division of Perkin-Elmer Corporation
American Tissue Culture Collection, Manassas, Va., USA
Amersham, Amersham International PLC, Little Chalfont, Buckinghamshire, UK
Australian Red Cross Blood Bank, Adelaide, Australia
Axygen, Inc, Union City, CA, USA
BDH, BDH Chemicals Australia Pty Ltd, Kilsyth Vic, Australia
Bexkman, Beckman Instruments Inc., Fullerton CA, USA
Bio-Rad, Bio-Rad Laboratories, Hercules CA, USA
Boeringer, Boeringer Mannheim, Mannheim, Germany
Cellstar, Greiner Bio-One GmbH, Germany
Clonetech Laboratories Inc, Palo Alto, CA, USA
Corgette Research, Australia
CSL, Commonwealth Serum Laboratories, Parkville, Australia
Falcon, BD Labware, Franklin Lakes, USA
Geneworks, Geneworks Pty Ltd, Adelaide SA Australia
Gibco BRL, Grand Island, USA
Immuntech, France
Kodak, Eastman Kodak, Rochester NY, USA
Lab-Tek, Nalge Nunc International, Naperville, IL, USA
Merck, Merck Biochemica, Darmstadt, Germany
Millipore Coorporation, Bedford, MA, USA
Molecular Dynamics, Inc., Beverly MA, USA
Molecular Probes, Eugene, Oregon, USA
National Centre for HIV-1 Virology Research, Melbourne, Australia

National Institutes of Health (NIH) AIDS Research and Reference Reagent Program, Division of AIDS, NIAID, NIH USA

New England Biolabs, Inc. Beverly, MA, USA

Perkin-Elmer Corporation, Roche Molecular Systems, Inc., Branchberg NY, USA

Perkin Elmer Life Sciences, Boston, MA, USA

Pharmacia, Pharmacia Biotech, Uppsala, Sweden

PharMingen, BD, NSW, Australia

Promega, Promega Corporation, Madison WI, USA

Qiagen, Victoria, Australia

Sartorius, Hannover, Germany

Savilllex, Techmate Ltd, UK

Sigma, Sigma Chemical Company, Sigma-Aldrich Pty Ltd, St. Lois MO, USA

Stratagene, Stratagene Cloning Systems, La Jolla CA, USA

Terumo, Tokyo, Japan

Whatman, Whatman International Ltd., MAIDStone, UK

Zymed, Invitrogen, NSW, Australia

Chapter 3

Cell to Cell infection of Astrocytes *in vitro*

3.1 Introduction

3.1.1 Background

The infection of astrocytes by HIV-1 results in a restricted infection typified by low level expression of viral regulatory proteins and the absence of viral structural proteins. The apparent low efficiency of this infection presents a challenge to characterising aspects of the infection of astrocytes by HIV-1. In this thesis the HIV-1 infection of astrocytes is analysed with both a "cell-to-cell" (this chapter) and a "cell free" (Chapters 4 to 6) *in vitro* model of infection. A cell-to-cell infection model was established because there were several indications in the literature that this mode of astrocyte infection may result in a more efficient infection than cell-free inoculation (Brack-Werner, 1999; Nath *et al*, 1995) (Section 1.5.1i). Previous work also suggested that astrocytes may be more susceptible to *in vitro* infection by T-cell tropic strains of HIV-1 than macrophage trophic strains (McCarthy *et al*, 1998; Nath *et al*, 1995; Schweighardt *et al*, 2001) (Section 1.5.1). The transmission of T-cell and macrophage tropic HIV-1 strains were investigated in this chapter by measuring reverse transcribed HIV-1 DNA transcripts over time. Viral reverse transcription was analysed with the primary aims of i) assessing and comparing the transmission to, and replication of, T-cell and macrophage tropic HIV-1 strains in astrocytes, and ii) characterising the kinetics of reverse transcription of HIV-1 in astrocytes. An additional aim was to compare the efficiency of the cell-to-cell infection (as measured by viral reverse transcription) with the cell-free model (Chapter 5).

To investigate transmission of T-cell tropic strains of HIV-1 to astrocytes, U251-MG astrocytes were cocultured with persistently HIV-1 infected T-cell lines (Section 3.2). Two T-cell lines were used as "virus-donor" cells; HIIIB cells (a clonal cell line persistently infected with HIV-1_{IIIB}) and E12 (a cell line persistently infected with HIV-1_{SF2}). HIIIB cells were chosen as these have previously been used successfully to study the transmission

of HIV-1 infection to T-cells (Karageorgos *et al*, 1993; Karageorgos *et al*, 1995; Li *et al*, 1993a; Li and Burrell, 1992; Li *et al*, 1992; Li *et al*, 1994). As a comparison, the chronically infected T-cell line, E12, was also used in these transmission experiments. E12 cells are persistently infected with a fully competent strain of HIV-1.

To investigate transmission of macrophage tropic strains of HIV-1 to astrocytes, U251-MG astrocytes were cocultured with chronically HIV-1 infected MDMs (Section 3.4). The HIV-1_{BaL} virus strain was chosen as it has previously been used successfully to characterise the transmission of HIV-1 from macrophages to T-cells (Carr *et al*, 1999).

3.2 Preliminary Investigations on the Culture of Astrocytes with Persistently infected T-cell lines

3.2.1 Characterisation of the persistently infected T-cell lines

HIIIB cells have been characterised previously (Section 2.1.1iii). Personal communication with Dr Jay Levy verified that E12 cells are a clonal cell line derived from infection of HuT-78 cells with the HIV-1_{SF2} virus. The HIV-1_{SF2} virus used for this infection was derived from the original SF2 viral isolate (previously known as ARV (Section 1.1.1)), and not from the molecular clone of SF2, which was subsequently derived from the same viral isolate.

To determine the proportion of the E12 cells that expressed virus, the cells were assessed for intracellular expression of the HIV-1 core protein p24 by FACS analysis. p24 protein was detected in between 30 to 40% of the cell population. To confirm whether these cells produced virus, the supernatants were tested for the secretion of p24 and infectious virus. These cells were shown to secrete >1ng p24 / ml / hour /10^6 cells. Incubation of filtered (0.2μm) E12 supernatant with HuT-78 cells (HIV-1 susceptible cells) and coculture of E12 cells with HuT-78 cells both resulted in the infection of the HuT-78 cells, as evident by syncytia formation (light microscopy), elevated p24 secretion (ELISA), and an elevation in viral DNA as a result of reverse transcription (PCR).

3.2.2 Minimising the contribution of HIV-1 replication in the virus-donor cell population

As the level of HIV-1 replication in the astrocyte population was expected to be low, the detection could be "masked" by viral replication in the virus-donor cell population. It was therefore anticipated that it would be necessary to minimise the contribution of HIV-1 replication in the virus-donor cells. For this reason, chronically infected donor cells were used rather than acutely infected donor cells, as the level of ongoing reverse transcription would be expected to be lower in chronically infected cells.

To further minimise the detection of viral reverse transcription in the virus-donor cells, several additional strategies were employed. These included i) separation of the astrocytes from the virus-donor cells after a period of coculture, and ii) pre-treatment of the virus-donor cells with an inhibitor of transcription (including HIV-1 reverse transcription), Actinomycin C_1 ($ActC_1$), and iii) pre-treatment with a specific inhibitor of reverse transcription, 3'-azido-3'-deoxythymidine (AZT), to distinguish between *de novo* reverse transcribed and pre-existing reverse transcribed HIV-1 DNA.

3.2.2i Separation of cell populations after coculturing

The separation of virus-donor cells from astrocyte cells after a period of coculture (2 - 24 hours) was initially attempted by washing away the donor cells (suspension cells) from the U251-MG astrocytes (adherent) (Section 2.3.1i). However, a significant proportion of the persistently infected lymphocytic cells were observed (by light microscopy) to adhere to U251-MG astrocyte cells within an hour of coculture. This lymphocyte-astrocyte interaction occurred with all persistently infected T-cell lines tested in this thesis (HIIIB, E12 and ACH2), and has been previously reported (Nath *et al*, 1995; Tornatore *et al*, 1991). Whilst the majority of virus-donor cells could be removed by washing, light microscopy observations of the astrocyte cultures over the subsequent days clearly revealed the outgrowth of lymphocytic cells, indicating that not all of the virus-donor cells had been washed away. No cytopathic effect (no syncytia or giant cell formation) was observed in either the virus-donor cells or the U251-MG astrocytes.

To improve the efficiency of removal of the virus-donor cells, after washing the excess donor cells away the astrocytes and remaining donor cells were resuspended by trypsin treatment. The remaining virus-donor cells were depleted with anti-CD3 magnetic beads, and the $CD3^-$ U251-MG cell population re-seeded. However, the recovery of U251-MG astrocyte cells after this procedure was poor, with the cell loss estimated to be up to 40%. Furthermore, a low level of lymphocytic cells persisted in the U251-MG cultures despite the $CD3^+$ cell depletion step, as evident by anti-CD3 FACS analysis of the re-seeded population on subsequent days of culture.

The tendency of the lymphocytes to adhere to the U251-MG astrocytes raised the concern that any potentially infected U251-MG cells may be selectively removed by virtue of their interaction with the donor cells during the $CD3^+$ cell depletion step. This concern was heightened by the considerable loss of U251-MG cells upon $CD3^+$ depletion. It was not possible to positively select the astrocyte cells whilst maintaining their viability for ongoing culture, due to the lack of an available astrocyte specific cell surface marker.

Even if positive selection of the U251-MG cells were possible, it would be likely that the recovered U251-MG population would still contain adhered virus-donor cells, or, if this could be prevented, be biased to those astrocyte cells which had not interacted with the donor cells. Removal of donor cells with an appropriate antibody and complement mediated lysis was considered, but was not attempted as this method was not expected to be 100% effective either. The presence of complement may also affect the infection, as astrocytes express complement receptors and complement can be toxic to certain cell types. Thus it was decided to analyse the astrocyte / virus-donor cell cocultures without attempting to separate the cell populations. This would allow the contribution of HIV-1 replication within the donor cell population to be controlled and hence accurately taken into account when evaluating HIV-1 replication in the cocultures. The level of viral reverse transcription in the donor cell population could also be minimised by $ActC_1$ treatment.

3.2.2ii Coculturing with Actinomycin C_1 pretreated virus-donor cells

Optimisation of $ActC_1$ pretreatment of virus-donor cells

As it was possible that coculturing with astrocytes could activate and upregulate virus replication in the viral donor cells, the donor cells were pretreated with or without the transcription (and reverse transcription) inhibitor, $ActC_1$. This was to reduce the background level of viral reverse transcription in the donor cell population. To minimise the potential toxicity of $ActC_1$ treatment, the drug was titrated to determine the minimum effective dose (Section 2.3.1ii). The viral donor T-cells (10^6 cells/ml) were treated for 2 hours with $ActC_1$ at concentrations from 2μg/ml up to 64μg/ml, after which the cells were washed twice to remove excess drug. The inhibition of transcription was assessed by the reduction in tritiated uridine uptake (Section 2.3.1ii). The minimum $ActC_1$ dose that gave maximal inhibition of transcription was found to be between 8 to 12 μg/ml for all persistently infected T-cell lines tested (HIIIB, E12, ACH2 and 8E5 cells). Therefore 12 μg/ml $ActC_1$ was used in all subsequent experiments, and in each experiment the inhibition of transcription was verified by assessing tritiated uridine uptake in a sample of the treated cells.

Preliminary experiments to analyse the transmission of HIV-1 from ±$ActC_1$ pretreated virus-donor cells to U251-MG astrocytes.

In preliminary experiments to analyse the transmission of HIV-1 from ±$ActC_1$ pretreated virus-donor cells (HIIIB and E12 cells) to U251-MG astrocytes, the U251-MG astrocytes (as well as the virus-donor cells) were counted immediately prior to coculturing. Accurate counting of the virus-recipient and virus-donor cell populations enabled the contribution of HIV-1 DNA and virus replication in the virus-donor cells to be accurately taken into account, with respective virus-donor cell monoculture controls. Accurate counting of the U251-MG cells was facilitated by first detaching the cells with trypsin. The detached U251-MG cells were then cocultured with ±$ActC_1$ pretreated E12 or HIIIB cells at a ratio of 2 U251-MG cells: 1 virus-donor cell. (±$ActC_1$ pretreated cells were washed twice prior to the experiment to remove excess drug).

Immediately after coculture (T = 0h), and 24 hours after coculture the extrachromosomal DNA was extracted from the cocultures and respective monoculture controls. To adjust for any variation in the extrachromosomal DNA extraction efficiency, semi-quantitative mitochondrial PCR and Southern hybridisation was performed (Figures 3.1A and 3.2A). The presence of extended minus strand reverse transcribed HIV-1 DNA transcripts in the extrachromosomal DNA samples was assessed by semi-quantitative HIV-1 *gag* PCR and Southern hybridisation (Figures 3.1B and 3.2B), and presented graphically as a the number of HIV-1 *gag* DNA copies present per 100 or 5000 cells of coculture (or the respective number of cells in the monoculture controls) (Figures 3.1C and 3.2C).

These preliminary experiments did not show any increase in the level of extrachromosomal HIV-1 DNA in the cocultures from 0 to 24 hours with untreated virus-donor cells (Figures 3.1C and 3.2C). The level of HIV-1 DNA present at 0 hours represents initial amount of HIV-1 DNA present in the virus-donor cells, as no HIV-1 DNA was detectable in the uninfected U251-MG cells, as expected. The lack of increase of HIV-1 DNA over 24 hours of coculture indicated that viral reverse transcription was either absent in the U251-MG cells, or below the background level of ongoing reverse transcription in the virus-donor cells.

$ActC_1$ pretreatment of the virus-donor cells was included to discern which cell population viral reverse transcription was occurring in, if an increase in extrachromosomal HIV-1 DNA had been observed over time in the cocultures. However, in the experiment shown in Figure 3.2, an increase in the level of extrachromosomal HIV-1 DNA was seen from 0 to 24 hours with $ActC_1$ but not untreated E12 virus-donor cells. Taken on its own, this data would suggest that viral reverse transcription was stimulated upon coculture, and as transcription was inhibited in the E12 cell population by $ActC_1$ (verified by the inhibition of tritiated uridine uptake in a sample of the $ActC_1$ treated E12 cells), indicating that the viral reverse transcription occurred in the U251-MG astrocyte cell population. However, this scenario of transmission of infection from the ($ActC_1$ treated) E12 cells to the U251-MG cells is not consistent with the results of the coculture with untreated E12 cells in the same experiment, nor the results of the U251-MG cocultures with $\pm ActC_1$ treated E12 cells in the previous experiment (Figure 3.1).

Figure 3.1 Analysis of transmission of HIV-1_{SF2} upon coculture of E12 cells with trypsin-treated U251-MG astrocytes.

U251-MG cells were detached with trypsin and combined with ± $ActC_1$ treated E12 cells at a ratio 2:1. The cocultures (and respective U251-MG and E12 control monocultures) were harvested immediately or (co-)cultured for 24 h, and the extrachromosomal DNA extracted.

To estimate the extrachromosomal DNA extraction efficiency, the volume of DNA which represented approximately 100 cells in the experiment at time 0h was subjected to mitochondrial PCR and Southern hybridisation, (**A**). The signal intensity of the amplified mitochondrial DNA from each sample was compared to the signal intensity of a known input of extrachromosomal U251-MG cell DNA (*), enabling the relative number of cells-worth of DNA present in the input of each sample to be estimated (†). Duplicate PCR reactions (27 cycles) were performed on each extrachromosomal DNA sample.

To determine the extent of HIV-1 reverse transcription which had occurred in these cultures, 100 cells-worth of extrachromosomal DNA from each cell mix or unmixed control culture was subjected to HIV-1 *gag* PCR (to detect the extended minus strand of viral reverse transcribed DNA, and any subsequent forms of HIV-1 DNA), followed by Southern hybridisation (**B**). The number of HIV-1 *gag* DNA copies per 100 cells of each culture was determined by comparison to HA8 HIV-1 DNA copy number standards. HIV-1 *gag* copy numbers in the control monocultures were adjusted to represent the proportion of these cells present in the cocultures, that is, 67 cells-worth of U251-MG cells and 33 cells-worth of E12 cells (**C**). Error bars represent the standard error between the duplicate HIV-1 *gag* PCR reactions (29 cycles) performed on each extrachromosomal DNA sample.

A.

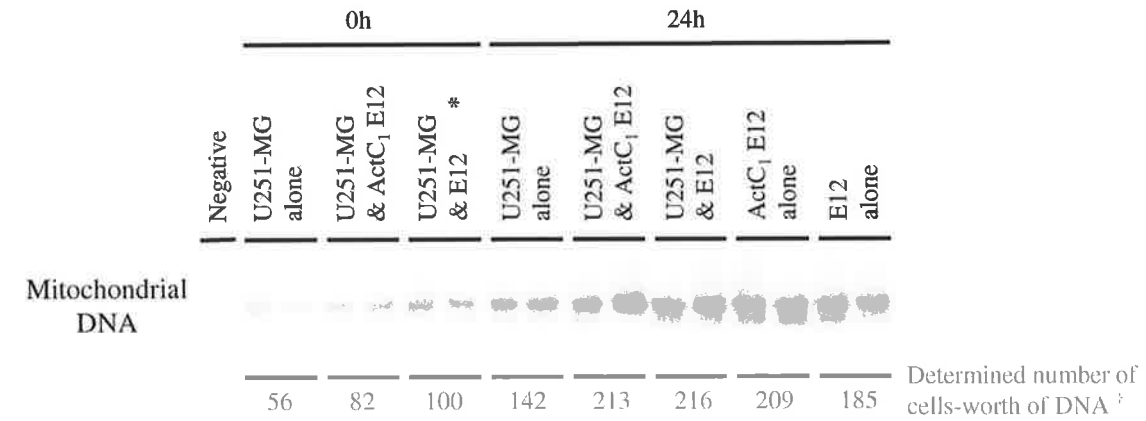
0h
24h
Negative
U251-MG alone
U251-MG & ActC1 E12
U251-MG * & E12
U251-MG alone
U251-MG & ActC1 E12
U251-MG & E12
ActC1 E12 alone
E12 alone
Mitochondrial DNA
56
82
100
142
213
216
209
185
Determined number of cells-worth of DNA

B.

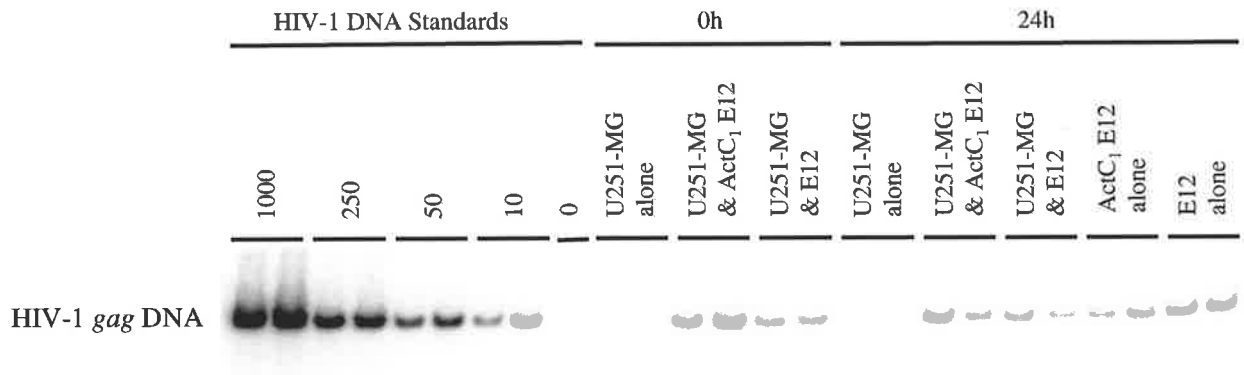
HIV-1 DNA Standards
0h
24h
1000
250
50
10
0
U251-MG alone
U251-MG & ActC1 E12
U251-MG & E12
U251-MG alone
U251-MG & ActC1 E12
U251-MG & E12
ActC1 E12 alone
E12 alone
HIV-1 gag DNA

C.

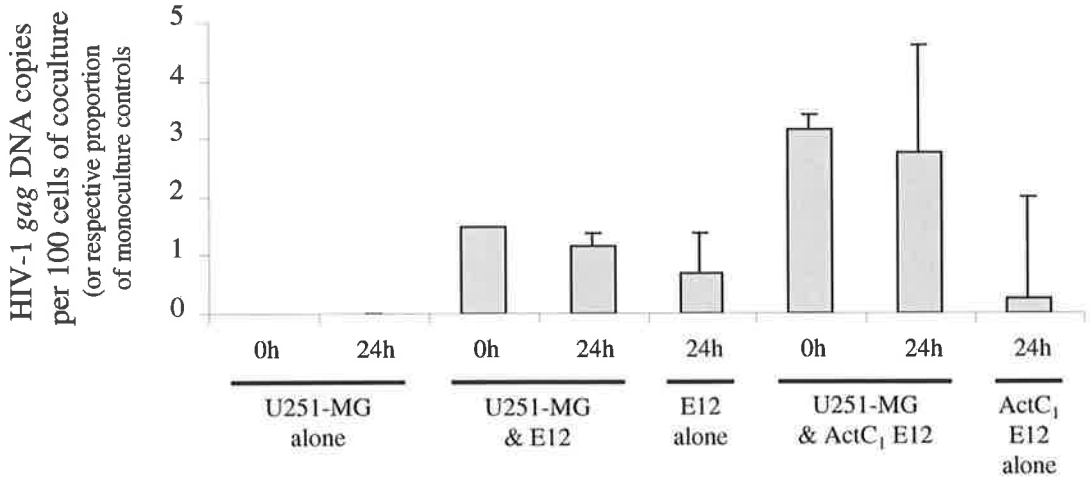
HIV-1 gag DNA copies per 100 cells of coculture (or respective proportion of monoculture controls
5
4
3
2
1
0
0h
24h
0h
24h
24h
0h
24h
24h
U251-MG alone
U251-MG & E12
E12 alone
U251-MG & ActC1 E12
ActC1 E12 alone

Figure 3.2 Analysis of transmission of HIV-1_{SF2} and HIV-1_{IIIB} upon coculture of E12 or HIIIB cells with trypsin-treated U251-MG astrocytes.

$ActC_1$ pre-treatment and cell-to-cell infections were performed as described in Figure 3.1, and the extrachromosomal DNA extracted at either 0 or 24h. The extrachromosomal DNA extraction efficiency was determined by subjecting the DNA from approximately 50 cells (0h cell counts) to mitochondrial PCR and Southern hybridisation (**A**). The relative extrachromosomal DNA extraction efficiency was determined by comparison to extrachromosomal DNA from U251-MG cell number standards, and the number of cells-worth of DNA present in each sample determined (†). Duplicate PCR reactions (22 cycles) were performed on each extrachromosomal DNA sample.

To determine the extent of HIV-1 reverse transcription which had occurred in these cultures, 5000 cells-worth of extrachromosomal DNA from each coculture or unmixed control monoculture was subjected to HIV-1 *gag* PCR followed by Southern hybridisation (**B**). The number of HIV-1 *gag* DNA copies per 5000 cells was determined by comparison to HA8 HIV-1 DNA copy number standards. HIV-1 *gag* DNA copy numbers in the control monocultures were adjusted to represent the proportion of these cells present in the cocultures, that is, 3333 U251-MG cells and 1667 of E12 cells (**C**). Error bars represent the standard error between the duplicate HIV-1 *gag* PCR reactions (29 cycles) performed on each extrachromosomal DNA sample.

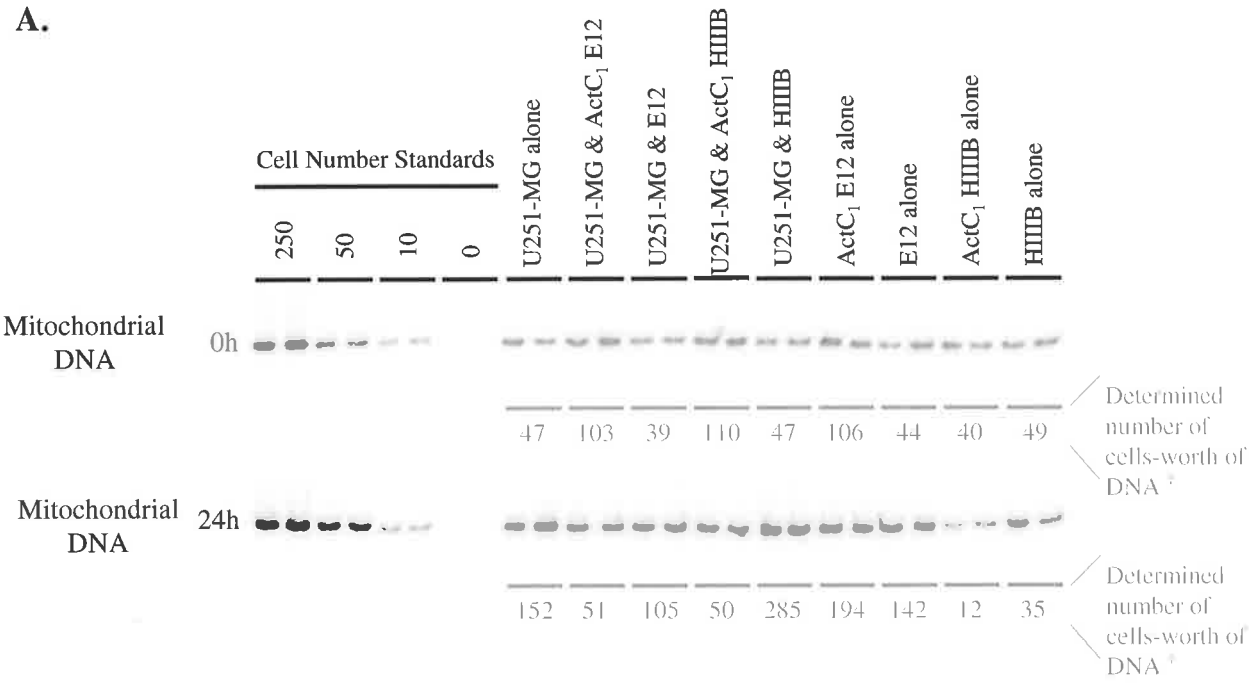
A.
Cell Number Standards
250
50
10
0
U251-MG alone
U251-MG & ActC1 E12
U251-MG & E12
U251-MG & ActC1 HIIIB
U251-MG & HIIIB
ActC1 E12 alone
E12 alone
ActC1 HIIIB alone
HIIIB alone
Mitochondrial DNA
0h
47 103 39 110 47 106 44 40 49
Determined number of cells-worth of DNA
Mitochondrial DNA
24h
152 51 105 50 285 194 142 12 35
Determined number of cells-worth of DNA

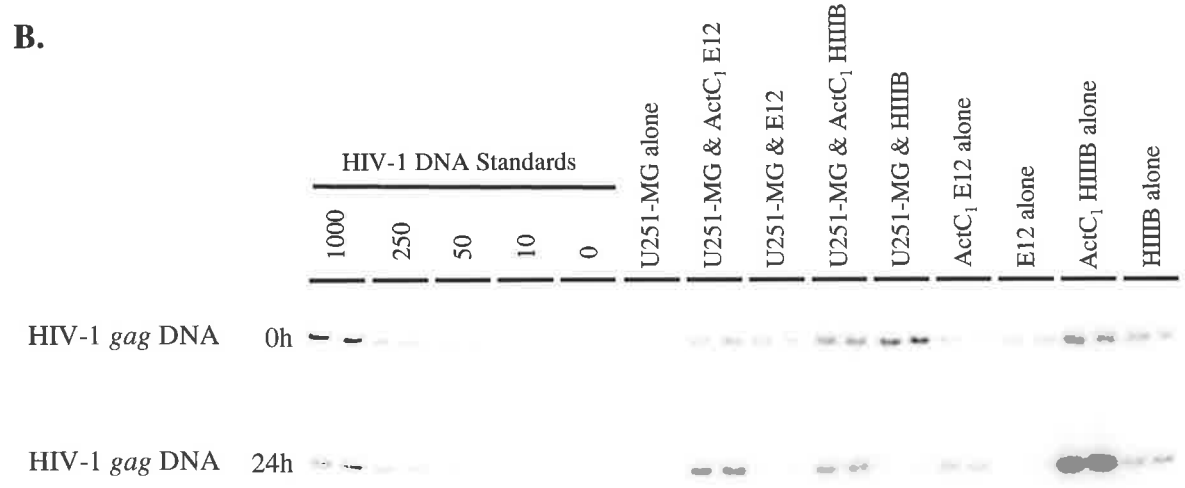
B.
HIV-1 DNA Standards
1000
250
50
10
0
U251-MG alone
U251-MG & ActC1 E12
U251-MG & E12
U251-MG & ActC1 HIIIB
U251-MG & HIIIB
ActC1 E12 alone
E12 alone
ActC1 HIIIB alone
HIIIB alone
HIV-1 gag DNA
0h
HIV-1 gag DNA
24h

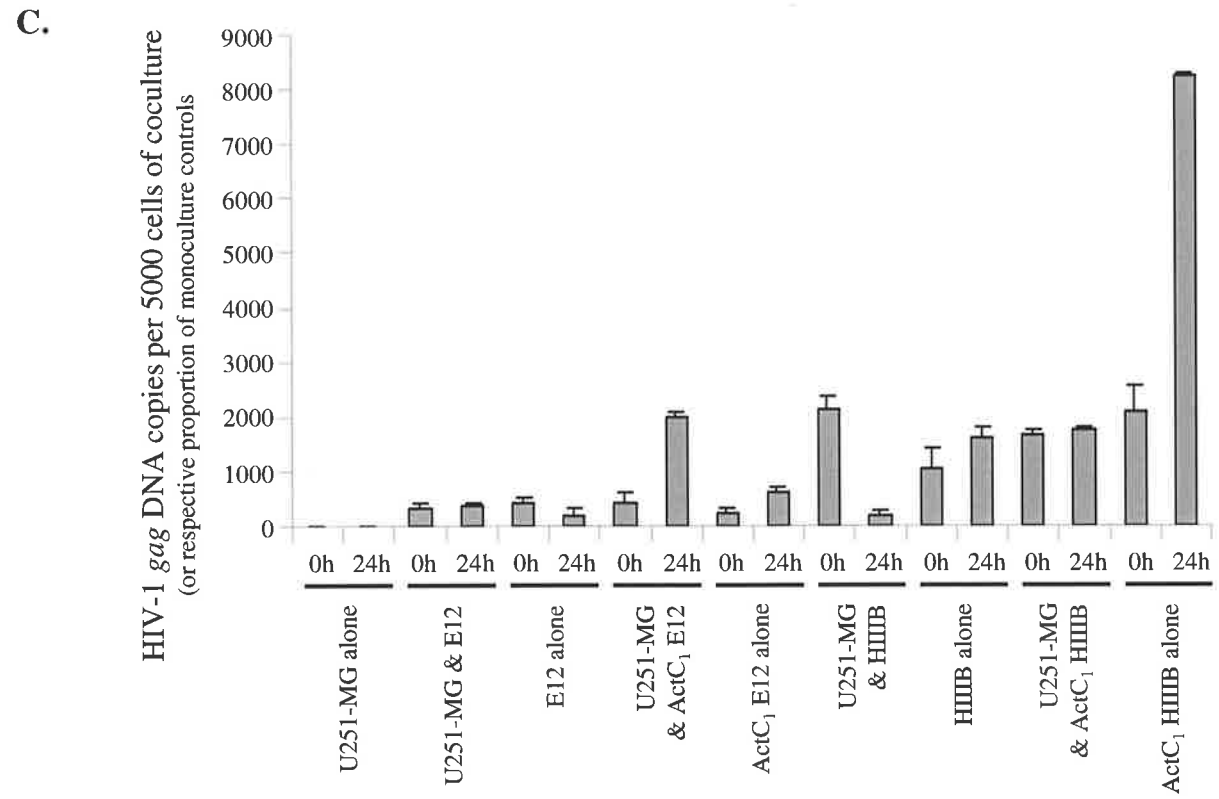
C.
HIV-1 gag DNA copies per 5000 cells of coculture
(or respective proportion of monoculture controls
9000
8000
7000
6000
5000
4000
3000
2000
1000
0
0h 24h 0h 24h 0h 24h 0h 24h 0h 24h 0h 24h 0h 24h 0h 24h 0h 24h
U251-MG alone
U251-MG & E12
E12 alone
U251-MG & ActC1 E12
ActC1 E12 alone
U251-MG & HIIIB
HIIIB alone
U251-MG & ActC1 HIIIB
ActC1 HIIIB alone

A similar phenomenon of increasing levels of extrachromosomal HIV-1 DNA was observed in the $ActC_1$ treated HIIIB monoculture control in the experiment shown in Figure 3.2. This was unexpected, as the inhibition of transcription by the $ActC_1$ treatment had been verified by tritiated uridine uptake analysis in these cells. This suggested that this increase in extrachromosomal HIV-1 *gag* DNA did not arise from reverse transcription. An alternative explanation may be the death of a proportion of the $ActC_1$ treated HIIIB cells, due to the toxicity of the drug. Apoptosis of these cells would result in fragmentation of their chromosomal DNA into small lengths. As the separation of chromosomal DNA from extrachromosomal DNA by the Hirt method (Section 2.6.3) is based on the size difference between of these two types of DNA molecules, small fragments of apoptotic chromosomal DNA would extract with the extrachromosomal, and not chromosomal, DNA fraction. As HIIIB cells contain an integrated copy of HIV-1 DNA in their chromosome, upon apoptosis this HIV-1 DNA may end up in the "extrachromosomal" DNA fraction, potentially explaining the increase in HIV-1 *gag* DNA detected in these cells. However this increase in extrachromosomal HIV-1 *gag* DNA in the $ActC_1$ treated HIIIB monoculture was not observed in the respective coculture. To better understand what was occurring in these cultures, the experiment was repeated with a more detailed time course of analysis (0, 12, 24 and 48h). Also, due to the possibility that HIV-1 was not being transmitted to the U251-MG cells due to the pretreatment of these cells with trypsin before coculture (trypsin treatment may have cleaved the cell surface receptors necessary for HIV-1 to attach to and enter U251-MG astrocytes), the U251-MG cells in the subsequent experiment were pre-seeded at least 18h prior to coculture. This would allow the cells to recover and re-express their normal complement of cell surface molecules.

3.3 Culture of Astrocytes with Persistently infected T-cell lines

3.3.1 Analysis of transmission of HIV-1 from E12 and HIIIB cells to U251-MG astrocytes

Cocultures and control monocultures were set up as described for the preliminary experiments in Section 3.2.2ii, except that the U251-MG astrocytes were *pre-seeded* approximately 18 h prior to coculturing (to enable any surface receptors which had been stripped by trypsin to be regenerated) and more time points were examined (0, 12, 24, and

48h post coculture). To confirm the ability of the persistently infected viral donor cell lines to transmit infection to uninfected cells, parallel cocultures were set up with a HIV-1 susceptible T-cell line (HuT-78) as virus recipient cells, in place of the U251-MG cells. Virus-donor cells (E12 and HIIIB cells) were again pre-treated with or without the transcriptional inhibitor, $ActC_1$.

a) E12 virus-donor cells

The coculture of (untreated) E12 cells with HuT-78 cells resulted in transmission of infection to the HuT-78 cells, confirming the ability of the E12 cells to transmit HIV-1. This was evident by the dramatic increase in extrachromosomal HIV-1 *gag* DNA in these cocultures within the first 12h of coculture, indicating significant viral reverse transcription had occurred (Figure 3.3Ci). It was expected that the products of reverse transcription would continue to accumulate over the 48h period, however this was not observed. This may have been due to the outgrowth of uninfected HuT-78 cells in this culture, or more likely, due to the cytopathogenicity of the viral infection, as by 48h syncytia formation and significant cell death was apparent in this culture. In contrast to the HuT-78 / E12 coculture, only a slight increase in the level of extrachromosomal HIV-1 *gag* DNA was detected in the E12 control monoculture. In the U251-MG / E12 coculture only a modest increase in extrachromosomal HIV-1 *gag* DNA was apparent over the 48h period (Figure 3.3Ci), and when compared to the E12 monocultures it was not clear whether this represented genuine *de novo* viral reverse transcription in the U251-MG cells or the background level of HIV-1 DNA in the virus-donor cells. If the increase in HIV-1 DNA in the U251-MG / E12 cocultures did indicate genuine reverse transcription in the U251-MG cell population, a similar increase in the level of extrachromosomal HIV-1 *gag* DNA would be expected in the U251-MG / $ActC_1$ treated E12 cocultures. However, unlike the findings in Figure 3.2, this was not the case (Figure 3.3Cii). Also, the level of HIV-1 *gag* DNA in the U251-MG / $ActC_1$ treated E12 cocultures in Figure 3.3Cii was much less at 12, 24 and 48h than in the $ActC_1$ treated E12 monoculture controls. Surprisingly the level of HIV-1 *gag* DNA in the $ActC_1$ treated E12 monoculture controls increased with time, similar to the anomaly seen with the $ActC_1$ treated HIIIB monoculture controls in the preliminary experiment described in Section 3.2.2ii and Figure 3.2C. The potential for the $ActC_1$ treated E12 cells to transmit infection to susceptible cells was verified by the dramatic increase in extrachromosomal HIV-1 DNA within the first 12 hours of coculture with HuT-78 cells, which was much

Figure 3.3 Analysis of transmission of HIV-1_{SF2} and HIV-1_{IIIB} upon coculture of E12 or HIIIB cells with pre-seeded U251-MG astrocytes.

U251-MG ("virus-recipient") cells were pre-seeded approximately 18h prior to coculture (mixing) with ±$ActC_1$ pre-treated E12 and HIIIB cells at an approximate ratio of 2 U251-MG cells per virus-donor cell. Control cocultures were also performed with HIV-1 susceptible cells (HuT-78 cells) as the virus-recipients. The cocultures and respective monoculture controls were harvested immediately or after 12, 24 or 48h of (co)culture, and the extrachromosomal DNA extracted.

The extrachromosomal DNA extraction efficiency was determined by subjecting the DNA from approximately 50 cells (0h cell counts) to mitochondrial PCR and Southern hybridisation (**A**). The relative extrachromosomal DNA extraction efficiency was determined by comparison to extrachromosomal DNA from U251-MG cell number standards, and the number of cells-worth of DNA present in each sample determined (†). * indicates a sample which was quantified from a repeat PCR reaction (not shown). Duplicate PCR reactions (15 cycles) were performed on each extrachromosomal DNA sample.

To determine the extent of HIV-1 reverse transcription which had occurred in these cultures, 5000 cells-worth of extrachromosomal DNA from each coculture or unmixed control monoculture was subjected to HIV-1 *gag* PCR followed by Southern hybridisation (**B**). The number of HIV-1 *gag* DNA copies per 5000 cells was determined by comparison to HA8 HIV-1 DNA copy number standards. HIV-1 *gag* DNA copy numbers in the control monocultures were adjusted to represent the proportion of these cells present in the cocultures, that is, 3333 U251-MG cells and 1667 E12 cells (**C**). Error bars represent the standard error between the duplicate HIV-1 *gag* PCR reactions (20 cycles) performed on each extrachromosomal DNA sample.

A. Mitochondrial DNA

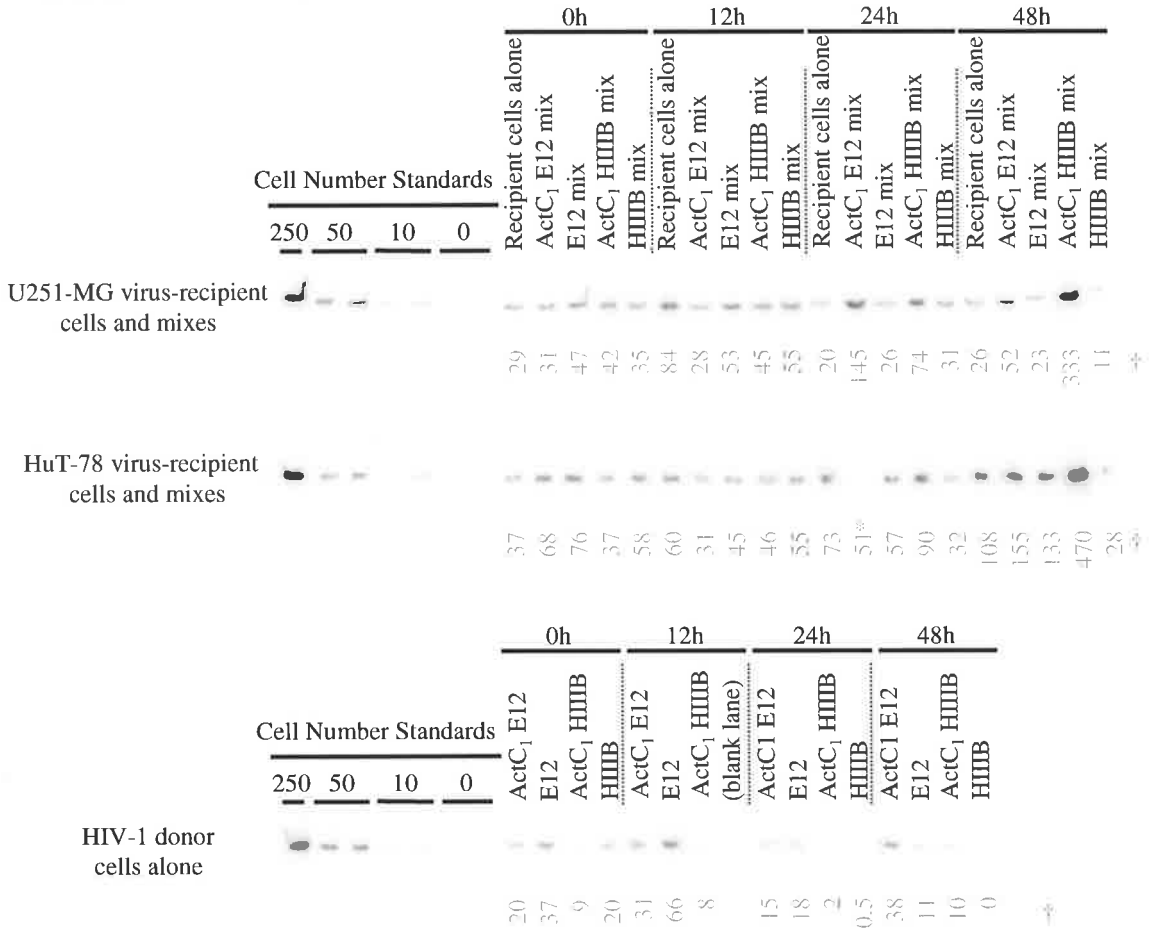

B. HIV-1 *gag* DNA

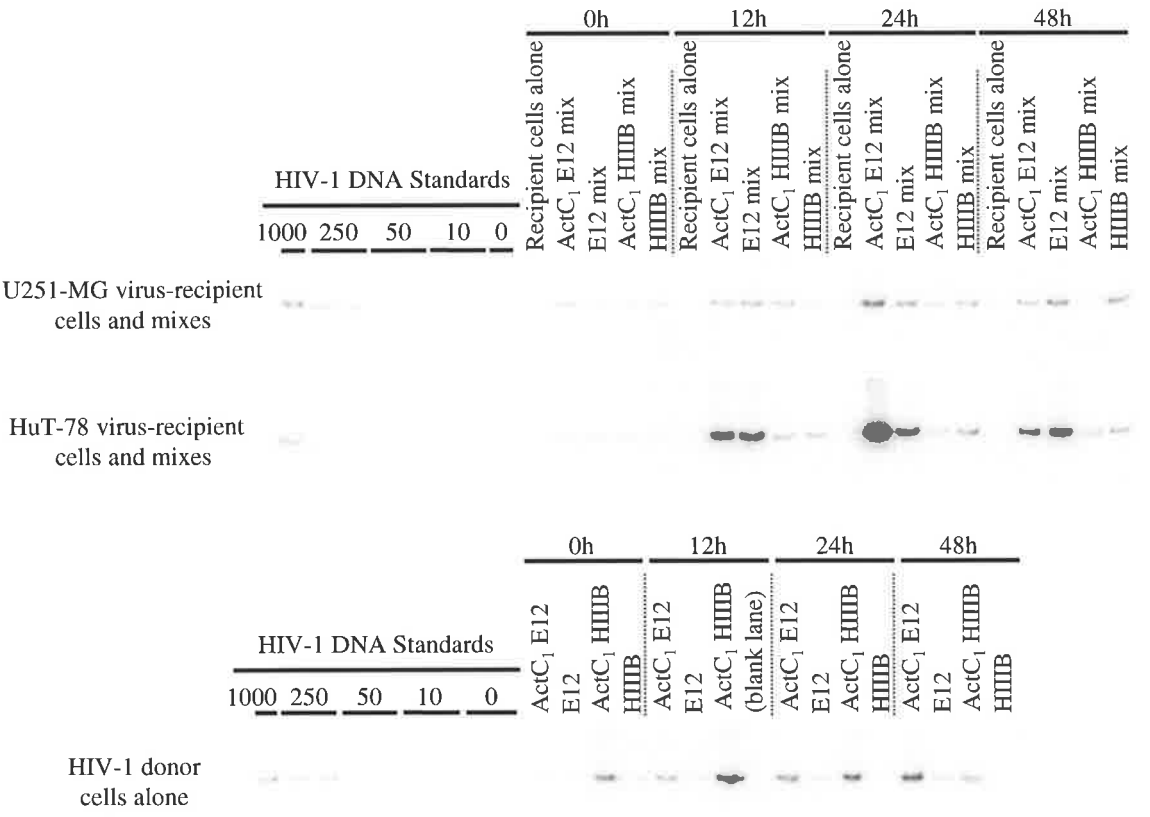

C.

i) E12 donor cells

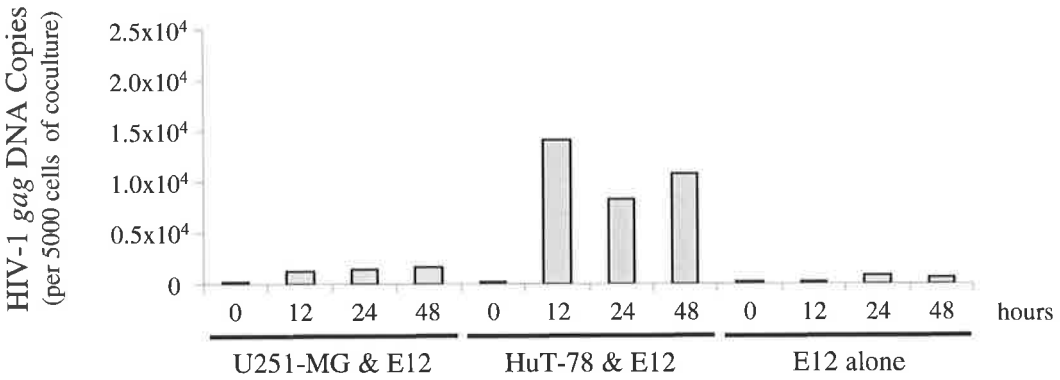

ii) ActC$_1$ E12 donor cells

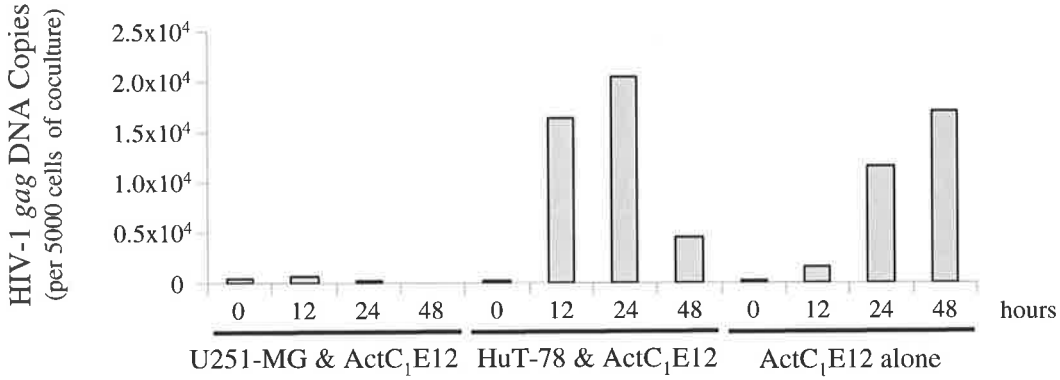

iii) HIIIB donor cells

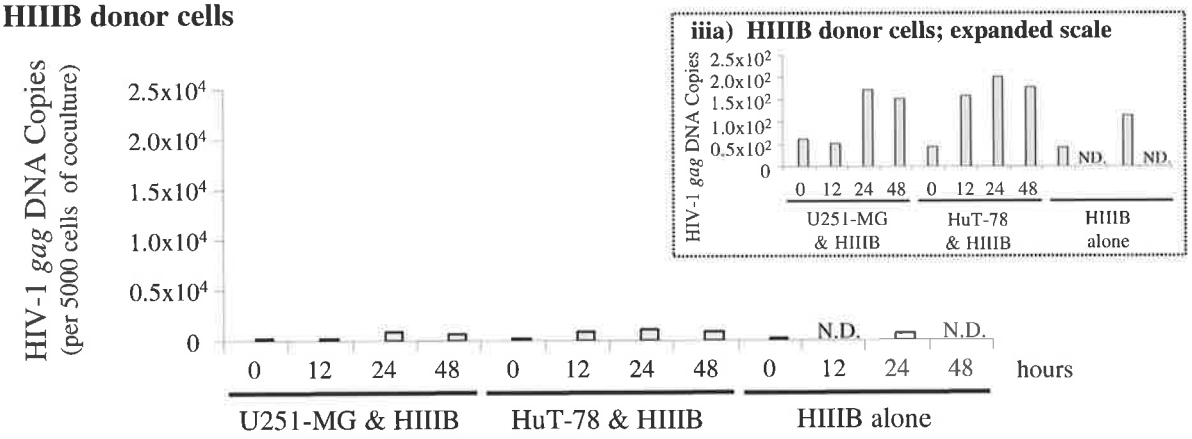

iiia) HIIIB donor cells; expanded scale

iv) ActC$_1$ HIIIB donor cells

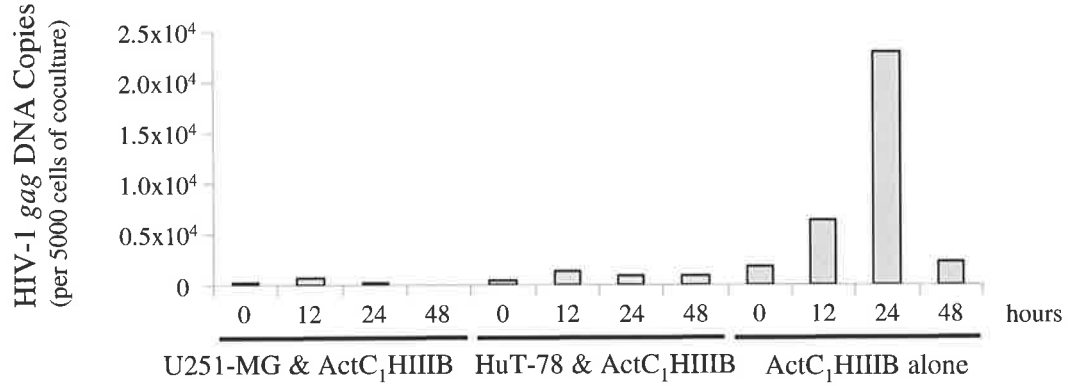

greater than the level of HIV-1 DNA in the $ActC_1$ treated E12 monoculture controls at 12 and 24h. The decline at 48h in the HuT-78 / $ActC_1$ treated E12 cocultures is likely to be due to the death of infected cells and possible outgrowth of uninfected cells.

b) HIIIB virus-donor cells

The level of HIV-1 *gag* DNA in cocultures and monoculture controls with ± $ActC_1$ treated HIIIB cells (Figure 3.3Ciii-iv) is presented on the same axis as the data from cocultures and monocultures with ± $ActC_1$ treated E12 cells (Figure 3.3Ci-ii), which demonstrates that, even with HuT-78 cells as the virus-recipient cells, the level of reverse transcription is much lower with HIIIB virus-donor cells than E12 virus-donor cells. Transmission and productive infection in the HuT-78 / HIIIB cocultures was indicated by the observation of syncytia at 48h. Yet, only a modest increase in extrachromosomal HIV-1 DNA was observed in this coculture by 12h (Figure 3.3Ciiia). Whether this represented a genuine increase in HIV-1 DNA compared to the HIIIB cells alone at 12h was not determined. At 24h the level of HIV-1 *gag* DNA is elevated in the U251-MG / HIIIB and the HuT-78 / HIIIB cocultures, however HIV-1 *gag* DNA is also elevated (to a lesser extent) in the HIIIB monoculture control. Due to the level of HIV-1 DNA in the extrachromosomal fraction of HIIIB monocultures, and due to the limited increase in the level of HIV-1 *gag* DNA upon coculture of these HIIIB cells with HIV-1 susceptible HuT-78 cells, it is difficult to interpret the ability of the HIIIB cells to transmit $HIV\text{-}1_{IIIB}$ virus to U251-MG astrocytes.

Cocultures with $ActC_1$ treated HIIIB cells did not appear to result in infection in either U251-MG or HuT-78 cells when compared to the $ActC_1$ treated HIIIB monoculture controls. However, the dramatic increase in the level of HIV-1 *gag* DNA in the extrachromosomal fraction of $ActC_1$ treated HIIIB cells from 0 to 24h (which was also observed in Experiment 2; Figure 3.2C), was unexpected. This was not expected because i) ongoing reverse transcription in this chronically infected cell line was expected to be minimal or absent, and ii) $ActC_1$ treatment should abolish the majority of reverse transcription and transcription in these cells. Indeed, analysis of titriated uridine uptake in these cells verified that the $ActC_1$ treatment gave maximal inhibition of transcription. Together this implied that the source of increasing extrachromosomal HIV-1 *gag* DNA levels (from 0 to 24h) in $ActC_1$ treated HIIIB cells did not represent *de novo* reverse transcription. As discussed in Section 3.2.2ii, this may be due to $ActC_1$ toxicity, causing cell death which may lead to the presence of degraded

chromosomal DNA (including the HIV-1 provirus) in the extrachromosomal DNA fraction. In this scenario, the use of $ActC_1$ would confound rather than clarify the interpretation of any increase in HIV-1 DNA in cocultures. Curiously, the increase in HIV-1 *gag* DNA seen in $ActC_1$ trcated HIIIB monocultures was not apparent in either the U251-MG or HuT-78 cocultures, suggesting HIIIB are less susceptible to $ActC_1$ toxicity in these coculture environments. The reasons for this are not clear, but may involve different cell growth kinetics in the different culture micro-environments. The recovery of extrachromosomal DNA from both ± $ActC_1$ treated HIIIB monocultures was also low (Figure 3.3A), which could indicate poor survival or growth of these cells. This may also reduce the accuracy of interpreting HIV-1 *gag* DNA content as a function of mitochondrial DNA content.

Summary

To summarise the findings thus far from the three experiments with ± $ActC_1$ treated viral donor cells, $ActC_1$ treatment was not useful in reducing reverse transcription in the viral donor cells. Instead of decreasing the amount of HIV-1 *gag* DNA detected in the extrachromosomal DNA fraction of the control monocultures, $ActC_1$ resulted in an increased level of HIV-1 *gag* DNA in these fractions. This is most likely due to cell death and the consequent degradation of chromosomal DNA, containing HIV-1 DNA, which would then separate into the "extrachromosomal" fraction upon Hirt DNA extraction. It is also difficult to assess the background level of HIV-1 *gag* DNA in untreated HIIIB cell monocultures compared to the respective cocultures as the growth / survival of these cells in the monocultures appeared poor according to the level of mitochondrial DNA in the extrachromosomal DNA extractions. E12 viral donor cells appear much more effective at transmitting HIV-1 infection to the HIV-1 susceptible HuT-78 cells than HIIIB viral donor cells. Indeed the amount of virus transmitted from the HIIIB cells appears very low, as only a modest increase in HIV-1 *gag* DNA occurred in HuT-78 / HIIIB cocultures compared to the HIIIB control monoculture in Experiment 3. Never-the-less, syncytia formation was observed after 48h of HuT-78 / HIIIB coculture, indicating that HIV-1 infection of the HuT-78 cells did occur. The experiment shown in Figure 3.3 suggested that E12 cells may be capable of transmission of $HIV\text{-}1_{SF2}$ to U251-MG cells, however this was not apparent in either of the preliminary experiments (Figures 3.1 and 3.2), and would require further clarification. However in the two preliminary experiments (Figures 3.1 and 3.2) the U251-MG cells had been treated with trypsin prior to coculturing. Trypsin may cleave the

astrocyte surface epitopes required for HIV-1 attachment and entry. Therefore, to clarify whether E12 cells could transmit HIV-1_{SF2} to pre-seeded U251-MG cells and whether viral reverse transcription subsequently occurred in these astrocyte cells, the experiment was repeated in the presence or absence of the reverse transcriptase inhibitor, AZT (see below).

3.3.2 AZT treatment to distinguish between *de novo* reverse transcription and pre-formed HIV-1 DNA

To clarify whether the modest increase in extrachromosomal HIV-1 *gag* DNA in the U251-MG / E12 coculture in Section 3.3.1 (Figure 3.3) represented transmission to, and subsequent reverse transcription of, HIV-1_{SF2} in the U251-MG astrocytes, the experiment was repeated with the inclusion of an inhibitor of reverse transcription, AZT. AZT is a thymidine analogue, and as such the phosphorylated form is included into the nascent reverse transcribing HIV-1 DNA strand. The inclusion of AZT into the nascent DNA strand terminates strand synthesis, thus inhibiting reverse transcription (Sections 2.3.1iii and 2.7.5i). AZT was tested and shown not to be cytotoxic to U251-MG cells, and has been previously shown not be toxic to HuT-78 cells (Section 2.7.5i). For the AZT treated cultures, both the virus-donor (E12) and virus-recipient cells (U251-MG or HuT-78) were pre-treated with 20μM AZT for 18h prior to coculture, and AZT was maintained at this concentration throughout the (co)culture. If HIV-1_{SF2} transmission and *de novo* reverse transcription occurred upon coculture of U251-MG astrocytes with E12 cells, an increase in extrachromosomal HIV-1 *gag* DNA would be expected in the in the drug-free cocultures (compared to the E12 monoculture controls) but not the AZT treated U251-MG / E12 cocultures.

E12 cells were confirmed to transmit infection to HIV-1 susceptible cells, as shown by the dramatic increase in extrachromosomal HIV-1 *gag* DNA from 0 to 24h of E12 / HuT-78 coculture, and compared to the E12 monoculture control (Figure 3.4A,B). The numerical difference in the number of HIV-1 *gag* DNA copies per 5000 cells-worth of DNA between this and previous experiments was most likely due to partial degradation of the HA8 standards in the analysis of previous experiments. This would result in the overestimation of HIV-1 *gag* DNA copies in the samples, but this does not alter the comparative interpretation provided above. In this experiment, and in all subsequent experiments in this thesis, fresh

Figure 3.4 Analysis of transmission of HIV-1_{SF2} infection upon coculture of ± AZT treated E12 cells with ± AZT treated, pre-seeded U251-MG astrocytes.

U251-MG astrocytes ("virus-recipients") were pre-seeded 18h prior to coculturing with E12 cells ("virus-donors"). These cocultures were either i) untreated, ii) treated with AZT*, or iii) used $ActC_1$ treated E12 cells[§], as described below:

Untreated: neither virus-recipient nor virus-donor cell population treated.

* AZT treated: both virus-recipient and virus-donor cells were pre-treated for 18h with 20μM AZT immediately prior to coculturing. The AZT was maintained at 20μM throughout the experiment.

[§] $ActC_1$ treated E12 cells were pre-treated with 12 μg/ml $ActC_1$ for 2h, then washed to remove excess drug, prior to coculturing with U251-MG cells. ($ActC_1$ was not maintained during the course of the experiment).

HIV-1 susceptible cells (HuT-78 cells) were included as an additional virus-recipient cell type as a positive control for virus transmission upon coculture. The cocultures and respective monoculture controls were harvested immediately or after 24 h of (co)culture, and the extrachromosomal DNA extracted.

Extrachromosomal DNA extraction efficiency was determined by subjecting the DNA from approximately 50 cells of coculture (0h cell counts), or the respective proportion of cells from the monoculture controls (ie. 33 cells of U251-MG or HuT-78 cultures and 16.7 cells of E12 cells) 15 cycles of mitochondrial PCR, followed by Southern hybridisation (**A**). The relative extrachromosomal DNA extraction efficiency was determined by comparison to extrachromosomal DNA from U251-MG cell number standards, and the number of cells-worth of DNA present in each sample determined.

To determine the extent of HIV-1 reverse transcription which had occurred in these cultures, 5000 cells-worth of extrachromosomal DNA from each coculture, or the respective amount of DNA from the monculture controls (3333 U251-MG cells or HuT-78 DNA and 1667 E12 cells) was analysed by 20 cycles of HIV-1 *gag* PCR followed by Southern hybridisation (**A**). Each lane represents a separate culture (each 24 h (co)culture was performed in duplicate). The number of HIV-1 *gag* DNA copies from each sample was determined by comparison to HA8 HIV-1 DNA copy number standards (**B**). The data from the U251-MG cells cocultured with the E12 cells, and the E12 cells alone (no virus recipient), are also presented on an expanded scale (**C**). Error bars represent the standard error between the duplicate 24h (co)cultures in the HIV-1 *gag* PCR reactions.

A.

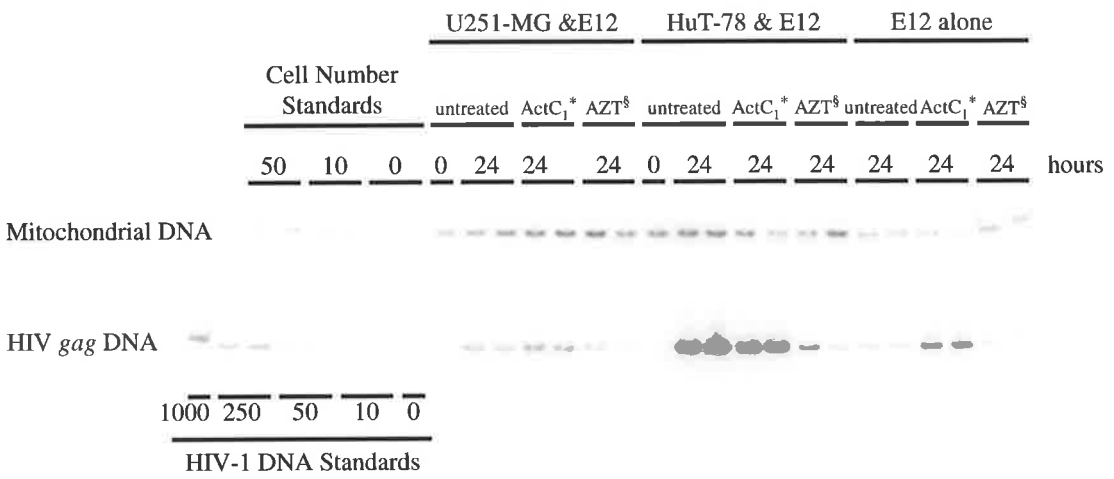
U251-MG &E12
HuT-78 & E12
E12 alone
Cell Number Standards
untreated
ActC1*
AZT§
untreated
ActC1*
AZT§
untreated
ActC1*
AZT§
50 10 0 0 24 24 24 0 24 24 24 24 24 24
hours
Mitochondrial DNA
HIV gag DNA
1000 250 50 10 0
HIV-1 DNA Standards

B.

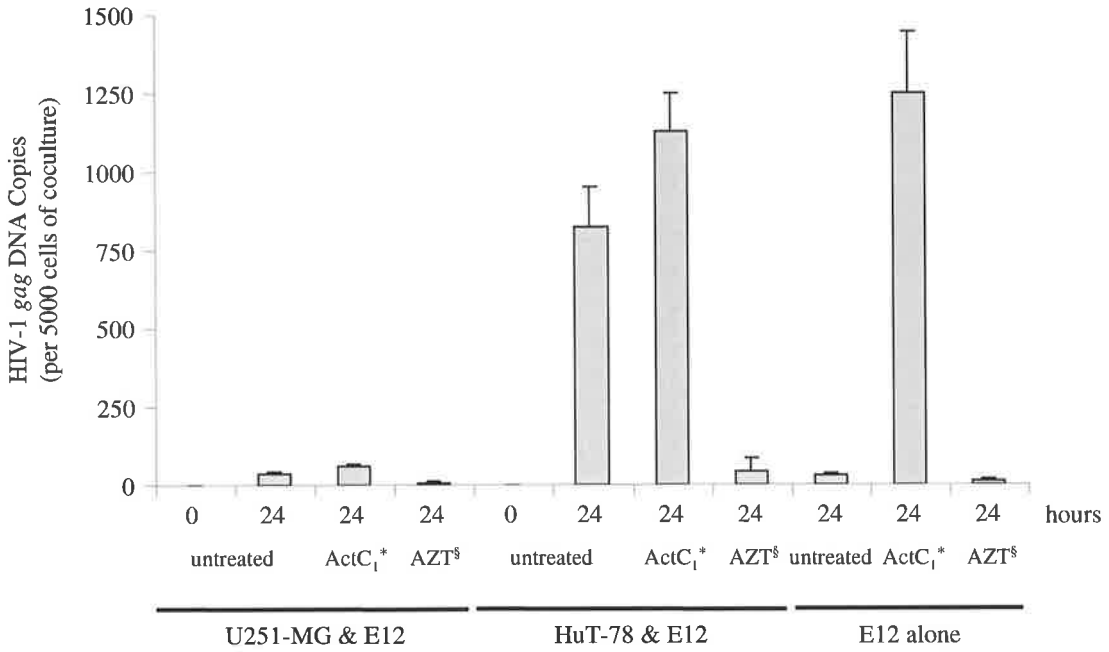
HIV-1 gag DNA Copies (per 5000 cells of coculture)
1500
1250
1000
750
500
250
0
0 24 24 24 0 24 24 24 24 24 24
hours
untreated
ActC1*
AZT§
untreated
ActC1*
AZT§
untreated
ActC1*
AZT§
U251-MG & E12
HuT-78 & E12
E12 alone

C.

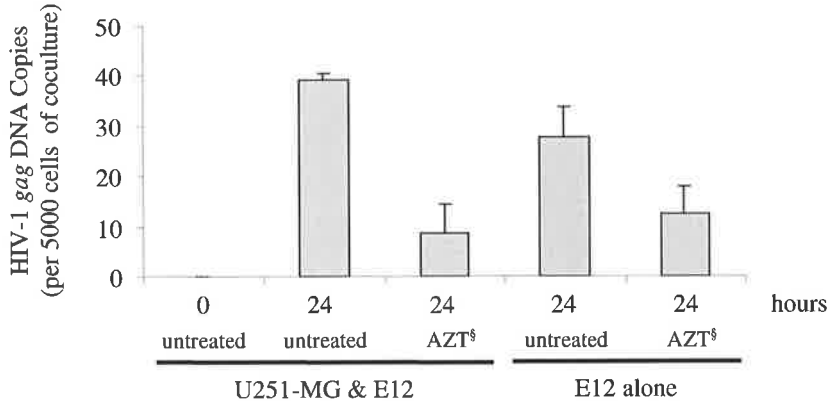
HIV-1 gag DNA Copies (per 5000 cells of coculture)
50
40
30
20
10
0
0 24 24 24 24
hours
untreated
untreated
AZT§
untreated
AZT§
U251-MG & E12
E12 alone

HA8 standards were thawed from the same batch of single use aliquots stored at –80°C, to ensure accuracy and consistency across experiments.

AZT abolished the accumulation of HIV-1 *gag* DNA in the 24h HuT-78 / E12 cocultures by >95%, demonstrating that AZT effectively inhibited reverse transcription in this coculture, and that the increase in HIV-1 *gag* DNA in the untreated HuT-78 / E12 coculture at 24h (compared to the E12 monoculture) was indeed due to *de novo* viral reverse transcription. As in previous experiments, treatment of the virus-donor cells with $ActC_1$ gave elevated levels of HIV-1 *gag* DNA in the extrachromosomal DNA fractions and did not assist the experimental analysis. The level of extrachromosomal HIV-1 *gag* DNA increased from 0 to 24h in the untreated U251-MG / E12 cocultures, and >75% of this increase was abolished in the presence of AZT. However the level of extrachromosomal HIV-1 *gag* DNA in these cocultures was similar to or less than the respective E12 monoculture controls. Therefore, within the level of sensitivity of this assay, reverse transcription could not be demonstrated in the U251-MG astrocytes upon coculture with E12 cells, although a very low level of U251-MG infection (<0.1%) cannot be excluded. Whilst astrocytes are reportedly more susceptible to infection with T-cell tropic HIV-1, the transmission of macrophage tropic HIV-1 would be of greater physiological significance to astrocyte infection *in vivo*, as astrocytes in the brain may come into contact with HIV-1 infected macrophages and microglia. The cell-to-cell transmission of HIV-1 from chronically infected macrophages to astrocytes is explored below.

3.4 Culture of Astrocytes with Chronically infected Macrophages

To investigate the cell to cell transmission of macrophage tropic HIV-1 from infected macrophages to uninfected astrocytes, cocultures were performed and the level of extrachromosomal HIV-1 DNA (as an indicator of HIV-1 entry and reverse transcription) analysed. MDMs were infected with $HIV\text{-}1_{BaL}$ 2 to 4 weeks prior to coculturing with U251-MG astrocytes. This was to establish a chronic infection in the MDMs in order to minimise the degree of *de novo* reverse transcription in the MDM population by the time of coculture. To prevent the carryover of HIV-1 DNA from MDMs which may have lysed during the course of infection, the MDMs were treated with DNase I overnight (then washed to removed excess DNase) prior to coculturing with U251-MG astrocytes. The U251-MG cells

were then cocultured with infected MDMs and the extrachromosomal DNA extracted at designated times. To assess the contribution of extrachromosomal HIV-1 *gag* DNA from the HIV-1_{BaL} infected MDMs, parallel MDM monocultures or "mock" cocultures were performed. For mock cocultures the respective numbers of infected MDMs and U251-MG astrocytes were cultured separately for the duration of the experiment, and combined immediately prior to harvesting the cells for extrachromosomal DNA extraction. The relative extraction efficiency was assessed by semi-quantitative Mitochondrial PCR and Southern hybridisation, and the level of HIV-1 reverse transcription assessed by semi-quantitative HIV-1 *gag* PCR and Southern hybridisation.

3.4.1 Coculture of U251-MG astrocytes with HIV-1_{BaL} infected MDMs

Analysis of transmission of HIV-1 from pre-seeded infected MDMs to trypsin-treated U251-MG astrocytes

To combine U251-MG astrocytes with the chronically infected MDMs (both are adherent cell types), in the first experiment described below U251-MG cells were resuspended with trypsin in order to be added to pre-seeded infected MDMs at a ratio of 5:1. The level of extrachromosomal HIV-1 DNA in the U251-MG cells which had been cocultured with infected MDMs for 24 h was not elevated in comparison to the infected MDM monoculture controls (Figure 3.5). Indeed, the level of HIV-1 DNA in the chronically infected MDMs was quite high, and so, a very low level of transmission of infection to the U251-MG cells would not have been discerned. The presence of the HIV-1 DNA in the MDM population is most likely due to ongoing *de novo* reverse transcription in these cultures, despite being used 3 weeks after the original infection. The pre-treatment of these infected MDMs with DNase I prior to coculture suggested that the source of the HIV-1 DNA in the extrachromosomal fraction is unlikely to be degraded chromosomal DNA. Ongoing reverse transcription in chronically infected MDMS has been observed previously (Dr Jillian Carr, personal communication). It is also possible that by treating the U251-MG cells with trypsin the surface molecules required for cell-cell transmission of HIV-1 to astrocytes may have been digested. Subsequent experiments avoided the use of trypsin on the U251-MG cells prior to coculturing, and attempted to minimise the contribution of extrachromosomal HIV-1 *gag*

Figure 3.5 Analysis of transmission of HIV-1_{BaL} upon coculture of infected MDMs with trypsin-treated U251-MG astrocytes.

Primary monocyte-derived macrophages (MDMs) were infected with HIV-1_{BaL} for 3 weeks, treated with 50μg/ml DNase I overnight and washed. U251-MG cells were detached with trypsin and added to the infected MDMs at a ratio of approximately 5 U251-MG cells per MDM. After 24h of coculture, the extrachromosomal DNA was extracted. To control for the potential contribution of HIV-1 DNA present in the infected MDMs, replica cultures of infected MDMs were maintained separately and harvested at the same time.

Extrachromosomal DNA extraction efficiency was determined by subjecting the DNA from approximately 50 cells of coculture (0h cell counts), or the respective proportion of cells from the MDM monoculture controls (ie. 8.3 cells) to 17 cycles of mitochondrial PCR, followed by Southern hybridisation (**A**). The relative extrachromosomal DNA extraction efficiency was determined by comparison to extrachromosomal DNA from U251-MG cell number standards, and the number of cells-worth of DNA present in each sample determined. The experiment included duplicate cocultures ("Mix A" and "Mix B") and MDM monoculture controls ("MDM A" and "MDM B"), and duplicate PCRs were performed on the DNA sample from each (co)culture.

To determine the level of HIV-1 reverse transcription occurring in these cultures, 1000 or 200 cells-worth of extrachromosomal DNA from each cell mix (or the respective proportion of extrachromosomal DNA from the MDM monoculture controls, ie 167 or 33 cells, respectively) was subjected to 22 cycles of HIV-1 *gag* PCR, followed by Southern hybridisation (**B**). Lanes represent separate cultures analysed at each of the two different dilutions. The number of HIV-1 *gag* DNA copies per 200 cells of coculture (or 33 cells of MDM alone) was determined by comparison to HA8 HIV-1 DNA copy number standards (**B**) and is represented in (**C**). Error bars represent the standard error between the average number of HIV-1 *gag* DNA copies derived from each of the duplicate (co)cultures.

A.

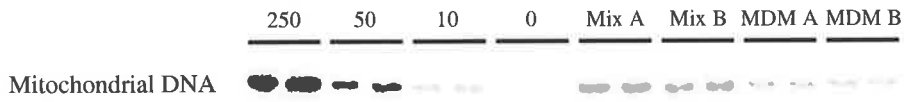
250
50
10
0
Mix A
Mix B
MDM A
MDM B
Mitochondrial DNA

B.

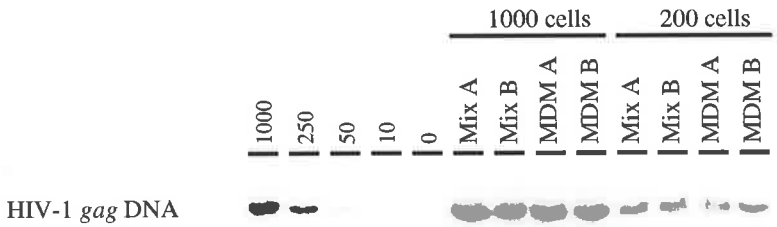
1000 cells
200 cells
1000
250
50
10
0
Mix A
Mix B
MDM A
MDM B
Mix A
Mix B
MDM A
MDM B
HIV-1 gag DNA

C.

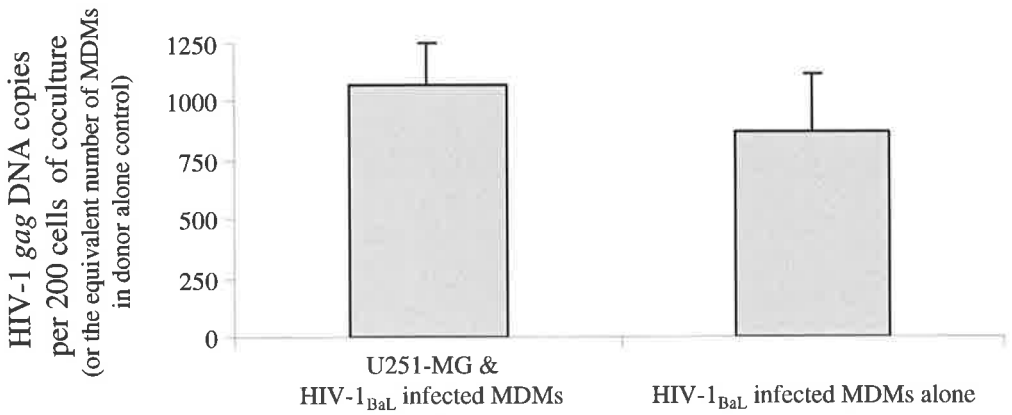
HIV-1 gag DNA copies per 200 cells of coculture
(or the equivalent number of MDMs in donor alone control)
1250
1000
750
500
250
0
U251-MG & HIV-1BaL infected MDMs
HIV-1BaL infected MDMs alone

DNA in the virus-donor MDMs by inhibiting reverse transcription in the MDMs or by separation of the two cell types after a period of coculture.

3.4.2 Minimising the contribution of HIV-1 replication in the virus-donor cell population.

To minimise the high level of HIV-1 *gag* DNA present in the infected viral donor MDM population (despite overnight treatment with DNase 1), in order to increase the potential to detect viral reverse transcription in the U251-MG cells upon coculture, the infected MDMs were pretreated with AZT pretreatment to inhibit ongoing HIV-1 reverse transcription in these viral donor cells, and separation of the two cell populations after coculturing was attempted. In these experiments, to avoid the use of trypsin, the astrocytes were suspended by cell scraping, and subsequent pipetting to obtain a relatively even cell suspension, then added to the pre-seeded MDMs.

Inhibiting transcription (including reverse transcription) in the MDM population with $ActC_1$ was not attempted due to the $ActC_1$ related complications described with T-cell line virus-donor cells (Sections 3.2.2ii and 3.3) and because previous studies in our laboratory have found that $ActC_1$ is toxic to MDMs, even at low concentrations (for example, 5µg/ml for 2 hours) and reduces their ability to transmit virus (Ms Helen Hocking and Dr Jillian Carr, personal communication).

3.4.2i AZT pre-treatment of the infected MDMs

Despite 48h of AZT treatment, a significant amount of HIV-1 DNA was detected in the extrachromosomal fraction of the mock cocultures, indicating a substantial amount of pre-formed intracellular extrachromosomal HIV-1 *gag* DNA was present in the infected MDMs (Figure 3.6). Similar to observations in the previous experiment with untreated, infected MDMs (Figure 3.5), no significant increase in extrachromosomal HIV-1 *gag* DNA was observed in the 24h U251-MG cocultures with AZT treated, infected MDMs compared to the mock coculture controls (Figure 3.6). This indicated that, within the sensitivity limitations of this assay, no reverse transcription in the U251-MG astrocytes could be detected upon coculture with infected MDMs over and above the background level of pre-

A.

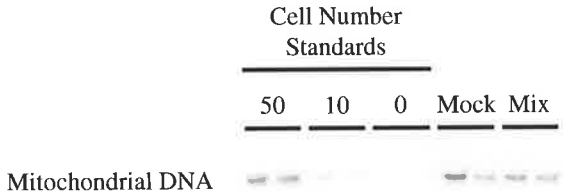

B.

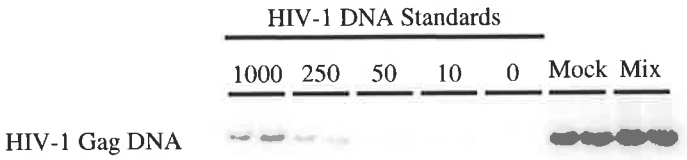

Figure 3.6 Analysis of transmission of HIV-1_{BaL} upon coculture of infected, AZT treated MDMs with *scraped* U251-MG astrocytes.

MDMs were infected with HIV-1_{BaL} for 12d, treated with AZT (20μM for 48h), and washed. U251-MG cells were detached by cell-scraping and added to the AZT treated infected MDMs and cocultured for 24h at a ratio of approximately 5 U251-MG cells per MDM, after which time the extrachromosomal DNA extracted. To control for the potential contribution of HIV-1 DNA present in the AZT treated HIV-1_{BaL} infected MDMs, replica cultures of infected MDMs and uninfected U251-MG cells were maintained separately and combined upon DNA harvest at 2 h ("mock" cocultures).

To determine the extrachromosomal DNA extraction efficiency, the amount of extrachromosomal DNA estimated to represent approximately 100 cells was subjected to mitochondrial PCR, followed by Southern hybridisation (**A**), and the number of cells-worth of DNA present in each sample determined by comparison to the amplification from U251-MG cell number standards. Each coculture was analysed by duplicate PCRs (20 cycles). To determine the level of HIV-1 reverse transcription occurring in these cultures, 1000 cells-worth of extrachromosomal DNA from each sample was subjected to 25 cycles of HIV-1 *gag* PCR, followed by Southern hybridisation (**B**).

formed extrachromosomal HIV-1 DNA in the infected MDMs alone, which persisted despite 2 days of AZT treatment. Again, the possibility that a low level of U251-MG infection was occurring could not be addressed by this assay.

3.4.2ii Separation of cell populations after coculturing.

To minimise the contribution of extrachromosomal HIV-1 DNA in the infected MDMs to the cocultures, separation of the two cell types after a period of coculture was attempted. It had been observed in previous experiments that the U251-MG cells settled onto the MDM monolayer within approximately one hour. (Whether this was merely due to gravity and adherent phenotype of the U251-MG cells, or whether specific interactions between the MDMs and U251-MGs were also involved, is not clear). $CD14^+$ cell depletion was trialed to selectively remove the MDMs from the U251-MG cells, and trypsin treatment was trialed to selectively remove the U251-MG cells from the MDMs. To assess the capacity of these techniques to separate the infected MDMs, they were applied after a short period of coculture (<4½h), when detection of HIV-1 DNA in the MDM-depleted U251-MG cell population could be used to assess persistence of MDM cells.

CD14 bead depletion of MDMs

To enable selection and removal of the CD14 positive MDMs from the cocultures by anti-CD14 magnetic beads, cocultures were performed in teflon pots to prevent cell adherence. Both the 14d infected MDMs and the U251-MG cells were suspended by cell scraping, and a relatively even cell suspension obtained for each culture by gentle pipetting. The cells were cocultured at a ratio of 10 U251-MG cells:1 infected MDM. After 4 hours of coculture, a sample was taken for microscopic analysis, which revealed single, unfused cells. The MDMs were then selectively removed by CD14 magnetic bead depletion. To control for any remaining MDMs, mock mixes were performed where the two cell populations were kept separate for the 4 hours of coculture and combined immediately prior to CD14 bead depletion. Analysis of the extrachromosomal DNA indicated a significantly lower level of mitochondrial DNA in the CD14 depleted coculture compared to the CD14 depleted mock coculture (Figure 3.7). This suggested that either the DNA extraction efficiency was poor in these particular samples, or that the majority of U251-MG cells were also lost upon CD14

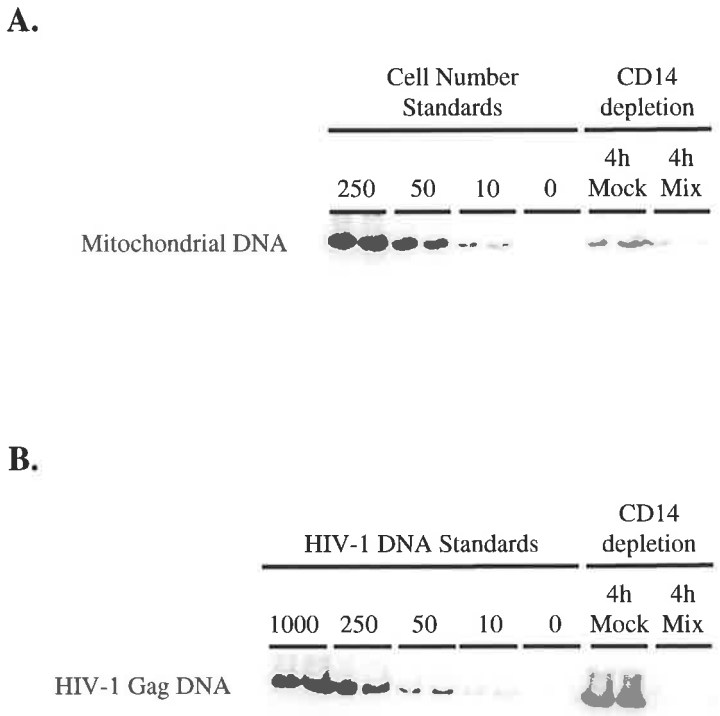

Figure 3.7 Separation of HIV-1_{BaL} infected MDM and U251-MG cell populations after coculture by CD14 bead depletion of the MDMs.

MDMs were infected with HIV-1_{BaL} for 14d, then suspended by cell-scraping. U251-MG cells were also detached by cell scraping. The U251-MG cells were cocultured with the infected MDMs at an approximate ratio of 10:1 in teflon pots. After 4h of coculture the infected MDMs were depleted from the coculture with anti-CD14 Magnetic Beads. Extrachromosomal DNA was extracted from the MDM depleted U251-MG cell population, and analysed for the relative presence of HIV-1 DNA by 24 and 29 cycles of mitochondrial and HIV-1 *gag* PCR respectively. To control for the proportion of infected MDMs which could persist in the MDM depleted U251-MG cell population, replica cultures of infected MDMs and uninfected U251-MG cells were maintained separately in teflon pots, treated with anti-CD14 magnetic beads, and the remaining cells pooled and harvested (mock coculture).

depletion, despite being CD14 negative. Surprisingly, a strong HIV-1 *gag* signal was detected from the mock coculture, indicating the presence of infected MDMs persisted despite the attempt to deplete $CD14^+$ cells from this sample. Yet HIV-1 *gag* DNA was not detectable in the 4 hour coculture after CD14 depletion, indicating that the CD14 positive MDM viral donor cells, which give rise to a background level of HIV-1 *gag* DNA, were removed from this sample. Together, this suggested that the bead depletion method was inconsistent between cell samples. Additionally, considerable loss of U251-MG cells during bead treatment of the cocultures was evidenced by the harvest of a visably smaller cell pellet for DNA extraction compared to the mock mix control, despite the fact that the starting cell numbers for each were the same at the commencement of the experiment, approximately 5 hours earlier. This indicated that a large proportion of the U251-MG cells were co-depleted with the MDMs via the affinity between these two cell types, even though the cells appeared separate by light microscopy.

Separation of U251-MG cells by trypsin treatment

Both astrocytes and macrophages are adherent cell types, but the adherence of astrocytes is trypsin sensitive whilst the adherence of macrophages is trypsin resistant. This difference was exploited in an attempt to selectively remove U251-MG cells from infected MDMS after a period of coculture. In a pilot experiment where U251-MG cells were cocultured with infected MDMs for 24h, it was observed that even exposure to 0.1% (v/v) trypsin for 30 min at 37°C the majority of the U251-MG cells remained adherent. In another experiment (Figure 3.8) the potential for trypsin to be used to separate U251-MG astrocytes from infected MDMs after a short period of coculture (2½ or 4½h) was assessed. At both time points it was clear by light microscopy that trypsin only detached a portion of the U251-MG cells and that some infected MDMs were also detached in this process. This was confirmed by the presence of extrachromosomal HIV-1 *gag* DNA in the trypsin sensitive subpopulation of mock and genuine U251-MG / infected MDM cocultures after brief coculture (2½ or 4½h).

Summary

Both the loss of U251-MG cells during CD14 depletion of the cocultures and the inability for U251-MG cells to be detached from the cocultures with trypsin indicated an interaction

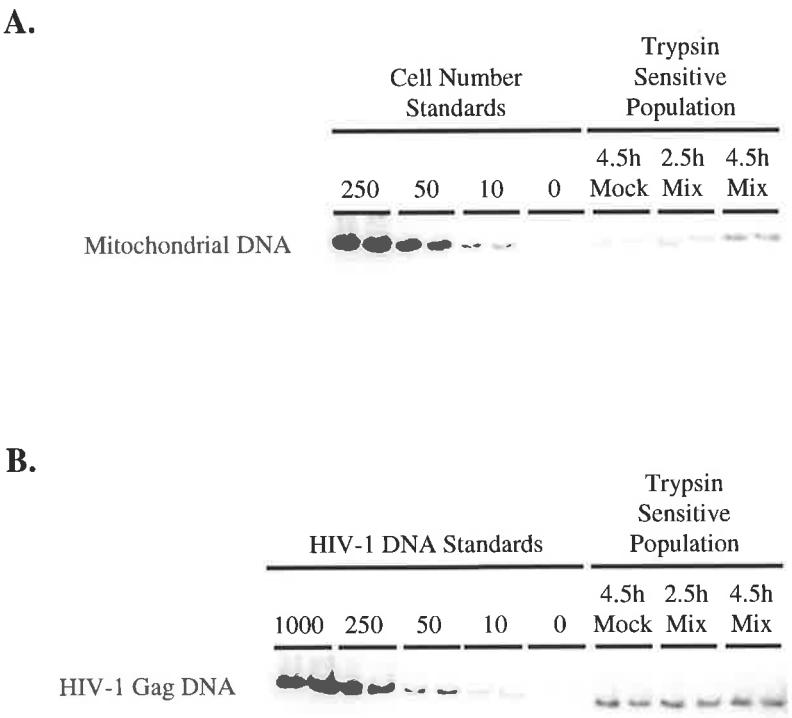

Figure 3.8 Separation of HIV-1_{BaL} infected MDM and U251-MG cell populations after coculture by trypsin treatment.

U251-MG cells were scraped and cocultured with 14d HIV-1_{BaL} infected, pre-seeded MDMs, at an approximate ratio of 5:1. After either 2½ or 4½ hours of coculture, selective separation of the U251-MG cells from the MDMs was attempted by trypsin treatment (0.1% for 15 min at RT). Extrachromosomal DNA was extracted from the U251-MG cell enriched, trypsin sensitive population, and analysed for the relative presence of HIV-1 DNA by 24 and 29 cycles of mitochondrial and HIV-1 *gag* PCR respectively. To control for the proportion of infected MDMs which may carry over into the trypsin-sensitive population, replica cultures of infected MDMs and uninfected U251-MG cells were maintained separately in the teflon pots, treated with trypsin, and the non-adherent populations combined (mock coculture).

between the astrocytes and the MDMs. It is likely then that any attempt to remove the MDMs from the astrocytes would result in the selective removal of the astrocytes most closely associated with the MDMs and most likely to be the recipients of the transmission of infection. (A positive selection cell surface marker specific for astrocytes was not available, and if one were, it would be likely that any interacting MDMs would also be harvested.) Harvesting the MDM-depleted portion of U251-MG cells after coculture would therefore be biased to the U251-MG cells least likely to have interacted with MDM virus-donor cells. Furthermore, the contribution of MDM-derived HIV-1 DNA in both the CD14 depletion and the trypsin-sensitive selection (Figures 3.7 and 3.8) could still potentially mask a low level of astrocyte infection.

3.5 Discussion

In summary, HIV-1 did not appear to be efficiently transferred from chronically infected T-cell lines or primary macrophages to astrocytes, or alternatively, if virus transmission did occur, reverse transcription did not proceed efficiently. Both chronically infected T-cell lines and macrophages had a higher level of background extrachromosomal HIV-1 DNA than initially expected, which limited the ability of the coculture reverse transcription assays to detect *de novo* reverse transcription in astrocytes. This background could be due to contamination of the extrachromosomal DNA fraction with chromosomal DNA and / or ongoing viral reverse transcription in these cells (Dr Jillian Carr, personal communication). Several strategies to minimise this "background" were attempted. Blocking transcription in the virus-donor cells by $ActC_1$ did not reduce the background level of HIV-1 DNA in the lymphocytic virus-donor cells, and was unsuitable for use with primary macrophages. Separation of the astrocytes from the viral donor cells could not be achieved due to the cell-cell interactions that occurred between the U251-MG astrocytes and the infected T-cells or MDMs. Because of this, a U251-MG population separated after a period of coculture would be intrinsically biased to the astrocytes that had minimal or no interaction with the viral donor cells, and thus least likely to have become infected. Furthermore, despite attempts to separate the cell populations after a period of coculture, the level of background HIV-1 DNA from both T-cell and macrophage virus-donor cells remained sufficient to potentially mask a low level of astrocyte infection. The reverse transcriptase inhibitor, AZT, did not abolish the presence of HIV-1 DNA in the MDM cocultures, further implying this HIV-1

DNA detection was due to pre-existing HIV-1 DNA in the viral donor cells, and not *de novo* reverse transcription.

The lack of detectable U251-MG astrocyte infection by HIV-1_{IIIB} was surprising, as cell free infection with HIV-1_{IIIB} has been shown to result in the restricted infection of some astrocyte cell lines (U373-MG and U87-MG) (Chesebro *et al*, 1990; Dewhurst *et al*, 1987a; Dewhurst *et al*, 1987b; Harouse *et al*, 1991; Harouse *et al*, 1989; Shapshak *et al*, 1991), HEA (Di Rienzo *et al*, 1998), HFA (Nath *et al*, 1995; Sabri *et al*, 1999) and PDA (Lawrence *et al*, 2004). In most of these reports restricted infection was demonstrated by the rescue of infectious virus upon coculture with CD4+ HIV-1 susceptible cells, sometimes coupled with the finding of initial p24 release, and / or HIV-1 nucleic acid (by PCR or RT-PCR), and / or HIV-1 proteins (immunodetection). HIV-1_{IIIB} has also been reported to be infectious to other CD4 negative cells (Ensoli *et al*, 1995; Ensoli *et al*, 1997). Interestingly, Choidi *et al* failed to demonstrate infection of U373-MG cells with HIV-1_{IIIB} (Chiodi *et al*, 1987), although other investigators have reported a restricted infection with this virus–cell combination (Dewhurst *et al*, 1987a; Harouse *et al*, 1989; Shapshak *et al*, 1991) indicating a different outcome could be due to subtle variations in infection methods, cell culture or virus source. Additionally, HIV-1_{IIIB} has been reported to infect several astrocyte cell lines (85HG-59, 85HG-63, 86HG-64 and 85HG-66) in a restricted manner upon cell-to-cell transmission (Brack-Werner *et al*, 1992). Like the experiments in this chapter, Brack-Werner *et al* cocultured astrocytic cells with chronically infected T-cell lines; KE37/1-IIIB and H9-IIIB. The H9-IIIB cells used by Brack-Werner *et al* are from the same source (Popovic *et al*, 1984) as the cloned HIV-1_{IIIB} H9 cells ("HIIIB" cells) used in this study. After 2 days of coculture, Brack-Werner *et al* removed the (majority of) H9-IIIB cells from the astrocytic cells by washing, and subsequently re-seeded the astrocytic cells as single cells. Up to 6% of these cells were found to be positive for HIV-1 antigen (p24 or Nef), however after 2-5 passages virtually none of the astrocytic cells continued to express detectable HIV-1 antigen (Brack-Werner *et al*, 1992). A persistently HIV-1_{IIIB} infected astrocyte cell line with a single integrated copy of the viral provirus was derived from a single cell clone (TH4-7-5) which did continue to express HIV-1 antigen (low p24 expression and disproportionately high Nef expression) (Brack-Werner *et al*, 1992). This indicated that, although it was a rare event, reverse transcription and integration was possible within the parent astrocyte cell line (85HG-66). The lack of detection of reverse transcription in U251-MG astrocytes upon coculture with HIIIB cells in this thesis may

reflect a lack of infectivity of this particular strain of HIV-1_{IIIB} for U251-MG cells, or limited capacity of this HIIIB cell clone to act as virus-donor cells. The latter possibility is supported by the coculture of the same HIIIB cells with the HIV-1 susceptible T-cell line, HuT-78 cells, in which only a modest amount of reverse transcription was observed. Whilst U251-MG cells have been shown to be susceptible to a restricted infection with other strains of HIV-1 including SF2 (see below), SF117, SF128A (Cheng-Mayer *et al*, 1987) and SF162 (Kort, 1998), it is possible that this cell line is resistant to infection by HIV-1_{IIIB}. The rationale for this is not clear, but may involve the lack of surface epitopes on U251-MG cells required for viral entry by the IIIB strain of HIV-1. It is notable that, in all the examples of astrocyte infection by HIV-1_{IIIB} outlined above, the level of infection ranged from very low to low. Due to the "background" level of HIV-1 *gag* DNA in the extrachromosomal fraction of the virus-donor cells, the possibility of a very low level of U251-MG infection could not be excluded.

The lack of detectable U251-MG astrocyte infection by HIV-1_{SF2} was also surprising, as cell free infection of with HIV-1_{SF2} has been reported to give rise to productive astrocyte infection in HFAs, in both cell free and cell-to-cell infection paradigms (Nath *et al*, 1995) (Prof. Cecilia Cheng-Mayer, personal communication). Furthermore, a restricted astrocyte infection has been previously observed upon cell-free infection of U251-MG astrocytes with HIV-1_{SF2} (Cheng-Mayer *et al*, 1987; Clapham *et al*, 1989; Dewhurst *et al*, 1987a; Dewhurst *et al*, 1987b). Each of these reports used different means to demonstrate a restricted infection of U251-MG cells; Cheng-Mayer *et al* demonstrated this by the rescue of infectious virus upon coculture with $CD4^+$ HIV-1 susceptible cells, Dewhurst *et al* by detection of HIV-1 RNA, and Clapham *et al* by a long term Tat-assay. These methods of detection would be more sensitive than the reverse transcription assay employed in this chapter. They also target later steps in the viral replication cycle, indicating viral reverse transcription had occurred. In a coculture system, however, these assays would not distinguish between low level astrocyte infection or the persistence of viral donor cells either. As discussed above for HIV-1_{IIIB}, the assays of cocultures used in this chapter lacked the resolution to distinguish between a low level astrocyte infection (which, if it were possible to separate the astrocytes from the virus-donor cells, could have been detected by a variety of means) and no infection at all. The occurrence of a low level infection would be consistent with previous reports of restricted infection of U251-MG astrocytes with HIV-1_{SF2} (Cheng-Mayer *et al*, 1987; Clapham *et al*, 1989; Dewhurst *et al*, 1987a; Dewhurst *et al*,

1987b). Alternatively, a lack of infection in U251-MG cells in this coculture model, in contrast to previous studies of U251-MG cells and HIV-1_{SF2} could be due to subtle inter-laboratory differences in the cells or the virus, or due to differences between E12 coculture and HIV-1_{SF2} cell-free infection. The HIV-1_{SF2} in the E12 cells is derived from the original HIV-1_{SF2} isolate, not the molecular clone of HIV-1_{SF2} isolate. Some of the other studies use the molecular HIV-1_{SF2} clone (Cheng-Mayer *et al*, 1987), which, although this is also derived from the original isolate, may be subtly different.

Cell-free infection with HIV-1_{BaL} has previously been demonstrated to give rise to a restricted infection of human embryonic astrocytes (HEA) (Di Rienzo *et al*, 1998) and to be capable of infecting other CD4 negative cells (Ensoli *et al*, 1995; Ensoli *et al*, 1997). Using cell-free infection with the macrophage tropic strain, HIV-1_{JR-FL}, Fiala *et al* showed that HFA infection was much more efficient in the presence of MDMs compared to a monoculture of HFA (resulting in 100% versus 1-2% of astrocytes which expressed the HIV-1 regulatory protein, Nef) (Fiala *et al*, 1996). Fiala *et al* postulated that the interplay of the two cell types, and the productive infection of the macrophages, increased the susceptibility of the astrocytes to infection. This report suggested that, after initial cell-free infection of the macrophages, the infection was being efficiently transferred to the astrocytes in the coculture. This, in conjunction with the findings of Nath *et al* that a higher proportion of astrocytes expressed viral proteins when infected by a cell-to-cell mode of infection compared to cell-free (with T-cell tropic HIV-1_{SF2}; 20% of HFAs positive for HIV-1 gp41 after cell-to-cell infection versus 5% after cell-free infection), gave rise to the concept that cell-to-cell transmission of infection to astrocytes is more efficient than cell-free (Brack-Werner, 1999; Nath *et al*, 1995). Given HIV-1_{BaL} has been shown to give rise to a restricted infection of astrocytes, and that astrocyte infection has been reported to be enhanced in the presence of macrophages, it was unexpected that astrocyte infection with HIV-1_{BaL} in a macrophage coculture system was not detectable over and above the background viral replication in the macrophages. It is possible that U251-MG astrocytes are resistant to infection by the HIV-1_{BaL} strain, or that infection occurred below the resolution of the coculture assay.

To conclude, *de novo* reverse transcription could not be demonstrated in the astrocytes upon coculture with virus-donor cells that produced T-cell tropic HIV-1_{SF2} or HIV-1_{IIIB}, or macrophage tropic HIV-1_{BaL}. This indicates either that virus transfer did not occur, or that

virus replication was blocked prior to the synthesis of extended minus strand DNA. Alternatively, virus transmission and replication may have occurred at too low a level to be distinguished from the background level present in the virus-donor cells. Attempts to reduce the background level of virus replication in the virus-donor cells, using several different strategies, were unsuccessful. Dual immuno-labelling approaches that identify both the cell type and a stage of HIV-1 replication could be feasible. Detection of HIV-1 nucleic acid and proteins in the astrocytes is possible (immuno and *in situ* labelling with microscopic or FACS analysis), but to study the kinetics of HIV-1 replication via such an approach would be exceedingly challenging. Whilst a cell-to-cell mode of infection of astrocytes may indeed be more efficient and more physiologically relevant than cell-free infection, it is an inherently difficult system to analyse. The rest of this thesis used a cell-free infection model that enabled a very sensitive and specific analysis of HIV-1 replication in astrocytes.

Chapter 4

Entry of HIV-1 into Astrocytes

(following cell free infection)

4.1 Introduction

4.1.1 Background

The mode of HIV-1 entry into astrocytes has not been elucidated. As discussed in Section 1.5.1, astrocytes do not express surface CD4 (Harouse *et al*, 1989; Peudenier *et al*, 1991; Tornatore *et al*, 1991), which is the main receptor for HIV-1 (see Section 1.1.6i). Consistent with this, neither anti-CD4 monoclonal antibodies nor soluble CD4 block *in vitro* astrocyte infection (Clapham *et al*, 1989; Di Rienzo *et al*, 1998; Harouse *et al*, 1989; Liu *et al*, 2004; Ma *et al*, 1994; Sabri *et al*, 1999; Tornatore *et al*, 1991). Immuno-detection on brain sections (Lavi *et al*, 1997; Muller-Ladner *et al*, 1996; Rottman *et al*, 1997; Sanders *et al*, 2000), HFAs (Andjelkovic *et al*, 2002; Andjelkovic *et al*, 1999; Guillemin *et al*, 2003; Harouse *et al*, 1989; Hesselgesser *et al*, 1997; Hesselgesser and Horuk, 1999; Klein *et al*, 1999; Lacy *et al*, 1995; Liu *et al*, 2004; McManus *et al*, 2000; Reeves *et al*, 1999; Rezaie *et al*, 2002; Sanders *et al*, 2000; Tornatore *et al*, 1994b; Zheng *et al*, 1999) and astrocyte cell lines (Brack-Werner *et al*, 1992; Harouse *et al*, 1989; Lacy *et al*, 1995; Speth *et al*, 2000) has demonstrated that human astrocytes may express or be induced to express a range of chemokine receptors (including CCR1, CCR2, CCR3, CCR5, CXCR2, and CXCR4) and orphan receptors (BOB, BONZO, Apj), which could potentially act as co-receptors for HIV-1 (if CD4 were also present). The relevance of viral tropism and coreceptor usage to astrocyte infection is unclear, as while "macrophage tropic" (CCR5-using) strains of HIV-1 predominate in the brain, some in vitro studies suggest that astrocytes are more susceptible to infection by CXCR4-using "T-cell tropic" strains (McCarthy *et al*, 1998; Nath *et al*, 1995; Schweighardt *et al*, 2001) (Section 1.5.1). TNFα, IFNγ, IL1β (Cota *et al*, 2000; Marcoux and Choi, 2002; Rottman *et al*, 1997; Wu *et al*, 2000) and quinolinic acid (Guillemin *et al*, 2003) have been reported to induce or up-regulate chemokine receptor expression by astrocytes (Section 1.2.4ii). These factors are produced by activated microglia (Section

1.2.4i) and are elevated in HIV-1 infected brains (Sections 1.3.4ii, 1.3.5ii and Figure 1.11). The profile of chemokine receptor expression on astrocytes varies between reports, possibly due to the different regions of brain studied (or from which HFAs were obtained), the heterogeneity of astrocytes and differences in the local micro-environments, as well as the sensitivity of the immuno-detection method employed. Despite the potential expression of co-receptors for HIV-1, antibodies and ligands to various co-receptors, including SDF-1β, RANTES, MIP-1β or MCP-1 (the natural ligands for CXCR4, CCR3, CCR5 and CCR2b / CCR1 respectively) fail to inhibit *in vitro* infection of astrocytes (Liu *et al*, 2004; Sabri *et al*, 1999). Galactosyl ceramide (also known as galactocerebroside) has also been proposed as a candidate receptor for HIV-1 on astrocytes (Section 1.5.1). This is based on the binding of HIV-1 gp120 to this molecule (Bhat *et al*, 1993; Harouse *et al*, 1991), and one report in which antibodies to galactosyl ceramide inhibited HIV-1 infection of the astrocyte cell line U373-MG (Harouse *et al*, 1989). However, infection of HFAs has been repeatedly shown to be independent of this molecule (Hao *et al*, 1997; Hao and Lyman, 1999; Ma *et al*, 1994).

The absence of CD4 on astrocytes and the apparent independence of astrocyte infection from chemokine receptor expression indicates that a non-conventional mode of HIV-1 attachment and entry underpins astrocyte infection. The level of expression of the astrocyte specific internal protein, GFAP, has been reported to correlate with the susceptibility of astrocyte cell lines to HIV-1 infection (Cheng-Mayer *et al*, 1987), but the mechanism for this is not known. The binding of HIV-1 to surface molecules present on HFAs has been reported, including a 65kDa and a 260kDa cell surface protein (Hao and Lyman, 1999; Ma *et al*, 1994). These proteins have not been identified, and whether this interaction leads to infection is yet to be demonstrated. Indeed the identification of receptor(s) for HIV-1 on astrocytes, despite persistent research efforts by several laboratories, has been highly elusive. Because of this, the aim of this chapter was to investigate the mode of entry of HIV-1 into astrocytes, rather than to attempt identification of the actual receptor(s) involved. At the time the experiments outlined in this chapter were performed, no receptors for HIV-1 had been identified on astrocytes, and consequently the mode of entry of HIV-1 into astrocytes was unknown. Recently the mannose receptor, a member of the C-type Lectin family, was identified as a receptor for HIV-1 on astrocytes and shown to be involved in infection (Liu *et al*, 2004; Trujillo *et al*, 2004) (refer Section 1.5.1). These studies also inferred the presence of additional, yet to be identified, receptors for HIV-1 on astrocytes

(Liu *et al*, 2004). C-type lectins have been implicated in HIV-1 infection of other cell types (DC-SIGN on dendritic cells, Langerin on langerhan cells) (Turville *et al*, 2003; Turville *et al*, 2002), however productive infection of these cell types still involves CD4 and a co-receptor. To investigate the mode of HIV-1 entry into astrocytes, astrocytic cells (U251-MG, U87-MG and CCF-STTG1 cell lines) were exposed to HIV-1 and fixed at various times within the first 75 minutes of virus exposure. The cellular location of HIV-1 proteins and virions was investigated by immunofluorescence and electron microscopy respectively.

4.2 Immunofluorescent tracking of HIV-1 entry into astrocytes

4.2.1 Preliminary Immunofluorescent Investigations

4.2.1i Confirmation that U251-MG, U87-MG and CCF-STTG1 cells are CD4 negative and GFAP positive.

The astrocyte cell lines used in this thesis (U251-MG, U87-MG, CCF-STTG1) have been previously documented to be negative for surface expression of CD4 (Barna *et al*, 1985; Bigner *et al*, 1981; Ponten and Macintyre, 1968) (Section 2.1.1i). To verify this, the cells were assessed for surface CD4 expression by FACS (Table 4.1). It was confirmed that none of these cell lines expressed detectable surface CD4. As controls, surface expression of CD4 was demonstrated in lymphocytic HuT-78 cells but not HeLa cells (Table 4.1).

Consistent with previous reports (Barna *et al*, 1985; Bigner *et al*, 1981) (see Section 2.1.1i), U251-MG and CCF-STTG1 astrocyte cells were confirmed to express the astrocyte marker, GFAP, by immunofluorescence (Figure 4.1). Reports of GFAP expression by U87-MG cells vary (Chesebro *et al*, 1990; Clapham *et al*, 1989; Ludwig *et al*, 1999) (see Section 2.1.1i). This could be due to the potential loss of GFAP expression by astrocytes, which has been reported to occur in some astrocytes upon culture (Cheng-Mayer *et al*, 1987; Collins, 1983; Keys *et al*, 1991). The current study used U87-MG within 8 passages of receipt from the ATCC, and GFAP expression was detected by immunofluorescence (Figure 4.1). Indeed, U87-MG cells in this study appeared to express a higher level of GFAP than U251-MG and CCF-STTG1 cells, as upon simultaneous immunofluorescent staining of GFAP in these three astrocyte cell lines U87-MG cells exhibited a greater degree of immunoreactivity

Cells	Antibody	% Positive[a]	Total % Postive[b]
U251-MG	Isotype control	0.3	0.0
	Anti CD4	0.0	
CCF-STTG1	Isotype control	0.2	0.0
	Anti CD4	0.2	
U87-MG	Isotype control	0.2	0.0
	Anti CD4	0.2	
HeLa[c]	Isotype control	0.1	0.8
	Anti CD4	0.9	
HuT-78[d]	Isotype control	0.1	29.1
	Anti CD4	29.2	

[a]Percent cells positive by FACS (10 000 cells counted)
[b]Percent of cells positive for CD4 minus percent of cells positive for isotype control (background)
[c]CD4 negative control cell line
[d]CD4 positive control cell line

Table 4.1 Examination of U251-MG, CCF-STTG1 and U87-MG cells for CD4 surface expression.

U251-MG, CCF-STTG1 and U87-MG astrocyte cell lines were examined for surface CD4 expression by Flow Cytometry. Fixed cells were incubated with either an antibody to CD4, or an isotype matched control antibody. Binding of the antibodies was detected by a FITC-conjugated secondary antibody, and the number of fluorescently (FITC) labelled cells measured by Flow Cytometry. Additional cell lines known to express surface CD4 (HuT-78 cells) and to be negative for CD4 expression (HeLa cells) were included as controls.

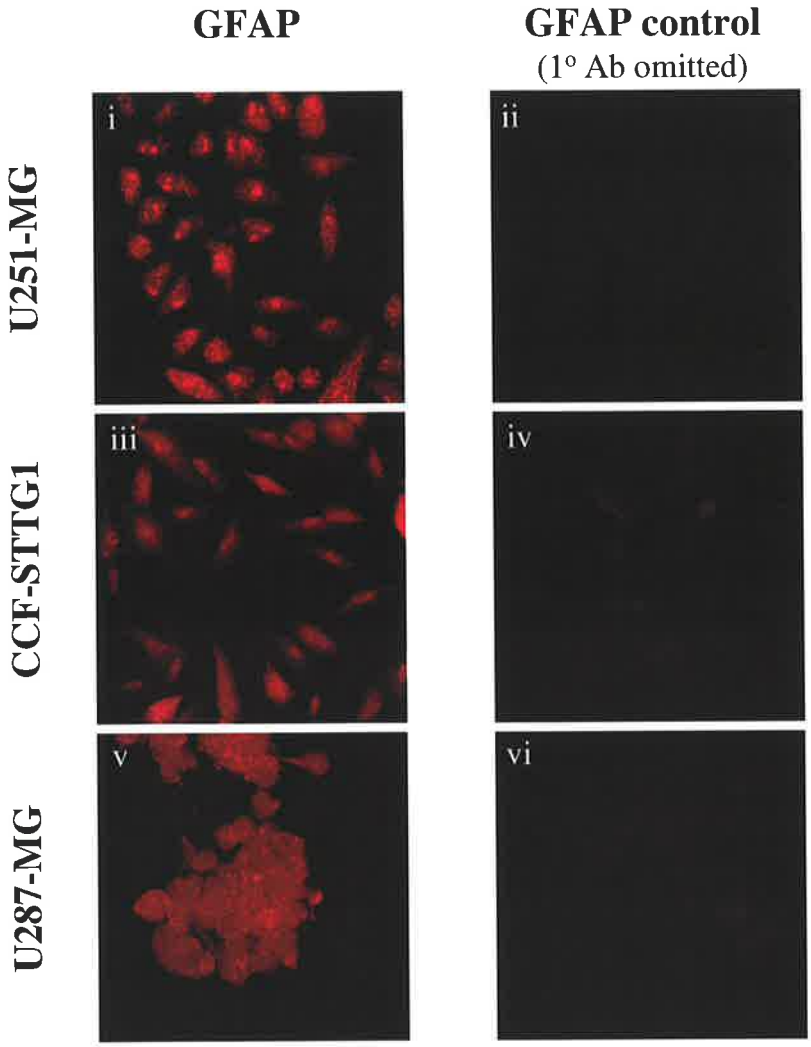

Figure 4.1 Examination of GFAP expression by U251-MG, CCF-STTG1 and U87-MG astrocytes.

U251-MG, CCF-STTG1 and U87-MG astrocyte cell lines were examined for expression of the astrocyte specific marker, glial fibrillary acidic protein (GFAP). Cells were cultured overnight on glass coverslips, then washed, fixed and processed for indirect immunofluorescence assay using a rabbit anti-GFAP polyclonal antibody and a Cyanine3-conjugated anti rabbit IgG secondary antibody (red fluorescence) (i, iii, v). To control for GFAP immunoreactivity, cells were processed with the omission of the GFAP primary antibody (ii, iv, vi). The images were captured by confocal microscopy at 200x magnification. Identical laser settings were used for image capture of control and experimental cells for each cell type. U87-MG cells were imaged with reduced excitation compared to the U251-MG and CCF-STTG1 cells, as the intensity of GFAP immunoreactivity was considerably higher in the U87-MG cells, despite concurrent preparation and analysis of all three cell types. (The U251-MG and CCF-STTG1 images were captured with the HeNe 543nm laser power set at 100%, the iris diaphram set to 8.7 and a gain of 14.4. U87-MG images were captured with the HeNe 543nm laser power reduced to 63.6% , the iris diaphragm reduced to 4.1, and a similar gain of 15.3).

to GFAP. Because of this, the amount of laser excitation used to for image capture of GFAP immunofluorescence was substantially reduced for U87-MG cells compared to U251-MG and CCF-STTG1 cells (Figure 4.1), in order to avoid saturation of the image intensity.

4.2.1ii Design and optimisation of fluorescent strategies to attain necessary sensitivity for detection of virus entry

Given the reported low level of infection of HIV-1 in astrocytes (Section 1.4), the lack of identified receptors for HIV-1 on astrocytes (Sections 1.4.1 and 4.1.1), and the indications that entry is a major restriction to astrocyte infection (Sections 1.5.1, 1.6.1vi, and 4.1.1), it was predicted that the amount of virus which would enter the astrocytes might be exceedingly low. Consequently, the detection of virus inside astrocytes early after infection (prior to production of new viral proteins) was expected to require particularly sensitive techniques. Additionally, the low level of infection could result from a moderate level of production of some viral proteins in a very small percentage of cells, perhaps due to their cell cycle phase and / or specific receptor expression. Alternatively, an exceedingly low level of viral production may occur in the majority of cells. Conventional (epi-) fluorescent microscopy and conventional fluorophores (for example, FITC) were unlikely to provide sufficient resolution or signal intensity for this study. The advent of more stable fluorophores (such as the Cyanine range, and later, the AlexaFluor range of fluorescent conjugates), and the more powerful laser excitation and greater resolution provided by confocal microscopy made this aim of detecting internalised virus by IFA feasible.

Fluorophore-labelled virions

In addition to using Cyanine- or AlexaFluor-conjugated antibodies in immunofluorescent studies, EGFP-labelled virions were produced by co-transfection of pNL4-3 proviral DNA with an expression plasmid for a fusion protein of Vpr-EGFP (pEGFP-C3-Vpr, kindly provided by Prof Warner Greene and Dr Carlos Noronha, see Section 2.1.2). Dual transfected cells were expected to produce virions which had incorporated the chimeric Vpr as previously shown (Schaeffer *et al*, 2001), as Vpr expressed from both the pNL4-3 proviral plasmid and the Vpr-EGFP expression vector are incorporated into the virions. Considerable optimisation of the co-transfection procedure was performed to maximise the

expression of both plasmids (Section 2.2.3iii). The optimised transfections exhibited EGFP expression in up to 50% of cells (epi-fluorescent microscopy) and up to 600ng/ml HIV-1 p24 core protein (ELISA) in the supernatant at 36 hours post transfection. However, no EGFP fluorescence was observed by confocal microscopy analysis of U251-MG cells that had been exposed to these transfection supernatants for 40 mintues.

Several factors may have accounted for the lack of detection of viral entry in this experiment, including insufficient titre of the chimeric virus, inefficient incorporation of Vpr-EGFP into virions (Dr Sabine Piller, personal communication), cleavage of the Vpr-EGFP fusion protein by viral (or cellular) proteases (Dr Sabine Piller, personal communication), and the potential dissemination of the EGFP-Vpr in the cytoplasm upon uncoating of the virus. Additionally, as discussed above, the lack of detection could be due to inefficient viral entry and the possibility that only a few rare cells may have contained virus. If successful, a significant advantage of this method would have been the potential to track viral entry in real time by live cell imaging. Whilst our confocal microscope facilities would not permit live HIV-1 studies (as this would require PC3 containment of the microscope facility), this could have be achieved with inactivated virus. For example, aldrithiol-2 treated EGFP-labelled virus stock could have been used for live cell studies of HIV-1 uptake, as aldrithiol-2 renders the virus non-infectious whilst preserving the conformational and functional integrity of the virus surface proteins, thus permitting studies of virus-cell binding and entry (Rossio *et al*, 1998). If intracellular fluorescence was observed upon infection of astrocyte cells with chimeric Vpr-EGFP HIV-1_{NL4-3} stock, controlling for the potential fluorescence due to non-virus associated (or virus-disassociated) Vpr-EGFP was likely to present further technical difficulties. Given this, and concurrent success with an immunofluorescence approach (see below), the chimeric fluorescent virus was not pursued further.

Immunofluorescence

To maximise the sensitivity of indirect immunofluorescence, pooled AIDS Patient Sera (APS) was used as the first antibody to label HIV-1 proteins. This was chosen as our laboratory had shown a greater sensitivity of HIV-1 immuno-detection with APS compared to antibodies to particular epitopes of HIV-1 (Dr Jillian Carr, personal communication). The high sensitivity of APS is most likely due to polyclonal reactivity to numerous HIV-1

proteins. However, as this serum is derived from humans, strict controls are required to differentiate between reactivity to HIV-1 epitopes and non-specific immunoreactivity to human epitopes present on the astrocyte cell lines, as these are human cells. Initial immunofluorescence was performed on chamber-slides pre-seeded with U251-MG cells which had been fixed 40 mpi with HIV-1_{NL4-3}, and with a secondary antibody conjugated with Cyanine2 (Cy2). (This was the latest and most photostable fluorophore available at the time, but was superseded in subsequent experiments with AlexaFluor (AF) conjugated secondary antibodies.) Some immunoreactivity, including nuclear immunoreactivity, was observed in these cells by confocal microscopy with both APS and normal human sera (NHS). However, preliminary results demonstrated punctate immunoreactivity in the cytoplasm of the infected U251-MG cells (Figure 4.2) which was not observed in infected cells treated with NHS, nor uninfected cells treated with APS (not shown). This HIV-1 specific punctate immunofluorescent pattern was suggestive of cytoplasmic vesicle staining, possibly of early endosomes (Sieczkarski and Whittaker, 2002) and was investigated further (Sections 4.2.2-4.2.5 and 4.3 below).

4.2.2 APS immunoreactivity in HIV-1 infected U251-MG astrocytes

At this time several reports had recently emerged in the literature which demonstrated uptake of HIV-1 by endocytosis in both CD4 positive and CD4 negative cells (Fredericksen *et al*, 2002; Grewe *et al*, 1990; Liu *et al*, 2002; Marechal *et al*, 1998; Marechal *et al*, 2001; Pauza and Price, 1988; Schaeffer *et al*, 2001) (see Section 1.1.6i). Of particular relevance were the demonstrations that HIV-1 is taken up into vesicle-like cytoplasmic compartments by HeLa cells, which are CD4 negative, within 45 minutes of infection, (Marechal *et al*, 1998; Schaeffer *et al*, 2001) (Figure 4.3). In both these reports, internalised HIV-1 was visualised as discrete punctate cytoplasmic fluorescence (by HIV-1 *gag* immunoreactivity and GFP-labelled virus, respectively), and found to colocalise with markers of clathrin-mediated endocytosis (Marechal *et al*, 1998; Schaeffer *et al*, 2001) (Figure 4.3B). Interestingly, electron microscopy observations of Hao and Lyman indicated that $HIV1_{RF}$ virions entered fetal astrocytes (HFAs) by clathrin-mediated endocytosis (Hao and Lyman, 1999). To determine if the punctate APS immunoreactivity seen in the preliminary analysis of HIV-1 infected U251-MG cells (Section 4.2.1ii and Figure 4.2) also represented clathrin-

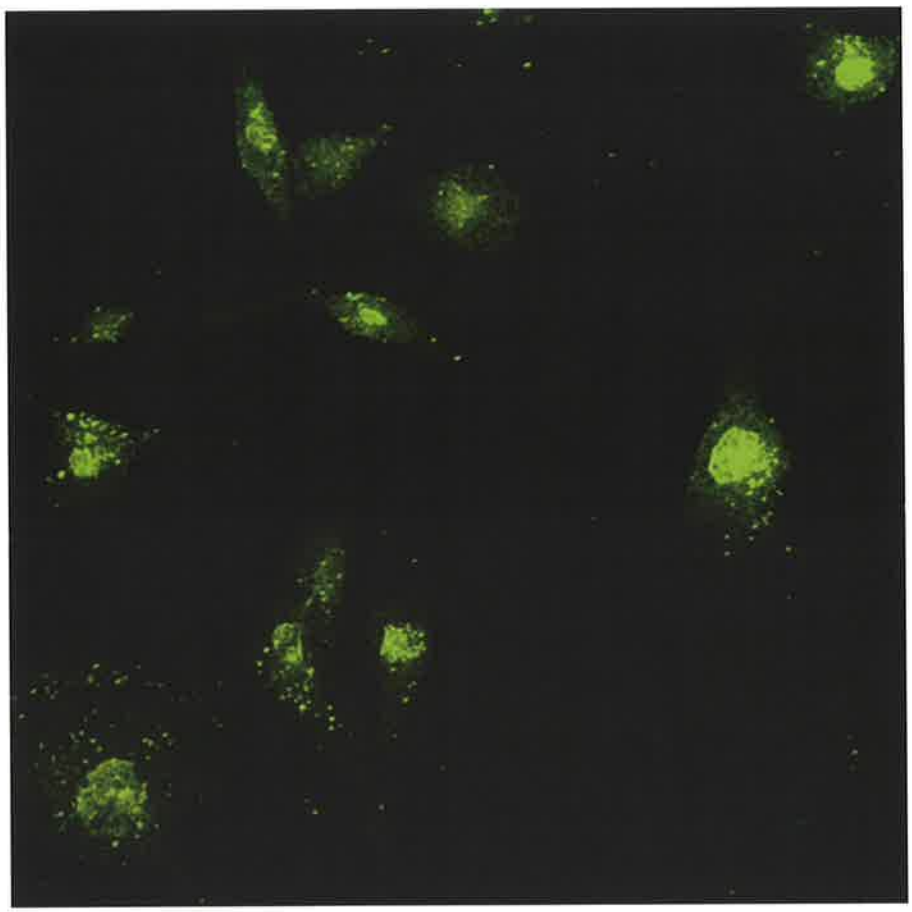

Figure 4.2 Preliminary immunofluorescence assay for AIDS Patient Sera immunoreactivity on HIV-$1_{NL4.3}$ infected U251-MG astrocytes.

U251-MG astrocytes were cultured overnight in chamber slides and subsequently exposed to HIV-$1_{NL4.3}$. After allowing the infection to proceed for 40 minutes, the cells were washed, fixed, and processed for indirect immunofluorescence assay using pooled AIDS Patient Serum (APS) and Cyanine2-conjugated anti-human IgG_1. Image captured by confocal microscopy at 400x magnification.

Figure 4.3 Previous observations of CD4-independent entry of HIV-1 into vesicular compartments in HeLa cells.

Marechal *et al.* (1998) demonstrated punctate immunoreactivity to HIV-1 Gag in both CD4 positive (P4 cells; HeLa cells transfected to express CD4) and CD4 negative (HeLa) cells, which had been fixed after 30 minutes of exposure to HIV-$1_{NL4.3}$ (**A**). This was shown by indirect immunofluorescence with a mixture of anti-HIV-1 Gag monoclonal antibodies and confocal microscopy. The HIV-1 Gag immunoreactivity was reported to partially colocalise with immunoreactivity to clathrin (indicating clathrin-mediated endocytosis), LAMP1 (a lysosomal marker, indicating vesicular trafficking to the lysosomal degradative pathway), and with live uptake of fluorescently labelled transferrin (a marker of clathrin-dependent endocytosis and the recycling endocytic pathway) (Marechal *et al*, 1998).

Similarly, in 2001, Schaeffer *et al.* demonstrated punctate fluorescence in HeLa cells (CD4 negative) which had been exposed to GFP-labelled HIV-$1_{NL4.3}$ virions for 45 minutes (**B**). The green fluorescence of the GFP-virus showed partial colocalisation with TAMRA (red) labelled human transferrin when this was included in the final 10 minutes of the infection (Biii). Colocalisation of GFP labelled virions and a lysosomal marker (LysoTracker Red) was not observed in this study (Bvi) (Schaeffer *et al*, 2001).

Figure (**A**) adapted from Marechal *et al*, (1998), Figure (**B**) adapted from Schaeffer *et al*, (2001).

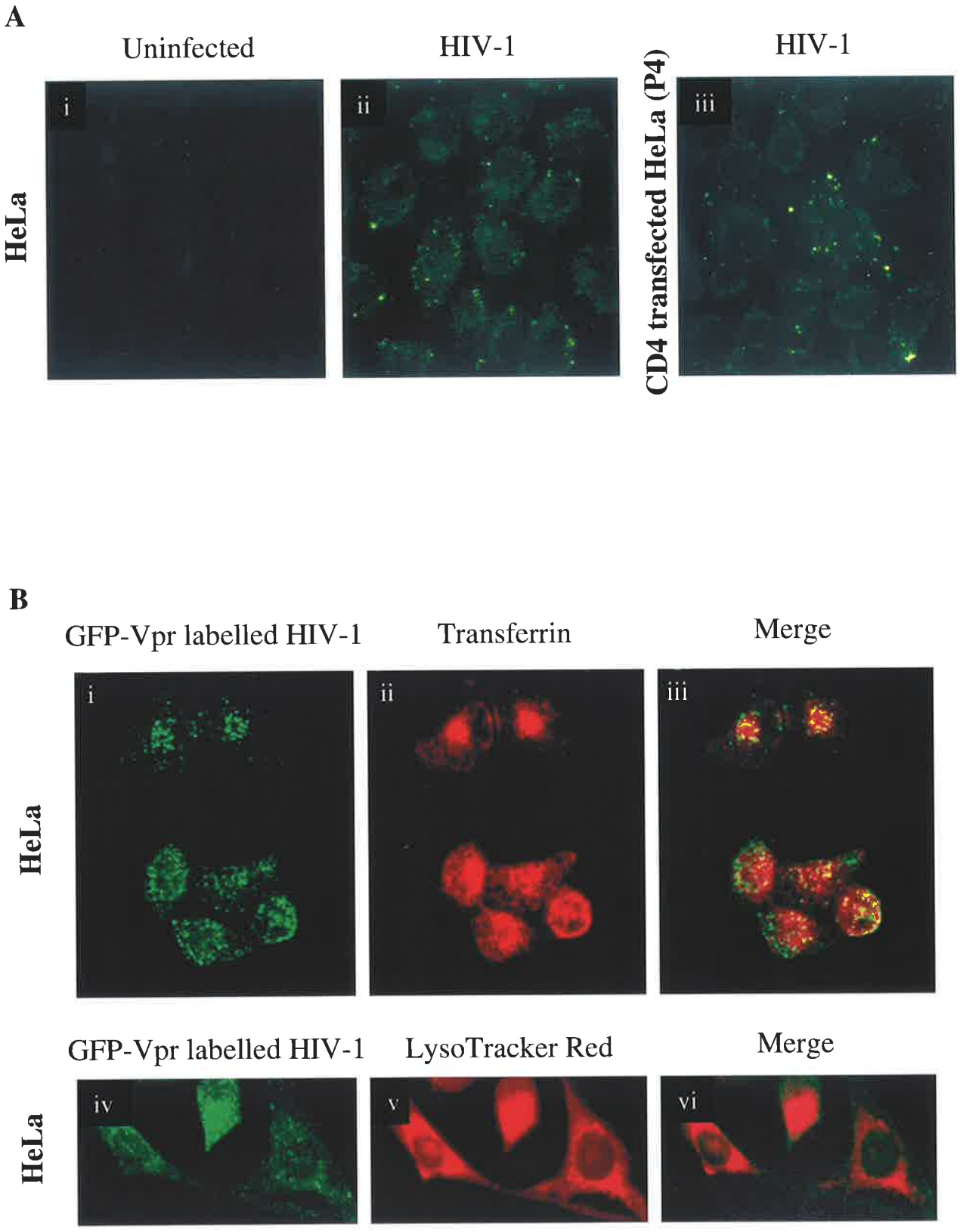
A
Uninfected
HIV-1
HIV-1
HeLa
CD4 transfected HeLa (P4)
i
ii
iii
B
GFP-Vpr labelled HIV-1
Transferrin
Merge
HeLa
i
ii
iii
GFP-Vpr labelled HIV-1
LysoTracker Red
Merge
HeLa
iv
v
vi

mediated endocytosis, colocalisation studies of HIV-1 immunoreactivity and labelled transferrin were performed.

4.2.2i Lack of colocalisation of punctate APS immunoreactivity with a marker of clathrin-mediated endocytosis.

U251-MG astrocytes and HeLa cells were pre-seeded in chamber-slides and infected with HIV-1_{NL4-3} for 40 minutes, in the presence of AlexaFluor546-conjugated human transferrin (AF546-Tf) (Section 2.3.3i). Uninfected controls were also prepared with and without labelled transferrin. HIV-1 immunoreactivity was detected with APS and Cyanine2-conjugated secondary antibodies. NHS controls were also prepared. Control NHS-treated infected U251-MG cultures, and uninfected U251-MG cultures treated with APS, exhibited low affinity for the secondary antibody, as minimal Cy2 fluorescence (green) was observed (Figure 4.4iv and v). This strongly suggested that the green punctate immunofluorescence seen only with APS-treated infected U251-MG cells was specific for HIV-1 immunoreactivity (Figure 4.4Aii). No surface staining was observed. Red fluorescence was only observed in U251-MG cultures that had been treated with AF546-Tf (Figure 4.4i). Similarly, APS immunoreactivity in infected HeLa cells (Figure 4.4vi) appeared to be specific for HIV-1 as Cy2 fluorescence was not observed in infected HeLa cells treated with NHS in place of APS (Figure 4.4ix). No surface staining for APS was observed on infected HeLa cells. This HIV-1 immunoreactivity appeared as punctate, cytoplasmic Cy2 fluorescence (green) in HeLa cells, and exhibited colocalisation with the red fluorescence of the AF546-Tf, visualised as yellow colouration upon merging the images from the green and red fluorescence detectors (Figures 4.4Aviii). This was confirmed to be genuine colocalisation (not merely overlapping fluorescence) as it was also observed upon optical "Z" sectioning (the capturing of a series of images focussed at precise depths through the cell monolayer) (Figures 4.4viii). This is consistent with previous reports of colocalisation of labelled transferrin with chimeric EGFP labelled HIV-1 virions (Schaeffer *et al*, 2001) (Figure 4.3B) and HIV-1 *gag* immunoreactivity in HIV-1 exposed HeLa cells (Marechal *et al*, 1998) (Figure 4.3A). However, the majority of the HIV-1 immunoreactivity of infected U251-MG astrocyte cells did not colocalise with labelled transferrin (Figures 4.4iii). This suggested that the vesicle-like immunoreactivity to HIV-1 seen in U251-MG cells did not represent clathrin-mediated uptake of HIV-1 virus / viral proteins.

Figure 4.4 Comparison of APS immunoreactivity and the localisation of labelled transferrin in U251-MG astrocytes and HeLa cells 40 minutes post HIV-1NL4.3 infection.

U251-MG astrocytes and HeLa cells were cultured overnight in chamber slides and subsequently exposed to HIV-1NL4.3 for 40 minutes. AlexaFluor 546-conjugated human transferrin (red fluorescence) was included during the infection, as a live-uptake marker of clathrin-mediated endocytosis and the recycling endocytosis pathway. The cells were then washed, fixed, and processed for indirect immunofluorescence assay using pooled AIDS Patient Serum and Cyanine2-conjugated anti-human IgG1 (green fluorescence). Infected cells treated with normal human sera and uninfected cells treated with APS were included as negative controls. The images were captured by confocal microscopy at 400x magnification, with a 1.5x optical zoom used in the capture of HeLa cell images. Identical laser settings were used for control and experimental cells.

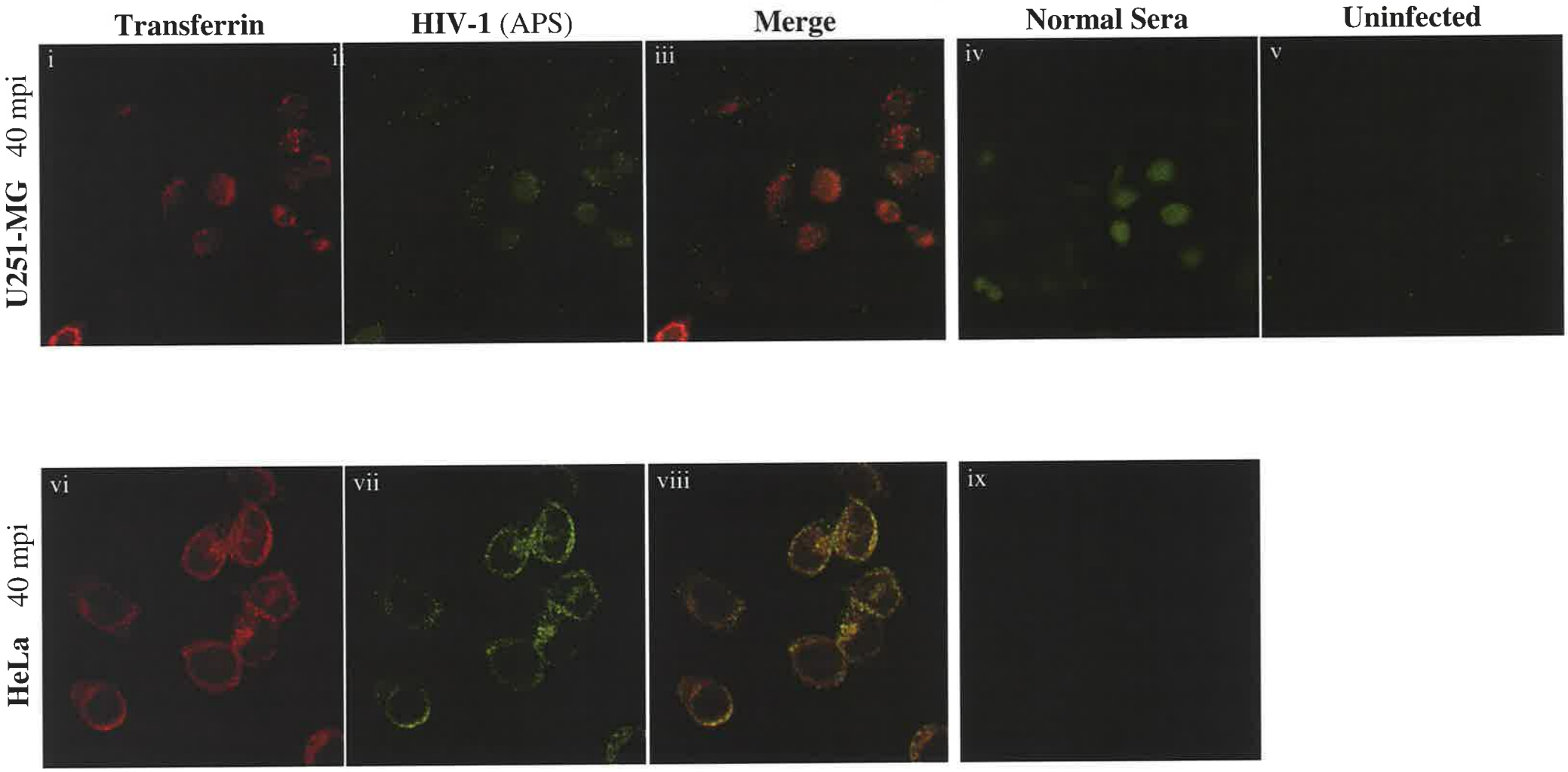
Transferrin
HIV-1 (APS)
Merge
Normal Sera
Uninfected
U251-MG 40 mpi
HeLa 40 mpi
i
ii
iii
iv
v
vi
vii
viii
ix

4.2.2ii Further optimisation and characterisation of the punctate APS immunoreactivity in HIV-1 infected U251-MG astrocytes.

The APS immunofluorescence shown in Figure 4.4 exhibited a significant level of background immunoreactivity and the assessment of the punctate reactivity was limited in part by the level of resolution which could be achieved with cells fixed on chamber-slides. To improve the sensitivity of detection of bound APS IgG, the Cy2-conjugated secondary antibody was replaced with the more photostable AF488-conjugated secondary antibody. To improve the resolution which could be achieved during confocal microscope analysis, U251-MG cells were pre-seeded onto glass coverslips rather than chamber slides. This permitted the capture of confocal images at a higher magnification in subsequent experiments. To confirm that the APS immunoreactivity was cytoplasmic, the nuclei were stained with fluorescent DNA label, Hoechst 33342 (blue).

APS immunoreactivity in U251-MG cells upon 5 to 75 minutes of HIV-1 exposure

To gain further insight into the apparent uptake of HIV-1 proteins into vesicle-like compartments, pre-seeded U251-MG cells (on coverslips) were infected with HIV-1_{NL4-3}, and fixed at a range of times post infection; 5, 15, 30, 45, 60 and 75 mpi. AF546-Tf was included for the last 15 min of each infection (or for the entire duration of infection for cultures fixed at 5 mpi and 15 mpi). Punctate immunoreactivity to APS was seen as early as 5 mpi (Figure 4.5A), but was observed to be relatively faint, and fewer bright spots / per cell were observed compared to cells fixed after longer periods of virus exposure. By 15 mpi almost all of the cells contained several distinct green fluorescence spots (Figure 4.5Biii). No surface staining was observed. As in previous experiments, a high level of laser excitation was required to capture this immunoreactivity, which also produced a low level of non-specific background or auto-fluorescence in control cells (for example, Figure 4.5Av). This did not appear to represent specific immunoreactivity as no punctate staining was observed in uninfected APS treated control cells, nor in NHS treated infected control cells (Figures 4.5Av, 4.5Cv and x). Punctate immunofluorescence at a similar level to that observed 15mpi was observed at the subsequent time points analysed, as illustrated by the analysis of cultures which were fixed at 75mpi (Figures 4.5Biii compared to 4.5Cviii and xiii), and again no surface staining was observed.

Figure 4.5 Analysis of APS immunoreactivity in U251-MG cells and the localisation of labelled transferrin after 5, 15 and 75 minutes of HIV-$1_{NL4.3}$ infection.

U251-MG astrocytes were cultured overnight on glass coverslips and subsequently exposed to HIV-$1_{NL4.3}$ for 5 (**A**), 15 (**B**), or 75 (**C**) minutes. AlexaFluor 546-conjugated human transferrin (red fluorescence) was included for the last 10 minutes of the infection. The cells were then washed, fixed, and processed for indirect immunofluorescence assay using APS and AlexaFluor488-conjugated anti-human IgG_1 (green fluorescence). Infected cells treated with normal human sera and uninfected cells treated with APS were included as negative controls. The cells were counterstained with the nuclear stain, Hoechst 33342. The images were captured by confocal microscopy at either 400x magnification (Ci-v), 600x magnification (A, Cvi-x) or 600x magnification with 1.5x optical zoom (B, Cxi-xiv). Identical laser settings were used for control and experimental cells.

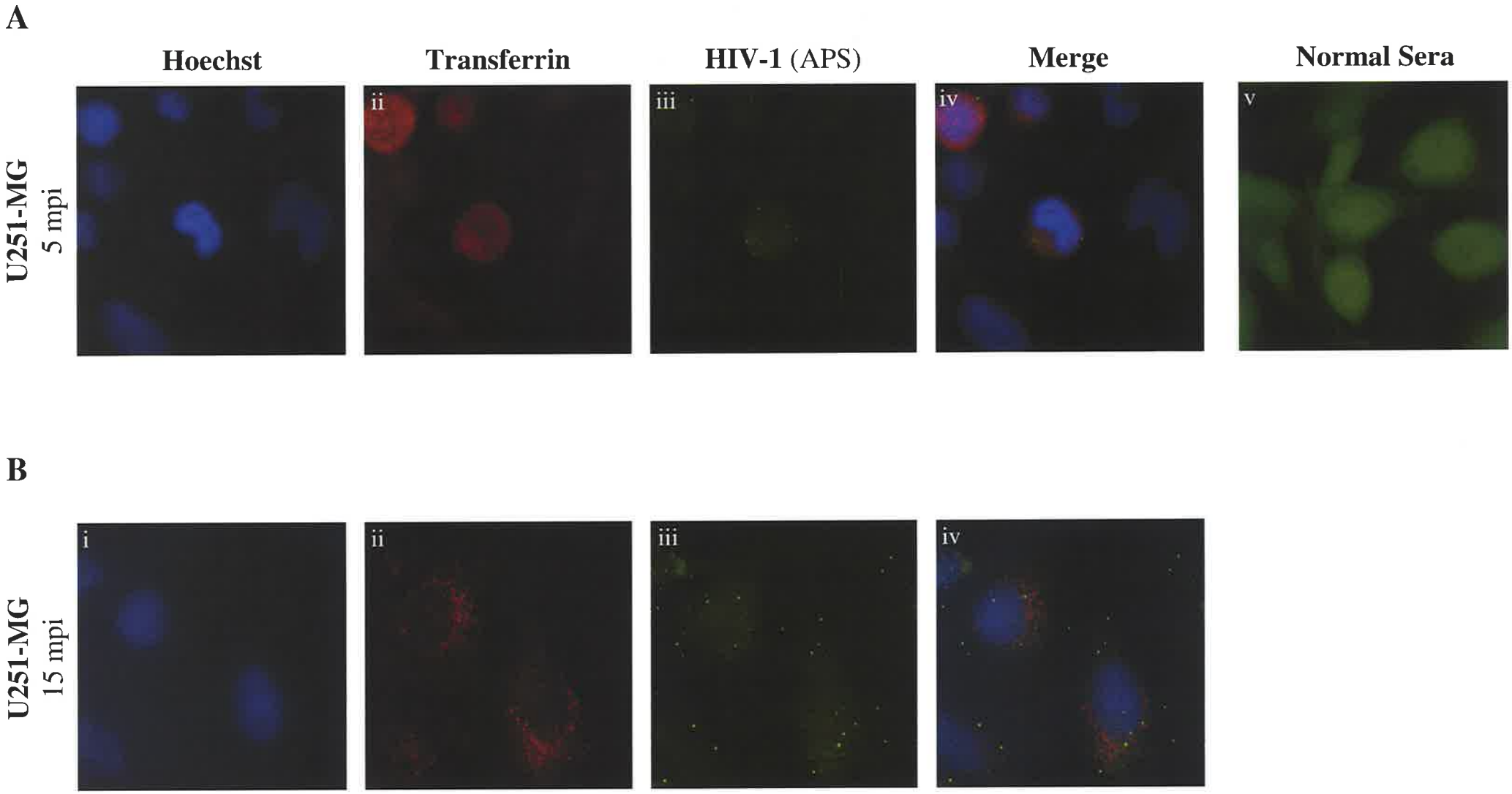
A
Hoechst
Transferrin
HIV-1 (APS)
Merge
Normal Sera
U251-MG
5 mpi
ii
iii
iv
v
B
U251-MG
15 mpi
i
ii
iii
iv

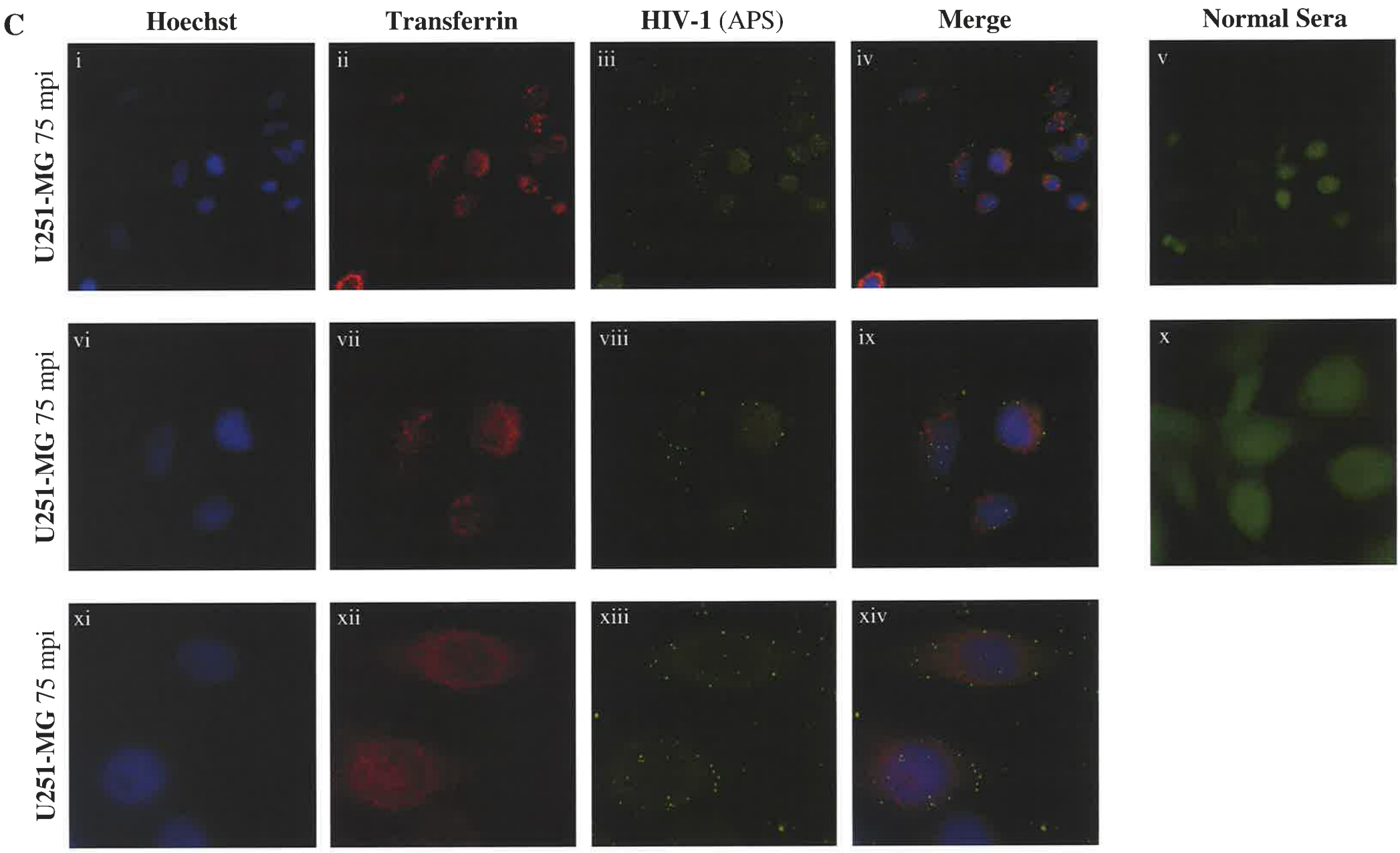
C
Hoechst
Transferrin
HIV-1 (APS)
Merge
Normal Sera
U251-MG 75 mpi
U251-MG 75 mpi
U251-MG 75 mpi
i
ii
iii
iv
v
vi
vii
viii
ix
x
xi
xii
xiii
xiv

Cellular location of the punctate APS immunoreactivity in the infected U251-MG cells

Consistent with the previous experiment (Figure 4.4), the punctate APS immunoreactivity in infected U251-MG cells did not appear to colocalise with the uptake of AF546-Tf at any of the time points assessed (Figures 4.5Aiv, 4.5Biv, 4.5Civ, ix and xiv). The majority of punctate AF488 APS green immunofluorescence did not overlap with the blue fluorescence of the Hoechst 33342 stained nucleus, indicating that this vesicle-like APS immunoreactivity was in the cytoplasm of the cells (Figures 4.5Aiv, 4.5Biv, 4.5Civ, ix and xiv). The location of the punctate APS immunoreactivity that did overlap with the nuclear-stained region of the cells could not be discerned, as this microscope could not assess the depth (Z-axis) of the blue fluorescence. (The confocal microscope used in these studies used an epi-fluorescent mercury UV lamp rather than a confocal laser to excite the Hoechst 33342, and consequently the nuclear localisation was determined by epi-fluorescence and could not be imaged in discrete optical Z sections (see Section 2.4.2)).

Summary

This data suggested that APS immunoreactive proteins (HIV-1 virions or HIV-1 proteins) were being taken up by the U251-MG cells into vesicle-like cytoplasmic compartments within the cells. The uptake of APS reactive proteins into U251-MG cells was quite rapid, as punctate immunoreactivity to APS was seen as early as 5mpi, with a notable increase in the number and intensity of the APS immunoreactive cytoplasmic spots seen by 15mpi. Whilst the absence of surface staining does not exclude the presence of surface bound virions or viral proteins (as they may be present at too low a level to detect), this is consistent with a process of rapid uptake of APS reactive proteins. Endocytosis of HIV-1 has been previously observed in other cell types (Fredericksen *et al*, 2002; Grewe *et al*, 1990; Liu *et al*, 2002; Marechal *et al*, 1998; Marechal *et al*, 2001; Pauza and Price, 1988; Schaeffer *et al*, 2001) (see Section 1.1.6i and 4.2.2 above), but remains to be well characterised, and is considered to result in viral degradation (Marechal *et al*, 1998; Schaeffer *et al*, 2001). The lack of colocalisation of the APS immunoreactivity in HIV-1_{NL4-3} infected U251-MG cells with labelled transferrin implies that the mode of HIV-1 uptake in these cells differs from the mode of uptake in HeLa cells, and, unlike the observations of Hao and Lyman (Hao and Lyman, 1999), appears unlikely to represent clathrin-dependent endocytosis. Whilst labelled transferrin is regarded as a marker of clathrin-mediated

endocytosis (Dautry-Varsat, 1986; Rothenberger *et al*, 1987; Schaeffer *et al*, 2001; Warren *et al*, 1988) and the recycling pathway of endocytosis (Bretscher, 1983), cell specific differences in the level of transferrin receptor expression, the mode of transferrin uptake, and the fate of internalised transferrin may exist. Hence it is possible, although unlikely, that, in U251-MG astrocytes, HIV-1 is taken up by a clathrin-dependent mechanism which excludes, or rapidly separates from, internalised transferrin. Further analysis of the mode of HIV-1 uptake into these astrocyte cells would require a combination of i) electron microscopy (to observe the morphology of the vesicular compartments) (Section 4.3), ii) immunofluorescence for other endocytosis markers, and iii) targeting various pathways of endocytosis with specific drugs (discussed in Sections 4.2.5 and 4.4). The specificity of APS immunoreactivity for HIV-1 proteins in infected U251-MG cells also requires confirmation with a separate and specific antibody (see Section 4.2.3 below).

4.2.3 Confirmation of HIV-1 immunoreactivity with an independent antibody

The punctate APS immunoreactivity seen in HIV-1_{NL4-3} infected U251-MG astrocytes was specific to infected U251-MG cells only, as it was not observed in uninfected cells. It required serum antibodies generated during HIV-1 infection, as punctate immunoreactivity was not observed when NHS was substituted for APS. This was an important control, as both APS and NHS are human sera, and these were being used on human cells (U251-MG). It was possible that auto-antibodies could be present in human sera with the potential to recognise epitopes present in the U251-MG cells. Similarly, it was possible (although unlikely) that the APS may have contained auto-antibodies, specific for human (not viral) epitopes, which may have become exposed or aggregated in the cytoplasm of U251-MG cells in response to exposure to the virus inoculum. To exclude any such anomaly or artefact due to the use of APS, and to confirm the previous findings presented in Sections 4.2.1 and 4.2.2, immunofluorescence was performed with an independent antibody; a mouse monoclonal antibody (MoAb) which is specific to the HIV-1 core protein, p24.

U251-MG infected with HIV-1_{NL4-3} as described in Section 4.2.2ii, and immunofluorescence performed for HIV-1 with a MoAb to HIV-1 p24 protein. Purified murine IgG of the same class as the p24 MoAb ($IgG_{1\kappa}$) was used as an isotype control on infected cultures to control

for any non-specific binding of mouse IgG. Bound murine IgG (p24 MoAb and isotype control) was detected with a Cy3-conjugated secondary antibody (red), and the cells were counterstained with Hoechst 33342 (blue). Similar to the results with APS (Figures 4.4 and 4.5), punctate HIV-1 immunoreactivity was observed in HIV-1 infected U251-MG cells (Figure 4.6ii and vi). This punctate immunoreactivity was not observed in either uninfected U251-MG cells (Figure 4.6iv) or infected U251-MG cells treated with isotype control IgG in place of the p24 MoAb (Figure 4.6iii, vii). The majority of the p24 MoAb reactive spots did not overlap with Hoechst 33342 nuclear fluorescence (comparison of Figure 4.6i and ii, v, and vi), indicating they were cytoplasmic. No surface staining was observed, however it was unlikely the sensitivity of this immuno-reaction was sufficient to have detected any surface p24. The number of immunoreactive punctate spots observed per cell appeared lower than had been previously observed with APS after at least 15 min of infection (Section 4.2.2, Figures 4.4 and 4.5). The intensity of fluorescence of the punctate staining was very low and only just detectable. A reduced intensity of staining was expected with a MoAb to HIV-1 compared to APS, as only one HIV-1 epitope was being detected. Additionally, the fluorescent emission from the Cy3 fluorophore was expected to be less intense than that from the AF488 fluorophore used for APS detection, as: i) Cy3 is less photostable than AF488 and exhibits more photo-bleaching upon excitation, and ii) as the HeNe 543 laser used to excite Cy3 is not as powerful as the Argon ion 488 laser used to excite AF488. A lower level of excitation results in less emission from the fluorophore. The relatively low number of p24 immunoreactive spots per cell could be because fewer vesicle-like compartments exhibited sufficient fluorescence to be detected, or due to the use of a different HIV-1_{NL4-3} virus stock to that used in previous experiments with APS (Figures 4.4 and 4.5). This virus stock is the same as that used for the APS analysis of infected U251-MG, CCF-STTG1 and U87-MG cells in Section 4.2.4 (below), which also exhibits a relatively low number of immunoreactive spots compared to previous experiments.

The observation of the same pattern of punctate immunreactivity with the p24 MoAb confirmed that fluorescence detected in the presence of APS represented immunoreactivity to HIV-1 proteins, indicating that U251-MG cells internalise either virions or virus protein(s) into cytoplasmic vesicles. To ascertain whether this phenomenon also occurred in other types of astrocytes, immunofluorescence for HIV-1 was performed in two other astrocyte cell lines (Section 4.2.4 below). APS was used to detect HIV-1 proteins as this pooled polyclonal sera provided more sensitive detection than p24 MoAb.

Figure 4.6 Determination of HIV-1 immunoreactivity in HIV-$1_{NL4.3}$ infected U251-MG astrocytes with an independent monoclonal antibody.

U251-MG astrocytes were cultured overnight on glass coverslips and subsequently exposed to HIV-$1_{NL4.3}$ for 40 minutes. The cells were then washed, fixed, and processed for indirect immunofluorescence assay using a monoclonal antibody specific for the HIV-1 core protein, p24, and Cyanine3-conjugated anti-mouse IgG_1 (red fluorescence). Infected cells treated with an isotype control antibody (purified murine IgG_1) and uninfected cells treated with the anti-p24 antibody were included as negative controls. The cells were counterstained with the nuclear stain, Hoechst 33342. The images were captured by confocal microscopy at 600x magnification. Identical laser settings were used for control and experimental cells.

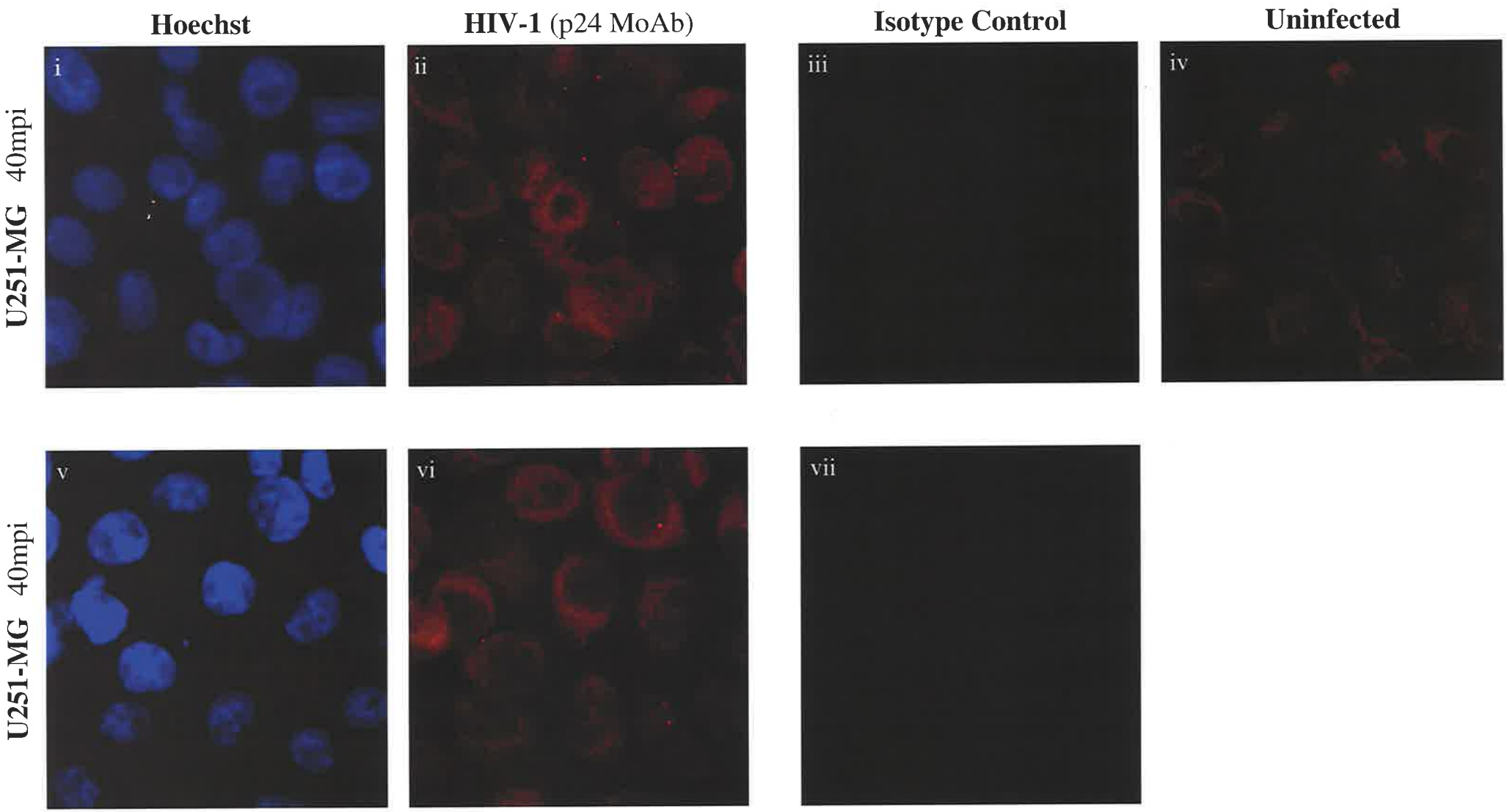
Hoechst
HIV-1 (p24 MoAb)
Isotype Control
Uninfected
U251-MG 40mpi
U251-MG 40mpi
i
ii
iii
iv
v
vi
vii

4.2.4 APS immunoreactivity in HIV-1 infected U251-MG, CCF-STTG1 and U87-MG astrocytes

CCF-STTG1, U87-MG and U251-MG astrocytes were prepared and exposed to HIV-1_{NL4-3} for 40 minutes as described in Section 4.2.2ii, and immunofluorescence assays performed for APS and GFAP immunoreactivity, as described in Sections 2.3.3, 2.4, 4.2.1i and 4.2.2ii.

Punctate, cytoplasmic immunoreactivity (green fluorescence) to APS was seen in infected U251-MG, CCF-STTG1 and U87-MG astrocytes (Figure 4.7iii, ix, xv and Figure 4.8i-iii), consistent with the previous analyses of HIV-1 immunoreactivity in HIV-1 exposed U251-MG cells (Sections 4.2.1ii, 4.2.2 and Figures 4.2, 4.4, 4.5 and 4.6). The frequency and intensity of the immunoreactive spots in the U251-MG cells appeared reduced compared to previous experiments (Section 4.2.2, Figures 4.4 and 4.5), possibly as a different virus stock was used (the same virus stock which was used in the experiment with the MoAb to HIV-1 p24; Section 4.2.3 and Figure 4.6). These bright spots were observed in greater abundance in CCF-STTG1 cells than in U251-MG cells and U87-MG cells, although these three cell types had been infected with the same HIV-1_{NL4-3} stock, for the same period of time in the same experiment. Distinct punctate immunoreactivity was frequently observed in long cytoplasmic processes protruding from CCF-STTG1 cell bodies (Figure 4.7ix, and Figure 4.8i-iii).

The assessment of HIV-1 immunoreactivity in HIV-1_{NL4-3} exposed U87-MG astrocytes was hindered by the altered morphology observed in these cells upon culturing overnight on glass coverslips, compared to their growth in tissue culture flasks. (No morphological difference had been observed when U251-MG or CCF-STTG1 astrocytes were cultured on glass coverslips). The growth rate of U87-MG astrocytic cells also appeared to be reduced when cultured on glass, and the cells adopted a more rounded morphology, with a distinct reduction in the number of cytoplasmic processes. This made it difficult to assess HIV-1 immunoreactivity in U87-MG cells by confocal microscopy. Ideally, the analysis of HIV-1 immunoreactivity in U87-MG cells should have been repeated with the cells grown on plastic coverslips or chamber-slides, however the use of plastic would impinge on the resolution obtainable with confocal microscopy, due to the limiting optical properties of plastics (increased light scatter, diffraction, refraction and reflection compared to that of

Figure 4.7 APS and GFAP immunoreactivity in U251-MG, CCF-STTG1 and U87-MG astrocytes 40 minutes post HIV-$1_{NL4.3}$ infection.

U251-MG, CCF-STTG1 and U87-MG astrocytes were cultured overnight on glass coverslips and subsequently infected with HIV-$1_{NL4.3}$ for 40 minutes. The cells were then washed, fixed, and processed for indirect immunofluorescence assay using APS to detect HIV-1 immunoreactivity (AlexaFluor488-conjugated secondary antibodies; green fluorescence; iii, ix, xv), and a rabbit anti-GFAP polyclonal antibody (AlexaFluor546 conjugated secondary antibodies; red fluorescence; ii, viii, xiv). To control for GFAP immunoreactivity, cells were processed with the omission of the GFAP primary antibody (iv, x, xvi). To control for APS immunoreactivity, infected cells treated with normal human sera (v, xi, xvii) and uninfected cells treated with the APS (vi, xii, xviii) were included as negative controls. The cells were counterstained with the nuclear stain, Hoechst 33342 (i, vii, xiii). The images were captured by confocal microscopy at 600x magnification. Identical laser settings were used for control and experimental cells for each cell type. (The GFAP immunoreactivity of the U87-MG cells was imaged with reduced laser excitation compared to imaging of the GFAP immunoreactivity in U251-MG and CCF-STTG1 cells (as described in Figure 4.1 and Section 4.2.1i), as the intensity of GFAP immunoreactivity was considerably higher in U87-MG cells).

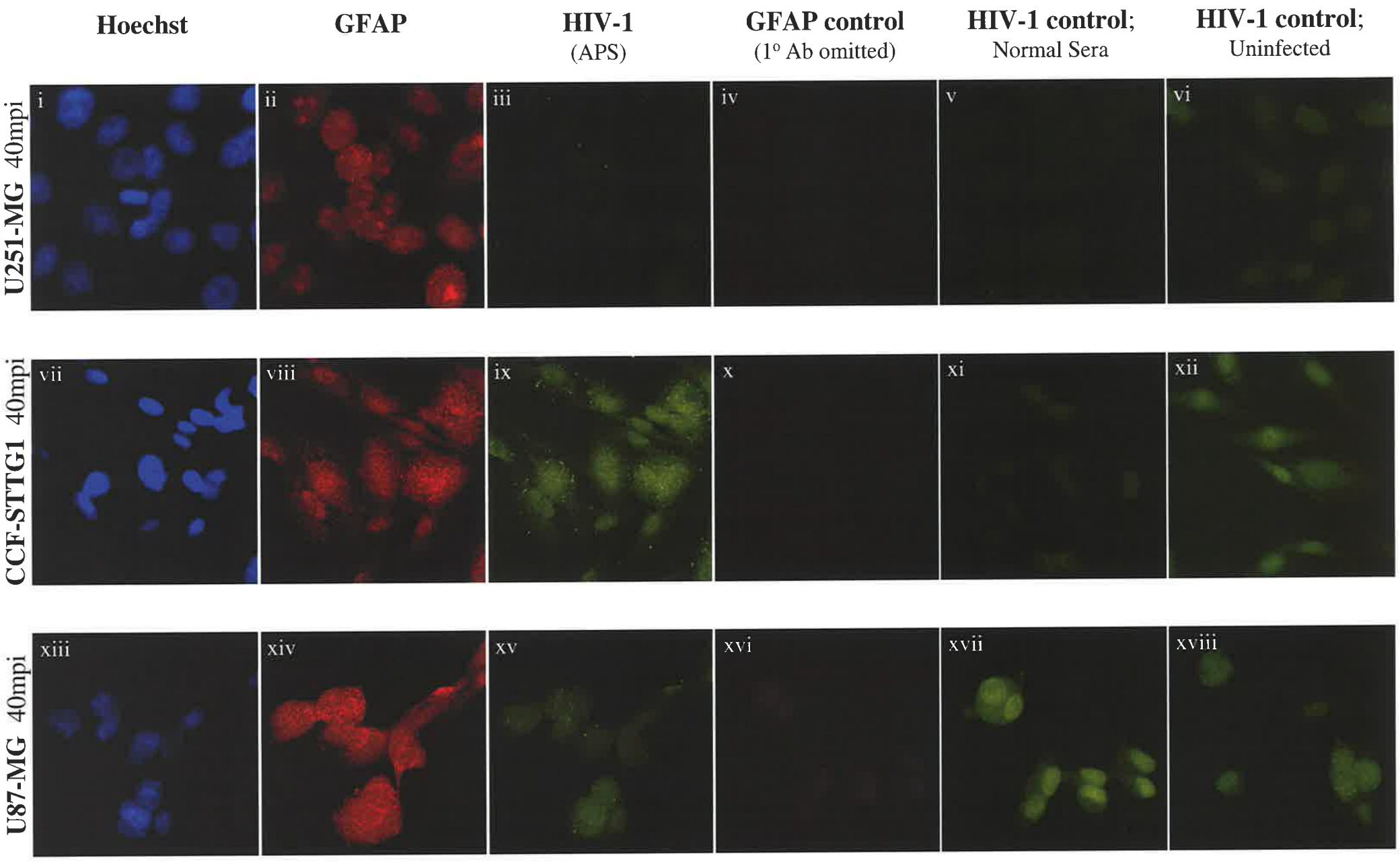
Hoechst
GFAP
HIV-1
(APS)
GFAP control
(1° Ab omitted)
HIV-1 control;
Normal Sera
HIV-1 control;
Uninfected
U251-MG 40mpi
CCF-STTG1 40mpi
U87-MG 40mpi
i
ii
iii
iv
v
vi
vii
viii
ix
x
xi
xii
xiii
xiv
xv
xvi
xvii
xviii

Figure 4.8 APS immunoreactivity in CCF-STTG1 astrocytes 40 minutes post HIV-$1_{NL4.3}$ infection.

CCF-STTG1 astrocytes were cultured overnight on glass coverslips and subsequently infected with HIV-$1_{NL4.3}$ for 40 minutes, as described in Figure 4.7. The cells were then washed, fixed, and processed for indirect immunofluorescence assay using APS to detect HIV-1 immunoreactivity (i, ii, iii) or normal human sera as a control (iv). Uninfected cells treated with the APS (v) were also included as controls. The images were captured by confocal microscopy at 400x magnification. Identical laser settings were used for control and experimental cells for each cell type.

CCF-STTG1 40mpi
HIV-1 (APS)

CCF-STTG1 40mpi
HIV-1 control; Normal Sera

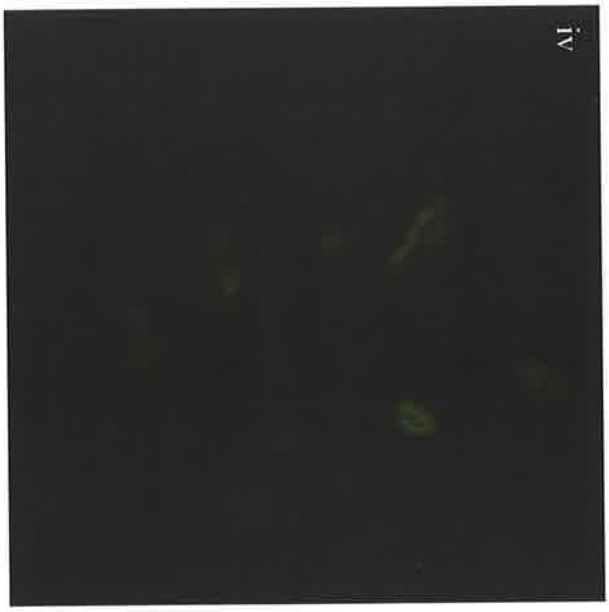

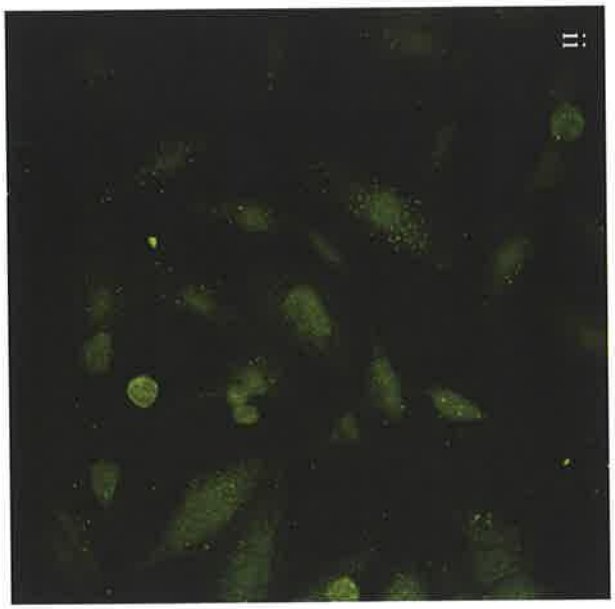

CCF-STTG1
HIV-1 control; Uninfected

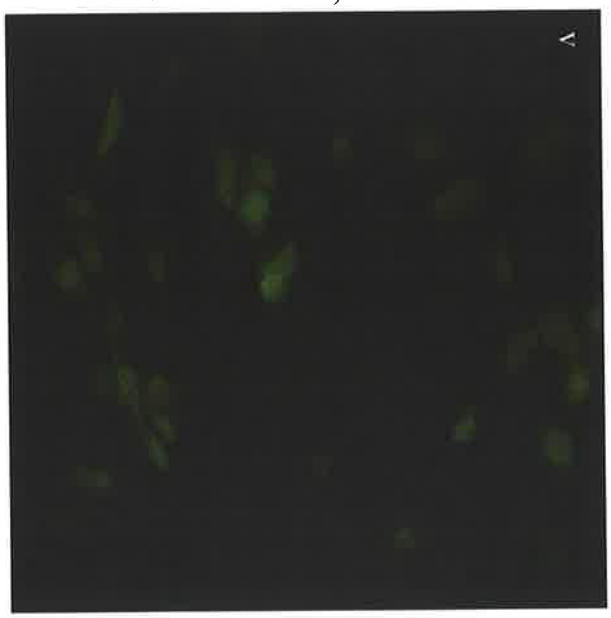

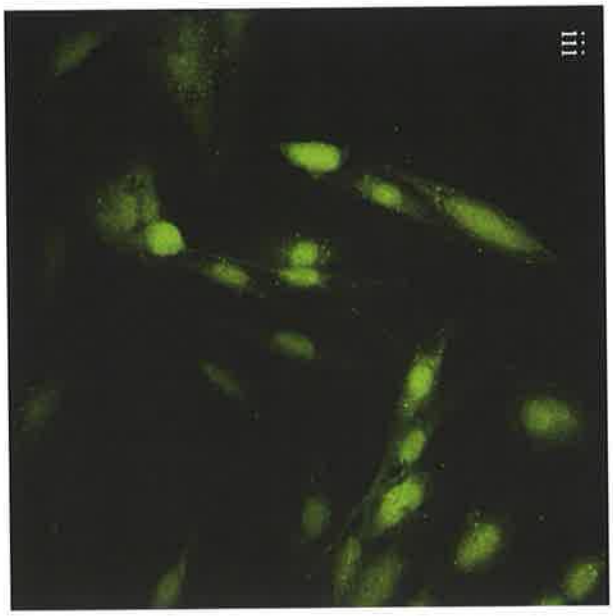

glass, and glass to oil, water and air interfaces).

The majority of punctate immunoreactivity in HIV-1 exposed U251-MG and CCF-STTG1 cells was confirmed to be cytoplasmic by comparison to the Hoechst 33342 staining of the nucleus (blue fluorescence) (Figure 4.7i, vii). In infected U87-MG cells, some of the punctate immunoreactivity to APS was clearly cytoplasmic, however, due to the rounded morphology of these cells, this could not be determined for the majority of APS immunoreactive spots. Optical Z-sectioning confirmed that the punctate APS immunoreactivity was intracellular in all three astrocyte cell lines, and no surface staining was observed on any of the cells.

4.2.5 Summary and consideration of the modes of endocytosis which could be involved in the uptake of virus / viral proteins by the astrocyte cells

Whilst U87-MG expressed a higher level of GFAP than the other two cell lines, the frequency of punctate APS immunoreactivity per cell (Figure 4.7xv) was no higher than in U251-MG cells (Figure 4.7iii), and less than that observed in CCF-STTG1 cells (Figure 4.7ix). The relationship of this result to a previous finding that the level of GFAP expression may correlate with the susceptibility of astrocyte cell lines to HIV-1 infection (Cheng-Mayer *et al*, 1987) is unclear. The APS immunoreactivity observed and presented in this chapter indicates a mechanism by which HIV-1 proteins are internalised by astrocytes, but this line of investigation does not address whether the astrocytes subsequently produce virus as a result of this internalisation. Also, the obvious morphological difference seen with U87-MG cells grown on glass coverslips indicates cellular changes which may affect their capacity to uptake HIV-1. The punctate immunoreactivity to APS which was seen in all three astrocyte lines when fixed 40mpi indicated that each internalised APS immunoreactive proteins into vesicle-like cytoplasmic compartments, suggestive of virus / viral protein uptake by endocytosis. This immunoreactivity appeared specific for HIV-1 proteins, as it was not observed in uninfected cells, nor infected cells treated with NHS in place of APS, and, in U251-MG cells, punctate immunoreactivity was also observed with a MoAb to the HIV-1 core protein, p24. This internalisation of viral proteins was seen as early as 5mpi in U251-MG cells, although it was more pronounced at later time points (15-75mpi). These vesicle-like compartments did not

exhibit colocalisation with the uptake of labelled transferrin in U251-MG cells, suggesting the mode of viral protein internalisation was unlikely to be clathrin-dependent endocytosis (Section 4.2.2i, ii).

Several other endocytic pathways exist (Figure 4.9), which may be exploited by various viruses to gain entry into cells (Sieczkarski and Whittaker, 2002). Indeed, the majority of virus families use endocytosis as a means of entry into cells, with many viruses exploiting the pH changes for conformational change, membrane fusion and / or uncoating, and / or exploiting the vesicle trafficking pathway for perinuclear localisation (Sieczkarski and Whittaker, 2002). Caveoli-dependent endocytosis of HIV-1 is considered unlikely, as vesicles formed by this mode of endocytosis are smaller (50 to 80nm in diameter (Conner and Schmid, 2003; Marechal *et al*, 2001)) than the HIV-1 virion itself (100-120nm in diameter (Coffin *et al*, 1997) (Section 1.1.1)). Clathrin-independent and caveoli-independent mechanisms of endocytosis are known to exist, although these remain to be characterised (Sieczkarski and Whittaker, 2002). Pinocytosis, a non-specific, non-receptor mediated, form of fluid uptake, usually results in vesicles smaller than the HIV-1 virion (Casey *et al*, 1986; Daher *et al*, 2001). Phagocytosis, and the less characterised process of macropinocytosis, result in cytoplasmic vesicles which are large enough to entrap entire virions (>0.2μm (Marechal *et al*, 2001; Swanson and Watts, 1995)).

Characterisation of the mode of endocytosis involved in viral uptake can be addressed by either i) drug studies with inhibitors of endocytosis, ii) colocalisation with proteins associated with particular stages or pathways of endocytosis, or iii) by electron microscopy. Traditional inhibitors of endocytosis such as brefeldin A and chlorpromazine, and low-pH shock treatment or potassium depletion, need to be used with caution as they are non-specific and have multiple effects on cell function. Newer, dominant-negative mutant versions of cellular proteins involved in various endocytosis pathways are more specific in their mechanism of action, however still need to be used with caution as cells expressing these proteins may compensate by upregulating other endocytic pathways (Sieczkarski and Whittaker, 2002).

Several antibodies are now commercially available for detection of members of the Rab family of GTPases, which are involved in specific stages of intracellular vesicle-sorting

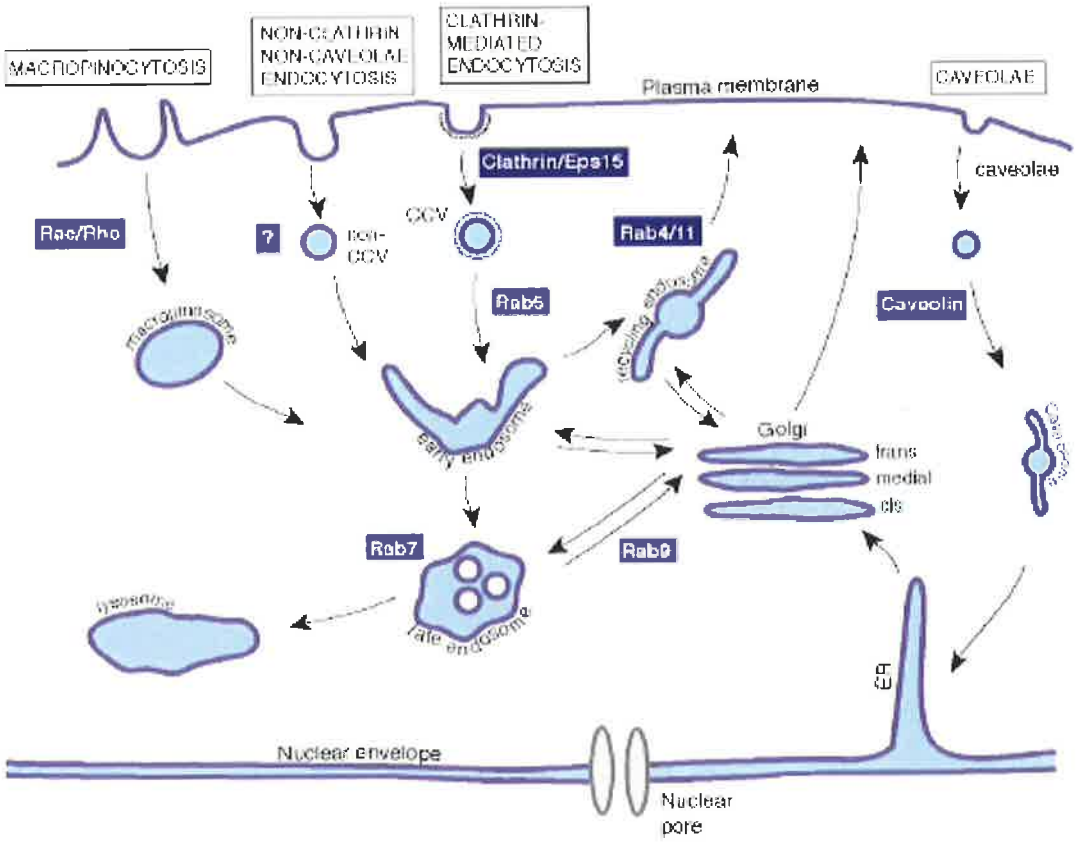

Figure 4.9 Summary of the major routes of endocytosis used by viruses.

Viruses can gain entry into cell cytoplasm by either direct penetration of the plasma membrane or by entering the cell via endocytosis, and subsequently gaining access to the cell cytoplasm. The most characterised route of endocytosis is via the formation of clathrin-coated pits. A number of viruses have been shown to enter cells via clathrin-mediated endocytosis. Several other mechanisms of endocytosis exist, which also have been shown to be exploited for cell-entry by various viruses. These include caveolin-mediated endocytosis and an apparent range of non-clathrin, non-caveolin mediated endocytic processes which remain to be well characterised. Other viruses gain entry via phagocytosis or macropinocytosis. Endocytosed vesicles become progressively acidified and undergo complex vesicle-sorting and intracellular trafficking events. The two main fates of endocytic vesicles are recycling of the contents to the cell surface and degradation via lysosomal targeting. The progress and pathway of vesicular trafficking may be identified by the morphology, intracellular location, pH, and the markers (such as Rab4, Rab5, Rab7, Rab11, Clathrin, Eps1, Caveolin, Rac and Rho) expressed on the vesicle. Many viruses exploit the low pH environment of endosomes to undergo conformational changes, membrane fusion and / or uncoating. A number of viruses also exploit the intracellular vesicular trafficking events to travel to the nucleus.

Figure taken from Sieczkarski and Whittaker (2002).

processes. These include antibodies to Rab5 (early endosomes), Rab4 and Rab11 (recycling endosomes), Rab7 (late endosomes), and Rab9 (transport between late endosomes and the Golgi apparatus) (Chavrier *et al*, 1992; Miyazawa *et al*, 2001; Novick and Brennwald, 1993; Somsel Rodman and Wandinger-Ness, 2000) (Figure 4.9). Additional antibodies directed against proteins specific to early endosomes (early endosome protein 1 (EEA1) (Mu *et al*, 1995) and lysosomes (lysosomal associated membrane proteins 1 and 2 (LAMP1 and LAMP2) (Chen *et al*, 1988; Febbraio and Silverstein, 1990)), as well as fluorescent pH indicators suggestive of the stage of endocytosis and fusion with lysosomes, are also commercially available. Analysis of the endocytic compartment at the ultrastructural level is the "gold standard" for identification of several modes of endocytosis, and can provide crucial morphological information on the nature of the vesicle / endocytic pathway involved. Electron microscopy was therefore pursued in this study, as it has the potential to distinguish intact virions from soluble viral proteins as well as provide important information on the mode of viral uptake.

4.3 Analysis of virus entry into astrocytes by electron microscopy

4.3.1 Preliminary Electron Microscopic Analysis

4.3.1i Maximising the probability of locating intracellular virions by EM.

The probability of locating intracellular virions by EM analysis was anticipated to be very low, due to the low level of infection of HIV-1 in astrocytes (Section 1.4) and the indications that entry is a major restriction to astrocyte infection (Sections 1.5.1, 1.6.1vi, 4.1.1 and 4.2.1ii). The observation of punctate APS immunoreactivity in almost all U251-MG and CCF-STTG1 astrocytes, and in the majority of U87-MG astrocytes, 40mpi (Section 4.2 above), however, did suggest that HIV-1 virions or HIV-1 proteins were readily internalised by most of these cells. The uptake of HIV-1 by the majority of cells would increase the probability of locating intracellular virions. However, the probability of locating a section upon EM analysis that contained a cross-section of clearly recognisable virions was low. It was anticipated that the identification of internalised virus by EM analysis might be further compounded by a brief window of time during which virions may

maintain their characteristic morphology. This is because HIV-1 virions shed their outer membrane (visible as an electron dense ring) during fusion with the cell membrane, and upon gaining access to the cytoplasm the viral core "uncoats". As a consequence virions would lose their distinctive electron dense envelope ring and cylindrical form encompassed by the envelope. If the virus is entrapped within vesicles, as suggested by the immunofluorescent observations (Section 4.2), the morphology of the viral core may be lost due to the progressive acidification which occurs within endosomes (Sieczkarski and Whittaker, 2002), as the conformation (and electron density) of the viral capsid protein which forms the viral core is pH dependent (Ehrlich *et al*, 2001).

Therefore, to maximise the probability of locating HIV-1 virions within astrocytes, virus stocks of the highest available titre were employed. These included a HIV-1_{IIIB} stock with a titre of 3.16×10^6 $TCID_{50}$/ml (kindly provided by Dr Nick Vandegraaff) and a HIV-1_{NL4-3} stock with a p24 content of 5.97 μg/ml (Section 2.3.4). U251-MG cells were cultured overnight in chamber-slides and exposed to HIV-1 for 40 minutes (the infection time was chosen based on the immunofluorescent observations in Section 4.2), washed with PBS and immediately fixed for EM analysis. Dr Peter Sutton-Smith performed further processing of the cells and EM analysis. Preliminary experiments revealed cells of poor ultrastructural morphology, which prevented the potential identification of any virion-like structures. No alteration of cell morphology upon infection had been observed by light microscopy in this experiment, nor in any previous or subsequent experiments. The poor ultrastructural morphology could have been due to certain cellular stresses imposed on the cells in the change from relatively fresh media to virus inoculum. In addition to intact virions, the virus inoculum (stored culture supernatant collected from virus-producing cells) may also contain a variety of viral proteins and spent cellular metabolites, and would also be depleted of serum and growth factors. The osmolarity and pH of the virus inoculum may also deviate from that of fresh cell culture medium. To address this, and to improve the chance of locating intracellular virions, a number of strategies were trialed in order to infect the cells in the presence of fresh medium, and / or with concentrated virus inoculum.

Optimisation of virus inoculation to preserve the ultrastructural integrity of the cells and to maximise the chance of locating intracellular virions.

To address the issue of U251-MG cell ultrastructural morphology, a pilot study of infection procedures were addressed (Section 2.3.4i). As the high titre HIV-1_{IIIB} stock was more abundant than the high titre HIV-1_{NL4-3} stock, the latter was used for this optimisation. To minimise the potential shock of the medium change, inoculations were performed with a dilution series (½, ¼, ⅛) of the virus in fresh media. Diluting the virus, however, would concomitantly decrease the probability of detecting internalised virions. Virus inoculations were also performed where, after a 40 minute period of infection, the inoculum was replaced with fresh medium, and the cells allowed to recover for a period of time (0.5, 1, 2, 4, 6, 8 hours) before being fixed for EM analysis. This may also decrease the chance of identifying internalised virions, as they may have uncoated in the cytoplasm or degraded within endosomes during this time. Several methods of virus concentration were attempted, including ultracentrifugation (the resulting viral pellet was resuspended in fresh medium), and centrifugation with high molecular weight retention columns manufactured by Centricon and Millipore. Virus in the Centricon columns required several spins of 30 minutes to reduce the virus stock volume 8 fold, after which the virus stock was diluted ½ in fresh medium (to minimise the shock of medium change to the cells). Virus retained in the Millipore column was concentrated 40 fold in one 30 minute centrifugation, and was subsequently washed twice with PBS and once with fresh media, and the final preparation diluted ½ in fresh medium. Due to the labour required for EM analysis, the cells treated with ultracentrifuged and Millipore column concentrated virus were analysed first, as these methods resulted in the most concentrated virus in fresh medium.

4.3.2 Identification of enveloped, mature virion-like particles within a vesicle-like structure in U251-MG astrocyte 40 mpi

Analysis of U251-MG astrocytes that had been infected with Millipore column concentrated HIV-1_{IIIB} revealed one section in which several virion-like structures were observed (Figure 4.10). The ultrastructural morphology of these virion-like particles was consistent with mature, enveloped HIV-1 virions (Figure 1.4 and Section 1.1.5). In particular, the structures appeared to possess an electron-dense perimeter in the form of a roughly circular ring with a diameter of approximately 100–120 nm, consistent with the envelope and size of HIV-1 particles. Within these electron-dense rings, a denser inner portion could be identified. In one of the rings the inner portion had cone-shape morphology (Figure 4.10B arrow). This is

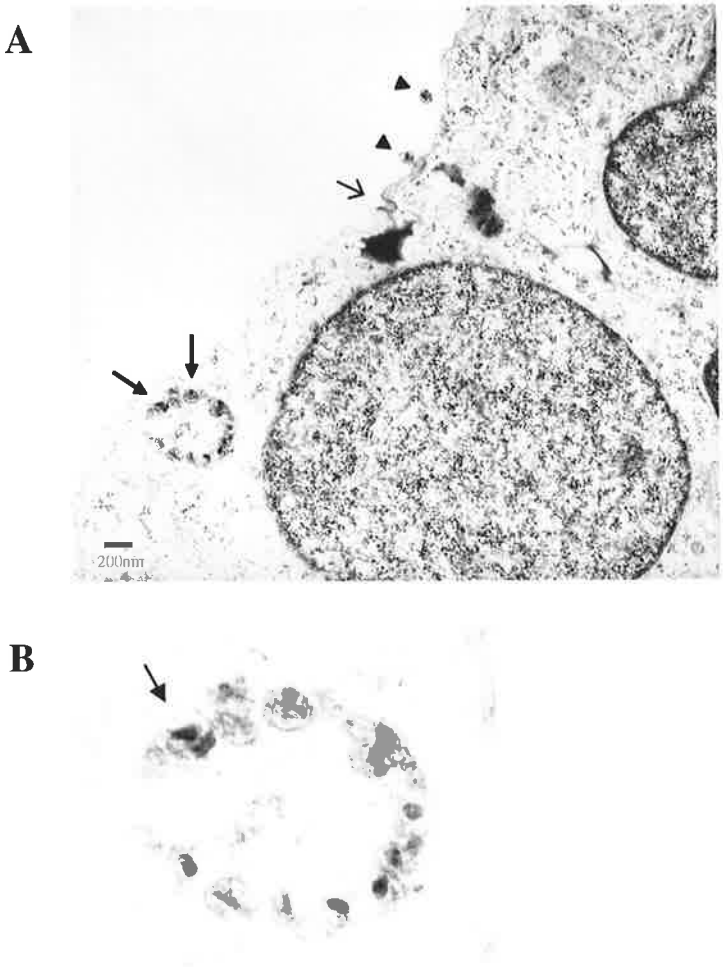

Figure 4.10 Electron microscopy of U251-MG astrocytes fixed 40 minutes post infection with HIV-1_{IIIB}.

U251-MG astrocytes were cultured overnight in chamber slides and subsequently exposed to HIV-1_{IIIB}. After 40 minutes of infection, the cells were washed, fixed, and processed for electron microscopy analysis.

consistent with a cross-section lengthwise through the cone-shaped core which is typical of virions of the Retroviridae family (Sections 1.1.1 and 1.1.5). Up to eleven virus-like structures appeared to line the inner membrane of a large vesicle-like structure within the cytoplasm of the cell. The observation that the inner portion was not distinctly cone shaped in all of these structures is consistent with virions that have been sectioned at different angles. The dimensions of the vesicle-like structure harbouring the virions were approximately 400 x 600 nm. These dimensions are too large to represent caveolin-coated vesicles (50 to 80nm in diameter (Conner and Schmid, 2003; Marechal *et al*, 2001)) or clathrin-coated vesicles (85-110nm diameter (Bretscher and Thomson, 1983; Conner and Schmid, 2003; Swanson and Watts, 1995). In addition, structures resembling clathrin-coated pits were observed (electron dense invaginations of the plasma membrane which occur early in the process of clathrin-dependent endocytosis) (Figure 4.10A, thin arrow), and virion-like structures were not observed near these electron-dense invaginations. The dimensions of the large vesicle-like structure harbouring the virion-like particles was consistent with a phagosome or macropinosome, or possibly a multi-vesicular body (MVB, also referred to as a "late endosome") (Figure 4.9). The attributes of these possibilities are presented below and discussed in the context of HIV-1 and astrocytes. Despite scanning additional sections from this and other HIV-1 exposed U251-MG astrocytes, no other convincing virus-like structures were observed inside the cells. CCF-STTG1 astrocyte cells which were exposed to Millipore column concentrated HIV-1_{IIIB} for 40 minutes did show similar, but less convincing, virus-like particles within vesicle-like structures, although the cellular morphology in these preparations was poor.

4.3.2i Phagocytosis, macropinocytosis and multivesicular bodies; consideration of the identity of the virion-filled vesicle

Phagocytosis

Phagocytosis is a cellular receptor-mediated internalisation process of ingestion, and is involved in the uptake of pathogens, apoptotic bodies and debris (Henneke and Golenbock, 2004). Macrophages, dendritic cells and granulocytes act as "professional phagocytes", and are involved in the recognition, uptake and processing of foreign bodies by phagocytosis. These cells express so-called "pattern-recognition receptors" (PRRs) (Janeway, 1989) which

include the C Type Lectin family of receptors (of which the Mannose Receptor is a member), Toll-like Receptors and Scavenger Receptors. These receptors enable broad-spectrum recognition of a variety of types of surface antigens, which are present on pathogens. Upon receptor binding, cell membrane pseudopods form and encompass the foreign body. This process is driven by actin polymerisation, and, in conventional phagocytosis, the pseudopod extension is guided by molecules on the surface of the particle which is being ingested. The dimensions of formed phagosomes usually exceed 500μm in diameter (Marechal *et al*, 2001), but depend on the size of the particle being ingested. Newly formed phagosomes proceed to fuse with lysosomes, generating "phagolysosomes" in which the foreign body is partially degraded. The subsequent vesicular trafficking and fate of the internalised particle is governed, at least in part, by the PRRs involved. The contents of the phagolysosome may be routed to antigen presentation in conjunction with MHC class II molecules (adaptive immune response), to stimulation of certain Toll-like receptors which upregulate an inflammatory cytokine response (innate immunity), or to nutrient recycling (Stuart and Ezekowitz, 2005). A subpopulation of astrocytes express the Mannose Receptor (Liu *et al*, 2004) which can bind HIV-1 (Liu *et al*, 2004; Nguyen and Hildreth, 2003), and can facilitate phagocytosis (see above). As astrocytes may be capable of phagocytosis (Shrikant and Benveniste, 1996) (Section 1.2.4ii), it is possible that the virion-filled vesicle observed in Figure 4.10 could be a phagosome.

Macropinocytosis

The term macropinosome describes giant pinosomes and usually infers a diameter of ≥ 0.2 μm (Marechal *et al*, 2001; Swanson and Watts, 1995). Macropinosomes of up to 5μm have been observed (Fawcett, 1965; Hewlett *et al*, 1994; Swanson, 1989). Unlike conventional phagocytosis (and clathrin-dependent or caveoli-dependent endocytosis), macropinocytosis (and pinocytosis) is considered to be a process of non-receptor mediated, fluid-phase endocytosis in which receptors are not concentrated (Racoosin and Swanson, 1992). Macropinosomes form from actin-driven membrane ruffling events, upon fusion of "ruffles" such that a portion of extracellular fluid becomes entrapped in an intracellular vesicle (Swanson and Baer, 1995; Swanson and Watts, 1995). The morphology of the membrane ruffling, the extent of macropinocytosis, and the subsequent intracellular processing and fate of these vesicles varies between cell types and their activation state (Racoosin and Swanson,

1989; Racoosin and Swanson, 1993; Swanson, 1989). In some cells, such as human A431 cells, macropinosomes eventually recycle their contents to the cell surface (Hewlett *et al*, 1994). In other cells (for example, macrophages) macropinosomes rarely fuse again with the cell surface. Instead, they acquire then lose markers of late endosomes / MVBs (Rab7) and, later, markers of lysosomes (Lgp-A) (Racoosin and Swanson, 1993). Immature dendritic cells constitutively perform a high level of macropinocytosis (Sallusto *et al*, 1995) which is targeted to MVB compartments rich in MHC class II molecules (Kleijmeer *et al*, 1997; Kleijmeer *et al*, 1996; Peters *et al*, 1991b) and associated with antigen processing and presentation (Sallusto *et al*, 1995; Sallusto and Lanzavecchia, 1994). As such macropinocytosis has been hypothesised to represent a mechanism of antigenic sampling (Swanson and Watts, 1995). Whether astrocytes perform macropinocytosis has not been investigated, but is plausible given astrocytes may be induced to express MHC class II (Malipiero *et al*, 1990) (Section 1.2.4ii), may be capable of antigen presentation (Fierz *et al*, 1985; Fontana *et al*, 1986; Fontana *et al*, 1984; Gehrmann *et al*, 1995; Shrikant and Benveniste, 1996) (Section 1.2.4ii), and U87-MG astrocytes with ruffled membranes have been observed (Liu *et al*, 2004). Also, reports of phagocytosis, including one suggesting astrocytes may be capable of phagocytosis (Shrikant and Benveniste, 1996), do not always differentiate between conventional phagocytosis and the phenomenon of macropinocytosis, which has only been recently described.

Distinguishing between phagocytosis and macropinocytosis

Distinguishing between phagocytosis and macropinocytosis with pharmacological agents is not straightforward. As both processes depend on actin polymerisation, drugs which affect actin dynamics (for example, cytochalasins) are not specific to either. Other inhibitors of macropinocytosis (phosphatidylinositol 3-kinase, Rho-GTPase and Na+/H+ exchange inhibitors, eg Wortmannin, toxin B and amiloride respectively) are also limited in their specificity and may interfere with other forms of endocytosis (Apodaca, 2001; Corvera, 2001; Sieczkarski and Whittaker, 2002). It may be possible to specifically target macropinocytosis with new dominant-negative forms of specific members of the ARF and Rho GTPases or Rac-dependent kinases (Dharmawardhane *et al*, 2000; Nichols and Lippincott-Schwartz, 2001; West *et al*, 2000), but these methods are yet to be established and have not been applied to virus entry. The identification of GTPases or kinases specific to macropinocytosis may support the labelling of macropinosomes by specific

immunofluorescence antibodies. At present, dextran particles of specific sizes can be used to assess the vesicle size of fluid-phase endocytic uptake, but a strategy to specifically immuno-label macropinosomes does not yet exist.

Phagocytosis and macropinocytosis are also not easily distinguishable by morphology. In conventional phagocytosis the vesicle closely envelops the internalised particle. Newly formed macropinosomes represent seemingly random fluid enclosures formed by the fusion of membrane ruffles, however within 15 minutes of enclosure they may shrink considerably (Berthiaume *et al*, 1995; Racoosin and Swanson, 1993) and, where particulate matter is entrapped, their appearance may not be dissimilar to that of a phagosome. The identification of macropinocytosis as a route of virus entry requires a timely assessment of ultrastructure and the visualisation of virus particles at sites of membrane ruffles and within large irregular vesicles (Sieczkarski and Whittaker, 2002). Indeed HIV-1 has been demonstrated to enter macrophages in this manner (Marechal *et al*, 2001).

Multivesicular Bodies

Multivesicular bodies are late endosomes so named because they contain intra-luminal membrane-bound vesicles (Pho *et al*, 2000; Sotelo and Porter, 1959). The identification of virions in MVBs would not indicate a specific mode of internalisation, but rather the fate of trafficking and vesicle sorting processes of a given vesicle. All modes of endocytosis may undergo trafficking events that result in MVBs. Aside from virus-like particles, no other internal vesicle structures were observed in the large virion-like filled vesicle shown in Figure 4.10. This structure is therefore unlikely to represent a MVB. If relevant, MVBs can also be identified with antibodies to specific GTPases associated with late endosomes, for example, Rab7 (Miyazawa *et al*, 2001; Somsel Rodman and Wandinger-Ness, 2000), or by fluorescent pH indicators ("lysotrackers" or "lysosensors"). Even if HIV-1 uptake was routed to MVBs, this pathway is unlikely to result in astrocyte infection as MVBs are usually targeted for lysosomal degradation (Kornfeld and Mellman, 1989), although in some scenarios, including the presentation of MHC associated antigen by antigen presenting cells, the internal vesicles of MVBs can be shunted to the cell surface ("exocytosis") as an outgoing vesicle ("exosome") (Denzer *et al*, 2000).

4.4 Discussion

The aim of this chapter was to investigate the mode of HIV-1 entry into astrocytes by characterising the cellular localisation of HIV-1 proteins and virions after brief virus exposure (5-75 min), by immunoreactivity and electron microscopy. Previous investigations of HIV-1 immunoreactivity in astrocytic cells have been performed after at least 24 hpi (Brack-Werner *et al*, 1992; Brengel-Pesce *et al*, 1997; Chesebro *et al*, 1990; Chiodi *et al*, 1987; Clapham *et al*, 1989; Keys *et al*, 1991; Nath *et al*, 1995; Shapshak *et al*, 1991; Tornatore *et al*, 1994b; Tornatore *et al*, 1991; Weber *et al*, 1989), to identify cells in which viral protein production was occurring. In this chapter, by fixing the cells within 75 minutes of virus contact, HIV-1 immunoreactivity indicated the cellular location of the input virus (or viral proteins) rather than the expression of viral proteins (which would require at least 16 hpi). Immunofluorescent observations (Section 4.2) of all three astrocyte cell lines within the first 75 minutes of HIV-1 infection demonstrated punctate HIV-1 immunoreactivity in almost all cells. This was seen as early as 5 mpi (Figure 4.5A), and with both AIDS Patient Sera (Figures 4.2, 4.4, 4.5, 4.7) and a monoclonal antibody to HIV-1 p24 (Figure 4.6). This vesicle-like immunoreactivity did not appear to colocalise with a marker of clathrin-dependent endocytosis (Figures 4.4, 4.5). Electron microscopy (Section 4.3) revealed the presence of mature, enveloped virion-like structures within a vesicle consistent with a phagosome or macropinosome, after 40 minutes of exposure to HIV-1 (Figure 4.10). This is concordant with the immunofluorescence findings, and confirms that entire virions are taken up into vesicles in astrocytic cells. Shortly after this EM finding, Liu *et al*. demonstrated intact HIV-1 virions with a phagosome- or macropinosome-like structure in HFAs (at 30 mpi) and U87-MG cells transfected to express the Mannose Receptor (at 5-60 mpi) (Liu *et al*, 2004). Internalised virions were visible at sites of plasma membrane ruffling in these U87-MG-Mannose Receptor expressing cells, suggestive of active macropinocytosis at the site of virus internalisation. This group also demonstrated that the Mannose Receptor acts a receptor for HIV-1 infection of astrocytes (Liu *et al*, 2004). This is the only receptor demonstrated to be involved in HIV-1 infection of astrocytes, although the involvement of additional receptors is also implicated (Liu *et al*, 2004). Prior to this, Hao and Lyman had also proposed that HIV-1 is internalised by astrocytes by a receptor-mediated vesicular route (Hao and Lyman, 1999). They demonstrated that the gp120 envelope molecular of HIV-1_{RF} bound to an astrocyte membrane associated protein of

65kDa, and visualised virions in clathrin-coated pits within the first 90 minutes of HFA infection by EM analysis. The apparent discrepancy in the mode of virus internalisation between the results of Hao and Lyman and the observations in this chapter and Liu *et al.*, in which virus uptake appears clathrin-independent, may be due to the strain of HIV-1 studied. Taken together, these results suggest more than one mode of HIV-1 uptake may occur in astrocytes, and that this may depend on the virus strain, and potentially also the phenotype of the astrocyte cell.

The mannose receptor (MR), belongs to the large C-type lectin receptor superfamily, and its ligand binding is mediated by mannosylated and / or mannose-rich glycan moieties present in its ligands (East and Isacke, 2002; Pontow *et al*, 1992). MR (also known as CD206) has well characterised roles in both the innate and adaptive immune system, and is expressed on macrophages and dendritic cells (East and Isacke, 2002). It is involved in internalisation of particles via both clathrin-mediated endocytic (usually recycling between early endosomes and the cell surface) and phagocytic pathways. The MR acts as a PRR, exhibiting binding to terminally mannosylated carbohydrate molecules which are present on the surface of a variety of pathogens (East and Isacke, 2002), including HIV-1 (Nguyen and Hildreth, 2003). Macrophages and dendritic cells internalise MR bound antigens and process them for antigen presentation (Stahl and Ezekowitz, 1998). There is also increasing evidence that MR may play a role in antigen recognition and processing (Prigozy *et al*, 1997). MR is also expressed on a range of other cell types including certain epithelial, endothelial, and muscle cells, suggesting it has several other functions (Lew *et al*, 1994; Linehan *et al*, 1999; Shepherd *et al*, 1991). MR plays a key role in the initial binding events of HIV-1 to dendritic cells (Geijtenbeek *et al*, 2000) and macrophages (Nguyen and Hildreth, 2003). MR is reported to be expressed on almost 50% of HFAs and has been demonstrated on astrocytes in fixed brain sections (Liu *et al*, 2004).

With the exception of the report by Liu *et al.* and Hao and Lyman, all previous attempts to identify virion structures in astrocytes by electron microscopy have investigated later time points post infection. Brack-Werner *et al.* performed EM analysis on their laboratory chronically HIV-1_{IIIB} infected astrocyte cell line (TH4-7-5 cells, see Sections 1.4.2, 1.5.2 and 1.5.3i). Whilst these cells were able to transmit infection upon coculture, they saw no signs of intra- or extra-cellular virus structures (Brack-Werner *et al*, 1992). Interestingly Nath *et al.* observed uncoated viral particles within the cytoplasm of infected HFAs by EM

analysis after 24 hours of coculture with HIV-1_{SF2} producing cells. Nath *et al.* specifically noted that the viral particles were not in endocytic or phagocytic vesicles (Nath *et al*, 1995). This could be because the majority of endocytosed virus would have been subjected to low pH environments by this time, potentially altering the conformation of the virus such that any vesicle-enclosed virus structures may not be readily identifiable by EM. The finding of uncoated virus particles in the cytoplasm and absence of virus particles within vesicles in this study could also be due to the strain of HIV-1 used, as it has since been demonstrated that HIV-1_{SF2}, known for its unique ability to productively infect astrocytes (Nath *et al*, 1995) (Prof Cecilia Cheng-Mayer, personal communication), exhibits unique membrane fusion properties at low pH (Fackler and Peterlin, 2000) (Sections 1.6.1iii). However, Epstein *et al.* also observed virus particles within the cytoplasm of astrocytes by EM on brain sections from a paediatric AIDS patient, and reported that the particles were "usually scattered among the subcellular organelles and intermediate filaments" (Epstein *et al*, 1984).

This chapter did not attempt to identify the receptors involved in the binding and uptake of HIV-1, and it is quite probable that other receptors were involved in addition to MR. Whilst the expression of MR on U251-MG and CCF-STTG1 cells has not been investigated, the proportion of U87-MG cells which express surface MR is low (~2.5% by FACS) (Liu *et al*, 2004). This suggests additional receptors may have been involved in the uptake of HIV-1 immunoreactive proteins observed in U87-MG cells (Figure 4.7xv). The elusive HIV-1 receptors on astrocytes could include other PRRs as, with the exception of MR, the expression of PRRs on astrocytes has not been assessed.

The ultrastructural observation of virion-like structures within a large vesicle in U251-MG cells 40 mpi in this study (Figure 4.10), and in fetal astrocytes (Liu *et al*, 2004), indicate that the virus is gaining entry to the cells via either macropinocytosis or phagocytosis. It is technically difficult to conclusively discern the mode of entry, although the membrane ruffling observed by Liu *et al* (2004) is suggestive of macropinocytosis. Further characterisation of the receptors involved may not necessarily distinguish between these two possibilities either, as, for example, MR can act as a receptor for both phagocytosis and macropinocytosis. It is perhaps more relevant to address the fate of the virions in these vesicular compartments. It is plausible that additional modes of HIV-1 entry into astrocytes may also occur. For example, virions which may have fused at the plasma membrane would be difficult to observe as the core would have separated from the envelope and possibly

commenced uncoating. Within the cell cytoplasm, the viral pre-integration complex would be difficult to detect by confocal immunofluoresence, possibly requiring a combination of sophisticated fluorescent labelling techniques and deconvolution analysis of the confocal images. Ultrastructural analysis alone would not be able to identify these viral replication complexes either, unless immuno-EM was employed. Virus which is internalised into vesicles in which the pH is rapidly decreased would also be difficult to detect, as epitopes for antigen binding may be pH sensitive, and the virus core structure is pH sensitive (Ehrlich *et al*, 2001).

Thus, this chapter demonstrates that HIV-1 can enter astrocytes via vesicular uptake, consistent with the recently published observations of (Liu *et al*, 2004). However, this is not necessarily the only route of entry of HIV-1 into these cells, and the subsequent fate of HIV-1 internalised in this manner is unknown. Endocytosed HIV-1 may subsequently fuse with the vesicle membrane, allowing subsequent virus replication (Fackler and Peterlin, 2000; Marechal *et al*, 2001), or may merely result in viral degradation (Fredericksen *et al*, 2002; Marechal *et al*, 1998; Schaeffer *et al*, 2001). To attempt to address this would require highly sophisticated microscopic analysis in conjunction with endocytosis inhibition and receptor blocking studies. To determine whether uptake of HIV-1_{NL4-3} by U251-MG, CCF-STTG1 and U87-MG astrocytes can lead to viral replication, the next chapter assessed the next step in the viral replication cycle after viral entry; reverse transcription.

Chapter 5

Reverse Transcription of HIV-1 in Astrocytes

(following cell free infection)

5.1 Introduction

5.1.1 Background

Once HIV-1 has gained entry into a target cell, the next step in viral replication is the uncoating of the viral core in conjunction with reverse transcription of the viral RNA genome into a linear, double stranded DNA molecule (see Section 1.1.6 and Figure 1.6). Reverse transcription of the viral DNA is an essential step in the virus life cycle, and is a highly organised and ordered process (Figure 1.7) (Karageorgos *et al*, 1995; Li *et al*, 1993b). The kinetics of the process of reverse transcription have been described for $CD4^+$ cells which support productive HIV-1 infection (Karageorgos *et al*, 1995; Li *et al*, 1993b), but have not been previously characterised in astrocytes. Evidence that HIV-1 reverse transcription can proceed in astrocytes *in vitro* includes; i) the initial phase of productive infection (Brack-Werner *et al*, 1992; Di Rienzo *et al*, 1998; Lawrence *et al*, 2004; McCarthy *et al*, 1998; Messam and Major, 2000; Sabri *et al*, 1999), ii) the detection of a low level of HIV-1 DNA in infected astrocytes (Brengel-Pesce *et al*, 1997; Keys *et al*, 1991; Kort, 1998; Sabri *et al*, 1999), which in some reports is still detectable up to 3 or 4 weeks after infection (Di Rienzo *et al*, 1998; Nath *et al*, 1995) and iii) the ability for so-called "latently" infected astrocytes to transmit infection upon coculture with HIV-1 susceptible cells (Cheng-Mayer *et al*, 1987; Chiodi *et al*, 1987; Dewhurst *et al*, 1987b; Di Rienzo *et al*, 1998; Sabri *et al*, 1999) (Section 1.4). The establishment of a chronically-infected astrocyte cell line by Brack-Werner *et al* (TH4-7-5 cells, refer Sections 1.4.2, 1.5.2 and 1.5.3i) is further evidence that HIV-1 reverse transcription proceeds in infected astrocytes (Brack-Werner *et al*, 1992). The detection of HIV-1 DNA in astrocytes in brain sections from HIV-1 infected individuals indicates that viral reverse transcription also occurs during astrocyte infection *in vivo* (An *et al*, 1999a; An *et al*, 1999b; Chiodi *et al*, 1996; Epstein *et al*, 1984; Nuovo *et al*, 1994; Ranki

et al, 1995; Saito *et al*, 1994; Sharer *et al*, 1986; Takahashi *et al*, 1996; Thompson *et al*, 2004; Tornatore *et al*, 1994a; Wiley, 1996).

As astrocytes are capable of restricting other steps of HIV-1 replication (Bannwarth *et al*, 2001; Gorry *et al*, 1998; Gorry *et al*, 1999; Li *et al*, 2002a; Ludwig *et al*, 1999; Neumann *et al*, 1995; Ong *et al*, 2005) (Section 1.5.3), this chapter investigated whether the process of reverse transcription was inhibited in astrocytes. Past studies which have characterised the post transcriptional restrictions to HIV-1 replication in astrocytes used infection models which bypassed reverse transcription by transfecting the astrocytes with proviral plasmid DNA, or by analysing an astrocyte cell line with an integrated provirus, in order to increase the efficiency of virus expression (Section 1.6.1iv and 1.6.1v). HIV-1 infection of astrocytes has also been studied by transfecting astrocytes to express the main receptor for HIV-1, CD4 (and a coreceptor if necessary), or pseudotyping the virus with VSV or MLV envelope, and in these models a productive infection is seen (Section 1.6.1vi). While this indicates that under certain conditions astrocytes can support productive infection (and thus reverse transcription), these models do not simulate *in vivo* infection in the CNS (Section 1.3.2ii). The aim of this chapter was to characterise the kinetics of HIV-1 reverse transcription upon infection of astrocytes with wild type enveloped HIV-1. A cell-free infection model was adopted to enable accurate and sensitive measurement of *de novo* viral DNA transcripts in astrocytes without the background HIV-1 DNA from the non-astrocyte virus donor cells which confounded the analysis of the cell-to-cell infection model (Chapter 3).

It was anticipated that quantitation of viral reverse transcription should reflect the extent of productive infection, since not all modes of virus entry necessarily lead to viral replication (Fredericksen *et al*, 2002; Marechal *et al*, 1998; Schaeffer *et al*, 2001) (Section 4.4). Consequently, this study of reverse transcription was intended to complement the characterisation of HIV-1 entry into astrocytes in Chapter 4. Evidence that the astrocytes had indeed become infected upon exposure to HIV-1 in our model was sought in all experiments by the ability of the infected astrocytes to transmit virus to HIV-1 susceptible cells upon coculture. All infections were also monitored by measureing the level of viral core protein in the astrocyte culture supernatants. To determine the kinetics of HIV-1 reverse transcription in astrocytes, three astrocyte cell lines (U251-MG, CCF-STTG1 and U87-MG) were exposed to cell-free HIV-1_{NL4-3} virus and the extrachromosomal DNA

extracted and assessed by PCR for the levels of specific reverse transcribed HIV-1 DNA transcripts (Figure 2.1) during the first two days of infection.

5.2 Preliminary Investigations

5.2.1 Establishing a model of cell-free infection of U251-MG astrocytes

5.2.1i Conventional Infection

In initial experiments U251-MG astrocytes were pre-seeded 18 hours prior to infection. The adhered astrocyte cells were exposed to cell-free HIV-1_{IIIB} or HIV-1_{NL4-3} (at approximately 0.05 – 0.1 $TCID_{50}U$/cell, 0.2 - 0.4 pg p24/cell) virus for 2 to 6 hours (Section 2.3.5i), followed by replacement or addition of fresh medium. However, these HIV-1 exposed astrocyte cultures tested negative for transmission of infection to HIV-1 susceptible cells upon coculture which was initiated 7 days later (refer to Section 2.3.5i). This indicated that the U251-MG cells had not actually become infected (Sections 1.4, 1.4.3 and 1.5.4). This was not surprising, as many previous *in vitro* studies of astrocyte infection employ methods to enhance viral inoculation (including the use of agents to alter the cell-surface charge, transfection of plasmids encoding HIV-1 or to express CD4 and a coreceptor for HIV-1 infection, and pseudotyping of the virus; refer to Sections 1.6.1iv-vi) in order to overcome the low efficiency of astrocyte infection. It is possible that a detectable level of infection may have been achieved with higher titre virus stocks than was available at the time ($>10^4$ $TCID_{50}U$/ml).

5.2.1ii Centrifugal Enhancement of Infection ("Spinoculation")

In this thesis, to improve the efficiency of infection, a modified centrifugally enhanced infection protocol (also known as "spinoculation') was adopted (Section 2.3.5ii). The astrocyte cells were suspended by trypsin treatment, and, to prevent adherence during the infection procedure, the centrifugally enhanced inoculation procedure was performed in teflon tubes. The cells were then washed three times (to remove excess inoculum) and seeded into 6-well culture trays. The cell viability and recovery after this procedure was assessed, and no adverse effects were apparent (Section 2.3.5ii).

Preliminary experiments indicated that spinoculation of U251-MG cells was successful, as astrocyte cultures infected by this method were shown to be capable of transmitting infection to HIV-1 susceptible (HuT-78) cells upon coculture initiated after 7 days (refer Section 2.3.5ii). Transmission of infection to the HuT-78 cells in the cocultures was evident by the formation of syncytia in the HuT-78 cell population and the detection of HIV-1 p24 protein in the coculture supernatants, after 2 to 6 days of coculture. This is consistent with the virus "rescue" or "reactivation" phenomenon, characteristic of the restricted HIV-1 infection of astrocytes observed *in vitro* (Cheng-Mayer *et al*, 1987; Chiodi *et al*, 1987; Dewhurst *et al*, 1987b; Di Rienzo *et al*, 1998; Messam and Major, 2000; Sabri *et al*, 1999; Tornatore *et al*, 1991) (Sections 1.4.3). Furthermore, p24 protein was detectable during the first few days of infection, after which it was undetectable (≤6 pg/ml). This was consistent with an initial release of p24 and the subsequent suppression of viral structural protein production, typical of astrocytes infected *in vitro* (Di Rienzo *et al*, 1998; Lawrence *et al*, 2004; Messam and Major, 2000; Sabri *et al*, 1999; Tornatore *et al*, 1994b; Tornatore *et al*, 1991) (Sections 1.4.1, 1.4.2).

The observation of the 3 stages of infection, i) initial p24 protein release, ii) undetectable virus production, and iii) transmission of virus upon coculture, validated this astrocyte infection model. The detection of p24 protein released during the first few days of U251-MG infection and the "rescue" of infection upon subsequent coculture indicated that HIV-1 could be produced by these cells, and that reverse transcription had therefore occurred. Thus this model of astrocyte infection was considered appropriate for the characterisation of the kinetics of HIV-1 reverse transcription in astrocytes.

5.2.2 Preliminary experiments and analysis of HIV-1 infected U251-MG cultures

5.2.2i Initial analysis of HIV-1 DNA and supernatant p24 protein during the course of U251-MG astrocyte infection.

Infection in the presence / absence of the reverse transcriptase inhibitor, AZT

To characterise viral reverse transcription upon HIV-1 infection of astrocytes, U251-MG cells were infected with 0.01 $TCID_{50}U$/cell (0.02 pg p24 / cell) of HIV-1_{NL4-3} by spinoculation. To aid the analysis of reverse transcription, infections were performed in the presence or absence of the reverse transcriptase inhibitor, AZT (20 μM), which had been shown not to be cytotoxic to U251-MG cells at concentrations up to 100 μM (Section 2.7.5i). To allow conversion of AZT into the active tri-phosphate form, U251-MG cells were pre-incubated in the presence of the drug for 18 hours prior to HIV-1 infection. The drug was maintained at 20 μM for the first 48 hpi, and then replaced with drug-free media. The drug-carrier, DMSO, was maintained at the same concentration in drug-free cultures as in AZT-treated cultures (0.2% v/v).

After spinoculation, the infected U251-MG cells were washed three times and then harvested to assess the initial level of HIV-1 DNA present (this was two hours after the initial contact of virus and cells at 37°C; "2 hpi"), or seeded into wells. The culture supernatants were sampled for p24 virus core protein at the time of seeding (2 hpi), and at 24 and 48 hpi. The culture media was changed at 48 hpi, and at 5 dpi the cells were washed, resuspended with trypsin (0.1% v/v), and re-seeded into 3 times as many fresh wells with fresh media (Section 2.3.5ii). At 7 dpi the culture media was again sampled for p24 content, the culture media changed, and $1x10^6$ HuT-78 cells added to each well to verify the ability of the astrocyte cultures to transmit infection to HIV-1 susceptible cells.

Monitoring the profile of infection by supernatant p24 protein levels

Up to 150 pg/ml p24 protein was present in the culture supernatants at the time the astrocytes were seeded (2hpi) (Figure 5.1A). This is prior to possible viral protein synthesis

Figure 5.1 Preliminary analysis of HIV-1 infection of U251-MG astrocytes (±AZT).

U251-MG astrocytes were cultured in the presence or absence of AZT for 18 hours prior to infection with HIV-1_{NL4-3}. The cells were trypsinised and infected by spinoculation and then washed 3 times to remove excess inoculum. After the last wash the cells were either seeded or harvested for extrachromosomal DNA extraction. The seeded cultures were subsequently harvested at 24 or 48 hpi, or maintained to verify successful infection by the ability of the infected astrocyte cultures to transmit infection to susceptible cells. At 5 dpi the cells were washed, resuspended with trypsin, and reseeded into 3x as many fresh wells. Transmission of infection was assessed by coculturing the infected U251-MG cultures at 7 dpi with HuT-78 cells. These cocultures were harvested for extrachromosomal DNA at 10 dpi. For infections in the presence of AZT, the drug was maintained at 20 μM throughout the pre-treatment of the cells and the first 48 hours after inoculation, after which the culture media was replaced with fresh media without AZT.

To assess the course of the infection, culture supernatants were sampled at designated times to measure the amount of HIV-1 core protein (p24) present. The supernatants were sampled at the time of seeding (2 hpi), and at 24 hpi, 48 hpi (the culture media was not changed until after sampling at 48 hpi), at 7 dpi (immediately prior to the addition of HuT-78 cells) and at 10 dpi, after 3 days of coculture. The p24 content was determined by ELISA, and the mean value at each time point (n=2) ± the standard error is shown (**A**).

To assess viral reverse transcription in the infected U251-MG cultures, extrachromosomal DNA was extracted from the harvested cells and assessed for DNA extraction efficiency (by relative Mitochondrial DNA levels) and mid-late stage HIV-1 reverse transcribed DNA (and all subsequent forms) assessed by PCR and Southern hybridisation targeting the extended minus strand of HIV-1 DNA (**B**). Duplicate U251-MG lanes represent true infection duplicates. Input DNA from U251-MG astrocytes represents approximately 100 cells (at 2 hpi) for Mitochondrial PCR and 2000 cells (at 2hpi) for HIV-1 PCR. The mitochondrial PCR was performed at 18 cycles and the extended minus strand HIV-1 PCR at 23 cycles.

* Cultures harvested at 10 dpi are cocultures of U251-MG and HuT-78 cells.

A

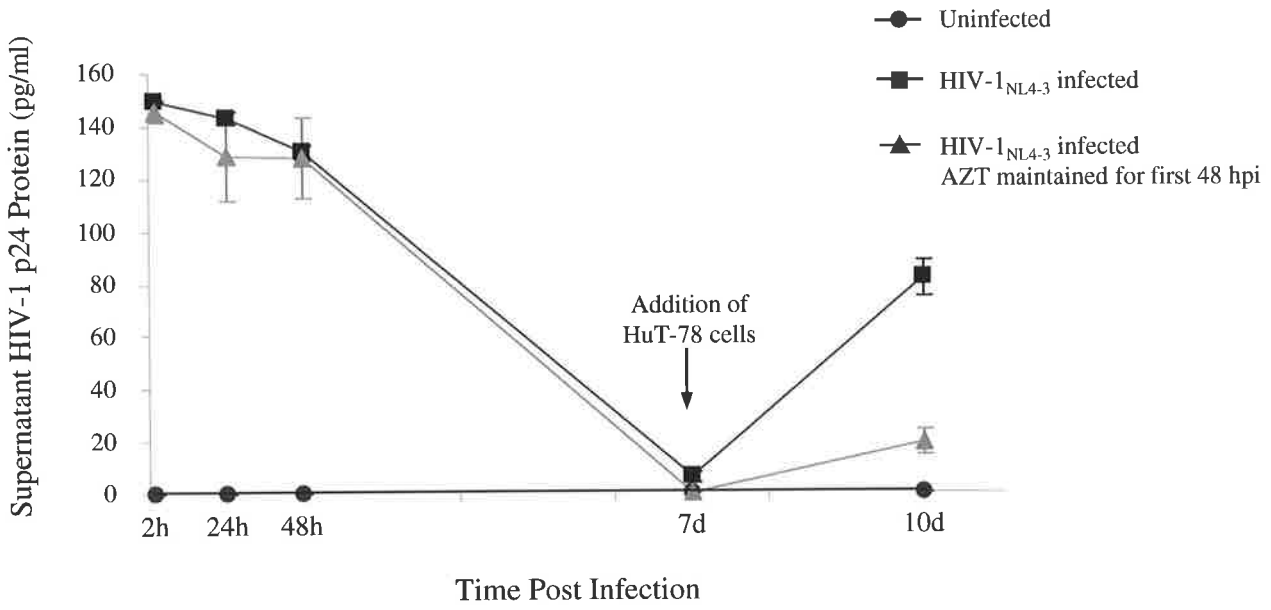
Uninfected
HIV-1NL4-3 infected
HIV-1NL4-3 infected
AZT maintained for first 48 hpi
Supernatant HIV-1 p24 Protein (pg/ml)
160
140
120
100
80
60
40
20
0
Addition of
HuT-78 cells
2h
24h
48h
7d
10d
Time Post Infection

B

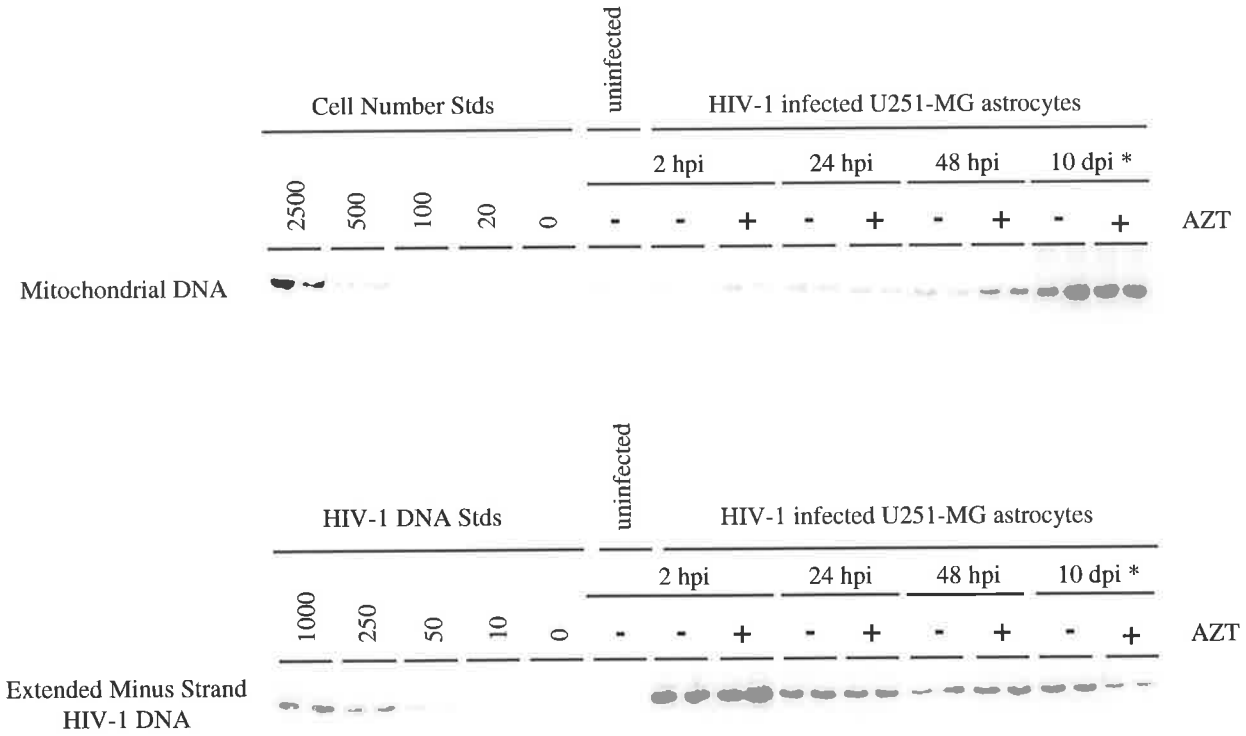
Cell Number Stds
uninfected
HIV-1 infected U251-MG astrocytes
2 hpi
24 hpi
48 hpi
10 dpi *
2500
500
100
20
0
- - + - + - + - +
AZT
Mitochondrial DNA
HIV-1 DNA Stds
uninfected
HIV-1 infected U251-MG astrocytes
2 hpi
24 hpi
48 hpi
10 dpi *
1000
250
50
10
0
- - + - + - + - +
AZT
Extended Minus Strand
HIV-1 DNA

in the infected astrocytes, and therefore indicates the persistence of p24 protein from the virus inoculum. There was no significant difference in the level of p24 detected in the presence or absence of AZT over the first 48 hpi. By 24 hpi *de novo* synthesis of p24 protein is possible, however, as no difference in the level of supernatant p24 was detected between the AZT treated and the drug free cultures, the source of the majority of the p24 protein detected at 24 and 48 hpi is likely to be residual inoculum.

By 7 dpi the p24 content of infected U251-MG cultures had declined to the limit of detection (6 pg/ml). This reduction in supernatant p24 protein from 48 hpi to 7 dpi is attributed to the media change at 48 hpi and subculturing of the cells at 5 dpi. The borderline detection of p24 at 7 dpi indicates that very little, if any, p24 protein was synthesised from 5 to 7 dpi. The infection of the U251-MG astrocytes was confirmed by transmission of the infection upon coculture with susceptible cells, as p24 protein synthesis occurred within 3 days of coculture (Figure 5.1). Interestingly, U251-MG cultures which had been infected in the presence AZT for the first 48 hpi were also capable of transmitting infection to HuT-78 cells, although the degree of p24 synthesis in these cocultures was less than in the cocultures with untreated, infected U251-MG cells.

Assessment of HIV-1 DNA levels during infection

To assess viral reverse transcription in the infected U251-MG cultures, extrachromosomal DNA was extracted from the cultures at 2, 24 and 48 hpi, and at 10 dpi (after 3 days of coculture with HuT-78 cells) (Sections 2.6.2i and 2.6.3i). The DNA extraction efficiency was assessed according to the comparative level of mitochondrial DNA present, as determined by semi-quantitative mitochondrial DNA PCR and Southern Hybridisation (Sections 2.7.2 and 2.7.3) (Figure 5.1B). The amount of viral DNA present was assessed by semi-quantitative PCR and Southern Hybridisation, targeting the extended minus strand DNA product of HIV-1 reverse transcription (a mid-late stage HIV-1 DNA product, refer Figure 2.1) and all subsequent forms of HIV-1 DNA. Extended minus strand HIV-1 DNA was detected in all infected U251-MG cultures, but was undetectable in control uninfected U251-MG cultures (Figure 5.1B). HIV-1 DNA was detectable in the cultures at the first time point sampled, 2 hpi, at >1000 HIV-1 DNA copies per ~100 – 500 cells, irrespective of the presence or absence of AZT. The relative amount of HIV-1 DNA in the cultures

declined considerably over the first 48 hpi, with no apparent difference in the presence of AZT.

Reverse transcribed HIV-1 DNA was detectable after 3 days of coculture of the infected U251-MG cells with HIV-1 susceptible cells (irrespective of the presence of AZT during the first 48 hours of U251-MG infection) (Figure 5.1B), consistent with productive infection and p24 synthesis in the cocultures at this time (Figure 5.1A). The ratio of HIV-1 DNA to mitochondrial DNA was lower in the cocultures (at 10dpi) from astrocytes which had been treated with AZT for the first 48h (Figure 5.1B). One explanation for this may be that a lower level of virus transmission occurred in the latter cocultures, as also indicated by the reduced supernatant p24 levels in cocultures of AZT treated astrocytes (Figure 5.1A). This would lead to reduced virus replication and greater cell growth in the HuT-78 population of the cocultures with AZT treated astrocytes.

The substantial presence of extended minus strand HIV-1 DNA products in the astrocyte cultures as early as 2 hpi was unexpected, although viral reverse transcription can commence within this time (Karageorgos *et al*, 1995) (discussed further in Section 5.4.1). However, the lack of repression of the viral DNA content by AZT suggests that either the drug was not effective in these cells, or, that the viral inoculum is the source of viral DNA, rather than *de novo* synthesis. To produce the virus stocks, 293T cells were transfected with pNL4-3 plasmid DNA (encoding fully competent HIV-1_{NL4-3}). The transfection supernatants (containing virus) were then passaged in CEM-SS cells for 9 to 14 days, and the CEM-SS culture supernatants collected, clarified and filtered for use as virus stocks (Section 2.2.3i). Consequently both the original pNL4-3 plasmid DNA and integrated proviral DNA from the infected CEM-SS cells, which may have lysed during virus culture, may be present in the virus stocks.

The detection of p24 protein and viral DNA in the infected astrocyte cultures as early as 2hpi indicated that the current regime of 3 post-inoculation washes was insufficient to remove excess virus inoculum. This persistence of p24 protein and HIV-1 DNA from the virus inoculum could potentially mask a low level of reverse trancription and virus production. To address this, in future experiments, virus stocks were treated with DNase I and additional post-inoculation washes were performed. The treatment of the inoculated

cells with trypsin to remove and inactivate surface-bound virus (Cheng-Mayer *et al*, 1987; Levy and Rowe, 1971; Tang and Levy, 1991) was also trialed.

5.2.2ii Minimising the persistence of excess virus inoculum

To reduce the amount of excess viral inoculum and p24 protein that persisted in the U251-MG cultures after inoculation, infections were trialed with additional post-infection washes and trypsin treatment. The detection of p24 protein in the supernatants of freshly seeded, virus-exposed U251-MG cells, despite 3 post infection washes, suggested that p24 protein, and possibly virus particles, may persist on the cell surface during the washes and subsequently be released into the supernatant.

Specifically, infections were performed with up to 7 post-inoculation washes, and with or without exposure to 0.05% (v/v) trypsin for 3 minutes (Section 2.3.5ii). To determine the effectiveness of the washes and trypsin treatment the washes were tested for p24 protein content (Figure 5.2A). Up to 115 pg/ml p24 protein was released into the washes, and no notable reduction in the amount of p24 protein was detected unless the cells had been washed 7 times, or at least 5 times with the inclusion of a trypsin treatment in the washing regime (Figure 5.2A). Even with 7 washes and a trypsin treatment ≥70 pg/ml p24 protein could be detected in the culture supernatants immediately upon seeding the cells. By 56 hpi, however, residual p24 protein was undetectable in the supernatants of cultures which had been washed 7 times and treated with trypsin, whilst supernatant p24 levels remained elevated in cultures which had only been washed 3 times and not treated with trypsin until after the cells had been subcultured with trypsin at 5 dpi (Figure 5.2B). The regime of 7 post-inoculation washes and a trypsin treatment was therefore adopted in all subsequent experiments. Although this protocol still permitted some persistence of the inoculum, further washes were not performed due to the delay this imposed on the first time point which could be analysed, which was important for the assessment of HIV-1 reverse transcription.

A

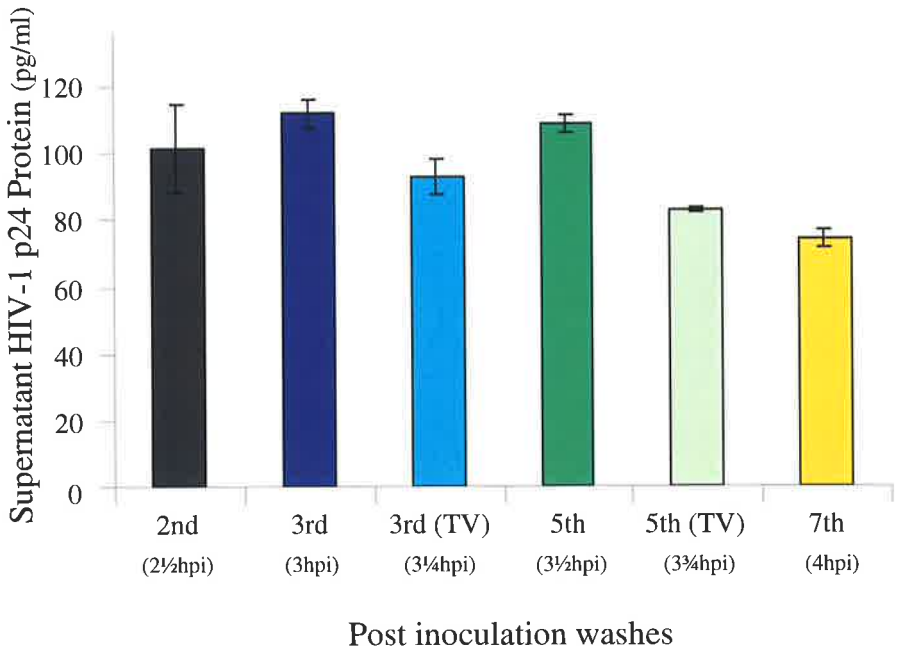

B

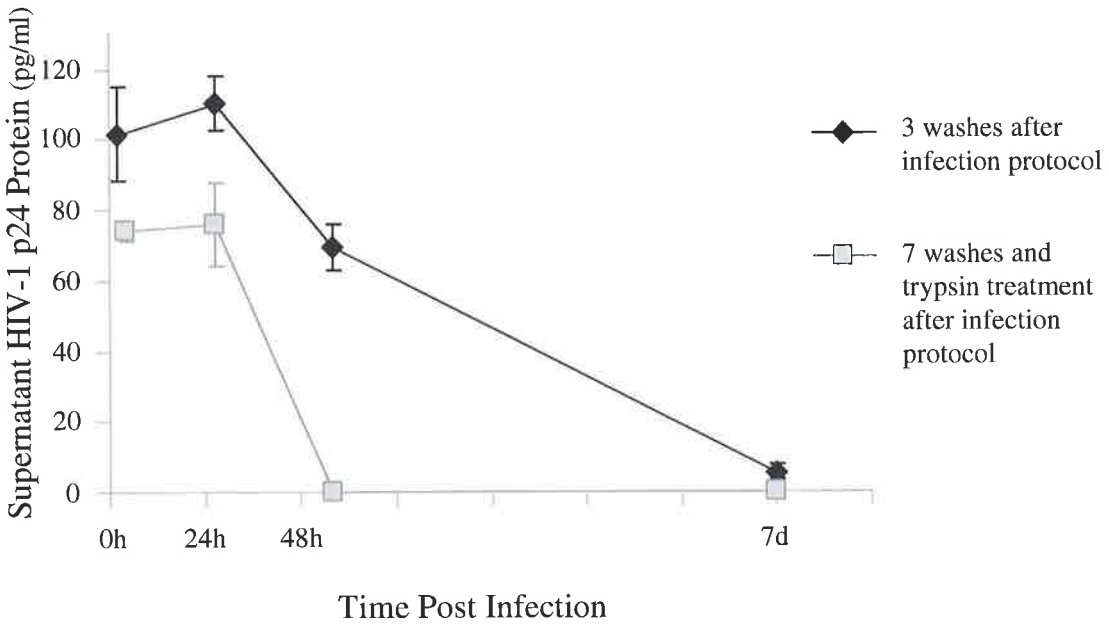

Figure 5.2 Effect of post-inoculation washes and trypsin treatment on the level of p24 protein present in the supernatant of HIV-1 infected U251-MG astrocytes.

U251-MG cells were infected with HIV-1_{NL4-3} by spinoculation with 3 post-inoculation washes. To assess the effectiveness of additional washes and trypsin treatment to remove excess HIV-1 core protein, additional washes ± trypsin treatment (0.05% v/v for 3 minutes) were performed. The post infection washes were sampled for p24 protein content (**A**), and the culture supernatants were sampled for p24 content over the subsequent course of infection (**B**).

5.2.2iii Minimising the DNA input from the initial inoculum

To prevent the carry-over of viral DNA from the virus inoculum, DNase I treatment of the virus stocks was trialed. The virus inoculum was treated 0, 1, 2 or 4 μg/ml DNase I, in the presence of 10 mM $MgCl_2$, for 30 minutes at room temperature, prior to inoculation of U251-MG cells, or added at the time of inoculation. Pre-treatment of virus stocks with 2 μg/ml DNase I has been reported to reduce contaminating DNA from cells lysed during virus culture (Korin and Zack, 1998). After spinoculation, excess virus inoculum was removed from the U251-MG cells with seven post-infection washes and a trypsin treatment as described in Section 5.2.2ii. Immediately after the washing regime (4 hours after the initial contact of the virus and cells at 37°C (4 hpi)), extrachromosomal DNA was harvested from the U251-MG cells. The relative DNA extraction efficiency was assessed by mitochondrial PCR and Southern hybridisation and the amount of HIV-1 DNA present assessed by PCR and Southern hybridisation for extended minus strand species of HIV-1 DNA. The amount of HIV-1 DNA present was only marginally reduced by any of the DNase I treatments, and a significant amount of HIV-1 DNA remained detectable, irrespective of the DNase I digestion (Figure 5.3). This indicated that either i) the HIV-1 DNA may be resistant to, or protected from, DNase I activity, ii) genuine *de novo* reverse transcription may be detectable in the infected U251-MG cells within 4 hpi, and / or iii) the DNAse I enzyme may be inactive.

The activity of the DNase I and the susceptibility of pNL4-3 plasmid DNA to DNase I digestion was verified by treating 1μg of pNL4-3 plasmid DNA (suspended in 4 ml complete U251-MG cell culture medium) with a range of DNase I concentrations (0.25 to 75 μg/ml) in presence of 10 mM $MgCl_2$ for 30 min at RT. The DNA was extracted and PCR revealed that HIV-1 DNA was readily amplified from untreated pNL4-3 DNA but could not be amplified from the DNase I treated plasmid, even with the lowest DNase I concentration (0.25μg/ml) (results not shown). This indicated that the batch of DNase I enzyme used in the experiments in this thesis was active, and that any pNL4-3 plasmid DNA which may have potentially carried-over into the virus stocks was susceptible to cleavage by DNase I. The only counter-argument to this may be that the DNA extraction efficiency may be reduced in samples with a very low DNA content, and consequently the yield of any DNase I resistant viral DNA may be low.

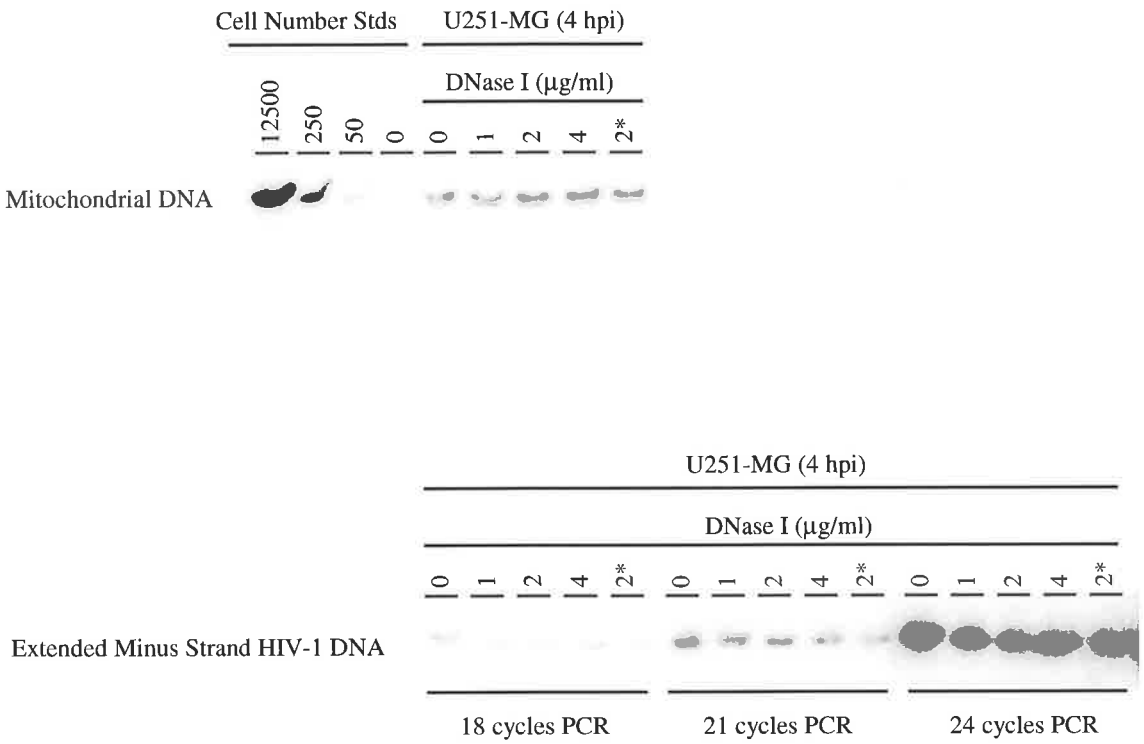

Figure 5.3 Effect of DNase I treatment of the virus inoculum on the level of HIV-1 DNA detected in the infected U251-MG cells at 4 hpi.

HIV- 1_{NL4-3} virus stocks were treated with 0, 1, 2 or 4 µg / ml DNase I in the presence of 10 mM $MgCl_2$ for 30 minutes prior to inoculation of U251-MG cells by spinoculation. In the infection denoted with an asterix (*), 2 µg/ml DNase I was added at the time of U251-MG cell inoculation. Following spinoculation, the cells were washed 5 times, treated with trypsin, and washed a further 2 times (7 washes in total). At this time (4 hpi) the cells were harvested and the extrachromosomal DNA extracted.

The DNA extraction efficiency was assessed by Mitochondrial PCR (18 cycles) and Southern hybridisation on an estimated DNA input of 250 cells. The relative amount of HIV-1 DNA present at 4 hpi with the different DNase I treatment regimes was assessed by PCR and Southern Hybridisation targeting the extended minus strand of HIV-1 DNA. The HIV-1 PCR was performed on an estimated DNA input of 5000 cells, and amplified with 18, 21 or 24 cycles of PCR, as indicated.

To ensure effectiveness of DNase I treatment on virus stocks, the HIV-1_{NL4-3} virus stocks used in the subsequent experiments were treated with 50 μg/ml DNase I in the presence of 10 mM $MgCl_2$ for 30 min at room temperature.

5.3 Analysis of the initial phase of viral protein release by infected U251-MG astrocytes

To characterise the initial phase of U251-MG infection, and to ascertain the source of p24 protein in the culture supernatants, p24 protein release from HIV-1 inoculated astrocytes was assessed over a more detailed time course. U251-MG cells were infected with DNase I treated HIV-1_{NL4-3} at 0.1 $TCID_{50}$U/cell (0.2 pg p24 / cell) by the spinoculation. Immediately after inoculation the cells were washed 5 times, treated with 0.05% trypsin for 5 minutes, and washed a further 3 times, and seeded in to 6-well trays. The (cell-free) supernatant was sampled immediately to assess the amount of residual p24 (Figure 5.4). To further discern the amount of p24 which persisted prior to *de novo* virus protein synthesis, a media change was performed at 18 hpi (the latest possible time before *de novo* p24 protein synthesis may occur), and the fresh supernatant sampled immediately to determine the base-line level of pre-existing p24 protein. These samples contained 94 ± 1 pg/ml p24 (n=2). At 24 hpi, by which time *de novo* p24 protein synthesis could have commenced, the p24 levels had declined to 33 ± 2 pg/ml (n=2), suggesting that degradation of released p24 protein had occurred since the sampling at 18 hpi. This decline continued, with 8.5 ± 1.7 pg/ml p24 detected at 48 hpi (n=2) and 4.6 ± 0.5 pg/ml p24 at 96 hpi (n=2), to undetectable levels by 6 dpi (Figure 5.4). The decline of p24 during the course of U251-MG infection is consistent with previous experiments (Section 5.2.1ii, Figure 5.2). The more detailed time course analysed in this experiment revealed that the detection of p24 in the first few days post infection is unlikely to represent *de novo* p24 synthesis, although definitive evidence for this, after 24 hpi, requires simultaneous analysis of another step of virus replication. The profile of supernatant p24 demonstrates the resilience of p24 protein in the initial inoculum despite extensive washing, and indicates that p24 protein may adhere to the cells and be subsequently released.

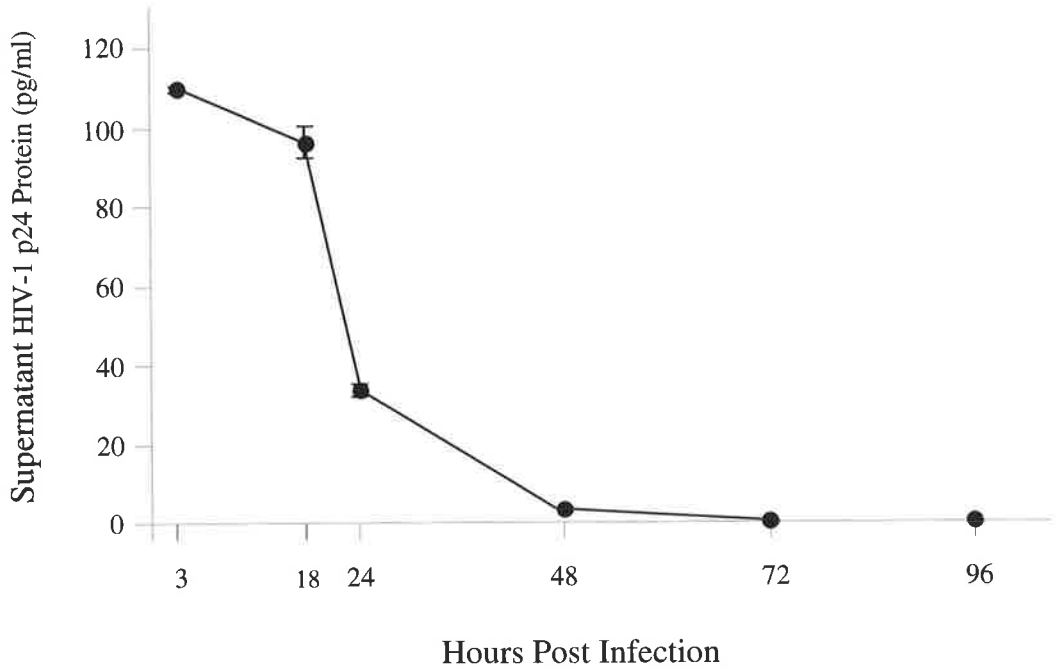

Figure 5.4 Supernatant p24 profile during acute U251-MG astrocyte infection.

U251-MG astrocyte cells were infected with HIV-1_{NL4-3} and the culture supernatants sampled for HIV-1 p24 content at designated times over the first 4 days of infection. After spinoculation, excess virus stock was removed by a series of 7 washes and trypsin treatment. The first sample was taken immediately after seeding the infected cells into wells, at 3 hpi. The media was changed again after the cells had adhered, as late as possible prior to potential *de novo* p24 protein synthesis, at 18 hpi. The fresh culture supernatant was sampled at this time to establish the background level of residual p24. The culture supernatants were subsequently sampled for p24 content at 24, 48, 72 and 96 hpi. Each data point represents the mean p24 concentration from two cultures ± standard error. The virus inoculum per culture in this experiment had a p24 content of 75.75 ng, and each culture was maintained in 4 ml of culture medium.

5.4 Analysis of *de novo* viral reverse transcription during the acute phase of U251-MG infection

5.4.1 Detection of HIV-1 DNA during acute infection of U251-MG astrocytes

U251-MG astrocytes were infected with DNase I treated (50 μg/ml for 30 minutes) HIV-1_{NL4-3} at 0.1 $TCID_{50}U$/cell (0.4 pg p24 / cell) by spinoculation, then seeded into 6-well trays. The cells were harvested at 3, 24, or 48 hpi (Section 2.6.2i), the extra-chromosomal DNA extracted (Section 2.6.3i) the relative DNA extraction efficiency assessed by mitochondrial DNA content, and the amount of HIV-1 reverse transcribed DNA quantified (Sections 2.7.2 and 2.7.3). Viral DNA products assessed at two stages of reverse transcription, one measuring the amount of extended minus strand HIV-1 DNA (a relatively late product of reverse transcription formed after the first template switch, see Section 1.1.6ii and Figures 1.7 and 2.1) and all subsequent products, and one measuring complete reverse transcribed products. Both forms of HIV-1 DNA were found to be detectable within the infected U251-MG astrocyte cultures as early 3 hpi (Figure 5.5).

Extrachromosomal HIV-1 DNA transcripts were more abundant in the U251-MG astrocyte cultures at 3 hpi than at 24 hpi, and, whilst still detectable, the amount of HIV-1 DNA transcripts present was further reduced by 48 hpi (Figure 5.5). Specifically, detection of extended minus strand and subsequent HIV-1 DNA transcripts declined from between 50-250 copies / 2500 cells at 3 hpi to approximately 10 copies / 2500 cells at 48 hpi. Complete reverse transcribed HIV-1 DNA was detected at a lower level than extended minus strand HIV-1 DNA (<10 copies complete HIV-1 DNA / 2500 cells at 3 hpi, compared to >50 copies extended minus strand HIV-1 DNA / 2500 cells at 3 hpi). The level of complete HIV-1 DNA also declined from 3 hpi to 48 hpi. The observation that extended minus strand HIV-1 transcripts were more abundant than completed transcripts is consistent with the kinetics of reverse transcription, and the requirement for a second template switch to occur for the nascent DNA strand to be synthesised to completion (Li *et al*, 1993b) (Section 1.1.6ii and Figure 1.7).

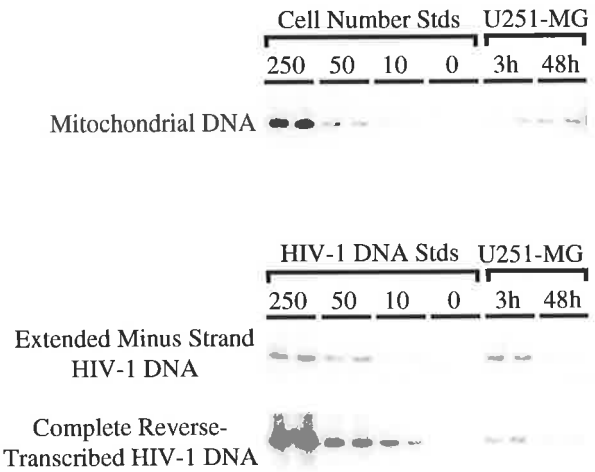

Figure 5.5 HIV-1 DNA is detected in HIV-1 infected U251-MG astrocytes as early as 3 hpi, and declines with time post infection.

U251-MG cells were infected with DNase I treated HIV- 1_{NL4-3} by spinoculation, and excess inoculum removed by 7 post infection washes and a trypsin treatment. The level of viral reverse transcribed DNA products was assessed in extrachromosomal DNA extracts harvested from U251-MG cells at 3 or 48 hpi by PCR followed by Southern hybridisation. Extended minus strand and complete HIV-1 reverse transcribed DNA was detected as early as 3 hpi in U251-MG astrocytes, and had declined in abundance by 48 hpi. U251-MG lanes represent true infection duplicates. Input DNA represents approximately 50 cells for mitochondrial PCR and 2500 cells for HIV-1 PCRs.

Mitochondrial PCRs were performed at 17 cycles, extended minus strand PCRs at 22 cycles, complete reverse transcribed PCRs at 30.

Early products of reverse transcription ("strong-stop DNA", refer Figure 1.7), have been reported to be detectable as early as 90 minutes after *in vitro* infection of $CD4^+$ cells (Karageorgos *et al*, 1995). In this cell-to-cell infection model, extended minus strand and even complete reverse transcription products were reported to be detectable by 2½ hpi, and to progressively accumulate over the following 48 hpi. Similarly, other analyses of extrachromosomal and total HIV DNA have also shown that full-length HIV-1 DNA can be detected as early as 3 to 4 hpi (Barbosa *et al*, 1994; Karageorgos *et al*, 1995; Kim *et al*, 1989; Li *et al*, 1993a; Li and Burrell, 1992). It is therefore possible that HIV-1 could enter U251-MG astrocytes and that reverse transcription may have proceeded to completion in some U251-MG cells within 3 hpi. This was somewhat unexpected, given that cell-free infection of $CD4^+$ cells has been reported to occur with slightly delayed kinetics compared to cell-to-cell infection models (Li and Burrell, 1992; Li *et al*, 1992), however the centrifugally enhanced protocol may have reduced this reported delay. Additionally, the standards used in this thesis (sensitivity of 10 HIV-1 DNA copies in Figure 5.5) allowed detection of lower levels of HIV-1 DNA than those used by Karageorgos *et al.* (lowest standard $2x10^5$ HIV-1 DNA copies), which may also explain the early detection of HIV-1 reverse transcription products in U251-MG astrocytes.

Whilst the early detection of HIV-1 DNA upon infection of astrocytes could indicate that reverse transcription proceeds initially in these cells, the decline in the level of reverse transcribed products from 3 hpi onwards is not consistent with the process of reverse transcription. Studies in $CD4^+$ permissive cells have shown that the products of reverse transcription continue to accumulate during the first few days of infection (Collin and Gordon, 1994; Gotte *et al*, 1999; Karageorgos *et al*, 1995; O'Brien, 1994; O'Brien *et al*, 1994). The decline in HIV-1 DNA transcripts in the U251-MG astrocytes during the first 48 hpi suggest that either i) the source of U251-MG cell-associated HIV-1 DNA was not *de novo* reverse transcription, or ii) that reverse transcription in these cells became restricted after an initial, brief period of *de novo* synthesis. To discern between these possibilities, specific inhibitors of reverse transcription were employed, and the base level of DNase I resistant HIV-1 DNA in the virus inoculum assessed.

5.5 Examination of the source of the detected HIV-1 DNA

To determine whether the source of HIV-1 DNA in infected U251-MG astrocytes was *de novo* reverse transcription, or persistence of DNase I resistant HIV-1 DNA in the virus inoculum, infections were performed with DNase I treated inoculum in the presence and absence of the reverse transcriptase inhibitors, AZT and 3TC (refer Section 2.7.5i). The amount of HIV-1 DNA present in the infected U251-MG cultures and in the DNase I treated virus inoculum was quantified.

5.5.1 Assessment of the DNase I treatment of the virus inoculum

To test whether the virus inoculum might be a source of the HIV-1 DNA detected in the infected U251-MG astrocytes, despite DNase I treatment, the effectiveness of the DNAse I treatment was assessed. In all subsequent experiments, duplicate samples of both the DNase I treated and non-DNase I treated virus inoculum was collected at the same time at which the astrocytes were inoculated with the DNase I treated virus. To prevent further DNase I activity in the virus samples, these samples were immediately mixed with phenol/chloroform/IAA, then stored for subsequent processing (Sections 2.3.5iii). To assess the DNA extraction efficiency in the inoculum samples, the ±DNase I treated inoculum samples were spiked with an irrelevant DNA, prior to extraction of the DNA (Section 2.6.4). The DNA content of the ±DNase I treated virus stock was assessed by PCR and Southern hybridisation targeting the spiked DNA, *β-globin* DNA, and early, mid-late and complete products of HIV-1 reverse transcription (Sections 2.7.3 and 2.7.4).

While some variation in the DNA extraction efficiency between the DNase I treated and the untreated virus stock was evident, the extraction efficiency did not appear to be reduced in the DNase I treated samples (Figure 5.6A). To assess the effectiveness of the DNase I treatment on cellular DNA, as DNA from lysed virus-producer cells may contaminate the virus stocks, the amount of *β-globin* DNA in the virus stocks was measured (Figure 5.6B). *β-globin* DNA was readily detected by PCR on the DNA extracted from the untreated virus stock, indicating cellular DNA was present in untreated virus inoculum. *β-globin* DNA could not be detected in the DNase I treated virus inoculum even at 35 cycles of PCR, despite the sensitivity of this PCR to 2 copies of the gene within 25 cycles. This suggested

Figure 5.6 Assessment of the HIV-1 DNA content of the HIV-1 inoculum used for the U251-MG infection shown in Figure 5.7.

DNA was extracted from the DNase I treated HIV-1_{NL4-3} virus inoculum used in the U251-MG infection experiment described in Section 5.5.2 and Figure 5.7. To assess the effectiveness of the DNase I treatment, a sample of the same virus stock was processed identically, with the omission of the DNase I enzyme. At the time of U251-MG inoculation with the DNase I treated virus, the DNase I digestion in the ± DNase I treated samples was terminated by the addition of phenol:chloroform:IAA, and stored for later analysis. To enable assessment of the DNA extraction efficiency from the ± DNase I treated inoculum samples they were spiked with an irrelevant DNA (pDengueCapsidcDNA) immediately prior to DNA extraction. The relative DNA extraction efficiency was assessed by a PCR targeting the spiked DNA (**A**). β-globin DNA content was assessed to indicate the level of contaminating cellular DNA (**B**). The level of strong-stop (early), extended minus strand (mid-late) and complete HIV-1 products of HIV-1 reverse transcription were assessed in the ± DNase I treated inoculum samples (**C**). Each lane represents a PCR input equating to 15µl of viral stock (which corresponds to the amount of inoculum used per 16 000 cells).

Dengue Capsid PCR was performed at 30 cycles, β–globin PCR at 30 cycles, strong stop PCR at cycles, extended minus strand PCR at 30 cycles, complete reverse transcribed PCR at 32 cycles, with subsequent Southern hybridisation to detect each amplicon. β-globin and HIV-1 PCRs were performed in duplicate.

A.

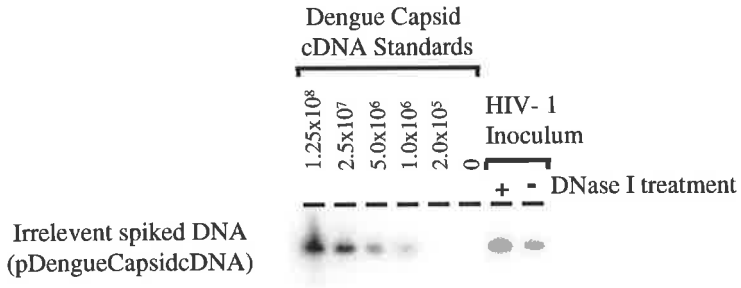
Dengue Capsid
cDNA Standards
1.25x10^8
2.5x10^7
5.0x10^6
1.0x10^6
2.0x10^5
0
HIV- 1
Inoculum
+ -
DNase I treatment
Irrelevent spiked DNA
(pDengueCapsidcDNA)

B.

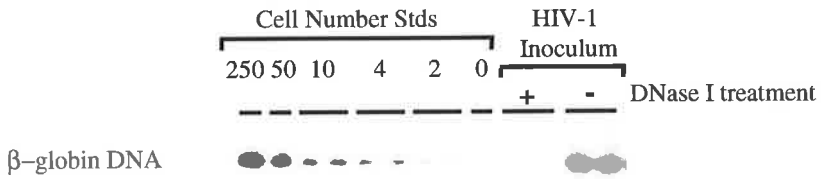
Cell Number Stds
HIV-1
Inoculum
250 50 10 4 2 0
+ -
DNase I treatment
β–globin DNA

C.

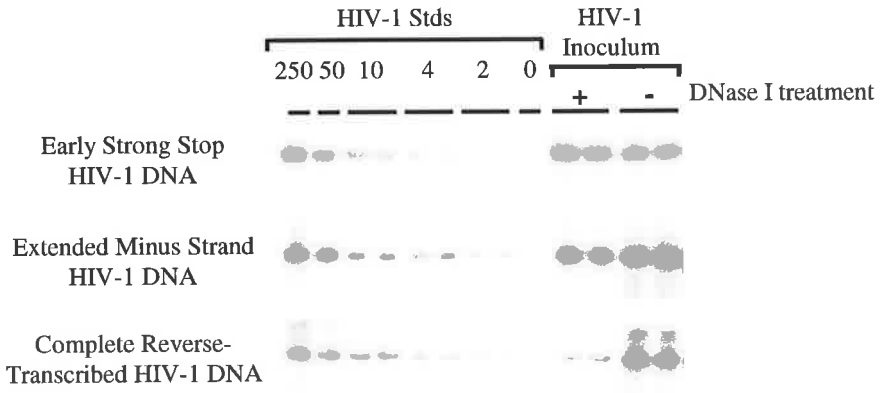
HIV-1 Stds
HIV-1
Inoculum
250 50 10 4 2 0
+ -
DNase I treatment
Early Strong Stop
HIV-1 DNA
Extended Minus Strand
HIV-1 DNA
Complete Reverse-
Transcribed HIV-1 DNA

that the DNase I treatment of the virus stock was effective in digesting cellular DNA. Despite this, however, HIV-1 DNA persisted in the DNase I treated virus inoculum (Figure 5.6C). Early, mid-late and, to a lesser extent, complete products of HIV-1 reverse transcription could be detected in both DNase I treated and untreated virus stocks. Considering the slightly more efficient DNA extraction efficiency of the DNase I treated sample, the DNase I treated sample had a relatively lower content of all three viral DNA species (Figure 5.6A,C).

At least 250 copies of the strong stop and extended minus strand reverse transcribed HIV-1 DNA species was detected per 15 µl of DNase I treated virus stock, the amount used to inoculate 1.6 x 10^4 U251-MG cells. The amount of complete reverse transcribed HIV-1 DNA species which was detected in the DNase I treated virus stock was much less; between 4 to 10 copies per 15 µl. The decrease in the level of complete virus transcripts compared to extended-minus strand transcripts in the DNase I treated virus stocks is consistent with the kinetics of reverse transcription, (Li *et al*, 1993b) (Section 1.1.6ii and Figure 1.7). In the untreated DNase I treated virus stocks there was no apparent decrease in the relative abundance of the three species of HIV-1 DNA tested.

The source of the DNase I resistant viral DNA in the inoculum was unlikely to be residual pNL4-3 plasmid DNA or integrated proviral DNA from lysed virus-producer cells, as these sources of DNA would have resulted in the detection of approximately equal amounts of early strong stop, extended minus strand, and complete viral DNA species. Also, these sources of DNA had been shown to be susceptible to DNase I digestion. However, the process of reverse transcription has been reported to commence within the virion, prior to entering a target cell, in a small proportion of virions (Section 1.1.6ii). Early, strong-stop HIV-1 DNA has been detected in up to 1% of virions (Arts *et al*, 1994; Lori *et al*, 1992; Trono, 1992; Zhang *et al*, 1994; Zhang *et al*, 1996a; Zhang *et al*, 1996b; Zhang *et al*, 1993). Lower levels of more complete HIV-1 DNA transcripts have also been detected (Zhang *et al*, 1996b; Zhang *et al*, 1993), and such intravirion DNA is reportedly protected from DNase I treatment, even when treated with 500 µg/ml (Arts *et al*, 1994). The higher level of complete reverse transcribed HIV-1 DNA (and slightly higher level of all three HIV-1 DNA species) in the untreated virus inoculum, compared to the DNase I treated inoculum, most

likely represents the presence of DNase I susceptible cellular or plasmid HIV-1 DNA, in addition to the DNase I resistant intravirion DNA.

5.5.2 Effect of reverse transcriptase inhibitors on the level of HIV-1 DNA present during acute infection of U251-MG astrocytes

5.5.2i Use of the nucleoside analogues; AZT and 3TC

The nucleoside analogues, AZT and 3TC, are converted by cellular kinases into active deoxy-nucleotide triphosphates (dNTPs), and are incorporated into the nascent reverse transcripts as substitutes for dTTP and dCTP respectively. The kinases required for phosphorylation of the respective nucleoside precursors into active tri-phosphate nucleotides are constitutively expressed by the majority of cell types, and the efficiency of this conversion varies between cell types depending on their mitochondrial content and stage of cell cycle (Brinkman *et al*, 1998; Kakuda, 2000; Lewis *et al*, 2003) (Section 2.7.5i). Both AZT and 3TC were tested and shown to be non-cytotoxic to U251-MG, CCF-STTG1 and U87-MG astrocytes (Section 2.7.5i). To allow time for conversion to their active triphosphate form, the cells were pre-incubated in the presence of the drug (or the drug-carrier, DMSO, alone) overnight (~18 hours), prior to infection. AZT and 3TC (or the respective drug-carrier alone) were maintained at concentrations shown to inhibit virus release from T cells (20μM and 50μM, respectively (Coates *et al*, 1992; Hazuda *et al*, 2000)) throughout the pre-incubation and infection.

5.5.2ii Infection of U251-MG cells in the presence of 3TC

U251-MG astrocytes and HuT-78 T cells were pre-incubated in the presence of 3TC (50μM, or the equivalent concentration of the drug-carrier, DMSO) overnight, then infected with DNase I treated HIV-1_{NL4-3} at 0.1 $TCID_{50}$U/cell (0.4 pg/cell p24 protein) by spinoculation and seeded into 6-well trays. The cells were harvested at 26 hpi and the extra-chromosomal DNA extracted by the Hirt method. The relative DNA extraction efficiency was assessed by mitochondrial DNA content, and the amount of HIV-1 reverse transcribed DNA products assessed by PCR targeting the extended minus strand and complete reverse transcribed HIV-1 DNA.

Assessment of the relative amount of mitochondrial DNA present demonstrated relatively uniform extrachromosomal DNA extractions (Figure 5.7). At 26 hpi the extended minus strand HIV-1 DNA was just detectable in the U251-MG astrocytes, at approximately 2 copies per 2500 cells (the limit of sensitivity of this assay). No complete HIV-1 reverse transcripts were detectable (assay sensitivity 2 copies / 2500 cells) at this time point. Notably, the amount of extended minus strand HIV-1 DNA in the U251-MG cells was the same for infections carried out in the presence of 3TC, as in the absence of this drug. The activity of 3TC in this experiment was confirmed by the inhibition of reverse transcription in HIV-1 permissive, $CD4^+$ HuT-78 cells (Figure 5.7). 5 fold less input HuT-78 cell extrachromosomal DNA was used in these PCR reactions, to prevent over-saturation of the PCR for HIV-1 DNA from productively infected cells. The presence of 3TC inhibited viral reverse transcription in the HuT-78 cells from ~50 copies of extended minus strand HIV-1 DNA / 500 cells to $\leq$2 copies / 500 cells at 26 hpi.

The level of extended minus strand HIV-1 DNA detected in the U251-MG cells at 26 hpi was completely accounted for by the levels in the DNase I treated virus inoculum (almost 20 fold more than that associated with the infected astrocyte cells at 26 hpi (2 copies / 2500 cells at 26 hpi (Figure 5.7) compared to $\geq$38 copies in the amount of DNase I treated inoculum used for this number of cells (Figure 5.6))). The absence of effect of 3TC on the level of HIV-1 DNA detected in U251-MG cells is also consistent with the source of cell-associated HIV-1 DNA being the DNase I treated inoculum and not *de novo* reverse transcription.

Whilst the amount of viral DNA present in the DNase I treated inoculum could account for the level of viral DNA associated with the infected U251-MG astrocytes, it was also plausible that *de novo* reverse transcription may have occurred, and that the 3TC may be ineffectual in U251-MG cells. Although 3TC was shown to be effective in inhibiting HIV-1 replication in HuT-78 cells, the effectiveness of 3TC may vary between cell types according to the efficiency of its conversion to the active triphosphate form within the cells. Poor conversion of 3TC to its active form in U251-MG cells was unlikely, however, as the cells were pre-treated with the drug overnight prior to infection. Never-the-less, to address this, the experiment was repeated with an alternative inhibitor of reverse transcription, AZT (Section 2.7.5i). This experiment also demonstrated that the amount of extended minus strand HIV-1 DNA detected in the U251-MG cultures was unaffected by the presence of

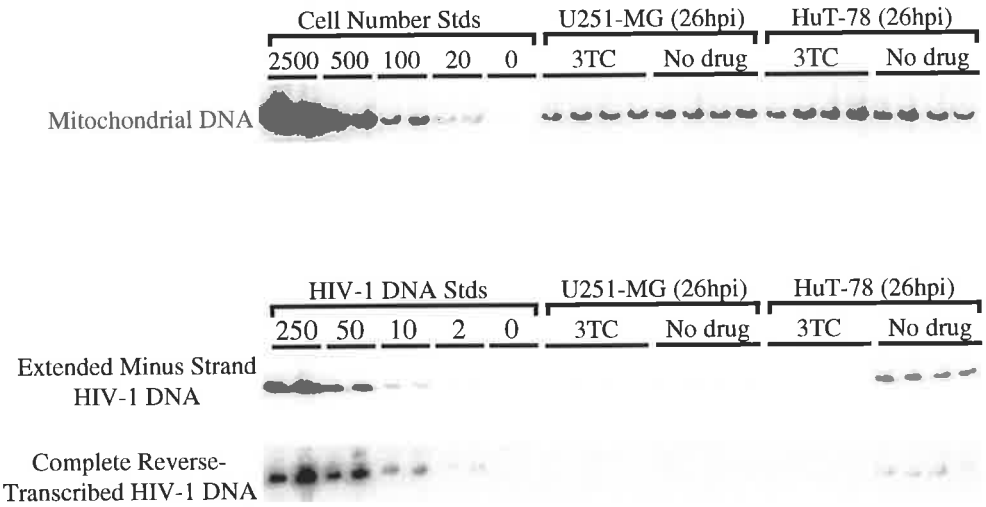

Figure 5.7 Detection of HIV-1 DNA upon infection of U251-MG astrocytes is independent of the reverse transcriptase inhibitor, 3TC.

U251-MG astrocytes were cultured in the presence or absence of 50 μM 3TC for 18 hours prior to infection with treated HIV-1_{NL4-3}. To assess the effectiveness of 3TC to inhibit HIV-1 reverse transcription, susceptible $CD4^+$ HuT-78 cells were included as controls. The respective cells were infected with DNase I treated (50 μg/ml for 30 min) HIV- 1_{NL4-3} by spinoculation, and excess inoculum removed by 7 post inoculation washes and a trypsin treatment. For infections in the presence of 3TC, the drug was maintained at 50 μM throughout all stages of the infection procedure until the cells were processed for DNA extraction.

To assess the level of viral reverse transcribed DNA products in infected U251-MG and HuT-78 cells, extrachromosomal DNA was extracted. The relative DNA extraction efficiency was assessed by PCR (17 cycles) and Southern hybridisation for Mitochondrial DNA on an estimated DNA input of 100 U251-MG cells or 20 HuT-78 cells (HuT-78 cells contain ~5x more mitochondrial DNA per cell than U251-MG cells). The level of extended minus strand and complete reverse transcribed HIV-1 DNA was assessed in the cultures by respective PCR and Southern hybridisation. 22 cycles PCR targeting extended minus strand forms of HIV-1 DNA and 26 cycles of PCR targeting complete reverse transcribed HIV-1 DNA was performed on an estimated DNA input of 2500 U251-MG or 500 HuT-78 cells. Duplicate PCRs were performed on true infection duplicates.

(The analysis of the DNA content of the DNase I treated virus inoculum is shown in Figure 5.6)

AZT during the infections, declined over the timecourse of the infection (3, 26, 52 hpi) and could be accounted for by the amount of HIV-1 DNA present in the DNase I treated inoculum.

5.5.2iii Subsequent transmission of HIV-1 from infected U251-MG cells upon coculture

The analysis of U251-MG infections in the presence and absence of 3TC and AZT, together with the analysis of the DNase I treated virus inoculum, indicated that the detection of HIV-1 DNA during the acute phase of infection of U251-MG cells did not represent *de novo* reverse transcription. Rather, the detection of HIV-1 DNA associated with the infected U251-MG astrocytes most likely represented the products of intravirion reverse transcription. In both these experiments, parallel (drug-free) infected U251-MG cultures were maintained until 7 dpi, when they were cocultured with HuT-78 cells. Interestingly, virus replication was subsequently detected in all cocultures within 3 days of coculture, as demonstrated by syncytia formation in the HuT-78 cell population and detection of p24 protein in the coculture supernatant. Taken together, this indicated that HIV-1 replication was inhibited at a stage prior to reverse transcription in U251-MG astrocytes during acute HIV-1 infection, but that these cells are yet able to subsequently release and transmit infectious virus. This suggests that *de novo* reverse transcription proceeds at a later stage of U251-MG infection, perhaps requiring some stimulus provided by the coculture. To confirm the lack of detectable *de novo* reverse transcription during the acute phase of U251-MG infection, and to determine whether this anomaly also occurred in other types of astrocytes, the study of viral protein production and reverse transcription during acute HIV-1 infection was repeated in U251-MG astrocytes and in two additional astrocyte cell lines (Section 5.6)

5.6 Analysis of acute infection of U251-MG, CCF-STTG1 and U87-MG astrocytes

U251-MG, CCF-STTG1 and U87-MG astrocytes and HuT-78 T cells were infected with DNase I treated HIV-1_{NL4-3} at 0.3 $TCID_{50}$U/cell (1.2 pg/cell p24 protein), in the presence or absence of 3TC, as described in Section 5.5.2ii. The infections were monitored by

measuring the level of p24 protein in the culture supernatants, and the cultures harvested at 3½, 26 and 48 hpi for analysis of the extra-chromosomal DNA. In these experiments, real-time PCR (Section 2.7.4) was used to assess the relative DNA extraction efficiency and to quantitate the amount of reverse transcribed HIV-1 DNA present. The real-time PCR used to detect HIV-1 DNA in this set of experiments targeted the U5 region of the HIV-1 genome using primers which span the PBS region, and hence only amplifies extended minus strand HIV-1 DNA formed by an intermolecular first template switch, or HIV-1 DNA which has undergone a second template switch, and all subsequent forms of HIV-1 DNA (Figure 2.1). Specific detection of this late stage of reverse transcription was chosen to minimise the potential detection of intra-virion reverse transcribed HIV-1 DNA.

5.6.1 Analysis of the initial phase of viral protein release by infected astrocytes

5.6.1i Profile of supernatant p24 protein during infection of U251-MG astrocytes

Consistent with previous experiments (Sections 5.2.2ii and 5.3), HIV-1 p24 protein was readily detectable within the first two days of U251-MG infection, and was detectable prior to possible *de novo* synthesis (at 8 hpi) (Figure 5.8A). As discussed previously, this therefore represented persistence of p24 protein from the original virus inoculum, despite 7 post-inoculation washes and a trypsin treatment to attempt to remove excess inoculum. The residual level of 200 - 400 pg/ml p24 protein per culture (4 ml culture, therefore the total residual amount of p24 was approximately 0.8 - 1.6 ng) is not surprising considering the virus inoculum per culture had a p24 content of 480 ng (1.2 pg p24 / cell, 4 x 10^5 cells / well). This represents a persistence at 8 hpi of 0.17 - 0.33% of p24 protein from the original inoculum. The difference observed between the amount of supernatant p24 in U251-MG infections in the presence / absence of 3TC appears to indicate a slight variation in the effectiveness of the washing procedure. (In this experiment each infection paradigm (each cell type ±3TC) was performed in a single tube, and, after the washing steps, the cells were seeded into multiple wells for culturing). As *de novo* p24 protein synthesis could not have occurred as early as 8 hpi, the difference in supernatant p24 levels between 3TC and

A. U251-MG cells

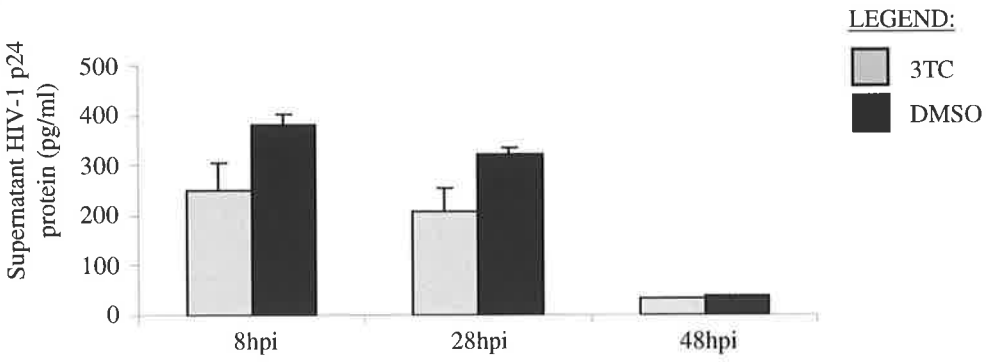

B. CCF-STTG1 cells

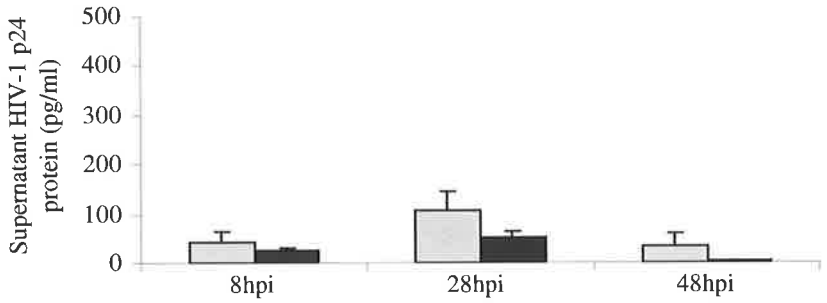

C. U87-MG cells

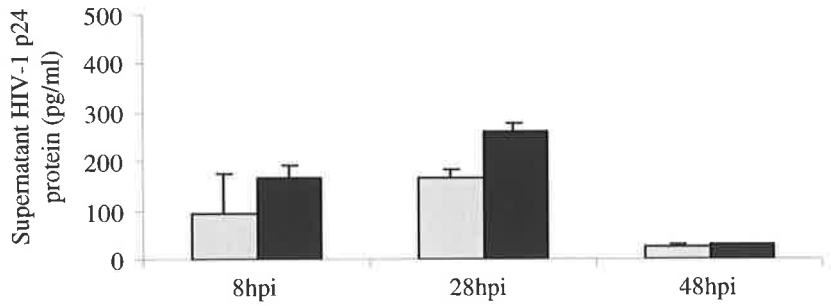

D. HuT-78 cells

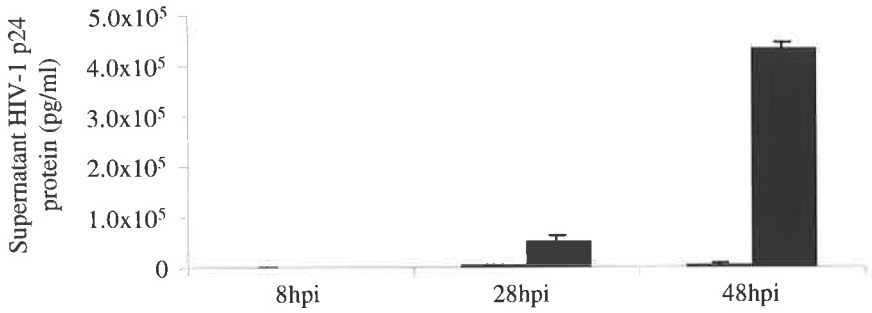

E. HuT-78 cells (3TC results on expanded axis)

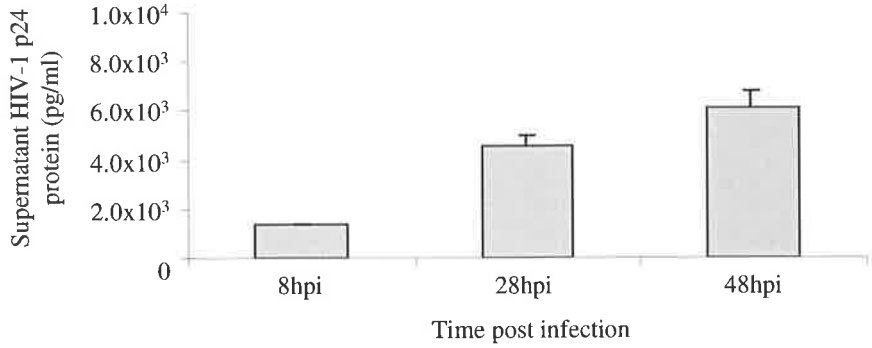

untreated (DMSO) cultures at 8 hpi does not indicate the progress of the respective infections.

The level of p24 protein present in the U251-MG culture supernatants declined from 8 hpi to 48 hpi, indicating the amount of residual p24 from the virus inoculum was degraded over time. The detection of p24 protein at 28 and 48 hpi most likely represented residual initial inoculum, although definitive evidence that this did not represent, at least in part, *de novo* p24 synthesis, requires simultaneous analysis of another step of virus replication (Section 5.6.2).

5.6.1ii Profile of supernatant p24 protein during infection of CCF-STTG1 amd U87-MG astrocytes

Infected CCF-STTG1 and U87-MG astrocyte cultures also had detectable levels of HIV-1 p24 protein in the supernatants during the first two days of infection (Figure 5.8B, C). Similar to observations of infected U251-MG cultures, HIV-1 p24 protein was detected in the supernatants of CCF-STTG1 and U87-MG cultures at 8 hpi, prior to the occurrence of *de novo* synthesis, indicating that this represented persistence of the initial virus inoculum. The amount of p24 / inoculum which persisted at 8hpi in CCF-STTG1 (0.02 – 0.06% of the initial inoculum) and U87-MG cultures (0.08 – 0.14% of the initial inoculum) was much less than that which persisted in the U251-MG cultures at this time (0.17 - 0.33% of the initial inoculum). By 28 hpi, the level of p24 protein in the CCF-STTG1 and U87-MG supernatants had increased, and assessment of p24 protein alone is insufficient to conclude whether this increase represents, at least in part, *de novo* p24 synthesis, or further release of cell-bound virus / p24 protein into the culture supernatants from 8 to 28 hpi. The higher level of p24 protein in the 3TC treated CCF-STTG1 cells at 28 hpi, compared to untreated CCF-STTG1 cells, suggests that the source of p24 protein detected in these culture supernatants is not *de novo* virus replication, but rather a reflection of the variable effectiveness of removing the initial inoculum by the post-inoculation washes and trypsin treatment, as indicated by the differing levels of p24 protein in the supernatants at 8 hpi. Persistence of the initial virus inoculum was also supported by the decline in p24 levels by 48 hpi in CCF-STTG1 and U87-MG cultures, although this could also be attributed to the infection entering a "restricted" phase whereby the expression of virus structural proteins

becomes limited. To summarise, the supernatant p24 data alone does not discern between these two possibilities, and analysis of additional aspects of the virus life cycle is required to discriminate between these two possibilities (Section 5.6.2).

5.6.1iii Infection of HuT-78 T-cells, and the effectiveness of 3TC to limit virus / p24 production

To confirm the infectivity of the DNase I treated virus stock and the effectiveness of 3TC to inhibit virus replication, the $CD4^+$, HIV-1 susceptible HuT-78 cells were included in this experiment as controls. Upon infection of CD4+ susceptible HuT-78 cells with the same infection protocol and virus inoculum, a low level of residual p24 protein (0.75 – 1.1% of the original inoculum) was detected at 8 hpi, prior to *de novo* synthesis (Figure 5.8D, E). This was higher than the amount of p24 / virus inoculum which persisted in the astrocyte infections, and suggested that the removal of excess virus / p24 may have been less efficient for HuT-78 cells than the astrocyte cells. However, by 28 hpi, the amount of supernatant p24 had increased 3.4-fold in the 3TC treated cultures (from 1.35 ± 0.03 ng/ml at 8 hpi to 4.5 ± 0.4 ng/ml at 28 hpi) and 56-fold in the untreated cultures (from 0.8 ± 0.8 ng/ml to 50 ± 12 ng/ml). By 48 hpi, the amount of p24 supernatant in the supernatants of the 3TC treated HuT-78 cultures had increased slightly (to 6.1 ± 0.7 ng/ml) in the 3TC treated cultures and significantly in the untreated cultures (to 435 ± 9 ng/ml). The amount of p24 detected in the untreated cultures at 28 and 48 hpi indicated that the majority of this protein must have arisen from *de novo* synthesis of virus and viral proteins, as it was much higher than the amount present prior to *de novo* synthesis (at 8 hpi) and the total amount in the initial inoculum. The repressed level of supernatant p24 in the 3TC treated HuT-78 cultures indicated that 3TC effectively inhibited the production of virus / p24 protein by 91% at 28 hpi (comparing the level of p24 in the supernatants of the untreated versus 3TC treated HuT-78 cultures at 28 hpi). The effect of the reverse transcriptase inhibitor was more pronounced by 48 hpi, where 98.6% inhibition of virus / p24 protein production was observed in the presence of 3TC (Figure 5.8D, E).

5.6.2 Analysis of the level of extrachromosomal HIV-1 DNA during astrocyte infection

To assess the process of HIV-1 reverse transcription during the infection of the three astrocyte cell lines described in Section 5.6.2, the extrachromosomal DNA was harvested from duplicate infected cultures (± 3TC) at 3½, 26 and 48 hpi and assessed by real-time PCR for relative DNA extraction efficiency and HIV-1 DNA content. To assess the HIV-1 DNA content of the DNase I treated virus inoculum, ±DNase I treated inoculum samples were collected and tested for strong stop, extended minus strand, and complete reverse transcribed HIV-1 DNA as described in Section 5.5.1 and Figure 5.6 (Figure 5.9). As a control for HIV-1 infection and for the efficacy of 3TC, extrachromosomal DNA was also prepared from duplicate cultures of HIV-1_{NL4-3} infected HuT-78 cells harvested at the same time points.

5.6.2i Assessment of the levels of HIV-1 reverse transcribed DNA species present in the DNase I treated virus inoculum

The analysis of the DNase I treated virus inoculum used in this experiment revealed that the DNase I treatment was effective in degrading cellular *β-globin* DNA, and some, but not all, of the HIV-1 DNA present in the virus stock (Figure 5.9). The relative abundance of the different HIV-1 DNA species correlated to the stage of reverse transcription, consistent with the previous analysis of another virus stock (Section 5.5.1, Figure 5.6). In the DNase I treated virus stock used in this experiment, approximately 10 to 50 copies of the extended minus strand reverse transcribed HIV-1 DNA, and approximately 2 to 4 copies of complete reverse transcribed HIV-1 DNA were detected per 15 µl of DNase I treated virus stock (Figure 5.9), the amount used to inoculate 1.6 x 10^4 astrocyte cells. This corresponds to the presence of approximately 1 to 6 copies of extended minus strand (and 0.25 to 0.5 copies of complete) reverse transcribed HIV-1 DNA in the inoculum used per 2000 cells, the number of cell-equivalents of extrachromosomal DNA analysed in Figures 5.11 and 5.12 (discussed below).

Figure 5.9 Assessment of the HIV-1 DNA content of the HIV-1 inoculum used for the U251-MG, CCF-STTG1 and U87-MG infections shown in Figures 5.10, 5.11 and 5.12.

DNA was extracted from the DNase I treated HIV-1_{NL4-3} virus inoculum used in the U251-MG, CCF-STTG1 and U87-MG infections described in Section 5.6 and Figures 5.10, 5.11 and 5.12. To assess the effectiveness of the DNase I treatment, a sample of the same virus stock was processed identically, with the omission of the DNase I enzyme. The DNase I treated virus stock was analysed as described in Figure 5.6. Specifically, at the time of U251-MG inoculation with the DNase I treated virus, the DNase I digestion in the ± DNase I treated samples was terminated by the addition of phenol:chloroform:IAA, and stored for later analysis. To enable assessment of the DNA extraction efficiency from the ± DNase I treated inoculum samples they were spiked with an irrelevant DNA (pDengueCapsidcDNA) immediately prior to DNA extraction. The relative DNA extraction efficiency was assessed by a PCR targeting the spiked DNA (**A**). β-globin DNA content was assessed to indicate the level of contaminating cellular DNA (**B**). The level of strong-stop (early), extended minus strand (mid-late) and complete HIV-1 products of reverse transcription were assessed in the ± DNase I treated inoculum samples (**C**). Each lane represents a PCR input equating to 15µl of viral stock (which corresponds to the amount of inoculum used per 16 000 cells).

Dengue Capsid PCRs were performed at 30 cycles, β–globin PCR at 30 cycles, strong stop PCR at cycles, extended minus strand PCRs at 30 cycles, complete reverse transcribed PCRs at 32 cycles, with subsequent Southern hybridisation performed to detect each amplicon. *β-globin* and HIV-1 PCRs were performed in duplicate.

A.

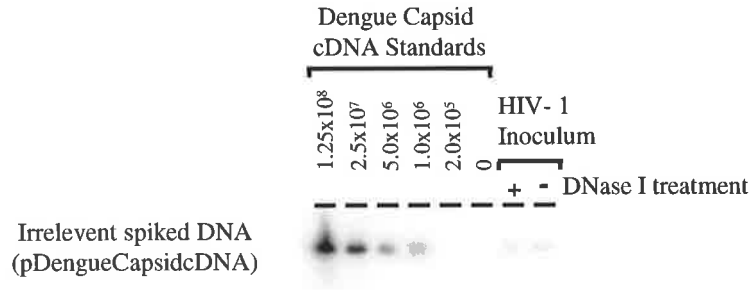
Dengue Capsid
cDNA Standards
1.25x10^8
2.5x10^7
5.0x10^6
1.0x10^6
2.0x10^5
0
HIV- 1
Inoculum
+ -
DNase I treatment
Irrelevent spiked DNA
(pDengueCapsidcDNA)

B.

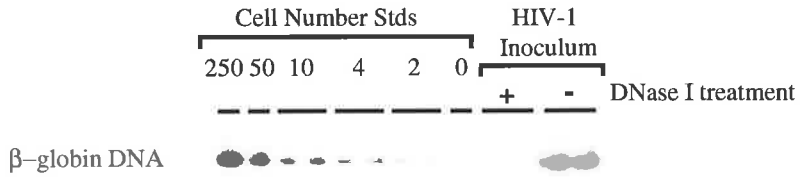
Cell Number Stds
HIV-1
Inoculum
250 50 10 4 2 0
+ -
DNase I treatment
β–globin DNA

C.

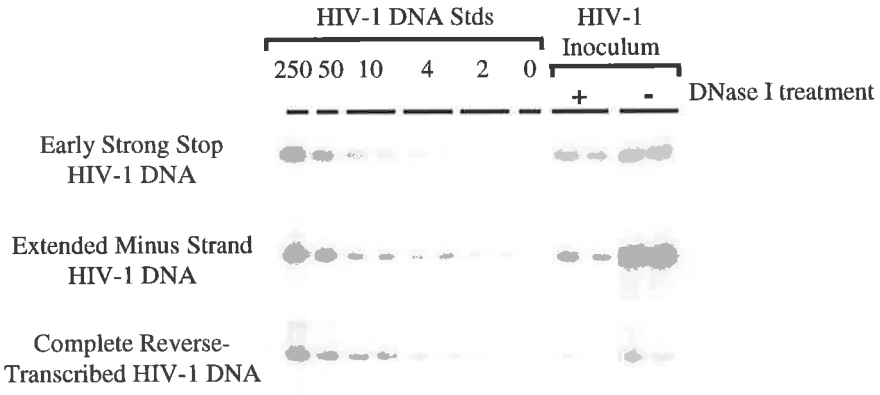
HIV-1 DNA Stds
HIV-1
Inoculum
250 50 10 4 2 0
+ -
DNase I treatment
Early Strong Stop
HIV-1 DNA
Extended Minus Strand
HIV-1 DNA
Complete Reverse-
Transcribed HIV-1 DNA

5.6.2ii Extrachromosomal HIV-1 DNA levels during astrocyte infections (± 3TC)

The efficiency of extrachromosomal DNA extractions from the U251-MG, CCF-STTG1 and U87-MG cells was assessed by real-time PCR for mitochondrial DNA (Figure 5.10). This quantitative PCR enabled accurate quantification of the samples for the subsequent analysis of HIV-1 DNA content. The analysis of the amount of HIV-1 DNA present in the extrachromosomal DNA extracts from the infected U251-MG, CCF-STTG1 and U87-MG cultures revealed that less than 10 copies of HIV-1 U5 DNA was present per 2000 cells, irrespective of the time at which the culture was harvested and the inclusion of 3TC in the infection (Figure 5.11). The mean HIV-1 copy number was determined for each of the duplicate cultures at each time point, and is presented graphically in Figure 5.12.

Analysis of the extrachromosomal HIV-1 DNA in infected U251-MG astrocyte cultures

In the infected U251-MG cultures, approximately 2 copies of extended minus strand HIV-1 reverse transcribed U5DNA was detectable per 2000 U251-MG cells at 3½ hpi, irrespective of the presence of 3TC in the infection (Figure 5.12A). After 3½ hpi, less than 1 copy of HIV-1 DNA was detectable in these cultures. This is consistent with the early detection of a low level of extrachromosomal HIV-1 DNA in infected U251-MG cells by conventional PCR (Figure 5.5 and Section 5.4.1), and the lack of effect of 3TC on the level of extrachromosomal HIV-1 DNA observed in previous experiments (Figure 5.6 and Section 5.5.2ii). The amount of HIV-1 DNA detected in the U251-MG astrocytes can be accounted for by the persistance of HIV-1 DNA in the DNase I treated virus stock, which was found to contain approximately 1 to 6 copies of extended minus strand strand (and 0.25 to 0.5 copies of complete) reverse transcribed HIV-1 DNA per 2000 U251-MG cells, the number of cells represented in Figures 5.11 and 5.12.

The lack of effect of 3TC and the fact that the amount of HIV-1 DNA in the U251-MG cells can be accounted for by the virus inoculum, taken together, strongly suggest that the level of HIV-1 DNA detected in the U251-MG astrocytes at 3½ hpi does not represent *de novo* reverse transcription. The subsequent decline in the level of HIV-1 DNA in the cultures (both ± 3TC treatment) (Figure 5.12A), as observed previously (Figure 5.5 and Section

A.

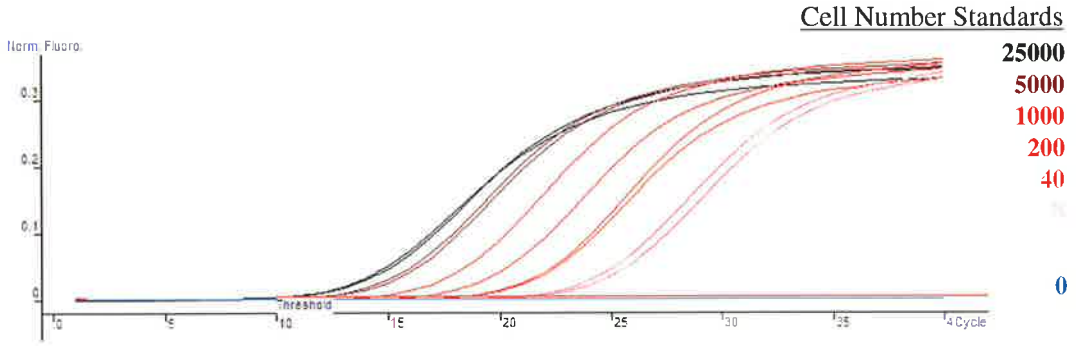

B.

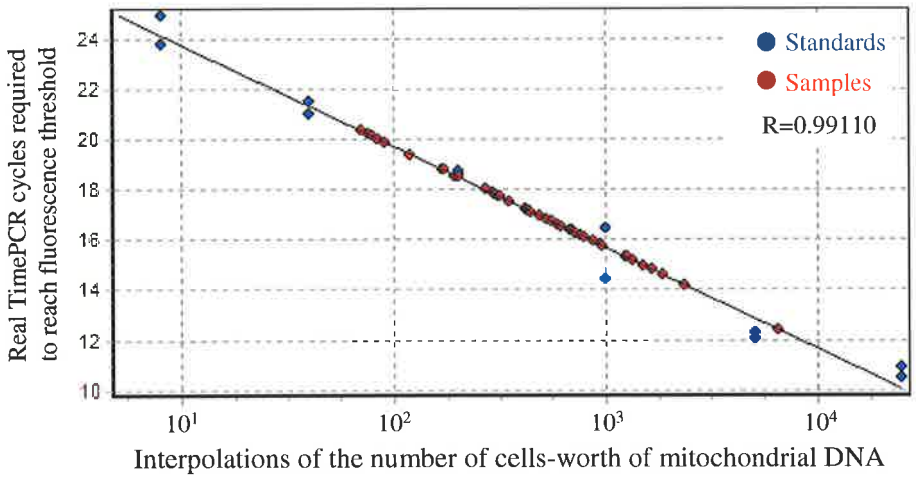

Figure 5.10 Determination of extrachromosomal mitochondrial DNA concentration by real-time PCR.

U251-MG, CCF-STTG1, U87-MG and HuT-78 cells were infected with HIV-1_{NL4-3} as described in Figure 5.8. The cultures were harvested for extrachromosomal DNA extraction at 3½, 26 or 48 hpi. To enable normalisation of the DNA extraction efficiency and quantification of extrachromosomal DNA in each sample, quantitative real time PCR for mitochondrial DNA was performed on samples which had been diluted 1 in 200 (as predicted for sample concentration to be within the range of the standards).

The fluorescence emission curves of the real-time PCR assay using different U251-MG cell number standards are shown (**A**). All samples fell within the quantitative range of the standard curve (**B**), enabling accurate quantification of the samples for subsequent analysis of HIV-1 DNA content (Figures 5.11 and 5.12).

A.

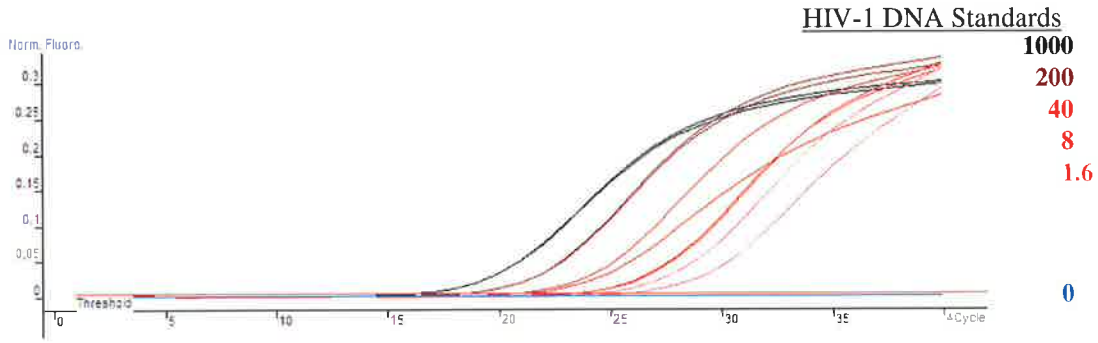

B.

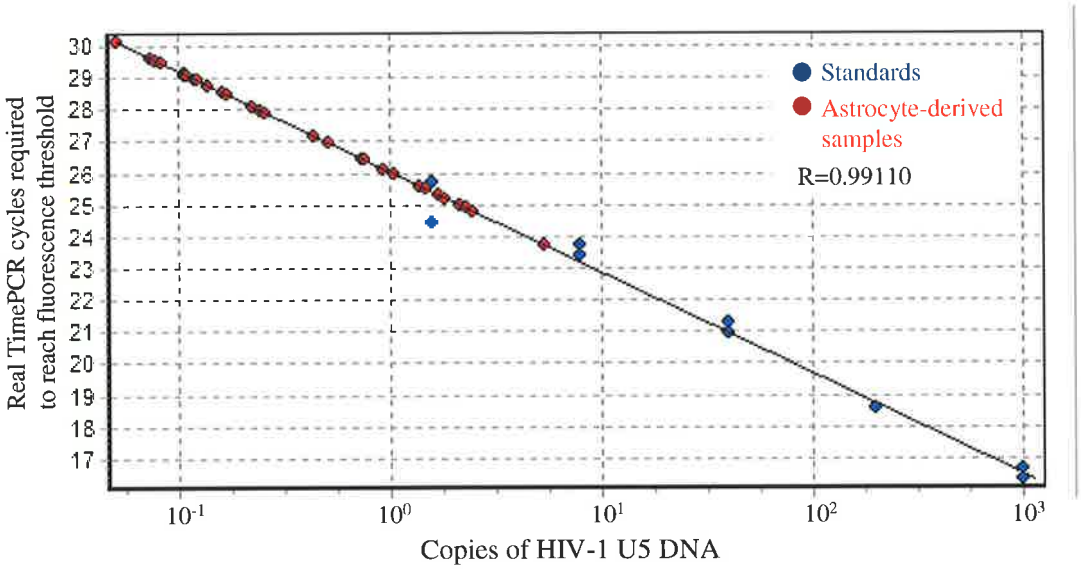

Figure 5.11 Determination of extrachromosomal HIV-1 DNA content by real time PCR.

U251-MG, CCF-STTG1, U87-MG and HuT-78 cells were infected with HIV-1_{NL4-3} as described in Figure 5.8, and the extrachromosomal DNA extracted at 3½, 26 or 48 hpi. The amount of extended minus strand (post second strand transfer) reverse transcribed viral DNA present in 2000 c.e. of extrachromosomal DNA was measured by quantitative real time HIV-1 U5 PCR (**A**).

A standard curve was generated from the amplification of the HIV-1 DNA standards (in the presence of 2000 cells-worth of uninfected extrachromosomal DNA) (**B**). This enabled the number of HIV-1 copies per 2000 cells to be determined for each sample, as shown in Figure 5.12.

Figure 5.12 Levels of HIV-1 DNA present in U251-MG, CCF-STTG1 and U87-MG cultures during HIV-1 infection (±3TC).

U251-MG, CCF-STTG1, U87-MG and HuT-78 cells were infected with HIV-1_{NL4-3} in the presence or absence of the nucleoside analogue, 3TC, as described in Figure 5.8. The extrachromosomal DNA was extracted at designated times post infection. The number of copies of HIV-1 DNA present per 2000 cells-worth of extrachromosomal DNA was determined by real time PCR (Figure 5.11), and is shown here as a function of time post infection. Each bar on the graphs represents the mean of two replicate cultures ± standard error.

(The analysis of the DNA content of the DNase I treated virus inoculum used in this experiment is shown in Figure 5.9)

A. U251-MG cells

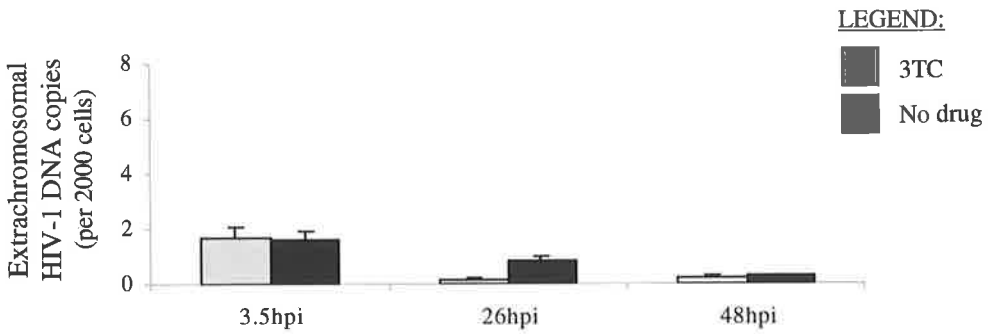

B. CCF-STTG1 cells

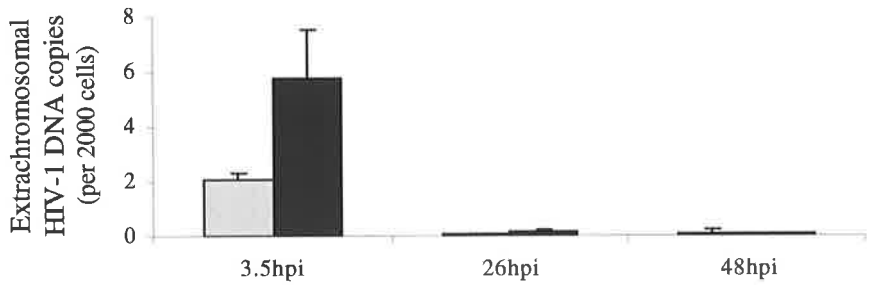

C. U87-MG cells

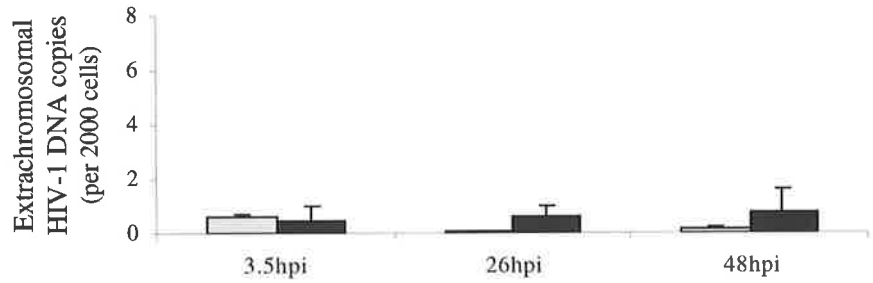

D. HuT-78 cells

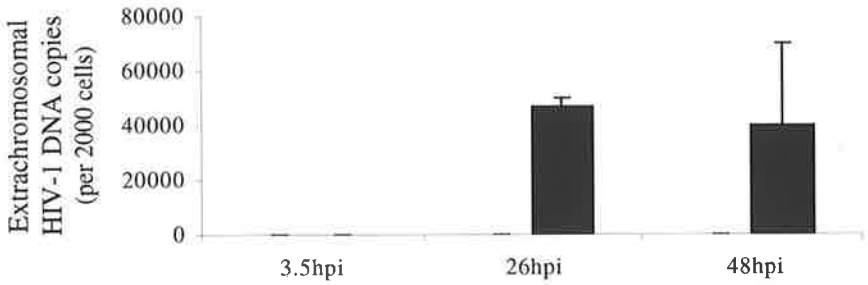

E. HuT-78 cells (3TC results on expanded axis)

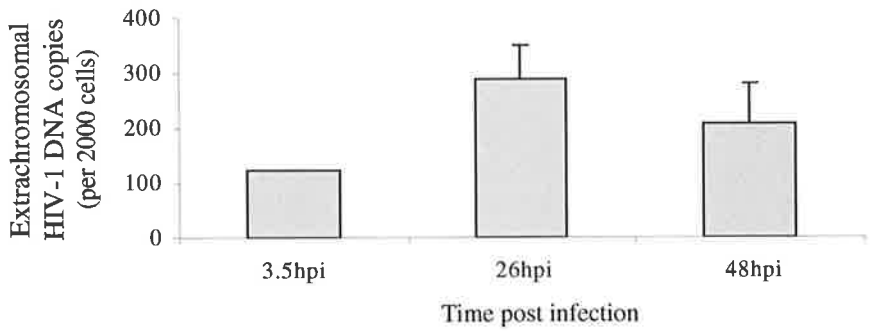

5.4.1), is also inconsistent with *de novo* HIV-1 reverse transcription (discussed in Section 5.4.1). The difference in HIV-1 DNA detection between the 3TC and untreated U251-MG cultures at 26 hpi is not significant as both samples fall below the lowest standard (1.6 copies of HIV-1 DNA), illustrating the high sensitivity of the assay. At 48 hpi the amount of HIV-1 DNA remained below the lowest standard.

The decline in the level of HIV-1 DNA associated with the infected U251-MG cells parallelled the decline in the level of p24 protein in the supernatants of these cultures (Figure 5.8A). The absence of detectable *de novo* reverse transcription in the infected U251-MG cultures in the first 48 hpi indicates that the detection of p24 protein in the culture supernatants during the first 48 hpi must also be due to persistence of the original inoculum, rather than *de novo* synthesis. Never-the-less, the two parallel (drug-free) infected U251-MG cultures which were maintained to test for the ability of the cultures to transmit infection, did indeed transmit HIV-1 infection to HuT-78 cells upon coculture initiated at 7 dpi. Specifically, virus replication was detected in both cocultures within 4 days of coculture, by syncytia formation and detection of p24 protein in the coculture supernatant. As discussed in Section 5.5.2iii, the ability of the infected U251-MG cultures to transmit infection, in spite of the absence of reverse transcription within the first 48 hpi, indicates that HIV-1 replication was inhibited at a stage prior to reverse transcription during acute HIV-1 infection, but that viral replication may occur later upon certain stimuli provided by coculture.

Analysis of the extrachromosomal HIV-1 DNA in infected CCF-STTG1 and U87-MG astrocyte cultures

The amount of HIV-1 DNA detected in the infected CCF-STTG1 and U87-MG cultures could also be accounted for by the amount of HIV-1 DNA present in the DNase I treated virus inoculum (Figures 5.9, 5.11 and 5.12). In the CCF-STTG1 cells, slightly higher levels of HIV-1 DNA was observed in the untreated cultures (5.95 ± 1.75 copies / 2000 cells), compared to the 3TC treated cultures (2.1 ± 0.2 copies 2000 cells), at 3½ hpi (Figure 5.12B). By 26 hpi, the level of HIV-1 DNA in the infected CCF-STTG1 cultures had declined below the limit of detection of the assay (1.6 HIV-1 DNA copies / 2000 cells). The detection of a higher level of HIV-1 DNA in the drug free cultures at 3½ hpi, compared to 3TC treated cultures, could possibly indicate the occurrence of a brief and very low level of *de novo*

reverse transcription in the absence of 3TC, which was inhibited by cellular mechanisms by 26 hpi. Given the very low level of HIV-1 DNA detected, and that this can be accounted for by HIV-1 DNA in the inoculum, it is more likely that the variation in the amount of HIV-1 DNA detected at 3½ hpi in both ±3TC treated CCF-STTG1 cultures was due to slight variations in the persistence of the original inoculum and the efficiency of post inoculation washing.

The amount of HIV-1 DNA detected in the infected U87-MG cultures was below the level of detection (<1.6 copies of HIV-1 DNA per 2000 cells) at all time points. The absence of detectable *de novo* reverse transcription in the infected CCF-STTG1 and U87-MG astrocytes during the first 48 hpi is consistent with the findings in U251-MG astrocytes, and indicates that the detection of p24 protein in the supernatants from CCF-STTG1 and U87-MG cultures over this time (Figure 5.8B and C) must also be due to persistence of the original inoculum, rather than *de novo* synthesis.

Despite the lack of detectable reverse transcription in infected CCF-STTG1 and U87-MG cultures, duplicate parallel (drug-free) infected CCF-STTG1 and U87-MG cultures from the same experiment, which were maintained to test for the ability of the cultures to transmit infection, did indeed transmit HIV-1 infection to HuT-78 cells upon coculture initiated at 7 dpi. As observed in cocultures of HuT-78 cells with infected U251-MG astrocytes, virus replication was detected in both HuT-78 / infected CCF-STTG1 and HuT-78 / infected U87-MG cocultures within 4 days of coculture, by syncytia formation and detection of p24 protein in the coculture supernatants. This is further evidence that, in astrocytes, HIV-1 replication may be inhibited at a stage prior to reverse transcription until certain stimuli are provided, and that these stimuli are provided by coculture with HuT-78 cells.

Analysis of reverse transcription in HuT-78 T-cells, and the effectiveness of 3TC

To control for the infectivity of the virus stock and the effectiveness of 3TC to inhibit viral reverse transcription, HuT-78 cells were included in this experiment as controls. For 3TC treated, and the 3½ hpi untreated infected Hut-78 cultures, 2000 cells-worth of extrachromosomal DNA from each culture were subjected to real-time PCR targeting the extended minus strand (post second strand transfer) HIV-1 DNA, and the results are presented in Figures 5.12D and E. For the extrachromosomal samples from untreated,

infected HuT-78 cells which had been harvested at 28 and 48 hpi, only 100 cells-worth of extrachromosomal DNA was subjected to this HIV-1 PCR, and an extra HIV-1 copy number standard of 5000 copies was included. This was done in order to ensure the number of copies of HIV-1 DNA in these productively infected cells was within the range of the standard curve, thus permitting interpolation and accurate quantification. This data is presented graphically in Figure 5.11D and E, and the number of HIV-1 copies detected has been extrapolated to represent the number present in 2000 cells, consistent with all other graphs in this figure.

At 3½ hpi HIV-1 DNA was detectable at low levels in both the 3TC and untreated HuT-78 cells, at a much higher level than was detected in any of the astrocyte cultures at this time (3TC treated HuT-78 cells; 122 ± 2 copies HIV-1 DNA / 2000 cells (Figure 5.12E), drug-free HuT-78 cells; 366 ± 16 copies HIV-1 DNA / 2000 cells (Figure 5.12D) compared to <8 copies / 2000 astrocytes cells (Figure 5.12A-C)). This suggests that, in contrast to the infection of astrocytes, reverse transcription had commenced in the HuT-78 cells by this time. In the absence of any inhibitor of reverse transcription, the amount of HIV-1 DNA present in the HuT-78 cells increased 128-fold from 3½ to 26 hpi (from 366 ± 16 copies to $4.7 \pm 0.3 \times 10^4$ copies per 2000 cells), consistent with the expected replication of HIV-1. From 26 to 48 hpi the amount of HIV-1 DNA present in the HuT-78 cells did not alter significantly, although a high degree of variation was seen between cultures ($4.0 \pm 3.0 \times 10^4$ copies per 2000 cells). This plateau, and the variation between HuT-78 cultures at 48 hpi, is most likely due to the cytotoxicity of the productive HIV-1 infection in these cells.

The level of HIV-1 DNA in the 3TC treated, infected HuT-78 cells increased 2.5 fold from 3½ to 26 hpi (from 122 ± 2 copies to 290 ± 62 copies per 2000 cells), with no further increase by 48 hpi (209 ± 70 copies per 2000 cells) (Figure 5.11 E). This demonstrated that, whilst the effectiveness of 50 μM 3TC on these cells was not absolute, it inhibited HIV-1 replication in HuT-78 cells by >99 % at 26 hpi (Figure 5.11 D, E).

5.6.2iii Summary of the analysis of HIV-1 reverse transcription in the infected astrocytes.

All three astrocyte lines appeared to become infected upon exposure to HIV-1_{NL4-3}, as evidenced by the ability of the infected cultures to transmit infectious virus upon coculture with susceptible cells. Yet, with the possible exception of the infected CCF-STTG1 at 3½ hpi, reverse transcription could not be detected in any of the infected astrocyte cultures during the first 48 hours of infection. HIV-1 DNA was detectable in the infected astrocyte cultures as early as 3½ hpi, but this did not represent *de novo* reverse transcription, as i) the level of HIV-1 DNA in the infected cultures could be accounted for by the amount HIV-1 DNA in the DNase I treated inoculum, ii) inhibitors of reverse transcription (3TC and AZT) had no effect, and iii) the amount of HIV-1 DNA associated with the astrocyte cultures declined over time. Definitive proof of whether the slight difference in the detection of HIV-1 DNA in the CCF-STTG1 cultures at 3½ hpi ±3TC may represent a low, transient period of *de novo* reverse transcription, or merely an arbitrary difference in the persistence of inoculum DNA between the two cultures, would require further experimentation. Regardless, reverse transcription was not detected at later time points in the infected CCF-STTG1 cells, and if a small degree of reverse transcription did occur in the drug-free CCF-STTG1 cultures within the first 3½ hpi, viral replication did not proceed to structural protein production, as the level of p24 protein in the supernatants of the untreated, infected CCF-STTG1 cultures did not exceed that in the 3TC treated, infected cultures (Section 5.6.1ii and Figure 5.8B). As *de novo* reverse transcription did not occur in either the infected U251-MG or U87-MG astrocytes during the first 48 hpi, the source of the p24 protein (shown in Figure 5.8A,C and discussed in Sections 5.6.1i and ii) in these culture supernatants is the persistence of viral inoculum. In summary, whilst p24 protein and HIV-1 DNA was detectable upon infection of all three astrocyte cell lines, the source of both viral protein and viral DNA was the inoculum rather than *de novo* synthesis.

5.5 Discussion

The model of cell-free HIV-1 astrocyte infection employed in this chapter exhibited the characteristic features of *in vitro* HIV-1 infection of astrocytes (Section 1.4). Specifically, the release of p24 protein into the culture supernatants was detected during the first few days

of infection, low levels of HIV-1 DNA were detected in the cultures, and transmission of infection upon coculture with HIV-1 susceptible cells was seen. This limited release of p24 protein has been previously interpreted as an initial phase of productive infection in some astrocyte models (Di Rienzo *et al*, 1998; Messam and Major, 2000; Sabri *et al*, 1999). The detailed analysis of p24 release into the supernatant during the initial phase of astrocyte infection in this chapter emphasises the need to critically evaluate the source of any initial p24 release, as a proportion of p24 protein from the initial inoculum can persist despite a comprehensive post-infection washing regime (Figures 5.2, 5.4 and 5.8).

In some reports the interpretation that early p24 protein release represents *de novo* synthesis is supported by an elevation of supernatant p24 levels above an earlier defined level (Messam and Major, 2000; Sabri *et al*, 1999). Specifically, Sabri *et al* document a convincing release of p24 protein by HFA cells infected with 2 primary HIV-1 isolates, as supernatant p24 protein levels are reduced to ≤50 pg/ml at 1 dpi by the post-infection washes, and rebound to > 200 pg/ml by 2 dpi (Sabri *et al*, 1999). In a review article by Messam and Major, the initial release of p24 protein from HIV-1 infected HFAs is associated with an initial phase of "productive infection". In their report, the detection of up to 1400 pg/ml p24 protein in the supernatant at 2 dpi does appear to represent *de novo* synthesis, as the supernatant contained less than 100 pg/ml p24 protein at around 36 hpi, and they report that "infectious progeny (HIV-1) are produced" during this initial productive phase (Messam and Major, 2000). This report was based on infection with HIV-1_{NL4-3}, however the dose and method of virus inoculation are not disclosed, nor is the method or data for the detection of infectious progeny virus.

In other reports, however, the background level of supernatant p24 protein is not established, and it is unclear whether the transient detection of p24 protein, which is highest at the first time point analysed (usually 1 or 2 dpi) represents transient *de novo* synthesis or persistent inoculum. This is particularly confusing when high dose virus inoculum is used. Nath *et al.* (1995) employed a very high dose inoculum to infect HFAs (2 μg / 10^6 cells) and detected a p24 protein release of between 110 and 160 pg/ml p24 protein at 2 dpi (the earliest supernatant sample), for each of three virus strains (HIV-1_{SF2}, HIV-1_{IIIB} and HIV-1_{Ada-M}). Interestingly, despite the detection of p24 protein in the supernatants of all three infections at 2 dpi, only two of three virus strains (HIV-1_{SF2} and HIV-1_{IIIB}) gave rise to HFA infection, as

determined by gp41 immunoreactivity, PCR detection of *env* and *nef* DNA, and the transmission of infection upon coculture. The HIV-1_{Ada-M} exposed HFAs are therefore an example of initial p24 protein release by astrocytes which do not exhibit any other signs of infection (and were not considered infected by Nath *et al.*). Like the data presented in this chapter, this therefore also challenges the concept that early p24 release by astrocytes necessarily represents an initial productive phase of infection.

Recently, Lawrence *et al* documented the detection of between 750 to 1250 pg/ml p24 protein in the culture supernatants of progenitor-derived astrocytes which were infected 1 day earlier with 10 ng p24 protein of HIV-1_{NL4-3} or HIV-1_{IIIB}. The level of supernatant p24 protein subsequently declined over the course of the infection. This group is the first to suggest an alternative interpretation for the initial detection of p24 protein upon HIV-1 infection of astrocytes; "Virus production by astrocytes was highest at 1 day postinfection, but may indicate the release of bound virus" (Lawrence *et al*, 2004).

The release of p24 protein during the acute phase of infection in this study demonstrated the capacity for cell-associated p24 protein to persist (despite numerous washes and trypsin treatment) and then rebound into the culture medium (Figures 5.2, 5.4 and 5.8). The number of post-infection washes corresponded to the reduction in the amount of p24 protein which persisted, although not even 7 washes and a trypsin treatment could completely remove p24 protein which persisted from the inoculum (Figure 5.2). The common use of relatively high dose HIV-1 inocula, coupled with the high sensitivity of commonly used p24 ELISA kits (sensitivity of 6 pg/ml in this thesis, and to 2.5 pg/ml in the literature (Di Rienzo *et al*, 1998)), highlight the need for caution in interpreting p24 data from any semi- or non-permissive cells and indicate that such p24 data should be coupled with additional assays for virus replication.

The detection of a low level of HIV-1 DNA in U251-MG, CCF-STTG1 and U87-MG astrocytes post HIV-1 infection is consistent with numerous reports of *in vitro* HIV-1 infection of astrocytes, including human fetal astrocytes (Brengel-Pesce *et al*, 1997; Di Rienzo *et al*, 1998; Keys *et al*, 1991; Nath *et al*, 1995; Sabri *et al*, 1999) and astrocyte cell lines (Keys *et al*, 1991), including U251-MG (Kort, 1998) and CCF-STTG1 (Brengel-Pesce *et al*, 1997). Data from this thesis, published recently in *Virology* (Clarke *et al*, 2006), comprise the first attempt to analyse the kinetics of HIV-1 reverse transcription upon

infection of astrocytes. The data in this chapter demonstrated that a low level of cell-associated HIV-1 DNA is detectable during the acute phase of astrocyte infection. The amount of HIV-1 DNA present declined with time post infection in infected U251-MG and CCF-STTG1 cells, over the first 48 hpi (Figures 5.1, 5.5 and 5.12). The level of HIV-1 DNA in U87-MG cells was below the detection limit (1.6 copies of HIV-1 DNA per 2000 cells) at all time points assessed (3½ , 26, 48 hpi) (Figure 5.12). A decline in the levels of HIV-1 DNA in infected astrocytes has been documented in several previous reports (Brengel-Pesce *et al*, 1997; Di Rienzo *et al*, 1998; Keys *et al*, 1991; Sabri *et al*, 1999).

Brengel-Pesce *et al* assessed the presence of HIV-1 DNA in two astrocyte cell lines (CCF-STTG1 and MOG-G-UVM) and HFAs over time post infection with four primary HIV-1 isolates (two syncytium-inducing and two non-syncytium-inducing strains). Eight out of the nine virus / cell combinations tested yielded detectable HIV-1 DNA at 16 hpi, using a PCR which targeted the *pol* region of the viral DNA genome, with a reported sensitivity of one copy per 1.5 x 10^5 cells (Brengel-Pesce *et al*, 1997). By 24 hpi, however, only 5 of these nine cultures tested positive for HIV-1 DNA, and by 3 dpi, only 3 of these cultures remained positive. By 6 dpi, HIV-1 DNA was only "weakly" detectable in one of these cultures, and tested negative at all subsequent time points.

Keys *et al* also observed a decline in the detection of HIV-1 DNA with time post infection of astrocyte cell lines (subclones of U138-MG). They reported the detection of HIV-1 DNA in their most susceptible subclone with 8 out of 9 HIV-1 isolates at 3 dpi, by a nested PCR targeting the pol region of the HIV-1 DNA genome (sensitivity of 1 copy per 10^5 cells). Their panel of virus isolates included HIV-1_{IIIB}, HIV-1_{BaL}, three blood-derived isolates, three CSF-derived isolates and a brain-derived isolate. However, by 10 dpi, HIV-1 DNA was only detectable in cultures infected with HIV-1_{BaL} and one of the blood-derived isolates. Interestingly, these cultures had supernatant p24 protein levels of around 2 ng/ml at 3 dpi, yet were negative for RT activity and virus production at all times assayed (1, 3, 7, 10 and 14 dpi). HIV-1 DNA was still detectable in the HIV-1_{BaL} infected U138-MG subclone as long as 28 dpi, but limiting dilution PCR analysis demonstrated that the number of HIV-1 DNA positive cells in these cultures declined with time, from between 1 in 4080 to 1 in 5067 (~0.022%) cells positive for HIV-1 DNA at 3 dpi, to 1 in 13 000 (0.0077%) at 10 dpi, a decrease of 35%. The decline in HIV-1 DNA positive cells in the HIV-1_{BaL} infected U138-MG population was postulated to be due to slower replication of the virus positive

cells (as suggested in an earlier report (Chiodi *et al*, 1987)), or cytopathic effect of the virus for the infected cells (Keys *et al*, 1991).

The above reports have not questioned the source of the viral DNA in astrocytes, and it was presumed to represent *de novo* synthesis since other components of viral replication were also detected, including regulatory viral mRNAs (Brengel-Pesce *et al*, 1997; Di Rienzo *et al*, 1998), Nef protein (Kort, 1998), gp41 protein (Nath *et al*, 1995), and the transmission of infection upon coculture (Di Rienzo *et al*, 1998; Sabri *et al*, 1999). Of note, the virus inoculum was not DNase treated in any of these studies, except that of Sabri *et al.* (1999). The studies in this chapter demonstrate that the amount of viral DNA present in the inoculum may be significant when studying low / non-productive infection (Figures 5.6 and 5.9), and that this potential source of HIV-1 DNA also needs to be considered when employing sensitive PCR based detection methods. Indeed, the low level of astrocyte-associated HIV-1 DNA described in this chapter can be completely accounted for by the level of HIV-1 DNA in the inoculum. Since the virus inoculum had been effectively treated with DNase I, the HIV-1 DNA detected in the astrocyte cultures was not loosely associated with the virus inoculum but most likely represented the products of intravirion reverse transcription (Arts *et al*, 1994; Lori *et al*, 1992; Trono, 1992; Zhang *et al*, 1994; Zhang *et al*, 1996a; Zhang *et al*, 1996b; Zhang *et al*, 1993), which is reportedly resistant to DNase digestion (Arts *et al*, 1994).

Furthermore, the detection of HIV-1 DNA in the infected U251-MG, CCF-STTG1 and U87-MG astrocytes was not dependent on *de novo* reverse transcription in these cells, as the amount of viral DNA detected was irrespective of the inclusion of the reverse transcriptase inhibitors, 3TC and AZT, during the infection (Figures 5.1, 5.7 and 5.12). The decay kinetics of viral DNA in the infected cells from 3½ hpi to 48 hpi (Figures 5.1, 5.5 and 5.11), are also not consistent with viral reverse transcription. The probability that both nucleoside analogue reverse transcriptase inhibitors (3TC and AZT) were ineffective in the astrocyte cell lines used is very low, given that the cells were pre-incubated with the respective drugs for 18 hours prior to inoculation, in order to allow conversion of the drugs into their active deoxynucleotide triphosphates. However, to exclude this possibility, the inclusion of a non-nucleoside based reverse transcriptase inhibitor, which does not require cellular conversion into an active form, would be recommended for future studies. Aldothriol-2 treated virus (which can bind and enter cells normally but is prevented from undergoing reverse

transcription) would also be a good control for similar studies. In this study, it is considered very unlikely that the detection of viral DNA at 3½ hpi may be due to an early, transient period of *de novo* reverse transcription in U251-MG and U87-MG cells, based on the lack of effect of 3TC and AZT in these experiments.

The demonstration in this chapter that the viral DNA in astrocytes can be accounted for by the viral DNA present in the inoculum raises this as a possibility in previous astrocyte studies and in future studies. Despite no evidence for viral reverse transcription in U251-MG, U87-MG, and possibly CCF-STTG1 cells, within the first 48 hpi, all the infected astrocyte cultures were capable of transmitting infectious HIV-1 to HuT-78 cells upon coculture initiated 7 dpi. Similar to previous reports (Cheng-Mayer *et al*, 1987; Di Rienzo *et al*, 1998; Sabri *et al*, 1999), at least 2 days (and up to 6 days) of coculture was required before increasing titres of supernatant p24 protein and syncytia were detectable (Section 1.4.3). This delay could indicate that release of virus from astrocytes is an inherently inefficient process and / or that viral replication may be restricted, prior to replication, until the occurrence of certain events triggered by coculture. To further characterise the HIV-1 infection of U251-MG, CCF-STTG1 and U87-MG astrocytes, and to determine whether viral replication was required for the release of infectious virus upon coculture or cytokine stimulation, the viral replication step of integration was analysed during the course of infection (Chapter 6).

Chapter 6

Integration of HIV-1 in Astrocytes

(following cell free infection)

6.1 Introduction

6.1.1 Background

After HIV-1 has entered a target cell, the viral core uncoated and the viral RNA genome reverse transcribed, the viral DNA, in the context of a pre-integration complex (PIC), is targeted for nuclear import (Section 1.1.6 and Figure 1.6). Upon entering the nucleus, the viral DNA has four potential fates; i) to persist as linear extrachromosomal DNA, ii) and iii); to form a circular episomal molecule with either one or two LTR regions, or iv) to be integrated into the host cell chromosome (Barbosa *et al*, 1994) (Section 1.1.6iii). Only the integrated proviral DNA has the potential to give rise to the production of progeny virions. Integration of the viral DNA is therefore an essential step in the virus life cycle (Englund *et al*, 1995; LaFemina *et al*, 1992; Sakai *et al*, 1993; Stevenson *et al*, 1990), and is a highly organised and ordered process mediated by both viral and cellular proteins associated with the viral DNA in the PIC (Bukrinsky *et al*, 1992; Bukrinsky *et al*, 1993; Chen and Engelman, 1998; Farnet and Bushman, 1997; Karageorgos *et al*, 1993; Li *et al*, 2000; Miller *et al*, 1997) (Section 1.1.6). The kinetics of HIV-1 integration has been described for $CD4^+$ cells which support productive HIV-1 infection (Stevenson *et al*, 1990; Vandegraaff *et al*, 2001a), but has not been previously characterised in astrocytes.

Like reverse transcription of HIV-1 DNA in astrocytes, the assumption that HIV-1 integration proceeds in astrocytes is based on; i) the initial phase of productive infection (Brack-Werner *et al*, 1992; Di Rienzo *et al*, 1998; Lawrence *et al*, 2004; McCarthy *et al*, 1998; Messam and Major, 2000; Nath *et al*, 1995; Sabri *et al*, 1999), ii) the detection of a low level of HIV-1 DNA in infected astrocytes (Brengel-Pesce *et al*, 1997; Di Rienzo *et al*, 1998; Keys *et al*, 1991; Kort, 1998; Nath *et al*, 1995; Sabri *et al*, 1999) which in some reports is still detectable up to three or four weeks after infection (Brengel-Pesce *et al*, 1997;

Di Rienzo *et al*, 1998; Keys *et al*, 1991; Kort, 1998; Nath *et al*, 1995; Sabri *et al*, 1999), and iii) the ability of so-called "latently" infected astrocytes to transmit infection upon coculture with susceptible cells (Cheng-Mayer *et al*, 1987; Chiodi *et al*, 1987; Dewhurst *et al*, 1987b; Di Rienzo *et al*, 1998; Sabri *et al*, 1999) (Section 1.4). The establishment of a chronically-infected astrocyte cell line by Brack-Werner *et al* (TH4-7-5 cells, see Sections 1.4.2, 1.5.2 and 1.5.3i) is further evidence that HIV-1 integration can proceed in infected astrocytes (Brack-Werner *et al*, 1992). The productive infection of astrocytes which occurs with VSV and MLV enveloped pseudotyped HIV-1, astrocytes transfected to express CD4 and HIV-1 coreceptors, and certain strains of HIV-1 (HIV-1_{SF2}) (Section 1.6.1vi), although not representative of the restricted infection of astrocytes observed *in vivo* (Section 1.3.2ii), indicate that under certain conditions astrocytes can support productive HIV-1 replication and therefore viral integration. In *in vivo* infected astrocytes, the occurrence of viral integration is supported by the detection of HIV-1 DNA in astrocytes in brain sections (An *et al*, 1999a; An *et al*, 1999b; Chiodi *et al*, 1996; Epstein *et al*, 1984; Nuovo *et al*, 1994; Ranki *et al*, 1995; Saito *et al*, 1994; Sharer *et al*, 1986; Takahashi *et al*, 1996; Thompson *et al*, 2004; Tornatore *et al*, 1994a; Wiley, 1996). None of the PCR based methods of HIV-1 DNA detection previously applied to astrocytes are specific for integrated provirus, as, without specific measures to demonstrate the positioning of the viral DNA within chromosomal DNA, other forms of viral DNA (episomal linear, 1-LTR circular and 2-LTR circular forms) would also be detected (Chun *et al*, 1995; Vandegraaff *et al*, 2001a; Zanussi *et al*, 2000).

Whilst observations from Chapter 4 demonstrated that HIV-1 was readily internalised by the three different astrocyte cell lines used in this thesis (U251-MG, CCF-STTG1 and U87-MG), Chapter 5 demonstrated that reverse transcription did not proceed within the first 48 hpi in any of these cell lines (upon infection by spinoculation). Yet, all three astrocyte cell lines subsequently transmitted infectious virus to susceptible cells upon coculture. This suggested that, whilst virus replication is blocked prior to reverse transcription during the first 48 hpi in these astrocytes, viral replication could proceed to the release of infectious virus when inoculated astrocytes are cocultured with $CD4^+$ HIV-1 susceptible cells. The ability of astrocytes to restrict virus replication, and for this restriction to be relieved upon coculture with $CD4^+$, HIV-1 susceptible cells, has been well documented for *in vitro* HIV-1 infection of astrocytes, with respect to post transcriptional mechanisms of virus restriction (Bannwarth *et al*, 2001; Gorry *et al*, 1998; Gorry *et al*, 1999; Li *et al*, 2002a; Ludwig *et al*,

1999; Neumann *et al*, 1995; Ong *et al*, 2005) (Section 1.5.3). With the exception of the chronically infected TH4-7-5 astrocyte cell line (discussed in Sections 1.4.2, 1.5.2 and 1.5.3i), these models bypassed reverse transcription by transfecting the astrocytes with proviral plasmid DNA. Whilst this plasmid DNA may integrate into the host cell chromosome, the process of plasmid integration is fundamentally different to the proviral integration which occurs during viral replication, as plasmid DNA is not in the context of pre-formed viral proteins. During HIV-1 infection viral proteins including the integrase enzyme in the PIC direct integration of the provirus (Bukrinsky *et al*, 1993; Miller *et al*, 1997).

The aim of this chapter was to characterise the kinetics of HIV-1 integration, in the context of the PIC, after inoculation of astrocytes with wild-type enveloped HIV-1. The absence of detectable reverse transcription during the first 48 hpi together with the recovery of infectious virus upon coculture with susceptible cells suggested that coculture might relieve astrocyte-specific restrictions to HIV-1 replication (Lawrence *et al*, 2004; Sabri *et al*, 1999; Tornatore *et al*, 1994b; Tornatore *et al*, 1991). This chapter therefore investigates viral integration in astrocytes both during the restricted phase of infection and during stimulation of virus release. To achieve this, U251-MG, CCF-SSTG1 and U87-MG astrocytes were infected with cell-free HIV-1_{NL4-3} by spinoculation, and the chromosomal DNA analysed for evidence for integrated proviral DNA. The course of the astrocyte infections were monitored by supernatant p24 levels, and infection of the astrocyte cultures were confirmed by the ability to transmit infection upon coculture with $CD4^+$ cells. To assess viral integration during the phase of virus transmission, the cytokine IL1β was used to model the stimulus of coculture (see Section 6.1.2 below) and the culture supernatants tested for the release of infectious virus. To further understand the nature of the HIV-1 infection being observed in our infection model, the expression of unspliced and multiply spliced viral RNAs was also assessed in one of these experiments (Section 6.6).

6.1.2 Use of IL1β as a model of coculture stimuli for the "rescue" of infectious virus from infected astrocytes.

The data in Chapter 5 suggested that viral replication did not proceed in U251-MG, CCF-STTG1 or U87-MG astrocytes until the occurrence of certain events triggered by coculture.

To further characterise HIV-1 infection of these astrocytes, and to determine whether virus replication was required for the release of infectious virus upon coculture, it was necessary to assess viral integration before and during the phase of coculture-induced virus transmission. The adherence of $CD4^+$ T-cells and macrophages upon coculture with astrocytes (Nath *et al*, 1995; Tornatore *et al*, 1991) (Sections 3.2.2i) renders the study of viral integration specifically in astrocytes exceedingly difficult, as the astrocyte population cannot be separated from the $CD4^+$ cells in which viral integration is readily occurring. To circumvent this problem, infected astrocyte cultures were treated with IL1β as a model of the stimulus provided by coculture. This proinflammatory cytokine has been previously reported to "reactivate" or "rescue" productive infection from the restricted state in astrocytes (Section 1.4.3). In the literature, this effect has been measured by the transient release of viral p24 protein after addition of IL1β to the culture medium of astrocytes which had been inoculated with cell-free virus (Sabri *et al*, 1999) or transfected with a proviral plasmid (Tornatore *et al*, 1991). In transfected astrocytes, infectious virus has also been demonstrated in culture supernatants after IL1β treatment, during the period of cytokine induced p24 release (Tornatore *et al*, 1991). Due to the inherent differences between HIV-1 plasmid transfection and HIV-1 infection, it was necessary to determine whether i) IL1β resulted in the release of p24 protein in the spinoculation model of astrocyte infection used in this thesis, and ii) whether this p24 release actually represented the release of infectious virions.

6.2 Preliminary investigations of integrated HIV-1 DNA, p24 protein and infectious virus release during HIV-1 infection of U251-MG cells with coculture or IL1β stimulation

To determine the temporal relationship between the integration of viral DNA and the release of viral products (p24 protein and infectious virus) upon stimulation by either coculture or IL1β, integrated provirus, p24 release and infectious virus release were measured during the course of U251-MG astrocyte infection, both before and after coculture or IL1β stimulation. U251-MG astrocytes were inoculated with 0.22 $TCID_{50}$U/cell of DNase I treated HIV-1_{NL4-3} by spinoculation (with 7 post-infection washes and a trypsin treatment to remove as much excess inoculum as possible (Section 5.2.2ii)) and seeded into 6-well culture trays. The cells

were subcultured with trypsin at 5 dpi into 3 times as many wells. At 7 dpi, the cultures were either left untreated, cocultured with $CD4^+$ HuT-78 cells or stimulated with IL1β. The cultures were analysed for the presence of the integrated provirus before (28 hpi and 7 dpi) and after (10, 13, 16 dpi) stimulation by coculture or IL1β. The ability of the infected U251-MG cultures to transmit infection to HuT-78 cells upon coculture was confirmed in all experiments by the formation of syncytia in the HuT-78 cell population and the release of p24 protein. To monitor the infection of the astrocyte cultures, and to assess the "rescue" of virus release upon stimulation with IL1β, the culture supernatants were sampled for p24 content and for infectious virus. Release of infectious virus from the astrocyte cultures was assayed by inoculating HIV-1 susceptible cells with filtered (0.2μm) supernatants from the astrocyte cultures, and looking for subsequent evidence of infection in the HIV-1 susceptible cell cultures (refer to the "Infectivity Assay", Sections 2.8 and 6.2.2).

6.2.1 Assaying astrocyte supernatants for the release of p24 protein.

Infected astrocyte cultures were treated with or without 10 U/ml IL1β from 7 dpi. This concentration of IL1β was based on a previous report which cited a modest and transient release of p24 protein (up to 20 pg/ml) from HIV-1 infected HFAs into the culture supernatants, 3 days after the addition of IL1β (Sabri *et al*, 1999). Figure 6.1 shows that a modest release of p24 protein was detected in two out of six IL1β treated, infected U251-MG cultures. In one of these cultures, p24 was detected in the supernatant 3 days after the addition of IL1β, and peaked at 99 pg/ml 4 days after the addition of IL1β (11 dpi). p24 protein remained detectable in the supernatant of this culture until 16 dpi, when the culture was harvested to assess viral integration. In another culture, p24 was undetectable in the culture supernatants until 13 dpi (6 days after the addition of IL1β), when 91 pg/ml p24 protein was detected. This particular culture was harvested at 13 dpi to assess viral integration. p24 protein was undetectable in the supernatants of the other four IL1β treated cultures, and all three untreated, infected astrocyte cultures, during the period tested (7 to 16 dpi). The release of p24 protein from some (but not all) IL1β treated, infected astrocyte cultures indicated that IL1β could be used to induce at least some components of virus replication. p24 protein was readily detectable within 3 days of coculture of HuT-78 cells with infected astrocytes, as expected.

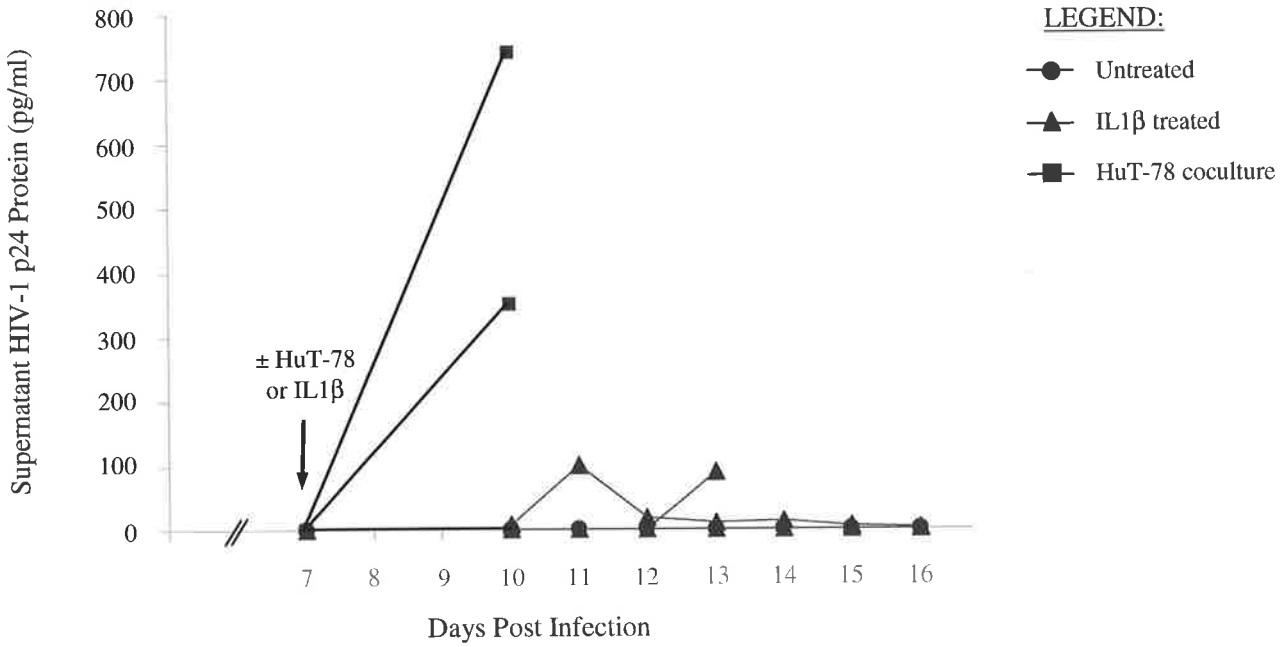

Figure 6.1 Supernatant p24 profile of the "rescue" of U251-MG astrocyte infection by CD4⁺ coculture and IL1β treatment.

U251-MG astrocyte cells were infected with HIV-1_{NL4-3} and the culture supernatants sampled for HIV-1 p24 content at designated times post infection. From 7dpi onwards the cultures were either i) untreated (●) (n=3), IL1β treated (▲) (n=6) or cocultured with HuT-78 cells (■) (n=2). Cultures were harvested at either 10, 13 or 16 dpi for analysis of HIV-1 integrated DNA (Figure 6.2). Taking into account the subculturing of the U251-MG

astrocytes at 5 dpi, the p24 content of the virus inoculum per culture was 69 ng.

6.2.2 Assaying astrocyte supernatants for the presence of infectious virus.

Release of infectious virus from the astrocyte cultures was assayed by inoculating HuT-78 cells with filtered (0.2μm) astrocyte culture supernatants. These HuT-78 cell cultures were observed for evidence of infection (syncytia formation and p24 protein release) over the following 10 to 14 days (Section 2.8). As a positive control, filtered supernatants from the cocultures were sampled at 10 dpi (after 3 days of coculture) and tested for infectivity by inoculation on fresh HuT-78 cells. Infection was subsequently detected in the latter HuT-78 cells by the formation of syncytia within 5 days (Table 6.1). Cytopathic effect, including syncytia, was not observed in HuT-78 cells passaged with supernatant from uninfected astrocytes. To test whether the presence of IL1β may affect the susceptibility of the HuT-78 cells to infection, the filtered 10 dpi coculture supernatants were tested for infectivity at various dilutions in the presence or absence of 10 U/ml IL1β. No apparent difference was observed in cultures with IL1β, suggesting the susceptibility of the HuT-78 cells to HIV-1 infection was not substantially altered by the presence of IL1β (Table 6.1).

None of the (filtered) supernatants from the infected astrocytes were infectious upon inoculation of HuT-78 cells, as no syncytia formation or p24 protein production was detectable in these HuT-78 cultures over the following 13 days (Table 6.1). This was unexpected, and indicated that either i) infectious virus was not released in the absence of coculture, not even in the IL1β treated cultures which released p24 protein (Figure 6.1), ii) the time of supernatant sampling did not coincide with the release of infectious virus, iii) the level of infectious virus in the astrocyte supernants was below the infectious dose required to infect the HuT-78 cells, and / or iv) that the presence of IL1β may have reduced the susceptibility of HuT-78 cells to infection at lower inoculum levels that that tested with the diluted coculture supernatants ± IL1β. The inability to detect infectious virus in the cultures which released p24 was surprising, especially in the culture which released 91 pg/ml p24 on 13 dpi, as the supernatant was sampled for infectivity on the same day (in this experiment, the supernatant from any given culture was only sampled for infectivity once, on the day the culture was harvested for assessment of viral integration). The culture which released p24 protein from 10 dpi onwards was not sampled for infectious virus release until 16 dpi, however p24 was still detectable in the culture supernatant at this time.

Infectivity of supernatants from HIV-1 infected U251-MG astrocytes																	
	No IL1β			IL1β treated						$CD4^+$ cocultured							
										No IL1β				IL1β			
Supernant dilution	n	n	n	n	n	n	n	n	n	n	0.1	0.03	0.01	n	0.1	0.03	0.01
10 dpi	-	-	-	-	-	-	-	-	-	+	+	+	+	+	+	+	+
13 dpi		-	-			-	-	-	-	+	+	+	+	+	+	+	+
16 dpi			-					-	-	+	+	+	+	+	+	+	+
			○				△	□	◊								

Table 6.1 Analysis of infectious virus release from HIV-1 infected U251-MG astrocytes.

U251-MG cells were inoculated with HIV-1_{NL4-3} and from 7 dpi onwards the cultures were either untreated (n=3), IL1β treated (n=6) or cocultured with HuT-78 cells (n=2). Culture supernatants were sampled from each culture at 10, 13, or 16 dpi, filtered and assayed for the presence of infectious virus by passage in HuT-78 cells (without spinoculation). The HuT-78 cultures were maintained for 14 days, and observed for evidence of infection (by syncytia formation and supernatant p24 elevation). Negative and positive controls for infectious virus (culture medium or diluted virus stock in place of astrocyte supernatant, respectively) were also passaged in HuT-78 cultures, which remained uninfected / become infected accordingly. As an internal positive control, supernatants from astrocytes which had been cocultured with HuT-78 cells from 7 dpi onwards were also assayed for the presence of infectious virus.

To assess whether the presence of IL1β in some astrocyte supernatants might impede infection of the HuT-78 cells, the infectivity of neat (n) and various dilutions of the coculture supernatants was tested in the presence and absence of IL1β. Each column in the Table represents an individual infected astrocyte culture, from which supernatants were sampled at 10, 13 and 16 dpi. Supernatants from the same cultures were also assayed for p24 protein (Figure 6.1), and the cultures were harvested at designated times for analysis of HIV-1 integration (Figure 6.2). Symbols △, ○, □ and ◊ indicate particular U251-MG cultures referred to in Figure 6.2. Cultures △ and □ were the two IL1β-treated U251-MG cultures that released p24 into their supernatant (Figure 6.1).

6.2.3 Assessment of HIV-1 integration.

The infected U251-MG cultures were harvested for chromosomal DNA extraction at 28 hpi, 7 dpi (prior to addition of HuT-78 cells or IL1β), and 10, 13 and 16 dpi (after 3, 6, or 9 days of coculture or IL1β stimulus, respectively). The chromosomal DNA extraction efficiency was assessed by *β-globin* PCR and Southern hybridisation, and the concentration of the DNA extracts estimated by comparison to cell-number standards. 10 000 cells-worth of chromosomal DNA was subjected to a modified nested *Alu* PCR (with the exception of the 28 hpi DNA harvest, from which 280 cells-worth of DNA was assayed) (Figure 6.2B). The *Alu* PCR technique is specific for the integrated form of HIV-1 DNA, and does not amplify other forms of HIV-1 DNA (Figure 2.2). The integrated form of HIV-1 DNA was not detectable in any of the infected U251-MG cultures, including the two IL1 β treated cultures which had released p24 protein (Section 6.2.1i and Figure 6.1), despite an assay sensitivity of 2 integrated provirus copies per 10 000 cells.

To negate the possibility that inhibitors to the *Alu* PCR reaction may have been present in the chromosomal DNA extracts, chromosomal DNA from four of the U251-MG cultures, including the two IL1β treated cultures which had released p24 protein were spiked with 10, 4 or 2 copies of chromosomal integrated provirus (Figure 6.2C). All spiked samples tested positive by the *Alu* PCR, indicating that the former negative result was genuine. As a control, chromosomal DNA was also extracted from the cocultures (harvested 3 days after initiation of coculture (10 dpi)), and these samples tested positive (Figure 6.2C). This *Alu* PCR assay was confirmed to be specific for the integrated form of HIV-1, as integrated provirus standards and chromosomal DNA from the cocultures tested negative when the Alu164 primer (which binds to *Alu* repeat sequences in the human genome) was omitted from the first round of PCR (Figure 6.2C). This control was performed to exclude the possibility that amplification from the PBS primer alone (which can bind to both unintegrated and integrated forms of HIV-1 DNA) could give rise to detectable amplification of viral DNA in the second round of the PCR (Vandegraaff *et al*, 2001a). As expected, no amplification could be detected in the absence of the Alu164 primer (Figure 6.2C).

Figure 6.2 Analysis of HIV-1 integration in infected U251-MG astrocytes.

Chromosomal DNA was extracted from the infected U251-MG astrocytes at 28 hpi and at 7, 10, 13 and 16 dpi. Cultures had been treated ± IL1β from 7dpi onwards, as indicated above the lanes in each Southern hybridisation (**A**, **B**). HuT-78 cells were added to each of two cultures at 7 dpi to confirm the transmission of infection upon coculture with $CD4^+$ cells (Figure 6.1 and Table 6.1). These cocultures were harvested for chromosomal DNA extraction after 6 days of coculture (13 dpi).

To estimate the chromosomal DNA extraction efficiency, *β-globin* PCR (27 cycles) and Southern hybridisation was performed on diluted chromosomal DNA samples (**A**). Amplification of *β-globin* from the DNA samples was compared to HA8 cell number standards. This enabled determination of chromosomal DNA input required to deliver approximately 10 000 cells-worth of DNA into the *Alu* PCR (†) (with the exception of the 28 hpi samples). Each lane represents an individual infected U251-MG culture.

To determine the level of HIV-1 integration in these cultures, 10 000 cells-worth of chromosomal DNA from each infected U251-MG culture (* with the exception of the 28hpi samples, from which the input DNA represented 280 cells-worth of chromosomal DNA) was subjected to modified nested *Alu* PCR, followed by Southern hybridisation (**B**). Alu PCR amplifications of integrated HIV-1 DNA copy number (HA8) standards were also performed in the presence of 10 000 cells-worth of (uninfected) chromosomal DNA. An overexposed scan of the same hybridised membrane is also shown. Open symbols (△, O, ◊, □) indicate the chromosomal DNA samples which were spiked in (**C**). Samples △ and □ were selected for further analysis as these are the two DNA samples from the IL1β treated cultures which released p24 protein into the culture supernatant (Figure 6.1).

To verify the *Alu* PCR results shown in (**B**), several additional controls were performed. To confirm that amplification could only be due to the integrated form of HIV-1 DNA, the 250 integrated HIV-1 DNA copy number standard was also assayed with the omission of the *Alu* primer in the first round of the nested *Alu* PCR. Chromosomal DNA extracts from HuT-78 cocultures were also assayed (10 000 cells-worth of DNA from each of 2 cultures) with and without the omission of the Alu primer. A subset of infected U251-MG chromosomal DNA samples from (**B**; open symbols; △, O, ◊, □) were spiked with either 10 (**C**; respective black symbols; ▲, ●, ♦, ■), 4 (■) or 2 (■) copies of integrated HIV-1 DNA standard.

A.

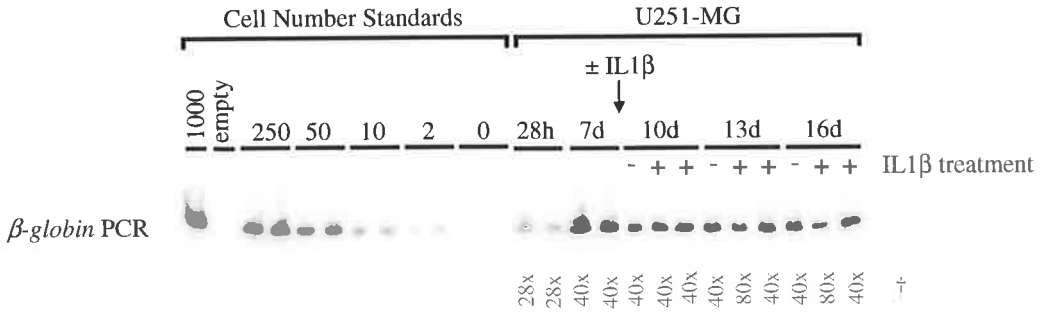

† Relative amount of input DNA for *Alu* PCR to represent approximately 10 000 cells, except 28h samples where the maximum input (of approximately 280 cells-worth of DNA) was used.

B.

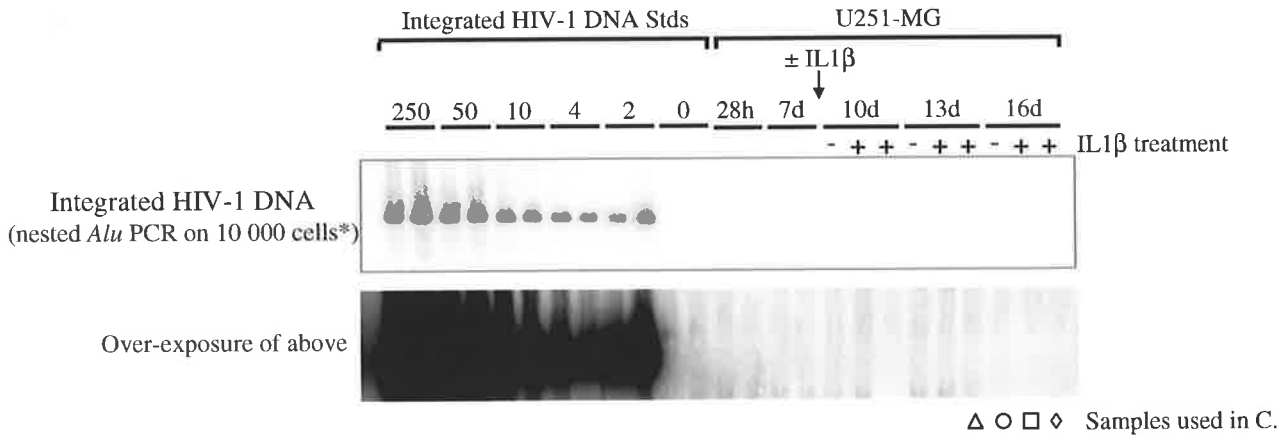

C.

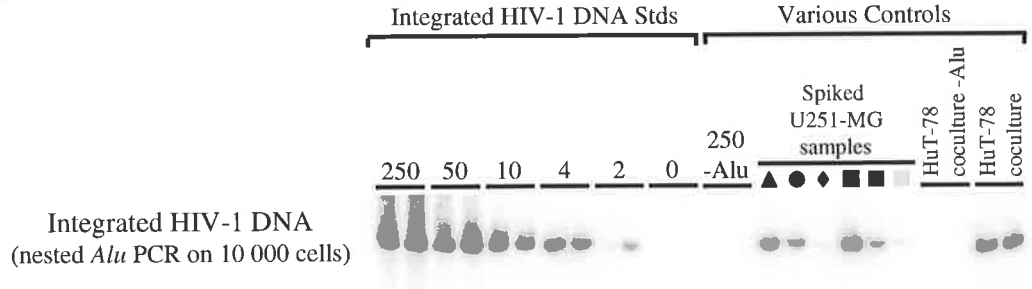

6.2.4 Consideration of the lack of detectable infectious virus release and integrated HIV-1 DNA in the IL1β-stimulated cultures which had released p24 protein.

The inability to detect integrated provirus in U251-MG astrocytes at 28 hpi (<2 copies of integrated provirus per 280 cells; Figure 6.2B) is consistent with the inability to detect the viral reverse transcription in these cells within the first 48 hpi (<2 copies / 2500 cells) (Chapter 5). That two of the infected astrocyte cultures released p24 protein upon IL1β stimulus (Figure 6.1), in the absence of detectable infectious virus release (Table 6.1) and the absence of viral integration (<2 copies / 10 000 cells) (Figure 6.2B) was unexpected. The failure to detect integrated provirus could be explained by virus replication in less than 0.02% of the cells, or the possibility that the cells which supported virus production may have died (with subsequent DNA degradation) by the time the cultures were harvested for extraction of chromosomal DNA. The latter hypothesis may be plausible for the culture in which the release of p24 protein peaked at 11 dpi and DNA was harvested at 16 dpi. In this scenario, the presence of a low level of supernatant p24 at 16 dpi may represent persistent p24 protein from earlier virus replication. This hypothesis, however, does not explain the inability to detect integrated DNA in the other IL1β treated culture, which released 91pg of p24 in the 24 hours prior to the harvest of the supernatant for infectivity assay and the DNA for integration assay (secreted p24 protein detected at 13 dpi and DNA and supernatants also harvested at 13 dpi). In this culture, the source of the p24 release may be from virus replication in less than 0.02% of the cells, and the amount of virus release at the time of sampling may have been below the infectious dose for HuT-78 cells in the presence of IL1β. It is also possible that the p24 production may have occurred without viral replication proceding to the formation and release of infectious virus particles, however *de novo* p24 synthesis would still require integration of the provirus.

An alternative but unlikely possibility is that the p24 protein released from IL1β treated culture may not necessarily have been produced by virus replication. p24 protein is present at high levels in the initial inoculum and the excess p24 protein is difficult to remove from astrocyte cells after inoculation (Chapter 5). Given the absence of detectable integrated provirus, p24 protein from the inoculum may be released from some intracellular or cell-associated store upon IL1β treatment. However the phenomenon of cell-associated p24

storage and subsequent release has not been documented previously. Although no cytotoxic effects of the IL1β treatment were observed by light microscopy or *β-globin* levels in the chromosomal DNA extractions, it could be postulated that IL1β treatment may result in the lysis of infected U251-MG cells, which may release cell-associated p24 protein, stored from the initial inoculum.

Despite the lack of detectable virus release in the IL1β treated cultures, infectious virus was transmitted upon coculture. IL1β treatment, therefore, may not necessarily be an adequate model for the "rescue" or "reactivation" of HIV-1 infection in astrocytes upon coculture. The ability of infected U251-MG astrocytes to transmit virus to susceptible cells upon coculture, without evidence of viral integration prior to coculture, indicates that virus replication is restricted in U251-MG cells prior to integration, until and unless the astrocytes are cocultured with $CD4^+$ cells. An additional possibility, although not previously described, is that the transmission of infection upon coculture may be due to low level persistence of the original virus inoculum. In this experiment, however, this is highly unlikely as the U251-MG astrocytes were treated with trypsin twice prior to initiation of the coculture (after inoculation and at 5 dpi), and trypsin reportedly inactivates and removes cell-bound HIV-1 (Cheng-Mayer *et al*, 1987; Levy and Rowe, 1971; Tang and Levy, 1991). Importantly it needs to be noted that as only two of the IL1β treated cultures gave a p24 release in this experiment, the intepretation is limited by the sample number of cultures in which coculture stimulus was simulated. To better understand the process of U251-MG infection with respect to virus replication and virus release, this experiment was repeated and analysed with more sensitive techniques, more cultures and more timepoints, for detection of virus integration and infectious virus release.

6.3 Detailed analysis of viral integration and the release of infectious virus during the course of U251-MG infection.

In this experiment, U251-MG astrocytes were inoculated with 0.01 $TCID_{50}$ U/cell (0.81 pg p24 protein / cell) DNase I treated HIV-1_{NL4-3} by spinoculation, with 7 post infection washes and a trypsin treatment. As in the previous experiment, the cells were subcultured with trypsin at 5 dpi into 3 times as many wells. At 7 dpi, the cultures were either untreated, cocultured with HuT-78 cells or stimulated with IL1β. In this experiment, in order to

analyse the release of infectious virus and viral integration in more detail, a greater number of cultures were assessed and assays with higher sensitivity were used for both the detection of infectious virus release and integrated HIV-1 DNA. The possibility that the presence of IL1β might affect either the release of infectious virus or the assay for the detection of infectious virus release was also addressed.

Because only one third of the IL1β treated cultures in the previous experiment subsequently gave a detectable release of viral p24 protein (Section 6.2.1 and Figure 6.1), the number of cultures treated with IL1β in this experiment was increased to 22, with the intention of obtaining a statistically significant number of cultures in which the phenomenon of "virus rescue" could be studied. Six cultures were left untreated as controls. To test the concern that the presence of IL1β might affect the release of infectious virus, or the susceptibility of HuT-78 cells to infection, 8 cocultures were performed; 4 in the presence and 4 in the absence of 10 U/ml IL1β. To further address this concern, the A3.01 T-cell line was used in addition to HuT-78 cells to test the infected U251-MG culture supernatants for the presence of infectious virus. A3.01 cells were chosen because they have been successfully used previously to test for infectious virus in supernatants from IL1β treated, transfected astrocyte cultures (Tornatore *et al*, 1991). Additionally, to increase the sensitivity of the assay for infectious virus in the U251-MG culture supernatants, the filtered supernatants were applied to the A3.01 and HuT-78 cells by spinoculation (Ho *et al*, 1993; Li and Burrell, 1992; Pietroboni *et al*, 1989) (Section 2.8).

Furthermore, to increase the probability of detecting infectious virus release, the culture supernatants were tested repeatedly for the presence of infectious virus. Cultures were tested daily for the release of infectious virus, starting 2 days after the addition of IL1β (9 dpi) (as previous reports, and observations in this thesis, indicated a delay of ≥48 hpi from the addition of IL1β until virus reactivation is detectable (Lawrence *et al*, 2004; Sabri *et al*, 1999; Tornatore *et al*, 1994b; Tornatore *et al*, 1991) (Figure 6.1)), until the culture was harvested for chromosomal DNA extraction and HIV-1 integration analysis.

To improve the sensitivity of detection of HIV-1 integration in the infected U251-MG cultures, a real-time PCR with a sensitivity of 2 copies of integrated HIV-1 DNA per 20 000 cells was used on chromosomal DNA extracts. Whilst this PCR, which targets the R-U5

region of the HIV-1 genome, is not specific for the integrated form of HIV-1 (as it would also detect the presence of circular and linear episomal HIV-1 DNA which may co-precipitate with the chromosomal DNA fraction (Barbosa *et al*, 1994; Pauza and Galindo, 1989; Stevenson *et al*, 1990; Vandegraaff *et al*, 2001a; Zanussi *et al*, 2000)), it was used because it is more economical, sensitive and rapid than the integrated provirus-specific *Alu* PCR. It was envisaged that any chromosomal DNA extracts which yeilded amplification of R-U5 HIV-1 DNA in the real-time PCR assay would then be subjected to the *Alu* PCR to determine whether the amplification was from unintegrated or integrated HIV-1 DNA. In addition, to better understand the nature of this astrocyte infection, RNA was also extracted from the same cultures, for subsequent analysis of various viral RNA species (Section 6.6).

6.3.1 Assaying astrocyte supernatants for the release of p24 protein.

p24 protein was readily detectable in the supernatants of the infected U251-MG cultures during the first few days of infection (Figure 6.3), as observed and discussed in Chapter 5. By 7 dpi, p24 protein was undetectable in all of the cultures, and remained undetectable in the untreated cultures for the duration of the experiment (16 days). Within 2 days of coculturing the infected astrocytes with HuT-78 cells syncytia formation was observed in the HuT-78 cell population, and within 3 days of coculture, p24 protein was detectable in the coculture supernatants, as expected, irrespective of the presence or absence of IL1β during the period of coculture (Figure 6.3). Surprisingly, only 1 of the 22 IL1β treated, infected U251-MG cultures released detectable levels of p24 protein into the supernatant (culture "u"). 47 pg/ml p24 protein was detected in the supernatant of this culture at 12 dpi (Figure 6.3). The lack of detectable p24 protein release from additional IL1β treated cultures was unexpected. This could be because a different HIV-1 virus stock was used in this experiment, compared to the previous experiment (Section 6.2), and / or because the multiplicity of infection was lower in this experiment.

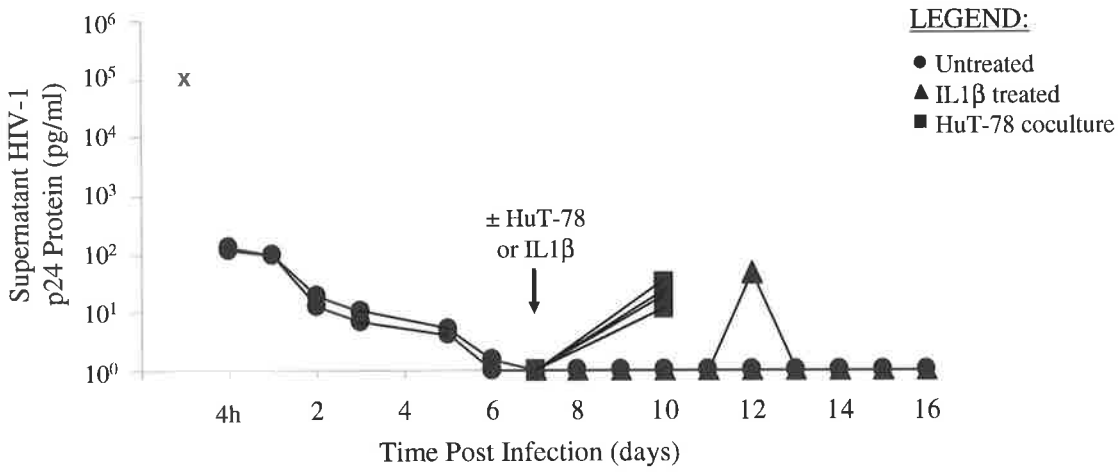

Figure 6.3 Supernatant p24 profile of the "rescue" of U251-MG astrocyte infection by CD4+ coculture and IL1β treatment (second, more detailed experiment).

U251-MG astrocyte cells were infected with HIV-1_{NL4-3} and the culture supernatants sampled for HIV-1 p24 content at designated times post infection. From 7dpi onwards the cultures were either i) untreated (●) (n=6), IL1β treated (▲) (n=22) or co-cultured with HuT-78 cells in the presence or absence of IL1β (■) (n=4). Taking into account the subculturing of the

U251-MG astrocytes at 5 dpi, the p24 content of the virus inoculum per culture was 161 ng.

Supernatants from the same cultures were tested for the presence of infectious virus (Table 6.2) and the cultures were harvested at either 10, 13 or 16 dpi for analysis of HIV-1 integrated DNA (Figure 6.4). The one IL1β treated culture which released p24 protein into the supernatant (supernatant p24 content of 47 pg/ml on 12 dpi, as shown in this Figure) is identified as Culture "u" in Table 6.2.

6.3.2 Assaying astrocyte supernatants for the presence of infectious virus.

6.3.2i Assaying for supernatant infectivity with A3.01 cells

Supernatants from the cocultures (±IL1β), as well as infectious virus stocks (positive controls) were infectious upon spinoculation of A3.01 cells, as expected. However, none of the supernatants from IL1β treated or untreated, infected U251-MG cultures were infectious to A3.01 cells, despite spinoculation, as no evidence of cytopathic effect was observed during 12 days of A3.01 culture.

6.3.2ii Assaying for supernatant infectivity with HuT-78 cells

Supernatants from some of the IL1β treated cultures were infectious upon spinoculation and passage in HuT-78 cells. Of the culture supernatants sampled at 9 and 10 dpi (cultures "a" – "n"), 79% (n=14) were infectious to HuT-78 cells (Table 6.2). Of the culture supernatants sampled daily from 11 to 13 dpi (cultures "h" – "v"), 40% (n=15) were infectious to HuT-78 cells. In this subset of cultures, two had supernatants which tested negative from 11 – 13 dpi despite testing positive on 9 dpi (supernatants from cultures "h" and "i"), suggesting the period of release of infectious virus may be transient. Over the 9 to 13 dpi period, the percentage of IL1β treated cultures which released infectious virus appeared to decline; from 79% (n=14) at 9 dpi to 13% (n=15) at 13 dpi. In some cultures, the release of detectable infectious virus into the culture supernant was sporadic. For example, released infectious virus was below detection on at least one of the days assayed in cultures "j", "k", "n" and "u", yet the presence of infectious virus was detected on at least one subsequent sampling. Infectious virus was not detectable in the supernatants from untreated infected U251-MG cultures (n=4), although these were only tested on 13 dpi, when the 87% (n=15) of IL1β treated cultures also tested negative. This indicated that more thorough testing of virus release from untreated, infected cultures was required in future experiments.

The detection of infectious virus in the IL1β treated U251-MG culture supernatants, in HuT-78 cells but not in A3.01 cells, suggested that HuT-78 cells may be more sensitive to infection and syncytia formation upon HIV-1_{NL4-3} inoculation than A3.01 cells. This was supported by the observation that, upon spinoculation of virus-containing coculture

dpi	Infectivity of supernatants from HIV-1 infected U251-MG astrocyte cells																												HuT-78 coculture							
	No IL1β						IL1β treated from 7dpi onwards																						No IL1β				IL1β			
	1	2	3	4	5	6	a	b	c	d	e	f	g	h	i	j	k	l	m	n	o	p	q	r	s	t	u	v	%+	1	2	3	4	1	2	3	4
9							-	+	+	+	+	+	+	+	+	+	+	-	-	+									**79**	+	+	+	+	+	+	+	+
10							-	+	+	-	+	+	+	-	-	-	-	-	-	-									**36**	+	+	+	+	+	+	+	+
11														-	-	-	+	-	-	-	-	+	-	-	-	-	-	+	**20**	+	+	+	+	+	+	+	+
12														-	-	+	+	-	-	+	-	-	-	-	-	-	+	-	**27**	+	+	+	+	+	+	+	+
13			-	-	-	-								-	-	-	+	-	-	+	-	-	-	-	-	-	-	-	**13**	+	+	+	+	+	+	+	+

Table 6.2 Analysis of infectious virus release from HIV-1 infected U251-MG astrocytes (second, more sensitive and detailed experiment).

U251-MG cells were infected with HIV-1_{NL4-3} and from 7 dpi onwards the cultures were either untreated (n=6), IL1β treated (n=22, labelled a – v) or cocultured with HuT-78 cells (n=4). Culture supernatants were sampled daily from 9 – 13 dpi, filtered and assayed for the presence of infectious virus by application to HuT-78 cells with spinoculation. The HuT-78 cultures were maintained for 12 days, and observed for evidence of infection (syncytia formation and supernatant p24 elevation). Uninfected and infected control HuT-78 cultures (inoculated with culture media or diluted virus stock in place of astrocyte supernatant, respectively) remained uninfected and become infected accordingly. As an internal positive control, the supernatants from astrocytes which had been cocultured with HuT-78 cells were also assayed for the presence of infectious virus. To assess whether the presence of IL1β in some astrocyte supernatants might impede infection of the HuT-78 cells, the infectivity of the latter supernatants was tested in the presence and absence of IL1β. Each column in the table represents an individual infected astrocyte culture, from which supernatants were sampled on consecutive days (rows). The percentage of IL1β treated culture supernatants which tested positive on each dpi assayed is indicated. Supernatants from the same cultures were also assayed for p24 protein (Figure 6.3), and the cultures were harvested at designated times for analysis of HIV-1 integration (Figure 6.4) and viral RNA species (Figures 6.8 and 6.9). The IL1β treated U251-MG culture "u" is the culture which released 47 pg/ml p24 protein into the supernatant on 12 dpi (Figure 6.3).

supernatants, or virus stock, a longer period of passage was required to detect syncytia in A3.01 cells compared to the same inoculation of HuT-78 cells. This is consistent with previous observations in our laboratory that HuT-78 cells are more sensitive to syncytia formation upon infection with HIV-1_{IIIB} than A3.01 cells (Dr Nick Vandegraaff, personal communication). These observations indicate that HuT-78 cells may be more sensitive to detecting minute amounts of infectious virus, and are thus better suited for detection of infectious virus release. The detection and amplification of infectious virus from IL1β treated U251-MG cultures in HuT-78 cells suggested the presence of IL1β did not adversely affect the susceptibility of HuT-78 cells to infection.

The inability to detect p24 protein in culture supernatants that were simultaneously shown to contain infectious virus is most likely due to the difference in sensitivity of the two methods with respect to virus release. The lower limit of p24 protein detection in the ELISA is 6 pg/ml, however it is possible that as little as one infectious particle, with an estimated p24 content of $2x10^{-7}$ pg (based on 200 capsid molecules / virion) (Arts *et al*, 1994; Davis and Rueckert, 1972)) may be detected in the infectivity assay. Even taking into account the fact that the majority (up to 99.9% or more (Layne *et al*, 1992)) of virus particles released from susceptible cells are non infectious, up to $3x10^7$ total virus particles / ml, with an estimated content of $\sim 3x10^4$ infectious particles, would be required for detection of 6 pg/ml p24 protein.

6.3.3 Assessment of HIV-1 integration.

The infected U251-MG cultures were harvested for chromosomal DNA extraction at 3½, 26, 54 hpi and 7 dpi (prior to ± IL1β treatment), and at 10, 13, 16 dpi (after ± IL1β treatment). The concentration of DNA in the chromosomal extracts was quantified according to the amplification of the *β-globin* gene (Figure 6.4A, B), and 20 000 cells-worth of chromosomal DNA tested for the presence of HIV-1 DNA by real-time PCR targeting the R-U5 region of the HIV-1 genome (Figure 6.4C).

With the exception of one of the two infected U251-MG cultures harvested at 3½ hpi, all of the chromosomal DNA samples from the infected U251-MG cultures were negative for the presence of HIV-1 DNA, to a sensitivity of 2 copies of HIV-1 DNA per 20 000 cells (Figure

Figure 6.4 Analysis of HIV-1 integration in infected U251-MG astrocytes
(second, more detailed and sensitive experiment)

Chromosomal DNA and total RNA was extracted from the infected U251-MG astrocytes at 3½, 26 and 54 hpi, and at 7, 10, 13 and 16 dpi. Cultures had been treated ± IL1β from 7 dpi onwards, as indicated. HuT-78 cells were added to each of four cultures ("HuT-78 cocultures") at 7 dpi to confirm the rescue of infection upon coculture with $CD4^+$ cells (Figure 6.3, Table 6.2), and harvested after 6 days of coculture (13 dpi).

To estimate the chromosomal DNA extraction efficiency, both conventional (**A**) and real time (**B**) *β-globin* PCRs were performed on diluted chromosomal DNA samples. Scanned ethidium bromide stained gels were used to approximate the chromosomal DNA content of the samples (26 cycles of PCR) (**A**). Each lane represents DNA extracted from an individual culture. Quantification of the DNA samples was achieved by real time PCR amplification compared to HA8 cell number standards (1000, 400, 80 and 16). All samples fell within the range of the standards (**B**), enabling accurate interpolation of the number of cells-worth of DNA in each sample. This quantification was used to determine the input of chromosomal DNA required to deliver approximately 20 000 cells-worth of DNA into the HIV-1 R-U5 real time PCR, with the exception of samples harvested prior to 10 dpi, where the maximum input was less than 20 000 cells-worth of DNA (see below).

To determine the level of HIV-1 integration occurring in these cultures, 20 000 cells-worth of chromosomal DNA (or 500, 700, 2700, 5700 cells-worth of chromosomal DNA from the samples harvested at 3½, 26 and 54 hpi and 7dpi, respectively) of chromosomal DNA from each infected U251-MG culture was subjected to real time HIV-1 R-U5 PCR (**C**). HIV-1 R-U5 PCR amplifications of integrated HIV-1 DNA copy number (HA8) standards were also performed in the presence of 20 000 cells-worth of (uninfected) chromosomal DNA. Each column in the graph represents an individual infected astrocyte culture.

(The analysis of viral RNA species in the same cultures is shown in Figures 6.8 and 6.9)

A.

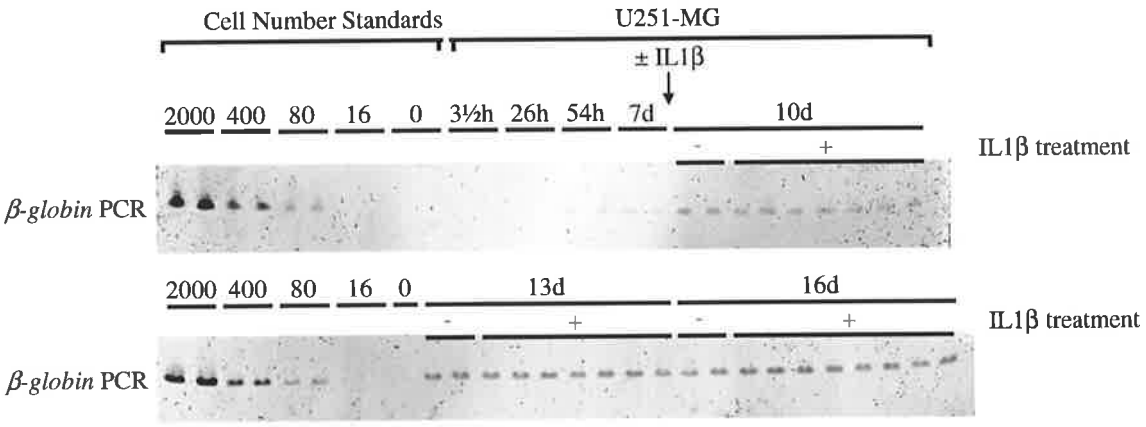
Cell Number Standards
U251-MG
± IL1β
2000 400 80 16 0 3½h 26h 54h 7d 10d
- +
IL1β treatment
β-globin PCR
2000 400 80 16 0 13d 16d
- + - +
IL1β treatment
β-globin PCR

B.

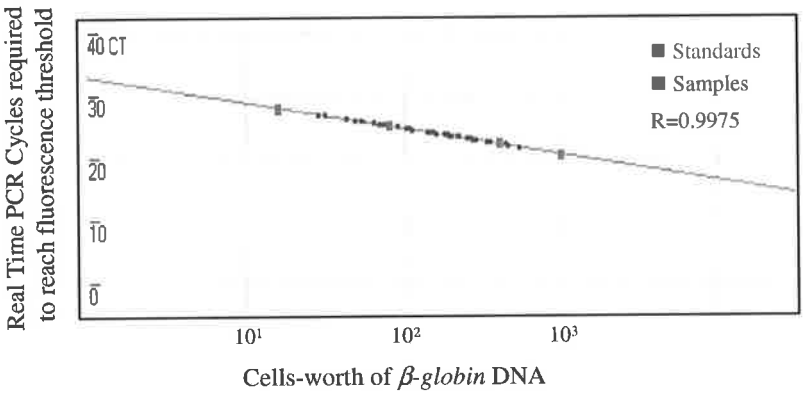
Real Time PCR Cycles required to reach fluorescence threshold
40 CT
30
20
10
0
Standards
Samples
R=0.9975
10¹
10²
10³
Cells-worth of β-globin DNA

C.

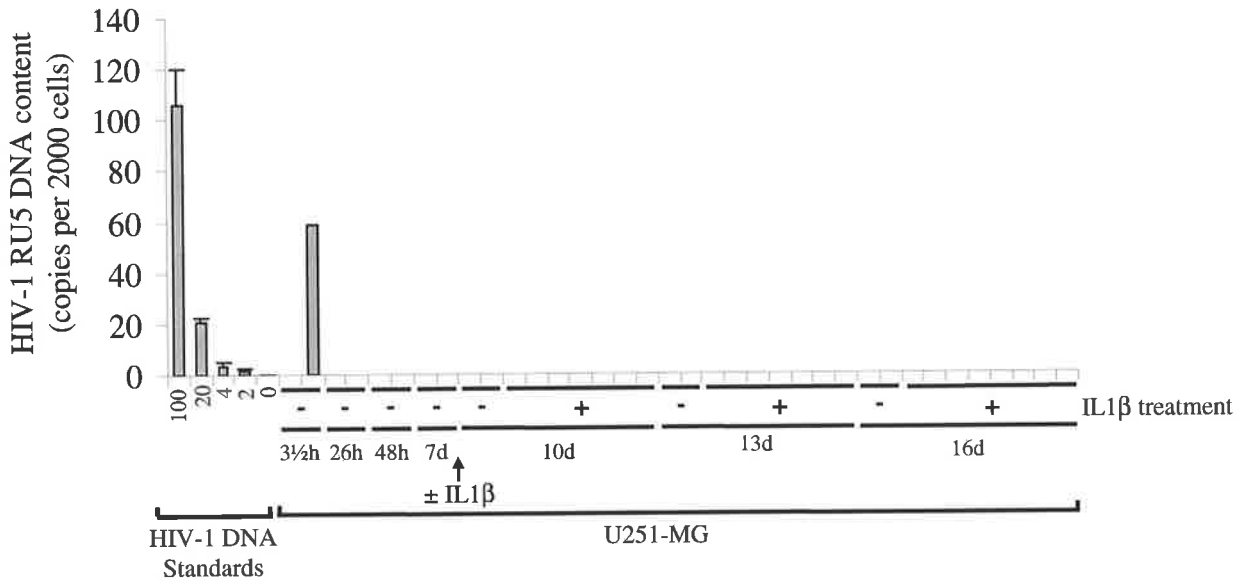
HIV-1 RU5 DNA content (copies per 2000 cells)
140
120
100
80
60
40
20
0
100
20
4
2
0
- - - - - + - + - +
IL1β treatment
3½h 26h 48h 7d 10d 13d 16d
± IL1β
HIV-1 DNA Standards
U251-MG

6.4C). The absence of HIV-1 DNA in the chromosomal fractions was observed irrespective of treatment of the cultures with IL1β, the detection of released infectious virus (Table 6.2), and the release of p24 protein (Figure 6.3). The detection of HIV-1 DNA in one of the cultures at 3½ hpi most likely represents input inoculum DNA, as extrachromosomal HIV-1 DNA was shown to be detectable as early as 3½ hpi in Chapter 5, and chromosomal DNA preparations isolated from HIV-1 infected cells invariably contain significant amounts of contaminating extrachromosomal HIV-1 DNA fraction (Barbosa *et al*, 1994; Pauza and Galindo, 1989; Stevenson *et al*, 1990; Vandegraaff *et al*, 2001a; Zanussi *et al*, 2000). The absence of detectable HIV-1 DNA in these cultures (at a sensitivity of 2 copies of HIV-1 DNA per 20 000 cells), including the 14 out of 22 (86%) IL1β treated cultures which released infectious virus into their supernatant (Table 6.2), indicates that either virus integration and replication is occurring at a level below detection, that is, in <0.01% of the cells, or that virus release is occuring without virus replication. To clarify these possibilities, and to ascertain whether these findings were unique to the U251-MG astrocyte cell line, or also pertained to other types of astrocytes, this experiment was repeated in U251-MG, CCF-STTG1 and U87-MG astrocytes (Section 6.4 below).

6.4 Detailed analysis of viral integration and the release of infectious virus during the course of U251-MG, CCF-STTG1 and U87-MG infection.

U251-MG, CCF-STTG1 and U87-MG astrocytes were infected with 1.58 pg p24 protein / cell of DNase I treated HIV-1_{NL4-3} by spinoculation as described in Section 6.3, and at 7 dpi the cultures were either untreated, cocultured with HuT-78 cells or stimulated with IL1β. The cultures were analysed for the presence of integrated virus, release of p24 protein, release of infectious virus, and the ability to transmit infection upon coculture, as described in Section 6.3.

6.4.1 Assaying astrocyte supernatants for the release of p24 protein.

p24 protein was readily detectable (approximately 40 to 95 pg/ml) in the supernatants of all three infected astrocyte cell lines during the first day of infection (Figure 6.5), as observed

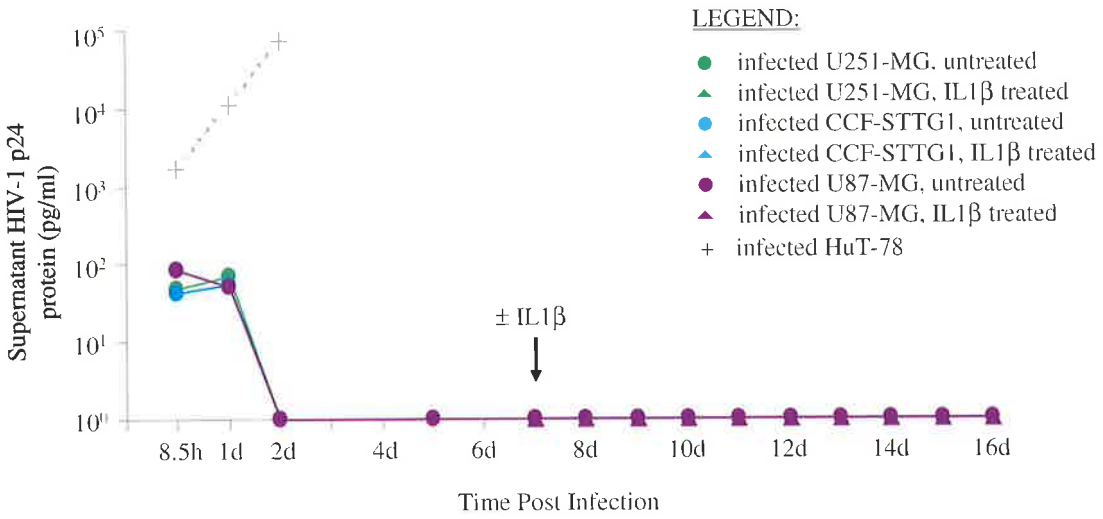

Figure 6.5 p24 profile of U251-MG, CCF-STTG1 and U87-MG infections for virus release and integration analysis.

Supernatant samples were collected from infected U251-MG, CCF-STTG1 and U87-MG astrocytes at 8½, 24 and 48 hpi, and at 5dpi and daily from 7dpi till 16dpi. Infected astrocyte cultures had been treated with (n=12 / cell line) or without (n=6 / cell line) IL1β from 7dpi onwards. Supernatant samples were collected from infected HuT-78 cells at 8.5, 24 and 48 hpi. The supernatants were tested for HIV-1 p24 protein content by ELISA.

Supernatants from the same cultures were tested for the presence of infectious virus (Table 6.3) and the cultures were harvested at either 10, 13 or 16 dpi for analysis of HIV-1 integrated DNA (Figure 6.7).

and discussed in Chapter 5. The infectivity of the virus stock used in this experiment was verified by infection of HuT-78 cells, which, upon infection with the same virus inoculum, produced approximately 80 ng/ml p24 by 48 hpi (Figure 6.5). By 2 dpi, p24 protein was undetectable in all of the astrocyte cultures, and remained undetectable in all astrocyte cultures for the duration of the experiment (16 days), irrespective of ±IL1β stimulation from 7 dpi onwards (for each of the three astrocyte cell lines there were 12 IL1β treated cultures, and 6 untreated cultures). As expected, within 4 days of coculturing the infected astrocytes with HuT-78 cells syncytia formation was observed in the HuT-78 cell population, and p24 protein was detectable in the coculture supernatants (results not shown).

6.4.2 Assaying astrocyte supernatants for the presence of infectious virus.

Filtered supernatants from the cocultures of the infected U251-MG, CCF-STTG1 and U87-MG astrocytes with HuT-78 cells were all shown to be infectious upon spinoculation of fresh HuT-78 cells, as expected. Supernatants from uninfected U251-MG, CCF-STTG1 and U87-MG astrocytes did not shown any cytopathic effect upon spinoculation and subsequent culture of HuT-78 cells.

In all three astrocyte cell lines, some of the filtered supernatants from both the untreated and the IL1β treated, infected astrocyte cultures were shown to contain infectious virus upon spinoculation of HuT-78 cells, at most of the time points assayed (Table 6.3A). For U251-MG astrocytes, 83% (n=6) of the untreated, infected cultures released detectable infectious virus into their supernatant on at least one of the days sampled (Tables 6.3A and 6.4). 92% (n=12) of the IL1β treated, infected U251-MG cultures released detectable infectious virus into their supernatant on *at least* one of the days sampled. For CCF-STTG1 astrocytes, all of the untreated, infected cultures released infectious virus on *at least* one of the days sampled (n=6), and 83% of the IL1β treated, infected cultures released infectious virus into their supernatant on *at least* one of the days sampled (Tables 6.3B and 6.4). All (n=18) of the infected U87-MG astrocyte cultures released detectable infectious virus into their supernatant on at least one of the days sampled, irrespective of IL1β treatement (Tables 6.3C and 6.4).

Table 6.3 Analysis of infectious virus release from HIV-1 infected U251-MG, CCF-STTG1 and U87-MG astrocytes

U251-MG, CCF-STTG1 and U87-MG astrocytes were infected with HIV-1_{NL4-3} and from 7 dpi onwards the cultures were either untreated (n=6 for each cell line), IL1β treated (n=12 for each cell line) or cocultured with HuT-78 cells (n=2 for each cell line). Culture supernatants were sampled daily from 9 – 16 dpi, filtered and assayed for the presence of infectious virus by spinoculation and passage in HuT-78 cells. The HuT-78 cultures were maintained for 12 days, and observed for evidence of infection (syncytia formation and supernatant p24 elevation). Positive and negative controls for infectious virus gave rise to infection or no infection in control HuT-78 cultures, respectively. Each column in each table represents an individual infected astrocyte culture, from which supernatants were sampled on consecutive days (rows). The percentage of untreated, IL1β treated and total culture supernatants which tested positive on each dpi assayed is indicated. Supernatants from the same cultures were also assayed for p24 protein (Figure 6.5), and the cultures were harvested at designated times for analysis of HIV-1 integration (Figure 6.7). Symbols △, ○, □ and ◊ indicate particular cultures referred to in Figure 6.7.

A.

dpi	Infectivity of supernatants from HIV-1 infected U251-MG astrocytes																			Total % +
	No IL1β						%+	IL1β treated from 7 dpi onwards												%+	
8	-	+	-	+	+	+	67	-	-	+	+	+	-	-	-	+	-	-	+	42	50
9	-	-	-	-	-	+	17	+	-	+	-	-	-	+	-	+	-	+	-	42	33
10	+	-	-	-	-	+	33	-	-	-	-	-	+	+	-	+	-	+	-	33	33
11			-	-	+	-	25					-	-	-	+	+	+	-	+	50	42
12			-	+	-	-	25					-	-	+	-	+	-	-	-	25	25
13			-	-	-	-	0					-	+	-	-	-	+	-	-	25	17
14					+	-	50									+	+	-	-	50	50
15					-	+	50									+	-	+	-	50	50
16					-	+	50									-	-	-	-	0	17

○ △ □ ◊

B.

dpi	Infectivity of supernatants from HIV-1 infected CCF-STTG1 astrocytes																			Total % +
	No IL1β						%+	IL1β treated from 7 dpi onwards												%+	
8	+	+	+	-	+	+	83	+	+	-	-	-	+	-	+	-	-	-	-	33	50
9	-	-	+	-	+	-	33	-	+	-	-	+	+	-	-	+	-	-	-	33	33
10	-	+	-	-	-	-	17	-	+	-	+	-	+	+	+	-	+	-	-	50	39
11			-	-	-	-	0					-	-	-	+	-	-	-	-	13	8
12			-	+	-	-	25					-	+	-	-	-	-	-	-	13	17
13			-	+	+	-	50					-	-	-	-	-	-	-	-	0	17
14					-	-	0									-	-	-	-	0	0
15					-	-	0									-	-	-	-	0	0
16					-	-	0									-	-	-	-	0	0

△ ○ □ ◊

C.

dpi	Infectivity of supernatants from HIV-1 infected U87-MG astrocytes																			Total % +
	No IL1β						%+	IL1β treated from 7 dpi onwards												%+	
8	+	+	+	-	+	+	83	+	+	+	+	+	-	+	-	+	+	+	+	83	83
9	+	+	+	-	-	+	67	+	+	+	+	+	+	+	-	+	-	+	+	83	78
10	-	-	+	+	+	+	67	+	+	+	+	+	+	+	+	+	-	+	+	92	83
11			+	+	+	+	100					+	-	+	-	+	-	+	+	63	75
12			+	+	+	+	100					+	+	+	+	-	-	+	+	75	83
13			+	+	+	+	100					-	+	+	+	-	-	+	+	20	75
14					+	-	50									+	+	+	-	75	67
15					+	-	50									+	+	+	-	75	67
16					+	-	50									-	-	+	+	50	50

△... ○ □ ◊

Infected astrocyte cell line	Cultures which released infectious virus			Cultures with chromosomal-associated HIV-1 DNA
	Untreated	IL1β treated	Total	
U251-MG (Table 6.3A)	83% (5/6)	92% (11/12)	89% (16/18)	0% (0/20)
U251-MG (Table 6.2)	(not tested)	64% (14/22)	64% (14/22)	0% (0/30)
CCF-STTG1 (Table 6.3B)	100% (6/6)	83% (10/12)	89% (16/18)	0% (0/20)
U87-MG (Table 6.3C)	100% (6/6)	100% (12/12)	100% (18/18)	0% (0/20)

Table 6.4 Summary of infectious virus release and proviral integration data from HIV-1 infected U251-MG, CCF-STTG1 and U87-MG astrocyte cultures

Infected astrocytes were cultured in the presence or absence of IL1β from 7 dpi onwards. Culture supernatants were sampled daily from 8 to 16 dpi, filtered, and applied to HuT-78 cells by spinoculation. The Hut-78 cultures were monitored for evidence of HIV-1 infection (by syncytia formation and p24 secretion) over 10 subsequent days. HuT-78 controls mock-inoculated with culture media or supernatant from uninfected astrocytes showed no evidence of infection. The percentage of cultures whose supernatant was infectious to HuT-78 cells (on at least one of the days sampled) is shown. The number of cultures whose samples tested positive, as a function of the total number tested, is indicated in brackets.

Chromosomal extracts from the same cultures, as well as cultures harvested prior to supernatant infectivity testing (≤7 dpi), were tested for HIV-1 DNA by R-U5 Real Time PCR. This table summarises the data in Figure 6.7 by showing the percentage of positive tests and number of positive tests as a function of the total number of cultures analysed.

The release of detectable infectious virus from a given culture into the supernatant varied across consecutive days of sampling (Table 6.3). This phenomenon was observed in all three astrocyte cell lines, and had also been observed in the previous U251-MG experiment (Section 6.3.2 and Table 6.2). The inconsistent release of infectious virus from the majority of cultures suggested that the release of infectious virus might be sporadic. Alternatively, the level of infectious virus present in the astrocyte culture supernatants may have bordered on the sensitivity of detection in the HuT-78 cells, and thus the seemingly sporadic detection of the release of infectious virus may be an artifact of the limit of sensitivity of the assay.

The thorough testing of supernatants from untreated, infected astrocytes in this experiment revealed that the release of infectious virus from the cultures occurred independently of the treatment with IL1β. This was unexpected, as p24 protein release (used as an indicator of infectious virus release) from astrocytes in the restricted phase of infection has been reported to require coculture, IL1β, or TNFα stimulus (Brack-Werner *et al*, 1992; Cheng-Mayer *et al*, 1987; Chiodi *et al*, 1987; Di Rienzo *et al*, 1998; Lawrence *et al*, 2004; Sabri *et al*, 1999; Tornatore *et al*, 1994b; Tornatore *et al*, 1991). However, release of infectious virus from infected astrocytes has not been previously measured with the heightened sensitivity of applying filtered supernatants to susceptible reporter cells by centrifugal inoculation. This method of inoculation has been reported to enhance the effective multiplicity of infection of HIV-1 by ten-fold (Ho *et al*, 1993; Li and Burrell, 1992; Pietroboni *et al*, 1989) (Sections 2.3.5ii and 2.8). Furthermore, while p24 protein release has been previously detected upon IL1β and TNFα stimulation of both infected and transfected astrocytes (Lawrence *et al*, 2004; Sabri *et al*, 1999; Tornatore *et al*, 1994b; Tornatore *et al*, 1991), measurement of infectious virus release has only been previously reported upon IL1β treatment of *transfected* astrocytes (Tornatore *et al*, 1991). In this experiment, secretion of p24 protein was not detected in any of the IL1β treated, infected astrocyte cultures (n=12 for each astrocyte cell line), nor any of the untreated infected cultures (n=6 for each astrocyte cell line), despite an assay sensitivity of 6 pg/ml p24 protein (Figure 6.5). The detection of infectious virus but not p24 protein in the majority of culture supernatants may reflect the superior sensitivity of the assay for infectious virus, as explained in Section 6.3.2ii.

The previous U251-MG experiment observed a declining trend in the number of cultures that released infectious virus over time (Section 6.3.2, Table 6.2). In this experiment, this

trend was not apparent in the U251-MG astrocyte cultures (Table 6.3A), however it was apparent in CCF-STTG1 astrocyte cultures (Table 6.3B). The proportion of infected CCF-STTG1 cultures which released infectious virus declined with time post infection, from 50% at 8dpi to 17% by 13 dpi, and was undetectable in the supernatants of both untreated and IL1β stimulated, infected CCF-STTG1 cultures from 14 dpi onwards. The proportion of infected U87-MG cultures which released infectious virus showed a modest decline with time post infection, from 83% at 8dpi to 67% at 14dpi, although infectious virus was still detectable in the supernatants of 50% (n=6) of the cultures at 16 dpi (Table 6.3C). Indeed, the proportion of U87-MG cultures, both with and without IL1β stimulation, which released infectious virus was higher than U251-MG and CCF-STTG1 cultures across all time points tested.

6.4.3 Assessment of HIV-1 integration.

The infected U251-MG, CCF-STTG1 and U87-MG cultures were harvested for chromosomal DNA extraction at 7 dpi (prior to IL1β treatment, n= 2 for each cell line), and at 10, 13, 16 dpi (untreated, n=2 for each cell line at each time point, IL1β treated; n=4 for each cell line at each time point). The concentration of DNA in the chromosomal extracts was quantified according to the amplification of the *β-globin* gene (Figure 6.6), and 20 000 cells-worth of chromosomal DNA tested for the presence of HIV-1 DNA by real time PCR targeting the R-U5 region of the viral DNA genome (Figure 6.7).

All of the chromosomal DNA samples from the three infected astrocyte cell lines were negative for the presence of HIV-1 DNA (n=20 for each cell line), to a sensitivity of 2 copies of HIV-1 DNA per 20 000 cells-worth of chromosomal DNA (Figure 6.7). The absence of HIV-1 DNA in the chromosomal fractions was observed irrespective of the detection of released infectious virus on at least one sampling in 89% of U251-MG cultures, 89% of CCF-STTG1 cultures, and 100% of U87-MG cultures (n=18 for each cell line, Section 6.4.2 and Tables 6.3 and 6.4). To negate the possibility that inhibitors to the R-U5 real time PCR reaction may have been present in the chromosomal extracts, chromosomal DNA from the infected astrocyte cultures which had repeatedly demonstrated release of infectious virus (n=4 for each astrocyte cell line; the cultures indicated by the symbols △, ○, □ and ◊ in Table 6.3 and Figure 6.7C (open symbols; unspiked samples)) were spiked with

Figure 6.6 Determination of the concentration of chromosomal DNA from HIV-1 infected U251-MG, CCF-STTG1 and U87-MG astrocytes.

Chromosomal DNA was extracted from the infected U251-MG, CCF-STTG1 and U87-MG astrocytes at 7, 10, 13 and 16 dpi. Cultures had been treated ± IL1β from 7dpi onwards. HuT-78 cells were added to each of four cultures ("HuT-78 cocultures") at 7 dpi to confirm rescue of infection upon coculture with $CD4^+$ cells, and harvested after 6 days of coculture (13 dpi).

To estimate the chromosomal DNA extraction efficiency real time *β-globin* PCRs were performed on diluted chromosomal DNA samples. The fluorescence emission curves of the HA8 cell-number standards from the real time PCR reactions used to quantitate the concentration of the U251-MG, CCF-STTG1 and U87-MG chromosomal DNA samples (**A, C**). All samples fell within the range of the standards enabling accurate interpolation of the concentration of cellular DNA in each sample (**B, D**). This quantification was used to determine the input of chromosomal DNA required to deliver approximately 20 000 cells-worth of DNA into the HIV-1 R-U5 real time PCR (Figure 6.7).

A.

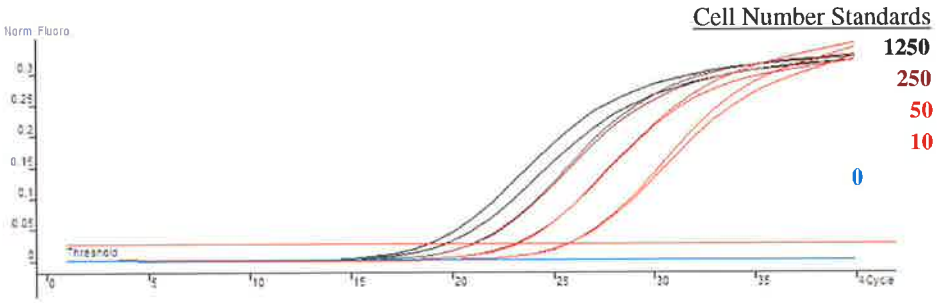
Cell Number Standards
1250
250
50
10
0
Norm. Fluoro
Threshold
Cycle

B.

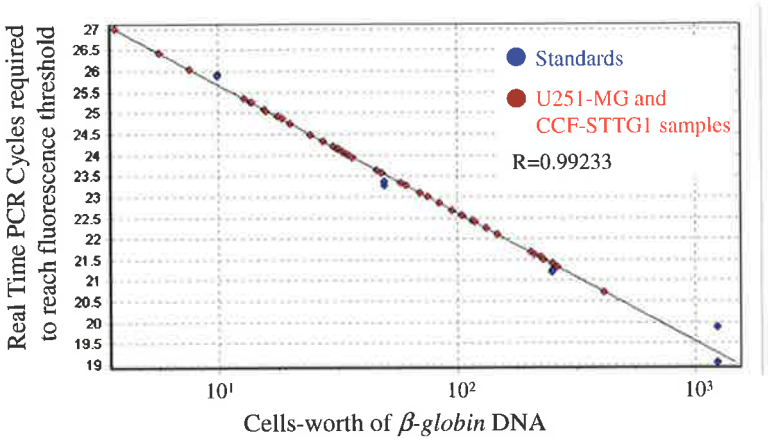
Real Time PCR Cycles required to reach fluorescence threshold
Standards
U251-MG and CCF-STTG1 samples
R=0.99233
Cells-worth of β-globin DNA

C.

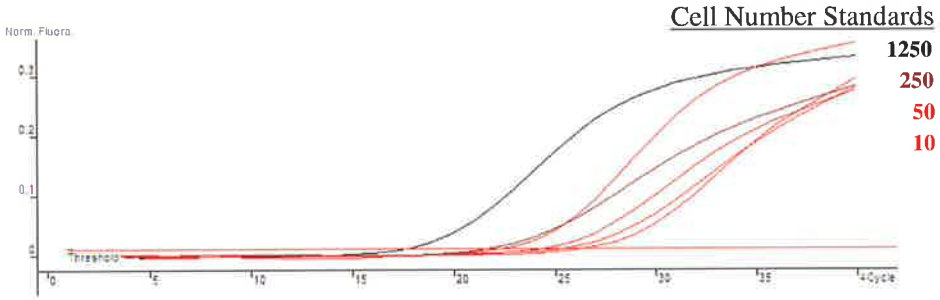
Cell Number Standards
1250
250
50
10
Norm. Fluoro
Threshold
Cycle

D.

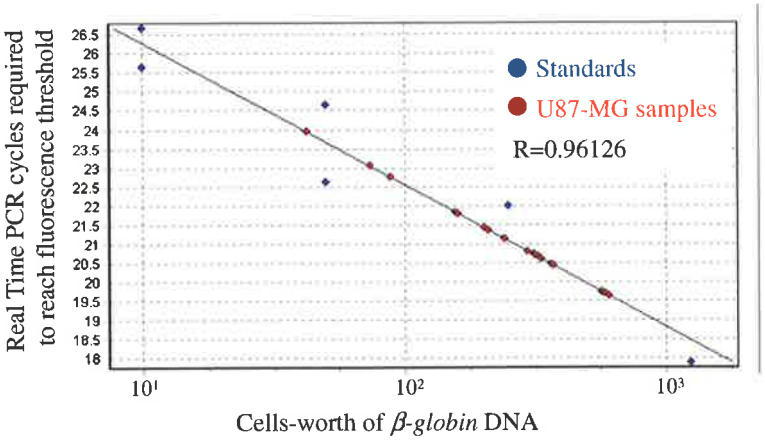
Real Time PCR cycles required to reach fluorescence threshold
Standards
U87-MG samples
R=0.96126
Cells-worth of β-globin DNA

Figure 6.7 Analysis of HIV-1 integration in infected U251-MG, CCF-STTG1 and U87-MG astrocytes

To determine the level of HIV-1 integration occurring in HIV-1 infected U251-MG (**A**), CCF-STTG1 (**B**) and U87-MG (**C**) astrocytes, chromosomal DNA was extracted from the infected cultures at 7, 10, 13 and 16 dpi. Cultures had been treated ± IL1β from 7 dpi onwards, as indicated, and the rescue of infection upon coculture with $CD4^+$ cells was confirmed upon the addition of HuT-78 cells to two of the infected U251-MG cultures at 7 dpi. To couple the integration data with assessment of the release of infectious virus, supernatants from the infected U251-MG, CCF-STTG1 and U87-MG cultures were assayed from 7 - 16 dpi for the release of infectious virus (Table 6.3).

To assess HIV-1 integration in these cultures, 20 000 cells-worth of chromosomal DNA (according to the *β-globin* DNA content, Figure 6.6) was subjected to real time PCR for HIV-1 R-U5 (**Ai**, **Bi** and **Ci**). HIV-1 R-U5 PCR amplifications of integrated HIV-1 DNA copy number (HA8) standards were also performed in the presence of 20 000 cells-worth of (uninfected) chromosomal DNA. The RU5 real time PCR fluorescence emission curves used to quantify the number of HIV-1 copies in the standards and samples is shown (**Ai**, **Aii**, **Bi**, **Bii**, **Ci** and **Cii**).

To verify the lack of HIV-1 R-U5 PCR amplification in the U251-MG, CCF-STTG1 and U87-MG cultures shown in **Ai**, **Bi** and **Ci**, 20 000 cells-worth of chromosomal DNA from each of four samples per cell line (selected samples indicated by the open symbols △, O, ◊ and □) were spiked with 4 copies of integrated HIV-1 DNA (HA8) standards, and subjected to HIV-1 R-U5 real time PCR (**Aii**, **Bii** and **Cii**). For each cell line, the four DNA samples to be spiked were selected from both ± IL1β treated cultures and represented cultures which had repeatedly released infectious virus into their supernatants (Table 6.3).

The determined copies of HIV-1 DNA in the standards, samples and spiked samples is presented graphically for each cell line (**Aiii**, **Biii** and **Ciii**). Each column represents an individual infected astrocyte culture. Treatment of each culture with or without IL1β is indicated below the graph. Spiked samples are indicated with respective black symbols: ▲, ●, ♦, ■.

A. U251-MG Astrocytes

i.

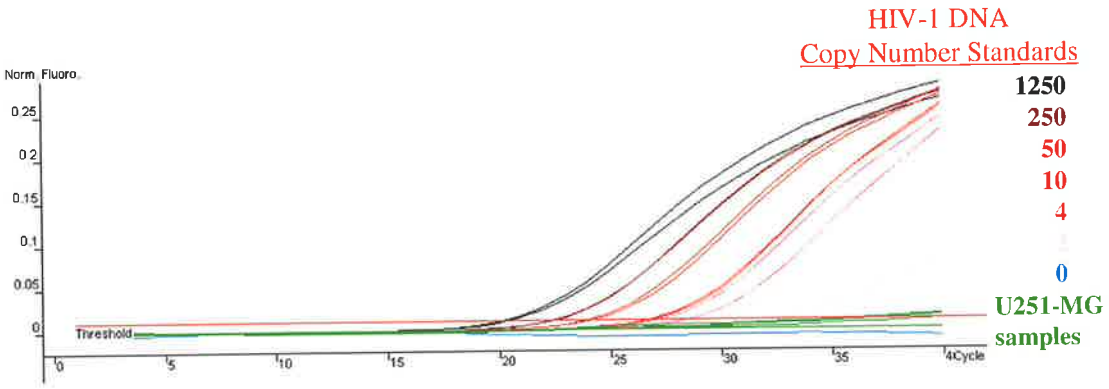

ii.

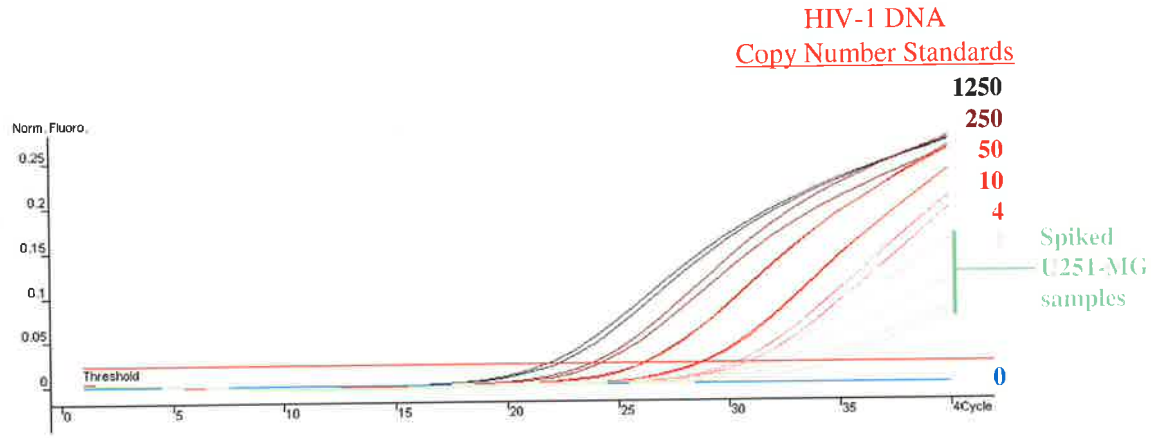

iii.

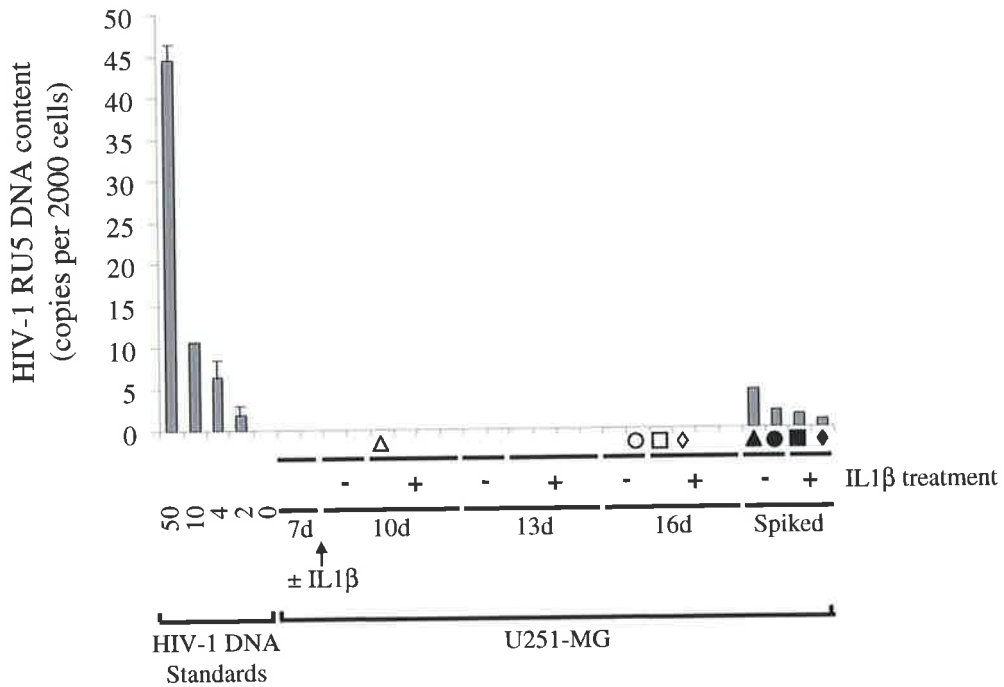

B. CCF-STTG1 Astrocytes

i.

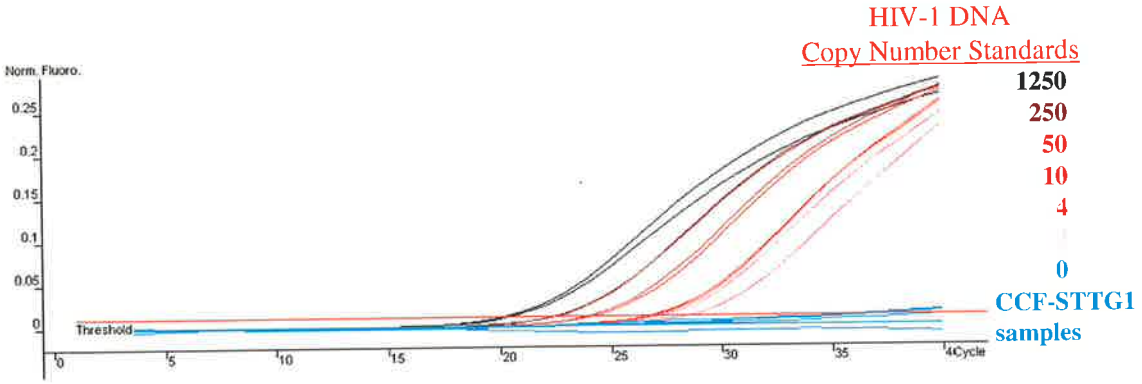

ii.

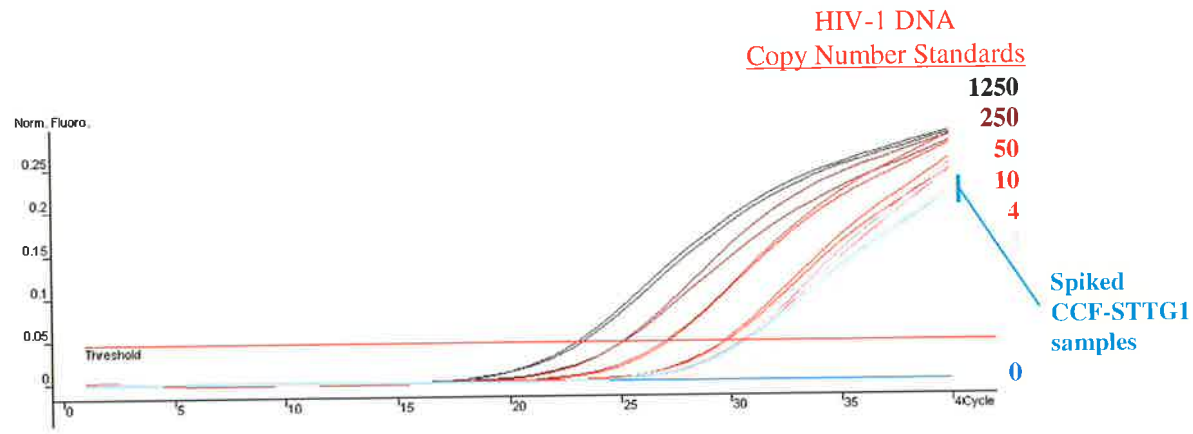

iii.

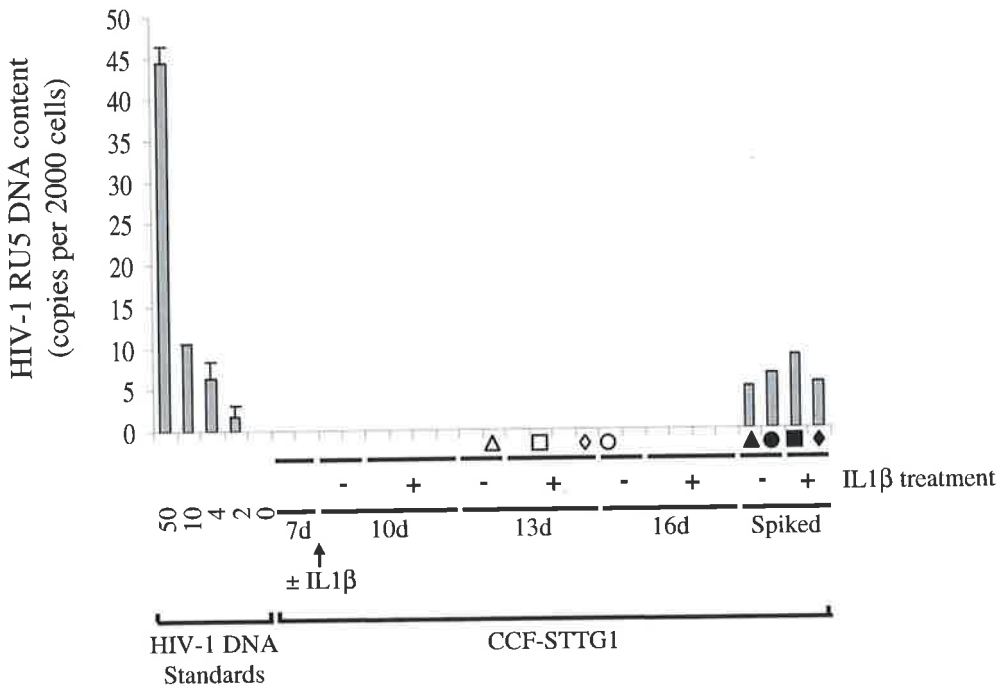

C. U87-MG Astrocytes

i.

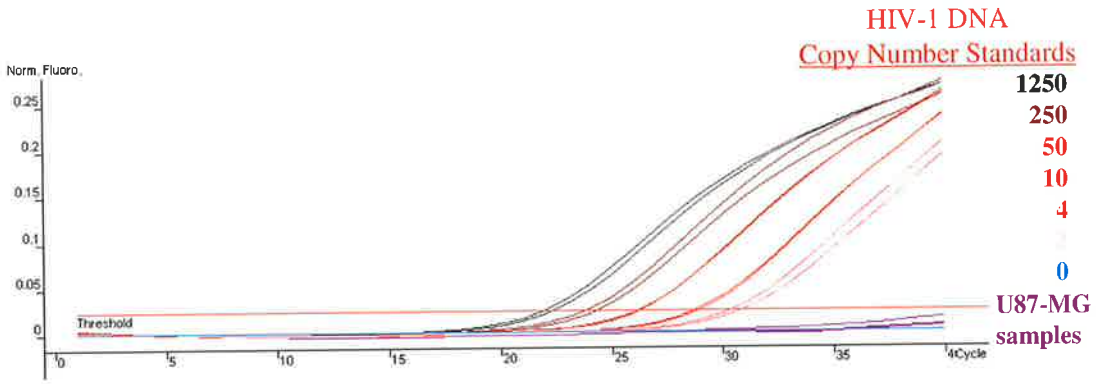

ii.

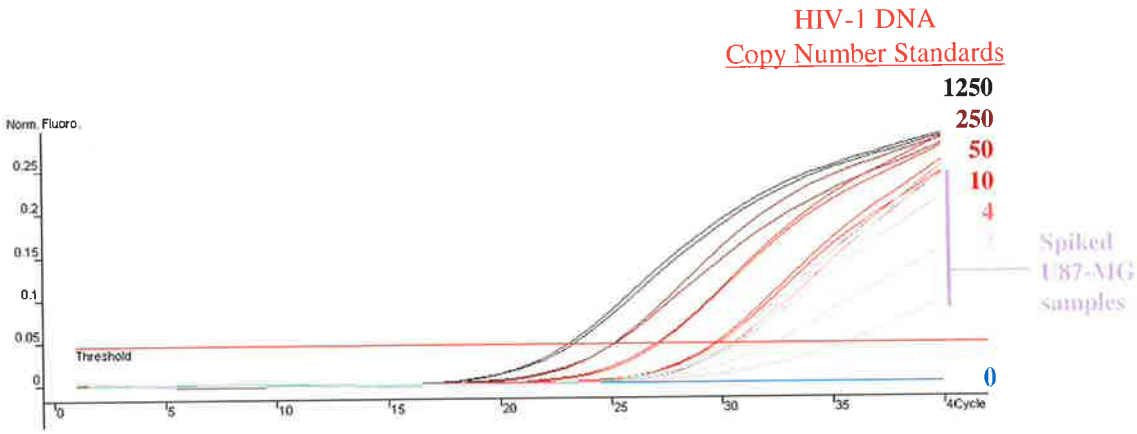

iii.

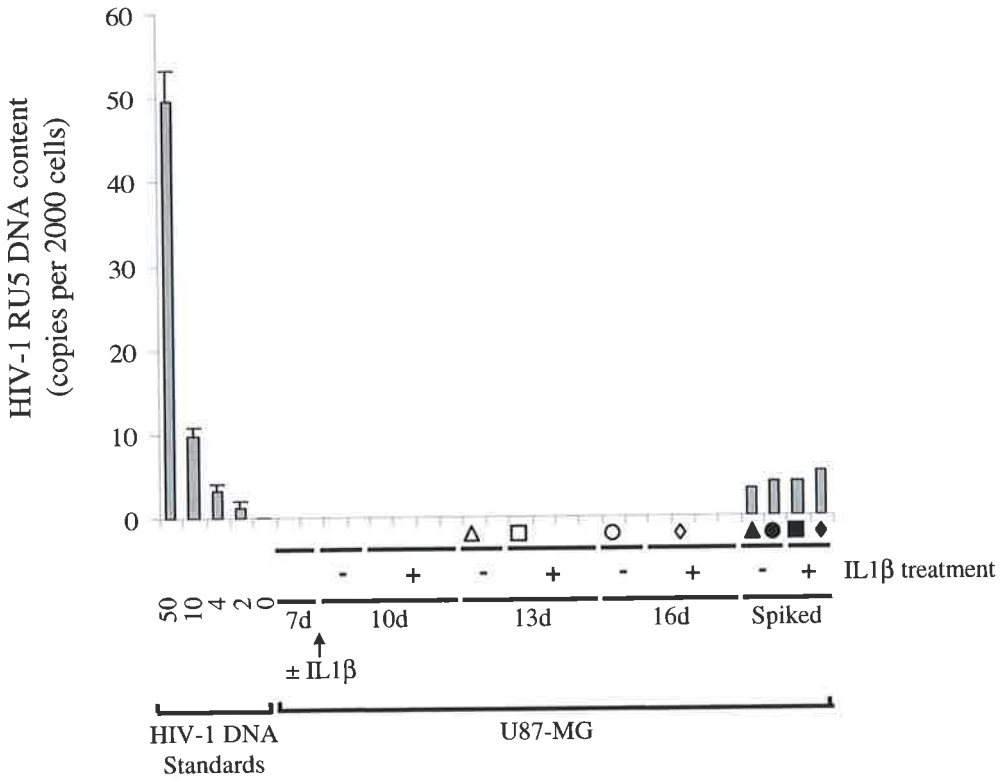

4 copies of integrated HIV-1 DNA (HA8) standard (identified by the respective black symbols; ▲, ●, ■ and ♦). All spiked samples tested positive by the R-U5 PCR (Figure 6.7C), as did chromosomal DNA from infected HuT-78 cells and cocultures of HuT-78 cells with infected astrocytes (results not shown). The absence of detectable HIV-1 DNA in cultures which released infectious virus into their supernatant indicates that either virus integration and replication is occurring at a level below detection (in <0.01% of the cells) or that virus release is occuring without virus replication.

6.5 Discussion of the lack of viral integration in the context of release of infectious virus.

6.5.1 Characteristics of the observed infectious virus release

The study of HIV-1_{NL4-3} infected U251-MG, CCF-STTG1 and U87-MG cultures in this chapter revealed the release of infectious virus in the absence of detectable proviral integration. Notably, the amount of infectious virus which was released from the cultures was very low, as spinoculation and up to 8 days of passage was required for amplification of the virus to be detectable in the HuT-78 reporter cells (by syncytia formation). A second consistent feature of this infectious virus release was that it appeared to occur sporadically from any given culture. The sporadic detection of the infectious virus release could be due to actual sporadic, random release of infectious virus, or it could be artifactual, as the amount of infectious virus in the supernatants may have bordered on the tissue culture infectious dose for spinoculation of HuT-78 cells, in which case detection may represent a chance event depending on the time of sampling and the probability of HuT-78 infection. Thirdly, in each cell line, the release of infectious virus was independent of IL1β treatment. Fourthly, the release of infectious virus did not appear to correlate with the release of detectable p24 protein and, in all but one culture (U251-MG culture "u"; Section 6.3.1, Figure 6.3, Table 6.2), the supernatant level of p24 protein was below 6 pg/ml. This is most likely due to the differential sensitivity of the two assays (discussed in Section 6.3.2ii). The three astrocyte cell lines appeared to display slightly different virus release kinetics, with release of infectious virus occurring less frequently from CCF-STTG1 cultures, and more

frequently from infected U87-MG cultures, compared to infected U251-MG cultures (Tables 6.2 and 6.3).

6.5.2 Hypotheses concerning the release of infectious virus in the absence of detectable provirus integration

The remarkable inability to detect integrated provirus in any of the 50 infected U251-MG cultures, 20 infected CCF-STTG1 cultures, or 20 infected U87-MG cultures, despite detection of released infectious virus in the majority of cultures tested (of the 40 U251-MG cultures tested for supernatant infectivity 30 were positive, of the 18 CCF-STTG1 cultures tested for supernatant infectivity 16 were positive, and of the 18 U87-MG cultures were also tested for supernatant infectivity 18 were positive) (Table 6.4), indicated that either i) virus replication occurred in less than 0.01% of the cells, or, ii) virus replication did not occur. These two possibilities are discussed below.

6.5.2i Possibility A: Viral replication in less than 0.01% of cells

The possibility that virus replication occurred in less than 0.01% of the cells in the astrocyte cultures cannot be completely excluded. However the inability to detect integrated virus, to a sensitivity of 2 copies / 20 000 cells, in a total of 64 astrocyte cultures (the sum of U251-MG, CCF-STTG1 and U87-MG cultures) in which release of infectious virus was detected suggests that, according to probability, the frequency of proviral integration was much lower than 0.01% of cells. It is also noteworthy that not all integration events lead to production of infectious virus (Section 1.1.6iii). In addition, the R-U5 real time PCR assay used to detect HIV-1 DNA in chromosomal DNA extracts would also detect episomal forms of HIV-1 DNA, including strong-stop HIV-1 DNA (the first species of HIV-1 DNA synthesised during reverse transcription) and all subsequent forms of HIV-1 DNA reverse transcribed in the cytoplasm, as well as linear, 1-LTR and 2-LTR circular forms which may accumulate in the nucleus. Whilst all of these forms are extrachromosomal, the Hirt method of separating extrachromosomal DNA from chromosomal DNA is only >80% effective (Vandegraaff *et al*, 2001a), as such chromosomal preparations of cellular DNA are invariably contaminated with a degree of extrachromosomal DNA (Barbosa *et al*, 1994; Pauza and Galindo, 1989; Stevenson *et al*, 1990; Vandegraaff *et al*, 2001a; Zanussi *et al*, 2000). (The amount of

extrachromosomal contamination of the astrocyte chromosomal extracts was not determined). Despite the potential for additional forms of HIV-1 DNA to be amplified as well as integrated provirus, R-U5 HIV-1 DNA could not be amplified from any of the astrocyte cultures.

6.5.2ii Possibility B: No viral replication

Given the very low probability that infectious virus release may have resulted from virus replication, the possibility of virus release without viral replication was considered. This concept, termed "*trans*-infection", has been demonstrated for CXCR4-coreceptor using strains of HIV-1 in dendritic cells, which are a specialised antigen presenting cell (Turville *et al*, 2003; Turville *et al*, 2004), and in certain epithelial cells, which are specialised in the cross-cell transport mechanism termed "transcytosis" (Bomsel, 1997; Hocini *et al*, 2001; Hocini and Bomsel, 1999). The possibility that astrocytes may transmit infectious virus without viral replication has not been previously described. Virus transmission without replication implies that infectious virus from the original virus inoculum has persisted, retained infectivity, and been subsequently released into the culture supernatant. Hypothetically, there are two possible scenarios for transmission of the original inoculum; a) preservation and persistence of infectious virus from the initial inoculum on the astrocyte cell surface, and b) internalisation and preservation of infectious virus from the initial inoculum with subsequent release into the extracellular milieu.

a) Persistence of virus inoculum on the cell surface.

The preservation and persistence of virus inoculum on the surface of cells for ≥7 days has not been previously described, and is unlikely because the cells were washed 7 times immediately after the centrifugally enhanced infection protocol and, after two of the PBS washes, the cells were also treated with 0.05% (v/v) trypsin for 3 minutes at room temperature. Trypin has been reported to inactivate retroviruses, including HIV-1, and remove cell-bound HIV-1 (Cheng-Mayer *et al*, 1987; Levy and Rowe, 1971; Tang and Levy, 1991). In addition, the cultures were split and re-seeded into 3 times as many wells by exposure to 0.1% (v/v) trypsin for 3 to 5 minutes at 37°C or until all the cells were detached. Trypsin treatment is thought to inactivate any persistent, surface bound HIV-1. However it

would be quite difficult to demonstrate the complete absence of any surface bound HIV-1 after trypsin exposure and to prove that the antiviral effect of trypsin treatment is absolute. Given that the amount of virus which is released from the astrocyte cultures from 8 to 16 dpi is minute, the persistence of a small amount of infectious virus despite trypsin treatment (although unlikely) cannot be definitively excluded.

b) Intracellular persistence of the original virus inoculum.

Internalisation of HIV-1 into intracellular compartments may protect the virus from physiological and enzymatic stresses, such as the exposure to trypsin. However, for virions to persist in an infectious form, they must retain an intact envelope with intact gp120 molecules in order to gain entry into a new, $CD4^+$ target cell. To do this, the membrane of the virus needs to avoid fusion with astrocyte cell membranes, which is plausible given astrocytes do not express surface CD4. It may be possible for virions that are internalised into vesicular compartments to maintain an intact, unfused membrane, as has been shown to occur in the trans-infection of dendritic cells and transcytosis of HIV-1 by epithelial cells. Indeed, HIV-1 has been demonstrated to enter a variety of cell types by endocytosis (Fredericksen *et al*, 2002; Grewe *et al*, 1990; Liu *et al*, 2002; Marechal *et al*, 1998; Marechal *et al*, 2001; Pauza and Price, 1988; Schaeffer *et al*, 2001) (Sections 1.1.6i and 4.2.2), including HFAs and the astrocyte cell lines used in this thesis (Hao and Lyman, 1999; Liu *et al*, 2004) (Chapter 4). Furthermore, enveloped HIV-1 virus-like particles have been observed by EM within intracellular vesicle-like structures in HFAs and U251-MG and U87-MG astrocytes (Liu *et al*, 2004) (Section 4.3.2 and Figure 4.10).

These observations of enveloped HIV-1 virions within astrocyte vesicles were made within 40 minutes of infection. How long the virus can remain viable within such a compartment has not been established. The contents of newly formed vesicles gradually become acidified, due to the incorporation of proton pumps (vacuolar H(+)-ATPases) into vesicle membranes (Van Dyke, 1996), and undergo complex intracellular vesicle sorting events (Sieczkarski and Whittaker, 2002) (Figure 4.9, discussed in Sections 4.2.5 and 4.3.2i). The two predominant fates of intracellular vesicles are i) progression to fusion with lysosomes (degradation pathway), and, ii) recycling of the vesicles back to the cell surface (recycling pathway) (Sieczkarski and Whittaker, 2002). The conformation and viability of HIV-1 virions is pH dependent (Dichtelmuller *et al*, 2002; Ehrlich *et al*, 2001), although

inactivation through exposure to mildly acidic environments has been reported to be reversible (Rawal and Vyas, 1996). Vesicular uptake of HIV-1 has been generally considered to lead to viral degradation (unless the viral envelope is able to fuse with the vesicle membrane) (Fackler and Peterlin, 2000; Marechal *et al*, 1998; Schaeffer *et al*, 2001). Two exceptions to this have been documented. Endocytic uptake and release of infectious virus has been characterised in primary dendritic cells (Turville *et al*, 2003; Turville *et al*, 2004), in which the virus may survive in an intracellular compartment for at least 24 hours. There is evidence to suggest that viral mechanisms subvert the vesicular sorting events such that at least some of the virus evades endolysosomal degradation (Garcia *et al*, 2005; Turville *et al*, 2004). Release of the preserved virus by exocytosis appears to be stimulated by contact with susceptible cells (Garcia *et al*, 2005; Turville *et al*, 2004). Vesicular uptake and release of viable HIV-1 by "transcytosis" has also been reported in primary epithelial cells (Bomsel, 1997; Hocini *et al*, 2001; Hocini and Bomsel, 1999). Interestingly, astrocytes have been shown to perform transcytosis (Tabernero *et al*, 2002) and perform exocytosis of the neurotransmitter, glutamate (Bezzi *et al*, 2004). The observations of vesicular uptake of HIV-1 by astrocytes (Hao and Lyman, 1999; Liu *et al*, 2004) (Chapter 4), coupled with the reports that HIV-1 can be internalised and released without replication in other specialised cell types, indicate that a "trans-infection" phenomenon is a plausible explanation for the release of infectious virus in the absence of viral replication, as observed in U251-MG, CCF-STTG1 and U87-MG astrocytes in this chapter.

In consideration of the various scenarios which may underly the release of infectious virus from U251-MG, CCF-STTG1 and U87-MG astrocytes in the absence of detectable viral replication, the expression of viral RNA was examined throughout the course of U251-MG astrocyte infection. Specifically, the expression and level of unspliced, genomic viral RNA and multiply spliced, regulatory (early) viral mRNA was investigated throughout the course of a U251-MG infection experiment in which the release of infectious virus (Table 6.2) in the absence detectable of integrated provirus (Figure 6.4) had already been demonstrated.

6.6 Analysis of viral RNA in infected astrocytes

(coupled with release of infectious virus and undetectable proviral integration)

6.6.1 Background to HIV-1 RNA synthesis during virus replication.

Upon HIV-1 infection of susceptible cells expressing CD4 and coreceptors the first viral transcripts to be detected (at around 12 hpi) are the multiply spliced transcripts which encode the major viral regulatory proteins; Tat, Rev and Nef (Davis *et al*, 1997; Greene, 1991; Kim *et al*, 1989) (Section 1.1.6iv). Singly and unspliced HIV-1 transcripts appear around 16 to 24 hpi, and, because they are incompletely spliced, they are dependent on Rev for nuclear export (Davis *et al*, 1997; Kim *et al*, 1989) (Section 1.1.6iv). The restricted phase of astrocyte infection, both *in vitro* and *in vivo*, resembles a Rev-defective phenotype, as viral gene expression is limited to the transcription and translation of the viral regulatory proteins (Brack-Werner *et al*, 1992; Di Rienzo *et al*, 1998; Gorry *et al*, 1998; Kohleisen *et al*, 1992; Kohleisen *et al*, 1999; Kort, 1998; Tornatore *et al*, 1994b; Tornatore *et al*, 1991) (Sections 1.3.2ii and 1.4.2). The reactivation of HIV-1 production in viral plasmid transfected HFAs by stimulation with IL1β or TNFα is reportedly coincident with an increase in the abundance of the multiply spliced viral transcripts (Tornatore *et al*, 1994b) (Section 1.4.2).

To further characterise the nature of the HIV-1 infection of astrocytes in this thesis, the level of unspliced and multiply spliced viral RNA was analysed during the course of U251-MG infection with HIV-1_{NL4-3}. To examine both the restricted phase of infection and the reactivation of virus release, infected U251-MG cultures were harvested for RNA extraction prior to and during IL1β stimulation. In order to couple the analysis of viral transcription with the analysis of viral integration and virus release, infected U251-MG cells had been harvested and stored for subsequent RNA extraction from a previous experiment in which viral integration and release have already been studied (Section 6.3.2i and Table 6.2, Section 6.3.3 and Figure 6.4). To enable assessment of both viral integration and viral transcription in the same cultures, upon harvesting the cells from each culture the resultant cell suspension was divided into two equal portions; one for DNA extraction and one for RNA extraction (Section 2.6.2i). Extracted RNA was treated with DNase I, re-extracted, and converted to cDNA (Section 2.6.5). The concentration of the cDNA preparations was

determined by semi-quantitative *β-actin* PCR and Southern hybridisation (Sections 2.7.2i, 2.7.2viii and 2.7.3).

6.6.2 Analysis of unspliced viral RNA.

To determine the amount of unspliced viral RNA present in the U251-MG cultures during the couse of HIV-1_{NL4-3} infection, the cDNA samples were subjected to semi-quantitative PCR and Southern hybridisation targeting the *gag* region of the HIV-1 genome (Sections 2.7.2i, 2.7.2iv and 2.7.3). Infected U251-MG cultures were found to contain a substantial amount of unspliced viral RNA immediately following infection, at 3½ hpi (Figure 6.8A). Because this is prior to possible *de novo* synthesis of viral RNA, this represents input viral RNA. In support of this conclusion, the viral inoculum was also found to contain up to 1250 copies of unspliced HIV-1 RNA per 30µl (Figure 6.8B), the volume of virus used to inoculate 30 000 cells. The high level of viral RNA detected immediately after inoculation, despite the post infection washes and trypsin treatment, indicated that a considerable amount of input viral RNA was cell-associated by 3½ hpi. This is consistent with the rapid uptake of viral proteins observed by confocal microscopy (Chapter 4) and the detection of cell-associated viral DNA within 3½ hpi (Chapter 5).

The amount of unspliced viral RNA detected in infected U251-MG cultures declined with time post infection over the next 7 days, and was undetectable (<50 copies / 12 000 cells) in 63% (17/27) of samples from 10-16 dpi (Figure 6.8A). This decline in cell associated viral RNA was not dissimilar to the decay in viral DNA levels observed from 3½ to 48 hpi (Chapter 5). The source of the unspliced viral RNA after 12 - 16 hpi, however, could be due to either the persistence of the initial viral inoculum or *de novo* viral transcription, or a combination of both. This experiment does not discriminate between these possibilities, and indeed it would be technically difficult to do so. The decay kinetics of the unspliced viral RNA is consistent with the hypothesis of virus persistence and absence of viral replication. Furthermore, synthesis of unspliced viral RNA would be unexpected during the "restricted" phase of a productive astrocyte infection. However, the detection of relatively high levels of unspliced viral RNA during the acute phase of infection, which subsequently declines over the following week, is also consistent with a hypothesis of initial productive infection followed by viral latency. Similarly, the detection of unspliced viral RNA in 63% (17/27) of

A.

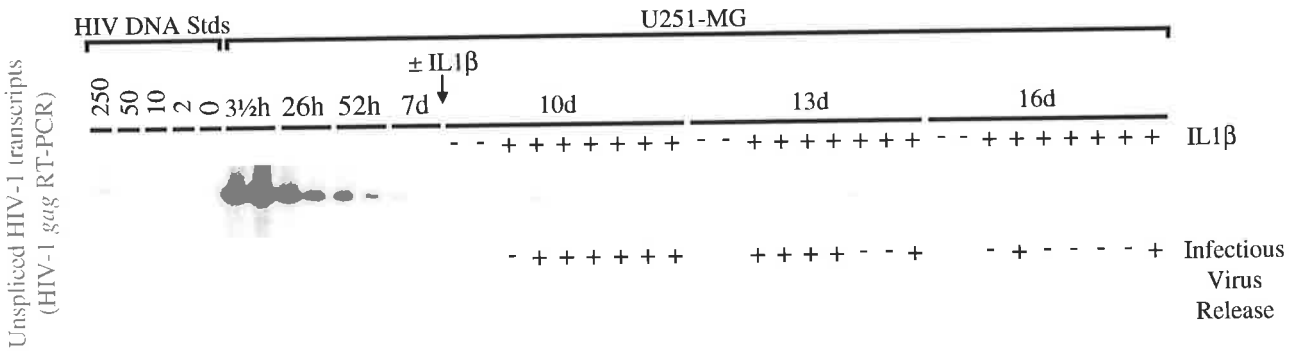

B.

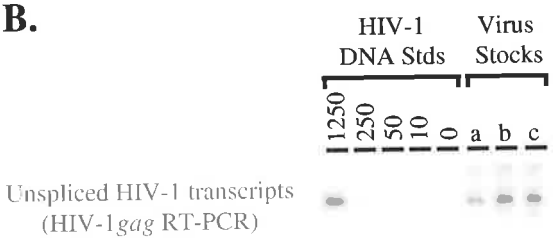

Figure 6.8 Analysis of unspliced HIV-1 RNA in infected U251-MG astrocytes and the virus inoculum

Total RNA was extracted from the HIV-1_{NL4-3} infected U251-MG cultures described in Figure 6.4, and from three virus stocks including the one used in this experiment. RNA samples were treated with DNase I and re-extracted. *β-actin* and viral RNA species were reverse transcribed into cDNA. Unspliced HIV-1 transcripts were assayed by HIV-1 *gag* PCR and Southern hybridisation on 12 000 cells-worth of cDNA (as determined by *β-actin* RT-PCR) (**A**). HIV-1 DNA standards were also assayed in the presence of 12 000 cells-worth of (uninfected) U251-MG cDNA. Each lane represents a replicate U251-MG culture. Treatment with or without IL1β from 7 dpi onwards is indicated above each lane. The results of the assay for infectious virus (Table 6.2) are summarised below each lane.

Unspliced HIV-1 RNA in the virus stocks were assayed by the same methods (**B**). Each lane represents a PCR input of cDNA equating to 30µl of virus from each of 3 virus stocks (a, b and c), which corresponds to the amount of inoculum used per 30 000 cells.

the cultures from 10 to 16 dpi could be interpreted either as the persistence of original viral inoculum or viral replication in the majority of cultures. Interestingly the detection of unspliced viral RNA in infected U251-MG cultures maintained for more than 7 days did not appear to correlate with IL1β stimulation or virus release (Figure 6.8A).

In summary, the identification of the source of unspliced viral RNA during the course of this U251-MG infection would be inconclusive if considered in isolation from other aspects of virus replication. However, given that viral reverse transcription (Chapter 5) and integration (Sections 6.2-6.4) are undetectable during the the first 48 hours of U251-MG infection, and that viral integration was undetectable in cells from the very same cultures as those analysed for viral RNA (Figure 6.4), it can be concluded that the detection of unspliced viral RNA during the first 2 days of infection must be due to persistence of the initial inoculum. Interpretation of the detection of unspliced viral RNA at later stages of U251-MG infection remains ambiguous, but given i) the high level of unspliced viral RNA initially associated with the cells, ii) the observation that unspliced viral RNA levels do not correlate with IL1β stimulation or the release of infectious virus (Figure 6.8A), and iii) the inability to detect integrated provirus in the same cultures (Figure 6.4), the most probable source of the unspliced viral RNA in the cultures harvested after 48hpi is also persistent initial inoculum.

6.6.3 Analysis of multiply-spliced viral mRNA.

To examine HIV-1 regulatory transcript expression during astrocyte infection, cDNA from virus stocks and infected U251-MG cultures were analysed for the presence of multiply-spliced viral transcripts (*nef*, *rev* and *tat*). The abundance of these transcripts was analysed by PCR using primers designed to co-amplify all multiply-spliced HIV-1 cDNA species and which discriminate between these transcript species according to the PCR product size (expected cDNA PCR product sizes for the predominant splice forms of *tat*, *rev* and *nef* are 393, 216 and 194 bp, respectively) (Davis *et al*, 1997) (Section 2.7.2ix). To increase the sensitivity of detection, Southern hybridisation was then performed with a cocktail of probes specific for each of the multipy-spliced viral cDNA amplicons (Section 2.7.3ii).

The analysis of virus stocks demonstrated the presence of *nef* transcripts at approximately 10-50 copies per 30μl (Figure 6.9B). This was not surprising as low levels of multiply

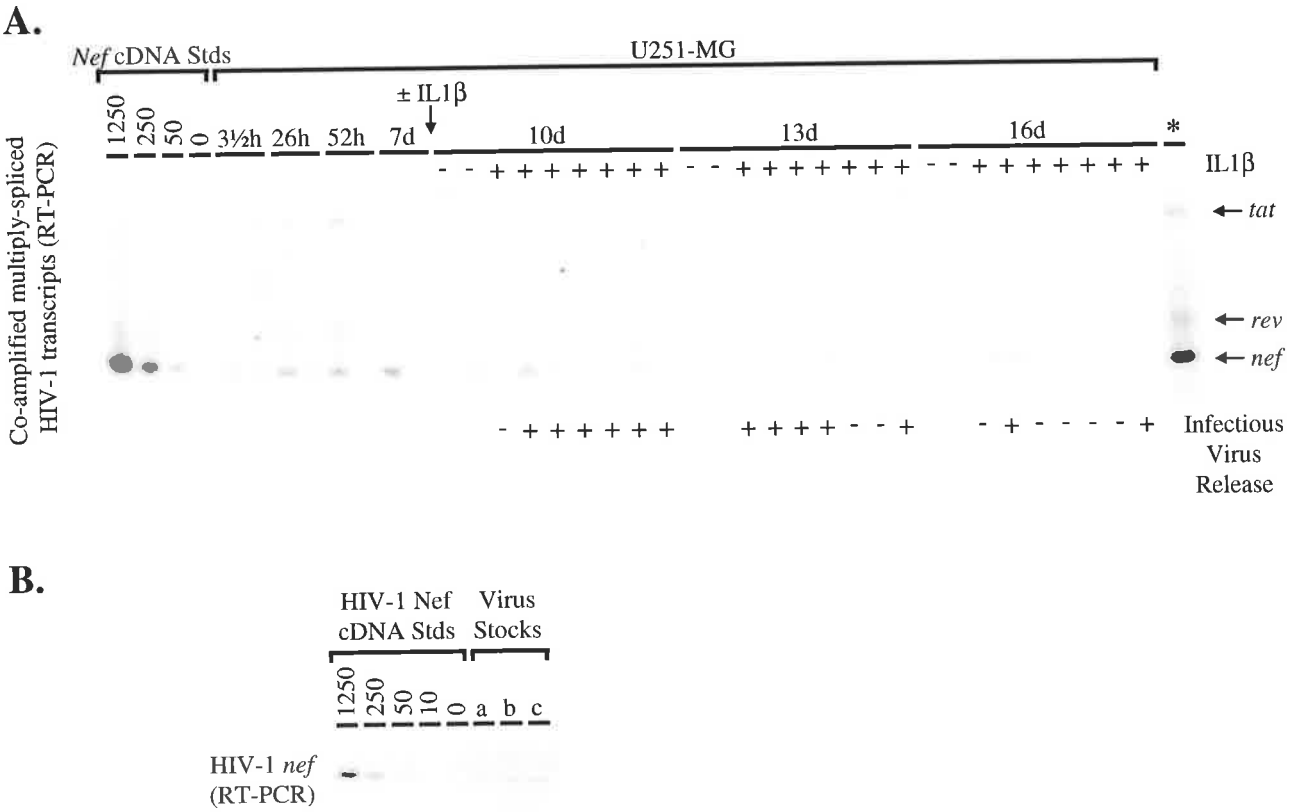

Figure 6.9 Analysis of multiply spliced HIV-1 mRNA in infected U251-MG astrocytes and the virus inoculum

Total RNA was extracted from the HIV-1_{NL4-3} infected U251-MG cultures described in Figure 6.4, and from three virus stocks, including the one used in this experiment, as described in Figure 6.8. RNA samples were treated with DNase I and re-extracted. *β-actin* and viral RNA species were reverse transcribed into cDNA. Multiply spliced HIV-1 transcripts were detected by HIV-1 2kb transcript RT-PCR on 250 000 - 35 000 cells-worth of cDNA (as determined by *β-actin* RT-PCR). This PCR, which amplifies all HIV-1 multiply spliced RNA species, was followed by Southern hybridisation with probes specific for the unique splice junction sites of *tat*, *rev* and *nef* (**A**). Each lane corresponds to the same cultures tested for HIV-1 *gag* cDNA in Figure 6.8. The marker lane in **A** (*) is derived from HIV-1_{NL4-3} infected HuT-78 cells. Treatment with or without IL1β from 7 dpi onwards is indicated above each lane. The results of the assay for infectious virus (Table 6.2) are summarised below each lane.

Multiply spliced *nef* HIV-1 mRNA in the virus stocks were assayed by the same methods (**B**). Each lane represents a PCR input of cDNA equating to 30μl of virus from each of 3 virus stocks (a, b and c), which corresponds to the amount of inoculum used per 30 000 cells.

spliced HIV-1 mRNA transcripts can be packaged, albeit inefficiently, into virions (Clever *et al*, 1999; Clever and Parslow, 1997; Luban and Goff, 1994). *Nef* transcripts were also detectable in infected U251-MG cultures at 3½, 26, 52 hpi and 7 dpi at varying levels (<250 copies per 250 000 cells) (Figure 6.9A). The abundance of *nef* transcripts did not decline with time post infection from 3hpi to 7dpi, but rather the abundance varied from culture to culture. This suggests that *de novo* synthesis of *nef* transcripts occurred in some of the U251-MG cultures. *Nef* transcripts were detectable in 44% (12/27) of infected U251-MG cultures from 10 dpi onwards, and did not appear to correlate with the release of infectious virus (Figure 6.9A). In some of the infected U251-MG cultures *rev* and *tat* transcripts were also detectable (Figure 6.9A). The most obvious template for transcription of multiply spliced transcripts is integrated provirus. However, the inability to detect integrated HIV-1 DNA in these cultures raises the additional possibility that the transcription may have occurred from unintegrated viral DNA (Kok *et al*, 1998; Liang *et al*, 2004; Spina *et al*, 1995; Wu and Marsh, 2001; Wu and Marsh, 2003a; Wu and Marsh, 2003b).

The possibility of transcription from unintegrated templates has not been previously entertained in the context of astrocyte infection, as it represents an unconventional and unlikely mode of HIV-1 transcription. Never-the-less, the expression of *nef* and, to a lesser extent, *tat* transcripts have been reported in the absence of detectable viral integration (by nested *Alu* PCR with a sensitivity of 1 copy per $5x10^4$ cells) in wild type HIV-1_{NL4-3} infected, quiescent primary $CD4^+$ T cells (Wu and Marsh, 2001). Expression of *nef* and *tat* has also been reported upon infection of quiescent primary $CD4^+$ T cells with an integrase defective HIV-1_{NL4-3} mutant (Wu and Marsh, 2001). Nef protein expression has also been observed in these cells (Wu and Marsh, 2001). This integration-independent transcription requires reverse-transcribed DNA template, in either a linear or circular episomal form (Wu and Marsh, 2003a). Other groups have also observed the transcription of regulatory mRNAs prior to, or in the absence of, proviral HIV-1 DNA integration (Kok *et al*, 1998; Spina *et al*, 1995). Recently, Liang *et al.* (2004) reported that multiply-spliced transcripts, which are present at a low level within virions, can be reverse transcribed into double-stranded cDNA, through the same mechanism by which full-length genomic HIV-1 RNA is reverse transcribed. Liang *et al.* (2004) found that reverse transcribed *nef* cDNAs were more abundant than *rev* and *tat* cDNAs, and these cDNAs can reportedly act as templates for subsequent mRNA transcription (Liang *et al*, 2004). The possibility that one of these mechanisms of integration-independent HIV-1 transcription may account for the detection of

nef (and, less frequently, *tat* and *rev*) transcripts in our model of HIV-1 infection of U251-MG cells is speculative and requires further experimentation. The detection of multiply-spliced viral transcripts does, however, suggest that the template DNA has gained access to the cell nucleus.

6.7 Discussion

6.7.1 Summary of Integration and virus release studies

The study of HIV-1 integration in the context of infectious virus release (discussed in detail in Section 6.5) revealed that;

i) IL1β only induced a release of p24 protein from a subset of HIV-1 infected U251-MG cultures
ii) IL1β induced p24 protein release occurred in the absence of detectable integrated provirus
iii) Viral infection was readily transmitted from infected U251-MG, CCF-STTG1 and U87-MG astrocyte cultures upon coculture with HuT-78 cells
iv) Even in the absence of HuT-78 cell coculture, the majority of infected U251-MG, CCF-STTG1 and U87-MG cultures released infectious virus into the supernatant
v) This infectious virus release occurred at a very low level, appeared to be sporadic, and was independent of IL1β stimulation
vi) Infectious virus release occurred in the absence of detectable integrated proviral DNA.

Together, the studies described in Sections 6.2, 6.3 and 6.4 indicate that the source of the release of infectious virus is either viral replication in less than 0.01% of cells (discussed in Section 6.5.2i), or the persistence of the original inoculum, either on the cell surface or within an intracellular compartment (discussed in Section 6.5.2ii). The possibility that infectious virus might persist on the surface of the astrocyte cells is quite unlikely due to the trypsin treatments, but cannot be excluded (Section 6.5.2iia). Alternatively, the original virus may persist in an intracellular compartment, and be subsequently released without having undergone replication (Section 6.5.2iib). This would require the virus to be

internalised into a vesicular-compartment in order to avoid fusion with cellular membranes, evade lysosomal degradation pathways, and subsequently be released from the cell. Indeed, intact, enveloped HIV-1 virions have been recently described within large vesicular compartments within astrocytes by the studies in this thesis (Chapter 4, Figure 4.10), and by others (Liu *et al*, 2004). This mode of HIV-1 trafficking, involving uptake and release of infectious virus without viral replication, has been demonstrated in other cell types (Bomsel, 1997; Hocini *et al*, 2001; Hocini and Bomsel, 1999; Turville *et al*, 2003; Turville *et al*, 2004).

The analysis of unspliced viral RNA during the course of HIV-1 infection of U251-MG astrocytes (Section 6.6.2, Figure 6.8), does not clarify whether the source of infectious virus release is a very low level of viral replication or persistent inoculum. The initial detection of viral RNA occurs prior to possible *de novo* synthesis (3½ hpi), indicating this is due to persistence of the viral inoculum. The declining level of unspliced viral RNA over the subsequent 2 dpi, in the absence of viral reverse transcription or viral integration, indicates that this is also due to persistence (and decay) of the initial inoculum. The source of the unspliced RNA detected from 10 to 16 dpi in the majority of the infected U251-MG cultures is unclear, but is likely to also represent initial inoculum rather than virus replication given i) viral integration is undetectable in the same cultures (Figure 6.4, Section 6.3) and ii) detection of unspliced viral RNA does not appear to correlate with the release of infectious virus (nor with IL1β stimulation).

Two other studies have assessed unspliced RNA levels during the course of HIV-1 infection of astrocytes, and both of these report the detection of unspliced viral RNA within the first 16 hpi (Brengel-Pesce *et al*, 1997; Di Rienzo *et al*, 1998). In both these studies, like the current study, the level of unspliced viral RNA then declines over the subsequent period of analysis. With two primary HIV-1 isolates, Brengel-Pesce *et al* detected around 3000 to 4000 copies of unspliced viral RNA per 10^6 CCF-STTG1 cells by 16 hpi, by reverse-transcribed PCR targeting the *gag* region of the unspliced viral RNA genome. Unspliced viral RNA levels had declined to ~ 40 copies per 10^6 cells by 1 dpi, and were undetectable by 2 dpi (sensitivity of <25 copies per 10^6 cells). With a third HIV-1 isolate; Brengel-Pesce *et al* detected approximately 72 000 copies of unspliced viral RNA per 10^6 cells at 16 hpi, which declined to ~470 copies per 10^6 cells by 2 dpi. This was considered to represent a

"transient expression" of late HIV-1 mRNAs (Brengel-Pesce *et al*, 1997). Similarly, Di Rienzo *et al* detected a high level of unspliced HIV-1 RNA 10 hours after HIV-1_{IIIB} infection of HEAs, by reverse-transcribed PCR and Southern hybridisation targeting the *gag* region of the unspliced viral RNA genome. The amount of unspliced RNA declined dramatically by 24 hpi, was barely detectable by 4 dpi, and was undetectable by 7 dpi (Di Rienzo *et al*, 1998). Di Rienzo *et al* raised the possibility that the transient initial detection of the unspliced transcripts may be "largely ascribed to the input virus" (Di Rienzo *et al*, 1998).

The detection of HIV-1 regulatory transcripts in the infected U251-MG cultures does not conform to the decay trend observed for unspliced viral transcripts (and viral DNA (Chapter 5)). Although the amount of *nef* transcripts present in the virus inoculum could account for the detection of *nef* transcripts in infected U251-MG cells at 3½ hpi (Figure 6.9), a higher level of *nef* was detectable in some of the cultures harvested at later time points, indicating that *de novo* synthesis of *nef* mRNA occurred in some cultures. Given HIV-1 integration could not be detected in these cultures, *nef* transcription may have occurred from unintegrated templates. The transcription of regulatory HIV-1 mRNAs, predominantly *nef*, from unintegrated viral DNA templates has been reported previously (Kok *et al*, 1998; Liang *et al*, 2004; Spina *et al*, 1995; Wu and Marsh, 2001; Wu and Marsh, 2003a; Wu and Marsh, 2003b). Additionally, regulatory transcripts, which are packaged at low levels within HIV-1 virions (Clever *et al*, 1999; Clever and Parslow, 1997; Luban and Goff, 1994), can undergo subsequent reverse transcription upon entering a host cell, thus generating further DNA templates for transcription (Liang *et al*, 2004). This process reportedly occurs most efficiently for *nef* (Liang *et al*, 2004). For either of these processes to occur in our model of astrocyte infection, the reverse transcribed viral DNAs would need to gain access to the cellular transcriptional machinery in the nucleus.

HIV-1 regulatory transcript and protein expression, in particular *nef* and Nef, has been reported in *in vivo* (Blumberg *et al*, 1994; Ranki *et al*, 1995; Saito *et al*, 1994; Tornatore *et al*, 1994a) and *in vitro* astrocyte infections (Brengel-Pesce *et al*, 1997; Di Rienzo *et al*, 1998; Kort, 1998). Upon HIV-1_{IIIB} infection of HEAs, Di Rienzo *et al* found *nef* and *tat* transcripts to be low or undetectable at 10 hpi and 1 dpi, much higher at 2 dpi, and variable from 4 to 14 dpi (Di Rienzo *et al*, 1998), which is not dissimiar to the findings presented in

Section 6.6.3. Kort *et al* also investigated HIV-1 infection of the U251-MG cell line, and observed Nef protein expression, which persisted to at least 42 dpi (Kort, 1998).

Two mechanisms have been previously characterised which explain the selective expression of HIV-1 regulatory genes, but not structural proteins, in astrocytes (Section 1.5.3). One mechanism involves an aberrant Rev / RRE regulatory axis in astrocytes, such that only multiply spliced, and not singly or unspliced, viral transcripts undergo nuclear export to the cytoplasm for translation (Ludwig *et al*, 1999; Neumann *et al*, 1995). These studies analysed an astrocyte cell line (TH4-7-5) with a single integrated provirus, and HIV-1 proviral plasmid transfected HFAs and astrocyte cell lines (Ludwig *et al*, 1999; Neumann *et al*, 1995). An additional mechanism has been described in HIV-1 proviral plasmid transfected astrocytes, where the limited expression of viral structural proteins is attributed to the very low level of an endogenous protein, TRBP, in astrocytes. TRBP normally restricts the inhibitory effects of cellular PKR on viral translation, which affects translation of the structural transcripts (Bannwarth *et al*, 2001; Gorry *et al*, 1998; Gorry *et al*, 1999; Gorry *et al*, 2003; Ong *et al*, 2005; Park *et al*, 1994). The detection of HIV-1 regulatory transcripts in our model of astrocyte infection is intriguing, as it indicates that transcription from unintegrated templates may be a third mechanism which underlies the selective expression of regulatory transcripts and the absence of structural HIV-1 gene expression in astrocytes. To better understand this possibility, further studies would be required to i) determine whether Nef protein expression occurs (by immuno-labelling of Nef protein), ii) determine whether singly-sliced HIV-1 transcripts and the respective translated proteins are detectable (by reverse-transcribed PCR), and iii) confirm the absence of HIV-1 structural protein expression (by sensitive immunolabelling) in our model of astrocyte infection.

Aside from the curious expression of *nef*, the data in this chapter, supported by the data in Chapter 5, suggest that a replication-independent pathway of HIV-1 infection and transmission occurred in the U251-MG, CCF-STTG1 and U87-MG astrocytes. As this non-replicative pathway of astrocyte infection displayed the features previously considered characteristic of the restricted-productive HIV-1 infection of astrocytes, this pathway may have proceeded, unnoticed, in previously reported models of astrocyte infection. The observations of the initial p24 release, early detection of extrachromosomal HIV-1 DNA and rescue of productive infection upon coculture in this non-replicative model indicate that

these features of astrocyte infection do not necessarily indicate that viral replication, including integration, has occurred. However, there is also considerable evidence for a restricted-productive pathway of infection in astrocytes, in which integration of the HIV-1 provirus was required (Brack-Werner *et al*, 1992; Nath *et al*, 1995). Recently the presence of integrated HIV-1 DNA has been demonstrated in astrocytes by the integrated provirus-specific *Alu* PCR on astrocytes which have been captured by laser-microdissection from HIV-1+ post mortem brains (Dr Melissa Churchill, personal communication). This clearly demonstrates that virus integration can occur in infected astrocytes *in vivo*. The results presented in this chapter, from three independent astrocyte cell lines, raise the possibility that a replication-independent pathway of HIV-1 infection may occur in astrocytes *in vivo*, in addition to the restricted-productive pathway.

Chapter 7

General Discussion

7.1 Summary and Discussion

The major aims of this thesis were to characterise the mode of HIV-1 entry into astrocyte cells, the subsequent reverse transcription and integration of the virus within astrocytes, and the transmission of virus from these cells upon coculture or IL1β stimulation. A minor aim was to compare the relative efficiency of astrocyte infection after cell-cell or cell-free inoculation. Cell-cell inoculation of the U251-MG astrocyte cell line by coculture with HIV-1_{IIIB} or HIV-1_{SF2} infected T-cell lines or with HIV-1_{BaL} infected MDMs did not result in demonstrable viral replication within the astrocytes (Chapter 3). However, viral replication in the U251-MG cells could not be excluded in these studies, as it may have been masked by the replication of HIV-1 in the virus-donor cells. The cell-free infection model permitted a more detailed analysis of the interaction between HIV-1 and astrocytes, and was used to examine the entry, reverse transcription, integration and virion release steps of the virus life cycle. Using cell-free HIV-1_{NL4-3} inoculum and three astrocyte cell lines, the cell-free infection model employed in this thesis displayed all the classical signs of *in vitro* HIV-1 infection of astrocytes. The features of the cell-free model of astrocyte infection used in this thesis are summarised in Table 7.1. In particular, this model displayed i) initial HIV-1 p24 protein release, ii) low levels of HIV-1 DNA, and iii) transmission of HIV-1 upon coculture with $CD4^+$ cells. However, more careful examination of these features revealed that each of these observations was likely to be due to the input virus inoculum rather than virus replication as currently assumed.

Comprehensive analyses of the initial p24 release demonstrated that, in this model, the source of the viral core protein was the original inoculum and not *de novo* synthesis (Chapter 5). Inoculum p24 protein was shown to persist in spite of a rigorous post-infection washing regime that included a trypsin treatment. Detailed analyses of the viral DNA sequences present during the first few days of astrocyte infection demonstrated a decline in levels over the time course assessed (3 hpi to 48 hpi) (Chapter 5). The data from this

	HIV-1 infected astrocyte cells (alone)		**HIV-1 infected astrocytes cocultured with HuT-78 cells** (from 7dpi onwards)
	Untreated	IL1β treated (from 7dpi onwards)	
Initial p24 release	+		
HIV-1 DNA	+		
Newly reverse transcribed HIV-1 DNA	-		
p24 release (after 7 dpi)	-	±	+++
Syncytia	-	-	+++
Integrated HIV-1 DNA	-	-	+++
Release of infectious virus Into culture supernatant	+	+	+++

Table 7.1 Summary of the observed features of cell-free HIV-1 infections of U251-MG, CCF-STTG1 and U87-MG astrocytes.

The features of untreated U251-MG, CCF-STTG1 and U87-MG astrocyte infection observed upon cell-free inoculation with DNase I treated HIV-1_{NL4-3} (Chapters 5 and 6) are summarised. The findings after IL1β treatment or coculture of the astrocytes with HIV-1 susceptible $CD4^+$ cells (from 7 dpi onwards) are compared to untreated astrocytes.

chapter also demonstrated that HIV-1 DNA did not arise from *de novo* reverse transcription after virus entry into astrocytes, but rather from the input viral inoculum even though this had been DNase treated and the excess inoculum had been removed. Transmission of HIV-1 occurred upon coculture of the astrocyte cells with $CD4^+$ cells in all experiments. Therefore, in Chapter 5, it was proposed that the lack of detectable reverse transcription in U251-MG, CCF-STTG1 and U87-MG astrocytes during the first 48 hpi indicated that HIV-1 replication was inhibited prior to reverse transcription, until the occurrence of certain cellular events which are stimulated by coculture.

In Chapter 6, the coculture stimulus was simulated with IL1β (as had been previously reported (Sabri *et al*, 1999; Tornatore *et al*, 1991) (Section 6.1.2)), and the viral replication steps of integration and release of infectious virus were examined. Despite highly sensitive assays for integrated HIV-1 proviral DNA, no viral integration could be demonstrated during the course of the U251-MG, CCF-STTG1 or U87-MG infections (3½ hpi to 16 dpi). Yet, with a highly sensitive assay to amplify and detect the infectious virus, most of the infected astrocyte cultures were shown to release infectious virus into their culture supernatants. In astrocyte cultures that had been inoculated with HIV-1 $\geq$ 7 days prior to testing for virus-release, this virus-release occurred at a very low level and was independent of IL1β treatment. The release of infectious virus in the absence of detectable viral replication suggested that a low level of the original virus could persist in an infectious state and be subsequently released from the astrocytes. The original virus is more likely to persist in an intracellular compartment than on the cell-surface, because the infected astrocyte cells were treated with trypsin immediatedly after inoculation and again at 5dpi, and the virus appeared to be readily internalised by confocal and EM studies (Chapter 4).

Replication independent HIV-1 uptake and release has not been previously described in astrocytes, however this phenomenon has been previously described in dendritic (Turville *et al*, 2003; Turville *et al*, 2004:Bernhard, 2004 #212) and epithelial cells (Bomsel, 1997; Hocini *et al*, 2001; Hocini and Bomsel, 1999). As already discussed in Chapter 6, for virus particles to be internalised and retain infectivity upon release, they need to maintain the integrity of their envelope. During "*trans*-infection" of dendritic cells, and "transcytosis" of epithelial cells, virus particles are internalised into a vesicular compartment and the virus envelope does not fuse with cellular membranes. The virus thereby retains an intact, gp120-

studded envelope that is capable of initiating infection via fusion upon contact with a subsequent susceptible cell. There is now convincing evidence from Chapter 4 of this thesis and a previous study (Liu *et al*, 2004) that astrocytes can also internalise whole enveloped virions into vesicular compartments. This process of virion internalisation appears to involve macropinocytosis or phagocytosis, although further investigations are required to confirm this.

The observation of internalised, enveloped virions within astrocytes shortly after exposure to HIV-1, coupled with the inability to detect viral replication in spite of the release of a low level of virus, indicates that a replication-independent pathway of HIV-1 infection occurred in this model of astrocyte infection (Figure 7.1). The scope of this thesis, however, did not analyse the fate of virions in the macropinosome-like vesicles beyond 75 mpi, and the hypothesis that the released virions have arisen from this mode of virus uptake is speculative. Additional routes of virus uptake may be occurring simultaneously in the astrocytes, which could be responsible for the subsequent release of virions. It should also be pointed out that the method of cell-free infection in this thesis differed for the microscopy and viral replication analyses. The immunofluorescent and EM studies presented in Chapter 4 were performed on pre-seeded astrocytes, in order to maintain the morphology of the cells. However the cell-free infection studies of virus replication were performed on astrocyte cells which had been suspended by trypsin treatment and subjected to centrifugally enhanced inoculation, in order to improve the efficiency of infection.

Centrifugally enhanced inoculation reportedly enhances virus-cell contact but does not alter the mode of virus entry (O'Doherty *et al*, 2000), although this has not been established for CD4 independent entry mechanisms. Trypsin treatment, however, would cleave certain surface molecules on the astrocytes. The absence of a restricted-productive infection in this cell-free model of astrocyte infection, and the apparent discrepancy compared to other astrocyte infection paradigms, may relate to the infection method used, as well as the subtype or phenotype of the astrocytes investigated. Previous *in vitro* studies of the restricted HIV-1 infection of astrocytes have used other methods to enhance the efficiency of infection, including virus inoculation in the presence of polybrene and DEAE dextran, which enhance virus-cell interactions by interfering with the electrostatic charge of the cell surface, and transfection of the astrocytes with a plasmid encoding HIV-1. In our model, the treatment of the cells with trypsin prior to infection revealed an additional, replication-

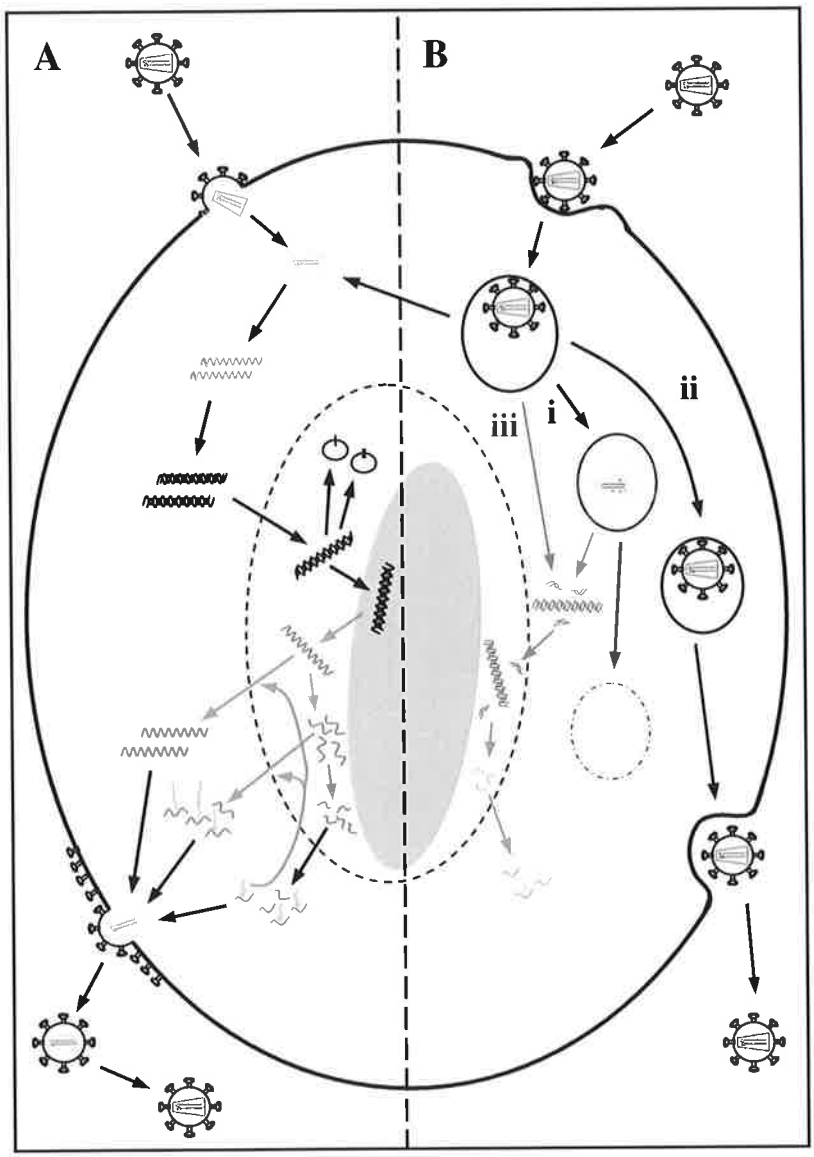

Legend:

Mature HIV-1 virion

Partially uncoated or immature virus core

Viral RNA genome

Double stranded viral genomic cDNA

Integrated proviral DNA in the cellular chromatin

Single and double LTR circular forms of HIV-1 DNA

Singly and multiply spliced viral mRNA transcripts

Nascent viral protein synthesis

HIV-1 gp120 trimer

Lysosomal degradation

independent pathway of infection, which may have otherwise been masked by restricted-productive infection (although a restricted-productive infection could not be detected upon cell-cell HIV-1 inoculation of pre-seeded U251-MG astrocytes (Chapter 3)). It is worth noting that the only receptor which has been shown to be involved in astrocyte infection to date, the mannose receptor (Liu *et al*, 2004), is reportedly resistant to trypsin (Turville *et al*, 2004).

In retrospect, in previous studies of the HIV-1 infection of astrocytes, the initial p24 protein release and early HIV-1 DNA detection may have also been due to persistence of the virus inoculum rather than *de novo* synthesis. A replication-independent pathway may also account for some of the virus release observed in previous models of astrocyte infection. However, in the presence of restricted-productive infection, a replication-independent pathway would not be noticed unless it was specifically looked for.

Based on the data in this thesis, we hypothesise that a replication-independent pathway of HIV-1 infection may occur in certain types of astrocytes (Figure 7.1). Taken together with previous models of astrocyte infection, this supports the notion that multiple pathways of HIV-1/cell interaction may occur in astrocytes in the brain microenvironment. The previously recognised pathway gives rise to inducible virus production (Figure 7.1A), involving a conventional HIV-1 life cycle with restrictions to virus structural protein synthesis. The occurrence of this pathway *in vivo* is supported by recent data which demonstrated that HIV-1 DNA sequences in astrocytes from post mortem HIV-1+ brain sections were distinct from viral sequences found macrophages / microglia from the same section, suggestive of the evolution of astrocyte-tropic virus *in vivo* (Thompson *et al*, 2004), and the demonstration of integrated proviral HIV-1 DNA (by *Alu* PCR) in astrocytes from post mortem HIV-1+ brains (Churchill *et al*, 2006).

An additional pathway which may exist in some types of astrocytes, supported by the data in this thesis, involves virus uptake and transmission without the virus actually replicating (Figure 7.1B). It is likely that the majority of virus which is endocytosed by astrocytes may be degraded by the lysosomal pathway. This would account for the decay of inoculum-derived HIV-1 DNA and unspliced viral RNA during the first few days of infection. However, a proportion of endosome-captured virus may avoid the degradation pathway and subsequently be released as infectious virus. This process appears to account for the

sporadic, very low level of infectious virus release observed in this thesis. Whether the more consistent and efficient "rescue" of virus upon coculture with $CD4^+$ cells represents a more efficient amplification of released virus or actually stimulates the release of virus from the astrocytes remains to be determined.

This replication-independent pathway does not account directly for the *de novo nef* transcription observed. We hypothesise that some viral DNA (the intravirion DNA present in a proportion of virions, or viral cDNA derived from intravirion multiply-spliced mRNAs) may escape the vesicular compartment and gain access to the nucleus, facilitating transcription, however this is speculative. The source of the p24 release, which occurred in a minority of cultures in this thesis, a few days after the addition of IL1β and in the absence of detectable integrated provirus, remains unclear.

Infectious HIV-1 has been recovered from astrocytes as long as 4 or 5 months post infection (Chiodi *et al*, 1987; Dewhurst *et al*, 1987b). The possibility that astrocytes in the CNS may harbour and transmit virus without replication may represent an important mechanism by which HIV-1 may evade anti-retroviral therapy. This non-replicative mode of HIV-1 persistence and transmission may also be important in the entry and spread of HIV-1 in the CNS. This novel mode of virus/astrocyte interaction may also represent an additional way in which HIV-1 can disrupt normal astrocyte function, as the interplay between the virus and intracellular vesicle sorting events could alter the normal astrocyte vesicle sorting events required for recycling of neurotransmitters and export of neurotropic factors. Further understanding of the non-replicative mode of astrocyte infection will be important for a comprehensive understanding of HIV-1 entry, spread and persistence in the CNS as well as for understanding the mechanims by which HIV-1 induces astrocyte dysfunction and apoptosis, and the subsequent impact on the pathogenesis of HIV-1 induced neurological diseases.

7.2 Future Directions

The evidence from this thesis that an alternative, replication-independent pathway of HIV-1 infection can occur in three astrocyte cell lines raises numerous further questions. The principle questions are;

i) Does this pathway occur in primary astrocytes and in astrocytes *in vivo*?

ii) What is the effect of this pathway on astrocyte function?

iii) Is this pathway significant in virus entry and spread in the CNS?

iv) Does this pathway consistitute a major source of antiretroviral evasion and virus persistence in the CNS?

Several mechanistic questions are also raised, in particular;

v) What is the nature of the intracellular trafficking route of the virus from uptake to subsequent release?

vi) What is the source of the regulatory transcript expression in this model?

Possible approaches to addressing these questions are discussed below.

i) Does a replication-independent pathway of HIV-1 infection occur in primary astrocytes and in astrocytes* in vivo*?

The first question to be addressed is whether this pathway occurs in primary astrocytes. It would be exceedingly difficult to demonstrate whether or not this pathway occurs *in vivo*, as no diagnostic marker is known which could discern a replication-independent pathway from a restricted-productive infection in a fixed-time point study of post mortem brain tissue. The occurrence of a replication independent pathway of HIV-1 in primary astrocytes could be investigated by *in vitro* studies in HFAs or PDAs. It would be anticipated that both pathways of infection may occur within the same culture (and possibly even the same cell) in HFAs and PDAs due to the heterogeneity of these astrocyte populations. Because of this, techniques that can differentiate between these two pathways would be required. The occurrence of a replication-independent pathway, in the presence of a restricted-productive infection, could be tested using antiretroviral agents that would block the restricted-productive pathway but not the replication-independent pathway. Such drugs would need to be applied to the astrocyte cells (not the virus stock), be irreversible, and excess drug removable, if the replication-independent pathway is to proceed and be detected by assays for infectious virus. Another strategy to discern between replication-independent and

restricted-productive infections pathways could involve the assessment of virus transfer / release prior to possible synthesis (within the first 20 hours of infection). A combination of these strategies have been successfully used in the characterisation of the *trans*-infection pathway in dendritic cells, as conventional, replication-dependent infection can also occur concurrently in dendritic cells with CCR5-using virus strains (Turville *et al*, 2003).

The source of any virus release within the first 20 hpi would need to be identified as either the rebound of surface-bound virus, or release of internalised virus. To exclude the release of surface-bound virus the primary astrocytes could treated with trypsin or an organic acid after viral inoculation, to remove or inactivate surface bound virus (Dichtelmuller *et al*, 2002; Rawal and Vyas, 1996), so long as such treatment did not interfere with subsequent detection of virus-release. Microtubule and endosomal inhibitors could also be employed to demonstrate that virus release requires intracellular trafficking.

An alternative strategy could involve inoculating astrocytes with virions which are labelled for the one round of infection only, such that the release of original labelled virus from the astrocytes could be discerned from unlabelled progeny virions. For example, chimeric virions that have incorporated β-lactamase-Vpr fusion proteins could be used to inoculate the astrocytes. The infected astrocytes could be subsequently cocultured with $CD4^+$ susceptible cells which are pre-loaded with an indicator of the β–lactamase enzyme, such as the fluorescent dye CCF2, enabling sensitive detection of the original virus by the change in the emission spectra of CCF2 in the $CD4^+$ virus-detector cells (Cavrois *et al*, 2002). A similar approach would be to infect the astrocytes with an integrase mutant virus, and to investigate transmission of the virus to $CD4^+$ susceptible cells that have been transfected to express integrase in *trans* (to enable amplification and detection of the virus transfer).

ii) What is the effect of this pathway on astrocyte function?

If it is established that a replication-independent pathway of infection can occur in primary astrocytes, then the relevance of this pathway should be investigated. Given the vital roles of astrocytes for normal neuronal function, and their apparent dysfunction and demise in HIVD, it would be important to determine if and how the intracellular trafficking of HIV-1 may affect their function. Such a study could be approached initially by physiological testing of astrocytes infected with HIV-1 by the replication-independent pathway for

impairment of calcium signalling, neurotransmitter signalling and recycling and glucose metabolism. Indeed it has been shown recently that binding of HIV-1 to the mannose receptor on astrocytes is sufficient to alter intracellular signalling through the mannose receptor (Lopez-Herrera *et al*, 2005).

iii) Is this pathway significant in virus entry and spread in the CNS?

The potential involvement of the replication-independent pathway of HIV-1 in the entry of HIV-1 into the CNS could be investigated *in vitro* using cell-culture models of the BBB, comprising a monolayer of HFAs or PDAs grown on a monolayer of primary endothelial cells on a membrane. Virus could be added to the culture media on the endothelial cell side (representing the peripheral side of the BBB), and mode of transmission of virus across the BBB model could be investigated. The question of whether virus exiting on the astrocyte side of the BBB model is input virus inoculum or requires virus replication (in either the endothelial or the astrocyte cells) could be addressed by the same strategies outlined above for the study of the replication-independent pathway in primary astrocytes (**i**)).

To determine whether the replication-independent pathway is important in virus entry and spread in the CNS *in vivo*, the actual vesicle-trafficking route involved in the replication-independent pathway would need to be identified (**vi**)). This would enable determination of how much HIV-1 is associated with this vesicle route across the BBB and in the brain parenchyma by *in situ* studies of post mortem tissue.

iv) Does this pathway constitute a major source of antiretroviral evasion and virus persistence in the CNS?

This is an exceedingly difficult question to address directly by experimental means. Rather, the importance of the replication-independent pathway of HIV-1 anti-retroviral evasion and virus persistence in the CNS may be determined indirectly, by a combination of *in situ* studies to determine the extent of HIV-1 virions involved in this vesicular pathway in the brain (**iii**)), and molecular sequencing studies to investigate the probability that a major source of virus rebound upon therapy cessation comes from brain-derived virus.

v) What is the nature of the intracellular trafficking route of the virus from uptake to subsequent release?

The route of endocytosis involved in the HIV-1 replication-independent pathway in astrocytes could be characterised by confocal and immuno-EM studies by labelling both the virus and markers of different stages and pathways of endocytosis. Identified pathways could be confirmed by employing drugs which target specific endocytosis routes in *in vitro* infection models. The question of whether virus release from this pathway is "random" or regulated or stimulated by cell-cell contact could also be investigated by a combination of microscopic and *in vitro* culture experiments.

vi) What is the source of the regulatory transcript expression in this model of astrocyte infection?

The mechanism of *nef* transcription from unintegrated templates could be investigated by careful molecular dissection at different stages of culture to address whether the DNA template for *nef* transcription was preformed in the virion, or derived from reverse transcription of unspliced or spliced RNA in the virion. Also, the mechanism by which the potentially vesicle-trapped DNA template may gain access to the cytoplasm, to subsequently gain access to the nucleus to be transcribed, could be characterised.

Bibliography

(1981). Pneumocystis pneumonia--Los Angeles. *MMWR Morb Mortal Wkly Rep* **30:** 250-2.

(1994). XVII Congress of the International Society for Analytical Cytology. Lake Placid, New York, 16-21 October 1994. Abstracts. *Cytometry Suppl* **7:** 1-92.

(2005). AIDS epidemic update: December 2005. UNAIDS/WHO.

Adamson DC, Wildemann B, Sasaki M, Glass JD, McArthur JC, Christov VI, Dawson TM, Dawson VL (1996). Immunologic NO synthase: elevation in severe AIDS dementia and induction by HIV-1 gp41. *Science* **274:** 1917-21.

An SF, Groves M, Giometto B, Beckett AA, Scaravilli F (1999a). Detection and localisation of HIV-1 DNA and RNA in fixed adult AIDS brain by polymerase chain reaction/in situ hybridisation technique. *Acta Neuropathol (Berl)* **98:** 481-7.

An SF, Groves M, Gray F, Scaravilli F (1999b). Early entry and widespread cellular involvement of HIV-1 DNA in brains of HIV-1 positive asymptomatic individuals. *J Neuropathol Exp Neurol* **58:** 1156-62.

Anders K, Steinsapir KD, Iverson DJ, Glasgow BJ, Layfield LJ, Brown WJ, Cancilla PA, Verity MA, Vinters HV (1986a). Neuropathologic findings in the acquired immunodeficiency syndrome (AIDS). *Clin Neuropathol* **5:** 1-20.

Anders KH, Guerra WF, Tomiyasu U, Verity MA, Vinters HV (1986b). The neuropathology of AIDS. UCLA experience and review. *Am J Pathol* **124:** 537-58.

Andjelkovic AV, Song L, Dzenko KA, Cong H, Pachter JS (2002). Functional expression of CCR2 by human fetal astrocytes. *J Neurosci Res* **70:** 219-31.

Andjelkovic AV, Spencer DD, Pachter JS (1999). Visualization of chemokine binding sites on human brain microvessels. *J Cell Biol* **145:** 403-12.

Apodaca G (2001). Endocytic traffic in polarized epithelial cells: role of the actin and microtubule cytoskeleton. *Traffic* **2:** 149-59.

Arthur FE, Shivers RR, Bowman PD (1987). Astrocyte-mediated induction of tight junctions in brain capillary endothelium: an efficient in vitro model. *Brain Res* **433:** 155-9.

Arts EJ, Mak J, Kleiman L, Wainberg MA (1994). DNA found in human immunodeficiency virus type 1 particles may not be required for infectivity. *J Gen Virol* **75 (Pt 7):** 1605-13.

Ausubel FM, Brent R, Kingston RE, Moore DD, Seidman JG, Smith JA, Struhl K, (eds). (1995). *Current Protocols in Molecular Biology*. John Wiley & Sons, Inc.

Bagasra O, Lavi E, Bobroski L, Khalili K, Pestaner JP, Tawadros R, Pomerantz RJ (1996). Cellular reservoirs of HIV-1 in the central nervous system of infected individuals: identification by the combination of in situ polymerase chain reaction and immunohistochemistry. *AIDS* **10:** 573-85.

Banks WA, Akerstrom V, Kastin AJ (1998). Adsorptive endocytosis mediates the passage of HIV-1 across the blood-brain barrier: evidence for a post-internalization coreceptor. *J Cell Sci* **111 (Pt 4):** 533-40.

Banks WA, Kastin AJ, Brennan JM, Vallance KL (1999). Adsorptive endocytosis of HIV-1gp120 by blood-brain barrier is enhanced by lipopolysaccharide. *Exp Neurol* **156:** 165-71.

Bannwarth S, Talakoub L, Letourneur F, Duarte M, Purcell DF, Hiscott J, Gatignol A (2001). Organization of the human tarbp2 gene reveals two promoters that are repressed in an astrocytic cell line. *J Biol Chem* **276:** 48803-13.

Barbosa P, Charneau P, Dumey N, Clavel F (1994). Kinetic analysis of HIV-1 early replicative steps in a coculture system. *AIDS Res Hum Retroviruses* **10:** 53-9.

Barna BP, Chou SM, Jacobs B, Ransohoff RM, Hahn JF, Bay JW (1985). Enhanced DNA synthesis of human glial cells exposed to human leukocyte products. *J Neuroimmunol* **10:** 151-8.

Barnes DA, Huston M, Holmes R, Benveniste EN, Yong VW, Scholz P, Perez HD (1996). Induction of RANTES expression by astrocytes and astrocytoma cell lines. *J Neuroimmunol* **71:** 207-14.

Barnum SR (1995). Complement biosynthesis in the central nervous system. *Crit Rev Oral Biol Med* **6:** 132-46.

Barres BA (1991). New roles for glia. *J Neurosci* **11:** 3685-94.

Barres BA, Chun LL, Corey DP (1990). Ion channels in vertebrate glia. *Annu Rev Neurosci* **13:** 441-74.

Barre-Sinoussi F, Chermann JC, Rey F, Nugeyre MT, Chamaret S, Gruest J, Dauguet C, Axler-Blin C, Vezinet-Brun F, Rouzioux C, Rozenbaum W, Montagnier L (1983). Isolation of a T-lymphotropic retrovirus from a patient at risk for acquired immune deficiency syndrome (AIDS). *Science* **220:** 868-71.

Belayev L, Busto R, Zhao W, Ginsberg MD (1996). Quantitative evaluation of blood-brain barrier permeability following middle cerebral artery occlusion in rats. *Brain Res* **739:** 88-96.

Bell JE (1998). The neuropathology of adult HIV infection. *Rev Neurol (Paris)* **154:** 816-29.

Bellander BM, von Holst H, Fredman P, Svensson M (1996). Activation of the complement cascade and increase of clusterin in the brain following a cortical contusion in the adult rat. *J Neurosurg* **85:** 468-75.

Bennett BA, Rusyniak DE, Hollingsworth CK (1995). HIV-1 gp120-induced neurotoxicity to midbrain dopamine cultures. *Brain Res* **705:** 168-76.

Benos DJ, Hahn BH, Bubien JK, Ghosh SK, Mashburn NA, Chaikin MA, Shaw GM, Benveniste EN (1994). Envelope glycoprotein gp120 of human immunodeficiency virus type 1 alters ion transport in astrocytes: implications for AIDS dementia complex. *Proc Natl Acad Sci U S A* **91:** 494-8.

Berrada F, Ma D, Michaud J, Doucet G, Giroux L, Kessous-Elbaz A (1995). Neuronal expression of human immunodeficiency virus type 1 env proteins in transgenic mice: distribution in the central nervous system and pathological alterations. *J Virol* **69:** 6770-8.

Berthiaume EP, Medina C, Swanson JA (1995). Molecular size-fractionation during endocytosis in macrophages. *J Cell Biol* **129:** 989-98.

Bezzi P, Carmignoto G, Pasti L, Vesce S, Rossi D, Rizzini BL, Pozzan T, Volterra A (1998). Prostaglandins stimulate calcium-dependent glutamate release in astrocytes. *Nature* **391:** 281-5.

Bezzi P, Gundersen V, Galbete JL, Seifert G, Steinhauser C, Pilati E, Volterra A (2004). Astrocytes contain a vesicular compartment that is competent for regulated exocytosis of glutamate. *Nat Neurosci* **7:** 613-20.

Bezzi P, Volterra A (2001). A neuron-glia signalling network in the active brain. *Curr Opin Neurobiol* **11:** 387-94.

Bhat S, Mettus RV, Reddy EP, Ugen KE, Srikanthan V, Williams WV, Weiner DB (1993). The galactosyl ceramide/sulfatide receptor binding region of HIV-1 gp120 maps to amino acids 206-275. *AIDS Res Hum Retroviruses* **9:** 175-81.

Bieth E, Gabus C, Darlix JL (1990). A study of the dimer formation of Rous sarcoma virus RNA and of its effect on viral protein synthesis in vitro. *Nucleic Acids Res* **18:** 119-27.

Bigner DD, Bigner SH, Ponten J, Westermark B, Mahaley MS, Ruoslahti E, Herschman H, Eng LF, Wikstrand CJ (1981). Heterogeneity of Genotypic and phenotypic characteristics of fifteen permanent cell lines derived from human gliomas. *J Neuropathol Exp Neurol* **40:** 201-29.

Binder GK, Griffin DE (2003). Immune-mediated clearance of virus from the central nervous system. *Microbes Infect* **5:** 439-48.

Blankson JN, Persaud D, Siliciano RF (2002). The challenge of viral reservoirs in HIV-1 infection. *Annu Rev Med* **53:** 557-93.

Blumberg BM, Gelbard HA, Epstein LG (1994). HIV-1 infection of the developing nervous system: central role of astrocytes in pathogenesis. *Virus Res* **32:** 253-67.

Bomsel M (1997). Transcytosis of infectious human immunodeficiency virus across a tight human epithelial cell line barrier. *Nat Med* **3:** 42-7.

Bonfoco E, Krainc D, Ankarcrona M, Nicotera P, Lipton SA (1995). Apoptosis and necrosis: two distinct events induced, respectively, by mild and intense insults with N-methyl-D-aspartate or nitric oxide/superoxide in cortical cell cultures. *Proc Natl Acad Sci U S A* **92:** 7162-6.

Booss J, Esiri MM (2003). *Viral Encephalitis in Humans*. American Society for Microbiology Press: Washington, D. C.

Botchkina GI, Meistrell ME, 3rd, Botchkina IL, Tracey KJ (1997). Expression of TNF and TNF receptors (p55 and p75) in the rat brain after focal cerebral ischemia. *Mol Med* **3:** 765-81.

Bowerman B, Brown PO, Bishop JM, Varmus HE (1989). A nucleoprotein complex mediates the integration of retroviral DNA. *Genes Dev* **3:** 469-78.

Brack-Werner R (1999). Astrocytes: HIV cellular reservoirs and important participants in neuropathogenesis. *AIDS* **13:** 1-22.

Brack-Werner R, Kleinschmidt A, Ludvigsen A, Mellert W, Neumann M, Herrmann R, Khim MC, Burny A, Muller-Lantzsch N, Stavrou D, et al. (1992). Infection of human brain cells by HIV-1: restricted virus production in chronically infected human glial cell lines. *AIDS* **6:** 273-85.

Brengel-Pesce K, Innocenti-Francillard P, Morand P, Chanzy B, Seigneurin JM (1997). Transient infection of astrocytes with HIV-1 primary isolates derived from patients with and without AIDS dementia complex. *J Neurovirol* **3:** 449-54.

Bretscher MS (1983). Distribution of receptors for transferrin and low density lipoprotein on the surface of giant HeLa cells. *Proc Natl Acad Sci U S A* **80:** 454-8.

Bretscher MS, Thomson JN (1983). Distribution of ferritin receptors and coated pits on giant HeLa cells. *Embo J* **2:** 599-603.

Brew B (2001). AIDS dementia complex. In: *HIV Neurology*. Oxford University Press: New York, pp p53-90.

Brew B (2004). In: *6th International Symposium on Neurovirology*. Journal of Neurovirology: Sardinia, Italy.

Brew BJ, Corbeil J, Pemberton L, Evans L, Saito K, Penny R, Cooper DA, Heyes MP (1995). Quinolinic acid production is related to macrophage tropic isolates of HIV-1. *J Neurovirol* **1:** 369-74.

Brew BJ, Dunbar N, Pemberton L, Kaldor J (1996). Predictive markers of AIDS dementia complex: CD4 cell count and cerebrospinal fluid concentrations of beta 2-microglobulin and neopterin. *J Infect Dis* **174:** 294-8.

Brinkman K, ter Hofstede HJ, Burger DM, Smeitink JA, Koopmans PP (1998). Adverse effects of reverse transcriptase inhibitors: mitochondrial toxicity as common pathway. *AIDS* **12:** 1735-44.

Brodal P, (ed). (1998). *The Central Nervous System. Structure and Function*, 2nd edn. Oxford University Press: New York.

Budka H (1991). The definition of HIV-specific neuropathology. *Acta Pathol Jpn* **41:** 182-91.

Budka H, Wiley CA, Kleihues P, Artigas J, Asbury AK, Cho ES, Cornblath DR, Dal Canto MC, DeGirolami U, Dickson D, et al. (1991). HIV-associated disease of the nervous system: review of nomenclature and proposal for neuropathology-based terminology. *Brain Pathol* **1:** 143-52.

Buee L, Hof PR, Bouras C, Delacourte A, Perl DP, Morrison JH, Fillit HM (1994). Pathological alterations of the cerebral microvasculature in Alzheimer's disease and related dementing disorders. *Acta Neuropathol (Berl)* **87:** 469-80.

Bukovsky AA, Dorfman T, Weimann A, Gottlinger HG (1997). Nef association with human immunodeficiency virus type 1 virions and cleavage by the viral protease. *J Virol* **71:** 1013-8.

Bukrinsky MI, Sharova N, Dempsey MP, Stanwick TL, Bukrinskaya AG, Haggerty S, Stevenson M (1992). Active nuclear import of human immunodeficiency virus type 1 preintegration complexes. *Proc Natl Acad Sci U S A* **89:** 6580-4.

Bukrinsky MI, Sharova N, McDonald TL, Pushkarskaya T, Tarpley WG, Stevenson M (1993). Association of integrase, matrix, and reverse transcriptase antigens of human immunodeficiency virus type 1 with viral nucleic acids following acute infection. *Proc Natl Acad Sci U S A* **90:** 6125-9.

Burkala EJ, He J, West JT, Wood C, Petito CK (2005). Compartmentalization of HIV-1 in the central nervous system: role of the choroid plexus. *AIDS* **19:** 675-84.

Buttke TM, Folks TM (1992). Complete replacement of membrane cholesterol with 4,4',14-trimethyl sterols in a human T cell line defective in lanosterol demethylation. *J Biol Chem* **267:** 8819-26.

Canki M, Potash MJ, Bentsman G, Chao W, Flynn T, Heinemann M, Gelbard H, Volsky DJ (1997). Isolation and long-term culture of primary ocular human immunodeficiency virus type 1 isolates in primary astrocytes. *J Neurovirol* **3:** 10-5.

Canki M, Thai JN, Chao W, Ghorpade A, Potash MJ, Volsky DJ (2001). Highly productive infection with pseudotyped human immunodeficiency virus type 1 (HIV-1) indicates no intracellular restrictions to HIV-1 replication in primary human astrocytes. *J Virol* **75:** 7925-33.

Carr JM, Hocking H, Li P, Burrell CJ (1999). Rapid and efficient cell-to-cell transmission of human immunodeficiency virus infection from monocyte-derived macrophages to peripheral blood lymphocytes. *Virology* **265:** 319-29.

Casey KA, Maurey KM, Storrie B (1986). Characterization of early compartments in fluid phase pinocytosis: a cell fractionation study. *J Cell Sci* **83:** 119-33.

Cavert W, Haase AT (1998). A national tissue bank to track HIV eradication and immune reconstruction. *Science* **280:** 1865-6.

Cavrois M, De Noronha C, Greene WC (2002). A sensitive and specific enzyme-based assay detecting HIV-1 virion fusion in primary T lymphocytes. *Nat Biotechnol* **20:** 1151-4.

Chavrier P, Simons K, Zerial M (1992). The complexity of the Rab and Rho GTP-binding protein subfamilies revealed by a PCR cloning approach. *Gene* **112:** 261-4.

Chen H, Engelman A (1998). The barrier-to-autointegration protein is a host factor for HIV type 1 integration. *Proc Natl Acad Sci U S A* **95:** 15270-4.

Chen H, Wood C, Petito CK (2000). Comparisons of HIV-1 viral sequences in brain, choroid plexus and spleen: potential role of choroid plexus in the pathogenesis of HIV encephalitis. *J Neurovirol* **6:** 498-506.

Chen JW, Cha Y, Yuksel KU, Gracy RW, August JT (1988). Isolation and sequencing of a cDNA clone encoding lysosomal membrane glycoprotein mouse LAMP-1. Sequence similarity to proteins bearing onco-differentiation antigens. *J Biol Chem* **263:** 8754-8.

Cheng J, Nath A, Knudsen B, Hochman S, Geiger JD, Ma M, Magnuson DS (1998). Neuronal excitatory properties of human immunodeficiency virus type 1 Tat protein. *Neuroscience* **82:** 97-106.

Cheng-Mayer C, Rutka JT, Rosenblum ML, McHugh T, Stites DP, Levy JA (1987). Human immunodeficiency virus can productively infect cultured human glial cells. *Proc Natl Acad Sci U S A* **84:** 3526-30.

Cheng-Mayer C, Weiss C, Seto D, Levy JA (1989). Isolates of human immunodeficiency virus type 1 from the brain may constitute a special group of the AIDS virus. *Proc Natl Acad Sci U S A* **86:** 8575-9.

Chesebro B, Buller R, Portis J, Wehrly K (1990). Failure of human immunodeficiency virus entry and infection in CD4-positive human brain and skin cells. *J Virol* **64:** 215-21.

Chiodi F, Britton S, Elovaara I (1996). Conference summary: pathogenic mechanisms of HIV type 1-associated neurological syndromes. *AIDS Res Hum Retroviruses* **12:** 1191-4.

Chiodi F, Fuerstenberg S, Gidlund M, Asjo B, Fenyo EM (1987). Infection of brain-derived cells with the human immunodeficiency virus. *J Virol* **61:** 1244-7.

Chomczynski P, Sacchi N (1987). Single-step method of RNA isolation by acid guanidinium thiocyanate-phenol-chloroform extraction. *Anal Biochem* **162:** 156-9.

Chu Y, Hughes S, Chan-Ling T (2001). Differentiation and migration of astrocyte precursor cells and astrocytes in human fetal retina: relevance to optic nerve coloboma. *Faseb J* **15:** 2013-5.

Chugani DC, Kedersha NL, Rome LH (1991). Vault immunofluorescence in the brain: new insights regarding the origin of microglia. *J Neurosci* **11:** 256-68.

Chun TW, Davey RT, Jr., Engel D, Lane HC, Fauci AS (1999). Re-emergence of HIV after stopping therapy. *Nature* **401:** 874-5.

Chun TW, Davey RT, Jr., Ostrowski M, Shawn Justement J, Engel D, Mullins JI, Fauci AS (2000). Relationship between pre-existing viral reservoirs and the re-emergence of plasma viremia after discontinuation of highly active anti-retroviral therapy. *Nat Med* **6:** 757-61.

Chun TW, Engel D, Berrey MM, Shea T, Corey L, Fauci AS (1998). Early establishment of a pool of latently infected, resting CD4(+) T cells during primary HIV-1 infection. *Proc Natl Acad Sci U S A* **95:** 8869-73.

Chun TW, Finzi D, Margolick J, Chadwick K, Schwartz D, Siliciano RF (1995). In vivo fate of HIV-1-infected T cells: quantitative analysis of the transition to stable latency. *Nat Med* **1:** 1284-90.

Chun TW, Stuyver L, Mizell SB, Ehler LA, Mican JA, Baseler M, Lloyd AL, Nowak MA, Fauci AS (1997). Presence of an inducible HIV-1 latent reservoir during highly active antiretroviral therapy. *Proc Natl Acad Sci U S A* **94:** 13193-7.

Churchill MJ, Gorry PR, Cowley D, Lal L, Sonza S, Purcell DF, Thompson KA, Gabuzda D, McArthur JC, Pardo CA, Wesselingh SL (2006). Use of laser capture microdissection to detect integrated HIV-1 DNA in macrophages and astrocytes from autopsy brain tissues. *J Neurovirol* **12:** 146-52.

Ciardi A, Sinclair E, Scaravilli F, Harcourt-Webster NJ, Lucas S (1990). The involvement of the cerebral cortex in human immunodeficiency virus encephalopathy: a morphological and immunohistochemical study. *Acta Neuropathol (Berl)* **81:** 51-9.

Cinque P, Vago L, Mengozzi M, Torri V, Ceresa D, Vicenzi E, Transidico P, Vagani A, Sozzani S, Mantovani A, Lazzarin A, Poli G (1998). Elevated cerebrospinal fluid levels of monocyte chemotactic protein-1 correlate with HIV-1 encephalitis and local viral replication. *AIDS* **12:** 1327-32.

Clapham PR, Weber JN, Whitby D, McIntosh K, Dalgleish AG, Maddon PJ, Deen KC, Sweet RW, Weiss RA (1989). Soluble CD4 blocks the infectivity of diverse strains of HIV and SIV for T cells and monocytes but not for brain and muscle cells. *Nature* **337:** 368-70.

Clapham PR, Weiss RA (1997). Immunodeficiency viruses. Spoilt for choice of co-receptors. *Nature* **388:** 230-1.

Clarke JN, Lake J, Burrell CJ, Wesselingh SL, Gorry PR, Li P (2006). Novel pathway of human immunodeficiency virus type 1 uptake and release in astrocytes. *Virology* **348:** 141-155.

Claudio L, Raine CS, Brosnan CF (1995). Evidence of persistent blood-brain barrier abnormalities in chronic-progressive multiple sclerosis. *Acta Neuropathol (Berl)* **90:** 228-38.

Clever JL, Eckstein DA, Parslow TG (1999). Genetic dissociation of the encapsidation and reverse transcription functions in the 5' R region of human immunodeficiency virus type 1. *J Virol* **73:** 101-9.

Clever JL, Parslow TG (1997). Mutant human immunodeficiency virus type 1 genomes with defects in RNA dimerization or encapsidation. *J Virol* **71:** 3407-14.

Clouse KA, Powell D, Washington I, Poli G, Strebel K, Farrar W, Barstad P, Kovacs J, Fauci AS, Folks TM (1989). Monokine regulation of human immunodeficiency virus-1 expression in a chronically infected human T cell clone. *J Immunol* **142:** 431-8.

Coates JA, Cammack N, Jenkinson HJ, Jowett AJ, Jowett MI, Pearson BA, Penn CR, Rouse PL, Viner KC, Cameron JM (1992). (-)-2'-deoxy-3'-thiacytidine is a potent, highly selective inhibitor of human immunodeficiency virus type 1 and type 2 replication in vitro. *Antimicrob Agents Chemother* **36:** 733-9.

Coffin J, Haase A, Levy JA, Montagnier L, Oroszlan S, Teich N, Temin H, Toyoshima K, Varmus H, Vogt P, et al. (1986). Human immunodeficiency viruses. *Science* **232:** 697.

Coffin JM, Hughes SH, Varmus HE, (eds). (1997). *Retroviruses*, 1 edn. Cold Spring Harbour Laboratory Press.

Collin M, Gordon S (1994). The kinetics of human immunodeficiency virus reverse transcription are slower in primary human macrophages than in a lymphoid cell line. *Virology* **200:** 114-20.

Collins VP (1983). Cultured human glial and glioma cells. *Int Rev Exp Pathol* **24:** 135-202.

Conant K, Garzino-Demo A, Nath A, McArthur JC, Halliday W, Power C, Gallo RC, Major EO (1998). Induction of monocyte chemoattractant protein-1 in HIV-1 Tat-stimulated astrocytes and elevation in AIDS dementia. *Proc Natl Acad Sci U S A* **95:** 3117-21.

Conner SD, Schmid SL (2003). Regulated portals of entry into the cell. *Nature* **422:** 37-44.

Corvera S (2001). Phosphatidylinositol 3-kinase and the control of endosome dynamics: new players defined by structural motifs. *Traffic* **2:** 859-66.

Cota M, Kleinschmidt A, Ceccherini-Silberstein F, Aloisi F, Mengozzi M, Mantovani A, Brack-Werner R, Poli G (2000). Upregulated expression of interleukin-8, RANTES and chemokine receptors in human astrocytic cells infected with HIV-1. *J Neurovirol* **6:** 75-83.

da Cunha A, Jefferson JJ, Tyor WR, Glass JD, Jannotta FS, Vitkovic L (1993). Control of astrocytosis by interleukin-1 and transforming growth factor-beta 1 in human brain. *Brain Res* **631:** 39-45.

Daher A, Longuet M, Dorin D, Bois F, Segeral E, Bannwarth S, Battisti PL, Purcell DF, Benarous R, Vaquero C, Meurs EF, Gatignol A (2001). Two dimerization domains in

the trans-activation response RNA-binding protein (TRBP) individually reverse the protein kinase R inhibition of HIV-1 long terminal repeat expression. *J Biol Chem* **276:** 33899-905.

Dallasta LM, Pisarov LA, Esplen JE, Werley JV, Moses AV, Nelson JA, Achim CL (1999). Blood-brain barrier tight junction disruption in human immunodeficiency virus-1 encephalitis. *Am J Pathol* **155:** 1915-27.

Dautry-Varsat A (1986). Receptor-mediated endocytosis: the intracellular journey of transferrin and its receptor. *Biochimie* **68:** 375-81.

Davey RT, Jr., Bhat N, Yoder C, Chun TW, Metcalf JA, Dewar R, Natarajan V, Lempicki RA, Adelsberger JW, Miller KD, Kovacs JA, Polis MA, Walker RE, Falloon J, Masur H, Gee D, Baseler M, Dimitrov DS, Fauci AS, Lane HC (1999). HIV-1 and T cell dynamics after interruption of highly active antiretroviral therapy (HAART) in patients with a history of sustained viral suppression. *Proc Natl Acad Sci U S A* **96:** 15109-14.

Davis AJ, Li P, Burrell CJ (1997). Kinetics of viral RNA synthesis following cell-to-cell transmission of human immunodeficiency virus type 1. *J Gen Virol* **78 (Pt 8):** 1897-906.

Davis EJ, Foster TD, Thomas WE (1994). Cellular forms and functions of brain microglia. *Brain Res Bull* **34:** 73-8.

Davis LE, Hjelle BL, Miller VE, Palmer DL, Llewellyn AL, Merlin TL, Young SA, Mills RG, Wachsman W, Wiley CA (1992). Early viral brain invasion in iatrogenic human immunodeficiency virus infection. *Neurology* **42:** 1736-9.

Davis NL, Rueckert RR (1972). Properties of a ribonucleoprotein particle isolated from Nonidet P-40-treated Rous sarcoma virus. *J Virol* **10:** 1010-20.

Dayton AI, Sodroski JG, Rosen CA, Goh WC, Haseltine WA (1986). The trans-activator gene of the human T cell lymphotropic virus type III is required for replication. *Cell* **44:** 941-7.

Deacon NJ, Tsykin A, Solomon A, Smith K, Ludford-Menting M, Hooker DJ, McPhee DA, Greenway AL, Ellett A, Chatfield C, Lawson VA, Crowe S, Maerz A, Sonza S, Learmont J, Sullivan JS, Cunningham A, Dwyer D, Dowton D, Mills J (1995). Genomic structure of an attenuated quasi species of HIV-1 from a blood transfusion donor and recipients. *Science* **270:** 988-91.

Denzer K, Kleijmeer MJ, Heijnen HF, Stoorvogel W, Geuze HJ (2000). Exosome: from internal vesicle of the multivesicular body to intercellular signaling device. *J Cell Sci* **113 Pt 19:** 3365-74.

Depienne C, Mousnier A, Leh H, Le Rouzic E, Dormont D, Benichou S, Dargemont C (2001). Characterization of the nuclear import pathway for HIV-1 integrase. *J Biol Chem* **276:** 18102-7.

Depienne C, Roques P, Creminon C, Fritsch L, Casseron R, Dormont D, Dargemont C, Benichou S (2000). Cellular distribution and karyophilic properties of matrix, integrase,

and Vpr proteins from the human and simian immunodeficiency viruses. *Exp Cell Res* **260:** 387-95.

Dewhurst S, Bresser J, Stevenson M, Sakai K, Evinger-Hodges MJ, Volsky DJ (1987a). Susceptibility of human glial cells to infection with human immunodeficiency virus (HIV). *FEBS Lett* **213:** 138-43.

Dewhurst S, Sakai K, Bresser J, Stevenson M, Evinger-Hodges MJ, Volsky DJ (1987b). Persistent productive infection of human glial cells by human immunodeficiency virus (HIV) and by infectious molecular clones of HIV. *J Virol* **61:** 3774-82.

Dewhurst S, Sakai K, Zhang XH, Wasiak A, Volsky DJ (1988). Establishment of human glial cell lines chronically infected with the human immunodeficiency virus. *Virology* **162:** 151-9.

Dharmawardhane S, Schurmann A, Sells MA, Chernoff J, Schmid SL, Bokoch GM (2000). Regulation of macropinocytosis by p21-activated kinase-1. *Mol Biol Cell* **11:** 3341-52.

Di Rienzo AM, Aloisi F, Santarcangelo AC, Palladino C, Olivetta E, Genovese D, Verani P, Levi G (1998). Virological and molecular parameters of HIV-1 infection of human embryonic astrocytes. *Arch Virol* **143:** 1599-615.

Dichtelmuller H, Rudnick D, Kloft M (2002). Inactivation of lipid enveloped viruses by octanoic Acid treatment of immunoglobulin solution. *Biologicals* **30:** 135-42.

Diop AG, Lesort M, Esclaire F, Dumas M, Hugon J (1995). Calbindin D28K-containing neurons, and not HSP70-expressing neurons, are more resistant to HIV-1 envelope (gp120) toxicity in cortical cell cultures. *J Neurosci Res* **42:** 252-8.

Dore GJ, Correll PK, Li Y, Kaldor JM, Cooper DA, Brew BJ (1999). Changes to AIDS dementia complex in the era of highly active antiretroviral therapy. *AIDS* **13:** 1249-53.

Dornadula G, Zhang H, VanUitert B, Stern J, Livornese L, Jr., Ingerman MJ, Witek J, Kedanis RJ, Natkin J, DeSimone J, Pomerantz RJ (1999). Residual HIV-1 RNA in blood plasma of patients taking suppressive highly active antiretroviral therapy. *Jama* **282:** 1627-32.

Dreyer EB, Kaiser PK, Offermann JT, Lipton SA (1990). HIV-1 coat protein neurotoxicity prevented by calcium channel antagonists. *Science* **248:** 364-7.

East L, Isacke CM (2002). The mannose receptor family. *Biochim Biophys Acta* **1572:** 364-86.

Eddleston M, Mucke L (1993). Molecular profile of reactive astrocytes--implications for their role in neurologic disease. *Neuroscience* **54:** 15-36.

Ehrlich LS, Liu T, Scarlata S, Chu B, Carter CA (2001). HIV-1 capsid protein forms spherical (immature-like) and tubular (mature-like) particles in vitro: structure switching by pH-induced conformational changes. *Biophys J* **81:** 586-94.

Eigen M, Nieselt-Struwe K (1990). How old is the immunodeficiency virus? *AIDS* **4 Suppl 1:** S85-93.

Eng LF, D'Amelio FE, Smith ME (1989). Dissociation of GFAP intermediate filaments in EAE: observations in the lumbar spinal cord. *Glia* **2:** 308-17.

Englund G, Theodore TS, Freed EO, Engelman A, Martin MA (1995). Integration is required for productive infection of monocyte-derived macrophages by human immunodeficiency virus type 1. *J Virol* **69:** 3216-9.

Ensoli F, Cafaro A, Fiorelli V, Vannelli B, Ensoli B, Thiele CJ (1995). HIV-1 infection of primary human neuroblasts. *Virology* **210:** 221-5.

Ensoli F, Wang H, Fiorelli V, Zeichner SL, De Cristofaro MR, Luzi G, Thiele CJ (1997). HIV-1 infection and the developing nervous system: lineage-specific regulation of viral gene expression and replication in distinct neuronal precursors. *J Neurovirol* **3:** 290-8.

Epstein LG, Gendelman HE (1993). Human immunodeficiency virus type 1 infection of the nervous system: pathogenetic mechanisms. *Ann Neurol* **33:** 429-36.

Epstein LG, Kuiken C, Blumberg BM, Hartman S, Sharer LR, Clement M, Goudsmit J (1991). HIV-1 V3 domain variation in brain and spleen of children with AIDS: tissue-specific evolution within host-determined quasispecies. *Virology* **180:** 583-90.

Epstein LG, Sharer LR, Cho ES, Myenhofer M, Navia B, Price RW (1984). HTLV-III/LAV-like retrovirus particles in the brains of patients with AIDS encephalopathy. *AIDS Res* **1:** 447-54.

Esiri MM, McGee JO (1986). Monoclonal antibody to macrophages (EMB/11) labels macrophages and microglial cells in human brain. *J Clin Pathol* **39:** 615-21.

Everall IP, Heaton RK, Marcotte TD, Ellis RJ, McCutchan JA, Atkinson JH, Grant I, Mallory M, Masliah E (1999). Cortical synaptic density is reduced in mild to moderate human immunodeficiency virus neurocognitive disorder. HNRC Group. HIV Neurobehavioral Research Center. *Brain Pathol* **9:** 209-17.

Everall IP, Luthert PJ, Lantos PL (1991). Neuronal loss in the frontal cortex in HIV infection. *Lancet* **337:** 1119-21.

Fackler OT, Peterlin BM (2000). Endocytic entry of HIV-1. *Curr Biol* **10:** 1005-8.

Farnet CM, Bushman FD (1997). HIV-1 cDNA integration: requirement of HMG I(Y) protein for function of preintegration complexes in vitro. *Cell* **88:** 483-92.

Fawcett DW (1965). Surface Specializations of Absorbing Cells. *J Histochem Cytochem* **13:** 75-91.

Febbraio M, Silverstein RL (1990). Identification and characterization of LAMP-1 as an activation-dependent platelet surface glycoprotein. *J Biol Chem* **265:** 18531-7.

Felber BK, Hadzopoulou-Cladaras M, Cladaras C, Copeland T, Pavlakis GN (1989). rev protein of human immunodeficiency virus type 1 affects the stability and transport of the viral mRNA. *Proc Natl Acad Sci U S A* **86:** 1495-9.

Fenyo EM, Albert J, Asjo B (1989). Replicative capacity, cytopathic effect and cell tropism of HIV. *AIDS* **3 Suppl 1:** S5-12.

Ffrench-Constant C, Miller RH, Kruse J, Schachner M, Raff MC (1986). Molecular specialization of astrocyte processes at nodes of Ranvier in rat optic nerve. *J Cell Biol* **102:** 844-52.

Fiala M, Rhodes RH, Shapshak P, Nagano I, Martinez-Maza O, Diagne A, Baldwin G, Graves M (1996). Regulation of HIV-1 infection in astrocytes: expression of Nef, TNF-alpha and IL-6 is enhanced in coculture of astrocytes with macrophages. *J Neurovirol* **2:** 158-66.

Fierz W, Endler B, Reske K, Wekerle H, Fontana A (1985). Astrocytes as antigen-presenting cells. I. Induction of Ia antigen expression on astrocytes by T cells via immune interferon and its effect on antigen presentation. *J Immunol* **134:** 3785-93.

Fine SM, Angel RA, Perry SW, Epstein LG, Rothstein JD, Dewhurst S, Gelbard HA (1996). Tumor necrosis factor alpha inhibits glutamate uptake by primary human astrocytes. Implications for pathogenesis of HIV-1 dementia. *J Biol Chem* **271:** 15303-6.

Finzi D, Blankson J, Siliciano JD, Margolick JB, Chadwick K, Pierson T, Smith K, Lisziewicz J, Lori F, Flexner C, Quinn TC, Chaisson RE, Rosenberg E, Walker B, Gange S, Gallant J, Siliciano RF (1999). Latent infection of CD4+ T cells provides a mechanism for lifelong persistence of HIV-1, even in patients on effective combination therapy. *Nat Med* **5:** 512-7.

Finzi D, Hermankova M, Pierson T, Carruth LM, Buck C, Chaisson RE, Quinn TC, Chadwick K, Margolick J, Brookmeyer R, Gallant J, Markowitz M, Ho DD, Richman DD, Siliciano RF (1997). Identification of a reservoir for HIV-1 in patients on highly active antiretroviral therapy. *Science* **278:** 1295-300.

Fisher AG, Feinberg MB, Josephs SF, Harper ME, Marselle LM, Reyes G, Gonda MA, Aldovini A, Debouk C, Gallo RC, et al. (1986). The trans-activator gene of HTLV-III is essential for virus replication. *Nature* **320:** 367-71.

Flanders KC, Ren RF, Lippa CF (1998). Transforming growth factor-betas in neurodegenerative disease. *Prog Neurobiol* **54:** 71-85.

Foley GE, Lazarus H, Farber S, Uzman BG, Boone BA, McCarthy RE (1965). Continuous Culture of Human Lymphoblasts from Peripheral Blood of a Child with Acute Leukemia. *Cancer* **18:** 522-9.

Folks T, Benn S, Rabson A, Theodore T, Hoggan MD, Martin M, Lightfoote M, Sell K (1985). Characterization of a continuous T-cell line susceptible to the cytopathic effects of the acquired immunodeficiency syndrome (AIDS)-associated retrovirus. *Proc Natl Acad Sci U S A* **82:** 4539-43.

Folks TM, Clouse KA, Justement J, Rabson A, Duh E, Kehrl JH, Fauci AS (1989). Tumor necrosis factor alpha induces expression of human immunodeficiency virus in a chronically infected T-cell clone. *Proc Natl Acad Sci U S A* **86:** 2365-8.

Folks TM, Justement J, Kinter A, Schnittman S, Orenstein J, Poli G, Fauci AS (1988). Characterization of a promonocyte clone chronically infected with HIV and inducible by 13-phorbol-12-myristate acetate. *J Immunol* **140:** 1117-22.

Folks TM, Powell D, Lightfoote M, Koenig S, Fauci AS, Benn S, Rabson A, Daugherty D, Gendelman HE, Hoggan MD, et al. (1986). Biological and biochemical characterization of a cloned Leu-3- cell surviving infection with the acquired immune deficiency syndrome retrovirus. *J Exp Med* **164:** 280-90.

Fontana A, Erb P, Pircher H, Zinkernagel R, Weber E, Fierz W (1986). Astrocytes as antigen-presenting cells. Part II: Unlike H-2K-dependent cytotoxic T cells, H-2Ia-restricted T cells are only stimulated in the presence of interferon-gamma. *J Neuroimmunol* **12:** 15-28.

Fontana A, Fierz W, Wekerle H (1984). Astrocytes present myelin basic protein to encephalitogenic T-cell lines. *Nature* **307:** 273-6.

Fouchier RA, Malim MH (1999). Nuclear import of human immunodeficiency virus type-1 preintegration complexes. *Adv Virus Res* **52:** 275-99.

Fox L, Alford M, Achim C, Mallory M, Masliah E (1997). Neurodegeneration of somatostatin-immunoreactive neurons in HIV encephalitis. *J Neuropathol Exp Neurol* **56:** 360-8.

Fredericksen BL, Wei BL, Yao J, Luo T, Garcia JV (2002). Inhibition of endosomal/lysosomal degradation increases the infectivity of human immunodeficiency virus. *J Virol* **76:** 11440-6.

Frei K, Malipiero UV, Leist TP, Zinkernagel RM, Schwab ME, Fontana A (1989). On the cellular source and function of interleukin 6 produced in the central nervous system in viral diseases. *Eur J Immunol* **19:** 689-94.

Fu DX, Jinno A, Shimizu N, Haraguchi Y, Hoshino H (1999). Isolation and characterization of a monoclonal antibody that inhibits HIV-1 infection. *Microbes Infect* **1:** 677-84.

Furtado MR, Callaway DS, Phair JP, Kunstman KJ, Stanton JL, Macken CA, Perelson AS, Wolinsky SM (1999). Persistence of HIV-1 transcription in peripheral-blood mononuclear cells in patients receiving potent antiretroviral therapy. *N Engl J Med* **340:** 1614-22.

Gadient RA, Otten UH (1997). Interleukin-6 (IL-6)--a molecule with both beneficial and destructive potentials. *Prog Neurobiol* **52:** 379-90.

Gallo RC, Salahuddin SZ, Popovic M, Shearer GM, Kaplan M, Haynes BF, Palker TJ, Redfield R, Oleske J, Safai B, et al. (1984). Frequent detection and isolation of cytopathic retroviruses (HTLV-III) from patients with AIDS and at risk for AIDS. *Science* **224:** 500-3.

Garcia E, Pion M, Pelchen-Matthews A, Collinson L, Arrighi JF, Blot G, Leuba F, Escola JM, Demaurex N, Marsh M, Piguet V (2005). HIV-1 trafficking to the dendritic cell-T-cell infectious synapse uses a pathway of tetraspanin sorting to the immunological synapse. *Traffic* **6:** 488-501.

Garcia JV, Miller AD (1991). Serine phosphorylation-independent downregulation of cell-surface CD4 by nef. *Nature* **350:** 508-11.

Gartner S (2000). HIV infection and dementia. *Science* **287:** 602-4.

Gartner S, Markovits P, Markovitz DM, Betts RF, Popovic M (1986). Virus isolation from and identification of HTLV-III/LAV-producing cells in brain tissue from a patient with AIDS. *Jama* **256:** 2365-71.

Gasque P, Chan P, Fontaine M, Ischenko A, Lamacz M, Gotze O, Morgan BP (1995). Identification and characterization of the complement C5a anaphylatoxin receptor on human astrocytes. *J Immunol* **155:** 4882-9.

Gasque P, Singhrao SK, Neal JW, Wang P, Sayah S, Fontaine M, Morgan BP (1998). The receptor for complement anaphylatoxin C3a is expressed by myeloid cells and nonmyeloid cells in inflamed human central nervous system: analysis in multiple sclerosis and bacterial meningitis. *J Immunol* **160:** 3543-54.

Gazdar AF, Carney DN, Bunn PA, Russell EK, Jaffe ES, Schechter GP, Guccion JG (1980). Mitogen requirements for the in vitro propagation of cutaneous T-cell lymphomas. *Blood* **55:** 409-17.

Gehrmann J, Matsumoto Y, Kreutzberg GW (1995). Microglia: intrinsic immuneffector cell of the brain. *Brain Res Brain Res Rev* **20:** 269-87.

Geijtenbeek TB, Torensma R, van Vliet SJ, van Duijnhoven GC, Adema GJ, van Kooyk Y, Figdor CG (2000). Identification of DC-SIGN, a novel dendritic cell-specific ICAM-3 receptor that supports primary immune responses. *Cell* **100:** 575-85.

Gelman BB, Soukup VM, Schuenke KW, Keherly MJ, Holzer C, 3rd, Richey FJ, Lahart CJ (2004). Acquired neuronal channelopathies in HIV-associated dementia. *J Neuroimmunol* **157:** 111-9.

Genis P, Jett M, Bernton EW, Boyle T, Gelbard HA, Dzenko K, Keane RW, Resnick L, Mizrachi Y, Volsky DJ, et al. (1992). Cytokines and arachidonic metabolites produced during human immunodeficiency virus (HIV)-infected macrophage-astroglia interactions: implications for the neuropathogenesis of HIV disease. *J Exp Med* **176:** 1703-18.

Giangaspero F, Scanabissi E, Baldacci MC, Betts CM (1989). Massive neuronal destruction in human immunodeficiency virus (HIV) encephalitis. A clinico-pathological study of a pediatric case. *Acta Neuropathol (Berl)* **78:** 662-5.

Giulian D, Baker TJ (1986). Characterization of ameboid microglia isolated from developing mammalian brain. *J Neurosci* **6:** 2163-78.

Giulian D, Baker TJ, Shih LC, Lachman LB (1986). Interleukin 1 of the central nervous system is produced by ameboid microglia. *J Exp Med* **164:** 594-604.

Giulian D, Corpuz M, Richmond B, Wendt E, Hall ER (1996a). Activated microglia are the principal glial source of thromboxane in the central nervous system. *Neurochem Int* **29:** 65-76.

Giulian D, Li J, Bartel S, Broker J, Li X, Kirkpatrick JB (1995). Cell surface morphology identifies microglia as a distinct class of mononuclear phagocyte. *J Neurosci* **15:** 7712-26.

Giulian D, Vaca K, Noonan CA (1990). Secretion of neurotoxins by mononuclear phagocytes infected with HIV-1. *Science* **250:** 1593-6.

Giulian D, Wendt E, Vaca K, Noonan CA (1993). The envelope glycoprotein of human immunodeficiency virus type 1 stimulates release of neurotoxins from monocytes. *Proc Natl Acad Sci U S A* **90:** 2769-73.

Giulian D, Yu J, Li X, Tom D, Li J, Wendt E, Lin SN, Schwarcz R, Noonan C (1996b). Study of receptor-mediated neurotoxins released by HIV-1-infected mononuclear phagocytes found in human brain. *J Neurosci* **16:** 3139-53.

Glass JD, Fedor H, Wesselingh SL, McArthur JC (1995). Immunocytochemical quantitation of human immunodeficiency virus in the brain: correlations with dementia. *Ann Neurol* **38:** 755-62.

Glass JD, Wesselingh SL, Selnes OA, McArthur JC (1993). Clinical-neuropathologic correlation in HIV-associated dementia. *Neurology* **43:** 2230-7.

Gonda MA, Wong-Staal F, Gallo RC, Clements JE, Narayan O, Gilden RV (1985). Sequence homology and morphologic similarity of HTLV-III and visna virus, a pathogenic lentivirus. *Science* **227:** 173-7.

Gorry P, Purcell D, Howard J, McPhee D (1998). Restricted HIV-1 infection of human astrocytes: potential role of nef in the regulation of virus replication. *J Neurovirol* **4:** 377-86.

Gorry PR, Howard JL, Churchill MJ, Anderson JL, Cunningham A, Adrian D, McPhee DA, Purcell DF (1999). Diminished production of human immunodeficiency virus type 1 in astrocytes results from inefficient translation of gag, env, and nef mRNAs despite efficient expression of Tat and Rev. *J Virol* **73:** 352-61.

Gorry PR, Ong C, Thorpe J, Bannwarth S, Thompson KA, Gatignol A, Wesselingh SL, Purcell DF (2003). Astrocyte infection by HIV-1: mechanisms of restricted virus replication, and role in the pathogenesis of HIV-1-associated dementia. *Curr HIV Res* **1:** 463-73.

Gotte M, Li X, Wainberg MA (1999). HIV-1 reverse transcription: a brief overview focused on structure-function relationships among molecules involved in initiation of the reaction. *Arch Biochem Biophys* **365:** 199-210.

Gray F, Gherardi R, Scaravilli F (1988). The neuropathology of the acquired immune deficiency syndrome (AIDS). A review. *Brain* **111 (Pt 2):** 245-66.

Gray F, Haug H, Chimelli L, Geny C, Gaston A, Scaravilli F, Budka H (1991). Prominent cortical atrophy with neuronal loss as correlate of human immunodeficiency virus encephalopathy. *Acta Neuropathol (Berl)* **82:** 229-33.

Greene WC (1991). The molecular biology of human immunodeficiency virus type 1 infection. *N Engl J Med* **324:** 308-17.

Grewe C, Beck A, Gelderblom HR (1990). HIV: early virus-cell interactions. *J Acquir Immune Defic Syndr* **3:** 965-74.

Griffin DE, Hess JL, Moench TR (1987). Immune responses in the central nervous system. *Toxicol Pathol* **15:** 294-302.

Grist NR, Ross CA, Bell EJ, (eds). (1974). *Diagnostic Methods in Clinical Virology*, 2nd edn. Blackwell Scientific Publications: Oxford.

Guillemin GJ, Croitoru-Lamoury J, Dormont D, Armati PJ, Brew BJ (2003). Quinolinic acid upregulates chemokine production and chemokine receptor expression in astrocytes. *Glia* **41:** 371-81.

Gunthard HF, Frost SD, Leigh-Brown AJ, Ignacio CC, Kee K, Perelson AS, Spina CA, Havlir DV, Hezareh M, Looney DJ, Richman DD, Wong JK (1999). Evolution of envelope sequences of human immunodeficiency virus type 1 in cellular reservoirs in the setting of potent antiviral therapy. *J Virol* **73:** 9404-12.

Gupta P, Balachandran R, Ho M, Enrico A, Rinaldo C (1989). Cell-to-cell transmission of human immunodeficiency virus type 1 in the presence of azidothymidine and neutralizing antibody. *J Virol* **63:** 2361-5.

Guy B, Kieny MP, Riviere Y, Le Peuch C, Dott K, Girard M, Montagnier L, Lecocq JP (1987). HIV F/3' orf encodes a phosphorylated GTP-binding protein resembling an oncogene product. *Nature* **330:** 266-9.

Haase AT (1986). Pathogenesis of lentivirus infections. *Nature* **322:** 130-6.

Hammarskjold ML, Heimer J, Hammarskjold B, Sangwan I, Albert L, Rekosh D (1989). Regulation of human immunodeficiency virus env expression by the rev gene product. *J Virol* **63:** 1959-66.

Hao HN, Chiu FC, Losev L, Weidenheim KM, Rashbaum WK, Lyman WD (1997). HIV infection of human fetal neural cells is mediated by gp120 binding to a cell membrane-associated molecule that is not CD4 nor galactocerebroside. *Brain Res* **764:** 149-57.

Hao HN, Lyman WD (1999). HIV infection of fetal human astrocytes: the potential role of a receptor-mediated endocytic pathway. *Brain Res* **823:** 24-32.

Harouse JM, Bhat S, Spitalnik SL, Laughlin M, Stefano K, Silberberg DH, Gonzalez-Scarano F (1991). Inhibition of entry of HIV-1 in neural cell lines by antibodies against galactosyl ceramide. *Science* **253:** 320-3.

Harouse JM, Kunsch C, Hartle HT, Laughlin MA, Hoxie JA, Wigdahl B, Gonzalez-Scarano F (1989). CD4-independent infection of human neural cells by human immunodeficiency virus type 1. *J Virol* **63:** 2527-33.

Harrigan PR, Whaley M, Montaner JS (1999). Rate of HIV-1 RNA rebound upon stopping antiretroviral therapy. *AIDS* **13:** F59-62.

Harris RS, Bishop KN, Sheehy AM, Craig HM, Petersen-Mahrt SK, Watt IN, Neuberger MS, Malim MH (2003). DNA deamination mediates innate immunity to retroviral infection. *Cell* **113:** 803-9.

Hartley CA, Gilbert MJ, Brigido L, Elbeik T, Levy JA, Crowe SM, Mills J (1996). Human immunodeficiency virus grown in CD4-expressing cells is associated with CD4. *J Gen Virol* **77 (Pt 9):** 2015-23.

Hazuda DJ, Felock P, Witmer M, Wolfe A, Stillmock K, Grobler JA, Espeseth A, Gabryelski L, Schleif W, Blau C, Miller MD (2000). Inhibitors of strand transfer that prevent integration and inhibit HIV-1 replication in cells. *Science* **287:** 646-50.

Henneke P, Golenbock DT (2004). Phagocytosis, innate immunity, and host-pathogen specificity. *J Exp Med* **199:** 1-4.

Henrich-Noack P, Prehn JH, Krieglstein J (1994). Neuroprotective effects of TGF-beta 1. *J Neural Transm Suppl* **43:** 33-45.

Herrmann CH, Carroll RG, Wei P, Jones KA, Rice AP (1998). Tat-associated kinase, TAK, activity is regulated by distinct mechanisms in peripheral blood lymphocytes and promonocytic cell lines. *J Virol* **72:** 9881-8.

Hesselgesser J, Halks-Miller M, DelVecchio V, Peiper SC, Hoxie J, Kolson DL, Taub D, Horuk R (1997). CD4-independent association between HIV-1 gp120 and CXCR4: functional chemokine receptors are expressed in human neurons. *Curr Biol* **7:** 112-21.

Hesselgesser J, Horuk R (1999). Chemokine and chemokine receptor expression in the central nervous system. *J Neurovirol* **5:** 13-26.

Hewlett LJ, Prescott AR, Watts C (1994). The coated pit and macropinocytic pathways serve distinct endosome populations. *J Cell Biol* **124:** 689-703.

Heyes MP, Brew BJ, Martin A, Price RW, Salazar AM, Sidtis JJ, Yergey JA, Mouradian MM, Sadler AE, Keilp J, et al. (1991). Quinolinic acid in cerebrospinal fluid and serum in HIV-1 infection: relationship to clinical and neurological status. *Ann Neurol* **29:** 202-9.

Hickey WF (1991). Migration of hematogenous cells through the blood-brain barrier and the initiation of CNS inflammation. *Brain Pathol* **1:** 97-105.

Hirt B (1967). Selective extraction of polyoma DNA from infected mouse cell cultures. *J Mol Biol* **26:** 365-9.

Ho WZ, Cherukuri R, Ge SD, Cutilli JR, Song L, Whitko S, Douglas SD (1993). Centrifugal enhancement of human immunodeficiency virus type 1 infection and human cytomegalovirus gene expression in human primary monocyte/macrophages in vitro. *J Leukoc Biol* **53:** 208-12.

Hocini H, Becquart P, Bouhlal H, Chomont N, Ancuta P, Kazatchkine MD, Belec L (2001). Active and selective transcytosis of cell-free human immunodeficiency virus through a tight polarized monolayer of human endometrial cells. *J Virol* **75:** 5370-4.

Hocini H, Bomsel M (1999). Infectious human immunodeficiency virus can rapidly penetrate a tight human epithelial barrier by transcytosis in a process impaired by mucosal immunoglobulins. *J Infect Dis* **179 Suppl 3:** S448-53.

Hofman FM, Dohadwala MM, Wright AD, Hinton DR, Walker SM (1994). Exogenous tat protein activates central nervous system-derived endothelial cells. *J Neuroimmunol* **54:** 19-28.

Holmes EC (2001). On the origin and evolution of the human immunodeficiency virus (HIV). *Biol Rev Camb Philos Soc* **76:** 239-54.

Hori K, Burd PR, Kutza J, Weih KA, Clouse KA (1999). Human astrocytes inhibit HIV-1 expression in monocyte-derived macrophages by secreted factors. *AIDS* **13:** 751-8.

Hu WS, Temin HM (1990). Retroviral recombination and reverse transcription. *Science* **250:** 1227-33.

Huang MB, Weeks O, Zhao LJ, Saltarelli M, Bond VC (2000). Effects of extracellular human immunodeficiency virus type 1 vpr protein in primary rat cortical cell cultures. *J Neurovirol* **6:** 202-20.

Hughes ES, Bell JE, Simmonds P (1997). Investigation of the dynamics of the spread of human immunodeficiency virus to brain and other tissues by evolutionary analysis of sequences from the p17gag and env genes. *J Virol* **71:** 1272-80.

Iadecola C (1992). Does nitric oxide mediate the increases in cerebral blood flow elicited by hypercapnia? *Proc Natl Acad Sci U S A* **89:** 3913-6.

Ilyin SE, Plata-Salaman CR (1997). HIV-1 envelope glycoprotein 120 regulates brain IL-1beta system and TNF-alpha mRNAs in vivo. *Brain Res Bull* **44:** 67-73.

Imamichi H, Crandall KA, Natarajan V, Jiang MK, Dewar RL, Berg S, Gaddam A, Bosche M, Metcalf JA, Davey RT, Jr., Lane HC (2001). Human immunodeficiency virus type 1 quasi species that rebound after discontinuation of highly active antiretroviral therapy are similar to the viral quasi species present before initiation of therapy. *J Infect Dis* **183:** 36-50.

Inoue H, Nojima H, Okayama H (1990). High efficiency transformation of Escherichia coli with plasmids. *Gene* **96:** 23-8.

Irani DN, Griffin DE (1996). Regulation of lymphocyte homing into the brain during viral encephalitis at various stages of infection. *J Immunol* **156:** 3850-7.

Irani DN, Lin KI, Griffin DE (1996). Brain-derived gangliosides regulate the cytokine production and proliferation of activated T cells. *J Immunol* **157:** 4333-40.

James W, Weiss RA, Simon JH (1996). The receptor for HIV: dissection of CD4 and studies on putative accessory factors. *Curr Top Microbiol Immunol* **205:** 137-58.

Janeway CA, Jr. (1989). Approaching the asymptote? Evolution and revolution in immunology. *Cold Spring Harb Symp Quant Biol* **54 Pt 1:** 1-13.

Janzer RC, Raff MC (1987). Astrocytes induce blood-brain barrier properties in endothelial cells. *Nature* **325:** 253-7.

Johnson RT, McArthur JC, Narayan O (1988). The neurobiology of human immunodeficiency virus infections. *Faseb J* **2:** 2970-81.

Jurka J, Smith T (1988). A fundamental division in the Alu family of repeated sequences. *Proc Natl Acad Sci U S A* **85:** 4775-8.

Kakuda TN (2000). Pharmacology of nucleoside and nucleotide reverse transcriptase inhibitor-induced mitochondrial toxicity. *Clin Ther* **22:** 685-708.

Kandel ER, Schwartz JH, Jessell TM (1991). *Principles of Neural Science*, 2 edn. Elsevier: New York.

Kao S, Akari H, Khan MA, Dettenhofer M, Yu XF, Strebel K (2003). Human immunodeficiency virus type 1 Vif is efficiently packaged into virions during productive but not chronic infection. *J Virol* **77:** 1131-40.

Karageorgos L, Li P, Burrell C (1993). Characterization of HIV replication complexes early after cell-to-cell infection. *AIDS Res Hum Retroviruses* **9:** 817-23.

Karageorgos L, Li P, Burrell CJ (1995). Stepwise analysis of reverse transcription in a cell-to-cell human immunodeficiency virus infection model: kinetics and implications. *J Gen Virol* **76 (Pt 7):** 1675-86.

Kaul M, Lipton SA (1999). Chemokines and activated macrophages in HIV gp120-induced neuronal apoptosis. *Proc Natl Acad Sci U S A* **96:** 8212-6.

Kelder W, McArthur JC, Nance-Sproson T, McClernon D, Griffin DE (1998). Beta-chemokines MCP-1 and RANTES are selectively increased in cerebrospinal fluid of patients with human immunodeficiency virus-associated dementia. *Ann Neurol* **44:** 831-5.

Keys B, Albert J, Kovamees J, Chiodi F (1991). Brain-derived cells can be infected with HIV isolates derived from both blood and brain. *Virology* **183:** 834-9.

Keys B, Karis J, Fadeel B, Valentin A, Norkrans G, Hagberg L, Chiodi F (1993). V3 sequences of paired HIV-1 isolates from blood and cerebrospinal fluid cluster according to host and show variation related to the clinical stage of disease. *Virology* **196:** 475-83.

Khan MA, Aberham C, Kao S, Akari H, Gorelick R, Bour S, Strebel K (2001). Human immunodeficiency virus type 1 Vif protein is packaged into the nucleoprotein complex through an interaction with viral genomic RNA. *J Virol* **75:** 7252-65.

Kim SY, Byrn R, Groopman J, Baltimore D (1989). Temporal aspects of DNA and RNA synthesis during human immunodeficiency virus infection: evidence for differential gene expression. *J Virol* **63:** 3708-13.

Kimelberg HK, Norenberg MD (1989). Astrocytes. *Sci Am* **260:** 66-72, 74, 76.

Kirchhoff F, Greenough TC, Brettler DB, Sullivan JL, Desrosiers RC (1995). Brief report: absence of intact nef sequences in a long-term survivor with nonprogressive HIV-1 infection. *N Engl J Med* **332:** 228-32.

Kleijmeer MJ, Morkowski S, Griffith JM, Rudensky AY, Geuze HJ (1997). Major histocompatibility complex class II compartments in human and mouse B lymphoblasts represent conventional endocytic compartments. *J Cell Biol* **139:** 639-49.

Kleijmeer MJ, Raposo G, Geuze HJ (1996). Characterization of MHC Class II Compartments by Immunoelectron Microscopy. *Methods* **10:** 191-207.

Klein RS, Williams KC, Alvarez-Hernandez X, Westmoreland S, Force T, Lackner AA, Luster AD (1999). Chemokine receptor expression and signaling in macaque and human fetal neurons and astrocytes: implications for the neuropathogenesis of AIDS. *J Immunol* **163:** 1636-46.

Kleinschmidt A, Neumann M, Moller C, Erfle V, Brack-Werner R (1994). Restricted expression of HIV1 in human astrocytes: molecular basis for viral persistence in the CNS. *Res Virol* **145:** 147-53.

Klotman ME, Kim S, Buchbinder A, DeRossi A, Baltimore D, Wong-Staal F (1991). Kinetics of expression of multiply spliced RNA in early human immunodeficiency virus type 1 infection of lymphocytes and monocytes. *Proc Natl Acad Sci U S A* **88:** 5011-5.

Knipe DM, Howley PM, (eds). (2001). *Fields Virology*, Vol.2, 4th edn. Lippincott Williams & Wilkins: Philadelphia.

Koenig S, Gendelman HE, Orenstein JM, Dal Canto MC, Pezeshkpour GH, Yungbluth M, Janotta F, Aksamit A, Martin MA, Fauci AS (1986). Detection of AIDS virus in macrophages in brain tissue from AIDS patients with encephalopathy. *Science* **233:** 1089-93.

Kohleisen B, Neumann M, Herrmann R, Brack-Werner R, Krohn KJ, Ovod V, Ranki A, Erfle V (1992). Cellular localization of Nef expressed in persistently HIV-1-infected low-producer astrocytes. *AIDS* **6:** 1427-36.

Kohleisen B, Shumay E, Sutter G, Foerster R, Brack-Werner R, Nuesse M, Erfle V (1999). Stable expression of HIV-1 Nef induces changes in growth properties and activation state of human astrocytes. *AIDS* **13:** 2331-41.

Kok TW, Li P, Burrell CJ (1998). Further characterization of HIV RNA synthesis early after cell-to-cell transmission infection. *Arch Virol* **143:** 1911-26.

Kolson DL, Lavi E, Gonzalez-Scarano F (1998). The effects of human immunodeficiency virus in the central nervous system. *Adv Virus Res* **50:** 1-47.

Korber BT, Kunstman KJ, Patterson BK, Furtado M, McEvilly MM, Levy R, Wolinsky SM (1994). Genetic differences between blood- and brain-derived viral sequences from human immunodeficiency virus type 1-infected patients: evidence of conserved elements in the V3 region of the envelope protein of brain-derived sequences. *J Virol* **68:** 7467-81.

Korin YD, Zack JA (1998). Progression to the G1b phase of the cell cycle is required for completion of human immunodeficiency virus type 1 reverse transcription in T cells. *J Virol* **72:** 3161-8.

Kornfeld S, Mellman I (1989). The biogenesis of lysosomes. *Annu Rev Cell Biol* **5:** 483-525.

Kort JJ (1998). Impairment of excitatory amino acid transport in astroglial cells infected with the human immunodeficiency virus type 1. *AIDS Res Hum Retroviruses* **14:** 1329-39.

Kort JJ, Jalonen TO (1998). The nef protein of the human immunodeficiency virus type 1 (HIV-1) inhibits a large-conductance potassium channel in human glial cells. *Neurosci Lett* **251:** 1-4.

Kreutzberg GW (1996). Microglia: a sensor for pathological events in the CNS. *Trends Neurosci* **19:** 312-8.

Kumar R, Vandegraaff N, Mundy L, Burrell CJ, Li P (2002). Evaluation of PCR-based methods for the quantitation of integrated HIV-1 DNA. *J Virol Methods* **105:** 233-46.

Kure K, Lyman WD, Weidenheim KM, Dickson DW (1990). Cellular localization of an HIV-1 antigen in subacute AIDS encephalitis using an improved double-labeling immunohistochemical method. *Am J Pathol* **136:** 1085-92.

Kutsch O, Oh J, Nath A, Benveniste EN (2000). Induction of the chemokines interleukin-8 and IP-10 by human immunodeficiency virus type 1 tat in astrocytes. *J Virol* **74:** 9214-21.

Lacy M, Jones J, Whittemore SR, Haviland DL, Wetsel RA, Barnum SR (1995). Expression of the receptors for the C5a anaphylatoxin, interleukin-8 and FMLP by human astrocytes and microglia. *J Neuroimmunol* **61:** 71-8.

LaFemina RL, Schneider CL, Robbins HL, Callahan PL, LeGrow K, Roth E, Schleif WA, Emini EA (1992). Requirement of active human immunodeficiency virus type 1 integrase enzyme for productive infection of human T-lymphoid cells. *J Virol* **66:** 7414-9.

Lafrenie RM, Wahl LM, Epstein JS, Hewlett IK, Yamada KM, Dhawan S (1996). HIV-1-Tat modulates the function of monocytes and alters their interactions with microvessel endothelial cells. A mechanism of HIV pathogenesis. *J Immunol* **156:** 1638-45.

Laming PR (1989). Do glia contribute to behaviour? A neuromodulatory review. *Comp Biochem Physiol A* **94:** 555-68.

Lassmann H (1997). Basic mechanisms of brain inflammation. *J Neural Transm Suppl* **50:** 183-90.

Lavi E, Strizki JM, Ulrich AM, Zhang W, Fu L, Wang Q, O'Connor M, Hoxie JA, Gonzalez-Scarano F (1997). CXCR-4 (Fusin), a co-receptor for the type 1 human immunodeficiency virus (HIV-1), is expressed in the human brain in a variety of cell types, including microglia and neurons. *Am J Pathol* **151:** 1035-42.

Lawrence DM, Durham LC, Schwartz L, Seth P, Maric D, Major EO (2004). Human immunodeficiency virus type 1 infection of human brain-derived progenitor cells. *J Virol* **78:** 7319-28.

Lawson LJ, Perry VH, Dri P, Gordon S (1990). Heterogeneity in the distribution and morphology of microglia in the normal adult mouse brain. *Neuroscience* **39:** 151-70.

Layne SP, Merges MJ, Dembo M, Spouge JL, Conley SR, Moore JP, Raina JL, Renz H, Gelderblom HR, Nara PL (1992). Factors underlying spontaneous inactivation and susceptibility to neutralization of human immunodeficiency virus. *Virology* **189:** 695-714.

Lecossier D, Bouchonnet F, Clavel F, Hance AJ (2003). Hypermutation of HIV-1 DNA in the absence of the Vif protein. *Science* **300:** 1112.

Lee SC, Liu W, Dickson DW, Brosnan CF, Berman JW (1993). Cytokine production by human fetal microglia and astrocytes. Differential induction by lipopolysaccharide and IL-1 beta. *J Immunol* **150:** 2659-67.

Levine B, Goldman JE, Jiang HH, Griffin DE, Hardwick JM (1996). Bc1-2 protects mice against fatal alphavirus encephalitis. *Proc Natl Acad Sci U S A* **93:** 4810-5.

Levine B, Griffin DE (1992). Persistence of viral RNA in mouse brains after recovery from acute alphavirus encephalitis. *J Virol* **66:** 6429-35.

Levine B, Hardwick JM, Griffin DE (1994). Persistence of alphaviruses in vertebrate hosts. *Trends Microbiol* **2:** 25-8.

Levy JA (1998). *HIV and the Pathogenesis of AIDS*, 2nd edn. American Society for Microbiology: Washington, D. C.

Levy JA, Hoffman AD, Kramer SM, Landis JA, Shimabukuro JM, Oshiro LS (1984). Isolation of lymphocytopathic retroviruses from San Francisco patients with AIDS. *Science* **225:** 840-2.

Levy JA, Rowe WP (1971). Lack of requirement of murine leukemia virus for early steps in infection of mouse embryo cells by murine sarcoma virus. *Virology* **45:** 844-7.

Lew DB, Songu-Mize E, Pontow SE, Stahl PD, Rattazzi MC (1994). A mannose receptor mediates mannosyl-rich glycoprotein-induced mitogenesis in bovine airway smooth muscle cells. *J Clin Invest* **94:** 1855-63.

Lewis W, Day BJ, Copeland WC (2003). Mitochondrial toxicity of NRTI antiviral drugs: an integrated cellular perspective. *Nat Rev Drug Discov* **2:** 812-22.

Li G, Simm M, Potash MJ, Volsky DJ (1993a). Human immunodeficiency virus type 1 DNA synthesis, integration, and efficient viral replication in growth-arrested T cells. *J Virol* **67:** 3969-77.

Li J, Liu Y, Kim BO, He JJ (2002a). Direct participation of Sam68, the 68-kilodalton Src-associated protein in mitosis, in the CRM1-mediated Rev nuclear export pathway. *J Virol* **76:** 8374-82.

Li J, Liu Y, Park IW, He JJ (2002b). Expression of exogenous Sam68, the 68-kilodalton SRC-associated protein in mitosis, is able to alleviate impaired Rev function in astrocytes. *J Virol* **76:** 4526-35.

Li L, Yoder K, Hansen MS, Olvera J, Miller MD, Bushman FD (2000). Retroviral cDNA integration: stimulation by HMG I family proteins. *J Virol* **74:** 10965-74.

Li P, Burrell CJ (1992). Synthesis of human immunodeficiency virus DNA in a cell-to-cell transmission model. *AIDS Res Hum Retroviruses* **8:** 253-9.

Li P, Kuiper LJ, Stephenson AJ, Burrell CJ (1992). De novo reverse transcription is a crucial event in cell-to-cell transmission of human immunodeficiency virus. *J Gen Virol* **73 (Pt 4):** 955-9.

Li P, Stephenson AJ, Brennan PA, Karageorgos L, Kok T, Kuiper LJ, Swift J, Burrell CJ (1994). Initiation of reverse transcription during cell-to-cell transmission of human immunodeficiency virus infection uses pre-existing reverse transcriptase. *J Gen Virol* **75 (Pt 8):** 1917-26.

Li P, Stephenson AJ, Kuiper LJ, Burrell CJ (1993b). Double-stranded strong-stop DNA and the second template switch in human immunodeficiency virus (HIV) DNA synthesis. *Virology* **194:** 82-8.

Liang C, Hu J, Russell RS, Kameoka M, Wainberg MA (2004). Spliced human immunodeficiency virus type 1 RNA is reverse transcribed into cDNA within infected cells. *AIDS Res Hum Retroviruses* **20:** 203-11.

Lindsberg PJ, Ohman J, Lehto T, Karjalainen-Lindsberg ML, Paetau A, Wuorimaa T, Carpen O, Kaste M, Meri S (1996). Complement activation in the central nervous system following blood-brain barrier damage in man. *Ann Neurol* **40:** 587-96.

Linehan SA, Martinez-Pomares L, Stahl PD, Gordon S (1999). Mannose receptor and its putative ligands in normal murine lymphoid and nonlymphoid organs: In situ expression of mannose receptor by selected macrophages, endothelial cells, perivascular microglia, and mesangial cells, but not dendritic cells. *J Exp Med* **189:** 1961-72.

Linskey ME (1997). Glial ontogeny and glial neoplasia: the search for closure. *J Neurooncol* **34:** 5-22.

Lipton SA (1993). Human immunodeficiency virus-infected macrophages, gp120, and N-methyl-D-aspartate receptor-mediated neurotoxicity. *Ann Neurol* **33:** 227-8.

Lipton SA (1994). AIDS-related dementia and calcium homeostasis. *Ann N Y Acad Sci* **747:** 205-24.

Lipton SA, Gendelman HE (1995). Seminars in medicine of the Beth Israel Hospital, Boston. Dementia associated with the acquired immunodeficiency syndrome. *N Engl J Med* **332:** 934-40.

Lipton SA, Sucher NJ, Kaiser PK, Dreyer EB (1991). Synergistic effects of HIV coat protein and NMDA receptor-mediated neurotoxicity. *Neuron* **7:** 111-8.

Lisziewicz J, Jessen H, Finzi D, Siliciano RF, Lori F (1998). HIV-1 suppression by early treatment with hydroxyurea, didanosine, and a protease inhibitor. *Lancet* **352:** 199-200.

Liu H, Wu X, Newman M, Shaw GM, Hahn BH, Kappes JC (1995). The Vif protein of human and simian immunodeficiency viruses is packaged into virions and associates with viral core structures. *J Virol* **69:** 7630-8.

Liu J, Zhao ML, Brosnan CF, Lee SC (1996). Expression of type II nitric oxide synthase in primary human astrocytes and microglia: role of IL-1beta and IL-1 receptor antagonist. *J Immunol* **157:** 3569-76.

Liu NQ, Lossinsky AS, Popik W, Li X, Gujuluva C, Kriederman B, Roberts J, Pushkarsky T, Bukrinsky M, Witte M, Weinand M, Fiala M (2002). Human immunodeficiency virus type 1 enters brain microvascular endothelia by macropinocytosis dependent on lipid rafts and the mitogen-activated protein kinase signaling pathway. *J Virol* **76:** 6689-700.

Liu Y, Jones M, Hingtgen CM, Bu G, Laribee N, Tanzi RE, Moir RD, Nath A, He JJ (2000). Uptake of HIV-1 tat protein mediated by low-density lipoprotein receptor-related protein disrupts the neuronal metabolic balance of the receptor ligands. *Nat Med* **6:** 1380-7.

Liu Y, Liu H, Kim BO, Gattone VH, Li J, Nath A, Blum J, He JJ (2004). CD4-independent infection of astrocytes by human immunodeficiency virus type 1: requirement for the human mannose receptor. *J Virol* **78:** 4120-33.

Lopez-Herrera A, Liu Y, Rugeles MT, He JJ (2005). HIV-1 interaction with human mannose receptor (hMR) induces production of matrix metalloproteinase 2 (MMP-2) through hMR-mediated intracellular signaling in astrocytes. *Biochim Biophys Acta* **1741:** 55-64.

Lori F, di Marzo Veronese F, de Vico AL, Lusso P, Reitz MS, Jr., Gallo RC (1992). Viral DNA carried by human immunodeficiency virus type 1 virions. *J Virol* **66:** 5067-74.

Lori F, Jessen H, Lieberman J, Finzi D, Rosenberg E, Tinelli C, Walker B, Siliciano RF, Lisziewicz J (1999). Treatment of human immunodeficiency virus infection with hydroxyurea, didanosine, and a protease inhibitor before seroconversion is associated with normalized immune parameters and limited viral reservoir. *J Infect Dis* **180:** 1827-32.

Luban J, Goff SP (1994). Mutational analysis of cis-acting packaging signals in human immunodeficiency virus type 1 RNA. *J Virol* **68:** 3784-93.

Ludwig E, Silberstein FC, van Empel J, Erfle V, Neumann M, Brack-Werner R (1999). Diminished rev-mediated stimulation of human immunodeficiency virus type 1 protein synthesis is a hallmark of human astrocytes. *J Virol* **73:** 8279-89.

Luo T, Foster JL, Garcia JV (1997). Molecular Determinants of Nef Function. *J Biomed Sci* **4:** 132-138.

Ma M, Geiger JD, Nath A (1994). Characterization of a novel binding site for the human immunodeficiency virus type 1 envelope protein gp120 on human fetal astrocytes. *J Virol* **68:** 6824-8.

Mabrouk K, Van Rietschoten J, Vives E, Darbon H, Rochat H, Sabatier JM (1991). Lethal neurotoxicity in mice of the basic domains of HIV and SIV Rev proteins. Study of these regions by circular dichroism. *FEBS Lett* **289:** 13-7.

Maddon PJ, McDougal JS, Clapham PR, Dalgleish AG, Jamal S, Weiss RA, Axel R (1988). HIV infection does not require endocytosis of its receptor, CD4. *Cell* **54:** 865-74.

Magnuson DS, Knudsen BE, Geiger JD, Brownstone RM, Nath A (1995). Human immunodeficiency virus type 1 tat activates non-N-methyl-D-aspartate excitatory amino acid receptors and causes neurotoxicity. *Ann Neurol* **37:** 373-80.

Malipiero UV, Frei K, Fontana A (1990). Production of hemopoietic colony-stimulating factors by astrocytes. *J Immunol* **144:** 3816-21.

Marcoux FW, Choi DW, (eds). (2002). *CNS Neuroprotection*, Vol.155. Springer-Verlag: Berlin.

Marechal V, Clavel F, Heard JM, Schwartz O (1998). Cytosolic Gag p24 as an index of productive entry of human immunodeficiency virus type 1. *J Virol* **72:** 2208-12.

Marechal V, Prevost MC, Petit C, Perret E, Heard JM, Schwartz O (2001). Human immunodeficiency virus type 1 entry into macrophages mediated by macropinocytosis. *J Virol* **75:** 11166-77.

Mariani R, Chen D, Schrofelbauer B, Navarro F, Konig R, Bollman B, Munk C, Nymark-McMahon H, Landau NR (2003). Species-specific exclusion of APOBEC3G from HIV-1 virions by Vif. *Cell* **114:** 21-31.

Masliah E, Ge N, Achim CL, Hansen LA, Wiley CA (1992a). Selective neuronal vulnerability in HIV encephalitis. *J Neuropathol Exp Neurol* **51:** 585-93.

Masliah E, Ge N, Morey M, DeTeresa R, Terry RD, Wiley CA (1992b). Cortical dendritic pathology in human immunodeficiency virus encephalitis. *Lab Invest* **66:** 285-91.

Masliah E, Heaton RK, Marcotte TD, Ellis RJ, Wiley CA, Mallory M, Achim CL, McCutchan JA, Nelson JA, Atkinson JH, Grant I (1997). Dendritic injury is a

pathological substrate for human immunodeficiency virus-related cognitive disorders. HNRC Group. The HIV Neurobehavioral Research Center. *Ann Neurol* **42:** 963-72.

Matlin KS, Reggio H, Helenius A, Simons K (1982). Pathway of vesicular stomatitis virus entry leading to infection. *J Mol Biol* **156:** 609-31.

Matthias LJ, Yam PT, Jiang XM, Vandegraaff N, Li P, Poumbourios P, Donoghue N, Hogg PJ (2002). Disulfide exchange in domain 2 of CD4 is required for entry of HIV-1. *Nat Immunol* **3:** 727-32.

McArthur JC (1987). Neurologic manifestations of AIDS. *Medicine (Baltimore)* **66:** 407-37.

McArthur JC, Hoover DR, Bacellar H, Miller EN, Cohen BA, Becker JT, Graham NM, McArthur JH, Selnes OA, Jacobson LP, et al. (1993). Dementia in AIDS patients: incidence and risk factors. Multicenter AIDS Cohort Study. *Neurology* **43:** 2245-52.

McCarthy M, He J, Wood C (1998). HIV-1 strain-associated variability in infection of primary neuroglia. *J Neurovirol* **4:** 80-9.

McClure MO, Sommerfelt MA, Marsh M, Weiss RA (1990). The pH independence of mammalian retrovirus infection. *J Gen Virol* **71 (Pt 4):** 767-73.

McDougal JS, Maddon PJ, Dalgleish AG, Clapham PR, Littman DR, Godfrey M, Maddon DE, Chess L, Weiss RA, Axel R (1986). The T4 glycoprotein is a cell-surface receptor for the AIDS virus. *Cold Spring Harb Symp Quant Biol* **51 Pt 2:** 703-11.

McManus CM, Weidenheim K, Woodman SE, Nunez J, Hesselgesser J, Nath A, Berman JW (2000). Chemokine and chemokine-receptor expression in human glial elements: induction by the HIV protein, Tat, and chemokine autoregulation. *Am J Pathol* **156:** 1441-53.

Meric C, Spahr PF (1986). Rous sarcoma virus nucleic acid-binding protein p12 is necessary for viral 70S RNA dimer formation and packaging. *J Virol* **60:** 450-9.

Merrill JE, Chen IS (1991). HIV-1, macrophages, glial cells, and cytokines in AIDS nervous system disease. *Faseb J* **5:** 2391-7.

Messam CA, Major EO (2000). Stages of restricted HIV-1 infection in astrocyte cultures derived from human fetal brain tissue. *J Neurovirol* **6 Suppl 1:** S90-4.

Meucci O, Fatatis A, Simen AA, Bushell TJ, Gray PW, Miller RJ (1998). Chemokines regulate hippocampal neuronal signaling and gp120 neurotoxicity. *Proc Natl Acad Sci U S A* **95:** 14500-5.

Michael NL, Chang G, d'Arcy LA, Tseng CJ, Birx DL, Sheppard HW (1995). Functional characterization of human immunodeficiency virus type 1 nef genes in patients with divergent rates of disease progression. *J Virol* **69:** 6758-69.

Michael NL, Morrow P, Mosca J, Vahey M, Burke DS, Redfield RR (1991). Induction of human immunodeficiency virus type 1 expression in chronically infected cells is associated primarily with a shift in RNA splicing patterns. *J Virol* **65:** 1291-303.

Michaels J, Price RW, Rosenblum MK (1988). Microglia in the giant cell encephalitis of acquired immune deficiency syndrome: proliferation, infection and fusion. *Acta Neuropathol (Berl)* **76:** 373-9.

Miller MD, Farnet CM, Bushman FD (1997). Human immunodeficiency virus type 1 preintegration complexes: studies of organization and composition. *J Virol* **71:** 5382-90.

Miyake T, Tsuchihashi Y, Kitamura T, Fujita S (1984). Immunohistochemical studies of blood monocytes infiltrating into the neonatal rat brain. *Acta Neuropathol (Berl)* **62:** 291-7.

Miyazawa N, Crystal RG, Leopold PL (2001). Adenovirus serotype 7 retention in a late endosomal compartment prior to cytosol escape is modulated by fiber protein. *J Virol* **75:** 1387-400.

Mu FT, Callaghan JM, Steele-Mortimer O, Stenmark H, Parton RG, Campbell PL, McCluskey J, Yeo JP, Tock EP, Toh BH (1995). EEA1, an early endosome-associated protein. EEA1 is a conserved alpha-helical peripheral membrane protein flanked by cysteine "fingers" and contains a calmodulin-binding IQ motif. *J Biol Chem* **270:** 13503-11.

Muesing MA, Smith DH, Cabradilla CD, Benton CV, Lasky LA, Capon DJ (1985). Nucleic acid structure and expression of the human AIDS/lymphadenopathy retrovirus. *Nature* **313:** 450-8.

Muller-Ladner U, Jones JL, Wetsel RA, Gay S, Raine CS, Barnum SR (1996). Enhanced expression of chemotactic receptors in multiple sclerosis lesions. *J Neurol Sci* **144:** 135-41.

Myers G, MacInnes K, Korber B (1992). The emergence of simian/human immunodeficiency viruses. *AIDS Res Hum Retroviruses* **8:** 373-86.

Nakielny S, Fischer U, Michael WM, Dreyfuss G (1997). RNA transport. *Annu Rev Neurosci* **20:** 269-301.

Nara PL, Fischinger PJ (1988). Quantitative infectivity assay for HIV-1 and-2. *Nature* **332:** 469-70.

Nara PL, Hatch WC, Dunlop NM, Robey WG, Arthur LO, Gonda MA, Fischinger PJ (1987). Simple, rapid, quantitative, syncytium-forming microassay for the detection of human immunodeficiency virus neutralizing antibody. *AIDS Res Hum Retroviruses* **3:** 283-302.

Nath A (2002). Human immunodeficiency virus (HIV) proteins in neuropathogenesis of HIV dementia. *J Infect Dis* **186 Suppl 2:** S193-8.

Nath A, Conant K, Chen P, Scott C, Major EO (1999). Transient exposure to HIV-1 Tat protein results in cytokine production in macrophages and astrocytes. A hit and run phenomenon. *J Biol Chem* **274:** 17098-102.

Nath A, Geiger J (1998). Neurobiological aspects of human immunodeficiency virus infection: neurotoxic mechanisms. *Prog Neurobiol* **54:** 19-33.

Nath A, Hartloper V, Furer M, Fowke KR (1995). Infection of human fetal astrocytes with HIV-1: viral tropism and the role of cell to cell contact in viral transmission. *J Neuropathol Exp Neurol* **54:** 320-30.

Nathanson N, Cook DG, Kolson DL, Gonzalez-Scarano F (1994). Pathogenesis of HIV encephalopathy. *Ann N Y Acad Sci* **724:** 87-106.

Navia BA (1997). Clinical and biologic features of the AIDS dementia complex. *Neuroimaging Clin N Am* **7:** 581-92.

Navia BA, Cho ES, Petito CK, Price RW (1986a). The AIDS dementia complex: II. Neuropathology. *Ann Neurol* **19:** 525-35.

Navia BA, Jordan BD, Price RW (1986b). The AIDS dementia complex: I. Clinical features. *Ann Neurol* **19:** 517-24.

Navia BA, Price RW (1987). The acquired immunodeficiency syndrome dementia complex as the presenting or sole manifestation of human immunodeficiency virus infection. *Arch Neurol* **44:** 65-9.

Neumann M, Felber BK, Kleinschmidt A, Froese B, Erfle V, Pavlakis GN, Brack-Werner R (1995). Restriction of human immunodeficiency virus type 1 production in a human astrocytoma cell line is associated with a cellular block in Rev function. *J Virol* **69:** 2159-67.

Nguyen DG, Hildreth JE (2003). Involvement of macrophage mannose receptor in the binding and transmission of HIV by macrophages. *Eur J Immunol* **33:** 483-93.

Nicholls D, Attwell D (1990). The release and uptake of excitatory amino acids. *Trends Pharmacol Sci* **11:** 462-8.

Nichols BJ, Lippincott-Schwartz J (2001). Endocytosis without clathrin coats. *Trends Cell Biol* **11:** 406-12.

Nishida K, Markey SP (1996). Platelet-activating factor in brain regions after transient ischemia in gerbils. *Stroke* **27:** 514-8; discussion 518-9.

Nitta T, Ebato M, Sato K, Okumura K (1994). Expression of tumour necrosis factor-alpha, -beta and interferon-gamma genes within human neuroglial tumour cells and brain specimens. *Cytokine* **6:** 171-80.

Nottet HS, Jett M, Flanagan CR, Zhai QH, Persidsky Y, Rizzino A, Bernton EW, Genis P, Baldwin T, Schwartz J, et al. (1995). A regulatory role for astrocytes in HIV-1 encephalitis. An overexpression of eicosanoids, platelet-activating factor, and tumor necrosis factor-alpha by activated HIV-1-infected monocytes is attenuated by primary human astrocytes. *J Immunol* **154:** 3567-81.

Nottet HS, Persidsky Y, Sasseville VG, Nukuna AN, Bock P, Zhai QH, Sharer LR, McComb RD, Swindells S, Soderland C, Gendelman HE (1996). Mechanisms for the transendothelial migration of HIV-1-infected monocytes into brain. *J Immunol* **156:** 1284-95.

Novick P, Brennwald P (1993). Friends and family: the role of the Rab GTPases in vesicular traffic. *Cell* **75:** 597-601.

Nuovo GJ, Gallery F, MacConnell P, Braun A (1994). In situ detection of polymerase chain reaction-amplified HIV-1 nucleic acids and tumor necrosis factor-alpha RNA in the central nervous system. *Am J Pathol* **144:** 659-66.

O'Brien WA (1994). HIV-1 entry and reverse transcription in macrophages. *J Leukoc Biol* **56:** 273-7.

O'Brien WA, Namazi A, Kalhor H, Mao SH, Zack JA, Chen IS (1994). Kinetics of human immunodeficiency virus type 1 reverse transcription in blood mononuclear phagocytes are slowed by limitations of nucleotide precursors. *J Virol* **68:** 1258-63.

O'Doherty U, Swiggard WJ, Malim MH (2000). Human immunodeficiency virus type 1 spinoculation enhances infection through virus binding. *J Virol* **74:** 10074-80.

Ong CL, Thorpe JC, Gorry PR, Bannwarth S, Jaworowski A, Howard JL, Chung S, Campbell S, Christensen HS, Clerzius G, Mouland AJ, Gatignol A, Purcell DF (2005). Low TRBP levels support an innate human immunodeficiency virus type 1 resistance in astrocytes by enhancing the PKR antiviral response. *J Virol* **79:** 12763-72.

Owens RJ, Dubay JW, Hunter E, Compans RW (1991). Human immunodeficiency virus envelope protein determines the site of virus release in polarized epithelial cells. *Proc Natl Acad Sci U S A* **88:** 3987-91.

Palmer DL, Hjelle BL, Wiley CA, Allen S, Wachsman W, Mills RG, Davis LE, Merlin TL (1994). HIV-1 infection despite immediate combination antiviral therapy after infusion of contaminated white cells. *Am J Med* **97:** 289-95.

Pandori MW, Fitch NJ, Craig HM, Richman DD, Spina CA, Guatelli JC (1996). Producer-cell modification of human immunodeficiency virus type 1: Nef is a virion protein. *J Virol* **70:** 4283-90.

Park H, Davies MV, Langland JO, Chang HW, Nam YS, Tartaglia J, Paoletti E, Jacobs BL, Kaufman RJ, Venkatesan S (1994). TAR RNA-binding protein is an inhibitor of the interferon-induced protein kinase PKR. *Proc Natl Acad Sci U S A* **91:** 4713-7.

Patel CA, Mukhtar M, Pomerantz RJ (2000). Human immunodeficiency virus type 1 Vpr induces apoptosis in human neuronal cells. *J Virol* **74:** 9717-26.

Patton HK, Zhou ZH, Bubien JK, Benveniste EN, Benos DJ (2000). gp120-induced alterations of human astrocyte function: Na(+)/H(+) exchange, K(+) conductance, and glutamate flux. *Am J Physiol Cell Physiol* **279:** C700-8.

Pauza CD, Galindo J (1989). Persistent human immunodeficiency virus type 1 infection of monoblastoid cells leads to accumulation of self-integrated viral DNA and to production of defective virions. *J Virol* **63:** 3700-7.

Pauza CD, Price TM (1988). Human immunodeficiency virus infection of T cells and monocytes proceeds via receptor-mediated endocytosis. *J Cell Biol* **107:** 959-68.

Pellerin L, Magistretti PJ (1994). Glutamate uptake into astrocytes stimulates aerobic glycolysis: a mechanism coupling neuronal activity to glucose utilization. *Proc Natl Acad Sci U S A* **91:** 10625-9.

Pellerin L, Stolz M, Sorg O, Martin JL, Deschepper CF, Magistretti PJ (1997). Regulation of energy metabolism by neurotransmitters in astrocytes in primary culture and in an immortalized cell line. *Glia* **21:** 74-83.

Pemberton LA, Brew BJ (2001). Cerebrospinal fluid S-100beta and its relationship with AIDS dementia complex. *J Clin Virol* **22:** 249-53.

Perry VH, Hume DA, Gordon S (1985). Immunohistochemical localization of macrophages and microglia in the adult and developing mouse brain. *Neuroscience* **15:** 313-26.

Persidsky Y, Stins M, Way D, Witte MH, Weinand M, Kim KS, Bock P, Gendelman HE, Fiala M (1997). A model for monocyte migration through the blood-brain barrier during HIV-1 encephalitis. *J Immunol* **158:** 3499-510.

Peters A, Palay SW, Webster FH, (eds). (1991a). *The fine structure of the nervous system: neurons and their supporting cells*. Saunders: Philadelphia.

Peters PJ, Neefjes JJ, Oorschot V, Ploegh HL, Geuze HJ (1991b). Segregation of MHC class II molecules from MHC class I molecules in the Golgi complex for transport to lysosomal compartments. *Nature* **349:** 669-76.

Peterson PK, Hu S, Salak-Johnson J, Molitor TW, Chao CC (1997). Differential production of and migratory response to beta chemokines by human microglia and astrocytes. *J Infect Dis* **175:** 478-81.

Petito CK, Cho ES, Lemann W, Navia BA, Price RW (1986). Neuropathology of acquired immunodeficiency syndrome (AIDS): an autopsy review. *J Neuropathol Exp Neurol* **45:** 635-46.

Pettigrew LC, Meyer JJ, Craddock SD, Butler SM, Tai HH, Yokel RA (1995). Delayed elevation of platelet activating factor in ischemic hippocampus. *Brain Res* **691:** 243-7.

Peudenier S, Hery C, Ng KH, Tardieu M (1991). HIV receptors within the brain: a study of CD4 and MHC-II on human neurons, astrocytes and microglial cells. *Res Virol* **142:** 145-9.

Pfrieger FW, Barres BA (1996). New views on synapse-glia interactions. *Curr Opin Neurobiol* **6:** 615-21.

Phillips DM, Bourinbaiar AS (1992). Mechanism of HIV spread from lymphocytes to epithelia. *Virology* **186:** 261-73.

Pho MT, Ashok A, Atwood WJ (2000). JC virus enters human glial cells by clathrin-dependent receptor-mediated endocytosis. *J Virol* **74:** 2288-92.

Pierson T, McArthur J, Siliciano RF (2000). Reservoirs for HIV-1: mechanisms for viral persistence in the presence of antiviral immune responses and antiretroviral therapy. *Annu Rev Immunol* **18:** 665-708.

Pietroboni GR, Harnett GB, Bucens MR (1989). Centrifugal enhancement of human immunodeficiency virus (HIV) and human herpesvirus type 6 (HHV-6) infection in vitro. *J Virol Methods* **24:** 85-90.

Poli G, Kinter A, Justement JS, Kehrl JH, Bressler P, Stanley S, Fauci AS (1990). Tumor necrosis factor alpha functions in an autocrine manner in the induction of human immunodeficiency virus expression. *Proc Natl Acad Sci U S A* **87:** 782-5.

Pomerantz RJ, Trono D, Feinberg MB, Baltimore D (1990). Cells nonproductively infected with HIV-1 exhibit an aberrant pattern of viral RNA expression: a molecular model for latency. *Cell* **61:** 1271-6.

Ponten J, Macintyre EH (1968). Long term culture of normal and neoplastic human glia. *Acta Pathol Microbiol Scand* **74:** 465-86.

Pontow SE, Kery V, Stahl PD (1992). Mannose receptor. *Int Rev Cytol* **137B:** 221-44.

Popovic M, Sarngadharan MG, Read E, Gallo RC (1984). Detection, isolation, and continuous production of cytopathic retroviruses (HTLV-III) from patients with AIDS and pre-AIDS. *Science* **224:** 497-500.

Power C, Johnson RT (1995). HIV-1 associated dementia: clinical features and pathogenesis. *Can J Neurol Sci* **22:** 92-100.

Power C, Kong PA, Crawford TO, Wesselingh S, Glass JD, McArthur JC, Trapp BD (1993). Cerebral white matter changes in acquired immunodeficiency syndrome dementia: alterations of the blood-brain barrier. *Ann Neurol* **34:** 339-50.

Power C, McArthur JC, Johnson RT, Griffin DE, Glass JD, Perryman S, Chesebro B (1994). Demented and nondemented patients with AIDS differ in brain-derived human immunodeficiency virus type 1 envelope sequences. *J Virol* **68:** 4643-49.

Power C, McArthur JC, Nath A, Wehrly K, Mayne M, Nishio J, Langelier T, Johnson RT, Chesebro B (1998). Neuronal death induced by brain-derived human immunodeficiency virus type 1 envelope genes differs between demented and nondemented AIDS patients. *J Virol* **72:** 9045-53.

Prats AC, Sarih L, Gabus C, Litvak S, Keith G, Darlix JL (1988). Small finger protein of avian and murine retroviruses has nucleic acid annealing activity and positions the replication primer tRNA onto genomic RNA. *Embo J* **7:** 1777-83.

Price RW, Brew B, Sidtis J, Rosenblum M, Scheck AC, Cleary P (1988). The brain in AIDS: central nervous system HIV-1 infection and AIDS dementia complex. *Science* **239:** 586-92.

Prigozy TI, Sieling PA, Clemens D, Stewart PL, Behar SM, Porcelli SA, Brenner MB, Modlin RL, Kronenberg M (1997). The mannose receptor delivers lipoglycan antigens to endosomes for presentation to T cells by CD1b molecules. *Immunity* **6:** 187-97.

Pulliam L, Gascon R, Stubblebine M, McGuire D, McGrath MS (1997). Unique monocyte subset in patients with AIDS dementia. *Lancet* **349:** 692-5.

Pulliam L, Herndier BG, Tang NM, McGrath MS (1991). Human immunodeficiency virus-infected macrophages produce soluble factors that cause histological and neurochemical alterations in cultured human brains. *J Clin Invest* **87:** 503-12.

Pulliam L, West D, Haigwood N, Swanson RA (1993). HIV-1 envelope gp120 alters astrocytes in human brain cultures. *AIDS Res Hum Retroviruses* **9:** 439-44.

Pumarola-Sune T, Navia BA, Cordon-Cardo C, Cho ES, Price RW (1987). HIV antigen in the brains of patients with the AIDS dementia complex. *Ann Neurol* **21:** 490-6.

Purcell DF, Martin MA (1993). Alternative splicing of human immunodeficiency virus type 1 mRNA modulates viral protein expression, replication, and infectivity. *J Virol* **67:** 6365-78.

Racoosin EL, Swanson JA (1989). Macrophage colony-stimulating factor (rM-CSF) stimulates pinocytosis in bone marrow-derived macrophages. *J Exp Med* **170:** 1635-48.

Racoosin EL, Swanson JA (1992). M-CSF-induced macropinocytosis increases solute endocytosis but not receptor-mediated endocytosis in mouse macrophages. *J Cell Sci* **102 (Pt 4):** 867-80.

Racoosin EL, Swanson JA (1993). Macropinosome maturation and fusion with tubular lysosomes in macrophages. *J Cell Biol* **121:** 1011-20.

Raff MC, Abney ER, Miller RH (1984). Two glial cell lineages diverge prenatally in rat optic nerve. *Dev Biol* **106:** 53-60.

Raff MC, Ffrench-Constant C, Miller RH (1987). Glial cells in the rat optic nerve and some thoughts on remyelination in the mammalian CNS. *J Exp Biol* **132:** 35-41.

Raff MC, Lillien LE (1988). Differentiation of a bipotential glial progenitor cell: what controls the timing and the choice of developmental pathway? *J Cell Sci Suppl* **10:** 77-83.

Ranki A, Nyberg M, Ovod V, Haltia M, Elovaara I, Raininko R, Haapasalo H, Krohn K (1995). Abundant expression of HIV Nef and Rev proteins in brain astrocytes in vivo is associated with dementia. *AIDS* **9:** 1001-8.

Ratner L, Haseltine W, Patarca R, Livak KJ, Starcich B, Josephs SF, Doran ER, Rafalski JA, Whitehorn EA, Baumeister K, et al. (1985). Complete nucleotide sequence of the AIDS virus, HTLV-III. *Nature* **313:** 277-84.

Rawal BD, Vyas GN (1996). Magnesium-mediated reversal of the apparent virucidal effect of ascorbic acid or congo red reacted in vitro with the human immunodeficiency virus. *Biologicals* **24:** 113-6.

Reeves JD, Hibbitts S, Simmons G, McKnight A, Azevedo-Pereira JM, Moniz-Pereira J, Clapham PR (1999). Primary human immunodeficiency virus type 2 (HIV-2) isolates

infect CD4-negative cells via CCR5 and CXCR4: comparison with HIV-1 and simian immunodeficiency virus and relevance to cell tropism in vivo. *J Virol* **73:** 7795-804.

Regnier-Vigouroux A (2003). The mannose receptor in the brain. *Int Rev Cytol* **226:** 321-42.

Reich E, Goldberg IH (1964). Actinomycin and nucleic acid function. *Prog Nucleic Acid Res Mol Biol* **3:** 183-234.

Reyes MG, Faraldi F, Senseng CS, Flowers C, Fariello R (1991). Nigral degeneration in acquired immune deficiency syndrome (AIDS). *Acta Neuropathol (Berl)* **82:** 39-44.

Rezaie P, Trillo-Pazos G, Everall IP, Male DK (2002). Expression of beta-chemokines and chemokine receptors in human fetal astrocyte and microglial co-cultures: potential role of chemokines in the developing CNS. *Glia* **37:** 64-75.

Rhodes RH (1987). Histopathology of the central nervous system in the acquired immunodeficiency syndrome. *Hum Pathol* **18:** 636-43.

Ridet JL, Malhotra SK, Privat A, Gage FH (1997). Reactive astrocytes: cellular and molecular cues to biological function. *Trends Neurosci* **20:** 570-7.

Rill RL, Hecker KH (1996). Sequence-specific actinomycin D binding to single-stranded DNA inhibits HIV reverse transcriptase and other polymerases. *Biochemistry* **35:** 3525-33.

Robert-Guroff M, Popovic M, Gartner S, Markham P, Gallo RC, Reitz MS (1990). Structure and expression of tat-, rev-, and nef-specific transcripts of human immunodeficiency virus type 1 in infected lymphocytes and macrophages. *J Virol* **64:** 3391-8.

Rosenberg ES, Altfeld M, Poon SH, Phillips MN, Wilkes BM, Eldridge RL, Robbins GK, D'Aquila RT, Goulder PJ, Walker BD (2000). Immune control of HIV-1 after early treatment of acute infection. *Nature* **407:** 523-6.

Rosenman SJ, Shrikant P, Dubb L, Benveniste EN, Ransohoff RM (1995). Cytokine-induced expression of vascular cell adhesion molecule-1 (VCAM-1) by astrocytes and astrocytoma cell lines. *J Immunol* **154:** 1888-99.

Rossio JL, Esser MT, Suryanarayana K, Schneider DK, Bess JW, Jr., Vasquez GM, Wiltrout TA, Chertova E, Grimes MK, Sattentau Q, Arthur LO, Henderson LE, Lifson JD (1998). Inactivation of human immunodeficiency virus type 1 infectivity with preservation of conformational and functional integrity of virion surface proteins. *J Virol* **72:** 7992-8001.

Rothenberger S, Iacopetta BJ, Kuhn LC (1987). Endocytosis of the transferrin receptor requires the cytoplasmic domain but not its phosphorylation site. *Cell* **49:** 423-31.

Rottman JB, Ganley KP, Williams K, Wu L, Mackay CR, Ringler DJ (1997). Cellular localization of the chemokine receptor CCR5. Correlation to cellular targets of HIV-1 infection. *Am J Pathol* **151:** 1341-51.

Rutka JT, Murakami M, Dirks PB, Hubbard SL, Becker LE, Fukuyama K, Jung S, Tsugu A, Matsuzawa K (1997). Role of glial filaments in cells and tumors of glial origin: a review. *J Neurosurg* **87:** 420-30.

Sabatier JM, Vives E, Mabrouk K, Benjouad A, Rochat H, Duval A, Hue B, Bahraoui E (1991). Evidence for neurotoxic activity of tat from human immunodeficiency virus type 1. *J Virol* **65:** 961-7.

Sabri F, Tresoldi E, Di Stefano M, Polo S, Monaco MC, Verani A, Fiore JR, Lusso P, Major E, Chiodi F, Scarlatti G (1999). Nonproductive human immunodeficiency virus type 1 infection of human fetal astrocytes: independence from CD4 and major chemokine receptors. *Virology* **264:** 370-84.

Sacktor N, Lyles RH, Skolasky R, Kleeberger C, Selnes OA, Miller EN, Becker JT, Cohen B, McArthur JC (2001). HIV-associated neurologic disease incidence changes:: Multicenter AIDS Cohort Study, 1990-1998. *Neurology* **56:** 257-60.

Saha K, Zhang J, Gupta A, Dave R, Yimen M, Zerhouni B (2001). Isolation of primary HIV-1 that target CD8+ T lymphocytes using CD8 as a receptor. *Nat Med* **7:** 65-72.

Sairanen TR, Lindsberg PJ, Brenner M, Siren AL (1997). Global forebrain ischemia results in differential cellular expression of interleukin-1beta (IL-1beta) and its receptor at mRNA and protein level. *J Cereb Blood Flow Metab* **17:** 1107-20.

Saito Y, Sharer LR, Epstein LG, Michaels J, Mintz M, Louder M, Golding K, Cvetkovich TA, Blumberg BM (1994). Overexpression of nef as a marker for restricted HIV-1 infection of astrocytes in postmortem pediatric central nervous tissues. *Neurology* **44:** 474-81.

Sakai H, Kawamura M, Sakuragi J, Sakuragi S, Shibata R, Ishimoto A, Ono N, Ueda S, Adachi A (1993). Integration is essential for efficient gene expression of human immunodeficiency virus type 1. *J Virol* **67:** 1169-74.

Sallusto F, Cella M, Danieli C, Lanzavecchia A (1995). Dendritic cells use macropinocytosis and the mannose receptor to concentrate macromolecules in the major histocompatibility complex class II compartment: downregulation by cytokines and bacterial products. *J Exp Med* **182:** 389-400.

Sallusto F, Lanzavecchia A (1994). Efficient presentation of soluble antigen by cultured human dendritic cells is maintained by granulocyte/macrophage colony-stimulating factor plus interleukin 4 and downregulated by tumor necrosis factor alpha. *J Exp Med* **179:** 1109-18.

Sambrook J, Fritsch EF, Maniatis T, (eds). (1989). *Molecular Cloning: A laboratory manual*, Vol.1, 2nd edn. Cold Spring Harbor Laboratory Press: Cold Spring Harbor.

Sanders VJ, Everall IP, Johnson RW, Masliah E (2000). Fibroblast growth factor modulates HIV coreceptor CXCR4 expression by neural cells. HNRC Group. *J Neurosci Res* **59:** 671-9.

Schaeffer E, Geleziunas R, Greene WC (2001). Human immunodeficiency virus type 1 Nef functions at the level of virus entry by enhancing cytoplasmic delivery of virions. *J Virol* **75:** 2993-3000.

Schilling T, Nitsch R, Heinemann U, Haas D, Eder C (2001). Astrocyte-released cytokines induce ramification and outward K+ channel expression in microglia via distinct signalling pathways. *Eur J Neurosci* **14:** 463-73.

Schrager LK, D'Souza MP (1998). Cellular and anatomical reservoirs of HIV-1 in patients receiving potent antiretroviral combination therapy. *Jama* **280:** 67-71.

Schulz TF, Jameson BA, Lopalco L, Siccardi AG, Weiss RA, Moore JP (1992). Conserved structural features in the interaction between retroviral surface and transmembrane glycoproteins? *AIDS Res Hum Retroviruses* **8:** 1571-80.

Schwartz O, Marechal V, Le Gall S, Lemonnier F, Heard JM (1996). Endocytosis of major histocompatibility complex class I molecules is induced by the HIV-1 Nef protein. *Nat Med* **2:** 338-42.

Schwartz S, Felber BK, Benko DM, Fenyo EM, Pavlakis GN (1990). Cloning and functional analysis of multiply spliced mRNA species of human immunodeficiency virus type 1. *J Virol* **64:** 2519-29.

Schwarze SR, Ho A, Vocero-Akbani A, Dowdy SF (1999). In vivo protein transduction: delivery of a biologically active protein into the mouse. *Science* **285:** 1569-72.

Schweighardt B, Atwood WJ (2001). HIV type 1 infection of human astrocytes is restricted by inefficient viral entry. *AIDS Res Hum Retroviruses* **17:** 1133-42.

Schweighardt B, Shieh JT, Atwood WJ (2001). CD4/CXCR4-independent infection of human astrocytes by a T-tropic strain of HIV-1. *J Neurovirol* **7:** 155-62.

Shahabuddin M, Bentsman G, Volsky B, Rodriguez I, Volsky DJ (1996). A mechanism of restricted human immunodeficiency virus type 1 expression in human glial cells. *J Virol* **70:** 7992-8002.

Shahabuddin M, Volsky B, Kim H, Sakai K, Volsky DJ (1992). Regulated expression of human immunodeficiency virus type 1 in human glial cells: induction of dormant virus. *Pathobiology* **60:** 195-205.

Shapshak P, Sun NC, Resnick L, Thornthwaite JT, Schiller P, Yoshioka M, Svenningsson A, Tourtellotte WW, Imagawa DT (1991). HIV-1 propagates in human neuroblastoma cells. *J Acquir Immune Defic Syndr* **4:** 228-37.

Sharer LR (1992). Pathology of HIV-1 infection of the central nervous system. A review. *J Neuropathol Exp Neurol* **51:** 3-11.

Sharer LR, Cho ES, Epstein LG (1985). Multinucleated giant cells and HTLV-III in AIDS encephalopathy. *Hum Pathol* **16:** 760.

Sharer LR, Epstein LG, Cho ES, Joshi VV, Meyenhofer MF, Rankin LF, Petito CK (1986). Pathologic features of AIDS encephalopathy in children: evidence for LAV/HTLV-III infection of brain. *Hum Pathol* **17:** 271-84.

Sharkey ME, Teo I, Greenough T, Sharova N, Luzuriaga K, Sullivan JL, Bucy RP, Kostrikis LG, Haase A, Veryard C, Davaro RE, Cheeseman SH, Daly JS, Bova C, Ellison RT, 3rd, Mady B, Lai KK, Moyle G, Nelson M, Gazzard B, Shaunak S, Stevenson M (2000). Persistence of episomal HIV-1 infection intermediates in patients on highly active anti-retroviral therapy. *Nat Med* **6:** 76-81.

Sharp PM, Shaw GM, Hahn BH (2005). Simian immunodeficiency virus infection of chimpanzees. *J Virol* **79:** 3891-902.

Shaw GM, Harper ME, Hahn BH, Epstein LG, Gajdusek DC, Price RW, Navia BA, Petito CK, O'Hara CJ, Groopman JE, et al. (1985). HTLV-III infection in brains of children and adults with AIDS encephalopathy. *Science* **227:** 177-82.

Shepherd VL, Tarnowski BI, McLaughlin BJ (1991). Isolation and characterization of a mannose receptor from human pigment epithelium. *Invest Ophthalmol Vis Sci* **32:** 1779-84.

Shi B, De Girolami U, He J, Wang S, Lorenzo A, Busciglio J, Gabuzda D (1996). Apoptosis induced by HIV-1 infection of the central nervous system. *J Clin Invest* **98:** 1979-90.

Shrikant P, Benveniste EN (1996). The central nervous system as an immunocompetent organ: role of glial cells in antigen presentation. *J Immunol* **157:** 1819-22.

Sieczkarski SB, Whittaker GR (2002). Dissecting virus entry via endocytosis. *J Gen Virol* **83:** 1535-45.

Siliciano JD, Siliciano RF (2000). Latency and viral persistence in HIV-1 infection. *J Clin Invest* **106:** 823-5.

Snider WD, Simpson DM, Nielsen S, Gold JW, Metroka CE, Posner JB (1983). Neurological complications of acquired immune deficiency syndrome: analysis of 50 patients. *Ann Neurol* **14:** 403-18.

Sodroski J, Goh WC, Rosen C, Dayton A, Terwilliger E, Haseltine W (1986). A second post-transcriptional trans-activator gene required for HTLV-III replication. *Nature* **321:** 412-7.

Somsel Rodman J, Wandinger-Ness A (2000). Rab GTPases coordinate endocytosis. *J Cell Sci* **113 Pt 2:** 183-92.

Sotelo JR, Porter KR (1959). An electron microscope study of the rat ovum. *J Biophys Biochem Cytol* **5:** 327-42.

Speck RF, Esser U, Penn ML, Eckstein DA, Pulliam L, Chan SY, Goldsmith MA (1999). A trans-receptor mechanism for infection of CD4-negative cells by human immunodeficiency virus type 1. *Curr Biol* **9:** 547-50.

Speth C, Joebstl B, Barcova M, Dierich MP (2000). HIV-1 envelope protein gp41 modulates expression of interleukin-10 and chemokine receptors on monocytes, astrocytes and neurones. *AIDS* **14:** 629-36.

Spina CA, Guatelli JC, Richman DD (1995). Establishment of a stable, inducible form of human immunodeficiency virus type 1 DNA in quiescent CD4 lymphocytes in vitro. *J Virol* **69:** 2977-88.

Stahl PD, Ezekowitz RA (1998). The mannose receptor is a pattern recognition receptor involved in host defense. *Curr Opin Immunol* **10:** 50-5.

Stanley LC, Mrak RE, Woody RC, Perrot LJ, Zhang S, Marshak DR, Nelson SJ, Griffin WS (1994). Glial cytokines as neuropathogenic factors in HIV infection: pathogenic similarities to Alzheimer's disease. *J Neuropathol Exp Neurol* **53:** 231-8.

Stella N, Estelles A, Siciliano J, Tence M, Desagher S, Piomelli D, Glowinski J, Premont J (1997). Interleukin-1 enhances the ATP-evoked release of arachidonic acid from mouse astrocytes. *J Neurosci* **17:** 2939-46.

Steuler H, Storch-Hagenlocher B, Wildemann B (1992). Distinct populations of human immunodeficiency virus type 1 in blood and cerebrospinal fluid. *AIDS Res Hum Retroviruses* **8:** 53-9.

Stevenson M, Stanwick TL, Dempsey MP, Lamonica CA (1990). HIV-1 replication is controlled at the level of T cell activation and proviral integration. *Embo J* **9:** 1551-60.

Strizki JM, Albright AV, Sheng H, O'Connor M, Perrin L, Gonzalez-Scarano F (1996). Infection of primary human microglia and monocyte-derived macrophages with human immunodeficiency virus type 1 isolates: evidence of differential tropism. *J Virol* **70:** 7654-62.

Stuart LM, Ezekowitz RA (2005). Phagocytosis: elegant complexity. *Immunity* **22:** 539-50.

Swanson JA (1989). Phorbol esters stimulate macropinocytosis and solute flow through macrophages. *J Cell Sci* **94 (Pt 1):** 135-42.

Swanson JA, Baer SC (1995). Phagocytosis by zippers and triggers. *Trends Cell Biol* **5:** 89-93.

Swanson JA, Watts C (1995). Macropinocytosis. *Trends Cell Biol* **5:** 424-8.

Swingler S, Easton A, Morris A (1992). Cytokine augmentation of HIV-1 LTR-driven gene expression in neural cells. *AIDS Res Hum Retroviruses* **8:** 487-93.

Tabernero A, Velasco A, Granda B, Lavado EM, Medina JM (2002). Transcytosis of albumin in astrocytes activates the sterol regulatory element-binding protein-1, which promotes the synthesis of the neurotrophic factor oleic acid. *J Biol Chem* **277:** 4240-6.

Takahashi K, Wesselingh SL, Griffin DE, McArthur JC, Johnson RT, Glass JD (1996). Localization of HIV-1 in human brain using polymerase chain reaction/in situ hybridization and immunocytochemistry. *Ann Neurol* **39:** 705-11.

Tang SB, Levy JA (1991). Inactivation of HIV-1 by trypsin and its use in demonstrating specific virus infection of cells. *J Virol Methods* **33:** 39-46.

Tardieu M, Hery C, Peudenier S, Boespflug O, Montagnier L (1992). Human immunodeficiency virus type 1-infected monocytic cells can destroy human neural cells after cell-to-cell adhesion. *Ann Neurol* **32:** 11-7.

Taylor AW, Streilein JW (1996). Inhibition of antigen-stimulated effector T cells by human cerebrospinal fluid. *Neuroimmunomodulation* **3:** 112-8.

Teichberg VI (1991). Glial glutamate receptors: likely actors in brain signaling. *Faseb J* **5:** 3086-91.

Thompson KA, Churchill MJ, Gorry PR, Sterjovski J, Oelrichs RB, Wesselingh SL, McLean CA (2004). Astrocyte specific viral strains in HIV dementia. *Ann Neurol* **56:** 873-7.

Thompson KA, McArthur JC, Wesselingh SL (2001). Correlation between neurological progression and astrocyte apoptosis in HIV-associated dementia. *Ann Neurol* **49:** 745-52.

Thorpe J (2001). TAR RNA-Binding Protein (TRBP) rescues highly productive HIV-1 expression in astrocytes. In: *Australian Virology Group Meeting*: Frazer Island, Queensland, Australia.

Toggas SM, Masliah E, Rockenstein EM, Rall GF, Abraham CR, Mucke L (1994). Central nervous system damage produced by expression of the HIV-1 coat protein gp120 in transgenic mice. *Nature* **367:** 188-93.

Tornatore C, Chandra R, Berger JR, Major EO (1994a). HIV-1 infection of subcortical astrocytes in the pediatric central nervous system. *Neurology* **44:** 481-7.

Tornatore C, Meyers K, Atwood W, Conant K, Major E (1994b). Temporal patterns of human immunodeficiency virus type 1 transcripts in human fetal astrocytes. *J Virol* **68:** 93-102.

Tornatore C, Nath A, Amemiya K, Major EO (1991). Persistent human immunodeficiency virus type 1 infection in human fetal glial cells reactivated by T-cell factor(s) or by the cytokines tumor necrosis factor alpha and interleukin-1 beta. *J Virol* **65:** 6094-100.

Trillo-Pazos G, McFarlane-Abdulla E, Campbell IC, Pilkington GJ, Everall IP (2000). Recombinant nef HIV-IIIB protein is toxic to human neurons in culture. *Brain Res* **864:** 315-26.

Trono D (1992). Partial reverse transcripts in virions from human immunodeficiency and murine leukemia viruses. *J Virol* **66:** 4893-900.

Trujillo JR, Jensen P, Maric D, Major EO (2004). Human Progenitor Derived Astrocytes Phagocytized HIV-1 through Mannose Receptor. In: *11th Conference on Retroviruses and Opportunistic Infections*: Mascone West, San Francisco.

Turville S, Wilkinson J, Cameron P, Dable J, Cunningham AL (2003). The role of dendritic cell C-type lectin receptors in HIV pathogenesis. *J Leukoc Biol* **74:** 710-8.

Turville SG, Cameron PU, Handley A, Lin G, Pohlmann S, Doms RW, Cunningham AL (2002). Diversity of receptors binding HIV on dendritic cell subsets. *Nat Immunol* **3:** 975-83.

Turville SG, Santos JJ, Frank I, Cameron PU, Wilkinson J, Miranda-Saksena M, Dable J, Stossel H, Romani N, Piatak M, Jr., Lifson JD, Pope M, Cunningham AL (2004). Immunodeficiency virus uptake, turnover, and 2-phase transfer in human dendritic cells. *Blood* **103:** 2170-9.

Vago L, Trabattoni G, Lechi A, Cristina S, Budka H (1990). Neuropathology of AIDS dementia. A review after 205 post mortem examinations. *Acta Neurol (Napoli)* **12:** 32-5.

Van Dyke RW (1996). Acidification of lysosomes and endosomes. *Subcell Biochem* **27:** 331-60.

Vandegraaff N, Kumar R, Burrell CJ, Li P (2001a). Kinetics of human immunodeficiency virus type 1 (HIV) DNA integration in acutely infected cells as determined using a novel assay for detection of integrated HIV DNA. *J Virol* **75:** 11253-60.

Vandegraaff N, Kumar R, Hocking H, Burke TR, Jr., Mills J, Rhodes D, Burrell CJ, Li P (2001b). Specific inhibition of human immunodeficiency virus type 1 (HIV-1) integration in cell culture: putative inhibitors of HIV-1 integrase. *Antimicrob Agents Chemother* **45:** 2510-6.

Vaughn JE, Grieshaber JA (1972). An electron microscopic investigation of glycogen and mitochondria in developing and adult rat spinal motor neuropil. *J Neurocytol* **1:** 397-412.

Vaux DL, Hacker G (1995). Hypothesis: apoptosis caused by cytotoxins represents a defensive response that evolved to combat intracellular pathogens. *Clin Exp Pharmacol Physiol* **22:** 861-3.

Vazeux R, Brousse N, Jarry A, Henin D, Marche C, Vedrenne C, Mikol J, Wolff M, Michon C, Rozenbaum W, et al. (1987). AIDS subacute encephalitis. Identification of HIV-infected cells. *Am J Pathol* **126:** 403-10.

Vidal N, Peeters M, Mulanga-Kabeya C, Nzilambi N, Robertson D, Ilunga W, Sema H, Tshimanga K, Bongo B, Delaporte E (2000). Unprecedented degree of human immunodeficiency virus type 1 (HIV-1) group M genetic diversity in the Democratic Republic of Congo suggests that the HIV-1 pandemic originated in Central Africa. *J Virol* **74:** 10498-507.

von Schwedler UK, Stemmler TL, Klishko VY, Li S, Albertine KH, Davis DR, Sundquist WI (1998). Proteolytic refolding of the HIV-1 capsid protein amino-terminus facilitates viral core assembly. *Embo J* **17:** 1555-68.

Wang TH, Donaldson YK, Brettle RP, Bell JE, Simmonds P (2001). Identification of shared populations of human immunodeficiency virus type 1 infecting microglia and tissue macrophages outside the central nervous system. *J Virol* **75:** 11686-99.

Warren G, Woodman P, Pypaert M, Smythe E (1988). Cell-free assays and the mechanism of receptor-mediated endocytosis. *Trends Biochem Sci* **13:** 462-5.

Weber J, Clapham P, McKeating J, Stratton M, Robey E, Weiss R (1989). Infection of brain cells by diverse human immunodeficiency virus isolates: role of CD4 as receptor. *J Gen Virol* **70 (Pt 10):** 2653-60.

Wei X, Ghosh SK, Taylor ME, Johnson VA, Emini EA, Deutsch P, Lifson JD, Bonhoeffer S, Nowak MA, Hahn BH, et al. (1995). Viral dynamics in human immunodeficiency virus type 1 infection. *Nature* **373:** 117-22.

Weiss JM, Downie SA, Lyman WD, Berman JW (1998). Astrocyte-derived monocyte-chemoattractant protein-1 directs the transmigration of leukocytes across a model of the human blood-brain barrier. *J Immunol* **161:** 6896-903.

Weiss JM, Nath A, Major EO, Berman JW (1999). HIV-1 Tat induces monocyte chemoattractant protein-1-mediated monocyte transmigration across a model of the human blood-brain barrier and up-regulates CCR5 expression on human monocytes. *J Immunol* **163:** 2953-9.

Wekerle H, Sun D, Oropeza-Wekerle RL, Meyermann R (1987). Immune reactivity in the nervous system: modulation of T-lymphocyte activation by glial cells. *J Exp Biol* **132:** 43-57.

Welker R, Kottler H, Kalbitzer HR, Krausslich HG (1996). Human immunodeficiency virus type 1 Nef protein is incorporated into virus particles and specifically cleaved by the viral proteinase. *Virology* **219:** 228-36.

Wesselingh SL, Gough NM, Finlay-Jones JJ, McDonald PJ (1990). Detection of cytokine mRNA in astrocyte cultures using the polymerase chain reaction. *Lymphokine Res* **9:** 177-85.

Wesselingh SL, Power C, Glass JD, Tyor WR, McArthur JC, Farber JM, Griffin JW, Griffin DE (1993). Intracerebral cytokine messenger RNA expression in acquired immunodeficiency syndrome dementia. *Ann Neurol* **33:** 576-82.

Wesselingh SL, Takahashi K, Glass JD, McArthur JC, Griffin JW, Griffin DE (1997). Cellular localization of tumor necrosis factor mRNA in neurological tissue from HIV-infected patients by combined reverse transcriptase/polymerase chain reaction in situ hybridization and immunohistochemistry. *J Neuroimmunol* **74:** 1-8.

West MA, Prescott AR, Eskelinen EL, Ridley AJ, Watts C (2000). Rac is required for constitutive macropinocytosis by dendritic cells but does not control its downregulation. *Curr Biol* **10:** 839-48.

Wiegers K, Rutter G, Kottler H, Tessmer U, Hohenberg H, Krausslich HG (1998). Sequential steps in human immunodeficiency virus particle maturation revealed by alterations of individual Gag polyprotein cleavage sites. *J Virol* **72:** 2846-54.

Wiley CA (1996). Polymerase chain reaction in situ hybridization--opening Pandora's box? *Ann Neurol* **39:** 691-2.

Wiley CA, Masliah E, Morey M, Lemere C, DeTeresa R, Grafe M, Hansen L, Terry R (1991). Neocortical damage during HIV infection. *Ann Neurol* **29:** 651-7.

Wiley CA, Schrier RD, Nelson JA, Lampert PW, Oldstone MB (1986). Cellular localization of human immunodeficiency virus infection within the brains of acquired immune deficiency syndrome patients. *Proc Natl Acad Sci U S A* **83:** 7089-93.

Wiley CA, Soontornniyomkij V, Radhakrishnan L, Masliah E, Mellors J, Hermann SA, Dailey P, Achim CL (1998). Distribution of brain HIV load in AIDS. *Brain Pathol* **8:** 277-84.

Wilkin GP, Marriott DR, Cholewinski AJ (1990). Astrocyte heterogeneity. *Trends Neurosci* **13:** 43-6.

Williams KC, Hickey WF (1995). Traffic of hematogenous cells through the central nervous system. *Curr Top Microbiol Immunol* **202:** 221-45.

Williams KC, Hickey WF (2002). Central nervous system damage, monocytes and macrophages, and neurological disorders in AIDS. *Annu Rev Neurosci* **25:** 537-62.

Williams RW, Herrup K (1988). The control of neuron number. *Annu Rev Neurosci* **11:** 423-53.

Winkler MK, Beveniste EN (1998). Transforming growth factor-beta inhibition of cytokine-induced vascular cell adhesion molecule-1 expression in human astrocytes. *Glia* **22:** 171-9.

Wong JK, Hezareh M, Gunthard HF, Havlir DV, Ignacio CC, Spina CA, Richman DD (1997). Recovery of replication-competent HIV despite prolonged suppression of plasma viremia. *Science* **278:** 1291-5.

Woodman SE, Benveniste EN, Nath A, Berman JW (1999). Human immunodeficiency virus type 1 TAT protein induces adhesion molecule expression in astrocytes. *J Neurovirol* **5:** 678-84.

Wortman MJ, Krachmarov CP, Kim JH, Gordon RG, Chepenik LG, Brady JN, Gallia GL, Khalili K, Johnson EM (2000). Interaction of HIV-1 Tat with Puralpha in nuclei of human glial cells: characterization of RNA-mediated protein-protein binding. *J Cell Biochem* **77:** 65-74.

Wu DT, Woodman SE, Weiss JM, McManus CM, D'Aversa TG, Hesselgesser J, Major EO, Nath A, Berman JW (2000). Mechanisms of leukocyte trafficking into the CNS. *J Neurovirol* **6 Suppl 1:** S82-5.

Wu Y, Marsh JW (2001). Selective transcription and modulation of resting T cell activity by preintegrated HIV DNA. *Science* **293:** 1503-6.

Wu Y, Marsh JW (2003a). Early transcription from nonintegrated DNA in human immunodeficiency virus infection. *J Virol* **77:** 10376-82.

Wu Y, Marsh JW (2003b). Gene transcription in HIV infection. *Microbes Infect* **5:** 1023-7.

Yeh MW, Kaul M, Zheng J, Nottet HS, Thylin M, Gendelman HE, Lipton SA (2000). Cytokine-stimulated, but not HIV-infected, human monocyte-derived macrophages produce neurotoxic levels of l -cysteine. *J Immunol* **164:** 4265-70.

Yerly S, Kaiser L, Perneger TV, Cone RW, Opravil M, Chave JP, Furrer H, Hirschel B, Perrin L (2000). Time of initiation of antiretroviral therapy: impact on HIV-1 viraemia. The Swiss HIV Cohort Study. *AIDS* **14:** 243-9.

Yu ACH, Hertz L, Norenberg MD, Sykova E, Waxman SG, (eds). (1992). *Neuronal-Astrocytic Interactions*, Vol.940-444-89537-X. Elsevier Science Publishers B. V.: Amsterdam.

Zanussi S, Bortolin MT, Giacca M, De Paoli P (2000). Quantitative assessment of integrated and episomal HIV DNA. *AIDS Res Hum Retroviruses* **16:** 931-3.

Zhang H, Bagasra O, Niikura M, Poiesz BJ, Pomerantz RJ (1994). Intravirion reverse transcripts in the peripheral blood plasma on human immunodeficiency virus type 1-infected individuals. *J Virol* **68:** 7591-7.

Zhang H, Dornadula G, Pomerantz RJ (1996a). Endogenous reverse transcription of human immunodeficiency virus type 1 in physiological microenviroments: an important stage for viral infection of nondividing cells. *J Virol* **70:** 2809-24.

Zhang H, Dornadula G, Wu Y, Havlir D, Richman DD, Pomerantz RJ (1996b). Kinetic analysis of intravirion reverse transcription in the blood plasma of human immunodeficiency virus type 1-infected individuals: direct assessment of resistance to reverse transcriptase inhibitors in vivo. *J Virol* **70:** 628-34.

Zhang H, Zhang Y, Spicer TP, Abbott LZ, Abbott M, Poiesz BJ (1993). Reverse transcription takes place within extracellular HIV-1 virions: potential biological significance. *AIDS Res Hum Retroviruses* **9:** 1287-96.

Zhang K, Rana F, Silva C, Ethier J, Wehrly K, Chesebro B, Power C (2003). Human immunodeficiency virus type 1 envelope-mediated neuronal death: uncoupling of viral replication and neurotoxicity. *J Virol* **77:** 6899-912.

Zhang L, Chung C, Hu BS, He T, Guo Y, Kim AJ, Skulsky E, Jin X, Hurley A, Ramratnam B, Markowitz M, Ho DD (2000). Genetic characterization of rebounding HIV-1 after cessation of highly active antiretroviral therapy. *J Clin Invest* **106:** 839-45.

Zhang L, Ramratnam B, Tenner-Racz K, He Y, Vesanen M, Lewin S, Talal A, Racz P, Perelson AS, Korber BT, Markowitz M, Ho DD (1999). Quantifying residual HIV-1 replication in patients receiving combination antiretroviral therapy. *N Engl J Med* **340:** 1605-13.

Zheng J, Ghorpade A, Niemann D, Cotter RL, Thylin MR, Epstein L, Swartz JM, Shepard RB, Liu X, Nukuna A, Gendelman HE (1999). Lymphotropic virions affect chemokine receptor-mediated neural signaling and apoptosis: implications for human immunodeficiency virus type 1-associated dementia. *J Virol* **73:** 8256-67.

Zigmond MJ, Bloom FE, Landis SC, Roberts JL, Squire LR, (eds). (1999). *Fundamental Neuroscience*. Academic Press: San Diego.